Oxidative Medicine and Cellular Longevity

Strategies for Modulating Oxidative Stress Under Diverse Physiological and Pathological Conditions 2020

Lead Guest Editor: Karolina Szewczyk-Golec
Guest Editors: Jolanta Czuczejko, Przemko Tylzanowski, Joanna Lecka, and Manjit Singh Rana

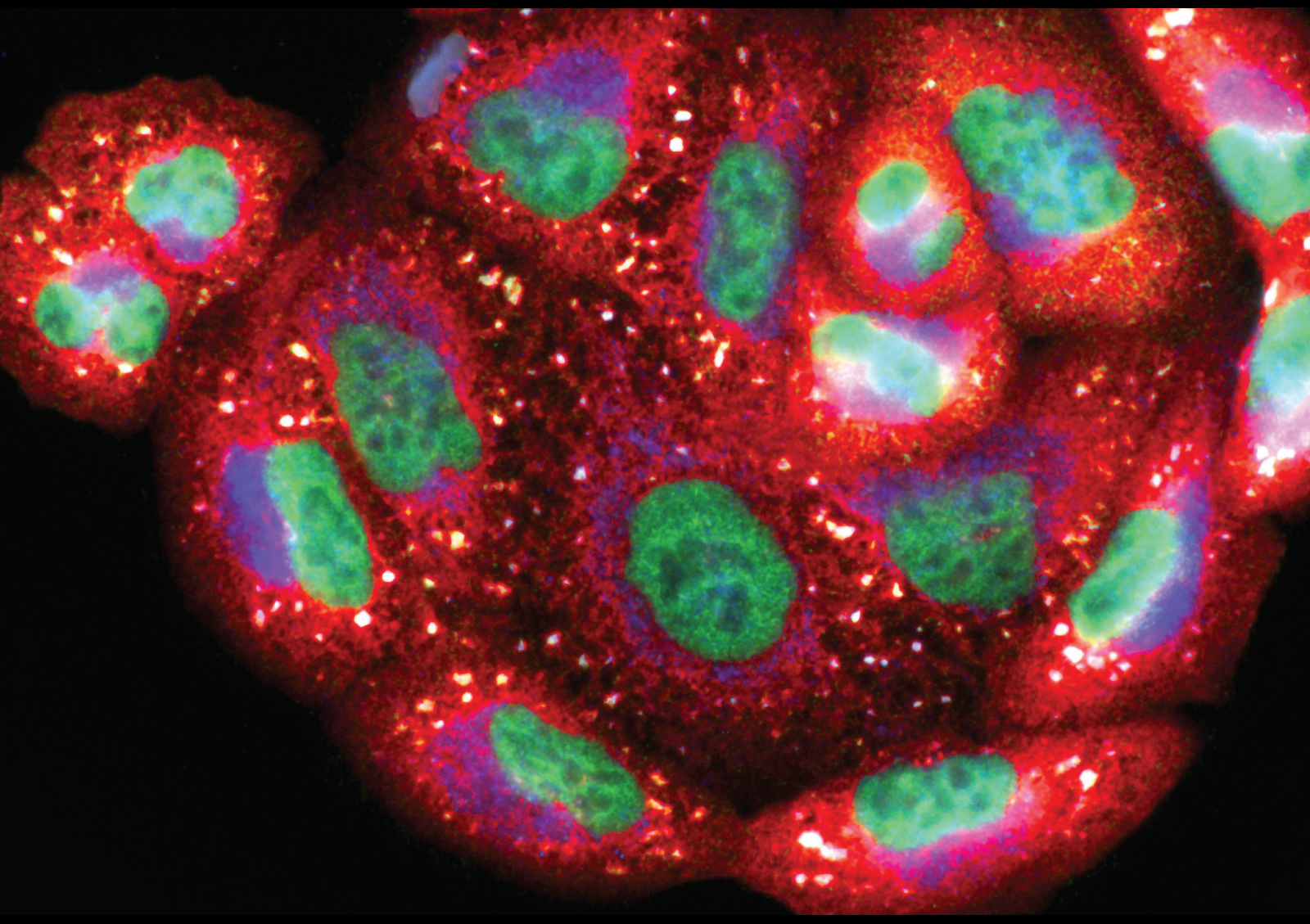

Strategies for Modulating Oxidative Stress Under Diverse Physiological and Pathological Conditions 2020

Oxidative Medicine and Cellular Longevity

Strategies for Modulating Oxidative Stress Under Diverse Physiological and Pathological Conditions 2020

Lead Guest Editor: Karolina Szewczyk-Golec
Guest Editors: Jolanta Czuczejko, Przemko Tylzanowski, Joanna Lecka, and Manjit Singh Rana

Copyright © 2021 Hindawi Limited. All rights reserved.

This is a special issue published in "Oxidative Medicine and Cellular Longevity." All articles are open access articles distributed under the Creative Commons Attribution License, which permits unrestricted use, distribution, and reproduction in any medium, provided the original work is properly cited.

Chief Editor

Jeannette Vasquez-Vivar, USA

Associate Editors

Amjad Islam Aqib, Pakistan
Angel Catalá, Argentina
Cinzia Domenicotti, Italy
Janusz Gebicki, Australia
Aldrin V. Gomes, USA
Vladimir Jakovljevic, Serbia
Thomas Kietzmann, Finland
Juan C. Mayo, Spain
Ryuichi Morishita, Japan
Claudia Penna, Italy
Sachchida Nand Rai, India
Paola Rizzo, Italy
Mithun Sinha, USA
Daniele Vergara, Italy
Victor M. Victor, Spain

Academic Editors

Ammar AL-Farga, Saudi Arabia
Mohd Adnan, Saudi Arabia
Ivanov Alexander, Russia
Fabio Altieri, Italy
Daniel Dias Rufino Arcanjo, Brazil
Peter Backx, Canada
Amira Badr, Egypt
Damian Bailey, United Kingdom
Rengasamy Balakrishnan, Republic of Korea
Jiaolin Bao, China
Ji C. Bihl, USA
Hareram Birla, India
Abdelhakim Bouyahya, Morocco
Ralf Braun, Austria
Laura Bravo, Spain
Matt Brody, USA
Amadou Camara, USA
Marcio Carocho, Portugal
Peter Celec, Slovakia
Giselle Cerchiaro, Brazil
Arpita Chatterjee, USA
Shao-Yu Chen, USA
Yujie Chen, China
Deepak Chhangani, USA
Ferdinando Chiaradonna, Italy
Zhao Zhong Chong, USA
Fabio Ciccarone, Italy
Alin Ciobica, Romania
Ana Cipak Gasparovic, Croatia
Giuseppe Cirillo, Italy
Maria R. Ciriolo, Italy
Massimo Collino, Italy
Manuela Corte-Real, Portugal
Manuela Curcio, Italy
Domenico D'Arca, Italy
Francesca Danesi, Italy
Claudio De Lucia, USA
Damião De Sousa, Brazil
Enrico Desideri , Italy
Francesca Diomede, Italy
Raul Dominguez-Perles, Spain
Joël R. Drevet, France
Grégory Durand, France
Alessandra Durazzo, Italy
Javier Egea, Spain
Pablo A. Evelson, Argentina
Mohd Farhan, USA
Ioannis G. Fatouros, Greece
Gianna Ferretti, Italy
Swaran J. S. Flora, India
Maurizio Forte, Italy
Teresa I. Fortoul, Mexico
Anna Fracassi, USA
Rodrigo Franco, USA
Juan Gambini, Spain
Gerardo García-Rivas, Mexico
Husam Ghanim, USA
Jayeeta Ghose, USA
Rajeshwary Ghosh, USA
Lucia Gimeno-Mallench , Spain
Anna M. Giudetti, Italy
Daniela Giustarini, Italy
José Rodrigo Godoy, USA
Saeid Golbidi, Canada
Guohua Gong, China
Tilman Grune, Germany
Solomon Habtemariam, United Kingdom
Eva-Maria Hanschmann, Germany
Md Saquib Hasnain, India
Md Hassan, India

Tim Hofer, Norway
John D. Horowitz, Australia
Silvana Hrelia, Italy
Dragan Hrncic, Serbia
Zebo Huang, China
Zhao Huang, China
Tarique Hussain, Pakistan
Stephan Immenschuh, Germany
Norsharina Ismail, Malaysia
Franco J. L, Brazil
Sedat Kacar, USA
Andleeb Khan, Saudi Arabia
Kum Kum Khanna, Australia
Neelam Khaper, Canada
Ramoji Kosuru, USA
Demetrios Kouretas, Greece
Andrey V. Kozlov, Austria
Chan-Yen Kuo, Taiwan
Gaocai Li, China
Guoping Li, USA
Jin-Long Li, China
Qiangqiang Li, China
Xin-Feng Li, China
Jialiang Liang, China
Adam Lightfoot, United Kingdom
Christopher Horst Lillig, Germany
Paloma B. Liton, USA
Ana Lloret, Spain
Lorenzo Loffredo, Italy
Camilo López-Alarcón, Chile
Daniel Lopez-Malo, Spain
Massimo Lucarini, Italy
Hai-Chun Ma, China
Nageswara Madamanchi, USA
Kenneth Maiese, USA
Marco Malaguti, Italy
Steven McAnulty, USA
Antonio Desmond McCarthy, Argentina
Sonia Medina-Escudero, Spain
Pedro Mena, Italy
Víctor M. Mendoza-Núñez, Mexico
Lidija Milkovic, Croatia
Alexandra Miller, USA
Sara Missaglia, Italy
Premysl Mladenka, Czech Republic
Sandra Moreno, Italy
Trevor A. Mori, Australia
Fabiana Morroni, Italy
Ange Mouithys-Mickalad, Belgium
Iordanis Mourouzis, Greece
Ryoji Nagai, Japan
Amit Kumar Nayak, India
Abderrahim Nemmar, United Arab Emirates
Xing Niu, China
Cristina Nocella, Italy
Susana Novella, Spain
Hassan Obied, Australia
Pál Pacher, USA
Pasquale Pagliaro, Italy
Dilipkumar Pal, India
Valentina Pallottini, Italy
Swapnil Pandey, USA
Mayur Parmar, USA
Vassilis Paschalis, Greece
Keshav Raj Paudel, Australia
Ilaria Peluso, Italy
Tiziana Persichini, Italy
Shazib Pervaiz, Singapore
Abdul Rehman Phull, Republic of Korea
Vincent Pialoux, France
Alessandro Poggi, Italy
Zsolt Radak, Hungary
Dario C. Ramirez, Argentina
Erika Ramos-Tovar, Mexico
Sid D. Ray, USA
Muneeb Rehman, Saudi Arabia
Hamid Reza Rezvani, France
Alessandra Ricelli, Italy
Francisco J. Romero, Spain
Joan Roselló-Catafau, Spain
Subhadeep Roy, India
Josep V. Rubert, The Netherlands
Sumbal Saba, Brazil
Kunihiro Sakuma, Japan
Gabriele Saretzki, United Kingdom
Luciano Saso, Italy
Nadja Schroder, Brazil

Anwen Shao, China
Iman Sherif, Egypt
Salah A Sheweita, Saudi Arabia
Xiaolei Shi, China
Manjari Singh, India
Giulia Sita, Italy
Ramachandran Srinivasan, India
Adrian Sturza, Romania
Kuo-hui Su, United Kingdom
Eisa Tahmasbpour Marzouni, Iran
Hailiang Tang, China
Carla Tatone, Italy
Shane Thomas, Australia
Carlo Gabriele Tocchetti, Italy
Angela Trovato Salinaro, Italy
Rosa Tundis, Italy
Kai Wang, China
Min-qi Wang, China
Natalie Ward, Australia
Grzegorz Wegrzyn, Poland
Philip Wenzel, Germany
Guangzhen Wu, China
Jianbo Xiao, Spain
Qiongming Xu, China
Liang-Jun Yan, USA
Guillermo Zalba, Spain
Jia Zhang, China
Junmin Zhang, China
Junli Zhao, USA
Chen-he Zhou, China
Yong Zhou, China
Mario Zoratti, Italy

Contents

Association between Vitamin D Supplements, Oxidative Stress Biomarkers, and Hyperbaric Therapy in Patients with Sudden Sensorineural Hearing Loss
Jarosław Paprocki, Paweł Sutkowy, Jacek Piechocki, and Alina Woźniak
Research Article (10 pages), Article ID 8895323, Volume 2021 (2021)

Gastric Electrical Pacing Reduces Apoptosis of Interstitial Cells of Cajal via Antioxidative Stress Effect Attributing to Phenotypic Polarization of M2 Macrophages in Diabetic Rats
Hongcai Wang, Kaile Zhao, Ying Ba, Tao Gao, Ning Shi, Qiong Niu, Chengxia Liu, and Yan Chen
Research Article (12 pages), Article ID 1298657, Volume 2021 (2021)

Activation of Nrf2 by miR-152 Inhibits Doxorubicin-Induced Cardiotoxicity via Attenuation of Oxidative Stress, Inflammation, and Apoptosis
Wen-Bin Zhang, Xin Lai, and Xu-Feng Guo
Research Article (14 pages), Article ID 8860883, Volume 2021 (2021)

Oxidative Stress-Related Mechanisms in Schizophrenia Pathogenesis and New Treatment Perspectives
Evgeny A. Ermakov, Elena M. Dmitrieva, Daria A. Parshukova, Daria V. Kazantseva, Alisa R. Vasilieva, and Liudmila P. Smirnova
Review Article (37 pages), Article ID 8881770, Volume 2021 (2021)

NAMPT/SIRT1 Attenuate Ang II-Induced Vascular Remodeling and Vulnerability to Hypertension by Inhibiting the ROS/MAPK Pathway
Lei Zhou, Sheng Zhang, Enkhbat Bolor-Erdene, Lingwei Wang, Ding Tian, and Yunqing Mei
Research Article (21 pages), Article ID 1974265, Volume 2020 (2020)

HSF1 Attenuates LPS-Induced Acute Lung Injury in Mice by Suppressing Macrophage Infiltration
Tao Li, Gui Xiao, Sipin Tan, Xueyan Shi, Leijing Yin, Chuyi Tan, Jia Gu, Yanjuan Liu, Huafei Deng, Ke Liu, Meidong Liu, Huali Zhang, and Xianzhong Xiao
Research Article (15 pages), Article ID 1936580, Volume 2020 (2020)

Early Enteral Nutrition Preserves Intestinal Barrier Function through Reducing the Formation of Neutrophil Extracellular Traps (NETs) in Critically Ill Surgical Patients
Qiongyuan Hu, Huajian Ren, Zhiwu Hong, Chenyang Wang, Tao Zheng, Yanhan Ren, Kai Chen, Song Liu, Gefei Wang, Guosheng Gu, Xiuwen Wu, and Jianan Ren
Research Article (8 pages), Article ID 8815655, Volume 2020 (2020)

Oxymatrine Ameliorates Memory Impairment in Diabetic Rats by Regulating Oxidative Stress and Apoptosis: Involvement of NOX2/NOX4
Yongpan Huang, Xinliang Li, Xi Zhang, and Jiayu Tang
Research Article (15 pages), Article ID 3912173, Volume 2020 (2020)

Natural Exogenous Antioxidant Defense against Changes in Human Skin Fibroblast Proteome Disturbed by UVA Radiation
Agnieszka Gęgotek, Pedro Domingues, and Elżbieta Skrzydlewska
Research Article (12 pages), Article ID 3216415, Volume 2020 (2020)

Protective Effect of Polydatin on Jejunal Mucosal Integrity, Redox Status, Inflammatory Response, and Mitochondrial Function in Intrauterine Growth-Retarded Weanling Piglets
Hao Zhang, Yanan Chen, Yue Li, and Tian Wang
Research Article (14 pages), Article ID 7178123, Volume 2020 (2020)

Bakuchiol Alleviates Hyperglycemia-Induced Diabetic Cardiomyopathy by Reducing Myocardial Oxidative Stress via Activating the SIRT1/Nrf2 Signaling Pathway
Wenshuai Ma, Wangang Guo, Fujun Shang, Yan Li, Wei Li, Jing Liu, Chao Ma, and Jiwei Teng
Research Article (15 pages), Article ID 3732718, Volume 2020 (2020)

The Impact of Modern Therapeutic Methods on the Oxidant-Antioxidant Equilibrium and Activities of Selected Lysosomal Enzymes and Serine Protease Inhibitor in Amateur Athletes
Łukasz Sielski, Paweł Sutkowy, Katarzyna Pawlak-Osińska, Alina Woźniak, Agnieszka Skopowska, Bartosz Woźniak, and Jolanta Czuczejko
Research Article (10 pages), Article ID 9792836, Volume 2020 (2020)

Two Faces of Heme Catabolic Pathway in Newborns: A Potential Role of Bilirubin and Carbon Monoxide in Neonatal Inflammatory Diseases
Wiktoria Osiak, Sławomir Wątroba, Lucyna Kapka-Skrzypczak, and Jacek Kurzepa
Review Article (14 pages), Article ID 7140496, Volume 2020 (2020)

Neuregulin-1β Protects the Rat Diaphragm during Sepsis against Oxidative Stress and Inflammation by Activating the PI3K/Akt Pathway
Hua Liu, Xiao-jian Weng, Jun-yan Yao, Jun Zheng, Xiang Lv, Xu-hui Zhou, Hong Jiang, and Shi-tong Li
Research Article (11 pages), Article ID 1720961, Volume 2020 (2020)

Body Mass Index (BMI) and Its Influence on the Cardiovascular and Operative Risk Profile in Coronary Artery Bypass Grafting Patients: Impact of Inflammation and Leptin
Katja Buschmann, Julius Wrobel, Ryan Chaban, Romina Rösch, Ahmed Ghazy, Alina Hanf, Katrin Schäfer, Andreas Daiber, Andres Beiras-Fernandez, and Christian Friedrich Vahl
Research Article (9 pages), Article ID 5724024, Volume 2020 (2020)

5α,6α-Epoxyphytosterols and 5α,6α-Epoxycholesterol Increase Nitrosative Stress and Inflammatory Cytokine Production in Rats on Low-Cholesterol Diet
Tomasz Wielkoszyński, Jolanta Zalejska-Fiolka, Joanna K. Strzelczyk, Aleksander J. Owczarek, Armand Cholewka, Katarzyna Kokoszczyk, and Agata Stanek
Research Article (9 pages), Article ID 4751803, Volume 2020 (2020)

Effects of Early Resveratrol Intervention on Skeletal Muscle Mitochondrial Function and Redox Status in Neonatal Piglets with or without Intrauterine Growth Retardation
Kang Cheng, Ting Wang, Simian Li, Zhihua Song, Hao Zhang, Lili Zhang, and Tian Wang
Research Article (12 pages), Article ID 4858975, Volume 2020 (2020)

Hindawi
Oxidative Medicine and Cellular Longevity
Volume 2021, Article ID 8895323, 10 pages
https://doi.org/10.1155/2021/8895323

Research Article

Association between Vitamin D Supplements, Oxidative Stress Biomarkers, and Hyperbaric Therapy in Patients with Sudden Sensorineural Hearing Loss

Jarosław Paprocki,[1] **Paweł Sutkowy**,[1] **Jacek Piechocki**,[2] **and Alina Woźniak**[1]

[1]*Department of Medical Biology and Biochemistry, Collegium Medicum of Nicolaus Copernicus University, Karłowicza 24, 85-092 Bydgoszcz, Poland*
[2]*Mazovian Centre for Hyperbaric Therapy and Wound Treatment in Warsaw, Wołoska 137, bud. "O", 02-507 Warszawa, Poland*

Correspondence should be addressed to Jarosław Paprocki; jaroslawpaprocki@interia.pl

Received 3 September 2020; Revised 21 October 2020; Accepted 16 February 2021; Published 11 March 2021

Academic Editor: Paola Rizzo

Copyright © 2021 Jarosław Paprocki et al. This is an open access article distributed under the Creative Commons Attribution License, which permits unrestricted use, distribution, and reproduction in any medium, provided the original work is properly cited.

The effect of vitamin D supplementation to patients with sudden sensorineural hearing loss (SSNHL), treated with hyperbaric oxygen (HBO) therapy, on the markers of the oxidant-antioxidant equilibrium was investigated. Patients were divided into two groups: those who did and did not receive vitamin D (cholecalciferol at 4000 IU/24 h). Concentrations of the following compounds, thiobarbituric acid reactive substances (TBARS), malondialdehyde (MDA), conjugated dienes (CD) in plasma and erythrocytes and activities of catalase (CAT), superoxide dismutase (SOD) and glutathione peroxidase (GPx) in erythrocytes, were determined. Haemoglobin (HGB) and haematocrit (HCT) were measured. Blood for analyses was collected from the basilic vein at three time points: before the first HBO procedure, up to 5 min after the first procedure, and after 14 procedures. No statistically significant differences in parameters tested were found between patients who did and did not receive vitamin D. In patients without supplementation, an increase of 53.2% ($P \leq 0.05$) in erythrocyte TBARS was observed after the first HBO treatment. In patients receiving vitamin D, a reduction of 27.6% ($P \leq 0.05$) was observed in erythrocyte MDA after 14 HBO treatments vs. that after the first treatment. In both groups, a decrease of 33.3% in plasma CD was observed after 14 treatments vs. that after the first treatment ($P \leq 0.05$ and $P \leq 0.01$, respectively). No statistically significant changes were observed in the erythrocyte SOD, GPx, and CAT activities and in HCT. A reduction of HGB concentration of 10.9% ($P \leq 0.05$) was demonstrated in nonsupplemented patients after 14 treatments compared with baseline. The results confirm that the effect of HBO therapy on oxidative stress markers is inconclusive and complex. Repeated HBO procedures can induce adaptive changes which protect against disruption of the oxidant-antioxidant equilibrium. It is possible that vitamin D supplementation inhibits the process of lipid peroxidation in erythrocytes.

1. Introduction

Vitamin D is a steroid hormone produced photochemically in the skin from 7-dehydrocholesterol [1]. This synthesis covers as much as 90% of the daily demand for this vitamin [2]. Cholecalciferol produced in the skin is an inactive form. It requires two hydroxylations to be fully activated. The first hydroxylation, at C25 in the side chain, occurs in the liver. It yields 25-hydroxy-cholecalciferol (calcidiol) which is the predominant metabolite of vitamin D in blood plasma [3]. The second hydroxylation, at C1, occurs both in the kidney and at extrarenal sites [4]. This reaction yields the most active metabolite of vitamin D (proper hormone)—,25-dihydroxycholecalciferol (calcitriol). Vitamin D is defined as fat soluble 9,10-secosteroids. D_3 (cholecalciferol) and D_2 (ergocalciferol) are the most important ones [3]. These compounds are not biologically active and are converted into active metabolites in the liver and kidney [5]. The most common form of vitamin D supplied with food and food supplements is cholecalciferol [3] present in products of

animal origin [6]. Vitamin D is mainly involved in calcium homoeostasis. By promoting mineralization of collagen matrix, this vitamin is crucial for normal bone growth [7]. However, the role of vitamin D is much broader, and its deficiency has been demonstrated in various anomalies and conditions, e.g., parathyroid hormone secretion disorders, osteoporosis, some cancers, cardiovascular diseases, type I diabetes, and obesity [8, 9]. Studies indicate that vitamin D can also be an antioxidant [7, 10]. This role of vitamin D helps to maintain the oxidant-antioxidant equilibrium. Any imbalance toward increased generation of reactive oxygen species (ROS) and/or compromised antioxidant mechanisms leads to oxidative stress whose involvement has been demonstrated in the aetiology and progression of several disease conditions [11]. The antioxidant properties of vitamin D have been demonstrated in, e.g., the liver of Sprague Dawley rats. The effectiveness of this vitamin was even greater than that of vitamin E—a well-known membrane antioxidant [12]. In addition to vitamins belonging to second line antioxidants, the body has at its disposal on enzymatic antioxidant barrier consisting of key three enzymes: superoxide dismutase (SOD), catalase (CAT), and glutathione peroxidase (GPx) [11]. One important mechanism of cell damage as a result of ROS action, including free oxygen radicals, is lipid peroxidation [13] whose products include conjugated diens (CD) and malondialdehyde (MDA) [14]. However, ROS also play a key role in the coordination of cellular signalling and, unexpectedly, protective antioxidant pathways [15]. Therefore, ROS can lead to both beneficial and adverse effects, which depends on their concentration and intracellular location. ROS are generated as natural by-products of metabolism, and their primary source in cells is the respiratory chain. In the process of cellular respiration, some oxygen naturally undergoes incomplete reduction, which leads to the formation of ROS [16].

Certain therapeutic methods can increase ROS generation in the body, especially those ones that are based on breathing 100% oxygen. These include hyperbaric oxygen (HBO) therapy [17] which consists of breathing pure oxygen in high-pressure conditions [18, 19]. HBO is used for treating, e.g., sudden sensorineural hearing loss (SSNHL) whose potential cause is cochlear ischaemia [20]. HBO therapy increases partial oxygen pressure in the perilymph. A study in animals showed an increase in oxygen concentration of up to 450% compared with the baseline value measured prior to treatment [21]. HBO has anti-inflammatory and angiogenic effects [17, 22].

HBO therapy is used in an increasing number of diseases and has beneficial health effects. Although it has been proven that oxidative stress can cause certain diseases, the effect of HBO therapy from the point of view of redox balance has not yet been fully understood. The aim of the study was to determine the effect of vitamin D supplementation to patients undergoing HBO therapy due to SSNHL on the levels of lipid peroxidation products: thiobarbituric acid reactive substances (TBARS), MDA, and CD in blood plasma and erythrocytes and on the activities of CAT, SOD, and GPx in peripheral blood erythrocytes.

2. Materials and Methods

2.1. Patients. The study included 24 patients with sudden sensorineural hearing loss (SSNHL) treated with hyperbaric oxygen (HBO) therapy, randomly selected from a total number of approx. 120 patients of hyperbaric therapy center (Warsaw, Poland). The patients formed two groups: patients receiving vitamin D (vitamin D_3, cholecalciferol) at a dose of 4000 IU/24 h (established by a physician; it is a tolerable upper intake level of vitamin D in adults, established by US Food and Nutrition Board [23]), daily throughout the experiment ($n = 12$, 4 women and 8 men, mean age 41.3 ± 14.3 years), and patients not receiving vitamin D ($n = 12$, 5 women and 7 men, mean age 41.5 ± 20.6 years). The criteria of exclusion from the study were smoking as well as associated conditions known to be caused by or to result in oxidative stress or involving disruption of the oxidant-antioxidant equilibrium (cancer, diabetes, and cardiovascular and infectious diseases). All study participants were informed of the aim and course of the experimental procedures planned. They provided their written consent for their participation in the study and declared they would abstain from drinking alcohol and taking vitamins and other preparations that could affect the oxidant-antioxidant equilibrium during the experiment, while the diet of the subjects did not change throughout the study. The study was conducted between October and April. In this period, sun exposure in Poland is insufficient to ensure that the cutaneous synthesis of vitamin D is appropriate to the needs [24]; therefore, the vitamin intake was recommended by a physician for some patients. In addition to HBO treatments, patients with SSNHL were treated with prednisone at a tapered dose until treatment was stopped (loading dose: 1 mg/kg of body weight per day, typically a maximum dose of 60 mg/day) (standard medical procedure in treatment of such disease). Treatment lasted two weeks starting from the diagnosis of SSNHL. Venous blood was collected before HBO therapy and after the first HBO treatment during prednisone therapy, while blood collection after 14 HBO treatments was performed after the end of prednisone therapy. The total number of HBO treatments was 15. The HBO therapy was a part of treatment covered by health insurance (the patients of public health service). However, it was not possible to perform the assays after the last, 15th HBO treatment. In 17 patients (9 of the supplemented group and 8 of the nonsupplemented group), hearing improvement (within the range of 10–20 dB) was observed after the end of therapy. The study was approved by the Bioethics Committee of Ludwik Rydygier Collegium Medicum in Bydgoszcz (approval no. 260/2016).

2.2. Hyperbaric Chamber Procedure. HBO treatments took place daily for 14 days, with each treatment lasting 90 minutes, and the pressure inside the chamber during the procedure was 2.5 MPa. Every session also included two 10-minute periods of compression and decompression at the beginning and end of the procedure, respectively. During these periods, the patients breathed air in the chamber. During oxygen therapy, whose total time was 60 minutes, the patients breathed pure oxygen through a special mask tightly

attached to their faces. The oxygen therapy periods were divided into 20-minute cycles separated by 5-minute break periods during which the patients breathed air in the chamber. The concentration of oxygen inside the chamber did not exceed 23%. The HBO treatments were conducted in the hyperbaric chamber Haux Starmed 2200 at the Mazovian Centre for Hyperbaric Therapy and Wound Treatment in Warsaw. This chamber is equipped with 12 treatment stations, a computerized treatment control system, a continuous video recording facility, and an integrated fire safety system. It provides constant environmental conditions in terms of humidity, temperature, and pressure. All patients in the chamber breathed 100% oxygen for the same period of time. A member of medical staff (physician or nurse) was present in the hyperbaric chamber with the patient throughout the procedure.

2.3. Laboratory Detection. Blood for biochemical analyses was collected from the basilic vein into EDTA-containing tubes, for plasma and erythrocytes, at three time points: before the first HBO procedure, up to 5 min after the end of the first procedure and up to 5 min after the end of the 14th procedure. The samples were analysed for the levels of lipid peroxidation products, i.e., thiobarbituric acid reactive substances (TBARS), malondialdehyde (MDA), and conjugated diens (CD), as well as for the activities of the main antioxidant enzymes: catalase (CAT), superoxide dismutase (SOD), and glutathione peroxidase (GPx). In addition, two blood count parameters were measured: haematocrit (HCT) and haemoglobin (HGB) levels. Determination of HCT and HGB was done at two time points: before the first and after the 14th HBO treatment.

Each sample was measured 5 times to determine intra- and interassay variation (the number of repetitions was limited by the amount of blood possible to take from each patient and method limitations associated with precision of absorbance measurement). Imprecision of the methods used for TBARS, MDA, and CD ranged between 3.4% and 8.5% in intra-assay coefficient of variation (CV) and in interassay CV between 2.6% and 11.4%, whereas ranges of intra- and interassay coefficients of variation for the methods of the enzyme activity determination amounted 6.8%–11.2% and 4.7%–13.4%, respectively.

2.3.1. Preparing of Erythrocytes and Blood Plasma. The tubes for blood plasma and erythrocytes were centrifuged for 10 minutes at 6000×g at +4°C. After centrifugation, the plasma constitutes the upper layer. The lower layer (blood cells) was washed three times with phosphate-buffered saline at a ratio of 1 : 3 and each time centrifuged (the same conditions). Supernatant was deleted to remove leukocytes and thrombocytes. The presence of white blood cells and platelets in the erythrocyte suspension was verified using microscopic observation of the performed smears, whereas the presence of the protein was checked with a 20% aqueous solution of sulfosalicylic acid. Erythrocyte suspension (haemolysate) was phosphate-buffered saline solution with 50% hematocrit index [25].

2.3.2. The TBARS Concentration. The TBARS in blood plasma and erythrocytes were determined using the methods by Buege and Aust [26] as modified by Esterbauer and Cheeseman [27]. In order to measure the TBARS concentration, a reaction mixture containing 0.375% thiobarbituric acid and 15% trichloroacetic acid in 0.25 N HCl was added to the haemolysate or blood plasma. 3,5-Di-tert-butyl-4-hydroxytoluene was also added to the tubes to inhibit lipid peroxidation during the reaction. The samples were then incubated at 100°C, refrigerated, and centrifuged at 2000×g. Absorbance was measured at a wavelength of 532 nm. The TBARS concentration was expressed as MDA concentration as the latter is the main product of lipid peroxidation reacting with thiobarbituric acid. TBARS concentration in erythrocytes (TBARS er) is presented as nmol MDA/g HGB and in plasma (TBARS pl) as nmol MDA/mL plasma [26, 27].

2.3.3. The MDA Concentration. The MDA concentration was determined using the method described by Wong et al. [28] based on high-performance liquid chromatography technique. A C18 (250 mm) column and 20 μl of the sample were used in the analysis. Mobile phase was a formic acid buffer with methanol (60%/40%). Flow rate was 1.0 mL/min, and MDA retention time was 1.55–1.60 min. The MDA level was determined using a fluorescence detector at λ: excitation = 532 nm, emission = 553 nm. MDA concentration in erythrocytes (MDA er) is presented in nmol/g HGB and in plasma (MDA pl) in nmol/mL plasma [28].

2.3.4. The CD Concentration. In order to determine the CD level (the method by Sergent et al. [29]), 0.5 mL of chloroform was added to 0.5 mL of haemolysate or blood plasma; the mixture was centrifuged, and 0.1 mL of the lower layer solution was taken for further analyses. The samples were subsequently evaporated under nitrogen and dissolved in cyclohexan, and absorbance was read at a wavelength of λ = 233 nm. The results are presented for CD in erythrocytes (CD er) as 10^{-2} absorbance unit per gram of haemoglobin (10^{-2} Abs./g HGB), whereas for CD measured in plasma (CD pl) as 10^{-2}Abs./mL [29].

2.3.5. The SOD Activity. The Zn/Cu-SOD (EC 1.15.1.1) activity was determined in erythrocytes using the method by Misra and Fridovich [30]. Measurement of the SOD activity was based on the inhibition of adrenaline autoxidation to adrenochrome in alkaline conditions. Absorbance was measured at a wavelength of 480 nm, and the SOD activity is expressed in the enzyme unit per gram of haemoglobin (U/g HGB). The unit of SOD activity is defined as that activity of SOD required to cause 50% inhibition of the oxidation of the adrenaline [30].

2.3.6. The CAT Activity. The CAT activity (EC 1.11.1.6) was determined according the method described by Beers and Sizer [31]. The method is based on measuring the decrease in the absorbance of a solution of H_2O_2 decomposed by the enzyme at a wavelength of 240 nm. The CAT activity is presented in international unit per gram of haemoglobin (IU/g HGB). The activity of the enzyme is equal to one unit when it decomposes 1.0 μmole of H_2O_2 per minute at pH 7.0 at

Table 1: The concentrations of TBARS, MDA, and CD in erythrocytes and blood plasma, and the activities of CAT, SOD, and GPx determined in the erythrocytes of patients with sudden sensorineural hearing loss (SSNHL) receiving hyperbaric oxygen (HBO) treatments without vitamin D supplementation.

Parameter	Before HBO therapy	After 1 HBO session	After 14 HBO sessions
TBARS er., nmol MDA/g HGB	20.66 ± 9.95	31.66 ± 8.68*	27.30 ± 13.42
TBARS pl., nmol MDA/mL	0.41 ± 0.12	0.51 ± 0.12	0.46 ± 0.06
MDA er., nmol/g HGB	0.81 ± 0.11	1.04 ± 0.18	0.89 ± 0.32
MDA pl., nmol/dL	1.17 ± 0.48	1.56 ± 0.39	1.01 ± 0.84
CD er., 10^{-2}Abs./g HGB	0.08 ± 0.03	0.09 ± 0.02	0.10 ± 0.01
CD pl., 10^{-2}Abs./mL	0.08 ± 0.02	0.09 ± 0.02	0.06 ± 0.01††
CAT, 10^{4}IU/g HGB	67.22 ± 8.50	65.81 ± 6.95	63.34 ± 9.87
SOD, U/g HGB	735.27 ± 92.23	695.37 ± 99.45	715.75 ± 44.25
GPx, U/g HGB	6.66 ± 4.09	8.18 ± 3.54	9.08 ± 3.92
HGB, g/dL	15.73 ± 1.93		14.02 ± 1.69*
HCT, %	43.08 ± 5.03		39.40 ± 4.07

TBARS: thiobarbituric acid reactive substances; MDA: malondialdehyde; CD: conjugated dienes; CAT: catalase; GPx: glutathione peroxidase; SOD: superoxide dismutase; HGB: haemoglobin; HCT: haematocrit. The values are expressed as means ± standard deviations (SD). *Statistically significant difference compared with measurement before the start of HBO therapy (*$P \leq 0.05$). †Statistically significant difference compared with measurement after the 1st HBO session (††$P \leq 0.01$).

25°C (the H_2O_2 concentration ranges between 10.3 mM and 9.2 mM) [31].

2.3.7. The GPx Activity. The measuring of GPx activity (EC 1.11.1.6) was performed using the method by Paglia and Valentine [32]. It was determined based on a reaction of reduced glutathione with hydrogen peroxide. Thus, oxidized glutathione is then reduced by glutathione reductase and a reduced form of nicotinamide adenine dinucleotide phosphate, which in this reaction turns into an oxidized form. Absorbance decreasing of reduced form of the dinucleotide was measured at a wavelength of 340 nm. The results are presented as the enzyme unit per gram of haemoglobin (U/g HGB). One unit is defined as the GPx activity which leads to production of 1.0 μmole oxidized form of the dinucleotide per minute [32].

2.3.8. HCT and HGB Levels. The HCT percentage and the HGB concentration in peripheral blood were determined using the Orphee-Mythic 22AL haematology analyser. The results are presented as % and g/dL, respectively.

2.4. Statistics. The Kolmogorov-Smirnov test was used to examine the normal distribution of variables. Results were expressed as the mean ± standard deviation. Uniformity of variance was checked using Levene's test. One-way analysis of variance with Tukey's post hoc test was used to compare measurements. Additional nonparametric testing was performed for groups that did not meet the aforementioned criteria (TBARS pl and MDA pl): Kruskal-Wallis test and Dunn's test as pairwise multiple comparisons of mean ranks. Correlations between the analysed parameters were assessed using a correlation matrix. A hypothesis of statistical significance of correlation coefficients (r) was tested (Pearson product-moment correlation coefficient). Correlation coefficients were determined between the parameters of oxidative stress only at a given study time point in order to establish the existence of a relationship/coexistence between them and to determine the strength of the relationship and nature (positive or negative coefficient).

Comparisons, including correlations, were considered as statistically significant when the calculated value of the tested probability was $P \leq 0.05$. Calculations were conducted in the Statistica 9.1 software package (Statsoft, 2011).

3. Results

All mean results are shown in Tables 1 and 2, while in Figure 1, the individual results are presented.

Comparison of the investigated parameters between both groups, i.e., patients with sudden sensorineural hearing loss (SSNHL) who did or did not receive vitamin D supplementation during hyperbaric oxygenation (HBO) procedures, showed no statistically significant differences at any of the three study time points, i.e., before the first HBO treatment and 5 min after the first and 14th HBO procedures.

In patients with SSNHL who did not receive vitamin D, a statistically significant increase of 53.2% ($P \leq 0.05$) in the erythrocyte thiobarbituric acid reactive substances (TBARS), concentration was found up to 5 min after the first HBO treatment compared with the baseline (pre-HBO) level. No statistically significant changes were demonstrated in patients receiving vitamin D in whom the TBARS concentration remained similar throughout the experiment. However, in patients receiving vitamin D, a reduction of 27.6% ($P \leq 0.05$) was observed in the erythrocyte malondialdehyde (MDA) concentration after 14 HBO treatments compared with that after the first treatment. Changes in the erythrocyte MDA concentration in nonsupplemented patients were not statistically significant at any study time point. In both groups, a decrease of 33.3% in the plasma conjugated diens (CD) level was observed after 14 HBO treatments compared with that after the first treatment ($P \leq 0.05$ and $P \leq 0.01$,

Table 2: The concentrations of TBARS, MDA, and CD in erythrocytes and blood plasma, and the activities of CAT, SOD, and GPx determined in the erythrocytes of patients with sudden sensorineural hearing loss (SSNHL) receiving hyperbaric oxygen (HBO) treatments with vitamin D supplementation.

Parameter	Before HBO therapy	After 1 HBO session	After 14 HBO sessions
TBARS er., nmol MDA/g HGB	25.69 ± 6.72	23.92 ± 6.72	25.16 ± 5.15
TBARS pl., nmol MDA/mL	0.43 ± 0.11	0.45 ± 0.10	0.45 ± 0.10
MDA er., nmol/g HGB	0.90 ± 0.15	0.98 ± 0.11	0.71 ± 0.28†
MDA pl., nmol/dL	1.07 ± 0.57	1.03 ± 0.63	1.17 ± 0.75
CD er., 10^{-2}Abs./g HGB	0.09 ± 0.03	0.09 ± 0.02	0.11 ± 0.02
CD pl., 10^{-2}Abs./mL	0.07 ± 0.02	0.09 ± 0.03	0.06 ± 0.01†
CAT, 10^{4}IU/g HGB	65.03 ± 12.43	60.68 ± 8.88	61.82 ± 10.08
SOD, U/g HGB	699.75 ± 51.81	728.48 ± 84.55	690.99 ± 73.20
GPx, U/g HGB	6.30 ± 4.13	11.31 ± 4.54	9.95 ± 4.99
HGB, g/mL	15.78 ± 0.98		15.02 ± 1.48
HCT, %	44.18 ± 2.66		42.20 ± 4.05

TBARS: thiobarbituric acid reactive substances; MDA: malondialdehyde; CD: conjugated dienes; CAT: catalase; GPx: glutathione peroxidase; SOD: superoxide dismutase; HGB: haemoglobin; HCT: haematocrit. The values are expressed as means ± standard deviations (SD). †Statistically significant difference compared with measurement after the 1st HBO session ($\dagger P \leq 0.05$).

respectively). No statistically significant changes in the plasma TBARS and MDA concentrations and in the erythrocyte CD concentration were found in either group throughout the experiment.

Similarly, no statistically significant changes were observed in the erythrocyte superoxide dismutase (SOD), glutathione peroxidase (GPx), and catalase (CAT) activities.

A reduction of haemoglobin (HGB) concentration of 10.9% ($P \leq 0.05$) was demonstrated in nonsupplemented patients after 14 HBO treatments compared with baseline. Such a statistically significant change was not found in supplemented patients throughout the experiment.

Several statistically significant correlations between the investigated parameters were determined in patients with SSNHL both with and without vitamin D supplementation (supplementary material (available here)).

4. Discussion

Lipids containing unsaturated fatty acids with more than one double bond are particularly susceptible to damage by reactive oxygen species (ROS) [33]. They are probably the first target of ROS action [34]. Hence, the concentration of products of lipid peroxidation, i.e., oxidation of polyunsaturated fatty acids, reflects the intensity of ROS generation. In this study, patients with SSNHL who did or did not receive vitamin D supplementation throughout the experiment were shown to have a statistically significant reduction of the plasma conjugated diens (CD pl) concentration after 14 hyperbaric oxygen (HBO) treatments compared with that measured after the first treatment. CD is produced during the first stage of lipid peroxidation as a result of removal of a hydrogen atom from a polyunsaturated fatty acid molecule [35]. The lack of statistically significant changes in CD pl level after the first HBO treatment compared with that measured prior to the start of HBO therapy, as well as the decrease in the CD pl level after 14 HBO treatments, may indicate a beneficial effect of HBO therapy on maintaining the oxidant-antioxidant equilibrium. Decreased CD pl level appears to be a result of adaptation to the repeated HBO procedures. The above observations are also confirmed by the observed changes in the erythrocyte thiobarbituric acid reactive substances (TBARS er) concentration. After the first HBO treatment in patients who did not receive vitamin D, a statistically significant increase in the TBARS er concentration was demonstrated, which is evidence of increased peroxidation of membrane lipids in erythrocytes. However, after 14 treatments, TBARS er level did not differ significantly from that measured before the start of HBO therapy, which may indicate the occurrence of adaptive changes. In our previous study, we showed that even a single HBO procedure resulted in a reduction of TBARS concentration in erythrocytes of patients with SSNHL aged over 50 years [36]. However, in another study, an increase in erythrocyte TBARS concentration was observed in patients with SSNHL after 14 HBO procedures, compared with that measured prior to the start of HBO therapy [37]. The literature lacks data on changes in CD level in conditions similar to those in the presented study. However, when examining the effects of HBO on the changes in mitochondria from heart cells, Nohl et al. [38] showed accumulation of these lipid peroxidation products in mitochondrial membrane. In contrast, HBO in rabbits has been shown to reduce diet-induced CD accumulation in the blood plasma of these animals, as well as to reduce low-density lipoprotein and high-density lipoprotein fractions of plasma, in the liver, and in the aortic diseases [39].

This study did not reveal any significant changes in the plasma TBARS (TBARS pl) in patients with SSNHL receiving or not receiving vitamin D, which can confirm that HBO therapy does not lead to a loss of the oxidant-antioxidant equilibrium in blood plasma. Similar results were obtained by Tepić et al. [40] in patients with type 2 diabetes mellitus

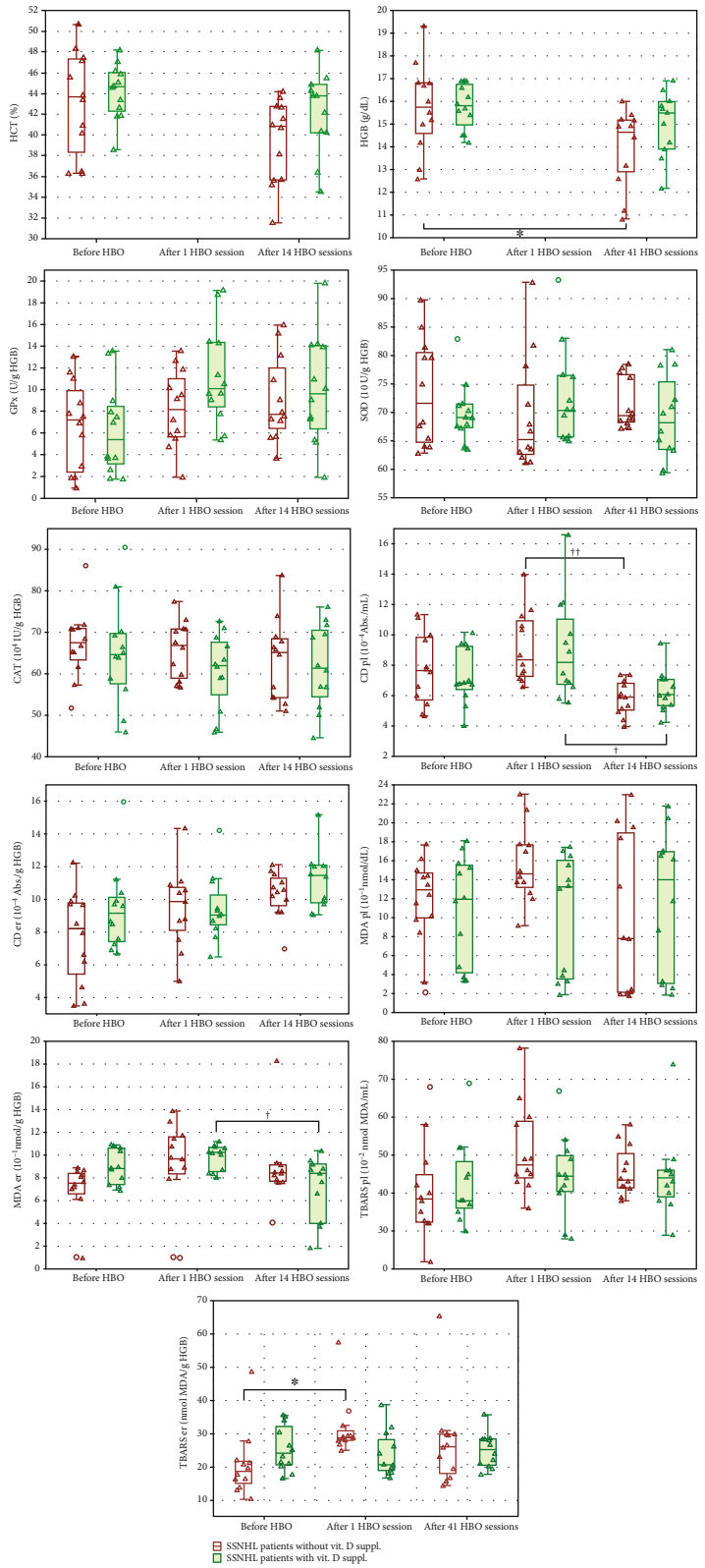

Figure 1: The individual levels of oxidative stress indicators in the venous blood of sudden sensorineural hearing loss (SSNHL) patients treated with hyperbaric oxygen (HBO) who did or did not receive vitamin D. TBARS, MDA, and CD er/pl: thiobarbituric acid reactive substances, malondialdehyde, and conjugated dienes in erythrocytes/plasma, respectively; CAT: catalase; SOD: superoxide dismutase; GPx: glutathione peroxidase; HGB: haemoglobin; HCT: haematocrit. Center lines show the medians, box limits indicate the 25th and 75th percentiles, whiskers denote ranges of nonoutliers, outliers are represented by circles. Statistically significant differences: compared with measurement before HBO treatment ($^*P \leq 0.05$) and in comparison to assay after 1 HBO session ($\dagger P \leq 0.05$, $\dagger\dagger P \leq 0.01$).

without vascular complications, who were subjected to 10 HBO treatments. However, in the group of patients with vascular complications, the plasma TBARS concentration on day 7 of HBO therapy increased in a statistically significant manner compared with that of day 5 of treatment. In our previous study, conducted in patients with difficult-to-heal skin conditions, no statistically significant changes in the plasma TBARS concentration were observed both after the first HBO procedure and after 25 procedures. Yet, we revealed a decreasing trend of TBARS in blood plasma after 25 HBO procedures [41]. A reduction in serum TBARS after a single HBO session was demonstrated in high performance runners, while in low performance runners that value did not change [42]. No changes in the whole blood malondialdehyde (MDA) concentration were observed in volunteer divers who underwent a single HBO treatment. However, a statistically significant increase in plasma isoprostanes was found after this treatment [43]. In rats with induced distal colitis, after 10 HBO sessions conducted over 5 days, lower TBARS concentrations in erythrocytes and blood plasma were demonstrated in comparison with those in rats with distal colitis that were not treated with HBO [44].

When comparing results obtained in patients with SSNHL who received vitamin D during HBO therapy with those obtained in patients without vitamin D supplementation, differences in MDA and TBARS levels in erythrocytes (MDA er and TABRS er) can be observed. In patients with vitamin D supplementation, MDA er level after 14 HBO treatments decreased significantly compared with that measured after the first HBO treatment. This significant change was not found in patients without vitamin D supplementation. In the latter group, after the first HBO treatment, the TBARS er concentration increased significantly, while in patients receiving vitamin D supplements, the observed changes were not statistically significant. The observed difference appears to confirm the antioxidant properties of this vitamin. Other scientific experiments support this observation. It has been shown, e.g., that vitamin D supplementation leads to increase in the concentration of reduced glutathione and in total antioxidant capacity in the blood serum of patients with major depressive disorder [45]. The literature lacks reports of studies in which HBO treatments would be combined with vitamin D supplementation. However, such studies have been conducted in rats which were given a combination of vitamins E plus C. Comparing the erythrocyte MDA concentrations in these animals after HBO (at a pressure of 2.8 atmospheres absolute, 1 hour daily, for 45 days), a lower MDA level was revealed in rats that received the above combination of vitamins three days before and during HBO treatments compared with rats that did not receive this combination [46]. In the presented study, in patients not receiving vitamin D supplementation, haemoglobin (HGB) concentration was decreased after 14 HBO treatments compared with the concentration measured before the first treatment. We did not identify any statistically significant changes in HGB concentration in the supplemented patients. Other blood count parameters were not analysed, so it is difficult to establish what could be a direct cause of decreased HGB concentration: an actual decrease in HGB level or, for example, reduction of the number of erythrocytes or their size. Decrease in haemoglobin concentration was demonstrated in our previous study after 14 HBO procedures in patients with SSNHL [37], while no statistically significant changes in HGB levels after 25 "stimulation" sessions in hyperbaric chamber were observed in patients with difficult-to-heal wounds [41]. In saturation divers during the decompression phase, a reduction of HGB concentration was observed as well, which was suggested to be associated with changes in erythropoietin level [47]. Kiboub et al. [48] showed a slight but statistically significant reduction of HGB in divers both immediately after decompression and 24 hours thereafter. In turn, the difference in HGB concentration change observed between patients who did and did not receive vitamin D supplements may be associated with the function of this vitamin. Effects of vitamin D on renal hormones such as renin and erythropoietin have been demonstrated [49].

Our study did not reveal any statistically significant changes in the activity of antioxidant enzymes in erythrocytes during the experiment in either group of patients. This lack of significant changes may indicate that there is no increased generation of superoxide radical anion (O_2^-), which would lead to an increase in superoxide dismutase (SOD), activity, or hydrogen peroxide, whose generation would induce changes in catalase (CAT) and glutathione peroxidase (GPx) activities. SOD is responsible for the dismutation of superoxide anion, while CAT and GPx remove H_2O_2 [11]. On the other hand, it has been shown that breathing 100% oxygen in hyperbaric conditions leads to increased ROS generation [50, 51], and it is these enzymes that are in the first line of antioxidant defence. Their important role in the removal of ROS in our study was indicated by the statistically significant negative correlations, as demonstrated after the completion of 14 HBO treatments between the TBARS er concentration and the SOD activity ($r = -0.741$; $P \leq 0.01$) in patients with SSNHL receiving vitamin D (Table 2 in the supplementary material), as well as prior to the start of HBO therapy: between the plasma MDA (MDA pl) concentration and the erythrocyte SOD activity in patients with vitamin D supplementation ($r = -0.646$; $P \leq 0.05$) (Table 2 in the supplementary material), and between the same parameters in patients not taking vitamin D ($r = -0.635$; $P \leq 0.05$) (Table 1 in the supplementary material).

It seems that virtually the lack of statistically significant changes in oxidative stress markers after HBO procedures can be linked to the function of ROS in cell signalling and regulation. It has been demonstrated that a modest increase in intracellular ROS during HBO procedures can modulate signalling pathways and induce expression of proteins which increase cell tolerance to harmful stimuli [52]. For example, it was observed that the upregulation of heat shock protein 32 induced by ROS in cultured rat spinal cord neurons protects cells from damage due to oxidative stress [53]. Therefore, it is possible that the nature of changes in oxidative stress markers (i.e., mainly lack thereof) revealed in this study is not due to the absence of effect of HBO therapy on ROS generation. Rather, it may be a result of activation of mechanisms preventing excessive ROS generation.

Lack of statistically significant changes in the SOD, CAT, and GPx activities was demonstrated in the whole blood in volunteer divers after a single HBO procedure during which the participants were breathing 100% oxygen at 2.5 atmosphere absolute for a total of 60 minutes [43]. Similarly, absence of effect of a single HBO session on the erythrocyte SOD activity has been demonstrated in runners. However, the activity of GPx in erythrocytes decreased, but only in high performance runners; no statistically significant change was recorded in low performance runners [42]. Ferrer et al. [54], in turn, observed an increase in the lymphocyte GPx activity after HBO exposure, while CAT activity did not change.

Prednisone therapy can be considered as a limitation in the interpretation of the results of this study. An effect of this treatment on the oxidative stress markers investigated in this study cannot be excluded, and potential impact may be not unequivocal. It has been shown that acute treatment with corticosteroids inhibits ROS generation [55]. In women with Crohn's disease, it has been proven that prednisone decreases lipid oxidation and increases protein oxidation [56]. However, earlier studies showed that prednisone treatment did not significantly affect the level of peroxides and the activity of SOD and CAT in patients with systemic vasculitides with autoimmune background [57]. In patients with active systemic lupus erythematosus, a statistically significant inverse correlation between daily prednisone doses and lipid peroxidation determined by CL-LOOH (tert-butyl hydroperoxide-initiated chemiluminescence) and a positive correlation between daily prednisone doses and the total antioxidant capacity were observed. In patients with nonactive systemic lupus erythematosus, the reported correlations were not statistically significant [58]. Another significant limitation of the present paper is a small number of participants in the study. Therefore, the statistical tests applied herein may have not demonstrated all important dependencies and differences, which may have influenced the process of inferring. Due to financial constraints and a limited quantity of material drawn for examination, there was no possibility to indicate other significant oxidative stress factors. A greater number of indicated parameters would have certainly influenced the interpretation of results obtained, allowing for a more precise determination of dependencies between vitamin D supplementation, hyperbaric oxygen therapy, and oxidative/antioxidative balance indicators. The quantity of material for examination also had a limiting impact on the number of repetitions possible to be performed. What additionally impacted the criticism of the results obtained, the number of time points at which indications were made, or the choice of indicated parameters, was the insubstantial experience in conducting scientific research and writing papers of the first and primary author of the present paper. Taking into account the abovementioned limitations, the present study should be treated as a pilot one. The results obtained, however, are interesting and allowed for assessment of usefulness of the tools applied as well as for verification of knowledge obtained from a small number of studies conducted so far on the issues analysed in the present paper. The questions arising in the course of performing of the present experiment prompt to continue research within this area.

5. Conclusions

The results confirm that the effect of hyperbaric oxygen therapy on oxidative stress markers is inconclusive and complex. A limitation of this study was certainly the small number of participants, which prevented us from proposing less-conservative conclusions. However, significant changes revealed allow us to conclude that repeated hyperbaric oxygen procedures perhaps induce adaptive changes which protect against disruption of the oxidant-antioxidant equilibrium. It is possible that vitamin D supplementation inhibits the process of lipid peroxidation in erythrocytes.

Data Availability

The study data used to support the findings of this study are included within the article.

Disclosure

The study was conducted as part of regular employment of the authors by the Ludwik Rydygier Collegium Medicum in Bydgoszcz, Nicolaus Copernicus University, Toruń, Poland.

Conflicts of Interest

The authors declare that they have no competing interests.

Authors' Contributions

Jarosław Paprocki is the author of the research concept and project. He also participated in patient recruitment for the study, obtaining and interpreting results and selection of literature. Jarosław Paprocki drafted the manuscript. Paweł Sutkowy was involved in the interpretation of study results and conducting statistical analysis. Jacek Piechocki was responsible for the selection of patients for the study and for providing them with medical care during the experiment. Alina Woźniak provided her critical revision of the manuscript. All authors read and approved the final version of the manuscript.

Supplementary Materials

Table 1: statistically significant correlation coefficients between parameters measured in patients with SSNHL not taking vitamin D supplements during the experiment. Table 2: statistically significant correlation coefficients between parameters measured in patients with SSNHL taking vitamin D supplements during the experiment. Table 2: statistically significant correlation coefficients between parameters measured in patients with SSNHL taking vitamin D supplements during the experiment. *(Supplementary Materials)*

References

[1] H. F. DeLuca, "Overview of general physiologic features and functions of vitamin D," *The American Journal of Clinical Nutrition*, vol. 80, no. 6, pp. 1689–1696, 2004.

[2] P. T. Alpert and U. Shaikh, "The effects of vitamin D deficiency and insufficiency on the endocrine and paracrine systems," *Biological Research for Nursing*, vol. 9, no. 2, pp. 117–129, 2007.

[3] A. Grafka, M. Łopucki, J. Kuna, A. Kuna, and B. Pęksa, "The role of vitamin D in the body," *Journal of Laboratory Diagnostics*, vol. 55, no. 1, pp. 55–60, 2019.

[4] M. Hewison and J. S. Adams, "Extrarenal 1α-hydroxylase," in *Vitamin D*, D. Feldman, J. W. Pike, and J. S. Adams, Eds., pp. 777–806, Academic Press, San Diego, CA, USA, 2011.

[5] P. Pludowski, M. F. Holick, W. B. Grant et al., "Vitamin D supplementation guidelines," *The Journal of Steroid Biochemistry and Molecular Biology*, vol. 175, pp. 125–135, 2018.

[6] G. Cardwell, J. F. Bornman, A. P. James, and L. J. Black, "A review of mushrooms as a potential source of dietary vitamin D," *Nutrients*, vol. 10, no. 10, article 1498, 2018.

[7] G. Murdaca, A. Tonacci, S. Negrini et al., "Emerging role of vitamin D in autoimmune diseases: an update on evidence and therapeutic implications," *Autoimmunity Reviews*, vol. 18, no. 9, article 102350, 2019.

[8] M. Holick, "The vitamin D epidemic and its health consequences," *The Journal of Nutrition*, vol. 135, no. 11, pp. 27395–27485, 2005.

[9] A. Lotito, M. Teramoto, M. Cheung, K. Becker, and D. Sukumar, "Serum parathyroid hormone responses to vitamin D supplementation in overweight/obese adults: a systematic review and meta-analysis of randomized clinical trials," *Nutrients*, vol. 9, no. 3, p. 241, 2017.

[10] J. Nuszkiewicz, A. Woźniak, and K. Szewczyk-Golec, "Ionizing radiation as a source of oxidative stress—the protective role of melatonin and vitamin D," *International Journal of Molecular Sciences*, vol. 21, no. 16, article 5804, 2020.

[11] O. M. Ighodaro and O. A. Akinloye, "First line defence antioxidants-superoxide dismutase (SOD), catalase (CAT) and glutathione peroxidase (GPX): their fundamental role in the entire antioxidant defence grid," *Alexandria Journal of Medicine*, vol. 54, no. 4, pp. 287–293, 2018.

[12] S. Sardar, A. Chakraborty, and M. Chatterjee, "Comparative effectiveness of vitamin D3 and dietary vitamin E on peroxidation of lipids and enzymes of the hepatic antioxidant system in Sprague–Dawley rats," *International Journal for Vitamin and Nutrition Research*, vol. 66, no. 1, pp. 39–45, 1996.

[13] K. H. Cheeseman, "Mechanisms and effects of lipid peroxidation," *Molecular Aspects of Medicine*, vol. 14, no. 3, pp. 191–197, 1993.

[14] A. M. Turpeinen, G. Alfthan, L. Valsta et al., "Plasma and lipoprotein lipid peroxidation in humans on sunflower and rapessed oil diets," *Lipids*, vol. 30, no. 6, pp. 485–492, 1995.

[15] M. Valko, D. Leibfritz, J. Moncol, M. T. Cronin, M. Mazur, and J. Telser, "Free radicals and antioxidants in normal physiological functions and human disease," *The International Journal of Biochemistry and Cell Biology*, vol. 39, no. 1, pp. 44–84, 2007.

[16] S. R. Thom, "Oxidative stress is fundamental to hyperbaric oxygen *therapy*," *Applied Physiology*, vol. 106, no. 3, pp. 988–995, 2009.

[17] J. Paprocki, P. Sutkowy, E. Krzyżańska-Malinowska, J. Piechocki, and A. Woźniak, "The indicators of oxidant – antioxidant balance in patients performed hyperbaric oxygenation," *Polish Hyperbaric Research*, vol. 43, no. 2, pp. 23–38, 2013.

[18] S. R. Thom, "Hyperbaric oxygen: its mechanisms and efficacy. Plastic and reconstructive surgery," *Plastic and Reconstructive Surgery*, vol. 127, no. 1, pp. 131–141, 2011.

[19] J. Paprocki, M. Gackowska, M. Pawłowska, and A. Woźniak, "The current use of hyperbaric oxygen treatment," *Medycyna Rodzinna*, vol. 4, no. 19, pp. 217–222, 2016.

[20] Y. Choi, H. L. Choi, A. Y. Jeong et al., "Hyperbaric oxygen (HBO) therapy as an effective approach to the treatment of patients with severe idiopathic sudden sensorineural hearing loss," *Acta Oto-Laryngologica*, vol. 140, no. 5, pp. 383–386, 2020.

[21] K. Lamm, C. Lamm, and W. Arnold, "Effect of isobaric oxygen versus hyperbaric oxygen on the normal and noise-damaged hypoxic and ischemic guinea pig inner ear," *Advances in Oto-Rhino-Laryngology*, vol. 54, pp. 59–85, 1998.

[22] J. Glik, A. Cholewka, A. Stanek et al., "Thermal imaging and planimetry evaluation of the results of chronic wounds treatment with hyperbaric oxygen therapy," *Advances in Clinical and Experimental Medicine*, vol. 28, no. 2, pp. 229–236, 2019.

[23] Institute of Medicine, Food and Nutrition Board, *Dietary reference intakes for calcium and vitamin D*, National Academy Press, Washington, DC, USA, 2010.

[24] E. Marcinowska-Suchowierska, M. Walicka, M. Tałałaj, W. Horst-Sikorska, M. Ignaczak-Szczepaniak, and E. Sewerynek, "Vitamin D supplementation in adults - guidelines," *Endokrynologia Polska*, vol. 61, no. 6, pp. 723–729, 2010.

[25] J. Krawczyński, *Diagnostyka Enzymologiczna w Medycynie Praktycznej*, Metodyka Badań, Wydawnictwo lekarskie PZWL, Warszawa, 1972.

[26] J. A. Buege and S. D. Aust, "[30] Microsomal lipid peroxidation," *Methods in Enzymology*, vol. 52, pp. 302–310, 1978.

[27] H. Esterbauer and K. H. Cheeseman, "Determination of aldehydic lipid peroxidation products: malonaldehyde and 4-hydroxynonenal," *Methods in Enzymology*, vol. 186, pp. 407–421, 1990.

[28] S. H. Wong, J. A. Knight, S. M. Hopfer, O. Zaharia, C. N. Leach, and F. W. Sunderman, "Lipoperoxides in plasma as measured by liquid-chromatographic separation of malondialdehyde-thiobarbituric acid adduct," *Clinical Chemistry*, vol. 33, no. 2, pp. 214–220, 1987.

[29] O. Sergent, I. Morel, P. Cogrel et al., "Simultaneous measurements of conjugated dienes and free malondialdehyde, used as a micromethod for the evaluation of lipid peroxidation in rat hepatocyte cultures," *Chemistry and Physics of Lipids*, vol. 65, no. 2, pp. 133–139, 1993.

[30] H. P. Misra and I. Fridovich, "The role of superoxide anion in the autoxidation of epinephrine and a simple assay for superoxide dismutase," *Journal of Biological Chemistry*, vol. 247, no. 10, pp. 3170–3175, 1972.

[31] R. F. Beers and J. Sizer, "A spectrophotometric method for measuring the breakdown of hydrogen peroxide by catalase," *Journal of Biological Chemistry*, vol. 195, no. 1, pp. 133–140, 1952.

[32] D. E. Paglia and W. N. Valentine, "Studies on the quantitative and qualitative characterization of erythrocyte glutathione peroxidase," *Journal of Laboratory and Clinical Medicine*, vol. 70, no. 1, pp. 158–169, 1967.

[33] T. P. Devasagayam, K. K. Boloor, and T. Ramasarma, "Methods for estimating lipid peroxidation: an analysis of

merits and demerits," *Indian Journal of Biochemistry and Biophysics*, vol. 40, no. 5, pp. 300–308, 2003.

[34] D. Praticò, "Lipid peroxidation and the aging proces," *Science of Aging Knowledge Environment*, vol. 2002, no. 50, article re5, 2002.

[35] L. I. Kolesnikova, M. A. Darenskaya, N. V. Semenova et al., "Lipid peroxidation and antioxidant protection in girls with type 1 diabetes mellitus during reproductive system development," *Medicina*, vol. 51, no. 2, pp. 107–111, 2015.

[36] J. Paprocki, M. Pawłowska, P. Sutkowy, J. Piechocki, and A. Woźniak, "The oxidant–antioxidant equilibrium in the blood of people with sudden sensorineural hearing loss after the first hyperbaric oxygen therapy session-a preliminary study," *Polish Hyperbaric Research*, vol. 4, no. 61, pp. 15–24, 2017.

[37] J. Paprocki, P. Sutkowy, J. Piechocki, and A. Wozniak, "Markers of oxidant-antioxidant equilibrium in patients with sudden sensorineural hearing loss treated with hyperbaric oxygen therapy," *Oxidative Medicine and Cellular Longevity*, vol. 2019, Article ID 8472346, 8 pages, 2019.

[38] H. Nohl, D. Hegner, and K. H. Summer, "The mechanism of toxic action of hyperbaric oxygenation on the mitochondria of rat-heart cells," *Biochemical Pharmacology*, vol. 30, no. 13, pp. 1753–1757, 1981.

[39] B. J. Kudchodkar, J. Wilson, A. Lacko, and L. Dory, "Hyperbaric oxygen reduces the progression and accelerates the regression of atherosclerosis in rabbits," *Arteriosclerosis Thrombosis and Vascular Biology*, vol. 20, no. 6, pp. 1637–1643, 2000.

[40] S. Tepić, A. Petković, I. Srejović et al., "Impact of hyperbaric oxygenation on oxidative stress in diabetic patients," *Undersea & Hyperbaric Medicine*, vol. 45, no. 1, pp. 9–17, 2018.

[41] J. Paprocki, M. Pawłowska, P. Sutkowy, J. Piechocki, and A. Woźniak, "Evaluation of oxidative stress in patients with difficult-to-heal skin wounds treated with hyperbaric oxygen," *Oxidative Medicine and Cellular Longevity*, vol. 2020, Article ID 1835352, 8 pages, 2020.

[42] A. Kormanovski, D. M. Hernandez-Garcia, E. Lara-Padilla, and R. Campos-Rodriguez, "Performance, metabolic and oxidant/antioxidant response were improved by hyperbaric oxygen in high performance runners," *Global Journal of Medical Research*, vol. 10, no. 2, pp. 11–17, 2010.

[43] C. M. Muth, Y. Glenz, M. Klaus, P. Radermacher, G. Speit, and X. Leverve, "Influence of an orally effective SOD on hyperbaric oxygen-related cell damage," *Free Radical Research*, vol. 38, no. 9, pp. 927–932, 2004.

[44] B. Gulec, M. Yasar, S. Yildiz et al., "Effect of hyperbaric oxygen on experimental acute distal colitis," *Physiological Research*, vol. 53, no. 5, pp. 493–499, 2004.

[45] Z. Sepehrmanesh, F. Kolahdooz, F. Abedi et al., "Vitamin D supplementation affects the beck depression inventory, insulin resistance, and biomarkers of oxidative stress in patients with major depressive disorder: a randomized, controlled clinical trial," *The Journal of Nutrition*, vol. 146, no. 2, pp. 243–248, 2016.

[46] O. Etlik, A. Tomur, K. Dündar, A. Erdem, and N. U. Gündoğan, "The effect of antioxidant vitamins E and C on lipoperoxidation of erythrocyte membranes during hyperbaric oxygenation," *Journal of Basic and Clinical Physiology and Pharmacology*, vol. 8, no. 4, pp. 269–277, 1997.

[47] D. Łuczyński, J. Lautridou, A. Hjelde, R. Monnoyer, and I. Eftedal, "Hemoglobin during and following a 4-Week commercial saturation dive to 200 m," *Frontiers in Physiology*, vol. 10, article 1494, 2019.

[48] F. Z. Kiboub, C. Balestra, Ø. Loennechen, and I. Eftedal, "Hemoglobin and erythropoietin after commercial saturation diving," *Frontiers in Physiology*, vol. 9, article 1176, 2018.

[49] D. Santoro, D. Caccamo, S. Lucisano et al., "Interplay of vitamin D, erythropoiesis, and the renin-angiotensin system," *BioMed Research International*, vol. 2015, Article ID 145828, 11 pages, 2015.

[50] S. J. Monstrey, P. Mullick, K. Narayanan, and S. S. Ramasastry, "Hyperbaric oxygen therapy and free radical production," *Annals of Plastic Surgery*, vol. 38, no. 2, pp. 163–168, 1997.

[51] M. Gröger, P. Radermacher, G. Speit, and C. M. Muth, "Genotoxicity of hyperbaric oxygen and its prevention: what hyperbaric physicians should know," *Diving and Hyperbaric Medicine*, vol. 38, no. 4, pp. 200–205, 2008.

[52] J. Hink and E. Jansen, "Are superoxide and/or hydrogen peroxide responsible for some of the beneficial effects of hyperbaric oxygen therapy?," *Medical Hypotheses*, vol. 57, no. 6, pp. 764–769, 2001.

[53] G. Huang, J. Diao, H. Yi, L. Xu, J. Xu, and W. Xu, "Signaling pathways involved in HSP32 induction by hyperbaric oxygen in rat spinal neurons," *Redox Biology*, vol. 10, pp. 108–118, 2016.

[54] M. D. Ferrer, A. Sureda, J. M. Batle, P. Tauler, J. A. Tur, and A. Pons, "Scuba diving enhances endogenous antioxidant defenses in lymphocytes and neutrophils," *Free Radical Research*, vol. 41, no. 3, pp. 274–281, 2007.

[55] S. S. Simons, "What goes on behind closed doors: physiological versus pharmacological steroid hormone actions," *BioEssays*, vol. 30, no. 8, pp. 744–756, 2008.

[56] R. Al-Jaouni, S. M. Schneider, T. Piche, P. Rampa, and X. Hébuterne, "Effect of steroids on energy expenditure and substrate oxidation in women with Crohn's disease," *The American Journal of Gastroenterology*, vol. 97, no. 11, pp. 2843–2849, 2002.

[57] S. Tănăseanu, M. G. Serban, and V. Niţă, "Lipid peroxidation and the activity of some antioxidant enzymes in patients with systemic vasculitides treated with corticoids," *Romanian Journal of Internal Medicine*, vol. 32, no. 1, pp. 47–50, 1994.

[58] M. A. B. Lozovoy, A. N. C. Simão, C. Panis et al., "Oxidative stress is associated with liver damage, inflammatory status, and corticosteroid therapy in patients with systemic lupus erythematosus," *Lupus*, vol. 20, no. 12, pp. 1250–1259, 2011.

Hindawi
Oxidative Medicine and Cellular Longevity
Volume 2021, Article ID 1298657, 12 pages
https://doi.org/10.1155/2021/1298657

Research Article

Gastric Electrical Pacing Reduces Apoptosis of Interstitial Cells of Cajal via Antioxidative Stress Effect Attributing to Phenotypic Polarization of M2 Macrophages in Diabetic Rats

Hongcai Wang,[1] Kaile Zhao,[2] Ying Ba,[2] Tao Gao,[2] Ning Shi,[2] Qiong Niu,[2] Chengxia Liu,[2] and Yan Chen[2]

[1]*Department of Neurology, Binzhou Medical University Hospital, Binzhou, Shandong, China*
[2]*Department of Gastroenterology, Binzhou Medical University Hospital, Binzhou, Shandong, China*

Correspondence should be addressed to Chengxia Liu; phdlcx@163.com and Yan Chen; chenyanfeihong0906@163.com

Received 9 April 2020; Accepted 8 February 2021; Published 28 February 2021

Academic Editor: Karolina Szewczyk-Golec

Copyright © 2021 Hongcai Wang et al. This is an open access article distributed under the Creative Commons Attribution License, which permits unrestricted use, distribution, and reproduction in any medium, provided the original work is properly cited.

Background. Gastric electrical pacing (GEP) could restore interstitial cells of Cajal in diabetic rats. M2 macrophages contribute to the repair of interstitial cells of Cajal injury though secreting heme oxygenase-1 (HO-1). The aim of the study is to investigate the effects and mechanisms of gastric electrical pacing on M2 macrophages in diabetic models. *Methods*. Sixty male Sprague-Dawley rats were randomized into control, diabetic (DM), diabetic with the sham GEP (DM+SGEP), diabetic with GEP1 (5.5 cpm, 100 ms, 4 mA) (DM+GEP1), diabetic with GEP2 (5.5 cpm, 300 ms, 4 mA) (DM+GEP2), and diabetic with GEP3 (5.5 cpm, 550 ms, 4 mA) (DM+GEP3) groups. The apoptosis of interstitial cells of Cajal and the expression of macrophages were detected by immunofluorescence technique. The expression levels of the Nrf2/HO-1 and NF-κB pathway were evaluated using western blot analysis or immunohistochemical method. Malonaldehyde, superoxide dismutase, and reactive oxygen species were tested to reflect the level of oxidative stress. *Results*. Apoptosis of interstitial cells of Cajal was increased in the DM group but significantly decreased in the DM+GEP groups. The total number of macrophages was almost the same in each group. In the DM group, M1 macrophages were increased and M2 macrophages were decreased. However, M2 macrophages were dramatically increased and M1 macrophages were reduced in the DM+GEP groups. Gastric electrical pacing improved the Nrf2/HO-1 pathway and downregulated the phosphorylation of NF-κB. In the DM group, the levels of malonaldehyde and reactive oxygen species were elevated and superoxide dismutase was lowered, while gastric electrical pacing reduced the levels of malonaldehyde and reactive oxygen species and improved superoxide dismutase. *Conclusion*. Gastric electrical pacing reduces apoptosis of interstitial cells of Cajal though promoting M2 macrophages polarization to play an antioxidative stress effect in diabetic rats, which associates with the activated Nrf2/HO-1 pathway and the phosphorylation of NF-κB pathway.

1. Introduction

For centuries, gastrointestinal motility disorders, one of the most frequently occurring diseases, have kept perplexed people's lives with decades of diabetes mellitus [1]. Gastroparesis, namely delayed gastric emptying, is a disorder that slows or reduces the food transit from the stomach to the small intestine without mechanical obstruction. However, effective therapies for gastroparesis remain elusive with limited roles and side effects. Fortunately, nondrug treatments, such as electroacupuncture (EA) and gastric electrical stimulation (GES), are gradually taken seriously because of its apparent efficacy without side effects. In particular, long pulse GES, for it induces slow waves also referred to as gastric electrical pacing (GEP), has a direct impact on gastric motility. At present, GEP develops as an alternative therapy of gastroparesis, but the mechanisms underlying its efficacy remain unclear.

Interstitial cells of Cajal (ICCs) serve as pacemakers and generate slow waves spontaneously in the stomach. Defect of ICCs has been consistently found in both humans and animal models with diabetic gastroparesis [2, 3]. We have reported that long-pulse GES could repair the injured ICCs

partly by IGF-1 signaling pathway and enhancing the proliferation of ICCs [4, 5]. However, apoptosis of ICCs was also certificated in the stomach of gastroparesis [6]; the effects and mechanisms of GEP on apoptosis of ICCs need to be further clarified.

Macrophages have two different phenotypes: proinflammatory M1 macrophages and anti-inflammatory M2 macrophages. They can be transformed into each other in a certain internal environment. Studies have shown that gastrointestinal motility disorder did not occur in diabetic mice with the absence of macrophages, suggesting that macrophages may participate in the development of gastroparesis [7]. It is also reported that phenotypic polarization of M2 macrophages could improve the delayed gastric emptying [8]. Further studies have shown that there was no significant change in the total number of macrophages in animal models and patients of diabetic gastroparesis, while CD206+ M2 macrophages were selectively decreased, accompanied by ICC deletion, resulting in delayed gastric emptying [9–11]. Accordingly, GEP may promote the phenotypic polarization of M2 macrophages to improve ICC expression and gastric emptying.

Heme oxygenase-1 (HO-1) is a widely existing antioxidant defense enzyme, which is not expressed or low expressed in normal tissues, but upregulated during stress playing an anti-inflammatory, antioxidative, and antiapoptotic role. In the gastrointestinal tract, HO-1 is mainly produced and expressed by resident M2 macrophages [12]. Recently, in a study of diabetic gastroparesis model, it has been found that the downregulation of HO-1 could not resist oxidative stress injury, which leads to the destruction of ICCs network and delayed gastric emptying, but upregulation of HO-1 could repair the injury of ICCs and improve the delayed gastric emptying [13, 14]. Similarly, Tian LG et al. reported that the expression of HO-1 in gastric antrum of diabetic gastroparesis mice was significantly decreased, and EA could improve the expression of HO-1 and gastric motility [15]. Therefore, we speculate that GEP may play a key role in improving gastric motility disorder by upregulating HO-1 to repair ICC injury.

Also, studies have shown that HO-1 can protect and reverse oxidative stress damage to ICCs [13]. Stem cell factor (also known as SCF, c-kit ligand) is essential for survival and maintenance of ICCs, but there are few reports about the correlation between HO-1 and SCF. Recent studies [16] have shown that the NF-κB signaling pathway was activated in diabetic gastrointestinal motility disorders and the decrease expression of SCF/c-kit causes the increase of ICC apoptosis, suggesting that the activation of NF-κB signaling may be an important factor in ICC apoptosis. It is also reported that nuclear factor erythroid 2-related factor 2 (Nrf2) plays a critical role in defending against inflammation in different tissues via activation of phase II enzyme HO-1 and inhibition of the NF-κB signaling pathway [17]. Other studies [18] have shown that HO-1 can inhibit the phosphorylation of NF-κB p65, promote the binding of anti-apoptotic genes to NF-κB, and promote gene transcription to play an antiapoptotic role. In addition, studies in human lung fibroblasts have shown that nuclear transcription factor NF-κB binds to enhancers of SCF gene and promotes SCF transcription [19]. We assumed that HO-1 may play an antiapoptotic role by inhibiting the phosphorylation of NF-κB p65.

In this study, we aimed to explore the effects of GEP on ICC apoptosis and phenotypic polarization of macrophages and to investigate the possible mechanisms of renovation of ICC injury in diabetic rats.

2. Materials and Methods

2.1. Animals. Male Sprague-Dawley rats (weighing 160-200 g, $N = 60$) were purchased from Jinan Pengyue Experimental Animal Breeding Co. Ltd. (Shandong, China) and were kept in the suitable laboratory conditions (22-23°C, 12/12 h light-dark cycle) with food and water *ad libitum*. The experimental procedures were implemented, following the ethical guidelines from the Animal Care and Use Committee of Binzhou Medical University Hospital Laboratory Animal Ethical Committee. The rats were randomly divided into the normal control, diabetes (DM), diabetic+sham GEP (DM+SGEP), and diabetic+GEP (DM+GEP) groups (Figure 1).

2.2. Surgical Procedures. After an overnight fast, the rat was anesthetized with sodium pentobarbital (37.5 mg/kg, ip). To implant stimulation electrodes, a 2 cm ventral midline incision was made and the stomach was exteriorized. A pair of electrodes was imbedded 2 cm above the pylorus in the serosa of the greater curvature. The ends of the electrode wires were inserted through the abdominal wall, tunneled subcutaneously out of the back neck, and fixed carefully. When doing stimulation, the wires were connected to a programmed electrical stimulator (YC-2, Chengdu Instrument Factory, China).

2.3. Diabetic Model. After 2 weeks of recovery from the surgery, diabetic models were established using streptozotocin (STZ, 60 mg/kg, ip, Alexis Biochemical, United States). Animals in the control group were given equal volume of solvent. After one week, blood glucose of the tail vein was measured and diabetes was confirmed twice with a blood glucose > 16.7 mmol/L.

2.4. Experimental Protocol. According to the parameters used in our previous study which were all effective in ICC alteration [4, 5], the DM+GEP group was further divided into three subgroups (each $n = 10$): DM+GEP1 (5.5 cpm, 100 ms, 4 mA), DM+GEP2 (5.5 cpm, 300 ms, 4 mA), and DM +GEP3 (5.5 cpm, 550 ms, 4 mA). The rats in the DM+GEP groups were treated with gastric electrical stimulation 30 min daily starting at 9 : 00 am, while the rats in the DM + SGEP group were treated with sham gastric electrical stimulation (stimulation electrodes connected to the stimulator without electric current). To avoid the influence of stress, the rats were put into a quiet and dark place during the stimulation. After stimulation for a period of 6 weeks, all rats were sacrificed to obtain gastric antrum tissues for western blot and immunostaining.

2.5. Immunostaining. The whole mount staining was used to test the apoptosis of ICCs. The tissue was blocked by normal rabbit serum and then the primary antibody c-kit (1 : 100, Invitrogen, USA) at 4°C overnight. The apoptosis of ICCs was detected

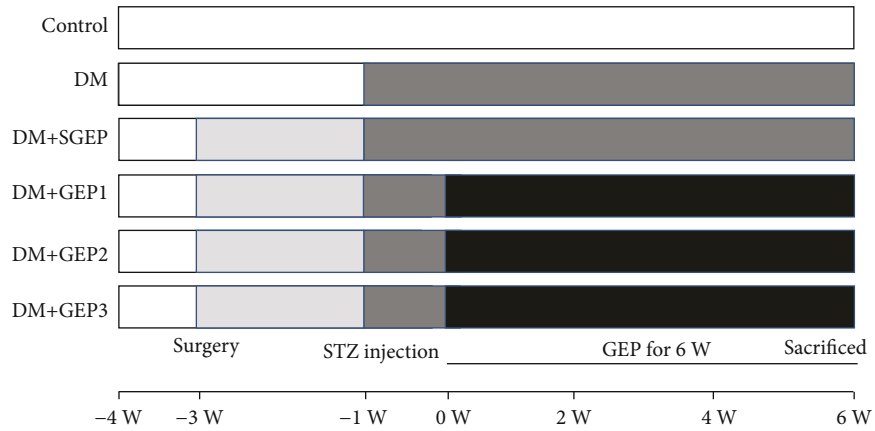

Figure 1: Sketch map of the experimental procedure. The six columns represent different groups as control (normal control group), DM (diabetes group), DM+SGEP (diabetic+sham GEP group), DM+GEP1 (diabetic+GEP1 group), DM+GEP2 (diabetic+GEP2 group), and DM+GEP3 (diabetic+GEP3 group). The whole experimental process maintained for 10 weeks. All rats were adapted to the laboratory conditions for one week (from -4 W to -3 W). All electrodes were implanted by the same surgeon in the serosa of the greater curvature of rats in the DM+SGEP and DM+GEP groups (-3 W). Two weeks later (-1 W), streptozotocin (STZ) was injected to establish diabetic models. Gastric electric pacing (GEP) was carried out in the DM+GEP group 30 min/day for 6 weeks.

with TUNEL Kit (labeling solution : enzyme solution = 9 : 1, Roche, Germany) for 1 h. After incubation with fluorescent labeled secondary antibodies, DAPI was used to label the nucleus. Then, the apoptotic ICCs could be observed under a fluorescence microscope.

For the section staining, the tissue of gastric antrum was fixed in 4% paraformaldehyde for 24 h and embedded into paraffin blocks and sliced about 6 μm. The sections were gradually deparaffinized in xylene and hydrated in a graded ethanol solution. After inhibiting the endogenous peroxidase activity by adding 0.3% hydrogen peroxide, the sections were microwaved (750 W) to expose antigens. Through nonspecific reaction blocked by normal rabbit serum, the primary antibodies NF-κB (1 : 100, Proteintech, USA), CD68 (1 : 100, Abcam, USA), CD86 (1 : 100, Novus, USA), CD206 (1 : 100, Proteintech, USA), and HO-1 (1 : 100, Proteintech, USA) were added to reveal different proteins.

With incubation with horseradish peroxidase-linked streptavidin marked secondary antibody for 1 h at room temperature, some sections were used to test the expression of NF-κB immunohistochemistry technology. And then a fresh 3,3′-diaminobenzidine solution was used to reflect the positive protein. After being counterstained and dehydrated, glass cover slips are mounted onto the slides.

To test immunoreactivity of CD68, CD86, CD206, and HO-1, fluorescent-labeled secondary antibodies were used for 1 h at room temperature. DAPI was added to stain the nucleus. All of sections were sealed with the antifluorescence quenching agent and observed under a fluorescence microscope.

2.6. Western Blot. Fresh-frozen distal stomach samples were grinded into cell suspension on ice using a homogenizer and homogenized in RIPA buffer with a protease inhibitor. After centrifugation at 12000 rpm for 5 min in 4°C, the supernatants were taken as the total protein. Loading buffer was mixed with the protein to scale prior to sodium dodecyl sulfate polyacrylamide gel electrophoresis. The total protein was separated by 10% SDS-PAGE and then transferred to a PVDF membrane. According to molecular weight, these membranes were incubated with primary antibodies against c-kit (1 : 200, Invitrogen, USA), SCF (1 : 1000, R&D Systems, USA), NF-κB (1 : 2000, Proteintech, USA), p-NF-κB (1 : 1000, CST, Germany), IKK (1 : 600, Proteintech, USA), HO-1 (1 : 1000, Proteintech, USA), Nrf2 (1 : 5000, Proteintech, USA), and GAPDH (1 : 1000, Beyotime, China) at 4°C overnight. Then, secondary antibody was added for 2 h at 37°C. Signal detection was visualized using an enhanced chemiluminescent agent, and the blot was present and detected by autoradiography.

2.7. Measurement of Malonaldehyde (MDA) Activity. MDA, a marker of oxidative stress, was determined by thiobarbituric acid method following the kit instruction (Nanjing Jiancheng Bioengineering Institute, China). Briefly, tissue was homogenized in Tris-HCl buffer at the ratio of 1 : 10 (mg/mL) under ice bath conditions. The supernatant was taken to be measured after centrifugation at 2500 rpm for 10 min. 2.5 mL thiobarbituric acid was added to the supernatant, and then, the solution was incubated at 95°C for 40 min. After that, samples were cooled with the flow water and centrifuged at 4000 rpm for 10 min. The MDA concentration (nmol/g) was measured spectrophotometrically at 532 nm.

2.8. Measurement of Superoxide Dismutase (SOD) Activity. SOD is a key enzyme in the dismutation of superoxide radicals, providing cellular defense against reactive oxygen species. SOD activity was ultimately determined using assay kits (Nanjing Jiancheng Bioengineering Institute, China). Distal stomach samples were homogenized in Tris-HCl buffer (1 : 10) under ice bath conditions and then centrifuged at 2500 rpm for 10 min. The supernatant was collected and mixed with working solutions, incubating at 37°C for 20 min. The absorbance of each well was determined by

enzyme-labeled instrument at 450 nm. The level of inhibition was measured, and the SOD level in U/g was thus determined.

2.9. Detection of Reactive Oxygen Species (ROS). Levels of ROS, a number of reactive molecules and free radicals derived from molecular oxygen, were detected by labeling with the oxidant-sensitive probe 2,7-dichlorofluorescein diacetate (DCF-DA) according to the instruction of Reactive Oxygen Species Assay Kit (Beyotime, China). After fresh tissues were homogenized and centrifuged at 1500 rpm for 5 min at 4°C, the supernatants were collected for the ROS assay. Briefly, cells were incubated with DCFH-DA at a final concentration of 10 μM for 20 min at 37°C. After removal of free DCFH-DA, the ROS levels were analyzed immediately with a flow cytometry (CytoFLEX, Beckman Coulter, USA).

2.10. Statistical Analysis. All values were expressed as the means ± SEM, and one-way ANOVA was adopted to analyze the difference among multiple groups. $P < 0.05$ was adopted as a statistically significant difference. All statistical analyses were done using SPSS 24.0 (SPSS Inc., Chicago, IL).

3. Results

3.1. Effects of GEP on Apoptosis of ICCs and SCF/c-Kit Pathway. The apoptosis of ICCs in each group is shown in Figure 2. In the control group, a lot of ICCs with few TUNEL+ cells were observed in the antrum. However, a lot of TUNEL+ cells were seen in the DM group, with significantly reduced c-kit+ cells. There was no significant difference of apoptotic ICCs between the DM+SGEP group and the DM group. From Figure 1, we could see a lot of ICCs with rare TUNEL+ cells distributed in the antrum of stomach in the DM+GEP groups.

Figure 3 demonstrates the expression of c-kit and SCF protein. In the DM group, the c-kit expression was significantly decreased compared with the control group ($P < 0.001$). The expression of c-kit in the DM+SGEP group was not significantly altered compared to that in the DM group ($P = 0.504$). However, the c-kit expression was dramatically improved in the DM+GEP groups compared with the DM group ($P = 0.042$, $P < 0.001$, and $P < 0.001$, respectively). For the expression of SCF protein, it was obviously decreased in the DM group compared with the control group ($P < 0.001$). There was no significantly difference in the DM +SGEP group compared to the DM group ($P = 1.000$). Nevertheless, the SCF expression was obviously increased in the DM+GEP groups compared with the DM group ($P = 0.080$, $P < 0.001$, and $P < 0.001$, respectively).

3.2. Effects of GEP on Macrophages. We used immunofluorescence technique to manifest the macrophages (Figure 4). In Figure 4(a), it showed that the macrophages labeled with CD68 were located in the submucosa, myenteric, and muscular layers. The expression of CD68+ cells was almost the same in each group.

M1 macrophages were marked by CD86 (Figure 4(b)). There were few M1 macrophages distributed in the submucosa, myenteric, and muscular layers in the control group. In the DM group, a lot of CD86+ cells were observed in the stomach wall. At the same time, this situation still could be seen in the DM+SGEP group. Thus, only a very few CD86-positive cells could be found in the DM+GEP groups.

Co-expression of CD206 and HO-1 were exhibited the M2 macrophages in stomach wall (Figure 4(c)). There was an abundance of CD206+/HO-1+ cells in the control group. Quite a few CD206-positive and HO-1-positive cells were observed in the DM and DM+SGEP groups, but a dramatically increased number of CD206+/HO-1+ cells were shown in the DM+GEP groups.

3.3. Effects of GEP on Nrf2/HO-1 Pathway. As shown in Figure 5, the expression of Nrf2 protein in the DM group was significantly decreased compared with that in the control group ($P = 0.020$), but HO-1 was not changed ($P = 0.365$). Compared with the DM group, no significant difference in the expression of Nrf2 and HO-1 protein could be found in the DM+SGEP group ($P = 0.618$, $P = 0.516$). However, they were dramatically increased in the DM+GEP groups compared with the DM group (for Nrf2: $P = 0.001$, $P < 0.001$, and $P < 0.001$; for HO-1: all $P < 0.001$).

3.4. Effects of GEP on the Phosphorylation of NF-κB. Immunohistochemical technique was employed to evaluate NF-κB expression (Figure 6(a)). There was a part of NF-κB+ nucleus in each layer of the control group. In the DM and DM+SGEP groups, lots of NF-κB+ nucleus and cytoplasm were demonstrated in the stomach wall. However, the expression of NF-κB+ nucleus in the DM+GEP2 and DM +GEP3 groups was significantly reduced compared with that in the DM group.

To further reveal the phosphorylation of NF-κB, western blot analysis was applied to detect the NF-κB, p-NF-κB, and IKK expression in the stomach wall (Figure 6(b)). Compared to the control group, the expression of NF-κB was obviously upregulated in the DM group ($P < 0.001$). There were no significant differences for the expression of NF-κB among the DM, DM+SGEP, and DM+GEP1 groups ($P = 0.966$, 0.180). Compared with that in the DM group, the protein expression level of NF-κB in the DM+GEP2 and DM+GEP3 groups were evidently reduced ($P = 0.002$ and $P < 0.001$).

P-NF-κB (p-p65) is the phosphorylation form of NF-κB (p65). Although the expression of p-NF-κB protein was increased in the DM group ($P = 0.084$) and the DM+SGEP group ($P = 0.143$), they still made no sense compared with the control group. Compared with the DM group, the p-NF-κB protein expression had a significant difference in the DM+GEP group ($P = 0.010$, 0.001, and 0.000).

NF-κB activation depends on the IκB kinase (IKK) complex. In the DM group, the expression of IKK was dramatically downregulated compared with the control group ($P < 0.001$). However, there were no marked differences between the DM group and the DM+SGEP group ($P = 0.703$). Greatly, when compared with the DM group, the IKK expression was distinctly upregulated in the DM +GEP groups ($P = 0.003$, <0.001, and <0.001).

3.5. Effects of EA on the Level of MDA, SOD, and ROS. MDA and SOD were detected following the instruction of the

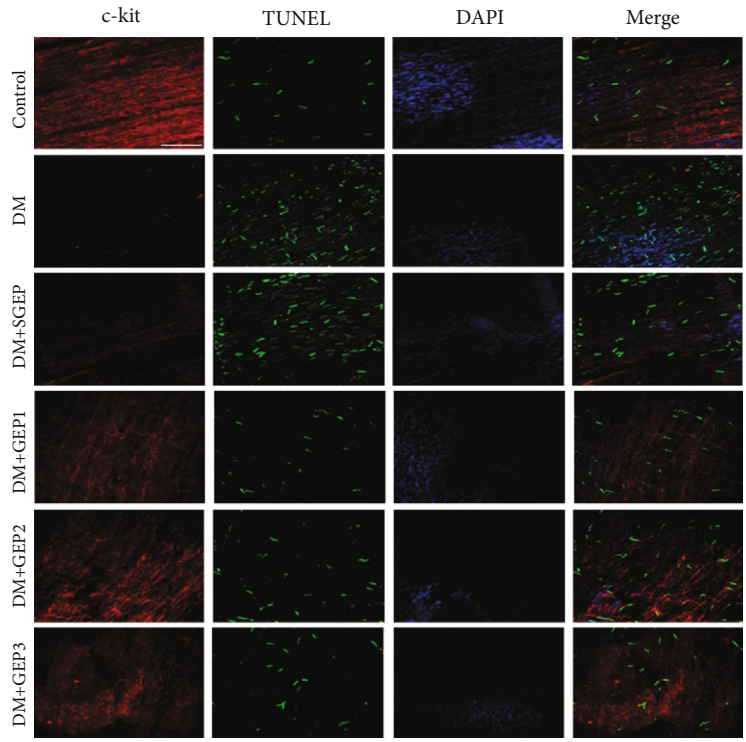

Figure 2: The alteration of the apoptosis of interstitial cells of Cajal (ICCs). The c-kit-positive ICC expression changes (staining with red) were investigated in different groups. The number of TUNEL-positive ICCs (staining with green) was counted to exhibit apoptotic cells ($n = 6$ in each group). Scale bar = 100 μm.

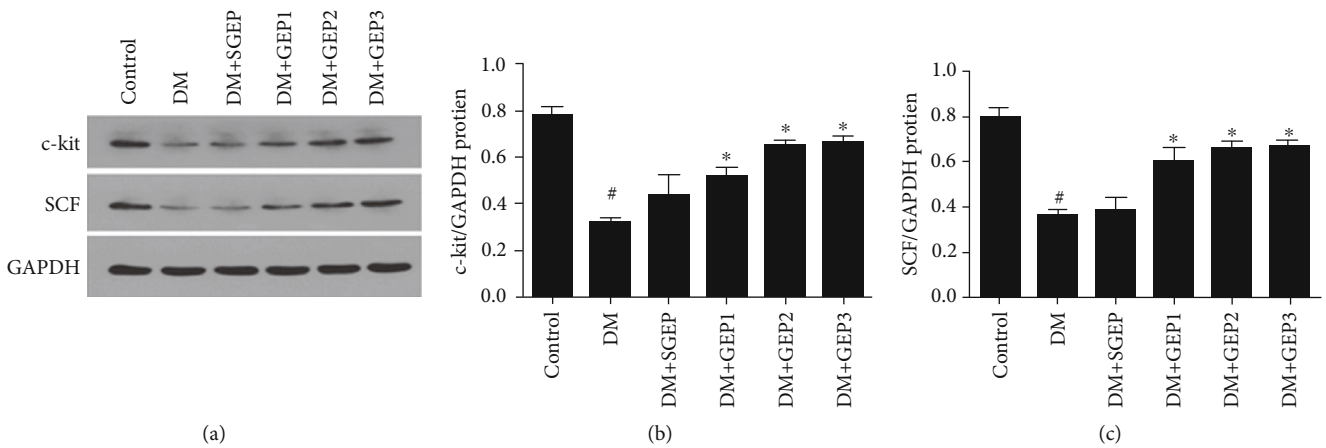

Figure 3: Expressions of c-kit and stem cell factor (SCF) protein in gastric antrum sample of different groups. (a) The altered expression of c-kit and SCF protein was tested in different groups by western blot analysis. GAPDH antibody was used as a loading control. (b, c) The relative grey ratio of protein bands was statistically evaluated in each group ($n = 6$ in each group). Data depicted as the mean ± SEM. $^{\#}$Compared with the control group, $P < 0.05$. *Compared with the DM group, $P < 0.05$.

manufacturer (Figures 7(a) and 7(b)). Compared with the control group, the MDA level was significantly elevated in the DM group ($P < 0.001$). There was no significant difference between the DM group and the DM+SGEP group ($P = 0.18$). However, the MDA level was dramatically reduced in the DM+GEP groups (all $P < 0.001$) compared with the DM group.

The SOD level in the stomach tissue was decreased distinctly in the DM group compared with the control group ($P < 0.001$). No obvious difference was found between the DM group and the DM+SGEP group ($P = 0.888$). However, the SOD level was clearly upregulated in the DM+GEP groups compared with the DM group (all $P < 0.001$).

The changes of ROS in the gastric antrum cells were detected by DCFH-DA fluorescence probe (Figure 7(c)). Compared with that in the control group, the expression of ROS in the DM group was significantly increased, the fluorescence signal of DCF was significantly enhanced, and the

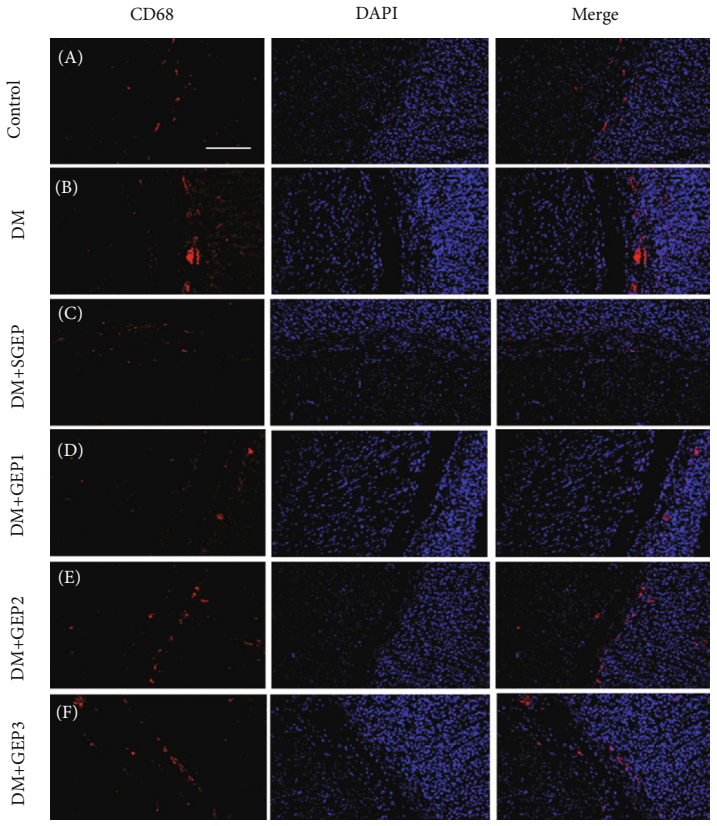

(a)

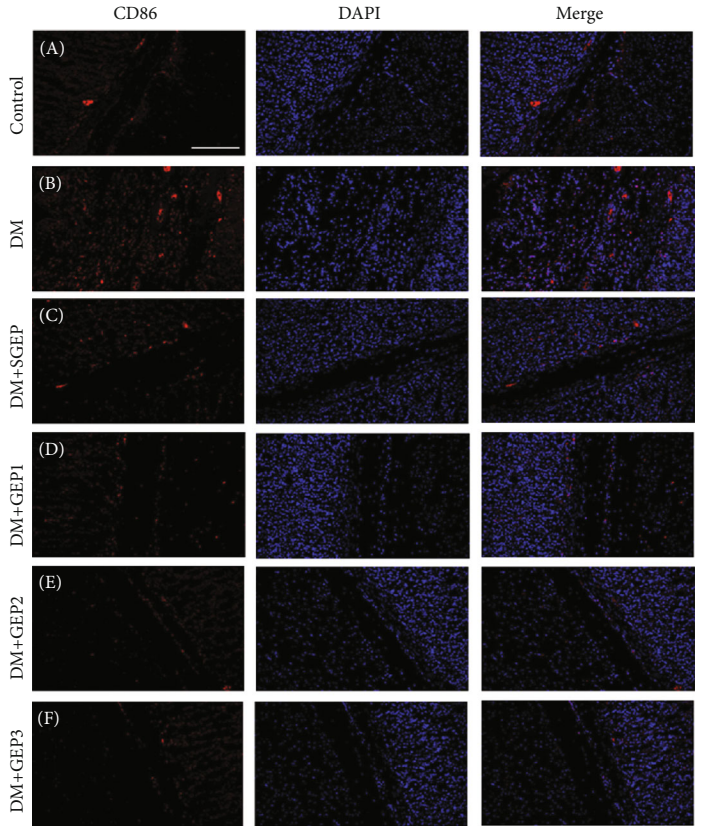

(b)

Figure 4: Continued.

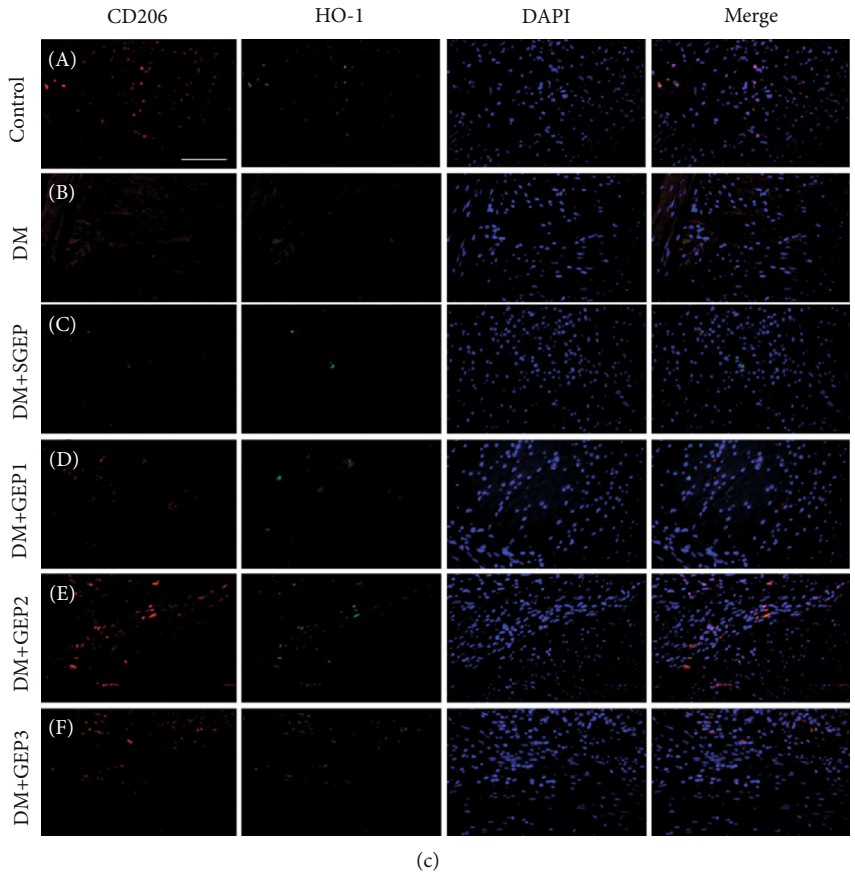

Figure 4: Differential effects of GEP stimulation on the polarization profiles of M1 and M2 macrophages. (a) The expression of CD68 positive macrophages was explored in the gastric antrum tissue of rats. (b) The expression of M1 macrophages (CD86 positive) was observed in different group. (c) The CD206- (red) and HO-1- (green) positive cells represent the expression of M2 macrophages ($n = 6$ in each group). All scale bars = 100 μm.

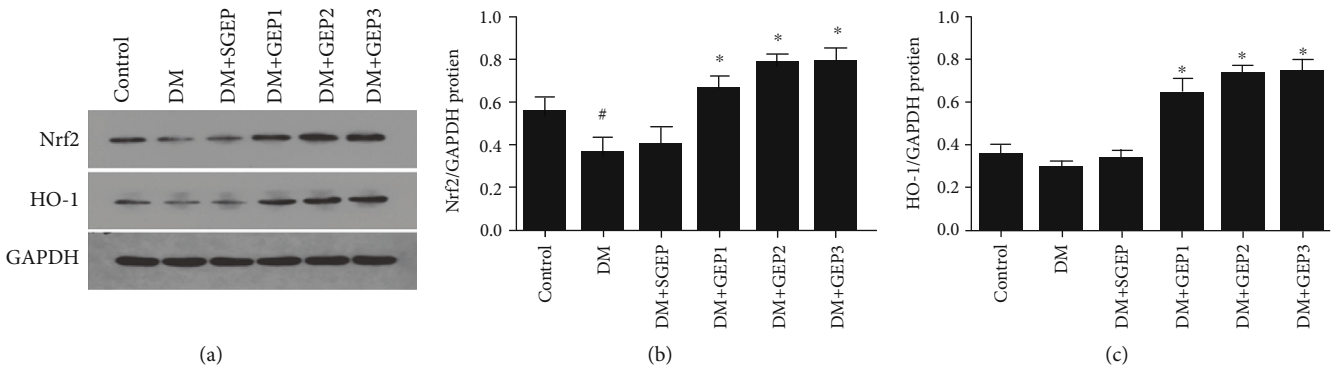

Figure 5: Expression of nuclear factor erythroid 2-related factor 2 (Nrf2) and hemeoxygenase-1 (HO-1) protein in the gastric antrum. (a) The expressions of Nrf2 and HO-1 were analyzed by western blot. (b, c) The representative quantification of Nrf2 and HO-1 protein was statistically evaluated ($n = 6$ per group). $^{\#}$Compared with the control group, $P < 0.05$. *Compared with the DM group, $P < 0.05$.

main peak of ROS shifted to the right side of the baseline. The same was seen in the DM+SGEP group. The fluorescence signal intensity in the DM+GEP groups was gradually weakened, and the main peak of ROS shifted to the left side of the baseline.

4. Discussion

In the present study, we demonstrated that GEP could decrease the apoptosis of ICCs via the improvement of phenotypic polarization of M2 macrophages, which promoted

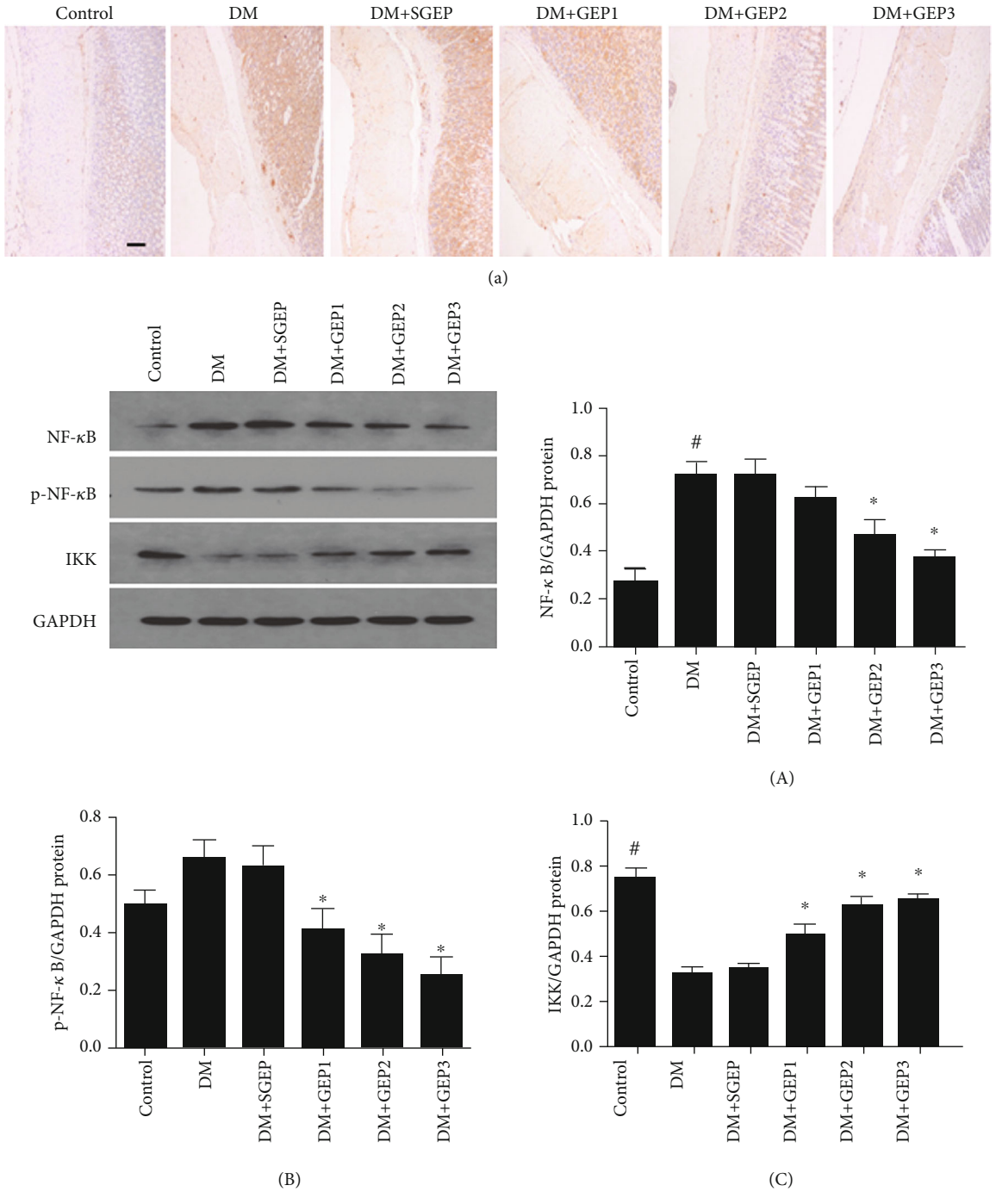

Figure 6: Effect of GEP on the phosphorylation of NF-κB in the gastric antrum. (a) The NF-κB expression was investigated by immunohistochemical staining. Scale bars = 500 μm. (b) The expressions of NF-κB and p-NF-κB were analyzed ($n = 6$ per group). #Compared with the control group, $P < 0.05$. *Compared with the DM group, $P < 0.05$.

the activation of the Nrf2/HO-1 pathway and ameliorated the phosphorylation of NF-κB. The effects of GEP were determined by frequency not pulse width of electrical stimulation. These underlying mechanisms indicated that GEP could reduce the oxidative stress, thus presenting a protective effect on ICCs.

Previous studies have demonstrated that loss and injury of ICCs have been verified in diabetic gastroparesis [2, 3, 20–22]. A further study reported that apoptotic ICC in the normal human colon was an ongoing process and the numbers of apoptotic ICC could be found [23]. The SCF/c-kit pathway is the basic guarantee to maintain of ICC quantity. We previously have reported that apoptosis of ICCs could be observed in the stomach and colon of diabetic rats, with downregulated SCF/c-kit pathway [6, 24, 25]. Wang et al. revealed that synchronized dual-pulse GES could decrease

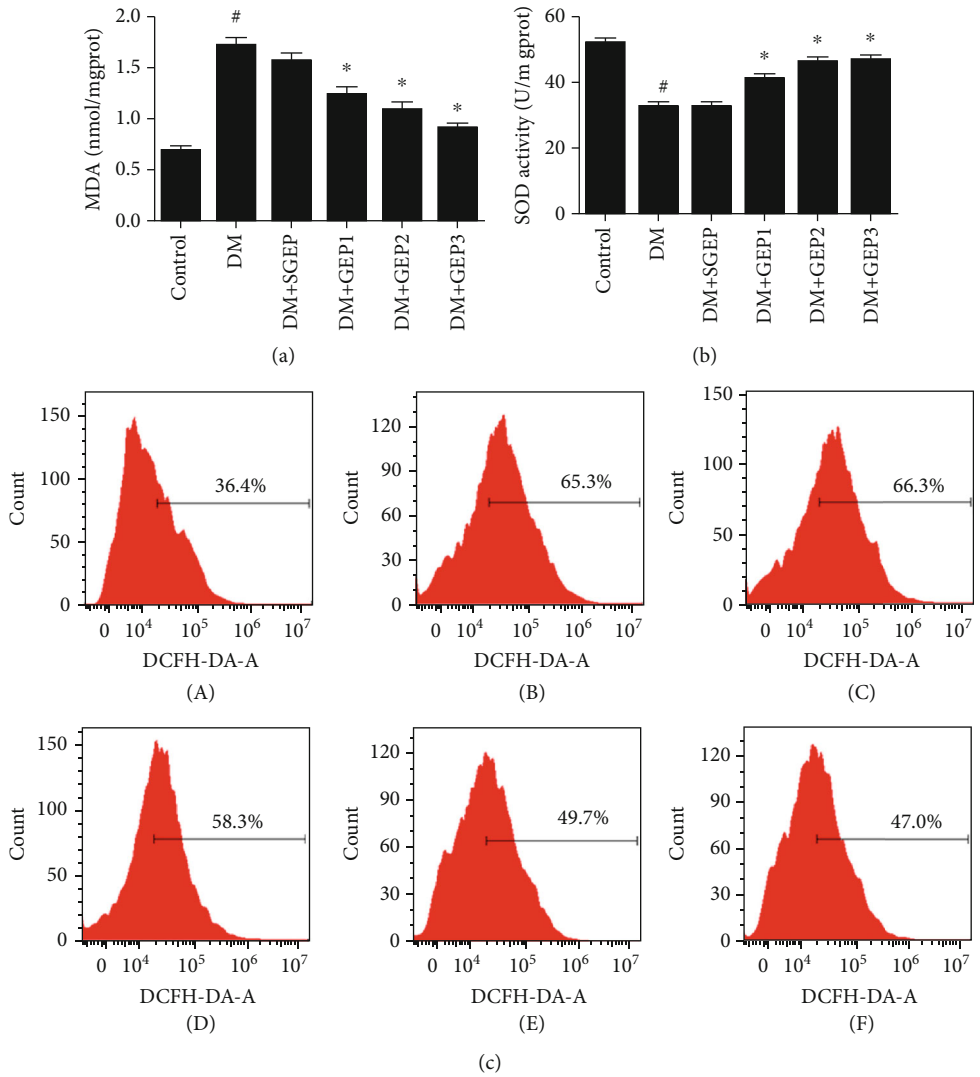

Figure 7: Measurement of malonaldehyde (MDA), superoxide dismutase (SOD), and reactive oxygen species (ROS) levels in different groups. (a) The MDA level was elevated in each group ($n = 6$ per group). #Compared with the control group, $P < 0.05$. *Compared with the DM group, $P < 0.05$. (b) The SOD level was shown in each group ($n = 6$ per group). #Compared with the control group, $P < 0.05$. *Compared with the DM group, $P < 0.05$. (c) The expression level of ROS from gastric antrum tissue in different groups was measured ($n = 3$ per group).

the apoptosis of enteric neurons in vagotomized rats [26]. The survival of ICCs could be rescued by long-pulse GES in light of our previous work [4, 5]. In the present study, we documented apoptosis of ICCs in the stomach of gastroparesis by immunofluorescence technique and GEP intervention could lessen the numbers of apoptotic of ICCs, with upregulated SCF/c-kit pathway. It implied that GEP played an antiapoptotic role of ICCs and further contributed to improved gastric motility.

To our knowledge, macrophages play a great role in gastric motility. Cipriani et al. found that diabetic *Csf1*$^{op/op}$ mice lacking macrophages were protected against the development of delayed gastric emptying [7]. A study also showed that delayed gastric emptying could be improved through phenotypic polarization of M2 macrophages [8]. Choi et al. revealed that CD206-positive M2 macrophages that expressed HO-1 protected against diabetic gastroparesis in mice [9]. Furthermore, Bernard et al. illustrated that low numbers of CD206-positive cells associated with loss of ICC in the gastric body of patients with diabetic gastroparesis [10]. Activation of macrophages with high levels of HO-1 expression protects against development of delayed gastric emptying in animal models of diabetes, while activation of macrophages that do not express HO-1 is linked to neuromuscular cell injury [11]. In our study, we observed different subtypes of macrophages and found that GEP increased the number of M2 macrophages and decreased the number of M1 macrophages, while the total number of macrophages was maintained. This result manifested that GEP promoted phenotypic polarization of M2 macrophages.

Oxidative stress plays a pivotal role in the development of diabetic complications, and antioxidant treatment could be a potential therapeutic procedure [27, 28]. Activation of the Nrf2/HO-1 signaling pathway contributes to the protective

effects against oxidative stress-induced DNA damage and apoptosis [29]. As a major protective mechanism against oxidative stress, HO-1 has been found to protect ICCs and prevent against gastroparesis. Choi et al. reported that HO-1 did not upregulate in the diabetic mice that developed delayed gastric emptying and loss of HO-1 upregulation increased levels of reactive oxygen species. Induction of HO-1 protected ICCs from oxidative stress and reversed diabetic gastroparesis in NOD mice [13]. In a rat model of streptozotocin-induced diabetes, impaired HO-1 induction in the gastric antrum induced disruption of the ICC network; thus, upregulated HO-1 expression could significantly restore the previously reduced ICC in the gastric antrum [14]. Although it is reported that EA could improve the expression of HO-1 in diabetic gastroparesis rats [15], the effects of GEP were to investigate as these two interventions had different mechanisms. We clarified that different pulse width with similar frequency GEP could promote the expression of the Nrf2/HO-1 signaling pathway, indicating the possible mechanism that GEP restore ICC in diabetic gastroparesis rats.

The NF-κB signaling pathway was considered both anti- and prooxidant roles in the setting of oxidative stress [30]. The NF-κB pathway was activated in diabetic gastroparesis, and oxidative stress was produced, resulting in the decreased expression of SCF/c-kit and the increase of ICC apoptosis [17]. Simultaneously, HO-1 could inhibit the phosphorylation of NF-κB p65, promote the binding of anti-apoptotic genes to NF-κB, and promote gene transcription to play an antiapoptotic role [19]. Our results showed that the expression of NF-κB and phosphorylated NF-κB p65 was increased in diabetic rats, with the expression of IKK (a central regulator of NF-κB activation) which was decreased. However, GEP could significantly suppress the phosphorylation of NF-κB p65, indicating that HO-1 may play an antiapoptotic role by inhibiting the phosphorylation of NF-κB p65.

Oxidative stress, an imbalance between the production of reactive oxygen species (ROS) and antioxidant defenses, is considered seriously in the production of tissue damage in diabetes mellitus [31]. MDA has been taken as an indirect marker of oxidative stress [32]. In our experiments, MDA was significantly increased in diabetic rats, which was consistent with previously reported findings [15], and GEP could lower the level of MDA. SOD, a main antioxidant enzyme, plays a role in the destruction of free superoxide radicals and blocks free radical-induced damage [33]. The SOD activity was significantly decreased in diabetic rat, while GEP could improve the activity of SOD. The present study indicates that GEP could ameliorate the balance of ROS production and antioxidant defenses. ROS are free radicals of unstable molecule that contains oxygen which may cause damage and cell death [34]. A previous study showed that oxidative stress resulted from high blood glucose through abundant ROS generation, which caused the complications of diabetes [35, 36]. In additional, we detected the ROS by flow cytometry and found that GEP could decrease the expression of ROS, suggesting that apoptosis of ICCs was reduced by GEP on the basis of lowering the ROS. This point coincides with the previous study [37].

5. Conclusions

Apoptosis of ICCs was verified in a diabetic rat with disturbance of oxidative stress, which were associated with the decreased number of M2 macrophages and downregulated Nrf2/HO-1 pathway. The progress was facilitated by activated NF-κB pathway resulting ICC apoptosis. However, GEP with different pulse width but the same frequency could reduce apoptosis of ICCs and promote phenotypic polarization of M2 macrophages via antioxidative stress effects in diabetic rats, which also optimized the Nrf2/HO-1 and NF-κB pathway. These results suggest that the protective effects of GEP targeting antioxidative stress might be a potential therapeutic strategy for diabetes dysmotility.

Abbreviations

GEP:	Gastric electrical pacing
ICCs:	Interstitial cells of Cajal
HO-1:	Heme oxygenase-1
DM group:	Diabetic group
DM+SGEP group:	Diabetic with sham GEP group
DM+GEP1 group:	Diabetic with GEP1 group
DM+GEP2 group:	Diabetic with GEP2 group
DM+GEP3 group:	Diabetic with GEP3 group
EA:	Electroacupuncture
GES:	Gastric electrical stimulation
SCF:	Stem cell factor
Nrf2:	Nuclear factor erythroid 2-related factor 2
MDA:	Malonaldehyde
ROS:	Reactive oxygen species
SOD:	Superoxide dismutase.

Data Availability

The data used to support the study can be available upon request.

Ethical Approval

All animal care and use complied with the ethical guidelines from the Animal Care and Use Committee.

Conflicts of Interest

The authors declare that they have no competing interests.

Authors' Contributions

HC W, CX L, and YC conceived and designed the study. HC W, KL Z, and YB performed the experiments. HC W and YC collected and analyzed the data. TG, NS, and QN interpreted the data. YC drafted the manuscript. All authors read and approved the final manuscript. Hongcai Wang and Kaile Zhao contributed equally to this work.

Acknowledgments

This work was supported by grants from the National Natural Science Foundation of China (No. 81700472), Medical and Health Science and Technology Development Program of Shandong Province (No. 2016WS0021), and Research Plan and Research Start-Up Fund of Binzhou Medical University (No. BY2015KYQD30).

References

[1] A. H. Kurniawan, B. H. Suwandi, and U. Kholili, "Diabetic gastroenteropathy: a complication of diabetes mellitus," *Acta Medica Indonesiana*, vol. 51, no. 3, pp. 263–271, 2019.

[2] V. J. Horváth, H. Vittal, A. Lörincz et al., "Reduced stem cell factor links smooth myopathy and loss of interstitial cells of cajal in murine diabetic gastroparesis," *Gastroenterology*, vol. 130, no. 3, pp. 759–770, 2006.

[3] S. Moraveji, M. Bashashati, S. Elhanafi et al., "Depleted interstitial cells of Cajal and fibrosis in the pylorus: novel features of gastroparesis," *Neurogastroenterology and Motility*, vol. 28, no. 7, pp. 1048–1054, 2016.

[4] Y. Chen, H. Wang, H. Li, and S. Liu, "Long-pulse gastric electrical stimulation repairs interstitial cells of Cajal and smooth muscle cells in the gastric antrum of diabetic rats," *Gastroenterology Research and Practice*, vol. 2018, Article ID 6309157, 10 pages, 2018.

[5] H. Li, Y. Chen, S. Liu, and X. H. Hou, "Long-pulse gastric electrical stimulation protects interstitial cells of Cajal in diabetic rats via IGF-1 signaling pathway," *World Journal of Gastroenterology*, vol. 22, no. 23, pp. 5353–5363, 2016.

[6] Y. Chen, J. J. Xu, S. Liu, and X. H. Hou, "Electroacupuncture at ST36 ameliorates gastric emptying and rescues networks of interstitial cells of Cajal in the stomach of diabetic rats," *PLoS One*, vol. 8, no. 12, article e83904, 2013.

[7] G. Cipriani, S. J. Gibbons, P. J. Verhulst et al., "Diabetic *Csf1*$^{o-p/op}$ mice lacking macrophages are protected against the development of delayed gastric emptying," *Cellular and Molecular Gastroenterology and Hepatology*, vol. 2, no. 1, pp. 40–47, 2016.

[8] G. Cipriani, S. J. Gibbons, K. E. Miller et al., "Change in populations of macrophages promotes development of delayed gastric emptying in mice," *Gastroenterology*, vol. 154, no. 8, pp. 2122–2136.e12, 2018.

[9] K. M. Choi, P. C. Kashyap, N. Dutta et al., "CD206-positive M2 macrophages that express heme oxygenase-1 protect against diabetic gastroparesis in mice," *Gastroenterology*, vol. 138, no. 7, pp. 2399–2409.e1, 2010.

[10] C. E. Bernard, S. J. Gibbons, I. S. Mann et al., "Association of low numbers of CD206-positive cells with loss of ICC in the gastric body of patients with diabetic gastroparesis," *Neurogastroenterology and Motility*, vol. 26, no. 9, pp. 1275–1284, 2014.

[11] L. Neshatian, S. J. Gibbons, and G. Farrugia, "Macrophages in diabetic gastroparesis–the missing link?," *Neurogastroenterology and Motility*, vol. 27, no. 1, pp. 7–18, 2015.

[12] Y. Naito, T. Takagi, and Y. Higashimura, "Heme oxygenase-1 and anti-inflammatory M2 macrophages," *Archives of Biochemistry and Biophysics*, vol. 564, pp. 83–88, 2014.

[13] K. M. Choi, S. J. Gibbons, T. V. Nguyen et al., "Heme oxygenase-1 protects interstitial cells of Cajal from oxidative stress and reverses diabetic gastroparesis," *Gastroenterology*, vol. 135, no. 6, pp. 2055–2064.e2, 2008.

[14] S. Mogami, H. Suzuki, H. Tsugawa, S. Fukuhara, and T. Hibi, "Impaired heme oxygenase-1 induction in the gastric antrum induces disruption of the interstitial cells of Cajal network in a rat model of streptozotocin-induced diabetes," *Neurogastroenterology and Motility*, vol. 25, no. 7, p. 609, 2013.

[15] L. Tian, S. Song, B. Zhu, and S. Liu, "Electroacupuncture at ST-36 protects interstitial cells of Cajal via sustaining heme oxygenase-1 positive M2 macrophages in the stomach of diabetic mice," *Oxidative Medicine and Cellular Longevity*, vol. 2018, Article ID 3987134, 9 pages, 2018.

[16] Q. H. Jin, H. X. Shen, H. Wang, Q. Y. Shou, and Q. Liu, "Curcumin improves expression of SCF/c-kit through attenuating oxidative stress and NF-κB activation in gastric tissues of diabetic gastroparesis rats," *Diabetology and Metabolic Syndrome*, vol. 5, no. 1, p. 12, 2013.

[17] L. Subedi, J. H. Lee, S. Yumnam, E. Ji, and S. Y. Kim, "Anti-inflammatory effect of sulforaphane on LPS-activated microglia potentially through JNK/AP-1/NF-κB inhibition and Nrf2/HO-1 activation," *Cell*, vol. 8, no. 2, p. 194, 2019.

[18] F. Christian, E. L. Smith, and R. J. Carmody, "The regulation of NF-κB subunits by phosphorylation," *Cell*, vol. 5, no. 1, p. 12, 2016.

[19] L. Reber, L. Vermeulen, G. Haegeman, and N. Frossard, "Ser276 phosphorylation of NF-kB p65 by MSK1 controls SCF expression in inflammation," *PLoS One*, vol. 4, no. 2, article e4393, 2009.

[20] J. Forster, I. Damjanov, Z. Lin, I. Sarosiek, P. Wetzel, and R. W. McCallum, "Absence of the interstitial cells of Cajal in patients with gastroparesis and correlation with clinical findings," *Journal of Gastrointestinal Surgery*, vol. 9, no. 1, pp. 102–108, 2005.

[21] T. Ordög, I. Takayama, W. K. Cheung, S. M. Ward, and K. M. Sanders, "Remodeling of networks of interstitial cells of Cajal in a murine model of diabetic gastroparesis," *Diabetes*, vol. 49, no. 10, pp. 1731–1739, 2000.

[22] X. Y. Wang, J. D. Huizinga, J. Diamond, and L. W. C. Liu, "Loss of intramuscular and submuscular interstitial cells of Cajal and associated enteric nerves is related to decreased gastric emptying in streptozotocin-induced diabetes," *Neurogastroenterology and Motility*, vol. 21, no. 10, p. 1095, 2009.

[23] S. J. Gibbons, R. De Giorgio, M. S. F. Pellegrini et al., "Apoptotic cell death of human interstitial cells of Cajal," *Neurogastroenterology and Motility*, vol. 21, no. 1, pp. 85–93, 2009.

[24] J. Xu, Y. Chen, S. Liu, and X. Hou, "Electroacupuncture regulates apoptosis/proliferation of intramuscular interstitial cells of cajal and restores colonic motility in diabetic constipation rats," *Evidence-based Complementary and Alternative Medicine*, vol. 2013, Article ID 584179, 10 pages, 2013.

[25] Y. Chen, J. Xu, S. Liu, and X. Hou, "Electroacupuncture at ST36 increases contraction of the gastric antrum and improves the SCF/c-kit pathway in diabetic rats," *The American Journal of Chinese Medicine*, vol. 41, no. 6, pp. 1233–1249, 2013.

[26] N. Wang, K. Li, S. Song, and J. Chen, "Gastric electrical stimulation improves enteric neuronal survival," *International Journal of Molecular Medicine*, vol. 40, no. 2, pp. 438–446, 2017.

[27] H. Wu, L. Cai, J. B. de Haan, and R. Giacconi, "Targeting oxidative stress in diabetic complications: new insights," *Journal Diabetes Research*, vol. 2018, article 1909675, 2 pages, 2018.

[28] U. Asmat, K. Abad, and K. Ismail, "Diabetes mellitus and oxidative stress–A concise review," *Saudi Pharmaceutical Journal*, vol. 24, no. 5, pp. 547–553, 2016.

[29] A. Loboda, M. Damulewicz, E. Pyza, A. Jozkowicz, and J. Dulak, "Role of Nrf2/HO-1 system in development, oxidative stress response and diseases: an evolutionarily conserved mechanism," *Cellular and Molecular Life Sciences*, vol. 73, no. 17, pp. 3221–3247, 2016.

[30] K. Lingappan, "NF-κB in oxidative stress," *Curr Opin Toxicol.*, vol. 7, pp. 81–86, 2018.

[31] O. M. Ighodaro, "Molecular pathways associated with oxidative stress in diabetes mellitus," *Biomedicine & Pharmacotherapy*, vol. 108, pp. 656–662, 2018.

[32] D. Tsikas, "Assessment of lipid peroxidation by measuring malondialdehyde (MDA) and relatives in biological samples: analytical and biological challenges," *Analytical Biochemistry*, vol. 524, pp. 13–30, 2017.

[33] G. Bresciani, I. B. da Cruz, and J. González-Gallego, "Manganese superoxide dismutase and oxidative stress modulation," *Advances in Clinical Chemistry*, vol. 68, pp. 87–130, 2015.

[34] T. Nakamura, I. Naguro, and H. Ichijo, "Iron homeostasis and iron-regulated ROS in cell death, senescence and human diseases," *Biochimica et Biophysica Acta - General Subjects*, vol. 1863, no. 9, pp. 1398–1409, 2019.

[35] V. R. Pasupuleti, C. S. Arigela, S. H. Gan et al., "A review on oxidative stress, diabetic complications, and the roles of honey polyphenols," *Oxidative Medicine and Cellular Longevity*, vol. 2020, Article ID 8878172, 16 pages, 2020.

[36] J. M. Dos Santos, S. Tewari, and R. H. Mendes, "The role of oxidative stress in the development of diabetes mellitus and its complications," *Journal Diabetes Research*, vol. 2019, article 4189813, 3 pages, 2019.

[37] R. Sghaier, A. Zarrouk, T. Nury et al., "Biotin attenuation of oxidative stress, mitochondrial dysfunction, lipid metabolism alteration and 7β-hydroxycholesterol-induced cell death in 158N murine oligodendrocytes," *Free Radical Research*, vol. 53, no. 5, pp. 535–561, 2019.

Hindawi
Oxidative Medicine and Cellular Longevity
Volume 2021, Article ID 8860883, 14 pages
https://doi.org/10.1155/2021/8860883

Research Article

Activation of Nrf2 by miR-152 Inhibits Doxorubicin-Induced Cardiotoxicity via Attenuation of Oxidative Stress, Inflammation, and Apoptosis

Wen-Bin Zhang,[1] **Xin Lai**,[2] **and Xu-Feng Guo**[1]

[1]*Department of Oncology, Renmin Hospital of Wuhan University, Wuhan 430060, China*
[2]*Department of Cardiology, Renmin Hospital of Wuhan University, Wuhan 430060, China*

Correspondence should be addressed to Xu-Feng Guo; guoxufeng007@126.com

Received 14 August 2020; Revised 23 December 2020; Accepted 11 January 2021; Published 27 January 2021

Academic Editor: Jolanta Czuczejko

Copyright © 2021 Wen-Bin Zhang et al. This is an open access article distributed under the Creative Commons Attribution License, which permits unrestricted use, distribution, and reproduction in any medium, provided the original work is properly cited.

Doxorubicin (DOX) could trigger congestive heart failure, which largely limited the clinical use of DOX. microRNAs (miRNAs) were closely involved in the pathogenesis of DOX-induced cardiomyopathy. Here, we aimed to investigate the effect of miR-152 on DOX-induced cardiotoxicity in mice. To study this, we used an adeno-associated viral vector to overexpress miR-152 in mice 6 weeks before DOX treatment, using a dose mimicking the concentrations used in the clinics. In response to DOX injection, miR-152 was significantly decreased in murine hearts and cardiomyocytes. After DOX treatment, mice with miR-152 overexpression in the hearts developed less cardiac dysfunction, oxidative stress, inflammation, and myocardial apoptosis. Furthermore, we found that miR-152 overexpression attenuated DOX-related oxidative stress, inflammation, and cell loss in cardiomyocytes, whereas miR-152 knockdown resulted in oxidative stress, inflammation, and cell loss in cardiomyocytes. Mechanistically, this effect of miR-152 was dependent on the activation of nuclear factor (erythroid-derived 2)-like 2 (Nrf2) in response to DOX. Notably, Nrf2 deficiency blocked the protective effects of miR-152 against DOX-related cardiac injury in mice. In conclusion, miR-152 protected against DOX-induced cardiotoxicity via the activation of the Nrf2 signaling pathway. These results suggest that miR-152 may be a promising therapeutic target for the treatment of DOX-induced cardiotoxicity.

1. Introduction

Doxorubicin (DOX), a quinone-containing anthracycline, is effective in the treatment of severe leukemia and malignant lymphomas [1]. Cardiomyocyte loss and congestive heart failure, however, compromised the clinical use of DOX [2]. The mechanism of DOX-induced cardiotoxicity was complex, but accumulating evidence indicated that oxidative stress and inflammation were closely involved [3, 4].

Available laboratory evidence showed that reactive oxygen species (ROS) and subsequent lipid peroxidation could be detected in the hearts within three hours after DOX treatment [5–8]. In addition, nuclear factor kappa-B (NF-κB) activation by DOX was observed very early in the hearts of mice [9]. Accumulation of ROS and inflammation caused caspase-3 activation and resulted in myocardial apoptosis [10]. Therefore, inhibition of these alterations would be of great significance to the treatment of DOX-related cardiac toxicity.

Nuclear factor (erythroid-derived 2)-like 2 (Nrf2) encodes multiple antioxidant genes and detoxifying enzymes [11]. Under physiological conditions, Nrf2 binds Kelch-like ECH-associated protein 1 (Keap1) and Cul3 ubiquitin ligase. Upon stimuli, Nrf2 is released from Keap1 and binds the antioxidant responsive element, leading to the transcription of Nrf2-dependent antioxidant genes [11]. Decreased Nrf2 expression was observed in DOX-treated hearts, and restoration of Nrf2 expression by a pharmacological agent could attenuate DOX-induced cardiotoxicity in mice [12]. Therefore, we speculated that activation of Nrf2 might largely rescue DOX-triggered cardiotoxicity.

microRNAs (miRNAs) bind to the 3′-untranslated

region (3′-UTR) of the targeted genes and cause degradation of protein expression [13]. miRNAs have been reported to regulate the activation of the Keap1-Nrf2 pathway [14, 15]. miR-200a could target Keap1 mRNA and promote degradation of Keap1, resulting in Nrf2 activation to protect against DOX-induced cardiotoxicity in mice [16]. The miR-152 family has been implicated in processes of immunomodulation, cell growth, and proliferation [17]. miR-152 overexpression improved cardiomyocyte viability and prevented hypoxia-induced cell injury in vitro [18]. In addition, miR-152 upregulation suppressed angiotensin II-induced cardiomyocyte apoptosis [19]. A previous study found that miR-152 protected against neuron injury through upregulation of the Nrf2 signaling pathway by targeting postsynaptic density protein-93 [20]. These observations raised the possibility that miR-152 would protect against DOX-triggered cardiotoxicity via regulation of Nrf2. In this study, we found that miR-152 targeted Keap1 to activate Nrf2 and protected mice from DOX-induced cardiotoxicity.

2. Materials and Methods

2.1. Antibodies and Reagents. Antibodies against NF-κB (ab16502), Lamin B (ab16048), Nrf2 (ab62352), Bax (ab32503), caspase3 (ab13847), cleaved-caspase3 (ab2302), Keap1 (ab119403) and GAPDH (ab181602) were provided by Abcam (Cambridge, UK). Mouse 3-nitrotyrosine (3-NT) ELISA kit (ab116691) and 4-hydroxynonenal (4-HNE)-protein adducts kit (ab238538) were acquired from Abcam. DOX (#D1515) and 2′,7′-dichlorodihydrofluorescein diacetate (DCFH-DA) were provided by Sigma. CardioTACS In Situ Apoptosis Detection Kit was obtained from Millipore (Billerica, MA, USA). Malondialdehyde (MDA, S0131), glutathione measurement kits (S0053), and total superoxide dismutase activity (SOD, S0101) were obtained from Beyotime Institute of Biotechnology (Shanghai, China).

2.2. Animals and Treatment. The protocols involving the use of animals were approved by the Institutional Animal Research Committee of Renmin Hospital of Wuhan University. An adeno-associated virus 9 (AAV9) system carrying miR-152 or miR-scramble under the cTnT promoter was generated by Genecopia (Shanghai, China). To overexpress miR-152 in the hearts, mice (male, age: 9-11 weeks) were given 5×10^{11} viral genome of AAV9-miR-152 or AAV9-miR-scramble by a single tail vein injection as described [21, 22]. These mice were injected with a single dose of DOX (15 mg/kg) at 6 weeks after AAV9 infection. We used normal saline (NS) to dissolve DOX. The animals were observed for 5 days after DOX injection; after that, animals were sacrificed. Cardiac Nrf2 depletion was achieved by a tail vein injection of AAV9 carrying Nrf2 small hairpin RNAs (shNrf2) or scrambled shRNA (5×10^{11} viral genome/-mouse) under the cTnT promoter (Genecopia).

2.3. Hemodynamics. After adequate anesthetization with 1.5% isoflurane, the hearts were excised and a pressure-volume catheter (Millar Instruments, USA) was inserted through an apical stab into the ventricle to measure cardiac function. Hemodynamic measurements were analyzed using an IOX software (EMKAtech).

2.4. RNA Extraction and Real-Time RT-PCR. Total RNA was extracted from the heart samples or cultured cardiomyocytes. Reverse transcriptional reactions were performed using the PrimeScript RT Reagent Kit (#RR036B, TaKaRa, Otsu, Japan). SYBR Green PCR Master Mix (04887352001, Roche) was used to detect the PCR amplification products. The mRNA levels of the target genes were normalized to those of GAPDH. The levels of miR-152 were detected using an All-in-One™ miRNA qPCR Kit (Genecopia).

2.5. Western Blot Analysis. Heart samples or cultured cardiomyocytes were lysed with a RIPA lysis buffer. An equal amount of proteins were separated in 10% SDS-PAGE gels and then transferred onto the PVDF membranes (Millipore, CA, USA). The membranes were incubated with the primary antibodies (dilution, 1 : 1000) overnight at 4°C. After that, these bands were incubated with appropriate horseradish peroxidase-conjugated secondary antibodies and visualized using enhanced chemiluminescent reagents (Promega, Madison, USA). Signals were quantified by the ImageJ software (Bio-Rad, Hercules, USA). GAPDH was used as the internal control. CelLytic™ NuCLEAR™ Extraction Kit (NXTRACT-1KT, Sigma) was used to extract the nuclear protein in our study.

2.6. NF-κB and Nrf2 Activation Assay. Transcription factor activation in heart samples and cell extracts were detected using TransAM® NFκB Activation Assay Kits and TransAM® Nrf2 Activation Assay Kits. The two kits are DNA-binding ELISAs that simplify the study of transcription factor activation, which were obtained from Active Motif.

2.7. Biochemical Detection. Fresh heart samples or cultured cardiomyocytes were homogenized in cold saline, and the supernatant fraction was collected to detect myocardial tumor necrosis factor-α (TNF-α), interleukin-6 (IL-6), IL-10, and interferon-γ (IFN-γ). TNF-α Mouse ELISA Kit (#BMS607-3), IL-6 Mouse ELISA Kit (#BMS603HS), and IL-10 Mouse Instant ELISA™ Kit (#BMS614INST) were provided by Invitrogen. IFN-γ (mouse) ELISA Kit, provided by Biovision (Shanghai, China), was used to detect myocardial IFN-γ. To evaluate oxidative damage, reduced glutathione (GSH), and oxidized GSH (GSSG), MDA, 4-HNE, and 3-NT were detected according to standard procedures.

To reflect cardiac injury after DOX treatment, lactate dehydrogenase (LDH), creatine kinase (CK), and cardiac troponin I (cTnI) were detected according to standard procedures. LDH Cytotoxicity Assay Kit (C0016) was obtained from Beyotime Institute of Biotechnology, and Creatine kinase assay kit (A032-1-1) was provided by Nanjing Jiancheng Bioengineering Institute (Nanjing, China). cTnI assay kit was obtained from Life Diagnostics, Inc. (West Chester, PA).

2.8. Apoptosis Assay. Heart paraffin sections were stained with terminal deoxynucleotidyl transferase-mediated nick-end labelling (TUNEL) staining to assess myocardial

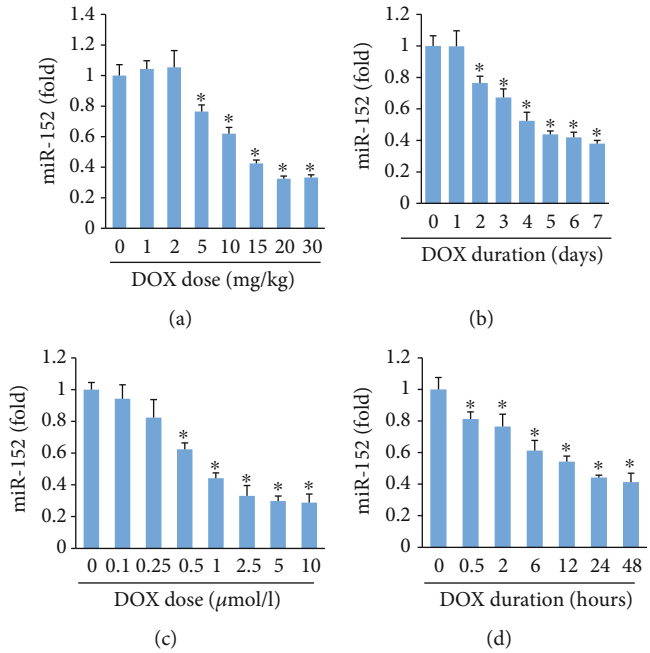

Figure 1: miR-152 expression after DOX treatment. (a, b) The miR-152 expression after DOX injection in mice ($n = 6$). (c, d) The miR-152 expression after DOX injection in neonatal rat cardiomyocytes ($n = 6$). $^*P < 0.05$ compared with NS (PBS) group. Values represent the mean ± SEM.

apoptosis. We also detected myocardial caspase 3 activity using the Caspase 3 Activity Assay Kit (C1116, Beyotime).

2.9. Cell and Treatment. Neonatal rat cardiac myocytes (NRCMs) were isolated according to a previous method [23, 24]. These cells were assigned into four groups: PBS+miR-scramble, PBS+miR-152, DOX+miR-scramble, and DOX+miR-152 groups. The cardiomyocytes were pretreated with micrON miR-152 (50 nmol/l) or scramble control for 48 hours and then incubated with DOX at 5 μg/ml or the same volume of PBS for 24 h. micrON miR-152 and scramble control were generated by Ribobio Technology (Guangzhou, China). To knock down miR-152 in NRCMs, these cells were subjected to a miR-152 inhibitor (50 nmol/l, Ribobio Technology) for 48 hours. To verify the hypothesis that the inflammatory response was secondary to the ROS production after miR-152 inhibition, NRCMs were pretreated with a nonspecific ROS inhibitor (*N*-acetyl-L-cysteine, NAC, 5 mmol/l) for 12 hours. To verify the hypothesis that miR-152 exerted protection via activation of Nrf2, cells were treated with siNrf2 (50 nmol/l) to knock down Nrf2. siNrf2 was generated by Invitrogen, and scrambled siRNA was used as a nonspecific control. Cell viability was determined by the cell counting assay (CCK-8; Dojindo Molecular Technologies, Rockville, USA) according to the manufacturer's instruction.

2.10. Intracellular ROS and Superoxide Detection. The levels of intracellular ROS were determined by spectrophotometry using DCFH-DA staining [25]. NRCMs were reacted with DCFH-DA (10 μmol/l) for 30 min at 37°C in the dark. And then, the cells were washed three times with PBS, and the fluorescence intensity was determined using a microplate reader (Biotek Instruments, VT, USA). We used Superoxide Anion Assay Kit (#CS1000, Sigma) to detect superoxide levels according to standard procedures.

2.11. Mitochondrial Respiration Complex I Activity and ATP Level Detection. Myocardial mitochondrial respiration complex I in the hearts was detected with a MitoCheck Complex I Activity Assay Kit. The ATP concentration was measured by using an ATP assay kit (Beyotime, Shanghai) according to the manufacturer's protocol.

2.12. Luciferase Assay. Keap1 3′-UTR reporter plasmid (containing the miR-152-binding sites) was generated by Genecopia, which was then transfected to NRCMs. The cardiomyocytes were treated with micrON miR-152 (50 nmol/l) or scramble control for 48 hours. Afterwards, Keap1 3′-UTR luciferase activity was tested via a Promega kit.

2.13. Statistical Analysis. All data are shown as means ± SEM. The two-tailed unpaired *T*-test was carried out to examine the significance between the two groups. Comparisons between multiple groups were performed using one-way ANOVA followed by a post hoc Bonferroni post hoc analysis for data meeting homogeneity of variance requirements. Statistical significance was accepted at a value of $P < 0.05$.

3. Results

3.1. miR-152 Level Was Downregulated in DOX-Treated Hearts and Cardiomyocytes. To investigate the involvement of miR-152 in the progression of DOX-related cardiac injury, we examined its levels in the hearts of DOX-treated mice. The cardiac miR-152 levels were significantly decreased in

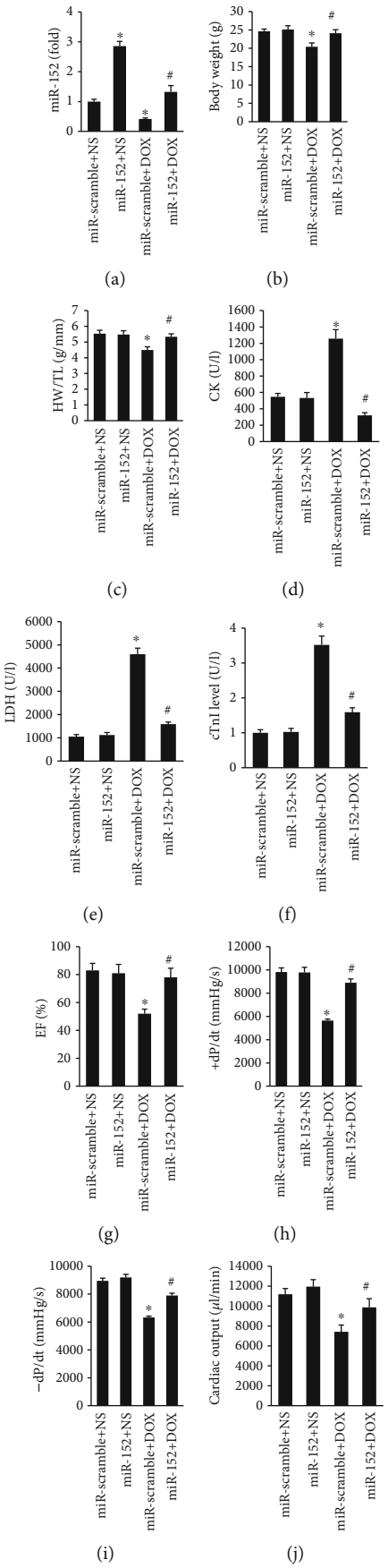

Figure 2: Continued.

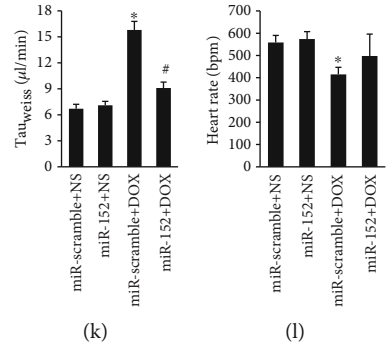

Figure 2: miR-152 overexpression improved cardiac function in mice with DOX treatment. (a) The miR-152 expression after AAV injection ($n = 6$). (b) Body weight of four groups ($n = 12$-13). (c) Statistical results of the heart weight (HW)/tibia length (TL) ($n = 12$-13). (d–f) The level of CK, LDH, and cTnI in DOX-treated mice ($n = 6$). (g–i) The alteration in EF, +dP/dt, and -dP/dt in mice ($n = 8$). (j, k) Cardiac output and Tau_{Weiss} in mice ($n = 8$). (l) Heart rate ($n = 8$). Values represent the mean ± SEM. $^{*}P < 0.05$ versus NS+miR-scramble; $^{\#}P < 0.05$ versus DOX+miR-scramble.

dose- and time-dependent manners after DOX exposure (Figures 1(a) and 1(b)). Using NRCMs, we also found that DOX treatment dose- and time-dependently decreased the expression of miR-152 in the cells (Figures 1(c) and 1(d)).

3.2. Overexpression of miR-152 Attenuated DOX-Induced Cardiac Injury and Improved Cardiac Function. To address the function of miR-152 in DOX-related cardia injury in vivo, mice were given 5×10^{11} viral genome of AAV9-miR-152 or AAV9-miR-scramble by a tail vein injection to overexpress miR-152 in the hearts. As indicated by Figure 2(a), the decreased myocardial miR-152 expression caused by DOX was successfully restored in the hearts of mice with AAV9-miR-152 injection (Figure 2(a)). After 5 days of DOX injection, mice with miR-152 expression exhibited higher body weights and heart-to-tibal length ratios than those of mice with AAV9-miR-scramble injection (Figures 2(b) and 2(c)). Furthermore, DOX-treated miR-152-overexpressed mice exhibited alleviated cardiac injury, as evidenced by the decreased plasma CK, LDH, and cTnI (Figures 2(d)–2(f)). DOX injection resulted in decreased ejection fraction (EF), maximum first derivative of ventricular pressure with respect to time (+dP/dt), -dP/dt, and cardiac output. However, these pathological alterations were attenuated after miR-152 overexpression in mice (Figures 2(g)–2(j)). miR-152 also decreased the elevation of Tau_{Weiss} in DOX-treated mice (Figure 2(k)). We also detected heart rate and found that miR-152 cannot affect the decreased heart rate in response to DOX (Figure 2(l)).

3.3. miR-152 Attenuated Myocardial Inflammation and Oxidative Damage in DOX-Treated Mice. In response to DOX, myocardial TNF-α, IL-6, and MCP-1 mRNA levels were significantly increased (Figures 3(a)–3(c)). However, these pathological elevations were decreased after miR-152 injection in mice (Figures 3(a)–3(c)). As indicated in Figures 3(d)–3(f), the overexpression of miR-152 significantly decreased myocardial cytokine protein levels, with the reduction found in TNF-α, IL-6, IL-10, and IFN-γ (Figures 3(d)–3(g)). Next, we detected the DNA binding of NF-κB and found that miR-152 significantly decreased the elevated NF-κB activation in DOX-treated hearts (Figure 3(h)). DOX-induced nuclear translocation of NF-κB was also inhibited by miR-152 supplementation (Figure 3(i)).

Next, we detected myocardial oxidative stress in mice. Elevated 3-NT, 4-HNE, and MDA in response to DOX were suppressed by miR-152 in mice (Figures 4(a)–4(c)). DOX injection decreased the ratio of GSH to GSSG and total SOD activity, and those downregulations were blocked by miR-152 (Figures 4(d) and 4(e)). Further detection revealed that the decreased mRNA levels of catalase (CAT), SOD1, SOD2, heme oxygenase 1 (HO-1), glutathione peroxidase 1 (Gpx1), and NAD(P)H:quinone oxidoreductase 1 (NQO1) were restored by miR-152 in DOX-treated mice (Figure 4(f)). The decreased Nrf2 protein expression in response to DOX treatment was also restored by miR-152 (Figure 4(g)). miR-152 significantly increased the decreased Nrf2 activation in DOX-treated hearts (Figure 4(h)). We next evaluated mitochondrial respiration complex I activity and ATP levels. Complex I activity and ATP levels were significantly reduced in the mitochondria of DOX mice compared with control mice and which were significantly increased by miR-152 (Figure S1A-B). In addition, miR-152 significantly decreased the percentage of TUNEL-positive nuclei in DOX-treated hearts (Figure 4(i)). Western analysis revealed that miR-152 decreased the protein expression of Bax and cleaved-caspase3 in DOX-treated hearts (Figures 4(j) and 4(k)).

3.4. miR-152 Attenuated DOX-Related Cardiomyocyte Injury In Vitro. To explore the effects of miR-152 in vitro, we infected NRCMs with micrON miR-152 or scramble control. DOX-induced cardiomyocyte inflammation accumulation and NF-κB activation in the miR-152 overexpression group were markedly ameliorated compared to those in the control group (Figures 5(a)–5(d)). miR-152 supplementation largely reduced the production of ROS, superoxide, and MDA in DOX-treated cells (Figures 5(e)–5(g)). The decreased cardiomyocyte viability was improved after miR-152 overexpression (Figure 5(h)). In contrast, miR-152 inhibition in NRCMs resulted in inflammation accumulation, ROS, and superoxide production, thus impairing cell viability even

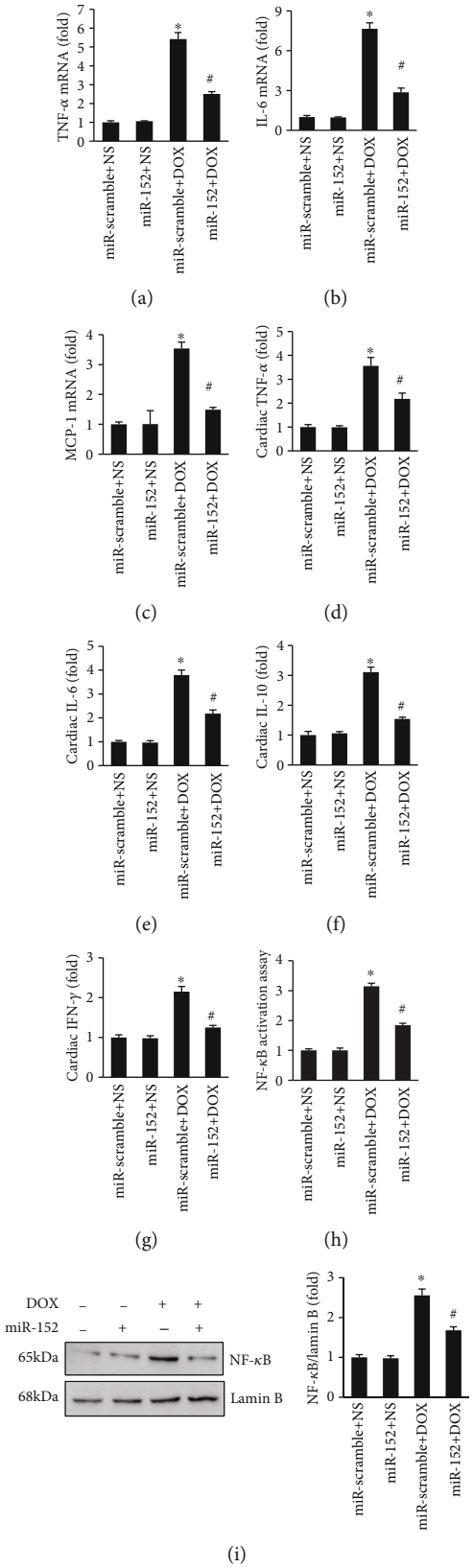

Figure 3: miR-152 supplementation attenuated myocardial inflammation accumulation in mice with DOX. (a–c) The mRNA levels of inflammatory factors in the hearts ($n = 6$). (d–g) Myocardial inflammatory factors as detected by ELISA ($n = 6$). (h) NF-κB activity in mice ($n = 6$). (i) NF-κB in the nucleus ($n = 6$). Values represent the mean ± SEM. $^{*}P < 0.05$ versus NS+miR-scramble, $^{\#}P < 0.05$ versus DOX+miR-scramble.

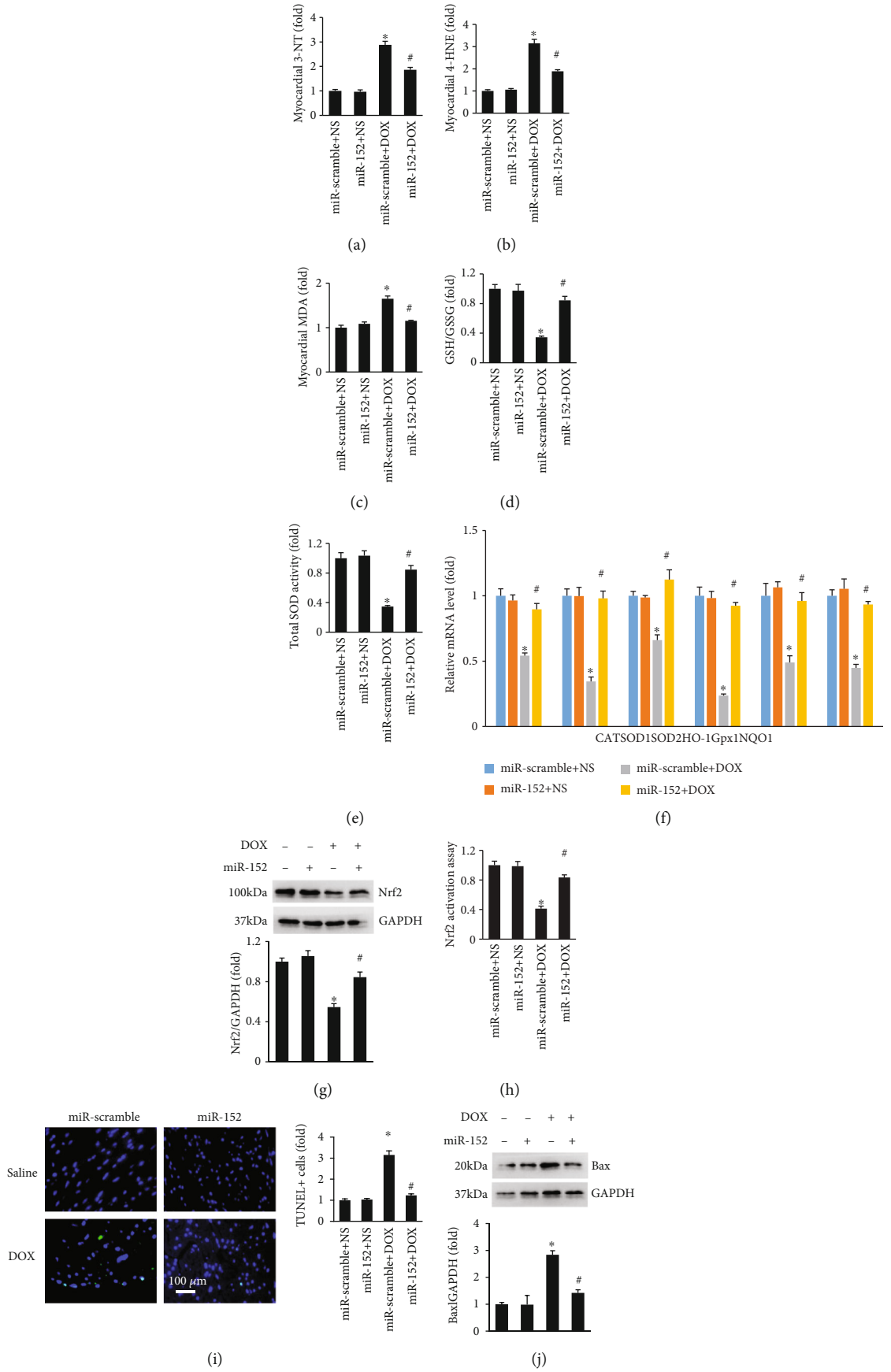

Figure 4: Continued.

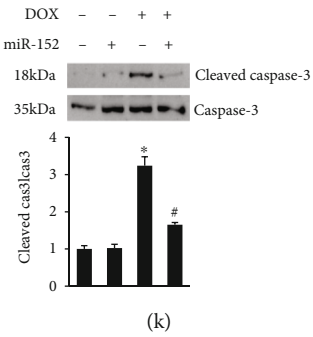

(k)

Figure 4: miR-152 reduced oxidative stress in DOX-treated mice. (a, b) The level of myocardial 3-NT and 4-HNE in the hearts ($n = 6$). (c, d) The levels of cardiac MDA and GSH/GSSG ($n = 6$). (e) Total SOD activity ($n = 6$). (f) The levels of Nrf2-regulated genes in the hearts ($n = 6$). (g) Protein expression of nuclear Nrf2 ($n = 6$). (h) Nrf2 activity assay ($n = 6$). (i) TUNEL staining ($n = 6$). (j, k) The protein expression of Bax and cleaved-caspase3 in the hearts ($n = 6$). Values represent the mean ± SEM. $^{*}P < 0.05$ versus NS+miR-scramble, $^{\#}P < 0.05$ versus DOX+miR-scramble.

without any stimuli (Figures 5(i)–5(m)). To verify the hypothesis that the inflammatory response was secondary to the production of ROS after miR-152 inhibition, NAC was used. NAC pretreatment abolished the accumulation of inflammation and NF-κB activation caused by miR-152 inhibition (Figures 5(n)–5(p)).

3.5. miR-152 Provided Cardiac Protection via Activation of Nrf2. The data in our study found that miR-152 could target the 3′-UTR of Keap1, and decreased Keap1 mRNA in cells with miR-152 overexpression (Figures 6(a) and 6(b)). Significantly, Keap1 protein expression was downregulated, and Nrf2 expression was upregulated in miR-152-overexpressed cells (Figure 6(c)). We also detected the mRNA levels of Nrf2 and found that miR-152 did not affect the mRNA levels of Nrf2 in cardiomyocytes (Figure 6(d)). Furthermore, mRNA expression of several key Nrf2-dependent genes, including HO1, NQO1, SOD1, and SOD2, was significantly restored in miR-152-overexpressing cells (Figure 6(e)). Next, we tested whether Nrf2 activation is essential for miR-152-induced cardiomyocyte protection against DOX-related cardiac injury. Cells were treated with siNrf2 to achieve Nrf2 knockdown, and Nrf2 depletion was confirmed by Western blotting (Figure 6(f)). As expected, miR-152 lost its protection in cardiomyocytes against DOX-related injury, as reflected by the TNF-α mRNA, NF-κB activation, ROS production, MDA content, and cell viability (Figures 6(g)–6(k)).

To further verify the hypothesis that miR-152 exerted its protection via activation of Nrf2 in mice, we knocked down myocardial Nrf2 in mice and found that there were no difference in plasma cTnI, EF, cardiac TNF-α level, GSH/GSSG, and caspase3 activity between miR-scramble+DOX+shNrf2 and miR-152+DOX+shNrf2 groups (Figures 7(a)–7(f)).

4. Discussion

The expression and potential function of miR-152 in DOX-related cardiac injury were unknown. The study by Zhang et al. showed that miR-152 was closely involved in the antiapoptotic effect of tanshinone IIA in cardiomyocytes [19]. miR-152 promoted the regeneration of the damaged neonatal heart through glycolysis [26]. However, there sounded quite a different voice that the upregulation of miR-152 expression in the failing myocardium contributed to heart failure pathophysiology [27]. Here, for the first time, we demonstrated that DOX decreased miR-152 expression, and supplementation of miR-152 resulted in cardioprotection from DOX-induced cardiotoxicity in mice and cardiomyocytes. More specifically, our data illustrated that miR-152 had the capacity to attenuate myocardial inflammation and oxidative damage and cardiomyocyte apoptosis, thus preventing cardiac dysfunction in mice. These findings positively suggest miR-152 supplementation may be a helpful approach to prevent DOX-related cardiac injury.

DOX-induced cardiomyopathy occurred primarily via the generation of ROS in the cardiomyocyte [28]. This mechanism separated DOX-induced cardiomyopathy from its antineoplastic activity. DOX could react with the hydrogen peroxide to yield hydroxyl radical, thus reacting with protein and lipids and thereby causing cell damage [29]. Here, we also found that DOX increased ROS, superoxide, and MDA production and decreased antioxidant activities in mice and cardiomyocytes. However, these pathological alterations were largely attenuated by miR-152 treatment, implying that the protection of miR-152 might be partly mediated by the amelioration of oxidative damage. In addition, NF-κB activation by DOX was observed in the hearts of mice, and DOX also could induce myocardial inflammation [4, 9]. Consistently, cardiac NF-κB activation and mRNA levels of inflammatory factors were found to be increased upon DOX treatment, but prevented by miR-152 supplementation, accompanied by an amelioration of cardiac dysfunction. These findings were consistent with a previous study [30]. Using NAC, we found that ROS depletion abolished the accumulation of inflammation and NF-κB activation caused by miR-152 inhibition, suggesting that the inflammatory response was secondary to the production of ROS in miR-152-deficient cardiomyocytes, which was also in line with a recent study found that inflammatory response was not the main biological factor and secondary to ROS production during acute DOX injury [31]. DOX-induced accumulation of ROS resulted in cytochrome c release followed by caspase-3

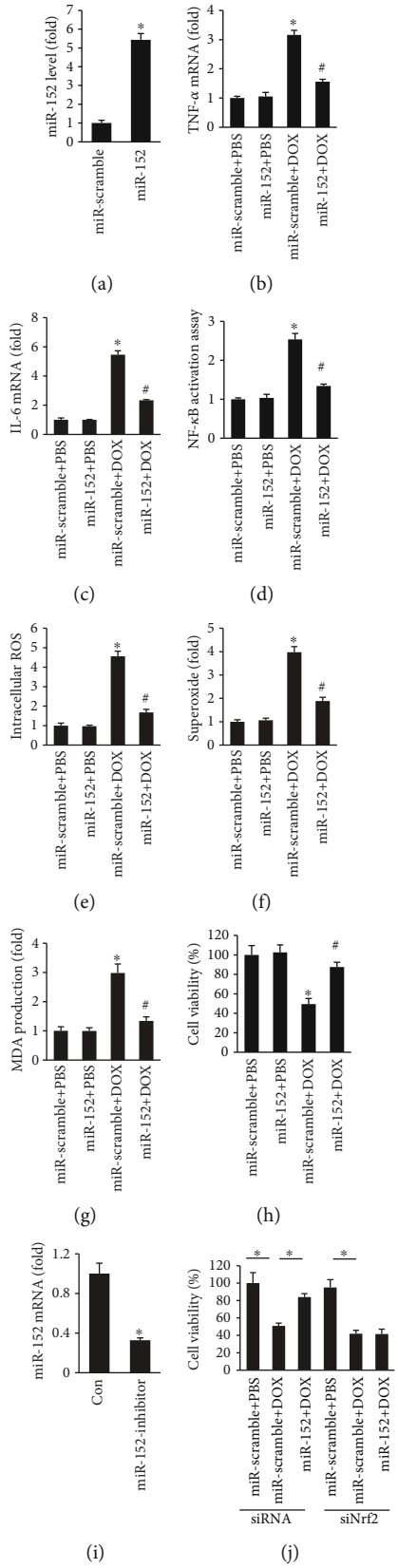

Figure 5: Continued.

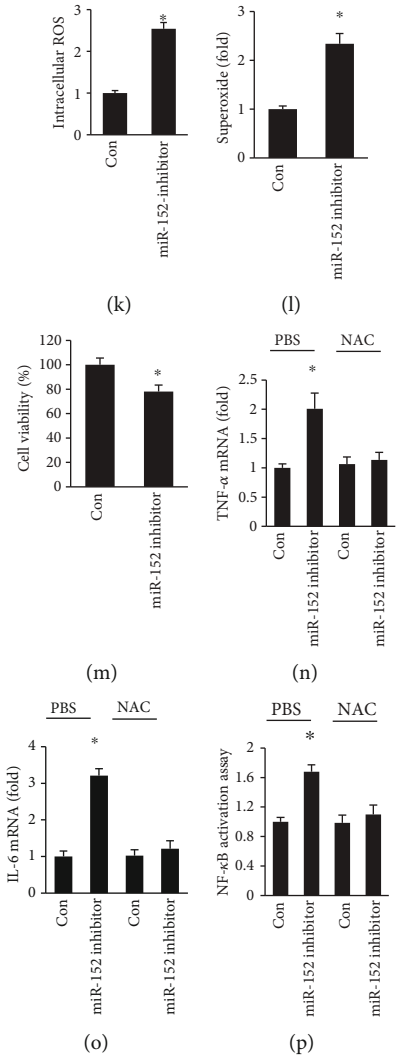

Figure 5: The role of miR-152 in cardiomyocytes. (a) miR-152 expression in cardiomyocytes ($n = 6$). (b, c) The mRNA levels of inflammatory factors in cardiomyocytes ($n = 6$). (d) NF-κB activity in cardiomyocytes ($n = 6$). (e, f) ROS and superoxide in cardiomyocytes ($n = 6$). (g) MDA production in cardiomyocytes ($n = 6$). (h) Cell viability in cardiomyocytes ($n = 6$). (i) miR-152 expression in cardiomyocytes ($n = 6$). (j) The mRNA levels of inflammatory factors in cardiomyocytes ($n = 6$). (k, l) ROS and superoxide in cardiomyocytes ($n = 6$). (m) Cell viability in cardiomyocytes ($n = 6$). (n, o) The mRNA levels of inflammatory factors in cardiomyocytes ($n = 6$). (p) NF-κB activity in cardiomyocytes ($n = 6$). Values represent the mean ± SEM. $^*P < 0.05$ versus the matched control.

activation and cell apoptosis [10]. In the present study, we observed a significant elevation in Bax and cleaved-caspase 3 expression after DOX injection compared with the control groups. Conversely, we found that miR-152 decreased the percentage of TUNEL-positive nuclei and the protein expression of Bax and cleaved-caspase 3 expression in DOX-treated hearts. These findings suggested that the improvement of cardiac function after miR-152 supplementation was partly dependent on the attenuation of myocardial inflammation, oxidative damage, and apoptosis.

Nrf2 was closely involved in the development of DOX-related oxidative damage and myocardial apoptosis. Decreased Nrf2 expression and activity were observed in DOX-induced acute cardiac injury [22], and restoration of Nrf2 by a pharmacological agent attenuated DOX-induced cardiotoxicity [12]. Recent studies demonstrate that miRNA-induced silencing of Keap1 is a novel strategy to regulate Nrf2 activation. miR-7 could target Keap1 and activate Nrf2 signaling in differentiated human neural progenitor cells [32]. miR-141 activated Nrf2 signaling by targeting and silencing Keap1 to protect cells against ultraviolet-induced oxidative stress [33]. It has been reported that miR-152 protected against neuron injury through the upregulation of Nrf2 signaling pathway by targeting postsynaptic density protein-93 [20]. The results of this study suggested that miR-152 was a direct and specific Keap1-targeting miRNA, which could regulate the Keap1-Nrf2 cascade in the hearts. In cardiomyocytes, forced miR-152 overexpression suppressed Keap1 3′-UTR reporter luciferase activity and downregulated Keap1 mRNA and protein expression,

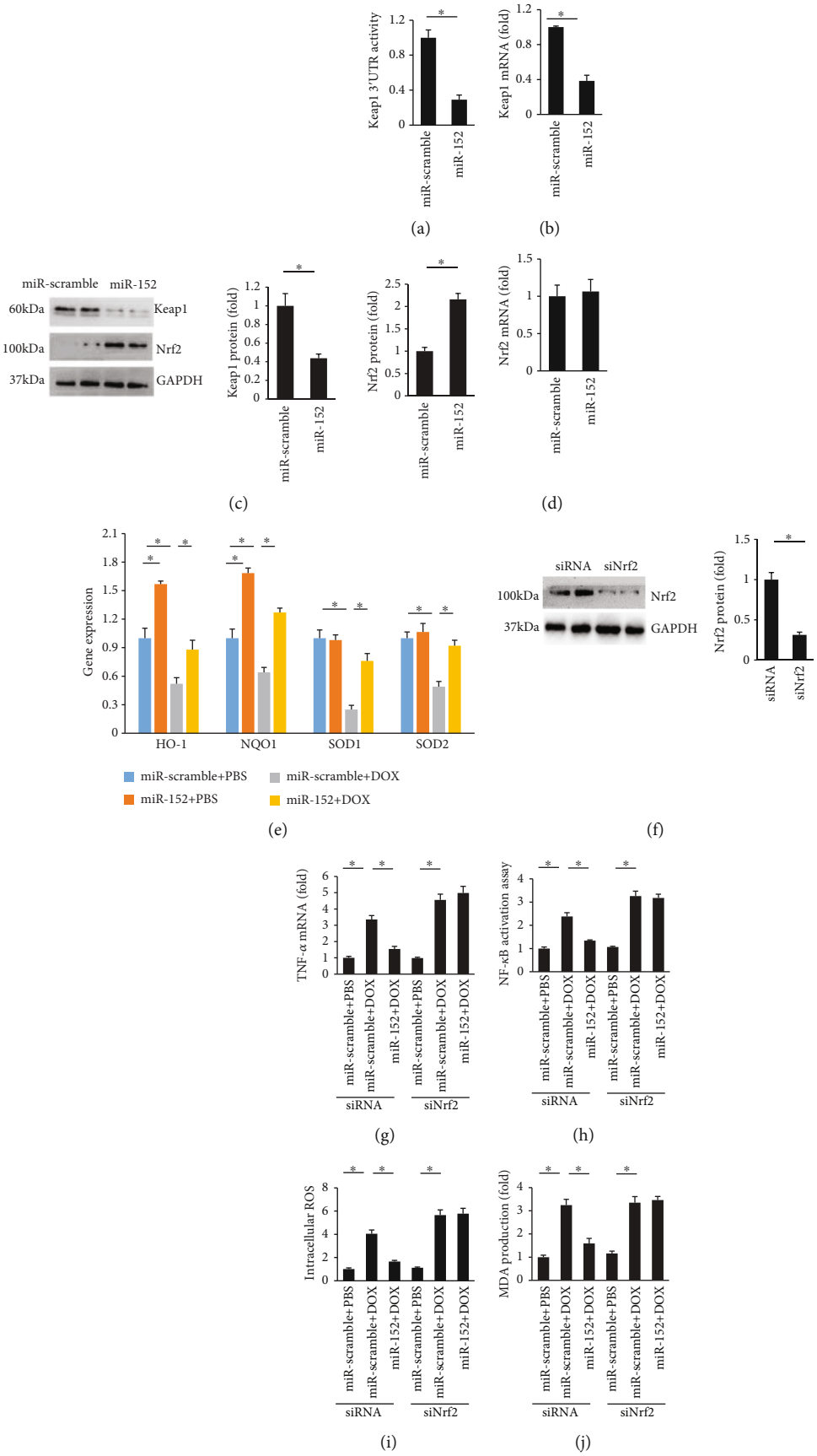

Figure 6: Continued.

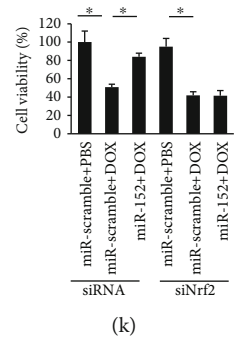

Figure 6: miR-152 targeted Keap1 and activated Nrf2. (a) Luciferase assay ($n = 6$). (b) Keap1 mRNA level ($n = 6$). (c) The protein expression of Nrf2 and Keap1 ($n = 6$). (d) Nrf2 mRNA level ($n = 6$). (e) The levels of Nrf2-regulated genes ($n = 6$). (f) The protein expression of Nrf2 ($n = 6$). (g, h) TNF-α mRNA level and NF-κB activity in cardiomyocytes ($n = 6$). (i, j) ROS and MDA production ($n = 6$). (k) Cell viability ($n = 6$). Values represent the mean ± SEM. $^*P < 0.05$ versus the matched control.

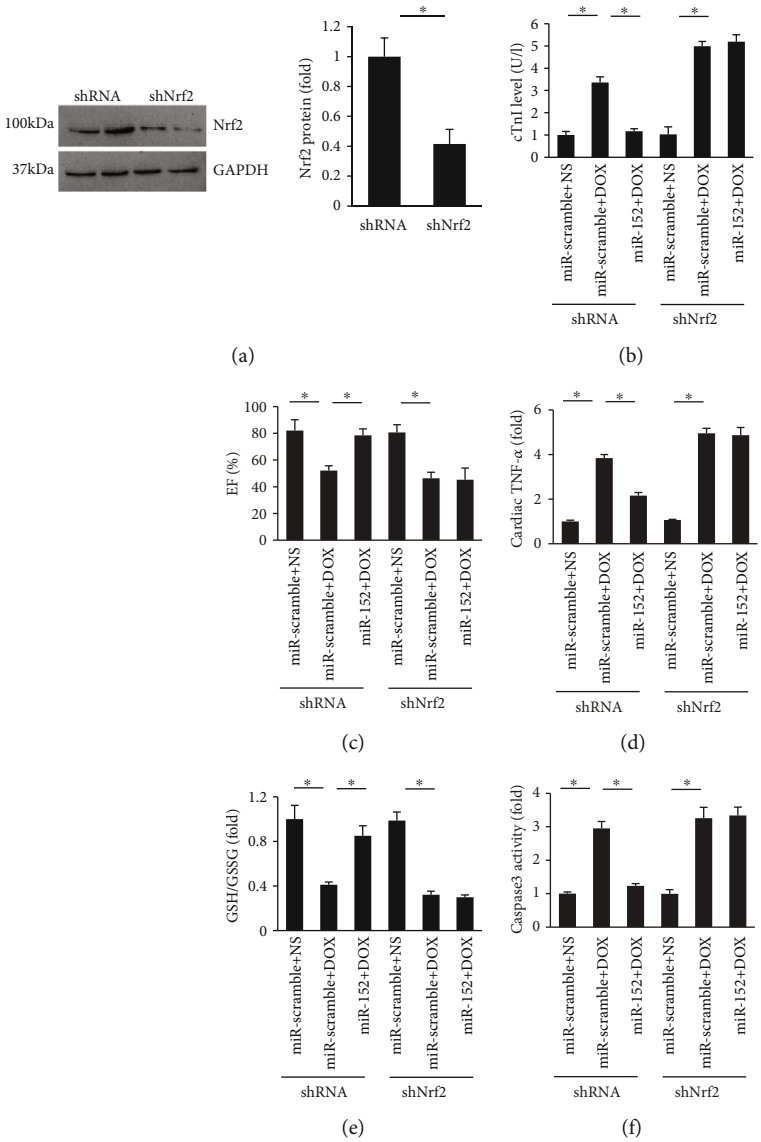

Figure 7: miR-152 lost protection in Nrf2-deficient mice. (a) Nrf2 expression ($n = 6$). (b) The level of plasma cTnI ($n = 8$). (c) EF in DOX-treated mice ($n = 8$). (d) Cardiac TNF-α level ($n = 6$). (e) GSH/GSSG ratio ($n = 6$). (f) The activity of caspase3 ($n = 6$). Values represent the mean ± SEM. $^*P < 0.05$ versus the matched control.

thus resulting in Nrf2 activation. To verify the hypothesis that miR-152 exerted cardiac protection via activation of Nrf2, we depleted Nrf2 expression in the hearts and found that miR-152 lost cardiac protection against DOX-related cardiac injury in Nrf2-deficient hearts, suggesting that the protection provided by miR-152 was dependent on the activation of Nrf2. Therefore, miR-152 overexpression provides a novel strategy to protect the hearts from DOX-related cardiac injuries.

In this study, we did not elevate whether miR-152 supplementation would promote tumor growth. We also did not elevate whether miR-152 supplementation compromises therapeutic DOX levels. These are the limitations of our study.

In conclusion, we discovered that miR-152 is a novel activator of Nrf2 in the setting of DOX-related cardiac injury. Cardiac miR-152 silenced Keap1 and activated Nrf2, leading to the attenuation of myocardial inflammation, oxidative stress, and apoptosis. This signaling cascade offers a potentially novel therapeutic target for the treatment of DOX-related cardiac injury.

Data Availability

The data that support the findings of this study are available from the corresponding author upon reasonable request.

Conflicts of Interest

The authors declare that they have no conflicts of interest.

Acknowledgments

This project was supported by the Fundamental Research Funds for the Central Universities (2042019kf0059, 2042020kf0046).

Supplementary Materials

Figure S1 The alterations in mitochondrial respiration complex I activity and ATP levels. (A) Mitochondrial respiration complex I activity ($n = 6$). (B) ATP levels ($n = 6$). Values represent the mean ± SEM. $^{*}P < 0.05$ versus NS+miR-scramble, $^{\#}P < 0.05$ versus DOX+miR-scramble. *(Supplementary Materials)*

References

[1] Y. Octavia, C. G. Tocchetti, K. L. Gabrielson, S. Janssens, H. J. Crijns, and A. L. Moens, "Doxorubicin-induced cardiomyopathy: from molecular mechanisms to therapeutic strategies," *Journal of Molecular and Cellular Cardiology*, vol. 52, no. 6, pp. 1213–1225, 2012.

[2] Y. A. Kim, H. Cho, N. Lee et al., "Doxorubicin-induced heart failure in cancer patients: a cohort study based on the Korean National Health Insurance Database," *Cancer Medicine*, vol. 7, no. 12, pp. 6084–6092, 2018.

[3] Y. J. Kang, Y. Chen, and P. N. Epstein, "Suppression of doxorubicin cardiotoxicity by overexpression of catalase in the heart of transgenic mice," *Journal of Biological Chemistry*, vol. 271, no. 21, pp. 12610–12616, 1996.

[4] Y.-P. Yuan, Z.-G. Ma, X. Zhang et al., "CTRP3 protected against doxorubicin-induced cardiac dysfunction, inflammation and cell death via activation of Sirt1," *Journal of Molecular and Cellular Cardiology*, vol. 114, pp. 38–47, 2018.

[5] L. Chaiswing, M. P. Cole, D. K. St. Clair, W. Ittarat, L. I. Szweda, and T. D. Oberley, "Oxidative damage precedes nitrative damage in adriamycin-induced cardiac mitochondrial injury," *Toxicologic Pathology*, vol. 32, no. 5, pp. 536–547, 2016.

[6] W. Yu, X. Qin, Y. Zhang et al., "Curcumin suppresses doxorubicin-induced cardiomyocyte pyroptosis via a PI3K/Akt/mTOR-dependent manner," *Cardiovascular Diagnosis and Therapy*, vol. 10, no. 4, pp. 752–769, 2020.

[7] X. Liang, S. Wang, L. Wang, A. F. Ceylan, J. Ren, and Y. Zhang, "Mitophagy inhibitor liensinine suppresses doxorubicin-induced cardiotoxicity through inhibition of Drp1-mediated maladaptive mitochondrial fission," *Pharmacological Research*, vol. 157, article 104846, 2020.

[8] S. Upadhyay, K. B. Gupta, A. K. Mantha, and M. Dhiman, "A short review: doxorubicin and its effect on cardiac proteins," *Journal of Cellular Biochemistry*, vol. 122, 2020.

[9] N. Nozaki, T. Shishido, Y. Takeishi, and I. Kubota, "Modulation of doxorubicin-induced cardiac dysfunction in toll-like receptor-2-knockout mice," *Circulation*, vol. 110, no. 18, pp. 2869–2874, 2004.

[10] A. C. Childs, S. L. Phaneuf, A. J. Dirks, T. Phillips, and C. Leeuwenburgh, "Doxorubicin treatment in vivo causes cytochrome C release and cardiomyocyte apoptosis, as well as increased mitochondrial efficiency, superoxide dismutase activity, and Bcl-2:Bax ratio," *Cancer Research*, vol. 62, no. 16, pp. 4592–4598, 2002.

[11] K. Itoh, K. I. Tong, and M. Yamamoto, "Molecular mechanism activating Nrf2-Keap1 pathway in regulation of adaptive response to electrophiles," *Free Radical Biology & Medicine*, vol. 36, no. 10, pp. 1208–1213, 2004.

[12] P. Singh, R. Sharma, K. McElhanon et al., "Sulforaphane protects the heart from doxorubicin-induced toxicity," *Free Radical Biology & Medicine*, vol. 86, pp. 90–101, 2015.

[13] E. L. Vegter, P. van der Meer, L. J. de Windt, Y. M. Pinto, and A. A. Voors, "MicroRNAs in heart failure: from biomarker to target for therapy," *European Journal of Heart Failure*, vol. 18, no. 5, pp. 457–468, 2016.

[14] S.-p. Li, W.-n. Cheng, Y. Li et al., "Keap1-targeting microRNA-941 protects endometrial cells from oxygen and glucose deprivation-re-oxygenation via activation of Nrf2 signaling," *Cell Communication and Signaling*, vol. 18, no. 1, p. 32, 2020.

[15] S. M. Kuosmanen, V. Sihvola, E. Kansanen, M. U. Kaikkonen, and A. L. Levonen, "MicroRNAs mediate the senescence-associated decline of NRF2 in endothelial cells," *Redox Biology*, vol. 18, pp. 77–83, 2018.

[16] X. Hu, H. Liu, Z. Wang, Z. Hu, and L. Li, "miR-200a attenuated doxorubicin-induced cardiotoxicity through upregulation of Nrf2 in mice," *Oxidative Medicine and Cellular Longevity*, vol. 2019, Article ID 1512326, 13 pages, 2019.

[17] X. Liu, J. Li, F. Qin, and S. Dai, "miR-152 as a tumor suppressor microRNA: target recognition and regulation in cancer," *Oncology Letters*, vol. 11, no. 6, pp. 3911–3916, 2016.

[18] J. Zhang, J. Ma, K. Long et al., "Overexpression of exosomal cardioprotective miRNAs mitigates hypoxia-induced H9c2

cells apoptosis," *International Journal of Molecular Sciences*, vol. 18, no. 4, 2017.

[19] Z. Zhang, Y. Li, C. Sheng, C. Yang, L. Chen, and J. Sun, "Tanshinone IIA inhibits apoptosis in the myocardium by inducing microRNA-152-3p expression and thereby downregulating PTEN," *American Journal of Translational Research*, vol. 8, no. 7, pp. 3124–3132, 2016.

[20] A. Zhang, Y. Qian, and J. Qian, "MicroRNA-152-3p protects neurons from oxygen-glucose-deprivation/reoxygenation-induced injury through upregulation of Nrf2/ARE antioxidant signaling by targeting PSD-93," *Biochemical and Biophysical Research Communications*, vol. 517, no. 1, pp. 69–76, 2019.

[21] Z.-G. Ma, Y.-P. Yuan, S.-C. Xu et al., "CTRP3 attenuates cardiac dysfunction, inflammation, oxidative stress and cell death in diabetic cardiomyopathy in rats," *Diabetologia*, vol. 60, no. 6, pp. 1126–1137, 2017.

[22] X. Zhang, C. Hu, C.-Y. Kong et al., "FNDC5 alleviates oxidative stress and cardiomyocyte apoptosis in doxorubicin-induced cardiotoxicity via activating AKT," *Cell Death and Differentiation*, vol. 27, no. 2, pp. 540–555, 2020.

[23] Z.-G. Ma, Y.-P. Yuan, X. Zhang et al., "C1q-tumour necrosis factor-related protein-3 exacerbates cardiac hypertrophy in mice," *Cardiovascular Research*, vol. 115, no. 6, pp. 1067–1077, 2019.

[24] Z.-G. Ma, J. Dai, Y.-P. Yuan et al., "T-bet deficiency attenuates cardiac remodelling in rats," *Basic Research in Cardiology*, vol. 113, no. 3, article 19, 2018.

[25] Z.-G. Ma, J. Dai, W.-B. Zhang et al., "Protection against cardiac hypertrophy by geniposide involves the GLP-1 receptor / AMPKα signalling pathway," *British Journal of Pharmacology*, vol. 173, no. 9, pp. 1502–1516, 2016.

[26] X. Wang, T. Ha, L. Liu et al., "TLR3 mediates repair and regeneration of damaged neonatal heart through glycolysis dependent YAP1 regulated miR-152 expression," *Cell Death and Differentiation*, vol. 25, no. 5, pp. 966–982, 2018.

[27] T. J. LaRocca, T. Seeger, M. Prado et al., "Pharmacological silencing of microRNA-152 prevents pressure overload-induced heart failure," *Circulation. Heart Failure*, vol. 13, no. 3, article e6298, 2020.

[28] C. Myers, "The role of iron in doxorubicin-induced cardiomyopathy," *Seminars in Oncology*, vol. 25, 4 Suppl 10, pp. 10–14, 1998.

[29] Y. J. Kang, Y. Chen, A. Yu, M. Voss-McCowan, and P. N. Epstein, "Overexpression of metallothionein in the heart of transgenic mice suppresses doxorubicin cardiotoxicity," *Journal of Clinical Investigation*, vol. 100, no. 6, pp. 1501–1506, 1997.

[30] T. Zhang, G. Gao, and F. Chang, "miR-152 promotes spinal cord injury recovery via c-Jun amino terminal kinase pathway," *European Review for Medical and Pharmacological Sciences*, vol. 23, no. 1, pp. 44–51, 2019.

[31] Z.-G. Ma, C.-Y. Kong, H.-M. Wu et al., "Toll-like receptor 5 deficiency diminishes doxorubicin-induced acute cardiotoxicity in mice," *Theranostics*, vol. 10, no. 24, pp. 11013–11025, 2020.

[32] S. Kabaria, D. C. Choi, A. D. Chaudhuri, M. R. Jain, H. Li, and E. Junn, "MicroRNA-7 activates Nrf2 pathway by targeting Keap1 expression," *Free Radical Biology & Medicine*, vol. 89, pp. 548–556, 2015.

[33] L.-B. Cheng, K.-R. Li, N. Yi et al., "miRNA-141 attenuates UV-induced oxidative stress via activating Keap1-Nrf2 signaling in human retinal pigment epithelium cells and retinal ganglion cells," *Oncotarget*, vol. 8, no. 8, pp. 13186–13194, 2017.

Hindawi
Oxidative Medicine and Cellular Longevity
Volume 2021, Article ID 8881770, 37 pages
https://doi.org/10.1155/2021/8881770

Review Article

Oxidative Stress-Related Mechanisms in Schizophrenia Pathogenesis and New Treatment Perspectives

Evgeny A. Ermakov,[1] **Elena M. Dmitrieva**,[2] **Daria A. Parshukova**,[2] **Daria V. Kazantseva**,[3] **Alisa R. Vasilieva**,[3] **and Liudmila P. Smirnova**[2]

[1]*Laboratory of Repair Enzymes, Institute of Chemical Biology and Fundamental Medicine, Siberian Division of Russian Academy of Sciences, Novosibirsk 630090, Russia*
[2]*Laboratory of Molecular Genetics and Biochemistry, Mental Health Research Institute, Tomsk National Research Medical Center of the Russian Academy of Sciences, Tomsk 634014, Russia*
[3]*Siberian State Medical University, Tomsk 634055, Russia*

Correspondence should be addressed to Liudmila P. Smirnova; lpsmirnova2016@gmail.com

Received 14 August 2020; Revised 15 December 2020; Accepted 2 January 2021; Published 23 January 2021

Academic Editor: Karolina Szewczyk-Golec

Copyright © 2021 Evgeny A. Ermakov et al. This is an open access article distributed under the Creative Commons Attribution License, which permits unrestricted use, distribution, and reproduction in any medium, provided the original work is properly cited.

Schizophrenia is recognized to be a highly heterogeneous disease at various levels, from genetics to clinical manifestations and treatment sensitivity. This heterogeneity is also reflected in the variety of oxidative stress-related mechanisms contributing to the phenotypic realization and manifestation of schizophrenia. At the molecular level, these mechanisms are supposed to include genetic causes that increase the susceptibility of individuals to oxidative stress and lead to gene expression dysregulation caused by abnormal regulation of redox-sensitive transcriptional factors, noncoding RNAs, and epigenetic mechanisms favored by environmental insults. These changes form the basis of the prooxidant state and lead to altered redox signaling related to glutathione deficiency and impaired expression and function of redox-sensitive transcriptional factors (Nrf2, NF-κB, FoxO, etc.). At the cellular level, these changes lead to mitochondrial dysfunction and metabolic abnormalities that contribute to aberrant neuronal development, abnormal myelination, neurotransmitter anomalies, and dysfunction of parvalbumin-positive interneurons. Immune dysfunction also contributes to redox imbalance. At the whole-organism level, all these mechanisms ultimately contribute to the manifestation and development of schizophrenia. In this review, we consider oxidative stress-related mechanisms and new treatment perspectives associated with the correction of redox imbalance in schizophrenia. We suggest that not only antioxidants but also redox-regulated transcription factor-targeting drugs (including Nrf2 and FoxO activators or NF-κB inhibitors) have great promise in schizophrenia. But it is necessary to develop the stratification criteria of schizophrenia patients based on oxidative stress-related markers for the administration of redox-correcting treatment.

1. Introduction

Schizophrenia is a complex and heterogeneous mental disorder. The heterogeneity of schizophrenia is associated with a wide range of causative biological pathways. However, the factor that unites these biological pathways is oxidative stress (OS). However, there is still no definite opinion on whether OS is the primary cause of the disease, or it occurs secondarily under the influence of environmental factors or long-term treatment. Nonetheless, it is generally accepted that OS plays an essential role in the pathogenesis of schizophrenia. In the first part of this comprehensive review, we will analyze the various mechanisms of schizophrenia pathogenesis associated with oxidative stress. In the second part, we will consider the effect of antipsychotic therapy on the parameters of redox balance, as well as review the prospects for the use of antioxidant therapy, and also propose new therapeutic strategies for redox correction based on transcription factor-targeting drugs.

2. Oxidative Stress in the Central Nervous System

Currently, there are a large number of facts that indicate the development of pronounced oxidative stress in various diseases of the central nervous system. It is due to a combination of many important factors and characteristics of the nervous tissue. The most significant of these is the high intensity of oxidative metabolism since 90% of the brain's energy needs are provided by aerobic processes [1]. Also important is the high content of unsaturated lipids in the nervous tissue [2] and metals of mixed valence (especially iron) [3], the participation of free radicals in neuroregulation [4], and the ability of several mediators and hormones to generate reactive oxygen species (ROS) [5].

The development of radical oxidative reactions in the nervous tissue is mainly local and depends on the metabolic characteristics of a particular type of tissue. CNS neurons are one of the primary consumers of glucose, oxygen, and ATP, high levels of which are necessary for maintaining membrane potentials, synthesizing neurotransmitters, and ensuring reorganization of synaptic connections and synaptic plasticity in postnatal development. All this provides an extreme sensitivity of neurons to OS; also, neurotransmitter metabolism itself generates prooxidants [6].

An imbalance of Ca^{2+} contributes to the aggravation of OS in neurons. ROS block the Ca^{2+} pumps of the endoplasmic reticulum and neurolemma, leading to an excessive concentration of Ca^{2+} ions in the cytoplasm of the neuron [7]. Intracellular Ca^{2+} regulates the release of neurotransmitters in the synaptic terminals, thus modulating synaptic activity and plasticity. In schizophrenia, there is a disruption of the synaptic transmission and plasticity [8], including the disruption of the N-methyl-D-aspartate receptor (NMDAR) activity, which is also modulated by Ca^{2+}. Besides, Ca^{2+} ions activate nNOS and the formation of NO, CO_3, and NO_2 anions that trigger neurodegeneration processes, via the heat shock protein 90 and apoptosis activation [9].

Increasing the concentration of the intracellular Ca^{2+} ion activates phospholipase A_2. Phospholipase A_2 hydrolyzes membrane phospholipids, which are rich in cell membranes and myelin oligodendrocytes, by oxidizing polyunsaturated fatty acids (PUFAs) [10]. During phospholipase hydrolysis, PUFA is released from the membrane and further participates in signal transduction directly or after conversion to bioactive derivatives. PUFAs and their mediators regulate brain processes, such as neurotransmission, neurogenesis, neuroinflammation, and neuron protection. Besides, in neurons, PUFA is used as a substrate for the synthesis of ATP by β-oxidation due to the higher yield of ATP, compared to the oxidation of glucose and lactate [11].

Metals with mixed valence (especially iron and copper) can contribute to the development of OS in neurons [12]. Iron in brain tissues is necessary for metabolic processes, synthesis of aminergic neurotransmitters, and synaptic connections in neurons [13]. However, the high content of Fe^{2+} in the central nervous system is potentially toxic due to iron-generated ROS in an oxygen-rich environment. Also, metals with mixed-valence properties can bind directly to DNA, changing the properties of reparative proteins. Neurons contain a "labile" pool of $Cu^{+}(\bullet)$, which is essential for transmitting cellular signals and excitability of neurons. Also, Cu^{2+} is a significant cofactor for enzymes. The high content of $Cu^{+}(\bullet)$ ions in neurons (from 0.1 μM to 1.3 μM) encourages Cu^{2+}-catalyzed protein oxidation and may be associated with a toxic increase in peroxidase activity, which can generate CO_3 through $HOOCO_2$ and thiol oxidase activity [14]. Copper ions can also participate in the generation of $OH^{\bullet}$ radicals by reacting with hydrogen hydroperoxide [15].

Having the factors mentioned above of vulnerability to OS, neurons have extremely weak antioxidant protection. Neurons have 50 times less catalase content compared to hepatocytes. The content of reduced glutathione (GSH) is ~50% lower in neurons compared to other cells (for example, ~5 μM in neurons compared to 10-11 μM in hepatocytes) [16]. The reduced ability to synthesize GSH due to the low content and activity of the transcription factor Nrf2 (nuclear factor erythroid 2-related factor 2), which binds the promoter, is responsible for the low level of cytosolic GSH in neurons. Cortical neurons have been shown to express Nrf2 approximately 100-1000 times less than astrocytes [17]. Additionally, the neuronal activity of Nrf2 is limited by the high content of the Cullin 3 protein, contributing to the proteasome degradation of Nrf2 [18]. All this contributes to the accumulation of ROS in neurons.

GSH enhances GABA-activated responses of inhibitory neurons via GABA receptors. Low GSH levels can lead to a decrease in GABA-mediated feedback inhibition and affect the normal function of GABAergic neurons in the prefrontal cortex by removing inhibitory effects on neurons in this area, which may be the cause of positive symptoms of schizophrenia [19]. In patients with schizophrenia, a decrease in the level of glutathione in the prefrontal cortex has been shown [20].

Astrocytes, in contrast, play a significant role in providing antioxidant support to neighboring neurons, and redox regulation of the Nrf2 astrocyte pathway is a potent homeostatic regulator of a large cohort of Nrf2-regulated antioxidant genes that are expressed by these cells. Even in an inactive state, astrocytes actively express antioxidant enzymes, including catalytic and regulatory subunits of glutamate-cysteine ligase (GCL), glutathione peroxidase (GPX), glutathione reductase (GSR), glutathione S-transferase (GST), as well as reduced glutathione (GSH), and vitamins C and E. Astrocytes also control the supply of energy substrates to the neurons to activate the pentose phosphate glucose utilization pathway that supports glutathione in its reduced state [21]. The NMDAR function is modulated by redox systems through the forming of disulfide bonds in receptor subunits that reduce NMDAR conductivity [22]. Astrocytic abnormalities in schizophrenia include disorders of glutamate reuptake, recycling, and turnover of endogenous NMDAR ligands [23]. The NMDAR hypofunction leads to cortical oxidative stress, GSH deficiency, and decreased activity of the thioredoxin/peroxiredoxin system through transcriptional control of several critical antioxidant genes [24].

Oligodendrocytes, which are necessary for maintaining a high speed of signal transmission through axons and maintaining the metabolism of neurons, are extremely vulnerable

to OS's effects. These cells require significant energy costs to maintain and form massive areas of the membrane, stacked in myelin sheets throughout the entire period of postnatal development. Also, myelin itself is a rich source of PUFA. Among all CNS cells, oligodendrocytes have the highest iron content, which is also necessary for the production of myelin [25]. When myelin is damaged, iron is released into the extracellular space and causes the formation of hydroxyl radicals during the transition of Fe^{2+} to Fe^{3+}, thereby contributing to the development of OS. This may also lead to the death of microglial cells caused by the absorption of Fe from the intercellular space [26].

Microglia, as the main immunological compartment of the central nervous system performing protective and immunoregulatory functions, is itself a ROS source. They are necessary as the central acting units of extracellular effector and intracellular signaling systems that regulate anti-inflammatory and antioxidant response and the main transcription programs via NF-κB and Nrf2, respectively [27]. However, in schizophrenia, excessive activation of microglia was detected, which leads to an increase in ROS production [28] and the development of neuroinflammation [29].

Different brain regions also differ in their susceptibility to OS. The regions of the brain that are most sensitive to OS are the amygdala, hippocampus, and cerebellar granule cells of the cerebellar cortex. Neurons with different sensitivity to OS can be found in each brain region [30].

The pyramidal neurons of the hippocampus of the adjacent CA1 and CA3 regions are similar in morphology, but not in their sensitivity to OS. A moderate decrease in GSH has been shown to cause a more pronounced OS in the CA1 region [31]. The accumulation of ROS in the CA1 area is accompanied by the significant destruction of neurons, which is observed in the CA3 region to a much lesser extent [32]. When creating an OS model by removing GPX4, it was shown that in the hippocampus, OS causes local neurodegeneration [33].

Neurons in the midbrain, namely the dopaminergic neurons of the pars compacta of substantia nigra (A9) and the adjacent ventral region (A10), also respond differently to OS. Despite the high content of Fe and Cu ions in these regions and the processes of dopamine autooxidation occurring in both parts of the midbrain, A9 neurons are more sensitive to OS effects [6].

Granular neurons in the cerebellum are susceptible to OS. It was shown that the superoxide generated by xanthine oxidase in granular cells induced apoptosis both directly through activation of caspase-3, and indirectly through a violation of the Ca^{2+} balance [34]. In neurons of the cerebral cortex (layers IV-VI), this reaction was almost not observed, so it can be argued that this area is less sensitive to OS [6].

Thus, many signaling and metabolic pathways in brain tissues provoke enhanced ROS formation, which is often exacerbated by the region-specific sensitivity of the brain to OS. In schizophrenia, these features become critical, compounded by the fact that OS plays a significant role in the pathogenesis of the disease, leading to the formation of stable disruptions of the redox balance.

3. Altered Redox Balance in Schizophrenia

Now, there is overwhelming evidence of redox imbalance in schizophrenia. This issue is considered thoroughly and in detail in numerous reviews [35–37] and meta-analyses [38–46]. The main markers of redox imbalance in schizophrenia are summarized in Table 1. Regardless of data heterogeneity, the predominance of prooxidant processes and deficiency of the antioxidant system, that is, the state of generalized oxidative stress, are mostly observed in schizophrenia. The main changes in the nonenzymatic antioxidant system consist of decreasing the concentrations of bilirubin, uric acid, ascorbic acid, tocopherol, pyridoxal, folate, and polyunsaturated fatty acids (PUFAs). The data on the reduction of folate and pyridoxal in blood serum of schizophrenia patients were confirmed by meta-analyses [42, 44]. The data on the reduction of PUFAs of the red blood cell membrane in patients treated with antipsychotic medication and antipsychotic-naïve patients were supported by meta-analysis [41] and seem convincing. Besides, the reduction of uric acid in the serum of patients was demonstrated and supported by meta-analysis [40]. Numerous data are indicative of the decreased concentration of reduced glutathione and increased concentration of oxidized glutathione in plasma [47, 48], erythrocytes [49], cerebrospinal fluid [50], and different brain regions [50–52] in first-episode, nonmedicated, medicated, and chronic schizophrenia patients.

The primary markers of disorders in the fermentative antioxidant system in schizophrenia are related to oppositely directed changes in the activity of antioxidant ferments (Table 1). According to the meta-analysis results, the level of activity of erythrocyte superoxide dismutase was reduced in acute relapse of psychosis, drug-naïve first-episode psychosis, stable medicated outpatients, and chronic inpatients [40]. The level of activity of erythrocyte catalase was decreased in the mentioned groups of patients, except for stable medicated outpatients, in whom this level was increased [40]. The level of activity of erythrocyte glutathione peroxidase was reduced in acute relapse of psychosis and chronic schizophrenia patients [40]. However, according to the results of other meta-analyses, the changes in the level of activity appeared to be statistically insignificant [43, 45]. This is explained by small samples of patients, high heterogeneity of groups, and the effect of therapy.

Markers of free radical oxidation products (Table 1) prove the predominance of prooxidant processes in schizophrenia. Numerous data indicate an increase in the concentration of thiobarbituric acid reactive substances (for example, malondialdehyde), lipid peroxides, 4-hydroxynonenal, 3-nitrotyrosine, 8-hydroxy-2-deoxyguanosine, and others. The most reliable proof of predominance of prooxidant processes is the increase of thiobarbituric acid reactive substances in drug-naïve first-episode psychosis, stable medicated outpatients, and chronic inpatients, which is confirmed by the results of meta-analysis [40, 46]. Another remarkable proof of redox imbalance in schizophrenia is the reduction of the total antioxidant status in drug-naïve first-episode psychosis, which is also confirmed by meta-analyses and reviews [35–37, 40, 45].

Table 1: Changes in oxidative stress-related markers in schizophrenia.

Parameters	Reviews				Meta-analyses		
	Yao J. K. and M. S. Keshavan, 2011 [35]	Boskovic M. et al., 2011 [36]	Koga M. et al., 2016 [37]	Zhang M. et al., 2010 [38]	Flatow J. et al., 2013 [40]	Fraguas D. et al., 2017 [43]	Fraguas D. et al., 2019 [45]	Carvalho A. F. et al., 2020 [46]
Nonenzymatic antioxidant system								
Bilirubin	↓		↓					
Biopyrrins[α]	↑		↓↑					
Thioredoxin	↑		↓↑					
Uric acid	↓	↓	↓		↓[ν] ↓[σ]		N.S.	
Ascorbic acid (vitamin C)[α]	↓	↓	↓		↓[σ]			
Tocopherol (vitamin E)[α]	↓	↓	↓		↓[σ]			
Pyridoxal (vitamin B6)								↓
Folate (vitamin B9)								↓
Glutathione[β]	↓		↓			N.S.	N.S.	
Free thiols	↓		↓					
PUFAs[γ]	↓		↓				↓[ν]	↓
Enzymatic antioxidant system								
Superoxide dismutase[δ]	↓↑	↓↑	↓↑	↓	↓[μ] ↓[ν] ↓[π] ↓[σ]	N.S.	N.S.	
Catalase[δ]	↓	↓	↓↑	N.S.	↓[μ] ↓[ν] ↑[π] ↓[σ]	N.S.	N.S.	
Glutathione peroxidase[δ]	↓↑	↓	↓↑	N.S.	↓[μ] N.S.[ν] N.S.[π] ↓[σ]	N.S.	N.S.	
Glutathione reductase[δ]		↓	↑					
Glutathione transferase[δ]			↑					
Free radical oxidation product markers								
Thiobarbituric acid reactive substances (TBARS)[ε]	↑	↑	↑	↑	↑[ν] ↑[π] ↑[σ]		N.S.	↑
Lipid peroxides	↑							
Pentane[θ]	↑		↑					
Ethane[θ]	↑		↑					
Isoprostanes[θ]	↑							
Carbonyl groups		↑	↑					
4-Hydroxynonenal	↑		↑					
3-Nitrotyrosine	↑	↑	↑					
8-Hydroxy-2-deoxyguanosine[λ]		↑						
Other markers								
NO	↑	↑		↑	↓[ν] ↑[π]			
Nitric oxide synthase[δ]	↓↑		↓↑					
Homocysteine		↑					↑[ν]	
Xanthine oxidase[δ]		↑						
Total antioxidant capacity			↓					
The ferric reducing ability of plasma			↓					
Total antioxidant potential			↓					
Total oxidant status		N.S.						
Total antioxidant status	↓		↓		↓[ν]	N.S.	↓[ν]	

Notes. Data are for plasma/serum unless otherwise indicated. [α]In plasma/serum or urine. [β]In plasma/serum, red blood cells, or brain tissues. [γ]In red blood cell membrane. [δ]In plasma/serum, red blood cells, platelets, or postmortem brain. [ε]In blood, plasma, cerebrospinal fluid, or red blood cells. [θ]In exhaled air. [λ]In urine or postmortem brain. [μ]Acute relapse of psychosis. [ν]Drug-naïve first-episode psychosis. [π]Stable medicated outpatients. [σ]Chronic inpatients. Abbreviations: PUFAs = polyunsaturated fatty acids. NO = nitric oxide. N.S. = not significant.

Only a limited number of studies indicate reductive stress in schizophrenia [53, 54]. Using phosphorus magnetic resonance spectroscopy studies, Kim et al. found a significant decrease in the NAD+/NADH ratio in both first-episode patients and chronic schizophrenia patients [53]. Chouinard et al. replicated this observation and extended it to siblings of schizophrenia patients with first-episode psychosis [54]. A decrease in the NAD+/NADH ratio indicates a shift in redox equilibrium towards a higher recovery potential. The reductive stress condition can lead to a paradoxical increase in

mitochondrial ROS production [55]. Thus, both oxidative stress and reductive stress can contribute to oxidative damage in schizophrenia.

4. Molecular Mechanisms of Oxidative Stress in the Pathogenesis of Schizophrenia

The redox imbalance can contribute to the development of schizophrenia at various levels and through various mechanisms. Diverse oxidative stress-associated molecular mechanisms (summarized in Figure 1) involved in the schizophrenia pathogenesis will be discussed in detail below.

4.1. Genetic Predisposition to Oxidative Stress in Schizophrenia. Polygenic deterministic predisposition to mental pathology is now proven. Schizophrenia, in particular, falls in the category of multifactorial diseases, whose development is a consequence of intergenic gene-environment impacts and interactions [56, 57]. Regarding schizophrenia, the significance of genetic factors is as high as up to 80%.

According to the literature data, some oxidative stress-related genetic polymorphisms are associated with schizophrenia (reviewed in [58]). First, GSH-related genes, such as glutathione synthesis genes and genes of glutathione-dependent antioxidant ferments, are associated with schizophrenia. In particular, the association with genes of glutamate-cysteine ligase subunits [59–61], being the main rate-limiting enzyme of glutathione synthesis, has been found. At the same time, no association with glutathione synthase genes has been observed in Danish and Swiss populations [61]. Besides, the association of single nucleotide polymorphisms (SNPs) of glutathione S-transferase genes with schizophrenia has been discovered [62–65], whereas no association of SNPs of glutathione peroxidase 1 genes has been revealed [66].

Second, the association of polymorphous variants of genes of antioxidant ferments with schizophrenia has been shown. The association of polymorphisms of manganese superoxide dismutase (Mn-SOD) genes has been demonstrated only for the Turkish sample, with negative reports from Korean, Japanese, and Caucasian samples [58]. In the Russian [67], Polish [68], Japanese [69], and Xhosa [70] populations, the association of Mn-SOD genes with tardive dyskinesia, which is a side effect of antipsychotic medications, has been observed. However, attempts to reproduce these observations in other populations failed [71–75]. No association of polymorphous variants of catalase genes with schizophrenia was found [76–78]. The association with genes of methionine sulfoxide reductase [79, 80], which regulates the activity of the central dopamine degradation ferment—catechol-O-methyl transferase [81], has been observed.

Third, the association of nitric oxide metabolism genes with schizophrenia has been revealed (reviewed in [82]). In particular, the association with genes of nitric oxide synthase 1 and nitric oxide synthase 1 adaptor protein has been shown [82].

Fourth, the association with mitochondrial genes was found [58]. Indeed, the association with the MTND4 gene (ND4 subunit of NADH-ubiquinone reductase) [83] and other genes of mitochondrial DNA was reported [84]. Besides, in nuclear DNA, the association of the DISC1 gene with schizophrenia was discovered [85–87]. This gene mostly expresses in mitochondria [87] and takes part in mitochondrial transport, neuronal axon, and dendrite outgrowth, as well as proliferation, differentiation, and migration of neuronal cells. However, the recent genome-wide association studies (GWASs) with large groups of patients and healthy donors failed to prove the mentioned associations with oxidative stress-related genetic polymorphisms [88–91]. It seems necessary to carry out GWASs with larger samples.

However, the most important result of the GWASs is proof of the polygenic nature of schizophrenia [88–91]. The association with numerous genes, each being a minor contributor to the disease's pathogenesis, has been revealed. According to the tentative estimate, the combination of 6,300 to 10,200 individual SNPs can provoke the development of schizophrenia [90]. Besides, many discovered associations can also be related to other mental diseases [92], which is indicative of some general mechanisms of the development of mental disorders. Also, the results of GWASs suggest that the disturbance of the regulation of gene expression is more significant for the etiopathogenesis of schizophrenia than changes in exonic regions of the genome (and, correspondingly, in protein sequences) because many associations were found beyond protein-coding regions of the genome [89, 90].

4.2. Gene Expression Dysregulation, Noncoding RNAs, Environmental Impact, and Oxidative Stress in Schizophrenia. Gene expression dysregulation in different tissues in schizophrenia is confirmed by numerous postmortem studies [93–96]. The transcription studies of the PsychENCODE consortium with the use of RNA-sequencing techniques and state-of-the-art analysis methods are indicative of complex spatiotemporal, sexual, cell-specific alterations in gene expression, splicing, and transcript isoforms levels in the brain of schizophrenia patients [97, 98]. It is noteworthy that the top pathways for diurnal rhythms in prefrontal cortex gene expression that were different in schizophrenia compared to healthy controls are oxidative phosphorylation and mitochondrial dysfunction [99]. The results of proteomic studies also confirm gene expression dysregulation in schizophrenia [100–102]. Prabakaran et al. showed that almost half of the proteins with altered expression were associated with oxidative stress responses and mitochondrial function [103]. Thus, genetic risk factors, along with gene expression dysregulation, form the basis of etiology and pathogenesis of schizophrenia and are associated with redox imbalance.

The available data on gene expression dysregulation in schizophrenia can be explained by dysregulation of transcriptional factors [96], particularly those participating in redox signaling. Indeed, SNPs of PDCD11 gene, coding the NF-κB-binding protein (NFBP) or the protein RRP5 homolog, have shown a statistically significant association with schizophrenia according to the GWAS results [91]. It is known that NFBP specifically binds to p50 and p65 subunits of nuclear factor kappa B (NF-κB) [104]. Besides, the association with TRIM8 (Tripartite Motif Containing 8) gene [91], coding E3 ubiquitin-protein ligase TRIM8, has been shown. E3 ubiquitin-protein ligase is known to potentiate TNFα-

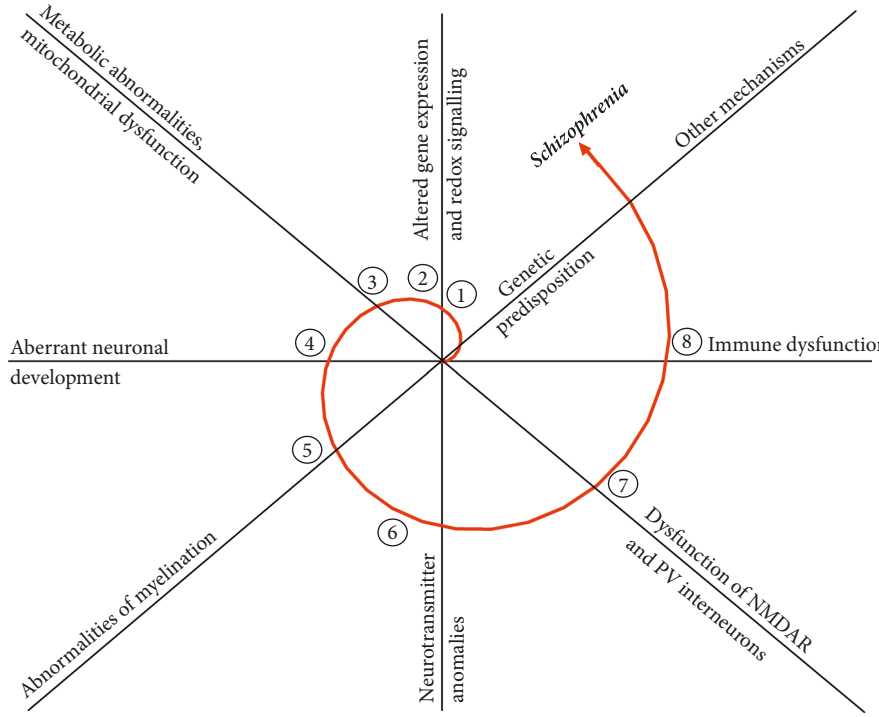

Figure 1: Oxidative stress-related mechanisms of schizophrenia pathogenesis. The involvement of each mechanism increases the likelihood of phenotypic realization and the manifestation of schizophrenia. The red line indicates the probability of developing schizophrenia; various causal mechanisms are plotted along the axes. All of these mechanisms can be involved both together and separately and during different critical periods. Various genetic causes (1) contribute to the increased susceptibility of individuals to oxidative stress. Genetic predisposition due to environmental impact at various critical periods contributes to redox imbalance, which leads to dysregulation of gene expression and redox signaling (2). These changes promote mitochondrial dysfunction and metabolic abnormalities (3). These processes, in turn, contribute to aberrant neuronal development (4) and abnormal myelination (5). These factors promote the neurotransmitter anomalies (6) and dysfunction of parvalbumin-positive interneurons (7). Immune dysfunction (8) also contributes to oxidative imbalance. All these mechanisms ultimately contribute to the manifestation of psychosis and the development of schizophrenia. Abbreviations: PV = parvalbumin; NMDAR = N-methyl-D-aspartate receptor.

and IL-1β-induced activation of NF-κB [105]. Shotgun proteomic analysis revealed that TRIM3 was upregulated in postmortem dorsolateral prefrontal cortex samples obtained from schizophrenia patients compared to its level in healthy individuals [106]. One of the missense mutations revealed in schizophrenia in TRIM genes is located in the catalytic RING domain. Therefore, this variant may alter ubiquitin ligase activity of this protein [106] and thus disturb NF-κB activation. Accordingly, some GWAS-identified SNPs associated with schizophrenia can affect NF-κB signaling. Taking into account that NF-κB participates in redox signaling, dysregulation of this factor can favor redox imbalance.

Gene expression dysregulation in schizophrenia is also associated with abnormalities in noncoding RNA-mediated regulation [107]. Noncoding RNAs (ncRNAs) are known to take part in redox regulation; moreover, ncRNAs affect ROS generation and ROS affect ncRNA transcription (reviewed in [108]). Among numerous ncRNAs dysregulated in schizophrenia [107], some are related to oxidative stress responses. Indeed, microRNA-30b expression was reduced [109], whereas the expression of microRNA-181a was increased [110] in brain samples of the prefrontal cortex of patients with schizophrenia. One of the target genes of microRNA-30b is CAT (encoding catalase), and the target gene of microRNA-181a is GPX1 (encoding glutathione peroxidase 1) [108]. In another example, the level of expression of microRNA-146a, which regulates the SOD2 gene (encoding superoxide dismutase 2) expression, was increased in peripheral blood mononuclear cells [111]. Besides, in the systematic review by Smigielski et al., dysregulation of microRNA-34a (mostly upregulation) and microRNA-132 (mixed pattern) was identified in different tissues of patients with schizophrenia [112]. These microRNAs take part in the regulation of nuclear factor erythroid 2-related factor 2 (Nrf2) that regulates the expression of numerous antioxidant proteins [113]. The increase in the level of expression of microRNA favors the silencing of the target gene. In contrast, the reduction of microRNA expression favors the increase of the target gene expression, although some exceptions are possible. Thus, the discovered abnormal level of microRNA expression in schizophrenia can globally affect the redox balance. However, it cannot be excluded that the change in the ncRNA level can also respond to a shift in redox balance [108].

Various environmental insults can contribute to gene expression dysregulation and redox imbalance in schizophrenia. Primarily, inflammation-mediated immune responses are also accompanied by abnormal gene expression, as well as by the oxidative stress. Indeed, animal model studies

confirm that lipopolysaccharide- (LPS-) induced maternal immune activation leads to an increase of expression profiles of oxidative stress-related genes and a decrease of expression profiles of critical neurodevelopmental genes in the fetal brain [114]. Other environmental insults associated with oxidative stress and schizophrenia are pre- and postnatal protein malnutrition [115] and hypoxia [116]. Besides, it was shown with the mouse model that prenatal hypovitaminosis D alters the gene expression of several biological pathways, including oxidative phosphorylation and redox balance [117]. Studies in the human population confirm the influence of neonatal vitamin D status on the risk of schizophrenia [118]. Early life adversity, for instance, maternal separation, favors oxidative stress in parvalbumin- (PV-) positive neurons [119] (more on the role of parvalbumin-expressing neurons is discussed further). Prenatal stress also supports oxidative stress and neuronal loss in the rat hippocampus [120]. At the same time, human epidemiological studies confirm that prenatal stress due to grief, famine, and major disasters has effects on vulnerability to schizophrenia [121]. It addition, it was shown that postweaning social isolation disturbs antioxidant defense mechanisms in cortical parvalbumin- (PV-) positive interneurons, supposedly mediated by downregulation of peroxisome proliferator-activated receptor-gamma coactivator 1-alpha (PGC-1α), which is a transcriptional coactivator and participates in the regulation of mitochondrial energy metabolism [122]. The oxidative stress after social isolation in rats was caused by increased expression of hypoxia-inducible factor-1α (HIF-1α) and redox-sensitive transcription factor c-fos. A treatment NOX inhibitor apocynin prevented histopathological and behavioral alterations [123].

Epigenetic mechanisms can serve a connecting link between environmental and genetic factors (reviewed in [112, 124, 125]). The following impairments of epigenetic regulation were found in schizophrenia: aberrant DNA methylation at approximately 100 loci, including genes regulating glutamatergic and GABAergic systems, genes of the stress response, and genes regulating the development of the nervous system, was shown; an alteration in the methylation status of different genes led to a change in symptoms of a disease; increased activity of DNA-methyltransferase 1 in interneurons of the hippocampus and striatum was found; increased levels of methyl group donor–S-adenosylmethionine was revealed in the prefrontal cortex of patients; increased level of homocysteine in blood serum was observed in acute schizophrenia; and histone modifications leading to dysregulation of different genes were found [112].

A considerable part of the epigenetic alterations in schizophrenia can be acquired through numerous environmental factors, and epigenetic changes can affect brain functions throughout the entire life. They can be inherited via epigenetic germline inheritance [91]. Besides, epigenetic modifications may be the molecular basis of the phenotypic heterogeneity of schizophrenia [125].

Thus, genetic susceptibility and gene expression dysregulation caused by abnormal regulation of transcriptional factors, noncoding RNAs, and epigenetic mechanisms favored by environmental insults form the basis of the prooxidant state underlying the pathogenesis of schizophrenia.

4.3. Altered Redox Regulation and Redox-Dependent Signaling in Schizophrenia. Maintenance of redox balance is essential for the cell and the entire organism. The redox regulation is controlled by different mechanisms [113] and is closely related to redox signaling [126]. Accurate redox regulation is necessary for cellular signaling because reactive oxygen and nitrogen species (ROS and RNS) participate in numerous signaling pathways [127, 128]. ROS or RNS in physiological concentrations take part in cell-signaling mechanisms, but in high levels, they favor oxidative stress [127, 128]. In the broad sense of the term, redox signaling is signaling processes accompanied by electron transfer reactions in which ROS and RNS or reductive equivalents are involved [129].

Oxidation and reduction of cysteine residues in transducing signal proteins are assumed to be the fundamental mechanisms by which ROS and RNS integrate into cellular signal transduction pathways [126]. Many signal events are accompanied by the generation of ROS serving as secondary messengers, thus leading to oxidative modifications of cysteine [127, 128]. Oxidative posttranslational modifications of cysteine residues in proteins under the effect of ROS include oxidation of cysteine thiols to sulfenic acid (SOH), sulfinic acid (SO_2H), and irreversible sulfonic acid (SO_3H) [130]. RNS interacts with cysteine thiols with the formation of reversible *S*-nitrosothiol [130]. The following reaction consists of intramolecular disulfide bond formation or conjugation with GSH (S-glutathionylation) [130]. S-glutathionylation can occur chemically or fermentatively via glutathione S-transferase (GST), peroxiredoxins, and occasionally glutaredoxins [130]. Reversing the oxidized cysteine residues in the sulfenic acid state occurs through the thioredoxin or GSH-dependent pathway [131]. Reversing the sulfinic acid state requires sulfiredoxin [131]. The reductive cellular environment (GSH) or catalysis by glutaredoxins remove protein-bound GSH and restore the protein cysteine [130]. Thus, glutathione is an essential molecule in signal transduction regulation. Oxidative stress and GSH deficiency, which are observed in schizophrenia [132, 133], can break the oxidation and reduction cycles of the cysteine residues, thereby disrupting redox signaling.

Many protein tyrosine phosphatases (PTPs) participating in signal cascades are direct targets of ROS and RNS [131]. Generation of ROS in response to, for example, receptor activation leads to inactivation of PTPs, thus leading to an increase of phosphorylation of numerous kinase targets, which is a necessary event for downstream signaling [131]. ROS inactivate not only PTPs but also dual-specificity phosphatases (for example, PTEN (phosphatase and tensin homolog deleted on chromosome 10)), low-molecular-weight PTPs, and cell cycle phosphatase [134]. Besides, ROS activate indirectly mitogen-activated protein kinases (MAPK), in particular, apoptosis signal-regulated kinase 1 (ASK1), through cysteine oxidation of thioredoxin, which directly inhibits its kinase activity [127]. The prooxidant state in schizophrenia can favor abnormal signaling.

Redox imbalance can also influence transcriptional factors. There are multiple ROS sensors and pathways involved in the redox-gene transcription regulation, in particular, Nrf2

(nuclear factor erythroid 2 related factor 2), NF-κB (nuclear factor kappa B), FoxO (forkhead box class O), AP-1 (activator protein 1), CREB (cAMP response element-binding protein), HSF1 (heat shock factor 1), TP53 (tumor protein p53), HIF-1 (hypoxia-inducible factor 1-alpha), SP1 (specificity protein 1), and other proteins [113].

The Nrf2-Keap1 (Kelch-like ECH-associated protein 1) pathway is one of the primary regulators of responses to oxidative stress [113]. Under normal conditions, Nrf2 is inactivated by Keap1-mediated ubiquitination and subsequent proteasomal degradation. Sulfhydryl groups of Keap1 act as ROS sensors, and their oxidation in the presence of ROS leads to nuclear translocation of Nrf2 and increased expression of antioxidant genes [113]. Transcription factor Nrf2 has shown the ability, both in *in vitro* and in *in vivo* experiments, to activate a series of vitagenes including (Hsp) Hsp32, Hsp70, and thioredoxin, conferring protection against oxidative stress, and contributing to establish a cytoprotective state in inflammation and neurodegenerative disorders [135, 136]. In the normal state, these pathways are considered as hormetic mechanisms of adaptive cellular stress response [137, 138]. In schizophrenia patients under conditions of systemic oxidative stress, the decreased Nrf2 expression in peripheral blood lymphocytes was discovered [139]. Besides, expressions of Nrf2 and Keap1 proteins in the parietal cortex from brain samples of schizophrenia patients were lower than those of healthy individuals [140].

NF-κB takes part not only in the regulation of genes of immune response, development, proliferation, and apoptosis but also in redox regulation [141]. ROS promote dissociation of inhibitory proteins and activation of NF-κB [113]. The increases in mRNA levels for NF-κB family members, NF-κB activation receptors, kinases, and inhibitor protein (IκBα) were found in the prefrontal cortex of schizophrenia patients [142].

The forkhead box class O (FoxO) family of transcription factors are critical regulators of the expression of genes involved in cellular oxidative stress response, ROS detoxification, DNA repair, energy homeostasis, and glucose metabolism (reviewed in [143]). FoxO transcription factors regulate numerous genes coding for intra- and extracellular antioxidant proteins such as Mn-SOD and Cu,Zn-SOD, peroxiredoxin-3 and peroxiredoxin-5, mitochondrial thioredoxin (Trx2) and mitochondrial thioredoxin reductase, glutathione peroxidase 1, and selenoprotein P [143]. Several protein kinases such as protein kinase B (Akt), extracellular signal-regulated kinase (ERK), p38 mitogen-activated protein kinases (p38MAPK), and c-Jun N-terminal kinase (JNK) phosphorylate FoxO transcription factors in response to elevated levels of ROS and upon exposure of cells to stressful stimuli [143]. Moreover, the effects are different depending on protein kinases; for instance, phosphorylation by Akt usually inactivates FoxO1a, FoxO3a, FoxO4, and FoxO6 proteins, whereas JNK activates FoxO4 and inactivates FoxO3a [143]. It was shown in the mouse model that behavioral stress can activate FoxO3a in the cerebral cortex through inactivation of Akt and is accompanied by activation of glycogen synthase kinase-3β (GSK3β) [144]. It was shown that the expression and activity of AKT1 were reduced in lymphocytes and in the frontal cortex and hippocampus of individuals with schizophrenia [145]. In another study, the reduction of expression of Akt and other Akt-mTOR signaling pathway proteins in the dorsolateral prefrontal cortex in schizophrenia was demonstrated [146]. The expression of JNK1 and JNK2 was decreased in the anterior cingulate cortex of schizophrenia patients, while the expression of ERK1/2 or p38 was unchanged [147]. Besides, different antipsychotics and psychoactive substances affect dopamine-associated behaviors through modulation of the Akt/GSK3β signaling pathway [148]. It is also known that clozapine can regulate the activity of the Akt/FoxO3a signaling pathway via phosphorylation of Akt and FoxO3a [149]. Thus, alteration of the activity of protein kinases, in particular, as a result of antipsychotic treatment, can modulate FoxO activities. This opens new ways of using inhibitors of protein kinases in the modulation of redox-regulated transcription factors.

Another mechanism of regulation of FoxO activities consists of acetylation and ubiquitination of lysine residues. Histone acetyltransferases and deacetylases catalyze reversible lysine acetylation. The ubiquitination of FoxOs proceeds by ubiquitin-protein ligases and promotes proteasomal degradation of FoxOs. Oxidative stress caused by increased intracellular levels of ROS and RNS, particularly H_2O_2, has been identified as a critical mediator of the state of acetylation and ubiquitination of FoxOs [143]. Indeed, exogenous H_2O_2 induces the formation of heterodimers between coactivators (p300 and CBP (CREB-binding protein) acetyltransferases) and FoxO4 through intermolecular disulfide bridges between redox-sensitive cysteine residues and stimulates acetylation of FoxO4 [150]. Brunet et al. have shown that NAD-dependent deacetylase sirtuin-1 (SIRT1) is a crucial regulator of the activity of FoxOs [151]. The activity of SIRT1 depends on the redox state of a cell, is regulated by the NAD+/NADH ratio, and is activated at a restriction of reduction equivalents [143]. SIRT1 is associated with the depression behavior in the mouse model [152] and with depressive symptoms in schizophrenia patients [153]. It is noticeable that there exist medicines increasing SIRT1 activity, for example, resveratrol [152] or salvianolic acid B [154], which can promote correction of redox imbalance through an increase in activity of Nrf2 [154] and, likely, FoxO, as well as through a decrease in the activity of NF-κB. However, an increase in the activity of SIRT1 in the nucleus accumbens may favor anxiety- and depression-like behaviors [152].

The transcriptional coactivator PGC-1α (peroxisome proliferator-activated receptor-gamma coactivator 1α) is an upstream regulator of energy metabolism and mitochondrial biogenesis. PGC-1α has been shown to regulate FoxO transcription factor activity in various cells [143]. GWASs have identified that PGC-1α is one of the candidate genes for schizophrenia [155]. PGC-1α knockout mice presented some characteristic features of schizophrenia [155]. Besides, PGC-1α gene deletion delayed maturation of PV interneurons, including their perineuronal nets [155]. As stated above, postweaning social isolation leads to the downregulation of PGC-1α in mice [122]. PGC-1α-dependent transcripts in postmortem cortical tissue from schizophrenia patients were

reduced and accompanied by a decrease in expression of Nrf1 as well as PV [156]. The data presented relate redox imbalance and altered redox regulation to the pathology of PV interneurons [156] (more on PV neuron pathology will be discussed below).

Thus, there are some data on the altered redox regulation and signaling in schizophrenia, which is related to prooxidant processes, glutathione deficiency, and impaired expression of transcriptional factors and multiple ROS sensors.

4.4. Effect of Oxidative Stress on Neuronal Development. The dysontogenetic hypothesis of schizophrenia was first formulated more than three decades ago [157, 158]. Today, it is proved by a wide range of studies whose results are indicative of neuroanatomical and cytoarchitecture brain disorders, such as disorders in the structure of synapsis and mediator systems, decrease of oligodendrocytes, and reduction of myelination. Many factors affecting the pre- and postnatal periods of development are considered as causes for these disorders. The prenatal causes include in utero exposure to viral and bacterial infections during pregnancy, maternal chronic diseases, severe nutritional disturbances of a mother during pregnancy, obstetric complications, and influence of alcohol, narcotic substances, and pharmaceutical products on the fetus. The main postnatal factors are social deprivation and psychogenic stress at an early age [159, 160].

Several studies are confirming the relation of schizophrenia to such viral diseases as influenza, herpes (Herpes Simplex Virus Type 2 (HSV-2)), and rubella [161]. The response of the maternal organism to an infectious disease leads to the activation of cytokines, which, in turn, gives rise to the risk of psychotic disorder. Buka et al. have found that the increased level of TNFα in mothers with infectious disease in the third trimester of pregnancy leads to an eightfold increase in the risk of psychotic disorder in the child as an adult [162]. Maternal TNFα penetrates through the placental barrier into fetal CNS [163] and leads to ROS generation through activation of NADPH oxidase [164]. The studies in animals show that cytokines penetrating through the fetal blood-brain barrier (BBB) significantly affect the survival and differentiation of neurons [165]. The paper by Simões et al. reports a significant increase in IL-1β, IL-6, and TNF$\alpha\beta$ levels in the offspring brain in response to maternal cytokines [166]. The inflammatory response leads to an increase in ROS generation by endothelial cells, and, consequently, to disruption of BBB permeability [167]. In addition to the disruption of BBB and placental barrier permeability, cytokines in the brain regulate the expression of major histocompatibility complex I (MHC I), coordinating synaptic pruning [168, 169]. Postmortem examination of the brain in schizophrenia patients shows that synaptic proteins interact with the complement system and other immunological pathways, causing changes in glial structures and synapse elimination [170].

Activation of cytokines in the maternal organism not only can be caused by the effect of an infectious agent but also can be induced by the action of ethanol on the fetus. The studies of González-Quintela et al. have demonstrated that the expression of IL-1α, IL-6, and TNFα can increase after single-dose administration of 60 g ethanol [171]. It has also been shown that chronic alcohol consumption increases the transcription of TNFα, IL-1β, and toll-like receptor 4 (TLR4) in the brain cortex and hypothalamus [172]. In the experiment with rats, at the intraperitoneal injection of ethanol in the concentration of 4 g/kg, a considerable increase of IL-6 expression in the hippocampus, paraventricular nucleus of the hypothalamus, and tonsil was observed [173]. Ethanol significantly affects neural membranes and synaptic contacts between developing neurons. In a fetus of an alcoholic mother at 9–12 weeks of pregnancy, the slower development of synapses, the shorter length of the postsynaptic density, and the smaller perimeter and area of the presynaptic terminal were observed. Ethanol-induced oxidative modification of proteins and lipids of cell membranes can be one of the mechanisms of the toxic effect of ethanol at neurogenesis [174].

At the chronic effect of ethanol, the amount of ROS and NO in the brain increases through induction of NADPH oxidase and NO synthase under the exposure to glial cytochrome P450-2E1 (CYP2E1) [175, 176]. In the study with mouse models, it was shown that an ethanol-induced disturbance of the redox homeostasis leads to activation of microglia by the M1 phenotype [177, 178]. Activation by the M1 phenotype leads to the secretion of proinflammatory cytokines and chemokines and ROS production.

The increased synthesis of proinflammatory cytokines is observed in obese pregnant women. It was revealed that the body mass index correlates directly with the concentration of proinflammatory cytokines in the mother and activation of proinflammatory pathways in the placenta [179]. In animal models, it was shown that obesity during pregnancy is related to systemic and placental inflammation, oxidative stress, and antioxidant deficit in the bodies of the mother and the fetus [180]. Edlow et al. have demonstrated that fetal expression of apolipoprotein D (APOD) gene was nine times higher in the case of an obese mother [181]. The increased APOD expression, in turn, was found in schizophrenia patients [182].

In addition to obesity, gestational diabetes and pregestational diabetes are possible factors of increased ROS generation [183, 184]. Under conditions of excess glucose in the mother's blood, the increased production of the superoxide anion radical ($O_2^{-\bullet}$) is observed [185]. Consequently, the disturbance of glucose exchange in the prenatal period leads to changes in the structure and functions of the plasmatic membrane of neurons and the receptor apparatus of neurotransmitters, thus increasing the risk of schizophrenia at adult age. The decreased placental levels of arachidonic acid (AA) and docosahexaenoic acid (DHA) were found in mothers and children with gestational diabetes [186]. These factors have a maximally unfavorable effect on the development of the child's brain: polyunsaturated fatty acids take part in synaptogenesis and synthesis of neuromodulators and prevent the synthesis of signal molecules associated with Alzheimer's disease and schizophrenia [187]. In postmortem studies, it was shown that schizophrenia patients had decreased AA and DHA levels in the frontal cortex [188]. The reduced level of polyunsaturated fatty acids is also assigned to the disruption of synaptic transmission of dopamine and GABA, which plays an essential role in the pathogenesis of schizophrenia [189, 190].

Recent studies demonstrate the relationship between the psychosocial stress in the postnatal period and the oxidative stress [191, 192]. It was assumed that the disturbance of the regulation of the hypothalamus-pituitary-adrenal axis could mediate the relationship between childhood trauma and psychosis. Colaianna et al. demonstrate that psychosocial stress leads to the increased ROS generation by NADPH oxidase 2 (NOX2) in the hypothalamus [193]. The oxidative stress in the hypothalamus disturbs the functions of the hypothalamus-pituitary-adrenal axis, contributing to psychosis development [194, 195]. Disorder in the development of the nervous system assumes that the prolonged exposure to stressors can cause the increased release of glucocorticoids, which stimulate the dopaminergic activity, thus increasing the risk of psychosis [196]. As is known, the increased dopamine synthesis is related to symptom severity at the prodromal stage. Besides, dopamine hyperactivation appears in schizophrenia patients in the acute stage and after psychological stress [196]. Glucocorticoid neurotoxicity favors the loss in hippocampus volume, which is observed in schizophrenia patients even at early stages [197].

Many investigators indicate that disorders of the prenatal brain development are related to the activation of oxidative stress. The activation of maternal immune reactions leads to the increased synthesis of cytokines and ROS, thus mediating inflammatory responses in the fetal brain. In addition to inflammatory responses, ROS affects the cell membranes of neurons, leading to the disturbance of the neurotransmission of dopamine, glutamate, and GABA, which are the main neuromediators involved in the pathogenesis of schizophrenia. Thus, maternal infectious diseases, obesity, diabetes, alcohol ingestion, and other factors lead to the development of oxidative stress in the fetal brain, which can be a predictor of schizophrenia development at adult age, in which the process of synaptic pruning in adolescence may be the starting point.

4.5. Metabolic Abnormalities and Mitochondrial Dysfunction. Mitochondria are not only the leading energy supplier of the cell but are also actively involved in other critical physiological processes, including redox signaling, calcium homeostasis, cellular differentiation, and apoptotic cell death. The role of mitochondria is especially crucial for the development and functioning of the nervous system. Mitochondria are involved in the regulation of neuronal differentiation, neuroplasticity, axogenesis, dendritogenesis, and the release of neurotransmitters by generating adenosine triphosphate (ATP) and regulating subcellular calcium concentration and redox homeostasis [198]. Mitochondrial dysfunction and decreased ATP production lead to the disruption of the transmembrane gradient and intracellular calcium buffering as well as enhancing ROS production [199].

Ample evidence has been accumulated, indicating a multifaceted mitochondrial dysfunction in schizophrenia (reviewed in [198, 200, 201]). Primarily, morphological and functional abnormalities of mitochondria in schizophrenia were detected. An electron microscopic study of the postmortem brain tissues of patients with schizophrenia showed a significant decrease in the number and density of mitochondria of oligodendroglial cells in the prefrontal cortex and caudate nucleus [202]. Besides, the functional activities of complexes IV and I+III of the mitochondrial electron transport chain were reduced in some areas of postmortem cortex tissues in patients with schizophrenia [203]. It is known that antipsychotic treatment reduces the activity of complex I in mitochondria [199]. In vivo imaging studies also confirm the functional changes in mitochondria in schizophrenia. The decreased metabolism in the frontal lobe, which was manifested by a decrease in creatine kinase, intracellular pH, and the concentration of macroergic compounds, was found in patients with schizophrenia [204]. Besides, increased ATP levels in white matter and decreased ATP levels in gray matter were found in the frontotemporal-striatal region in first-episode schizophrenia patients [205]. Metabolomics studies also confirmed metabolic abnormalities in schizophrenia [206].

These changes may be associated with impaired gene expression. Indeed, the decreased expression of numerous mitochondria-related genes (encoding, for example, NADH-ubiquinone oxidoreductase core subunits V1, V2, and S1 and cytochrome c oxidase) was observed in postmortem brain tissues of patients with schizophrenia in smaller-scale studies [201]. As stated above, transcriptomic and proteomic studies in large samples also confirmed the impaired expression of mitochondrial genes in brain tissues [98, 103, 207]. Remarkably, altered transcripts evaluated in parvalbumin- (PV-) containing interneurons were enriched for pathways involved in mitochondrial function [207]. A meta-analysis of microarray studies assessing gene coexpression network modules in the prefrontal cortex of schizophrenia patients showed that oxidative phosphorylation, myelination, and immune function are some of the most downregulated enriched modules [208]. A recent meta-analysis considering the gene expression, transcript isoform expression, local splicing, and coexpression network modules identified cell-specific dysregulation, including protein-coding, noncoding, splicing, and isoform-level changes in brain samples from individuals with schizophrenia, autism spectrum disorder, and bipolar disorder [98]. Among the confirmed differentially expressed genes, transcripts, and splicing isoforms in patients with schizophrenia, mitochondrial genes were also found [98]. The downregulation of coexpressed gene modules associated with mitochondria in a larger sample of schizophrenia patients was also shown [209].

Evidence also includes the genetic association of mitochondrial genes with schizophrenia. Among the 350 genes within 108 schizophrenia loci identified by GWAS [91], 22 are related to mitochondrial function [201]. For instance, the association of schizophrenia with the USMG5 gene encoding a small subunit of the mitochondrial ATP synthase (complex V), as well as with the SFXN2 gene encoding sideroflexin-2, which is involved in iron metabolism in mitochondria, has been shown [91].

Various animal models have shown that mitochondrial dysfunction leads to neurobehavioral abnormalities (reviewed in [201]). Ablation of the transcriptional coactivator PGC-1α reduced the expression of the Ca-binding protein parvalbumin (PV) in the GABAergic interneurons and also disrupted evoked synaptic responses in mice [210]. As stated above,

PGC-1α is the crucial regulator of mitochondrial biogenesis, including through the regulation of the activity of redox regulating transcription factors FoxOs. Thus, the impaired activity of PGC-1α is associated with altered redox regulation and mitochondrial dysfunction, which leads to the pathology of PV interneurons. Besides, the ablation of the cox10 gene in PV interneurons of mice resulted in progressive loss of cytochrome oxidase, which is a terminal enzyme of the electron transfer chain, and was accompanied by an excitation/inhibition imbalance, as well as behavioral alterations similar to schizophrenia [211]. Knockdown of Disrupted-In-Schizophrenia-1 (DISC1) or expression of a dominant-negative C-terminal truncated DISC1 led to a decrease in glucose transporter 4, oxidative phosphorylation, and glycolysis as well as diminished lactate production in mouse astrocytes [212]. These changes were accompanied by altered affective behavior and impaired spatial memory, while lactate treatment rescued these anomalies [212]. Hemizygous deletions of 22q11DS genes were accompanied by haploinsufficiency of mitochondrial large ribosomal subunit protein 40 and led to dysregulation of short-term potentiation via impaired calcium homeostasis in mitochondria [213]. The knockdown of Txnrd2, a 22q11 gene essential for ROS detoxification in brain mitochondria, led to the disruption of the axon and dendrite growth and violated mitochondrial and synaptic integrity in projection neurons; however, antioxidant treatment eliminated these alterations [214]. Therefore, Txnrd2-mediated oxidative stress led to cortical underconnectivity impairment and cognitive deficits [214]. Furthermore, the transfer of isolated mitochondria in induced pluripotent stem cells leads to increased mitochondrial function and improved differentiation into glutamatergic neurons [215]. Injection of isolated mitochondria into the cerebral cortex of adolescent rats in the maternal immune activation model prevents mitochondrial deficiency and behavioral abnormalities at adulthood [215]. These observations link mitochondrial dysfunction, immune disturbances, and impaired neuronal development.

Thus, mitochondrial dysfunction is accompanied by oxidative stress, functional anomalies in neuronal cells, and behavioral alterations and is a prerequisite for the development of schizophrenia.

4.6. Oxidative Stress and Abnormal Myelination. Myelination of the human brain proceeds actively in the postnatal period, but the myelin content in the brain peaks at middle age, which coincides in time with the massive remodeling of synaptic contacts in the cerebral cortex [216]. The excess prenatal formation of axons and considerable reduction of axon amount in the postnatal period [217] are compensated by the vast increase of subcortical myelination of residual axons, which are practically absent at birth but grow to up to 25% of the adult human brain volume [218]. These processes reflect the brain formation with gain in experience and optimization of information processes through myelination [219].

Myelin is produced by mature oligodendrocytes (OLs) formed from oligodendrocyte precursor cells (OPCs) in the infantile and adult brains. Neuronal activity can instruct OPCs to divide and mature and stimulate myelin sheath production by OLs [220], leading to increased myelination and improved behavioral performance [221]. Cortical-subcortical white matter (WM) pathways achieve maturation peaks at the age of 23 to 39. This data indicate that WM maturation in frontal regions continues at the time most characteristic of schizophrenia manifestation [222].

Several pathways regulate OL differentiation and myelination in the CNS [223]. The phosphatidylinositol-3-phosphate kinase (PI3K)/Akt/mTOR pathway controls the initiation of myelination in the CNS through mTORC1 signaling [224]. In conjunction, glycogen synthase kinase 3β (GSK3β) signaling regulates OL differentiation [225]. Moreover, extracellular signal-regulated kinases-1 and -2 (ERK1/2), the downstream mediators of the mitogen-activated protein kinase (MAPK) pathway, regulate myelin growth and maintain the integrity of myelinated axons [226]. These MEK/ERK1/2-MAPK-mediated functions are mostly independent of mTORC1 [227].

Oligodendrocytes can be damaged at the stage of their differentiation from precursors and at the stage of a mature cell. For example, 15-20% of changes in the redox balance in the OPCs, which are extremely sensitive to oxidative stress, may already affect signaling pathways [228]. Factors that cause high vulnerability to oxidative stress include exceptionally high amounts of ROS (six times higher) in OPCs and OLs, three times lower glutathione concentration, and 20-fold higher free-iron levels as compared with astrocytes [229]. These processes promote hypomyelination in the prefrontal cortex and hippocampus.

The decreased volume of cortical grey matter at schizophrenia cannot be fully explained by the loss of synaptic contacts or changes in the microcirculatory bloodstream. Uranova et al. have performed the electron-microscope morphometric study of myelinated fibers in the prefrontal cortex, caudatum, and hippocampus of schizophrenia patients [230]. Local destruction of myelin sheaths and atrophy of axons have been revealed in all the examined brain structures. Besides, the decreased density of WM oligodendrocytes in the frontal cortex was also shown [231]. It is known that uncompensated loss of myelin at schizophrenia forms immediately after the first episode and increases in the course of disease [232, 233]. The OPC dysfunction coincides with the relatively late start of myelination of the prefrontal cortex, causing hypomyelination and distorting connectivity in this part of the brain. It is also assumed that the disturbance of OPCs can affect hypomyelination in the hippocampus; this is confirmed by the results obtained with Gclm-KO mice [234] and the results of postmortem studies of patients with schizophrenia [235, 236].

Unlike astrocytes, which have powerful antioxidant defense mechanisms [237], oligodendrocytes are sensitive to hypoxia and oxidative stress, especially during the terminal phase of differentiation and formation of myelin sheaths. During CNS maturation, the resistance of OLs to oxidative damage increases due to the elevated glutathione levels [238], the transition from the oxidative to the glycolytic mechanism [239], the rise of the longevity of myelin proteins [240], and metabolic support of axons by myelin sheathes [241].

In the context of glutathione deficiency, an increase in the ROS level resulting from a high metabolic rate in the

mitochondria of OLs leads to hyperstimulation of the AMP-activated protein kinase (AMPK), which activates the tuberous sclerosis 1/2 complex. This complex prevents the activation of the rapamycin (mTOR)-P70S6K pathway, which leads to OPC proliferation arrest, apoptosis, and hypomyelination [242].

The death of mature oligodendrocytes also promotes neuroinflammation and oxidative stress stimulation. As mentioned above, OLs are rich in iron ions. Iron released by oligodendrocytes is accumulated in macrophages and microglia, which can release iron into the intercellular space, disturbing the integrity of axons [243]. These processes can also stimulate neuronal cell death through ferroptosis [244]. Thus, the wavelike release of iron stimulates the processes of neurodegeneration together with inflammation [245].

Thus, abnormal myelination and dysfunction of the white and gray matter of the brain have been identified in schizophrenia. The molecular mechanisms underlying these changes remain unclear, but undoubtedly oxidative stress also contributes to these processes.

4.7. Immune Dysfunction and Oxidative Stress. A growing body of evidence suggests that an "immunooxidative" pathway, including oxidative stress, mitochondrial dysfunction, neuroinflammation, and cell-mediated immune response may contribute to disruptions in brain activity in schizophrenia [53]. Inflammation and increased oxidative stress could constitute a common pathway between early genetic and environmental factors (such as prenatal infections, obstetric complications, hypoxia, or stress during pregnancy) and psychosis [246, 247]. In the immune system, ROS and H_2O_2 are not the only products of peripheral and tissue macrophages. Still, they have a physiological role in signaling cascades that controls activation, migration, and differentiation of immune cells [248].

4.7.1. Microglia and Oxidative Stress. An enormous array of sensitive receptors in microglia control the activation status of these immunological cells [249]. Signaling pathways of these receptors are associated with NADPH oxidase (NOX) expression and ROS generation. Thus, activated microglia and astrocytes can become sources of oxidants by activating NOX enzyme cascades; producing interleukins; and releasing glutamate, quinolinic, and arachidonic acid, which may all contribute to neuron damage [131]. Excessive activation of microglia can lead to the neuroinflammation that accompanies many forms of acute or chronic neuropathology, including schizophrenia.

Microglia, as the resident immune macrophages of the CNS, express high levels of superoxide-producing NADPH oxidases (NOX). The primary function of the members of the NOX family is to generate reactive oxygen species (ROS) or H_2O_2 that are important in maintaining cell homeostasis through the regulation of crucial redox-dependent pathways [131]. Overproduction of oxidants leads to an excess signal in strength or in time, both of which have pathological effects and cause oxidative stress. In pathological conditions, ROS production by microglia is considered a major cause of neuronal dysfunction [250] through direct oxidative damage to neuronal macromolecules [251] or derangement of neuronal redox signaling circuits.

Initial molecular signaling pathways underlying microglial activation includes activation of toll-like receptors (TLRs), cytokine receptors, complement receptor 3, CD36 receptors, ionotropic and metabotropic purinergic receptors, and neurotransmitter receptors [248]. Microglia express most TLRs, and their expression levels are altered by microglial activation [252]. Signaling through TLRs is essential for priming (hyperresponsiveness) of NOX2 in several ways.

TLR signaling activates IL-1 receptor-associated kinase 4 (IRAK4) in the MyD88-dependent TLR signaling axis. IRAK4 primes NOX and phosphorylates p47phox on several residues to activate the oxidase directly [251]. Microglia cells can have two phenotypes: the proinflammatory classic M1 phenotype, which is associated with anti-inflammatory cytokine production, antigen-presenting properties, and ROS production, and the M2 anti-inflammatory alternative phenotype possessing anti-inflammatory and immunoregulatory activity [253]. Treatment with LPS combined with the proinflammatory cytokine interferon-γ (IFN-γ) is frequently used to induce and study the M1 type of microglial activation in vitro. These factors activate toll-like receptor 4 (TLR4, also called CD14) and the IFN-γ receptor and induce the recruitment of cytosolic phox proteins to the membrane by the phosphorylation of p47phox (neutrophil cytosolic factor 1, NCF1) [254].

TLR engagement also leads to the activation of the GTP/GDP exchange factor VAV, which mediates nucleotide exchange on Rac1, a catalytic subunit of the NOX complex. In addition, Rac1 activated downstream of TLRs also activates p38MAPK (p38 mitogen-activated protein kinases), which may participate in the mobilization of p47phox [255].

Also, it has been found that TLRs depend on NOX activity. NOX-derived ROS directly regulate the partitioning of TLRs to lipid rafts in the membrane [256] or promote the assembly of signaling complexes, which are required for efficient signaling [257].

LPS stimulation of NOX2 activity in microglia may occur through binding with complement receptor 3 (CR3, MAC1, also called CD11b/CD18) [258]. CR3 acts as a phagocytic receptor for C3b/iC3b-opsonized targets including endogenous targets such as synapses [259] and neurites [260]. CR3 ligation leads to direct NOX2 activation as well as through tyrosine-based activation of receptors DAP12 (TYRO protein tyrosine kinase-binding protein) or FcγRs (Fc-gamma receptors) [261].

Ionotropic P2X and metabotropic P2Y purinergic receptors are important for the regulation of the microglial actin cytoskeleton [262]. Stimulation of the ionotropic P2X7 receptor by ATP, together with an increase in intracellular calcium, induces ROS production and release in microglia. Increased NOX activity is implemented through ERK1/2-dependent (mitogen-activated protein kinase 3) [263], p38MAPK-dependent, and PI3K-dependent (phosphoinositide 3-kinase) pathways [264].

Microglia express a large number of neurotransmitter receptors. In turn, disruptions of the neurotransmitter environment significantly affect the activation state of microglia

and neuronal integrity. NOX activation could be induced by agonists of glutamate metabotropic (mGlu3 and group III), GABAA, and purinergic P2X7 or mGlu5 receptors on the rodent BV2 microglial cell line [263]. A complementary study revealed that activation of microglia in vitro, following NMDA receptor stimulation, was accompanied by secretion of ROS that was toxic to neurons [265].

Furthermore, as in the case of TLR signaling or CR3 ligation in macrophages, NOX2-derived oxidants are implicated in the redox regulation of signaling pathways, in which ROS and H_2O_2 act as second messengers in cytokine responses [266]. H_2O_2 activates mitogen-activated protein kinase (MAPK) cascades, partly through oxidation of catalytic cysteines on MAPK-inactivating phosphatases [267], and induces nuclear factor kappa B (NF-κB) translocation from the cytosol to the nucleus [268]. The initiation of NF-κB-dependent gene transcription promotes the production of proinflammatory mediators. These include cell adhesion molecules ICAM and VCAM, ROS-producing enzymes like iNOS and NOX2, and cytokines IL-6, IL-8, and, importantly, TNF [269, 270]. Taking into account that TNF and ROS may induce NF-κB-dependent gene transcription, this potentially results in an amplification loop of TNF and ROS signaling [269].

Additionally, the release of cytokines or gliotransmitters by activated astroglia and microglia controls BBB permeability in brain pathologies associated with excessive angiogenesis, cerebrovascular remodeling, and blood-brain barrier-mediated neuroinflammation also observed in schizophrenia [253].

4.7.2. Cytokines and Oxidative Stress. The role of cytokines in the pathogenesis of schizophrenia has been demonstrated in many works [249, 271]. The study of the relationship between the level of cytokines and oxidative markers in schizophrenia using the Bradford Hill criteria to establish a causal relationship confirmed their pathogenic role [272]. A high level of proinflammatory cytokines is associated with a high probability of developing schizophrenia among people at risk compared with people at risk but with a low content of proinflammatory cytokines. According to many studies, the severity of clinical symptoms correlates with the level of cytokines [43].

The study of proinflammatory and oxidative markers in patients with schizophrenia revealed increased levels of proinflammatory cytokines (i.e., IL-1-β, IL-6, IL-12, IFN-γ, TNF-alpha, tumor growth factor-β) and reduced levels of antioxidants (total antioxidant status, catalase, plasma nitrites, and superoxide dismutase) in patients with the first episode of schizophrenia [273].

There are several suggested ways by which proinflammatory cytokines can contribute to schizophrenia development [272]:

(1) Inflammation-associated activation of IDO (indolamine 2,3-dioxygenase) enhancing the production of kynurenine metabolites 3-hydroxykynurenine and 3-hydroxyanthranilic acid, both of which are potent generators of radical oxygen species [274]. Thus, it can be proposed that inflammation contributes to neurodegeneration by converting oxidative stress to excitotoxic stress in the context of IDO activation [275]. Kynurenic acid also contributes to the hyperactivation of glutamatergic neurotransmission, which is considered one of the mechanisms for the development of positive symptoms in schizophrenia by itself [273]

(2) Proinflammatory cytokines activate microglia, promoting the development of neuroinflammation and oxidative stress [276]. There was a significant increase in the levels of TNFα, IL-1β, and IL-6 and a decrease in the levels of IFN-γ in patients with schizophrenia [249]. Lipid peroxides were elevated in serum, while total sulfhydryl levels were decreased. Superoxide dismutase and glutathione peroxidase were reduced, while the activities of catalase, glutathione reductase, and myeloperoxidase were found to be elevated [275]. Activated microglia are a source of oxidants, which lead to the development of oxidative stress and damage to the membranes of neurons, as described above

(3) Proinflammatory cytokines may disturb neurodevelopment (particularly when there is a prenatal inflammation), increasing the risk of psychosis [277]. Activation of the IL-6/Nox2 pathway in schizophrenia leads to the loss of the GABAergic phenotype of PV interneurons and decreased inhibitory activity in the prefrontal cortex [53]

(4) Inflammatory cytokines can affect the synthesis of monoamine neurotransmitters; increase reuptake of dopamine, serotonin, and norepinephrine; and influence neurotransmitters' release [251]

Thus, the generation of prooxidants, on the one hand, is an element of the signaling pathways in the immune system. On the other hand, stimulation of the generation of ROS and H_2O_2 helps to maintain the immune response; however, in overexpression, it can lead to neuroinflammation. In combination with an insufficient antioxidant system, this leads to damage to the membranes of neurons and glia and a violation of their functions.

This is confirmed by the results of the study using a 31P-MRS-based method to directly quantify NAD+ and NADH concentrations in the brain at ultra-high-field MR scanners. This study confirmed a significant reduction in the NAD+/NADH ratio in chronically ill schizophrenia patients compared to a healthy control group and in first-episode schizophrenia patients compared to both a first-episode bipolar disorder patient group and a healthy control group. These findings provide evidence for redox imbalance in the brain in all phases of schizophrenia, potentially reflecting oxidative stress [278].

The development of oxidative stress induces the antioxidant system response. Activated microglia and macrophages release glutamate [274] in exchange for cysteine with an extracellular transporter (xc-transporter) [279]. During inflammation, activation of the xc-system functions as an endogenous antioxidant response since the influx of cysteine helps preserve the redox status of the cell [280], consequently

increasing extracellular glutamate [35]. Several studies highlight the association between glutamate stimulation of microglia and decreased NOX activity by mGlu receptor activation [248].

Nevertheless, there is a decrease of canonical antioxidant systems, including peroxidases, oxidoreductases, oxidases, and dismutases, confirmed by multiple studies in schizophrenia [281, 282]. Recently, immunoglobulins with noncanonical properties have been discovered [283] that catalyze various reactions, including those similar to antioxidant enzymes. IgG antibodies with catalase-like activity in schizophrenia [284], IgG with peroxidase and oxidoreductase activities in healthy humans [285, 286], and IgG with SOD-like activity in patients with multiple sclerosis [287] were revealed. It can be assumed that such catalytic antibodies are involved in limiting oxidative damage at the inflammation areas, since antibodies can accumulate there. At the whole-organism level, catalytic antibodies with "antioxidant" properties can compensate for the deficiency of the canonical antioxidant systems in schizophrenia. Thus, human IgGs could probably also play a significant role in protecting humans from OS and toxic compounds.

4.8. ROS-Dependent Regulation of Neurotransmission and Changes Characteristic of Schizophrenia. Synaptic plasticity is characterized by the ability of the synapses to respond to stimulation and is determined by the change in the number of neurotransmitters or in the cell's ability to respond to neurotransmitters [288]. Controlled ROS production provides the optimal redox state for the activation of transductional pathways involved in synaptic changes. High ROS concentrations reportedly diminish synaptic signaling and brain plasticity mechanisms [289]. Intracellular calcium (Ca^{2+}) is also one of the critical factors of synaptic plasticity in excitatory glutamatergic neurons [290].

Glutamate accounts for 50-60% of all neurotransmission in the brain, and the remaining 40-50% is GABAergic. Therefore, 90-99% of neurons are modulated by glutamatergic or GABAergic neurotransmission and less than 10% by other monoamine, neuropeptide, and neuroendocrine neurotransmissions. Most neural energy is expended on sustaining excitatory signaling within the CNS with action potential firing, and glutamatergic transmission is proposed to contribute as much as 80% of the total expenditure. There is evidence indicating an equally high need for cellular metabolism of inhibiting GABAergic interneurons [291]. Accardi et al. show that mitochondrial-derived reactive oxygen species (mROS) regulate postsynaptic GABAA receptors' strength at inhibitory synapses of cerebellar stellate cells. The generation of mROS has been traditionally linked to the cellular damage that accompanies the chronic disease. This data identifies mROS as a putative homeostatic signaling molecule, coupling cellular metabolism to the strength of inhibitory transmission [292]. As stated above, mitochondrial dysfunction plays a significant role in the pathogenesis of schizophrenia [293].

An increase in functional changes associated with the level of oxidative stress is shown in several neurotransmitter systems. The site of redox modification on vulnerable molecules may undergo oxidative damage, resulting in an irreversible inhibitory action on proteins involved in synaptic transmission, as well as promoting mitochondrial dysfunction and excitotoxicity [294].

As mentioned above, glutamate is the major excitatory neurotransmitter of the central nervous system. Three groups represent ionotropic glutamate receptors, namely, AMPA, KA, and NMDA receptors, that mediate rapid transmembrane ion currents [295]. ROS and NO are essential mediators of NMDA receptor signaling [20]. Under normal physiological conditions, nitric oxide is generated by NMDA receptor-mediated activation of nNOS. In turn, nitric oxide regulates glutamate metabolism, the release of glutamate at the synapse, and transport out of the synapse [296]. Both NMDA receptor activation and blockade are reported to induce oxidative stress through an increase in NADPH oxidase (NOX) activity [297, 298]. Besides, the addition of glutamate to the culture of neurons at a concentration of 100 microns also causes the formation of ROS [299]. It has also been shown that prolonged exposure to glutamate damages motor neurons primarily through the activation of calcium/-calmodulin, neuronal synthase, and nitric oxide in the cytoplasm and leads to the apoptosis of neurons [300]. In turn, increased ROS results in NMDA receptor hypofunction, and the production of nitric oxide can reduce NMDA receptor activity through S-nitrosylation of cysteines on NMDA receptor subunits. Similarly, S-nitrosylation of serine racemase inhibits the formation of the NMDA receptor coagonist, D-serine, which would decrease NMDA receptor activity [301].

In addition to NMDA receptors, α-amino-3-hydroxy-5-methyl-4-isoxazole propionic acid (AMPA) receptors represent the other dominant class of ionic glutamate receptors. It has been shown that the AMPA receptor's function is not directly related to the redox state, and lipid peroxidation does not affect its synaptic transmission [302]. In schizophrenia, changes in subunit expression of AMPA receptors and protein expression regulating the forward trafficking of AMPA receptors through the cell have been reported. These facts are the basis of the mechanism of impaired regulation of glutamate in schizophrenia. It has been revealed that in schizophrenia, abnormal trafficking of AMPA receptors from the endoplasmic reticulum to the synaptic membrane occurs [303, 304].

Glutamate signaling dysfunction and dysregulation of oxidative stress have been considered to play essential roles in schizophrenic prodrome [22]. The question of the primacy of oxidative stress in schizophrenia has not yet been definitively resolved. Still, most studies suggest that its influence is interdependent with the violation of glutamatergic neurotransmission [24, 305].

The effect of redox processes on GABAergic synaptic transmission and GABA release is very ambiguous. Redox state may have opposing effects on GABAB and GABAA receptors. For example, synaptic GABAA receptors can be weakened under oxidizing conditions; however, in the hippocampus, tonic currents are increased by hydrogen peroxide [306, 307]. Finally, oxidative damage can decrease the synthesis of GABA.

The hypofunction of subpopulations of GABAergic interneurons in the prefrontal cortex and hippocampus has long been established in schizophrenia. Also, there is a lot of data showing that redox changes of NMDA receptor synaptic input to inhibitory interneurons can decrease the release of GABA and induce the loss of inhibitory interneurons in the PFC (prefrontal cortex). And the modern view of the pathogenesis of schizophrenia is based on the hypofunction of the NMDA receptor and the loss of GABAergic neurons [308]. Recent experimental work carried out by the Department of Psychiatry at Harvard Medical School showed that interneurons in schizophrenia had a significantly smaller nucleus, which indicates an innate state of oxidative stress. The antioxidant N-acetylcysteine increased the area of the cell nucleus in interneurons in schizophrenia and eliminated synapse deficits [309].

It has long been known that the catabolism of dopamine shifts the cellular redox state toward oxidative stress through the production of superoxide, hydrogen peroxide, quinones, and quinoprotein adducts [310, 311]. In the presence of Mn, the autooxidation of dopamine produces semiquinones (SQ) and superoxide radicals ($O_2^{-\bullet}$), as well as H_2O_2, which is readily converted to $OH^\bullet$ in the presence of Fe^{2+}. On the other hand, the enzymatic oxidation of dopamine by monoamine oxidase (MAO) can also produce H_2O_2 and, subsequently, generate the toxic $OH^\bullet$ [35]. Dopamine metabolites, when interacting with Fe^{3+} and Cu^{2+}, also produce ROS and thus exacerbate OS [311, 312].

It is now generally accepted that schizophrenia is based on a disruption of the interactions between the glutamatergic, GABAergic, and dopaminergic systems. At the present stage, an assumption is made that elevated baseline levels of dopamine observed in schizophrenia may be secondary to hypoglutamatergia. This is supported by evidence suggesting that NMDAR antagonists can enhance the release of dopamine and glutamate, leading to cortical disinhibition [313]. Besides, it was found that inhibition of NMDAR reduces the activity of putative GABA interneurons [314]. Thus, it is established that the main contribution to the pathogenesis of schizophrenia is made by mutually influencing disorders of neurotransmission of glutamate, dopamine, and GABA.

The contribution of other neurotransmitters to the pathogenesis of schizophrenia is less significant, but in any case, ROS signaling regulates neurotransmission to some extent. Noradrenaline in low concentrations, in contrast, increases neuroprotection for many types of neurons [315, 316]. There are isolated studies that indicate that OS disrupts the functioning of muscarinic cholinergic receptors, which is restored by GSH [317]. Acetylcholine, which is their mediator, is also involved in the development of schizophrenia [318]. Schizophrenia is also characterized by serotonin deficiency [319]. It has been shown that serotonin receptors can modulate dopaminergic functions, but their effect may have different tendencies. For example, serotonin can inhibit or stimulate the release of dopamine in the striatum [320, 321].

Thus, the entire neurotransmission of the CNS is regulated to some extent by ROS or RNS. All neurotransmitters are a close, mutually regulating system, and even with minor deviations from the norm, the homeostasis of this system is disrupted. Several morphological changes in cells in schizophrenia indicate that OS was present at an early stage of the morphosis. This area has already been studied in detail and is represented by a vast number of works. Here, we show only the most basic mechanisms. But the literature does not cover the following question: Are the described changes specific only for schizophrenia, or are they characteristic of other mental disorders?

4.9. Dysfunction of Parvalbumin-Positive Interneurons. Numerous studies, including postmortem, genetic, and in vivo electrophysiological experiments in murine models of schizophrenia, consider the disruption of parvalbumin-(PV-) positive GABAergic interneurons as a critical pathophysiological mechanism of schizophrenia [322]. PV interneurons are the most abundant type of GABAergic cells known for their high-frequency generation of action potentials [323]. PV interneurons form a common network that facilitates the processing of a massive flow of information from sensory systems and provides mechanisms for temporary memory, attention, learning, and social behavior. Parvalbumin is a Ca^{2+}-binding protein that has little effect on excitatory potentials but significantly increases the decay rate of the signal [324]. This function allows maintaining a balance of excitatory/inhibitory postsynaptic potentials, synchronizing the activity of neurons. Electroencephalography-(EEG-) measured synchronized oscillatory activity, particularly in the gamma range, is abnormal in patients with schizophrenia [325].

Disorders of PV interneurons can lead to schizophrenia not only in adulthood but also at the stages of early neurogenesis. Recent studies have shown that suppressed PV interneuron activity decreases the survival and maturation of hippocampal neurons in newborns [326]. Caballero et al. showed that a slight suppression of PV interneuron activity in adolescence significantly reduces GABAergic transmission, disrupting the balance of excitation/inhibition processes in the prefrontal cortex [327]. An increase in the expression of PV interneurons in adolescence is necessary for better GABAergic regulation of excitation/inhibition, contributing to the activation of cognitive functions. Consequently, the loss of PV interneurons leads to an increase in the excitation/inhibition ratio due to the GABAergic interneurons' inability to maintain a high generation of action potentials, which leads to impaired processing of afferent information from the ventral hippocampus [328].

Correct high-frequency synchronization of PV interneurons requires a high level of metabolism and oxidative phosphorylation [329], which leads to an increase in ROS synthesis. PV interneurons are known to be extremely sensitive to increased ROS levels. In transgenic mouse models, it has been found that reduced glutathione (GSH) correlates with a deficiency of PV interneurons in the prefrontal cortex and hippocampus and disrupts neuronal synchronization [330]. Prefrontal cortical PV interneurons are more vulnerable to ROS during postnatal development. GSH deficiency results in a rapid and long-term decrease in the density of PV interneurons in the anterior cingulate gyrus [19]. Using an assessment of the level of oxidized and reduced

glutathione in tissues, gamma fluctuations, and PV expression at different time points in transgenic Wistar rats, it was found that NMDA receptor (NMDAR) inhibition and GSH depletion during early postnatal development markedly alter gamma fluctuations [331]. It has been shown in vitro that during the early development of neurons, NMDAR inhibition primarily results in a sustained decrease in the peak gamma frequency. At the same time, a reduction of PV expression occurs only after a few days. These functional changes are expected to precede the suppression of PV expression. One of the possible mechanisms is assumed to be oxidative stress, which contributes to the loss of PV interneurons due to the suppression of internal antioxidant systems [332].

Damage to the perineuronal nets (PNNs) can be another critical factor in the disruption of PV interneurons. PNNs are reticular lattice structures composed of proteoglycans, chondroitin sulfate, hyaluronic acid, tenascin, and binding proteins, and braiding PV interneurons prevent the flow of cations spontaneously into the neuron [333]. The effect of oxidative stress on PNNs is to alter PV interneuron maturation and synapse formation [330]. Therefore, oxidative stress disrupts the plasticity of the PV interneuron network and may affect the ratio of excitatory and inhibitory synapses [334].

Mouse models were used to investigate the effects of oxidative stress on PV interneurons and PNNs. Indeed, mice with an alpha-7 nicotinic receptor (α-7-nAChR) deletion show reduced expression of PV, glutamate decarboxylase (GAD67), and NMDAR in PV interneurons [335]. α-7-nAChR activation inhibits NF-κB-dependent pathways and mediates Nrf2-induced antioxidant responses, providing anti-inflammatory and neuroprotective effects [336]. Patients with schizophrenia have disturbances in neuregulin-1 (NRG1) and its receptor tyrosine kinase ErbB4 [337]. Signaling through the NRG1/ErbB4 complex controls the development of inhibitory chains in the cerebral cortex. Fazzari et al. have demonstrated that signaling through the ErbB4 receptor promotes the formation of perisomatic and axo-axonal synapses, and NRG1 mediates these effects [301]. ErbB4 is also required for the formation and maintenance of excitatory synapses on GABAergic interneurons. NRG1 suppresses NMDAR activation in the prefrontal cortex in subjects with schizophrenia, consistent with the increased NRG1-ErbB4 signaling observed in this disease [338]. NRG1 modulates NMDAR activity through tyrosine phosphorylation on the NR2 subunit. Enhanced NRG1 signaling may contribute to NMDAR hypofunction in schizophrenia [338].

Thus, the functioning of the PV interneuron, which plays an essential role in human cognitive functions impaired in schizophrenia, is directly dependent on the level of oxidative stress. As stated above, a decrease in the activity of the antioxidant system leads to inhibition of NMDAR and disrupts the PV interneurons, which makes a significant contribution to the pathogenesis of schizophrenia.

5. Antipsychotic Medication and Redox Correction in Schizophrenia

5.1. Antipsychotic Therapy Promotes Oxidative Imbalance. Antipsychotics are the drugs of choice for the long-term management of schizophrenia. As mentioned above, patients with schizophrenia have endogenous oxidative stress, which can cause the development of pathology. However, antipsychotic treatment can also cause oxidative imbalance.

Typical and atypical antipsychotics vary significantly in their effects on redox balance [339–342]. Animal studies indicate that typical antipsychotics most often cause oxidative stress. It was shown that treatment with haloperidol (45 and 90 days), a typical antipsychotic, significantly reduced the activity of Mn-SOD, Cu,Zn-SOD, and catalase and increased lipid peroxidation in the rat's brain [340]. But treatment with atypical antipsychotics (risperidone, clozapine, and olanzapine) did not cause any changes in antioxidant enzyme levels [340]. A 28-day study in male Wistar rats that received haloperidol daily showed an increase in thiobarbituric acid (TBA) reactive substances (TBAR) inducing the production of superoxide in the hippocampus [343]. In other experiments in rats after the administration of haloperidol, an increase in the level of TBAR in the striatum, but a decrease in the cortex, was also observed [341, 342]. The long-term treatment (90 and 180 days) with haloperidol also significantly decreased the levels of Mn-SOD, Cu,Zn-SOD, and to a lesser extent, catalase [339]. In the same work, it was shown that atypical antipsychotics such as ziprasidone, risperidone, and olanzapine did not show significant changes in the lipid peroxidation products (hydroxyalkanals) after 90 days of treatment [339]. However, further treatment (up to 180 days) resulted in significantly increased levels of hydroxyalkanals in ziprasidone and risperidone, but not in olanzapine-treated rats [339]. These data indicate that long-term treatment, even with atypical antipsychotics, can contribute to prooxidant processes. At the same time, posttreatment with some atypical antipsychotics for 90 days after 90 days of typical antipsychotic treatment restores developed redox abnormalities [339]. These observations can be explained by the direct antioxidant activity of some atypical antipsychotics, such as olanzapine and clozapine [344].

Summarizing the available data from animal studies, we can conclude that oxidative damage of the brain during treatment with typical antipsychotics is due to the following mechanisms:

(i) A significant decrease in the activity of Mn-SOD, Cu,Zn-SOD, and catalase

(ii) Increased lipid peroxidation of membranes

(iii) Reduction of NO concentration [345]

(iv) Increased production of superoxide and H_2O_2 [345]

Human studies also indicate that antipsychotics contribute to oxidative stress [346]. It has been shown that MDA levels in patients treated with risperidone, amisulpride, quetiapine, and clozapine were significantly lower than in the first-generation antipsychotic group [347]. Treatment with typical antipsychotic haloperidol was associated with higher serum TBAR and lower antioxidant parameters in patients with schizophrenia [348]. Besides, an overdose of typical antipsychotics can cause oxidative stress [349]. Another

study reported that both typical and atypical antipsychotics contributed to patients' prooxidant state with various types of schizophrenia [350]. The specific activity of SOD and glutathione peroxidase was reduced, but MDA levels were increased in chronic patients, regardless of the type of antipsychotic [350]. Padurariu et al. [351] obtained similar results. An increase in the specific activity of SOD, mainly in patients receiving haloperidol and quetiapine, was shown [351]. Antipsychotic treatment also affects peripheral nonenzymatic antioxidants. Indeed, uric acid levels did not change after treatment, while albumin and total bilirubin levels decreased significantly after treatment [352]. Thioredoxin levels also decreased in patients receiving antipsychotic medication [353]. However, no correlation was found between thioredoxin levels and treatment with atypical antipsychotics [353]. Antipsychotic treatment also affects the serum lipid profile [354]. Indeed, serum lipid profiles of patients with first-episode psychosis before and after seven months of treatment were significantly different [354]. Our data also confirm the effect of therapy on the activity of antioxidant systems in schizophrenia [355]. We showed that atypical antipsychotics do not have a pronounced impact on the glutathione system, while treatment with typical antipsychotics leads to a further decrease in reduced glutathione, thereby exacerbating the imbalance in metabolic processes in schizophrenia [355]. Besides, metabolic syndrome and antipsychotic-induced weight gain may be associated with high levels of oxidative stress in patients [356].

However, there is clinical evidence of a decrease in oxidative stress markers after the antipsychotic treatment of schizophrenia patients [357–359]. Therapy with atypical antipsychotics improved the redox balance, together with the results of the Brief Psychiatric Rating Scale for schizophrenia [359]. The antipsychotic medication (7 months) of first-episode psychosis patients not only had a significant anti-inflammatory effect but also reduced lipid peroxidation and protein oxidation-related indices of oxidative stress [357]. A decrease in the neopterin levels and an increase in antioxidant levels were found after three months of treatment with antipsychotics [358]. Zhang et al. published evidence that clozapine treatment significantly increased SOD and decreased lipid peroxidation in patients with schizophrenia [350]. In our work, it was shown that therapy with typical antipsychotics leads to normalization of catalase activity. However, the activity of glucose-6-phosphate dehydrogenase continues to decrease [360]. Besides, we showed that antipsychotic therapy leads to a decrease in MDA in red blood cells and blood plasma but does not affect the level of oxidized and reduced glutathione [361].

Thus, despite contradictory data, nevertheless, there is an association between antipsychotic therapy and oxidative stress. Both typical and atypical antipsychotics have the most significant effect on redox balance in schizophrenia. Therefore, additional antioxidant treatment can have beneficial effects on the redox balance and, accordingly, on the condition of schizophrenia patients.

5.2. Antioxidant Therapeutics in Schizophrenia. Antioxidant treatment can be used at various stages of schizophrenia, from prenatal and postnatal development to acute and chronic phases of the illness [362]. However, the most realistic option is to use antioxidant therapy to treat the disease's active stage.

To assess the promise of prescribing antioxidants to patients with schizophrenia in the last decades, many different studies have been conducted (Table 2). Some effects of antioxidants were analyzed in detail in large-scale meta-analyses [36, 363, 364]. It was shown that additional antioxidant therapy could improve the mental state of patients with schizophrenia.

N-Acetylcysteine (NAC) is an L-cysteine precursor, an antioxidant, and a free radical-scavenging agent. NAC can regulate glutathione (GSH): this is a precursor for glutathione synthesis and a stimulator of the cytosolic enzymes involved in glutathione regeneration [365]. NAC is also able to regulate excessive brain glutamate through the cysteine-glutamate antiporter [366]. Symptoms of schizophrenia are associated with elevations in glutamatergic metabolites across several brain regions [367] and oxidative stress [40]. This determines the potential possibility of the use of NAC as adjunctive therapy for patients with schizophrenia [368–377]. The NAC study's frequent outcome as an adjunct to antipsychotic treatment was a significant reduction in PANSS total and the negative PANSS subscale, but not positive symptoms or cognition (Table 2). Also, some authors noted an improvement in the generation of negative mismatch (MMN) and working memory performance in patients with schizophrenia (Table 2). A recent meta-analysis of randomized controlled trials with N-acetylcysteine in the treatment of schizophrenia confirmed the effectiveness of NAC, but it is worth noting that therapeutic effects were observed at a later point in time (>24 weeks) [364]. This suggests that long-term administration of N-acetylcysteine is required for successful treatment.

Ginkgo biloba is the most widely studied plant antioxidant in the treatment of schizophrenia [378–381]. Published studies and meta-analyses demonstrated that Ginkgo as an adjunctive therapy could alleviate the symptoms of chronic schizophrenia and improve tardive dyskinesia (Table 2).

Selegiline and allopurinol have also been studied as an additional antioxidant treatment for schizophrenia patients [382–388]. In selegiline, the ability to reduce negative symptoms was noted; on the contrary, in allopurinol, the ability to interfere with positive symptoms was noted. However, the use of these drugs often did not make a performance compared with the control group (Table 2).

Vitamin E is a lipid-soluble antioxidant. Evaluation of the effectiveness of treatment with vitamin E in patients with schizophrenia showed a significant difference in Abnormal Involuntary Movement Scale (AIMS) score (Table 2) [389–395]. There is also evidence that vitamin E is more effective for patients using classic antipsychotics compared to patients using atypical antipsychotics [36].

There is very little data on the individual use of vitamin C as an antioxidant therapy for schizophrenia [396]. But since ascorbic acid has a synergistic effect with vitamin E, there is evidence of the effect of their combined action in patients with schizophrenia [397]. The effects are similar to those of

Table 2: The results of the use of redox regulatory drugs in schizophrenia and animal models.

Drugs	Class	Mechanism of action	Studies	Outcome
Antioxidant drugs				
N-Acetylcysteine (NAC)	Cysteine precursor	NAC (i) Activates the synthesis of glutathione, the main endogenous antioxidant mediator in the brain (the most important mechanism) (ii) Has its own nonspecific activity in neutralizing various free radical groups	Yolland et al., 2020 (meta-analysis) [364]	Total PANSS and in the negative PANSS subscale and total scores as well as the cognitive domain of working memory were significantly improved with N-acetylcysteine supplementation after 24 weeks of treatment
			Berk et al., 2008 [368]; Farokhnia et al., 2013 [369]	Significant reduction of the Positive and Negative Syndrome Scale (PANSS) negative, PANSS total, and Clinical Global Impression (CGI) scales in comparison to placebo
				No significant change on the PANSS positive subscale was seen
				There was no significant difference with the control group in the frequency of side effects.
			Lavoie et al., 2008 [370]	Administration of NAC to schizophrenia patients resulted in improved auditory cortical functioning, improved mismatch negativity (MMN) generation
			Zheng et al., 2018 [371]	Adjunctive NAC significantly improved total (positive and negative) symptoms in schizophrenia
			Rapado-Castro et al., 2017 [372]	Significantly higher working memory performance compared with placebo
			Sepehrmanesh et al., 2018 [373]	Significant improvement in total PANSS and in the positive and negative PANSS subscales
				Improvements in attention, short-term and working memory, executive functioning and speed of processing
			Conus et al., 2018 [374]	NAC therapy improved neurocognition and reduced positive symptoms among patients with high peripheral oxidative status
				No changes in negative or positive symptoms or functional outcome were observed with NAC
			Klauser et al., 2018 [375]	Significant improvements in neurocognition and a reduction of positive symptoms
				Increase in GSH levels in the medial prefrontal cortex
			Breier et al., 2018 [377]	Significant improvement in PANSS total, negative, and disorganized thought symptom scores
				No changes in PANSS positive symptoms and BACS cognitive scores

Table 2: Continued.

Drugs	Class	Mechanism of action	Studies	Outcome
			McQueen et al., 2020 [376]	A single dose of NAC was associated with decreases in rs-FC in prefrontal cortical regions of the DMN and SN network in patients with established schizophrenia
			Singh et al., 2010 (meta-analysis) [381]	Statistically significant moderate improvement in total and negative symptoms of chronic schizophrenia
Ginkgo biloba extract	Contains flavonoids, tricyclic diterpenes (ginkgolides A, B, C, and J), sesquiterpenes (bilobalide A)	Ginko biloba extract (i) Scavenger of superoxide anion, hydroxyl radicals, peroxyl (ii) Reduces the concentration of primary and secondary products of lipid peroxidation (diene conjugates, TBA-active products) (iii) Induces the enzymatic activity of superoxide dismutase and catalase	Doruk et al., 2008 [378]	Significant reduction of the PANSS negative No significant change on the PANSS total and in the positive PANSS subscale
			Zhang et al., 2011 [379]	A significant decrease in the Abnormal Involuntary Movement Scale (AIMS) total score No between-group differences in the PANSS total score or cognitive measures from baseline
			Rathbone et al., 2005 [380]	Treatment with Ginkgo biloba resulted in moderate improvement in total and negative symptoms of schizophrenia
Selegiline	Selective inhibitor of MAO-B	The antioxidant effect of selegiline may be associated with the protection of neurons from oxygen free radicals that are released as a result of MAO-B activity	Amiri et al., 2008 [382]	Decline of negative symptoms and PANSS total scores
			Bordbar et al., 2008 [383]	No significant change on the PANSS negative subscale was seen
			Bodkin et al., 2005 [384]	Significant improvements in negative symptoms
Allopurinol	Xanthine oxidase inhibitor	Allopurinol prevents the formation of free radicals: (i) Inhibits the xanthine oxidase reaction, during which superoxide anion radical is actively formed	Akhondzadeh et al., 2005 [385]	A significant superiority in the treatment of positive symptoms, general psychopathology symptoms as well as PANSS total scores Decreased Extrapyramidal Symptoms Rating Scale (ESRS)
			Brunstein et al., 2005 [386]	Significant improvement in PANSS total, positive, negative, and general scores, particularly for positive symptoms
			Dickerson et al., 2009 [387]	At least a 20% reduction in total PANSS score
			Weiser et al., 2012 [388]	No differences with control group on the PANSS
Vitamin E	Vitamin	Vitamin E is a natural antioxidant that neutralizes free radicals: (i) There is a transfer of hydrogen of the phenyl group to the peroxide radical (ii) Performs structural function by interacting with phospholipids of biological membranes	Adler et al., 1993 [389]	Significant reduction of AIMS score
			Adler et al., 1999 [390]	No significant reduction of AIMS and Brief Psychiatric Rating Scale (BPRS)
			Dorevitch et al., 1997 [391]	No significant differences between vitamin E and placebo-treated patients in AIMS score
			Lohr et al., 1996 [392]	Significant reduction of AIMS score Significant change on the PANSS positive subscale

Table 2: Continued.

Drugs	Class	Mechanism of action	Studies	Outcome
			Zhang et al., 2004 [393]	Significant reduction of AIMS score
			Sajjad, 1998 [394]	Significant reduction of AIMS score
			Soares-Weiser et al., 2018 [395]	No clear difference between vitamin E and placebo for the outcome of TD (not improved to a clinically important extent)
Vitamin C	Vitamin	Vitamin C antioxidant activity: (i) The formation of a redox pair of ascorbic acid/dehydroascorbic acid, restores the active form of vitamin E (ii) Prevents or reverses the oxidation process of reduced glutathione (GSH) to its functionally inactive form (GSSG)	Dakhale et al., 2005 [396]	Significant change on the BPRS
Vitamins C and E	Vitamins	Ascorbic acid has a synergistic effect for vitamin E: (i) Restores the oxidation product of tocopherol (α-tocopheroxide) to α-tocopherol	Nicolaus et al., 2002 [397]	Significant reduction in dyskinetic movement total score High dietary intake will lead to prooxidant action
Vitamins E and C and fatty acids	Vitamins and dietary supplements	Q.V. mechanisms of action of vitamins E and C and fatty acids	Arvindakshan et al., 2003 [398]	Significant reduction of PANSS and BPRS and increase of QOL (Henrich's Quality of Life scale)
			Sivrioglu et al., 2007 [399]	Significant reduction of BPRS, Scale for Assessment of Negative Symptoms, Simpson-Angus Rating Scale, and Barnes Akathisia Rating Scale
			Emsley et al., 2002 [400]	Significant reduction in PANSS total scale
			Emsley et al., 2006 [404]	No significant difference in the Extrapyramidal Symptom Rating Scale
Polyunsaturated fatty acids (PUFAs)	Dietary supplements	The detailed mechanisms of action are mostly unknown, but PUFAs have anti-inflammatory and antiatherogenic effects	Fenton et al., 2001 [405]	No significant change in PANSS, Abnormal Involuntary Movement Syndrome scale, Clinical Global Impression scale
			Peet et al., 2001 [401]; Peet et al., 2002 [402]	Significant reduction in PANSS total
			Amminger et al. 2010 [403]	Significantly reduced positive, negative, and general symptoms and improved functioning compared with placebo
Transcription factor-targeting drugs				
Sulforaphane	Nrf2 transcription factor activator	Inhibit Keap1 protein through electrophilic modification, which leads to Nrf2 activation. The transcription factor Nrf2 plays a central role in the inducible expressions of many cytoprotective genes in response to oxidative stress	Sedlak et al. 2017 [406]	Isothiocyanate sulforaphane increased blood and brain GSH levels in healthy human subjects following 7 days of administration
			Shiina et al. 2015 [407]	Sulforaphane may have the potential to improve cognitive impairments in patients with schizophrenia, but the differences before and after treatment are not significant

Table 2: Continued.

Drugs	Class	Mechanism of action	Studies	Outcome
			Shirai et al., 2015 (animal model) [408]	Sulforaphane exhibited an atypical antipsychotic activity in PCP-induced cognitive deficits in animal models. Genetic analysis showed an epistatic interaction between Nrf2 and Keap1 gene variants on working memory in schizophrenia
DDO-7263	Nrf2 transcription factor activator	Nrf2 activation and NLRP3 inflammasome inhibition	Xu et al., 2019 (animal model) [409]	The neuroprotective effects of DDO-7263 have been proven in mice, through Nrf2 activation and NLRP3 inflammasome inhibition
Curcumin	Polyphenolic compound	Inhibit Keap1 protein through electrophilic modification, which leads to Nrf2 activation	Miodownik et al. 2019 [410]	Significant reduction in total PANSS and in the negative symptoms subscale. There were no differences in the positive and general PANSS subscales, and the Calgary Depression Scale for Schizophrenia scores
Resveratrol	Anthocyanins	Resveratrol is (i) An activator of NAD-dependent deacetylase sirtuin-1 (SIRT1), which activates the transcription factor FoxO (ii) An inhibitor of NF-κB (anti-inflammatory effect)	Zortea et al., 2016 [411]	Oral resveratrol in sufficiently low doses has not brought improvement
			Zortea et al., 2016 [412]	No significant improvement in psychopathology severity
			Magaji et al., 2017 (animal model) [413]	Anxiolytic and antipsychotic potentials of resveratrol in murine models of anxiety and schizophrenia in mice was found
			Huang et al., 2019 (animal model) [414]	Study has confirmed the antidepressant activity in an induced depression rat model
Salvianolic acid B	Polyphenolic compound	Salvianolic acid B like resveratrol is an activator of SIRT1 and an inhibitor of NF-κB	Yu et al., 2016 (animal model) [415]	Treatment of stress-challenged rats with fluoxetine and fluoxetine combined with salvianolic acid could alleviate depression-like symptoms and cognitive deficit
			Liao et al., 2020 (animal model) [154]	SalB relieved CMS-induced depressive-like state in mice through the mitigation of inflammatory status, oxidative stress, and the activation of the AMPK/SIRT1 signaling pathway
Metformin	Antidiabetic agent	Activate FoxO3 via AMP-activated protein kinase activation	Jiang et al., 2020 [416]	Significantly reduce antipsychotic-induced weight gain, dyslipidemia, and metabolic abnormalities in schizophrenia

vitamin E. Supplements with polyunsaturated fatty acids (PUFAs) in schizophrenia help to reduce the PANSS scores [398–403], but in some cases [404, 405] the changes are not significant (Table 2). Despite all efforts, PUFA mechanisms of action are still poorly understood.

5.3. Promising Transcription Factor-Targeting Drugs. Insufficient efficiency of antioxidant therapy stimulates the search for new approaches to correct redox balance. The potential new therapeutic avenues are associated with activators of redox-regulated transcription factors (Nrf2, FoxO). The activation of Nrf2 or FoxO by low-molecular-weight drugs may have therapeutic potential to control redox balance by enhancing endogenous antioxidant responses. Numerous drugs such as dimethyl fumarate (DMF), sulforaphane, cyanoenone triterpenoids (in particular, bardoxolone methyl and omaveloxolone), nitro fatty acids, and hydroxylamine are considered promising Nrf2 activators [417]. Of these, only DMF was approved by the US Food and Drug Administration and the European Medicines Agency to treat remitting-relapsing MS. [417] Sulforaphane, curcumin, resveratrol, and metformin have been tested to treat schizophrenia (Table 2). The Keap1 inhibitor sulforaphane increased blood and brain GSH levels in healthy humans [406] and improved cognitive

impairments in schizophrenia individuals [407]. Sulforaphane exhibited an atypical antipsychotic activity in an animal model [408]. Another Keap1 inhibitor, curcumin, reduced total PANSS and the negative symptom subscale scores in schizophrenia [410]. Another Nrf2 activator (DDO-7263) showed a neuroprotective and anti-inflammatory effect through Nrf2 activation and NLRP3 inflammasome inhibition in an animal model [409]. It is noteworthy that there are some reversible Keap1-binding compounds with low off-target activity that protect cells from oxidative effects by preserving the ATP content and mitochondrial potential in the cell culture of primary astrocytes [418].

Some drugs can modulate the FoxO transcription factor activity (Table 2). Resveratrol activates NAD-dependent deacetylase sirtuin-1 (SIRT1), and thereby activates the transcription factor FoxO, and also inhibits NF-κB. Resveratrol demonstrated anxiolytic and antipsychotic potentials in murine models of anxiety and schizophrenia [413]. However, oral resveratrol is not effective in human trials [411, 412]. Another promising compound with a similar mechanism of action is salvianolic acid B, which has been shown to alleviate depression-like symptoms and cognitive deficits in animal models [154, 414, 415]. Metformin, an antidiabetic agent, was identified as a therapeutic activator of FoxO3. Metformin showed efficacy in the treatment of antipsychotic-induced weight gain, dyslipidemia, and metabolic abnormalities in schizophrenia [416]. Besides, there are specific FoxO activators. Cautain et al., using image-based high-content screening technology, identified the isothiazolonaphthoquinone-based compound (LOM612) as a specific FoxO3a protein activator [419]. This compound induced nuclear translocation of FoxO3a and FoxO1 proteins and also did not affect the translocation of NF-κB in U2OS cancer cells [419]. Some inhibitors of PI3K, Akt, and other protein kinases may also be considered as possible regulators of FoxO activity [420].

5.4. Stratification of Patients Based on Oxidative Stress-Related Markers for the Administration of Antioxidant Treatment. Heterogeneity and complexity are the main obstacles to developing etiopathogenetic treatments for schizophrenia. The lack of effectiveness of traditional antipsychotic therapy, especially in the treatment of negative and cognitive symptoms, leads to the search for new therapeutic avenues. Considering the above data about the involvement of oxidative stress in the molecular mechanisms of the schizophrenia pathogenesis, redox correction in conjunction with antipsychotic therapy is a promising therapeutic strategy. However, existing treatment approaches do not consider the multistage process of schizophrenia. Indeed, the redox markers in first-episode psychosis patients, people with acute relapse of psychosis, chronic inpatients, and stable medicated outpatients, as well as in people with different types of schizophrenia and depending on antipsychotic treatment, are different [40, 350]; therefore, it is necessary to take into consideration the characteristics of each person's redox status, including during clinical trials.

As stated above, clinical trial results indicate that additional antioxidant therapy has beneficial effects, including for treatment-resistant schizophrenia patients [421]. However, a shift in the redox balance towards an increase in the reduction potential leads to reductive stress and a paradoxical increase in ROS production [422]. Therefore, the appointment of antioxidant therapy should be strictly controlled. It is also necessary to consider that prolonged use of antioxidant drugs can have prooxidant effects [422]. Consequently, stratification criteria based on oxidative stress-related markers need to be developed. The stratification criteria may be blood-based biomarkers, since they may reflect the degree of redox imbalance in the brain, or noninvasive visualization-based markers. Genetic-based stratification may also be promising. Identification of subgroups of high-risk patients with common redox imbalance parameters will allow choosing the optimal targeted treatment strategy for each patient. This approach is an important step towards personalized and precision medicine.

6. Conclusions

The heterogeneity of schizophrenia is reflected in the diversity of oxidative stress-related mechanisms that contribute to the disease. In our opinion, genetic causes lead to a predisposition to redox imbalance. There is ample evidence that a variety of environmental factors contribute to the dysregulation of gene expression caused by abnormal regulation of redox-sensitive transcriptional factors, noncoding RNAs, and epigenetic mechanisms. These changes contribute to altered redox signaling. Thus, these processes form the basis of the redox imbalance and lead to mitochondrial dysfunction and metabolic abnormalities that contribute to aberrant neuronal development, abnormal myelination, NMDA receptor hypofunction, and dysfunction of parvalbumin-positive interneurons. Immune dysregulation through various mechanisms also enhances redox imbalance. All these mechanisms ultimately contribute to the phenotypic realization of predisposition to redox imbalance and the manifestation of schizophrenia. However, it should be noted that all these mechanisms are interconnected and, at the same time, can act both independently and jointly in different periods. But these mechanisms eventually increase the likelihood of developing schizophrenia. Knowledge of oxidative stress-related mechanisms could pave the way for novel treatment options in schizophrenia. We suggest that not only classical antioxidants but also transcription factor-targeting drugs have great promise in schizophrenia. Since dysregulation of redox-sensitive transcriptional factors (e.g., Nrf2, NF-κB, and FoxO) may play an important role in the development of schizophrenia, modulators of the activity of these factors may contribute to the normalization of redox balance. However, it is necessary to use redox regulatory drugs with caution, since any change in the redox balance towards oxidative stress and reductive stress has detrimental consequences. Therefore, we propose to develop the stratification criteria of schizophrenic patients based on oxidative stress-related markers for the administration of antioxidant treatment for high-risk patients. Nevertheless, there are still many unresolved questions about the role of oxidative stress in schizophrenia pathogenesis. We expect that further research will reveal new oxidative stress-related mechanisms in schizophrenia.

Data Availability

The presented data supporting this systematic review are from previously reported studies and datasets, which have been cited. The processed data are available from the corresponding author upon request.

Conflicts of Interest

The authors declare that there is no conflict of interest regarding the publication of this review.

Acknowledgments

The authors are grateful to all researchers of oxidative stress in schizophrenia for their contributions to this challenging but interesting area. This work was supported by the Russian Science Foundation (grant number 18-15-00053). E.A.E. is the recipient of a fellowship of the President of the Russian Federation (SP-2258.2019.4).

References

[1] J. B. Lohr and J. A. Browning, "Free radical involvement in neuropsychiatric illnesses," *Psychopharmacology Bulletin*, vol. 31, no. 1, pp. 159–165, 1995.

[2] J. M. Bourre, M. Boonneil, M. Clément et al., "Function of dietary polyunsaturated fatty acids in the nervous system," *Prostaglandins, Leukotrienes and Essential Fatty Acids*, vol. 48, pp. 5–15, 1993.

[3] R. A. Floyd, "Antioxidants, Oxidative Stress, and Degenerative Neurological Disorders," *Proceedings of the Society for Experimental Biology and Medicine*, vol. 222, pp. 236–245, 1999.

[4] K. Shibuki and D. Okada, "Endogenous nitric oxide release required for long-term synaptic depression in the cerebellum," *Nature*, vol. 349, pp. 326–328, 1991.

[5] C. M. Maier and P. H. Chan, "Book Review: Role of superoxide dismutases in oxidative damage and neurodegenerative disorders," *The Neuroscientist*, vol. 8, pp. 323–334, 2002.

[6] X. Wang and E. K. Michaelis, "Selective neuronal vulnerability to oxidative stress in the brain," *Frontiers in Aging Neuroscience*, vol. 2, p. 12, 2010.

[7] G. Ermak and K. J. Davies, "Calcium and oxidative stress: from cell signaling to cell death," *Molecular Immunology*, vol. 38, no. 10, pp. 713–721, 2002.

[8] A. J. Pocklington, M. O'Donovan, and M. J. Owen, "The synapse in schizophrenia," *European Journal of Neuroscience*, vol. 39, no. 7, pp. 1059–1067, 2014.

[9] M. C. Franco, Y. Ye, A. C. Refakis et al., "Nitration of Hsp90 induces cell death," *Proceedings of the National Academy of Sciences of the United States of America*, vol. 110, no. 12, pp. E1102–E1111, 2013.

[10] R. P. Bazinet and S. Layé, "Polyunsaturated fatty acids and their metabolites in brain function and disease," *Nature Reviews Neuroscience*, vol. 15, no. 12, pp. 771–785, 2014.

[11] P. Schönfeld and G. Reiser, "why does brain metabolism not favor burning of fatty acids to provide energy? - reflections on disadvantages of the use of free fatty acids as fuel for brain," *Journal of Cerebral Blood Flow & Metabolism*, vol. 33, no. 10, pp. 1493–1499, 2013.

[12] J. N. Cobley, M. L. Fiorello, and D. M. Bailey, "13 reasons why the brain is susceptible to oxidative stress," *Redox Biology*, vol. 15, pp. 490–503, 2018.

[13] L. Vallee, "Iron and neurodevelopment," *Archives de pediatrie*, vol. 24, no. 5S, pp. 5S18–5S22, 2017.

[14] E. L. Que, D. W. Domaille, and C. J. Chang, "Metals in neurobiology: probing their chemistry and biology with molecular imaging," *Chemical Reviews*, vol. 39, pp. 1517–1549, 2008.

[15] R. Brigelius, R. Spottl, W. Bors, E. Lengfelder, M. Saran, and U. Weser, "Superoxide dismutase activity of low molecular weight Cu2+-chelates studied by pulse radiolysis," *FEBS Letters*, vol. 47, no. 1, pp. 72–75, 1974.

[16] D. Dwivedi, K. Megha, R. Mishra, and P. K. Mandal, "Glutathione in brain: overview of its conformations, functions, biochemical characteristics, quantitation and potential therapeutic role in brain disorders," *Neurochemical Research*, vol. 45, no. 7, pp. 1461–1480, 2020.

[17] P. S. Baxter and G. E. Hardingham, "Adaptive regulation of the brain's antioxidant defences by neurons and astrocytes," *Free Radical Biology and Medicine*, vol. 100, pp. 147–152, 2016.

[18] D. Jimenez-Blasco, P. Santofimia-Castano, A. Gonzalez, A. Almeida, and J. P. Bolanos, "Astrocyte NMDA receptors' activity sustains neuronal survival through a Cdk5-Nrf2 pathway," *Cell death & Differentiation*, vol. 22, pp. 1877–1889, 2015.

[19] J. H. Cabungcal, D. Nicolas, R. Kraftsik, M. Cuénod, K. Q. Do, and J.-P. Hornung, "Glutathione deficit during development induces anomalies in the rat anterior cingulate GABAergic neurons: relevance to schizophrenia," *Neurobiology of Disease*, vol. 22, no. 3, pp. 624–637, 2006.

[20] I. Bókkon and I. Anta, "Schizophrenia: redox regulation and volume neurotransmission," *Current Neuropharmacology*, vol. 9, no. 2, pp. 289–300, 2011.

[21] S. Fernandez-Fernandez, A. Almeida, and J. P. Bolaños, "Antioxidant and bioenergetic coupling between neurons and astrocytes," *Biochemical Journal*, vol. 443, no. 1, pp. 3–11, 2012.

[22] C. H. Lin and H. Y. Lane, "Early identification and intervention of schizophrenia: insight from hypotheses of glutamate dysfunction and oxidative stress," *Frontiers in Psychiatry*, vol. 10, p. 93, 2019.

[23] N. S. Kolomeets, "Role of astrocytes in alterations of glutamatergic neurotransmission in schizophrenia," *Zhurnal nevrologii i psikhiatrii im. S.S. Korsakova*, vol. 115, no. 1, pp. 110–117, 2015.

[24] G. E. Hardingham and K. Q. Do, "Linking early-life NMDAR hypofunction and oxidative stress in schizophrenia pathogenesis," *Nature Reviews Neuroscience*, vol. 17, no. 2, pp. 125–134, 2016.

[25] B. Todorich, J. M. Pasquini, C. I. Garcia, P. M. Paez, and J. R. Connor, "Oligodendrocytes and myelination: the role of iron," *Glia*, vol. 57, no. 5, pp. 467–478, 2009.

[26] L. Haider, "Inflammation, iron, energy failure, and oxidative stress in the pathogenesis of multiple sclerosis," *Oxidative Medicine and Cellular Longevity*, vol. 2015, Article ID 725370, 10 pages, 2015.

[27] F. Vilhardt, J. Haslund-Vinding, V. Jaquet, and G. McBean, "Microglia antioxidant systems and redox signaling," *British Journal of Pharmacology*, vol. 174, no. 12, pp. 1719–1732, 2017.

[28] M. L. Block, "NADPH oxidase as a therapeutic target in Alzheimer's disease," *BMC Neuroscience*, vol. 9, no. 2, article S8, 2008.

[29] S. Najjar, S. Pahlajani, V. De Sanctis, J. N. H. Stern, A. Najjar, and D. Chong, "Neurovascular unit dysfunction and blood–brain barrier hyperpermeability contribute to schizophrenia neurobiology: a theoretical integration of clinical and experimental evidence," *Frontiers in Psychiatry*, vol. 8, p. 83, 2017.

[30] S. Salim, "Oxidative stress and the central nervous system," *Journal of Pharmacology and Experimental Therapeutics*, vol. 360, no. 1, pp. 201–205, 2016.

[31] S. Fernandez-Fernandez, V. Bobo-Jimenez, R. Requejo-Aguilar et al., "Hippocampal neurons require a large pool of glutathione to sustain dendrite integrity and cognitive function," *Redox Biology*, vol. 19, pp. 52–61, 2018.

[32] W. S. Hambright, R. S. Fonseca, L. Chen, R. Na, and Q. Ran, "Ablation of ferroptosis regulator glutathione peroxidase 4 in forebrain neurons promotes cognitive impairment and neurodegeneration," *Redox Biology*, vol. 12, pp. 8–17, 2017.

[33] B. B. Andersen, H. J. G. Gundersen, and B. Pakkenberg, "Aging of the human cerebellum: a stereological study," *Journal of Comparative Neurology*, vol. 466, no. 3, pp. 356–365, 2003.

[34] A. Valencia and J. Morán, "Role of oxidative stress in the apoptotic cell death of cultured cerebellar granule neurons," *Journal of Neuroscience Research*, vol. 64, no. 3, pp. 284–297, 2001.

[35] J. K. Yao and M. S. Keshavan, "Antioxidants, redox signaling, and pathophysiology in schizophrenia: an integrative view," *Antioxidants & Redox Signaling*, vol. 15, no. 7, pp. 2011–2035, 2011.

[36] M. Boškovic, T. Vovk, B. K. Plesničar, and I. Grabnar, "Oxidative stress in schizophrenia," *Current Neuropharmacology*, vol. 9, no. 2, pp. 301–312, 2011.

[37] M. Koga, A. V. Serritella, A. Sawa, and T. W. Sedlak, "Implications for reactive oxygen species in schizophrenia pathogenesis," *Schizophrenia Research*, vol. 176, no. 1, pp. 52–71, 2016.

[38] M. Zhang, Z. M. Zhao, L. He, and C. L. Wan, "A meta-analysis of oxidative stress markers in schizophrenia," *Science China Life Sciences*, vol. 53, no. 1, pp. 112–124, 2010.

[39] S. Grignon and J. M. Chianetta, "Assessment of malondialdehyde levels in schizophrenia: a meta-analysis and some methodological considerations," *Progress in Neuro-Psychopharmacology and Biological Psychiatry*, vol. 31, no. 2, pp. 365–369, 2007.

[40] J. Flatow, P. Buckley, and B. J. Miller, "Meta-analysis of oxidative stress in schizophrenia," *Biological Psychiatry*, vol. 74, no. 6, pp. 400–409, 2013.

[41] W. P. Hoen, J. G. Lijmer, M. Duran, R. J. A. Wanders, N. J. M. van Beveren, and L. de Haan, "Red blood cell polyunsaturated fatty acids measured in red blood cells and schizophrenia: a meta-analysis," *Psychiatry Research*, vol. 207, no. 1-2, pp. 1–12, 2013.

[42] D. Wang, J. X. Zhai, and D. W. Liu, "Serum folate levels in schizophrenia: a meta-analysis," *Psychiatry Research*, vol. 235, pp. 83–89, 2016.

[43] D. Fraguas, C. M. Díaz-Caneja, A. Rodríguez-Quiroga, and C. Arango, "Oxidative stress and inflammation in early onset first episode psychosis: a systematic review and meta-analysis," *International Journal of Neuropsychopharmacology*, vol. 20, no. 6, pp. 435–444, 2017.

[44] Y. Tomioka, S. Numata, M. Kinoshita et al., "Decreased serum pyridoxal levels in schizophrenia: meta-analysis and Mendelian randomization analysis," *Journal of Psychiatry & Neuroscience*, vol. 43, no. 3, pp. 194–200, 2018.

[45] D. Fraguas, C. M. Díaz-Caneja, M. Ayora et al., "Oxidative stress and inflammation in first-episode psychosis: a systematic review and meta-analysis," *Schizophrenia Bulletin*, vol. 45, no. 4, pp. 742–751, 2019.

[46] A. F. Carvalho, M. Solmi, M. Sanches et al., "Evidence-based umbrella review of 162 peripheral biomarkers for major mental disorders," *Translational Psychiatry*, vol. 10, no. 1, pp. 1–13, 2020.

[47] M. Raffa, F. Atig, A. Mhalla, A. Kerkeni, and A. Mechri, "Decreased glutathione levels and impaired antioxidant enzyme activities in drug-naive first-episode schizophrenic patients," *BMC Psychiatry*, vol. 11, no. 1, article 124, 2011.

[48] R. Reddy, M. Keshavan, and J. K. Yao, "Reduced plasma antioxidants in first-episode patients with schizophrenia," *Schizophrenia Research*, vol. 62, no. 3, pp. 205–212, 2003.

[49] I. Altuntas, H. Aksoy, I. Coskun, A. Cayköylü, and F. Akçay, "Erythrocyte superoxide dismutase and glutathione peroxidase activities, and malondialdehyde and reduced glutathione levels in schizophrenic patients," *Clinical Chemistry and Laboratory Medicine*, vol. 38, no. 12, pp. 1277–1281, 2000.

[50] K. Q. Do, A. H. Trabesinger, M. Kirsten-Krüger et al., "Schizophrenia: glutathione deficit in cerebrospinal fluid and prefrontal cortex in vivo," *European Journal of Neuroscience*, vol. 12, no. 10, pp. 3721–3728, 2000.

[51] J. K. Yao, S. Leonard, and R. Reddy, "Altered glutathione redox state in schizophrenia," *Disease Markers*, vol. 22, no. 1-2, 93 pages, 2006.

[52] J. Kumar, E. B. Liddle, C. C. Fernandes et al., "Glutathione and glutamate in schizophrenia: a 7 T MRS study," *Molecular Psychiatry*, vol. 25, no. 4, pp. 873–882, 2020.

[53] S. Y. Kim, B. M. Cohen, X. Chen et al., "Redox dysregulation in schizophrenia revealed by in vivo NAD+/NADH measurement," *Schizophrenia Bulletin*, vol. 43, no. 1, pp. 197–204, 2017.

[54] V. A. Chouinard, S. Y. Kim, L. Valeri et al., "Brain bioenergetics and redox state measured by ^{31}P magnetic resonance spectroscopy in unaffected siblings of patients with psychotic disorders," *Schizophrenia Research*, vol. 187, pp. 11–16, 2017.

[55] P. Korge, G. Calmettes, and J. N. Weiss, "Increased reactive oxygen species production during reductive stress: the roles of mitochondrial glutathione and thioredoxin reductases," *Biochimica et Biophysica Acta (BBA) - Bioenergetics*, vol. 1847, no. 6-7, pp. 514–525, 2015.

[56] V. E. Golimbet, "The genetics of schizophrenia," *Zhurnal nevrologii i psikhiatrii imeni S.S. Korsakova*, vol. 3, pp. 58–67, 2003.

[57] I. Escudero and M. Johnstone, "Genetics of schizophrenia," *Current Psychiatry Reports*, vol. 16, no. 11, article 502, 2014.

[58] K. V. Chowdari, M. N. Bamne, and V. L. Nimgaonkar, "Genetic association studies of antioxidant pathway genes and schizophrenia," *Antioxidants & Redox Signaling*, vol. 15, no. 7, pp. 2037–2045, 2011.

[59] R. Gysin, R. Kraftsik, J. Sandell et al., "Impaired glutathione synthesis in schizophrenia: convergent genetic and functional evidence," *Proceedings of the National Academy of Sciences of the United States of America*, vol. 104, no. 42, pp. 16621–16626, 2007.

[60] J. Ma, D. M. Li, R. Zhang et al., "Genetic analysis of glutamate cysteine ligase modifier (GCLM) gene and schizophrenia in Han Chinese," *Schizophrenia Research*, vol. 119, no. 1-3, pp. 273-274, 2010.

[61] M. Tosic, J. Ott, S. Barral et al., "Schizophrenia and oxidative stress: glutamate cysteine ligase modifier as a susceptibility gene," *The American Journal of Human Genetics*, vol. 79, no. 3, pp. 586–592, 2006.

[62] B. Rodríguez-Santiago, A. Brunet, B. Sobrino et al., "Association of common copy number variants at the glutathione S-transferase genes and rare novel genomic changes with schizophrenia," *Molecular Psychiatry*, vol. 15, no. 10, pp. 1023–1033, 2010.

[63] P. Gravina, I. Spoletini, S. Masini et al., "Genetic polymorphisms of glutathione S-transferases GSTM1, GSTT1, GSTP1 and GSTA1 as risk factors for schizophrenia," *Psychiatry Research*, vol. 187, no. 3, pp. 454–456, 2011.

[64] Y. Ci, D. Li, F. Chunfeng et al., "Association between glutathione S-transferase (GST) polymorphisms and schizophrenia in a Chinese Han population," *Neuropsychiatric Disease and Treatment*, vol. 16, pp. 479–487, 2020.

[65] C. Liu, S. Song, J. Zhang, X. Li, and H. Gao, "Effects of GSTA1 and GPX3 polymorphisms on the risk of schizophrenia in Chinese Han population," *Neuropsychiatric Disease and Treatment*, vol. 16, pp. 113–118, 2020.

[66] T. Shinkai, V. De Luca, G. Zai et al., "No association between the Pro197Leu polymorphism in the glutathione peroxidase (GPX1) gene and schizophrenia," *Psychiatric Genetics*, vol. 14, no. 3, pp. 177–180, 2004.

[67] A. F. Y. Al Hadithy, S. A. Ivanova, P. Pechlivanoglou et al., "Missense polymorphisms in three oxidative-stress enzymes (GSTP1, SOD2, and GPX1) and dyskinesias in Russian psychiatric inpatients from Siberia," *Human Psychopharmacology: Clinical and Experimental*, vol. 25, no. 1, pp. 84–91, 2010.

[68] P. Gałecki, T. Pietras, and J. Szemraj, "Manganese superoxide dismutase gene (MnSOD) polimorphism in schizophrenics with tardive dyskinesia from central Poland," *Psychiatria Polska*, vol. 40, no. 5, pp. 937–948, 2006.

[69] H. Hori, O. Ohmori, T. Shinkai et al., "Manganese superoxide dismutase gene polymorphism and schizophrenia: relation to tardive dyskinesia," *Neuropsychopharmacology*, vol. 23, no. 2, pp. 170–177, 2000.

[70] A. Hitzeroth, D. J. H. Niehaus, L. Koen, W. C. Botes, J. F. Deleuze, and L. Warnich, "Association between the MnSOD Ala-9Val polymorphism and development of schizophrenia and abnormal involuntary movements in the Xhosa population," *Progress in Neuro-Psychopharmacology and Biological Psychiatry*, vol. 31, no. 3, pp. 664–672, 2007.

[71] Z. Zhang, X. Zhang, G. Hou, W. W. Sha, and G. P. Reynolds, "The increased activity of plasma manganese superoxide dismutase in tardive dyskinesia is unrelated to the Ala-9Val polymorphism," *Journal of Psychiatric Research*, vol. 36, no. 5, pp. 317–324, 2002.

[72] C. U. Pae, T. S. Kim, A. A. Patkar et al., "Manganese superoxide dismutase (MnSOD: Ala–9Val) gene polymorphism may not be associated with schizophrenia and tardive dyskinesia," *Psychiatry Research*, vol. 153, no. 1, pp. 77–81, 2007.

[73] S. G. Kang, J. E. Choi, H. An et al., "Manganese superoxide dismutase gene Ala–9Val polymorphism might be related to the severity of abnormal involuntary movements in Korean schizophrenic patients," *Progress in Neuro-Psychopharmacology and Biological Psychiatry*, vol. 32, no. 8, pp. 1844–1847, 2008.

[74] C. C. Zai, A. K. Tiwari, V. Basile et al., "Oxidative stress in tardive dyskinesia: genetic association study and meta-analysis of NADPH quinine oxidoreductase 1 (NQO1) and superoxide dismutase 2 (SOD2, MnSOD) genes," *Progress in Neuro-Psychopharmacology and Biological Psychiatry*, vol. 34, no. 1, pp. 50–56, 2010.

[75] H. Liu, C. Wang, P. H. Chen et al., "Association of the manganese superoxide dismutase gene Ala–9Val polymorphism with clinical phenotypes and tardive dyskinesia in schizophrenic patients," *Progress in Neuro-Psychopharmacology and Biological Psychiatry*, vol. 34, no. 4, pp. 692–696, 2010.

[76] J. K. Park, H. K. Lee, G. H. Bahn, J. D. Park, J. H. Chung, and H. I. Chang, "The association between Korean schizophrenics and catalase gene polymorphism," *Korean Journal of Biological Psychiatry*, vol. 9, no. 1, pp. 62–67, 2002.

[77] M. Bošković, T. Vovk, M. Saje et al., "Association of SOD2, GPX1, CAT, and TNF genetic polymorphisms with oxidative stress, neurochemistry, psychopathology, and extrapyramidal symptoms in schizophrenia," *Neurochemical research*, vol. 38, no. 2, pp. 433–442, 2013.

[78] S. Mostafa, S. Safaie, and I. Saadat, "Genetic polymorphism of C-262T catalase and susceptibility to schizophrenia," *Macedonian Journal of Medical Sciences*, vol. 7, no. 1, pp. 74–77, 2014.

[79] C. Walss-Bass, M. C. Soto-Bernardini, T. Johnson-Pais et al., "Methionine sulfoxide reductase: a novel schizophrenia candidate gene," *American Journal of Medical Genetics Part B: Neuropsychiatric Genetics*, vol. 150, no. 2, pp. 219–225, 2009.

[80] X. Ma, W. Deng, X. Liu et al., "A genome-wide association study for quantitative traits in schizophrenia in China," *Genes, Brain and Behavior*, vol. 10, no. 7, pp. 734–739, 2011.

[81] J. Moskovitz, C. Walss-Bass, D. A. Cruz, P. M. Thompson, and M. Bortolato, "Methionine sulfoxide reductase regulates brain catechol-O-methyl transferase activity," *International Journal of Neuropsychopharmacology*, vol. 17, no. 10, pp. 1707–1713, 2014.

[82] R. F. Nasyrova, D. V. Ivashchenko, M. V. Ivanov, and N. G. Neznanov, "Role of nitric oxide and related molecules in schizophrenia pathogenesis: biochemical, genetic and clinical aspects," *Frontiers in physiology*, vol. 6, p. 139, 2015.

[83] R. M. Marchbanks, M. Ryan, I. N. M. Day, M. Owen, P. McGuffin, and S. A. Whatley, "A mitochondrial DNA sequence variant associated with schizophrenia and oxidative stress," *Schizophrenia Research*, vol. 65, no. 1, pp. 33–38, 2003.

[84] B. Verge, Y. Alonso, J. Valero, C. Miralles, E. Vilella, and L. Martorell, "Mitochondrial DNA (mtDNA) and schizophrenia," *European Psychiatry*, vol. 26, no. 1, pp. 45–56, 2011.

[85] P. A. Thomson, N. R. Wray, J. K. Millar et al., "Association between the TRAX/DISC locus and both bipolar disorder and schizophrenia in the Scottish population," *Molecular Psychiatry*, vol. 10, no. 7, pp. 657–668, 2005.

[86] J. E. Chubb, N. J. Bradshaw, D. C. Soares, D. J. Porteous, and J. K. Millar, "The DISC locus in psychiatric illness," *Molecular Psychiatry*, vol. 13, no. 1, pp. 36–64, 2008.

[87] R. James, R. R. Adams, and S. Christie, "Disrupted in Schizophrenia 1 (DISC1) is a multicompartmentalized protein that predominantly localizes to mitochondria," *Molecular and Cellular Neuroscience*, vol. 26, no. 1, pp. 112–122, 2004.

[88] International Schizophrenia Consortium, S. M. Purcell, and N. R. Wray, "Common polygenic variation contributes to risk

of schizophrenia and bipolar disorder," *Nature*, vol. 460, no. 7256, pp. 748–752, 2009.

[89] The Schizophrenia Psychiatric Genome-Wide Association Study (GWAS) Consortium, "Genome-wide association study identifies five new schizophrenia loci," *Nature Genetics*, vol. 43, no. 10, pp. 969–976, 2011.

[90] S. Ripke, C. O'Dushlaine, K. Chambert et al., "Genome-wide association analysis identifies 13 new risk loci for schizophrenia," *Nature Genetics*, vol. 45, no. 10, pp. 1150–1159, 2013.

[91] Schizophrenia Working Group of the Psychiatric Genomics Consortium, "Biological insights from 108 schizophrenia-associated genetic loci," *Nature*, vol. 511, no. 7510, pp. 421–427, 2014.

[92] The Brainstorm Consortium, "Analysis of shared heritability in common disorders of the brain," *Science*, vol. 360, no. 6395, article eaap8757, 2018.

[93] K. Mirnics, F. A. Middleton, A. Marquez, D. A. Lewis, and P. Levitt, "Molecular characterization of schizophrenia viewed by microarray analysis of gene expression in prefrontal cortex," *Neuron*, vol. 28, no. 1, pp. 53–67, 2000.

[94] S. J. Glatt, I. P. Everall, W. S. Kremen et al., "Comparative gene expression analysis of blood and brain provides concurrent validation of SELENBP1 up-regulation in schizophrenia," *Proceedings of the National Academy of Sciences of the United States of America*, vol. 102, no. 43, pp. 15533–15538, 2005.

[95] M. Fromer, P. Roussos, S. K. Sieberts et al., "Gene expression elucidates functional impact of polygenic risk for schizophrenia," *Nature Neuroscience*, vol. 19, no. 11, pp. 1442–1453, 2016.

[96] C. Chen, Q. Meng, Y. Xia et al., "The transcription factor POU3F2 regulates a gene coexpression network in brain tissue from patients with psychiatric disorders," *Science Translational Medicine*, vol. 10, no. 472, article eaat8178, 2018.

[97] M. Li, G. Santpere, Y. I. Kawasawa et al., "Integrative functional genomic analysis of human brain development and neuropsychiatric risks," *Science*, vol. 362, no. 6420, article eaat7615, 2018.

[98] M. J. Gandal, P. Zhang, E. Hadjimichael et al., "Transcriptome-wide isoform-level dysregulation in ASD, schizophrenia, and bipolar disorder," *Science*, vol. 362,, no. 6420, article eaat8127, 2018.

[99] M. L. Seney, K. Cahill, J. F. Enwright 3rd et al., "Diurnal rhythms in gene expression in the prefrontal cortex in schizophrenia," *Nature Communications*, vol. 10, no. 1, pp. 1–11, 2019.

[100] J. M. Nascimento and D. Martins-de-Souza, "The proteome of schizophrenia," *npj Schizophrenia*, vol. 1, no. 1, pp. 1–11, 2015.

[101] K. Davalieva, I. M. Kostovska, and A. J. Dwork, "Proteomics research in schizophrenia," *Frontiers in Cellular Neuroscience*, vol. 10, p. 18, 2016.

[102] L. Smirnova, A. Seregin, I. Boksha et al., "The difference in serum proteomes in schizophrenia and bipolar disorder," *BMC Genomics*, vol. 20, no. 7, article 535, 2019.

[103] S. Prabakaran, J. E. Swatton, M. M. Ryan et al., "Mitochondrial dysfunction in schizophrenia: evidence for compromised brain metabolism and oxidative stress," *Molecular Psychiatry*, vol. 9, no. 7, pp. 684–697, 2004.

[104] T. Sweet, B. E. Sawaya, K. Khalili, and S. Amini, "Interplay between NFBP and NF-κB modulates tat activation of the LTR," *Journal of Cellular Physiology*, vol. 204, no. 2, pp. 375–380, 2005.

[105] Q. Li, J. Yan, A. P. Mao et al., "Tripartite motif 8 (TRIM8) modulates TNFα- and IL-1β-triggered NF-κB activation by targeting TAK1 for K63-linked polyubiquitination," *Proceedings of the National Academy of Sciences of the United States of America*, vol. 108, no. 48, pp. 19341–19346, 2011.

[106] W. Masashi and S. Hatakeyama, "TRIM proteins and diseases," *Journal of Biochemistry*, vol. 161, no. 2, pp. 135–144, 2017.

[107] M. U. Gibbons and B. Dean, "Non-coding RNA as novel players in the pathophysiology of schizophrenia," *Noncoding RNA*, vol. 4, no. 2, p. 11, 2018.

[108] M. S. Leisegang, K. Schröder, and P. R. Brandes, "Redox regulation and noncoding RNAs," *Antioxidants & Redox Signaling*, vol. 29, no. 9, pp. 793–812, 2018.

[109] N. Mellios, M. Galdzicka, E. Ginns et al., "Gender-specific reduction of estrogen-sensitive small RNA, miR-30b, in subjects with schizophrenia," *Schizophrenia Bulletin*, vol. 38, no. 3, pp. 433–443, 2012.

[110] N. J. Beveridge, E. Gardiner, A. P. Carroll, P. A. Tooney, and M. J. Cairns, "Schizophrenia is associated with an increase in cortical microRNA biogenesis," *Molecular Psychiatry*, vol. 15, no. 12, pp. 1176–1189, 2010.

[111] H. Ghazaryan, R. Zakharyan, M. Petrek et al., "Expression of micro-RNAs miR-31, miR-146a, miR-181c and miR-155 and their target gene IL-2 are altered in schizophrenia: a case-control study," *F1000Research*, vol. 8, no. 2077, p. 2077, 2019.

[112] L. Smigielski, V. Jagannath, W. Rössler, S. Walitza, and E. Grünblatt, "Epigenetic mechanisms in schizophrenia and other psychotic disorders: a systematic review of empirical human findings," *Molecular Psychiatry*, vol. 25, pp. 1718–1748, 2020.

[113] C. Espinosa-Diez, V. Miguel, D. Mennerich et al., "Antioxidant responses and cellular adjustments to oxidative stress," *Redox Biology*, vol. 6, pp. 183–197, 2015.

[114] D. B. Oskvig, A. G. Elkahloun, K. R. Johnson, T. M. Phillips, and M. Herkenham, "Maternal immune activation by LPS selectively alters specific gene expression profiles of interneuron migration and oxidative stress in the fetus without triggering a fetal immune response," *Brain, Behavior, and Immunity*, vol. 26, no. 4, pp. 623–634, 2012.

[115] A. M. Feoli, I. R. Siqueira, L. Almeida et al., "Effects of protein malnutrition on oxidative status in rat brain," *Nutrition*, vol. 22, no. 2, pp. 160–165, 2006.

[116] Z. V. Niatsetskaya, S. A. Sosunov, D. Matsiukevich et al., "The oxygen free radicals originating from mitochondrial complex I contribute to oxidative brain injury following hypoxia–ischemia in neonatal mice," *Journal of Neuroscience*, vol. 32, no. 9, pp. 3235–3244, 2012.

[117] D. Eyles, L. Almeras, P. Benech et al., "Developmental vitamin D deficiency alters the expression of genes encoding mitochondrial, cytoskeletal and synaptic proteins in the adult rat brain," *The Journal of Steroid Biochemistry and Molecular Biology*, vol. 103, no. 3-5, pp. 538–545, 2007.

[118] J. J. McGrath, D. W. Eyles, C. B. Pedersen et al., "Neonatal vitamin D status and risk of schizophrenia: a population-based case-control study," *Archives of General Psychiatry*, vol. 67, no. 9, pp. 889–894, 2010.

[119] A. R. Soares, K. R. Gildawie, J. A. Honeycutt, and H. C. Brenhouse, "Region-specific effects of maternal separation on

oxidative stress accumulation in parvalbumin neurons of male and female rats," *Behavioural Brain Research*, vol. 388, article 112658, 2020.

[120] Z. Zhu, X. Li, W. Chen et al., "Prenatal stress causes gender-dependent neuronal loss and oxidative stress in rat hippocampus," *Journal of Neuroscience Research*, vol. 78, no. 6, pp. 837–844, 2004.

[121] D. Malaspina, C. Corcoran, K. R. Kleinhaus et al., "Acute maternal stress in pregnancy and schizophrenia in offspring: a cohort prospective study," *BMC psychiatry*, vol. 8, no. 1, article 71, 2008.

[122] Z. Jiang, G. R. Rompala, S. Zhang, R. M. Cowell, and K. Nakazawa, "Social isolation exacerbates schizophrenia-like phenotypes via oxidative stress in cortical interneurons," *Biological Psychiatry*, vol. 73, no. 10, pp. 1024–1034, 2013.

[123] S. Schiavone, S. Sorce, M. Dubois-Dauphin et al., "Involvement of NOX2 in the development of behavioral and pathologic alterations in isolated rats," *Biological Psychiatry*, vol. 66, no. 4, pp. 384–392, 2009.

[124] N. P. Maric and D. M. Svrakic, "Why schizophrenia genetics needs epigenetics: a review," *Psychiatria Danubina*, vol. 24, no. 1, pp. 2–18, 2012.

[125] J. Richetto and U. Meyer, "Epigenetic modifications in schizophrenia and related disorders: molecular scars of environmental exposures and source of phenotypic variability," *Biological Psychiatry*, vol. 89, no. 3, pp. 215–226, 2021.

[126] C. C. Winterbourn and M. B. Hampton, "Thiol chemistry and specificity in redox signaling," *Free Radical Biology and Medicine*, vol. 45, no. 5, pp. 549–561, 2008.

[127] P. D. Ray, B. W. Huang, and Y. Tsuji, "Reactive oxygen species (ROS) homeostasis and redox regulation in cellular signaling," *Cellular Signaling*, vol. 24, no. 5, pp. 981–990, 2012.

[128] M. Schieber and N. S. Chandel, "ROS function in redox signaling and oxidative stress," *Current biology*, vol. 24, no. 10, pp. R453–R462, 2014.

[129] H. J. Forman, J. M. Fukuto, and M. Torres, "Redox signaling: thiol chemistry defines which reactive oxygen and nitrogen species can act as second messengers," *American Journal of Physiology-Cell Physiology*, vol. 287, no. 2, pp. C246–C256, 2004.

[130] R. Matsui, B. Ferran, A. Oh et al., "Redox regulation via glutaredoxin-1 and protein S-glutathionylation," *Antioxidants & Redox Signaling*, vol. 32, no. 10, pp. 677–700, 2020.

[131] K. M. Holmström and T. Finkel, "Cellular mechanisms and physiological consequences of redox-dependent signalling," *Nature reviews Molecular Cell Biology*, vol. 15, no. 6, pp. 411–421, 2014.

[132] D. O. Perkins, C. D. Jeffries, and K. Q. Do, "Potential roles of redox dysregulation in the development of schizophrenia," *Biological Psychiatry*, vol. 88, no. 4, pp. 326–336, 2020.

[133] J. Kumar, E. B. Liddle, C. C. Fernandes et al., "Glutathione and glutamate in schizophrenia: a 7T MRS study," *Molecular Psychiatry*, vol. 25, no. 4, pp. 873–882, 2020.

[134] A. Salmeen and D. Barford, "Functions and mechanisms of redox regulation of cysteine-based phosphatases," *Antioxidants & Redox Signaling*, vol. 7, no. 5-6, pp. 560–577, 2005.

[135] V. Calabrese, C. Cornelius, A. T. Dinkova-Kostova, E. J. Calabrese, and M. P. Mattson, "Cellular stress responses, the hormesis paradigm, and vitagenes: novel targets for therapeutic intervention in neurodegenerative disorders," *Antioxidants & Redox Signaling*, vol. 13, no. 11, pp. 1763–1811, 2010.

[136] V. Calabrese, C. Cornelius, L. Maiolino et al., "Oxidative stress, redox homeostasis and cellular stress response in Ménière's disease: role of vitagenes," *Neurochemical Research*, vol. 35, no. 12, pp. 2208–2217, 2010.

[137] E. J. Calabrese, I. Iavicoli, and V. Calabrese, "Hormesis," *Human & Experimental Toxicology*, vol. 32, no. 2, pp. 120–152, 2013.

[138] V. Calabrese, M. Renis, A. Calderone, A. Russo, M. L. Barcellona, and V. Rizza, "Stress proteins and SH-groups in oxidant-induced cell damage after acute ethanol administration in rat," *Free Radical Biology and Medicine*, vol. 20, no. 3, pp. 391–397, 1996.

[139] G. V. Shmarina, M. D. Orlova, E. S. Ershova et al., "NRF2 and HMOX1 gene expression against the background of systemic oxidative stress in patients with acute psychosis," *Russian Journal of Genetics*, vol. 56, no. 1, pp. 96–102, 2020.

[140] J. C. Zhang, W. Yao, C. Dong, M. Han, Y. Shirayama, and K. Hashimoto, "Keap1–Nrf2 signaling pathway confers resilience versus susceptibility to inescapable electric stress," *European Archives of Psychiatry and Clinical Neuroscience*, vol. 268, no. 8, pp. 865–870, 2018.

[141] K. Lingappan, "NF-κB in oxidative stress," *Current Opinion in Toxicology*, vol. 7, pp. 81–86, 2018.

[142] D. W. Volk, A. E. Moroco, K. M. Roman, J. R. Edelson, and D. A. Lewis, "The role of the nuclear factor-κB transcriptional complex in cortical immune activation in schizophrenia," *Biological Psychiatry*, vol. 85, no. 1, pp. 25–34, 2019.

[143] L. O. Klotz, C. Sánchez-Ramos, I. Prieto-Arroyo, P. Urbánek, H. Steinbrenner, and M. Monsalve, "Redox regulation of FoxO transcription factors," *Redox Biology*, vol. 6, pp. 51–72, 2015.

[144] W. Zhou, L. Chen, S. Yang, F. Li, and X. Li, "Behavioral stress-induced activation of FoxO3a in the cerebral cortex of mice," *Biological Psychiatry*, vol. 71, no. 7, pp. 583–592, 2012.

[145] E. S. Emamian, D. Hall, M. J. Birnbaum, M. Karayiorgou, and J. A. Gogos, "Convergent evidence for impaired AKT1-GSK3β signaling in schizophrenia," *Nature Genetics*, vol. 36, no. 2, pp. 131–137, 2004.

[146] R. Chadha and J. H. Meador-Woodruff, "Downregulated AKT-mTOR signaling pathway proteins in dorsolateral prefrontal cortex in schizophrenia," *Neuropsychopharmacology*, vol. 45, no. 6, pp. 1059–1067, 2020.

[147] A. J. Funk, R. E. McCullumsmith, V. Haroutunian, and J. H. Meador-Woodruff, "Abnormal activity of the MAPK- and cAMP-associated signaling pathways in frontal cortical areas in postmortem brain in schizophrenia," *Neuropsychopharmacology*, vol. 37, no. 4, pp. 896–905, 2012.

[148] J. M. Beaulieu, R. R. Gainetdinov, and M. G. Caron, "The Akt-GSK-3 signaling cascade in the actions of dopamine," *Trends in Pharmacological Sciences*, vol. 28, no. 4, pp. 166–172, 2007.

[149] Z. Zeng, X. Wang, S. K. Bhardwaj et al., "The atypical antipsychotic agent, clozapine, protects against corticosterone-induced death of PC12 cells by regulating the Akt/FoxO3a Signaling pathway," *Molecular Neurobiology*, vol. 54, no. 5, pp. 3395–3406, 2017.

[150] T. B. Dansen, L. M. M. Smits, M. H. van Triest et al., "Redox-sensitive cysteines bridge p300/CBP-mediated acetylation and FoxO4 activity," *Nature Chemical Biology*, vol. 5, no. 9, pp. 664–672, 2009.

[151] A. Brunet, L. B. Sweeney, J. F. Sturgill et al., "Stress-dependent regulation of FOXO transcription factors by the SIRT1 deacetylase," *Science*, vol. 303, no. 5666, pp. 2011–2015, 2004.

[152] H. D. Kim, J. Hesterman, T. Call et al., "SIRT1 mediates depression-like behaviors in the nucleus accumbens," *Journal of Neuroscience*, vol. 36, no. 32, pp. 8441–8452, 2016.

[153] X. Fang, Y. Chen, Y. Wang, J. Ren, and C. Zhang, "Depressive symptoms in schizophrenia patients: a possible relationship between SIRT1 and BDNF," *Progress in Neuro- Psychopharmacology and Biological Psychiatry*, vol. 95, article 109673, 2019.

[154] D. Liao, Y. Chen, Y. Guo et al., "Salvianolic acid B improves chronic mild stress-induced depressive behaviors in rats: involvement of AMPK/SIRT1 signaling pathway," *Journal of Inflammation Research*, vol. Volume 13, pp. 195–206, 2020.

[155] J. Wang, H. R. Song, M. N. Guo et al., "PGC-1α regulate critical period plasticity via gene × environment interaction in the developmental trajectory to schizophrenia," *Biochemical and Biophysical Research Communications*, vol. 525, no. 4, pp. 989–996, 2020.

[156] L. J. McMeekin, E. K. Lucas, J. H. Meador-Woodruff et al., "Cortical PGC-1α-dependent transcripts are reduced in post-mortem tissue from patients with schizophrenia," *Schizophrenia Bulletin*, vol. 42, no. 4, pp. 1009–1017, 2016.

[157] D. R. Weinberger, "Implications of normal brain development for the pathogenesis of schizophrenia," *Archives of General Psychiatry*, vol. 44, no. 7, pp. 660–669, 1987.

[158] S. W. Lewis and R. M. Murray, "Obstetric complications, neurodevelopmental deviance, and risk of schizophrenia," *Journal of Psychiatric Research*, vol. 21, no. 4, pp. 413–421, 1987.

[159] R. M. Murray, V. Bhavsar, G. Tripoli, and O. Howes, "30 years on: how the neurodevelopmental hypothesis of schizophrenia morphed into the developmental risk factor model of psychosis," *Schizophrenia Bulletin*, vol. 43, no. 6, pp. 1190–1196, 2017.

[160] H. M. Sallis, J. Croft, A. Havdahl et al., "Genetic liability to schizophrenia is associated with exposure to traumatic events in childhood," *Psychological Medicine*, pp. 1–8, 2020.

[161] A. S. Brown, P. Cohen, J. Harkavy-Friedman et al., "Prenatal rubella, premorbid abnormalities, and adult schizophrenia," *Biological Psychiatry*, vol. 49, no. 6, pp. 473–486, 2001.

[162] S. L. Buka, M. T. Tsuang, E. F. Torrey, M. A. Klebanoff, R. L. Wagner, and R. H. Yolken, "Maternal cytokine levels during pregnancy and adult psychosis," *Brain, Behavior, and Immunity*, vol. 15, no. 4, pp. 411–420, 2001.

[163] B. Osburg, C. Peiser, D. Dömling et al., "Effect of endotoxin on expression of TNF receptors and transport of TNF-α at the blood-brain barrier of the rat," *American Journal of Physiology-Endocrinology and Metabolism*, vol. 283, no. 5, pp. E899–E908, 2002.

[164] L. De Biase, P. Pignatelli, L. Lenti et al., "Enhanced TNFα and oxidative stress in patients with heart failure: effect of TNFα on platelet O2 - production," *Thrombosis and Haemostasis*, vol. 90, no. 8, pp. 317–325, 2017.

[165] P. Boksa, "Effects of prenatal infection on brain development and behavior: a review of findings from animal models," *Brain, Behavior, and Immunity*, vol. 24, no. 6, pp. 881–897, 2010.

[166] L. R. Simões, G. Sangiogo, M. H. Tashiro et al., "Maternal immune activation induced by lipopolysaccharide triggers immune response in pregnant mother and fetus, and induces behavioral impairment in adult rats," *Journal of Psychiatric Research*, vol. 100, pp. 71–83, 2018.

[167] P. Singh, S. K. Agnihotri, M. C. Tewari, S. Kumar, M. Sachdev, and R. K. Tripathi, "HIV-1 Nef breaches placental barrier in rat model," *PLoS One*, vol. 7, no. 12, article e51518, 2012.

[168] M. W. Glynn, B. M. Elmer, P. A. Garay et al., "MHCI negatively regulates synapse density during the establishment of cortical connections," *Nature Neuroscience*, vol. 14, no. 4, pp. 442–451, 2011.

[169] M. L. Estes and A. K. McAllister, "Immune mediators in the brain and peripheral tissues in autism spectrum disorder," *Nature Reviews Neuroscience*, vol. 16, no. 8, pp. 469–486, 2015.

[170] H. Lee, B. K. Brott, L. A. Kirkby et al., "Synapse elimination and learning rules co-regulated by MHC class I H2-D^{b}," *Nature*, vol. 509, no. 7499, pp. 195–200, 2014.

[171] A. González-Quintela, M. J. Dominguez-Santalla, L. F. Pérez, C. Vidal, S. Lojo, and E. Barrio, "Influence of acute alcohol intake and alcohol withdrawal on circulating levels of IL-6, IL-8, IL-10 AND IL-12.," *Cytokine*, vol. 12, no. 9, pp. 1437–1440, 2000.

[172] D. J. Knapp, K. M. Harper, B. A. Whitman, Z. Zimomra, and G. R. Breese, "Stress and withdrawal from chronic ethanol induce selective changes in neuroimmune mRNAs in differing brain sites," *Brain Sciences*, vol. 6, no. 3, p. 25, 2016.

[173] T. L. Doremus-Fitzwater, H. M. Buck, K. Bordner, L. Richey, M. E. Jones, and T. Deak, "Intoxication- and withdrawal-dependent expression of central and peripheral cytokines following initial ethanol exposure," *Alcoholism: Clinical and Experimental Research*, vol. 38, no. 8, pp. 2186–2198, 2014.

[174] A. V. Solonsky, V. D. Prokopieva, and E. G. Yarygina, "Neuromorphological and molecular effects of ethanol," *Siberian Herald of Psychiatry and Addiction Psychiatry*, vol. 2, no. 99, pp. 28–32, 2018.

[175] N. Kapoor, A. B. Pant, A. Dhawan et al., "Differences in sensitivity of cultured rat brain neuronal and glial cytochrome P450 2E1 to ethanol," *Life Sciences*, vol. 79, no. 16, pp. 1514–1522, 2006.

[176] Y. Zhong, G. Dong, H. Luo et al., "Induction of brain CYP2E1 by chronic ethanol treatment and related oxidative stress in hippocampus, cerebellum, and brainstem," *Toxicology*, vol. 302, no. 2-3, pp. 275–284, 2012.

[177] S. A. Marshall, J. A. McClain, M. L. Kelso, D. M. Hopkins, J. R. Pauly, and K. Nixon, "Microglial activation is not equivalent to neuroinflammation in alcohol- induced neurodegeneration: The importance of microglia phenotype," *Neurobiology of Disease*, vol. 54, pp. 239–251, 2013.

[178] F. Akhtar, C. A. Rouse, G. Catano et al., "Acute maternal oxidant exposure causes susceptibility of the fetal brain to inflammation and oxidative stress," *Neuroinflammation*, vol. 14, no. 1, article 195, 2017.

[179] L. Aye, S. Lager, V. I. Ramirez et al., "Increasing maternal body mass index is associated with systemic inflammation in the mother and the activation of distinct placental inflammatory pathways," *Biology of Reproduction*, vol. 90, no. 6, p. 129, 2014.

[180] Y. Hatanaka, K. Wada, and T. Kabuta, "Maternal high-fat diet leads to persistent synaptic instability in mouse offspring via oxidative stress during lactation," *Neurochemistry International*, vol. 97, pp. 99–108, 2016.

[181] A. G. Edlow, N. L. Vora, L. Hui, H. C. Wick, J. M. Cowan, and D. W. Bianchi, "Maternal obesity affects fetal neurodevelopmental and metabolic gene expression: a pilot study," *PLoS One*, vol. 9, no. 2, article e88661, 2014.

[182] E. A. Thomas, D. L. Copolov, and J. G. Sutcliffe, "From pharmacotherapy to pathophysiology: emerging mechanisms of apolipoprotein D in psychiatric disorders," *Current Molecular Medicine*, vol. 3, no. 5, pp. 408–418, 2003.

[183] M. Shang, X. Dong, and L. Hou, "Correlation of adipokines and markers of oxidative stress in women with gestational diabetes mellitus and their newborns," *Journal of Obstetrics and Gynaecology*, vol. 44, no. 4, pp. 637–646, 2018.

[184] M. Jamilian, N. Mirhosseini, M. Eslahi et al., "The effects of magnesium-zinc-calcium-vitamin D co-supplementation on biomarkers of inflammation, oxidative stress and pregnancy outcomes in gestational diabetes," *BMC Pregnancy Childbirth*, vol. 19, no. 1, article 107, 2019.

[185] J. L. Rains and S. K. Jain, "Oxidative stress, insulin signaling, and diabetes," *Free Radical Biology and Medicine*, vol. 50, no. 5, pp. 567–575, 2011.

[186] D. Bitsanis, K. Ghebremeskel, T. Moodley, M. A. Crawford, and O. Djahanbakhch, "Gestational diabetes mellitus enhances arachidonic and docosahexaenoic acids in placental phospholipids," *Lipids*, vol. 41, no. 4, pp. 341–346, 2006.

[187] N. Chakraborty, S. Muhie, R. Kumar et al., "Contributions of polyunsaturated fatty acids (PUFA) on cerebral neurobiology: an integrated omics approach with epigenomic focus," *Journal of Nutritional Biochemistry*, vol. 42, pp. 84–94, 2017.

[188] K. Hamazaki, M. Maekawa, T. Toyota et al., "Fatty acid composition and fatty acid binding protein expression in the postmortem frontal cortex of patients with schizophrenia: a case-control study," *Schizophrenia Research*, vol. 171, no. 1-3, pp. 225–232, 2016.

[189] W. A. Cass, G. Larson, F. A. Fitzpatrick, and N. R. Zahniser, "Inhibitors of arachidonic acid metabolism: effects on rat striatal dopamine release and uptake," *Journal of Pharmacology and Experimental Therapeutics*, vol. 257, no. 3, pp. 990–996, 1991.

[190] I. A. Reddy, J. A. Pino, P. Weikop et al., "Glucagon-like peptide 1 receptor activation regulates cocaine actions and dopamine homeostasis in the lateral septum by decreasing arachidonic acid levels," *Translational Psychiatry*, vol. 6, no. 5, p. e809, 2016.

[191] S. M. Eick, E. S. Barrett, T. J. van 't Erve et al., "Association between prenatal psychological stress and oxidative stress during pregnancy," *Paediatric and Perinatal Epidemiology*, vol. 32, no. 4, pp. 318–326, 2018.

[192] F. H. Holland, P. Ganguly, D. N. Potter, E. H. Chartoff, and H. C. Brenhouse, "Early life stress disrupts social behavior and prefrontal cortex parvalbumin interneurons at an earlier time-point in females than in males," *Neuroscience letters Supplement*, vol. 566, pp. 131–136, 2014.

[193] M. Colaianna, S. Schiavone, M. Zotti et al., "Neuroendocrine profile in a rat model of psychosocial stress: relation to oxidative stress," *Antioxidants & Redox Signaling*, vol. 18, no. 12, pp. 1385–1399, 2013.

[194] J. Vetulani, "Early maternal separation: a rodent model of depression and a prevailing human condition," *Pharmacological Reports*, vol. 65, no. 6, pp. 1451–1461, 2013.

[195] I. Valli, N. A. Crossley, F. Day et al., "HPA-axis function and grey matter volume reductions: imaging the diathesis- stress model in individuals at ultra-high risk of psychosis," *Translational Psychiatry*, vol. 6, no. 5, p. e797, 2016.

[196] A. Egerton, L. R. Valmaggia, O. D. Howes et al., "Adversity in childhood linked to elevated striatal dopamine function in adulthood," *Schizophrenia Research*, vol. 176, no. 2-3, pp. 171–176, 2016.

[197] F. Adriano, C. Caltagirone, and G. Spalletta, "Hippocampal volume reduction in first-episode and chronic schizophrenia: a review and meta-analysis," *Neuroscientist*, vol. 18, no. 2, pp. 180–200, 2012.

[198] A. Rajasekaran, G. Venkatasubramanian, M. Berk, and M. Debnath, "Mitochondrial dysfunction in schizophrenia: pathways, mechanisms and implications," *Neuroscience & Biobehavioral Reviews*, vol. 48, pp. 10–21, 2015.

[199] D. Ben-Shachar, "Mitochondrial dysfunction in schizophrenia: a possible linkage to dopamine," *Journal of neurochemistry*, vol. 83, no. 6, pp. 1241–1251, 2002.

[200] D. Ben-Shachar, "Mitochondrial multifaceted dysfunction in schizophrenia; complex I as a possible pathological target," *Schizophrenia Research*, vol. 187, pp. 3–10, 2017.

[201] P. Ni and S. Chung, "Mitochondrial dysfunction in schizophrenia," *BioEssays*, vol. 42, no. 6, article e1900202, 2020.

[202] N. Uranova, D. Orlovskaya, O. Vikhreva et al., "Electron microscopy of oligodendroglia in severe mental illness," *Brain Research Bulletin*, vol. 55, no. 5, pp. 597–610, 2001.

[203] I. Maurer, S. Zierz, and H. J. Möller, "Evidence for a mitochondrial oxidative phosphorylation defect in brains from patients with schizophrenia," *Schizophrenia Research*, vol. 48, no. 1, pp. 125–136, 2001.

[204] F. du, A. J. Cooper, T. Thida et al., "In vivo evidence for cerebral bioenergetic abnormalities in schizophrenia measured using 31P magnetization transfer spectroscopy," *JAMA Psychiatry*, vol. 71, no. 1, pp. 19–27, 2014.

[205] J. E. Jensen, J. Miller, P. C. Williamson et al., "Grey and white matter differences in brain energy metabolism in first episode schizophrenia: ^{31}P-MRS chemical shift imaging at 4 Tesla," *Psychiatry Research: Neuroimaging*, vol. 146, no. 2, pp. 127–135, 2006.

[206] G. Nedic Erjavec, M. Konjevod, M. Nikolac Perkovic et al., "Short overview on metabolomic approach and redox changes in psychiatric disorders," *Redox biology*, vol. 14, pp. 178–186, 2018.

[207] J. F. Enwright III, Z. Huo, D. Arion, J. P. Corradi, G. Tseng, and D. A. Lewis, "Transcriptome alterations of prefrontal cortical parvalbumin neurons in schizophrenia," *Molecular Psychiatry*, vol. 23, no. 7, pp. 1606–1613, 2018.

[208] M. Mistry, J. Gillis, and P. Pavlidis, "Meta-analysis of gene coexpression networks in the post-mortem prefrontal cortex of patients with schizophrenia and unaffected controls," *BMC neuroscience*, vol. 14, no. 1, p. 105, 2013.

[209] M. J. Gandal, J. R. Haney, N. N. Parikshak et al., "Shared molecular neuropathology across major psychiatric disorders parallels polygenic overlap," *Science*, vol. 359, no. 6376, pp. 693–697, 2018.

[210] E. K. Lucas, S. J. Markwardt, S. Gupta et al., "Parvalbumin deficiency and GABAergic dysfunction in mice lacking *PGC-1*," *Journal of Neuroscience*, vol. 30, no. 21, pp. 7227–7235, 2010.

[211] M. Inan, M. Zhao, M. Manuszak et al., "Energy deficit in parvalbumin neurons leads to circuit dysfunction, impaired sensory gating and social disability," *Neurobiology of disease*, vol. 93, pp. 35–46, 2016.

[212] Y. Jouroukhin, Y. Kageyama, V. Misheneva et al., "DISC1 regulates lactate metabolism in astrocytes: implications for psychiatric disorders," *Translational Psychiatry*, vol. 8, no. 1, pp. 1–12, 2018.

[213] P. Devaraju, J. Yu, D. Eddins et al., "Haploinsufficiency of the 22q11.2 microdeletion gene *Mrpl40* disrupts short-term synaptic plasticity and working memory through dysregulation of mitochondrial calcium," *Molecular Psychiatry*, vol. 22, no. 9, pp. 1313–1326, 2017.

[214] A. Fernandez, D. W. Meechan, B. A. Karpinski et al., "Mitochondrial dysfunction leads to cortical under-connectivity and cognitive impairment," *Neuron*, vol. 102, no. 6, pp. 1127–1142.e3, 2019.

[215] O. Robicsek, H. M. Ene, R. Karry et al., "Isolated mitochondria transfer improves neuronal differentiation of schizophrenia-derived induced pluripotent stem cells and rescues deficits in a rat model of the disorder," *Schizophrenia Bulletin*, vol. 44, no. 2, pp. 432–442, 2018.

[216] R. D. Fields, "White matter in learning, cognition and psychiatric disorders," *Trends in Neurosciences*, vol. 31, no. 7, pp. 361–370, 2008.

[217] V. Haroutunian, P. Katsel, P. Roussos, K. L. Davis, L. L. Altshuler, and G. Bartzokis, "Myelination, oligodendrocytes, and serious mental illness," *Glia*, vol. 62, no. 11, pp. 1856–1877, 2014.

[218] P. I. Yakovlev, A. R. Lecours, A. Minkowski, and F. A. Davis, "Regional development of the brain in early life," pp. 3–70, 1967.

[219] H. Grydeland, K. B. Walhovd, C. K. Tamnes, L. T. Westlye, and A. M. Fjell, "Intracortical myelin links with performance variability across the human lifespan: results from T1- and T2-weighted MRI myelin mapping and diffusion tensor imaging," *Journal of Neuroscience*, vol. 33, no. 47, pp. 18618–18630, 2013.

[220] S. Mensch, M. Baraban, R. Almeida et al., "Synaptic vesicle release regulates myelin sheath number of individual oligodendrocytes *in vivo*," *Nature Neuroscience*, vol. 18, no. 5, pp. 628–630, 2015.

[221] E. M. Gibson, D. Purger, C. W. Mount et al., "Neuronal activity promotes oligodendrogenesis and adaptive myelination in the mammalian brain," *Science*, vol. 344, no. 6183, p. 1252304, 2014.

[222] P. Kochunov, D. E. Williamson, J. Lancaster et al., "Fractional anisotropy of water diffusion in cerebral white matter across the lifespan," *Neurobiology of Aging*, vol. 33, no. 1, pp. 9–20, 2012.

[223] D. Gouvêa-Junqueira, A. C. B. Falvella, A. S. L. M. Antunes et al., "Novel treatment strategies targeting myelin and oligodendrocyte dysfunction in schizophrenia," *Frontiers in Psychiatry*, vol. 11, no. 379, 2020.

[224] S. E. Wahl, L. E. McLane, K. K. Bercury, W. B. Macklin, and T. L. Wood, "Mammalian target of rapamycin promotes oligodendrocyte differentiation, initiation and extent of CNS myelination," *The Journal of Neuroscience*, vol. 34, no. 13, pp. 4453–4465, 2014.

[225] K. Azim and A. M. Butt, "GSK3β negatively regulates oligodendrocyte differentiation and myelination *in vivo*," *Glia*, vol. 59, no. 4, pp. 540–553, 2011.

[226] A. Ishii, M. Furusho, J. L. Dupree, and R. Bansal, "Role of ERK1/2 MAPK signaling in the maintenance of myelin and axonal integrity in the adult CNS," *The Journal of Neuroscience*, vol. 34, no. 48, pp. 16031–16045, 2014.

[227] A. Ishii, M. Furusho, W. Macklin, and R. Bansal, "Independent and cooperative roles of the Mek/ERK1/2-MAPK and PI3K/Akt/mTOR pathways during developmental myelination and in adulthood," *Glia*, vol. 67, no. 7, pp. 1277–1295, 2019.

[228] Z. Li, T. Dong, C. Pröschel, and M. Noble, "Chemically diverse toxicants converge on Fyn and c-Cbl to disrupt precursor cell function," *PLoS Biology*, vol. 5, no. 2, article e35, 2007.

[229] D. A. Maas, A. Vallès, and G. J. M. Martens, "Oxidative stress, prefrontal cortex hypomyelination and cognitive symptoms in schizophrenia," *Translational Psychiatry*, vol. 7, no. 7, article e1171, 2017.

[230] N. A. Uranova, N. S. Kolomeets, O. V. Vikhreva, I. S. Zimina, V. I. Rachmanova, and D. D. Orlovskaya, "Ultrastructural pathology of myelinated fibers in schizophrenia," *Zhurnal nevrologii i psikhiatrii imeni SS Korsakova*, vol. 113, no. 9, pp. 63–69, 2013.

[231] C. L. Beasley, A. J. Dwork, G. Rosoklija et al., "Metabolic abnormalities in fronto-striatal-thalamic white matter tracts in schizophrenia," *Schizophrenia Research*, vol. 109, no. 1-3, pp. 159–166, 2009.

[232] M. Y. Deng, G. M. McAlonan, C. Cheung et al., "A naturalistic study of grey matter volume increase after early treatment in anti-psychotic naïve, newly diagnosed schizophrenia," *Psychopharmacology*, vol. 206, no. 3, pp. 437–446, 2009.

[233] H. G. Bernstein, A. Ortmann, H. Dobrowolny et al., "Bilaterally reduced claustral volumes in schizophrenia and major depressive disorder: a morphometric postmortem study," *European Archives of Psychiatry and Clinical Neuroscience*, vol. 266, no. 1, pp. 25–33, 2016.

[234] J. H. Cabungcal, P. Steullet, A. Frank et al., "Redox dysregulation affects parvalbumine interneuron's integrity and neural synchronisation in ventral but not dorsal hippocampus," *Schizophrenia Research*, vol. 2, no. 117, p. 388, 2010.

[235] N. S. Kolomeets and N. A. Uranova, "Pathology of oligodendroglia and myelinated fibers of the hippocampus in schizophrenia (an ultrastructural and morphometric study)," *Zhurnal nevrologii i psikhiatrii imeni SS Korsakova*, vol. 108, no. 8, pp. 52–60, 2008.

[236] Y. Hao, Q. Yan, H. Liu et al., "Schizophrenia patients and their healthy siblings share disruption of white matter integrity in the left prefrontal cortex and the hippocampus but not the anterior cingulate cortex," *Schizophrenia Research*, vol. 114, no. 1-3, pp. 128–135, 2009.

[237] J. X. Wilson, "Antioxidant defense of the brain: a role for astrocytes," *Canadian journal of physiology and pharmacology*, vol. 75, no. 10-11, pp. 1149–1163, 1997.

[238] B. Back, K. Sere, and H. Vanharanta, "Managing complexity in large data bases using self-organizing maps," *Accounting Management and Information Technologies*, vol. 8, no. 4, pp. 191–210, 1998.

[239] U. Fünfschilling, L. M. Supplie, D. Mahad et al., "Glycolytic oligodendrocytes maintain myelin and long-term axonal integrity," *Nature*, vol. 485, no. 7399, pp. 517–521, 2012.

[240] B. H. Toyama and M. W. Hetzer, "Protein homeostasis: live long, won't prosper," *Nature reviews Molecular Cell Biology*, vol. 14, no. 1, pp. 55–61, 2013.

[241] J. Hirrlinger and K. A. Nave, "Adapting brain metabolism to myelination and long-range signal transduction," *Glia*, vol. 62, no. 11, pp. 1749–1761, 2014.

[242] B. Liu, X. Chen, Z. Q. Wang, and W. M. J. Tong, "DNA damage and oxidative injury are associated with hypomyelination in the corpus callosum of newborn Nbn CNS-del mice," *Journal of Neuroscience Research*, vol. 92, no. 2, pp. 254–266, 2014.

[243] E. Stephenson, N. Nathoo, Y. Mahjoub, J. F. Dunn, and V. W. Yong, "Iron in multiple sclerosis: roles in neurodegeneration and repair," *Nature Reviews Neurology*, vol. 10, no. 8, pp. 459–468, 2014.

[244] J. Li, F. Cao, H. L. Yin et al., "Ferroptosis: past, present and future," *Cell Death & Disease*, vol. 11, no. 2, pp. 1–13, 2020.

[245] S. Hametner, I. Wimmer, L. Haider, S. Pfeifenbring, W. Brück, and H. Lassmann, "Iron and neurodegeneration in the multiple sclerosis brain," *Annals of neurology*, vol. 74, no. 6, pp. 848–861, 2013.

[246] V. Bergink, S. M. Gibney, and H. A. Drexhage, "Autoimmunity, inflammation, and psychosis: a search for peripheral markers," *Biological Psychiatry*, vol. 75, no. 4, pp. 324–331, 2014.

[247] G. M. Khandaker, L. Cousins, J. Deakin, B. R. Lennox, R. Yolken, and P. B. Jones, "Inflammation and immunity in schizophrenia: implications for pathophysiology and treatment," *The Lancet Psychiatry*, vol. 2, no. 3, pp. 258–270, 2015.

[248] J. Haslund-Vinding, G. McBean, V. Jaquet, and F. Vilhardt, "NADPH oxidases in oxidant production by microglia: activating receptors, pharmacology and association with disease," *British Journal of Pharmacology*, vol. 174, no. 12, pp. 1733–1749, 2017.

[249] G. Z. Réus, G. R. Fries, L. Stertz et al., "The role of inflammation and microglial activation in the pathophysiology of psychiatric disorders," *Neuroscience*, vol. 300, pp. 141–154, 2015.

[250] M. L. Block, L. Zecca, and J. S. Hong, "Microglia-mediated neurotoxicity: uncovering the molecular mechanisms," *Nature Reviews Neuroscience*, vol. 8, no. 1, pp. 57–69, 2007.

[251] S. Pacquelet, J. L. Johnson, B. A. Ellis et al., "Cross-talk between IRAK-4 and the NADPH oxidase," *Biochemical Journal*, vol. 403, no. 3, pp. 451–461, 2007.

[252] C. S. Jack, N. Arbour, J. Manusow et al., "TLR signaling tailors innate immune responses in human microglia and astrocytes," *Journal of Immunology*, vol. 175, no. 7, pp. 4320–4330, 2005.

[253] E. A. Bordt and B. M. Polster, "NADPH oxidase- and mitochondria-derived reactive oxygen species in proinflammatory microglial activation: a bipartisan affair?," *Free Radical Biology and Medicine*, vol. 76, pp. 34–46, 2014.

[254] S. H. Choi, S. Aid, H. W. Kim, S. H. Jackson, and F. Bosetti, "Inhibition of NADPH oxidase promotes alternative and anti-inflammatory microglial activation during neuroinflammation," *Journal of neurochemistry*, vol. 120, no. 2, pp. 292–301, 2012.

[255] A. V. Miletic, D. B. Graham, V. Montgrain et al., "Vav proteins control MyD88-dependent oxidative burst," *Blood*, vol. 109, pp. 3360–3368, 2006.

[256] S. W. Wong, M. J. Kwon, A. M. Choi, H. P. Kim, K. Nakahira, and D. H. Hwang, "Fatty acids modulate Toll-like receptor 4 activation through regulation of receptor dimerization and recruitment into lipid rafts in a reactive oxygen species-dependent manner," *Journal of Biological Chemistry*, vol. 284, no. 40, pp. 27384–27392, 2009.

[257] C. S. Yang, D. M. Shin, H. M. Lee et al., "ASK1-p38 MAPK-p47phox activation is essential for inflammatory responses during tuberculosis via TLR2-ROS signalling," *Cellular Microbiology*, vol. 10, no. 3, pp. 741–754, 2008.

[258] L. Qin, Y. Liu, T. Wang et al., "NADPH oxidase mediates lipopolysaccharide-induced neurotoxicity and proinflammatory gene expression in activated microglia," *Journal of Biological Chemistry*, vol. 279, no. 2, pp. 1415–1421, 2004.

[259] D. P. Schafer, E. K. Lehrman, A. G. Kautzman et al., "Microglia Sculpt Postnatal Neural Circuits in an Activity and Complement- Dependent Manner," *Neuron*, vol. 74, no. 4, pp. 691–705, 2012.

[260] B. Linnartz, J. Kopatz, A. J. Tenner, and H. Neumann, "Sialic acid on the neuronal glycocalyx prevents complement C1 binding and complement receptor-3-mediated removal by microglia," *The Journal of Neuroscience*, vol. 32, no. 3, pp. 946–952, 2012.

[261] B. Linnartz and H. Neumann, "Microglial activatory (immunoreceptor tyrosine-based activation motif)- and inhibitory (immunoreceptor tyrosine-based inhibition motif)-signaling receptors for recognition of the neuronal glycocalyx," *Glia*, vol. 61, no. 1, pp. 37–46, 2013.

[262] C. Madry and D. Attwell, "Receptors, ion channels, and signaling mechanisms underlying microglial dynamics," *Journal of Biological Chemistry*, vol. 290, no. 20, pp. 12443–12450, 2015.

[263] G. Martel-Gallegos, G. Casas-Pruneda, F. Ortega-Ortega et al., "Oxidative stress induced by P2X7 receptor stimulation in murine macrophages is mediated by c-Src/Pyk2 and ERK1/2," *Biochimica et Biophysica Acta*, vol. 1830, no. 10, pp. 4650–4659, 2013.

[264] R. L. Stornetta and J. J. Zhu, "Ras and Rap signaling in synaptic plasticity and mental disorders," *The Neuroscientist*, vol. 17, no. 1, pp. 54–78, 2011.

[265] A. M. Kaindl, V. Degos, S. Peineau et al., "Activation of microglial N-methyl-D-aspartate receptors triggers inflammation and neuronal cell death in the developing and mature brain," *Annals of Neurology*, vol. 72, no. 4, pp. 536–549, 2012.

[266] H. J. Palmer and K. E. Paulson, "Reactive oxygen species and antioxidants in signal transduction and gene expression," *Nutrition Reviews*, vol. 55, no. 10, pp. 353–361, 1997.

[267] H. Kamata, S. Honda, S. Maeda, L. Chang, H. Hirata, and M. Karin, "Reactive Oxygen Species Promote TNFα-Induced Death and Sustained JNK Activation by Inhibiting MAP Kinase Phosphatases," *Cell*, vol. 120, no. 5, pp. 649–661, 2005.

[268] J. J. Haddad and S. C. Land, "Redox/ROS regulation of lipopolysaccharide-induced mitogen-activated protein kinase (MAPK) activation and MAPK-mediated TNF-α biosynthesis," *British Journal of Pharmacology*, vol. 135, no. 2, pp. 520–536, 2002.

[269] R. Fischer and O. Maier, "Interrelation of oxidative stress and inflammation in neurodegenerative disease: role of TNF," *Oxidative medicine and cellular longevity*, vol. 2015, Article ID 610813, 18 pages, 2015.

[270] D. R. Goldsmith, E. Haroon, A. H. Miller, G. P. Strauss, P. F. Buckley, and B. J. Miller, "TNF-α and IL-6 are associated with the deficit syndrome and negative symptoms in patients with chronic schizophrenia," *Schizophrenia research*, vol. 199, pp. 281–284, 2018.

[271] D. I. Lurie, "An integrative approach to neuroinflammation in psychiatric disorders and neuropathic pain," *Journal of experimental neuroscience*, vol. 12, 2018.

[272] S. Momtazmanesh, A. Zare-Shahabadi, and N. Rezaei, "Cytokine alterations in schizophrenia: an updated review," *Frontiers in Psychiatry*, vol. 10, p. 892, 2019.

[273] R. Upthegrove and G. M. Khandaker, "Cytokines, oxidative stress and cellular markers of inflammation in schizophrenia," *Current Topics in Behavioral Neurosciences*, vol. 44, pp. 49–66, 2019.

[274] R. Dantzer and A. K. Walker, "Is there a role for glutamate-mediated excitotoxicity in inflammation-induced depression?," *Journal of Neural Transmission*, vol. 121, no. 8, pp. 925–932, 2014.

[275] W. Hu, M. L. Macdonald, D. E. Elswick, and R. A. Sweet, "The glutamate hypothesis of schizophrenia: evidence from human brain tissue studies," *Annals of the New York Academy of Sciences*, vol. 1338, no. 1, pp. 38–57, 2015.

[276] A. K. Al-Asmari and M. W. Khan, "Inflammation and schizophrenia: alterations in cytokine levels and perturbation in antioxidative defense systems," *Human & Experimental Toxicology*, vol. 33, no. 2, pp. 115–122, 2014.

[277] U. Ratnayake, T. Quinn, D. Walker, and H. Dickinson, "Cytokines and the neurodevelopmental basis of mental illness," *Frontiers in Neuroscience*, vol. 7, p. 180, 2013.

[278] H. Takeuchi, S. Jin, J. Wang et al., "Tumor necrosis factor-α induces neurotoxicity via glutamate release from hemichannels of activated microglia in an autocrine manner," *Journal of Biological Chemistry*, vol. 281, no. 30, pp. 21362–21368, 2006.

[279] M. Conrad and H. Sato, "The oxidative stress-inducible cystine/glutamate antiporter, system x_c^-: cystine supplier and beyond," *Amino Acids*, vol. 42, no. 1, pp. 231–246, 2012.

[280] G. M. Khandaker and R. Dantzer, "Is there a role for immune-to-brain communication in schizophrenia?," *Psychopharmacology*, vol. 233, no. 9, pp. 1559–1573, 2016.

[281] A. Kulak, P. Steullet, J. H. Cabungcal et al., "Redox dysregulation in the pathophysiology of schizophrenia and bipolar disorder: insights from animal models," *Antioxidants & Redox Signaling*, vol. 18, no. 12, pp. 1428–1443, 2013.

[282] X. Y. Zhang, D. F. Zhou, L. Y. Qi et al., "Superoxide dismutase and cytokines in chronic patients with schizophrenia: association with psychopathology and response to antipsychotics," *Psychopharmacology*, vol. 204, no. 1, pp. 177–184, 2009.

[283] E. A. Ermakov, G. A. Nevinsky, and V. N. Buneva, "Immunoglobulins with non-canonical functions in inflammatory and autoimmune disease states," *International Journal of Molecular Sciences*, vol. 21, no. 15, p. 5392, 2020.

[284] E. A. Ermakov, L. P. Smirnova, N. A. Bokhan et al., "Catalase activity of IgG antibodies from the sera of healthy donors and patients with schizophrenia," *PLoS One*, vol. 12, no. 9, article e0183867, 2017.

[285] A. S. Tolmacheva, E. A. Blinova, E. A. Ermakov, V. N. Buneva, N. L. Vasilenko, and G. A. Nevinsky, "IgG abzymes with peroxidase and oxidoreductase activities from the sera of healthy humans," *Journal of Molecular Recognition*, vol. 28, no. 9, pp. 565–580, 2015.

[286] A. S. Tolmacheva, E. A. Ermakov, V. N. Buneva, and G. A. Nevinsky, "Substrate specificity of healthy human sera IgG antibodies with peroxidase and oxydoreductase activities," *Royal Society Open Science*, vol. 5, no. 1, article 171097, 2018.

[287] L. P. Smirnova, I. A. Mednova, N. M. Krotenko, V. M. Alifirova, and S. A. Ivanova, "IgG-dependent dismutation of superoxide in patients with different types of multiple sclerosis and healthy subjects," *Oxidative Medicine and Cellular Longevity*, vol. 2020, Article ID 8171020, 11 pages, 2020.

[288] G. C. Castellani, E. M. Quinlan, L. N. Cooper, and H. Z. Shouval, "A biophysical model of bidirectional synaptic plasticity: dependence on AMPA and NMDA receptors," *Proceedings of the National Academy of Sciences*, vol. 98, no. 22, pp. 2772–12777, 2001.

[289] M. Zhuo, S. A. Small, E. R. Kandel, and R. D. Hawkins, "Nitric oxide and carbon monoxide produce activity-dependent long-term synaptic enhancement in hippocampus," *Science*, vol. 260, no. 5116, pp. 1946–1950, 1993.

[290] R. S. Zucker, "Calcium- and activity-dependent synaptic plasticity," *Current Opinion in Neurobiology*, vol. 9, no. 3, pp. 305–313, 1999.

[291] D. Attwell and S. B. J. Laughlin, "An energy budget for signaling in the grey matter of the brain," *Journal of Cerebral Blood Flow & Metabolism*, vol. 21, no. 10, pp. 1133–1145, 2001.

[292] M. V. Accardi, B. A. Daniels, P. M. G. E. Brown, J. M. Fritschy, S. K. Tyagarajan, and D. Bowie, "Mitochondrial reactive oxygen species regulate the strength of inhibitory GABA-mediated synaptic transmission," *Nature Communications*, vol. 5, no. 1, pp. 1–12, 2014.

[293] D. Ben-Shachar and D. Laifenfeld, "Mitochondria, synaptic plasticity, and schizophrenia," *International Review of Neurobiology*, vol. 59, pp. 273–296, 2004.

[294] A. Kumar, B. Yegla, and T. C. Foster, "Redox signaling in neurotransmission and cognition during aging," *Antioxidants & Redox Signaling*, vol. 28, no. 18, pp. 1724–1745, 2018.

[295] J. G. Nicholls, A. R. Martin, B. G. Wallace, and P. A. Fuchs, *From Neuron to Brain*, Sinauer Associates, Sunderland (MA), 5th edition, 2012.

[296] K. Raju, P. T. Doulias, P. Evans et al., "Regulation of brain glutamate metabolism by nitric oxide and S-nitrosylation," *Science Signaling*, vol. 8, no. 384, pp. ra68–ra68, 2015.

[297] M. M. Behrens, S. S. Ali, D. N. Dao et al., "Ketamine-induced loss of phenotype of fast-spiking interneurons is mediated by NADPH-oxidase," *Science*, vol. 318, no. 5856, pp. 1645–1647, 2007.

[298] A. M. Brennan, S. Won Suh, S. Joon Won et al., "NADPH oxidase is the primary source of superoxide induced by NMDA receptor activation," *Nature Neuroscience*, vol. 12, no. 7, pp. 857–863, 2009.

[299] I. J. Reynolds and T. G. Hastings, "Glutamate induces the production of reactive oxygen species in cultured forebrain neurons following NMDA receptor activation," *The Journal of Neuroscience*, vol. 15, no. 5, pp. 3318–3327, 1995.

[300] M. Urushitani, Tomoki, Nakamizo et al., "N-Methyl-D-aspartate receptor-mediated mitochondrial Ca^{2+} overload in acute excitotoxic motor neuron death: a mechanism distinct from chronic neurotoxicity after Ca^{2+} influx," *Journal of Neuroscience Research*, vol. 63, no. 5, pp. 377–387, 2001.

[301] H. Takahashi, Y. Shin, S. J. Cho et al., "Hypoxia enhances S-nitrosylation-mediated NMDA receptor inhibition via a thiol oxygen sensor motif," *Neuron*, vol. 53, no. 1, pp. 53–64, 2007.

[302] C. Lu, S. L. Chan, N. Haughey, W. T. Lee, and M. P. Mattson, "Selective and biphasic effect of the membrane lipid peroxidation product 4-hydroxy-2,3-nonenal on N-methyl-D-aspartate channels," *Journal of Neurochemistry*, vol. 78, no. 3, pp. 577–589, 2001.

[303] H. W. Kessels and R. Malinow, "Synaptic AMPA receptor plasticity and behavior," *Neuron*, vol. 61, no. 3, pp. 340–350, 2009.

[304] J. Tucholski, M. S. Simmons, A. L. Pinner, V. Haroutunian, R. E. McCullumsmith, and J. H. Meador-Woodruff, "Abnormal N-linked glycosylation of cortical AMPA receptor subunits in schizophrenia," *Schizophrenia Research*, vol. 146, no. 1-3, pp. 177–183, 2013.

[305] P. Steullet, J. H. Cabungcal, A. Monin et al., "Redox dysregulation, neuroinflammation, and NMDA receptor hypofunction: A "central hub" in schizophrenia pathophysiology?," *Schizophrenia Research*, vol. 176, no. 1, pp. 41–51, 2016.

[306] Z. H. Pan, X. Zhang, and S. A. Lipton, "Redox modulation of recombinant human $GABA_A$ receptors," *Neuroscience*, vol. 98, no. 2, pp. 333–338, 2000.

[307] A. Penna, D. S. Wang, J. Yu et al., "Hydrogen peroxide increases $GABA_A$ receptor-mediated tonic current in hippocampal neurons," *The Journal of Neuroscience*, vol. 34, no. 32, pp. 10624–10634, 2014.

[308] J. E. Lisman, J. T. Coyle, R. W. Green et al., "Circuit-based framework for understanding neurotransmitter and risk gene interactions in schizophrenia," *Trends in Neurosciences*, vol. 31, no. 5, pp. 234–242, 2008.

[309] A. Kathuria, K. Lopez-Lengowski, B. Watmuff, D. McPhie, B. M. Cohen, and R. Karmacharya, "Synaptic deficits in iPSC-derived cortical interneurons in schizophrenia are mediated by NLGN2 and rescued by *N*-acetylcysteine," *Translational Psychiatry*, vol. 9, no. 1, article 321, 2019.

[310] I. Miyazaki and M. Asanuma, "Dopaminergic neuron-specific oxidative stress caused by dopamine itself," *Acta Medica Okayama*, vol. 62, no. 3, pp. 141–150, 2008.

[311] F. A. Zucca, J. Segura-Aguilar, E. Ferrari et al., "Interactions of iron, dopamine and neuromelanin pathways in brain aging and Parkinson's disease," *Progress in Neurobiology*, vol. 155, pp. 96–119, 2017.

[312] W. A. Spencer, J. Jeyabalan, S. Kichambre, and R. C. Gupta, "Oxidatively generated DNA damage after Cu(II) catalysis of dopamine and related catecholamine neurotransmitters and neurotoxins: role of reactive oxygen species," *Free Radical Biology and Medicine*, vol. 50, no. 1, pp. 139–147, 2011.

[313] X. Wang, A. Pinto-Duarte, T. J. Sejnowski, and M. M. Behrens, "How Nox2-containing NADPH oxidase affects cortical circuits in the NMDA receptor antagonist model of schizophrenia," *Antioxidants & Redox Signaling*, vol. 18, no. 12, pp. 1444–1462, 2013.

[314] H. Homayoun and B. Moghaddam, "NMDA receptor hypofunction produces opposite effects on prefrontal cortex interneurons and pyramidal neurons," *The Journal of Neuroscience*, vol. 27, no. 43, pp. 11496–11500, 2007.

[315] J. L. Madrigal, S. Kalinin, J. C. Richardson, and D. L. Feinstein, "Neuroprotective actions of noradrenaline: effects on glutathione synthesis and activation of peroxisome proliferator activated receptor delta," *Journal of Neurochemistry*, vol. 103, no. 5, pp. 2092–2101, 2007.

[316] J. D. Troadec, M. Marien, F. Darios et al., "Noradrenaline provides long-term protection to dopaminergic neurons by reducing oxidative stress," *Journal of Neurochemistry*, vol. 79, no. 1, pp. 200–210, 2001.

[317] E. M. Blanc, J. F. Kelly, R. J. Mark, G. Waeg, and M. P. Mattson, "4-Hydroxynonenal, an aldehydic product of lipid peroxidation, impairs signal transduction associated with muscarinic acetylcholine and metabotropic glutamate receptors: possible action on $G\alpha_{q/11}$," *Journal of Neurochemistry*, vol. 69, no. 2, pp. 570–580, 1997.

[318] A. V. Terry Jr., "Role of the central cholinergic system in the therapeutics of schizophrenia," *Current Neuropharmacology*, vol. 6, no. 3, pp. 286–292, 2008.

[319] A. Abi-Dargham, M. Laruelle, G. K. Aghajanian, D. Charney, and J. Krystal, "The role of serotonin in the pathophysiology and treatment of schizophrenia," *The Journal of Neuropsychiatry and Clinical Neurosciences*, vol. 9, no. 1, pp. 1–17, 1997.

[320] T. C. Westfall and V. Tittermary, "Inhibition of the electrically induced release of [^{3}H]dopamine by serotonin from superfused rat striatal slices," *Neuroscience Letters*, vol. 28, no. 2, pp. 205–209, 1982.

[321] P. De Deurwaerdère, M. L'hirondel, N. Bonhomme, G. Lucas, A. X. Cheramy, and U. Spampinato, "Serotonin stimulation of 5-HT4 receptors indirectly enhances *in vivo* dopamine release in the rat striatum," *Journal of Neurochemistry*, vol. 68, no. 1, pp. 195–203, 1997.

[322] D. A. Lewis, A. A. Curley, J. R. Glausier, and D. W. Volk, "Cortical parvalbumin interneurons and cognitive dysfunction in schizophrenia," *Trends in Neurosciences*, vol. 35, no. 1, pp. 57–67, 2012.

[323] Y. Kawaguchi, H. Katsumaru, T. Kosaka, C. W. Heizmann, and K. Hama, "Fast spiking cells in rat hippocampus (CA_1 region) contain the calcium-binding protein parvalbumin," *Brain Research*, vol. 416, no. 2, pp. 369–374, 1987.

[324] M. Müller, F. Felmy, B. Schwaller, and R. Schneggenburger, "Parvalbumin is a mobile presynaptic Ca^{2+} buffer in the calyx of Held that accelerates the decay of Ca^{2+} and short-term facilitation," *Journal of Neuroscience*, vol. 27, no. 9, pp. 2261–2271, 2007.

[325] J. M. McNally and R. W. McCarley, "Gamma band oscillations: a key to understanding schizophrenia symptoms and neural circuit abnormalities," *Current Opinion in Psychiatry*, vol. 29, no. 3, pp. 202–210, 2016.

[326] J. Song, J. Sun, J. Moss et al., "Parvalbumin interneurons mediate neuronal circuitry-neurogenesis coupling in the adult hippocampus," *Nature Neuroscience*, vol. 16, no. 12, pp. 1728–1730, 2013.

[327] A. Caballero, E. Flores-Barrera, D. R. Thomases, and K. Y. Tseng, "Downregulation of parvalbumin expression in the prefrontal cortex during adolescence causes enduring prefrontal disinhibition in adulthood," *Neuropsychopharmacology*, vol. 45, no. 9, pp. 1527–1535, 2020.

[328] A. J. Murray, M. U. Woloszynowska-Fraser, L. Ansel-Bollepalli et al., "Parvalbumin-positive interneurons of the prefrontal cortex support working memory and cognitive flexibility," *Scientific Reports*, vol. 5, no. 1, article 16778, 2015.

[329] J. J. Harris, R. Jolivet, and D. Attwell, "Synaptic energy use and supply," *Neuron*, vol. 75, no. 5, pp. 762–777, 2012.

[330] J. H. Cabungcal, P. Steullet, H. Morishita et al., "Perineuronal nets protect fast-spiking interneurons against oxidative stress," *Proceedings of the National Academy of Sciences of the United States of America*, vol. 110, no. 22, pp. 9130–9135, 2013.

[331] L. A. Hasam-Henderson, G. C. Gotti, M. Mishto et al., "NMDA-receptor inhibition and oxidative stress during hippocampal maturation differentially alter parvalbumin expression and gamma-band activity," *Scientific Reports*, vol. 8, no. 1, article 9545, 2018.

[332] Z. Jiang, R. M. Cowell, and K. Nakazawa, "Convergence of genetic and environmental factors on parvalbumin-positive interneurons in schizophrenia," *Frontiers in Behavioral Neuroscience*, vol. 7, p. 116, 2013.

[333] W. Härtig, A. Derouiche, K. Welt et al., "Cortical neurons immunoreactive for the potassium channel Kv3.1b subunit are predominantly surrounded by perineuronal nets presumed as a buffering system for cations," *Brain Research*, vol. 842, no. 1, pp. 15–29, 1999.

[334] H. Morishita, M. Kundakovic, L. Bicks, A. Mitchell, and S. Akbarian, "Interneuron epigenomes during the critical period of cortical plasticity: implications for schizophrenia," *Neurobiology of Learning and Memory*, vol. 124, pp. 104–110, 2015.

[335] H. Lin, F. C. Hsu, B. H. Baumann, D. A. Coulter, S. A. Anderson, and D. R. Lynch, "Cortical parvalbumin GABAergic deficits with $\alpha 7$ nicotinic acetylcholine receptor deletion: implications for schizophrenia," *Molecular and Cellular Neuroscience*, vol. 61, pp. 163–175, 2014.

[336] J. Egea, I. Buendia, E. Parada, E. Navarro, R. Leon, and M. G. Lopez, "Anti-inflammatory role of microglial alpha7 nAChRs and its role in neuroprotection," *Biochemical Pharmacology*, vol. 97, no. 4, pp. 463–472, 2015.

[337] P. Fazzari, A. V. Paternain, M. Valiente et al., "Control of cortical GABA circuitry development by Nrg1 and ErbB4 signalling," *Nature*, vol. 464, no. 7293, pp. 1376–1380, 2010.

[338] C. G. Hahn, H. Y. Wang, D. S. Cho et al., "Altered neuregulin 1-erbB4 signaling contributes to NMDA> receptor hypofunction in schizophrenia," *Nature Medicine*, vol. 12, no. 7, pp. 824–828, 2006.

[339] A. Pillai, V. Parikh Jr., A. V. Terry, and S. P. Mahadik, "Long-term antipsychotic treatments and crossover studies in rats: differential effects of typical and atypical agents on the expression of antioxidant enzymes and membrane lipid peroxidation in rat brain," *Journal of Psychiatric Research*, vol. 4, no. 5, pp. 372–386, 2007.

[340] V. Parikh, M. M. Khan, and S. P. Mahadik, "Differential effects of antipsychotics on expression of antioxidant enzymes and membrane lipid peroxidation in rat brain," *Journal of Psychiatric Research*, vol. 37, no. 1, pp. 43–51, 2003.

[341] A. Reinke, M. R. Martins, M. S. Lima, J. C. Moreira, F. Dal-Pizzol, and J. Quevedo, "Haloperidol and clozapine, but not olanzapine, induces oxidative stress in rat brain," *Neuroscience Letters*, vol. 372, no. 1-2, pp. 157–160, 2004.

[342] M. R. Martins, F. C. Petronilho, K. M. Gomes, F. Dal-Pizzol, E. L. Streck, and J. Quevedo, "Antipsychotic-induced oxidative stress in rat brain," *Neurotoxicity Research*, vol. 13, no. 1, pp. 63–69, 2008.

[343] M. Polydoro, N. Schröder, M. N. M. Lima et al., "Haloperidol- and clozapine-induced oxidative stress in the rat brain," *Pharmacology Biochemistry and Behavior*, vol. 78, no. 4, pp. 751–756, 2004.

[344] I. Sadowska-Bartosz, S. Galiniak, G. Bartosz, M. Zuberek, A. Grzelak, and A. Dietrich-Muszalska, "Antioxidant properties of atypical antipsychotic drugs used in the treatment of schizophrenia," *Schizophrenia research*, vol. 176, no. 2-3, pp. 245–251, 2016.

[345] S. L. Arnaiz, M. F. Coronel, and A. Boveris, "Nitric oxide, superoxide, and hydrogen peroxide production in brain mitochondria after haloperidol treatment," *Nitric Oxide*, vol. 3, no. 3, pp. 235–243, 1999.

[346] Z. L. Bai, X. S. Li, G. Y. Chen et al., "Serum oxidative stress marker levels in unmedicated and medicated patients with schizophrenia," *Journal of Molecular Neuroscience*, vol. 66, no. 3, pp. 428–436, 2018.

[347] S. Kropp, V. Kern, K. Lange et al., "Oxidative stress during treatment with first- and second-generation antipsychotics," *The Journal of Neuropsychiatry and Clinical Neurosciences*, vol. 17, no. 2, pp. 227–231, 2005.

[348] O. P. Singh, I. Chakraborty, A. Dasgupta, and S. Datta, "A comparative study of oxidative stress and interrelationship of important antioxidants in haloperidol and olanzapine treated patients suffering from schizophrenia," *Indian journal of psychiatry*, vol. 50, no. 3, pp. 171–176, 2008.

[349] B. Dejanović, V. Vuković-Dejanović, I. Stevanović, I. Stojanović, G. Mandić-Gajić, and S. Dilber, "Oxidative stress induced by chlorpromazine in patients treated and acutely poisoned with the drug," *Vojnosanitetski pregled*, vol. 73, no. 4, pp. 312–317, 2016.

[350] X. Y. Zhang, Y. L. Tan, L. Y. Cao et al., "Antioxidant enzymes and lipid peroxidation in different forms of schizophrenia treated with typical and atypical antipsychotics," *Schizophrenia Research*, vol. 81, no. 2-3, pp. 291–300, 2006.

[351] M. Padurariu, A. Ciobica, I. Dobrin, and C. Stefanescu, "Evaluation of antioxidant enzymes activities and lipid peroxidation in schizophrenic patients treated with typical and atypical antipsychotics," *Neuroscience Letters*, vol. 479, no. 3, pp. 317–320, 2010.

[352] Z. Lu, T. Wen, Y. Wang, W. Kan, and G. Xun, "Peripheral non-enzymatic antioxidants in patients with schizophrenia: a case-control study," *BMC Psychiatry*, vol. 20, no. 1, pp. 1–9, 2020.

[353] A. Bas, G. Gultekin, S. Incir, T. O. Bas, M. Emul, and A. Duran, "Level of serum thioredoxin and correlation with neurocognitive functions in patients with schizophrenia using clozapine and other atypical antipsychotics," *Psychiatry Research*, vol. 247, pp. 84–89, 2017.

[354] L. Leppik, M. Parksepp, S. Janno et al., "Profiling of lipidomics before and after antipsychotic treatment in first-episode psychosis," *European Archives of Psychiatry and Clinical Neuroscience*, vol. 270, no. 1, pp. 59–70, 2020.

[355] S. A. Ivanova, L. P. Smirnova, Y. G. Shchigoreva, A. V. Semke, and N. A. Bohan, "Glutathione in the blood serum of schizophrenic patients in the dynamics of antipsychotic therapy," *Bulletin of Experimental Biology and Medicine*, vol. 160, no. 8, pp. 255–258, 2015.

[356] H. An, X. du, X. Huang et al., "Obesity, altered oxidative stress, and clinical correlates in chronic schizophrenia patients," *Translational Psychiatry*, vol. 8, no. 1, article 258, 2018.

[357] K. Kriisa, L. Haring, E. Vasar et al., "Antipsychotic treatment reduces indices of oxidative stress in first-episode psychosis patients," *Oxidative Medicine and Cellular Longevity*, vol. 2016, Article ID 9616593, 7 pages, 2016.

[358] S. Chittiprol, G. Venkatasubramanian, N. Neelakantachar et al., "Oxidative stress and neopterin abnormalities in schizophrenia: a longitudinal study," *Journal of Psychiatric Research*, vol. 44, no. 5, pp. 310–313, 2010.

[359] G. Dakhale, S. Khanzode, S. Khanzode, A. Saoji, L. Khobragade, and A. Turankar, "Oxidative damage and schizophrenia: the potential benefit by atypical antipsychotics," *Neuropsychobiology*, vol. 49, no. 4, pp. 205–209, 2004.

[360] S. A. Ivanova, L. P. Smirnova, Y. G. Shchigoreva et al., "glucose-6-phosphate dehydrogenase and catalase activities in erythrocytes of schizophrenic patients under pharmacotherapy with traditional antipsychotics," *Neurochemical Journal*, vol. 8, no. 1, pp. 66–70, 2014.

[361] N. M. Krotenko, L. P. Smirnova, V. N. Loginov, A. S. Ivanova, and A. V. Semke, "Influence of neuroleptic therapy on state of lipids peroxidation and glutathione system in schizophrenic patients," *Siberian Herald of Psychiatry and Addiction Psychiatry*, vol. 2, no. 59, pp. 133–135, 2010.

[362] A. C. Rossetti, M. S. Paladini, M. A. Riva, and R. Molteni, "Oxidation-reduction mechanisms in psychiatric disorders: a novel target for pharmacological intervention," *Pharmacology & Therapeutics*, vol. 210, article 107520, 2020.

[363] P. V. Magalhaes, O. Dean, A. C. Andreazza, M. Berk, and F. Kapczinski, "Antioxidant treatments for schizophrenia," *Cochrane database of systematic reviews*, vol. 2, article CD008919, 2016.

[364] C. O. Yolland, D. Hanratty, E. Neill et al., "Meta-analysis of randomised controlled trials with N-acetylcysteine in the treatment of schizophrenia," *Australian & New Zealand Journal of Psychiatry*, vol. 54, no. 5, pp. 453–466, 2020.

[365] M. Arakawa and Y. Ito, "N-Acetylcysteine and neurodegenerative diseases: basic and clinical pharmacology," *The Cerebellum*, vol. 6, no. 4, pp. 308–314, 2007.

[366] R. J. Bridges, N. R. Natale, and S. A. Patel, "System xc- cystine/-glutamate antiporter: an update on molecular pharmacology and roles within the CNS," *British Journal of Pharmacology*, vol. 165, no. 1, pp. 20–34, 2012.

[367] K. Merritt, A. Egerton, M. J. Kempton, M. J. Taylor, and P. K. McGuire, "Nature of glutamate alterations in schizophrenia: a meta-analysis of proton magnetic resonance spectroscopy studies," *JAMA Psychiatry*, vol. 73, no. 7, pp. 665–674, 2016.

[368] M. Berk, D. Copolov, O. Dean et al., "N-Acetyl Cysteine as a Glutathione Precursor for Schizophrenia–A Double- Blind, Randomized, Placebo-Controlled Trial," *Biological Psychiatry*, vol. 64, no. 5, pp. 361–368, 2008.

[369] M. Farokhnia, A. Azarkolah, F. Adinehfar et al., "N-Acetylcysteine as an adjunct to risperidone for treatment of negative symptoms in patients with chronic schizophrenia: a randomized, double-blind, placebo-controlled study," *Clinical Neuropharmacology*, vol. 36, no. 6, pp. 185–192, 2013.

[370] S. Lavoie, M. M. Murray, P. Deppen et al., "Glutathione Precursor, *N*-Acetyl-Cysteine, Improves Mismatch Negativity in Schizophrenia Patients," *Neuropsychopharmacology*, vol. 33, no. 9, pp. 2187–2199, 2008.

[371] W. Zheng, Q. E. Zhang, D. B. Cai et al., "N-Acetylcysteine for major mental disorders: a systematic review and meta-analysis of randomized controlled trials," *Acta Psychiatrica Scandinavica*, vol. 137, no. 5, pp. 391–400, 2018.

[372] M. Rapado-Castro, S. Dodd, A. I. Bush et al., "Cognitive effects of adjunctive N-acetyl cysteine in psychosis," *Psychological Medicine*, vol. 47, no. 5, pp. 866–876, 2017.

[373] Z. Sepehrmanesh, M. Heidary, N. Akasheh, H. Akbari, and M. Heidary, "Therapeutic effect of adjunctive *N*-acetyl cysteine (NAC) on symptoms of chronic schizophrenia: A double-blind, randomized clinical trial," *Progress in Neuro-Psychopharmacology and Biological Psychiatry*, vol. 82, pp. 289–296, 2018.

[374] P. Conus, L. J. Seidman, M. Fournier et al., "N-Acetylcysteine in a double-blind randomized placebo-controlled trial: toward biomarker-guided treatment in early psychosis," *Schizophrenia Bulletin*, vol. 44, no. 2, pp. 317–327, 2018.

[375] P. Klauser, L. Xin, M. Fournier et al., "*N*-Acetylcysteine add-on treatment leads to an improvement of fornix white matter integrity in early psychosis: a double-blind randomized placebo-controlled trial," *Translational Psychiatry*, vol. 8, no. 1, article 220, 2018.

[376] G. McQueen, A. Lay, J. Lally et al., "Effect of single dose *N*-acetylcysteine administration on resting state functional connectivity in schizophrenia," *Psychopharmacology*, vol. 237, no. 2, pp. 443–451, 2020.

[377] A. Breier, E. Liffick, T. A. Hummer et al., "Effects of 12-month, double-blind *N*-acetyl cysteine on symptoms, cognition and brain morphology in early phase schizophrenia spectrum disorders," *Schizophrenia Research*, vol. 199, pp. 395–402, 2018.

[378] A. Doruk, Ö. Uzun, and A. Özsahin, "A placebo-controlled study of extract of ginkgo biloba added to clozapine in patients with treatment-resistant schizophrenia," *International Clinical Psychopharmacology*, vol. 23, no. 4, pp. 223–227, 2008.

[379] W. F. Zhang, Y. L. Tan, X. Y. Zhang, R. C. Chan, H. R. Wu, and D. F. Zhou, "Extract ofGinkgo bilobaTreatment for tardive dyskinesia in Schizophrenia," *The Journal of Clinical Psychiatry*, vol. 72, no. 5, pp. 615–621, 2011.

[380] J. Rathbone, L. Zhang, M. Zhang, J. Xia, X. Liu, and Y. Yang, "Chinese herbal medicine for schizophrenia," *Cochrane Database of Systematic Reviews*, vol. 4, article CD003444, 2005.

[381] V. Singh, S. P. Singh, and K. Chan, "Review and meta-analysis of usage of ginkgo as an adjunct therapy in chronic schizophrenia," *International Journal of Neuropsychopharmacology*, vol. 13, no. 2, pp. 257–271, 2010.

[382] A. Amiri, A. A. Noorbala, A. A. Nejatisafa et al., "Efficacy of selegiline add on therapy to risperidone in the treatment of the negative symptoms of schizophrenia: a double-blind randomized placebo-controlled study," *Human Psychopharmacology: Clinical and Experimental*, vol. 23, no. 2, pp. 79–86, 2008.

[383] M. R. Fayazi Bordbar, E. Abdollahian, K. Hojjat, and A. A. Samaric, "Effects of selegiline on negative symptoms in schizophrenia: a double-blind clinical trial," *Iranian Journal of Psychiatry and Clinical Psychology*, vol. 14, no. 2, pp. 131–139, 2008.

[384] J. A. Bodkin, S. G. Siris, P. C. Bermanzohn, J. Hennen, and J. O. Cole, "Double-blind, placebo-controlled, multicenter trial of selegiline augmentation of antipsychotic medication to treat negative symptoms in outpatients with schizophrenia," *American Journal of Psychiatry*, vol. 162, no. 2, pp. 388–390, 2005.

[385] S. Akhondzadeh, A. Safarcherati, and H. Amini, "Beneficial antipsychotic effects of allopurinol as add-on therapy for schizophrenia: a double blind, randomized and placebo controlled trial," *Progress in Neuro-Psychopharmacology and Biological Psychiatry*, vol. 29, no. 2, pp. 253–259, 2005.

[386] M. G. Brunstein, E. S. Ghisolfi, F. L. Ramos, and D. R. Lara, "A clinical trial of adjuvant allopurinol therapy for moderately refractory schizophrenia," *The Journal of Clinical Psychiatry*, vol. 66, no. 2, pp. 213–219, 2005.

[387] F. B. Dickerson, C. R. Stallings, A. E. Origoni et al., "A double-blind trial of adjunctive allopurinol for schizophrenia," *Schizophrenia Research*, vol. 109, no. 1-3, pp. 66–69, 2009.

[388] M. Weiser, A. A. Gershon, K. Rubinstein et al., "A randomized controlled trial of allopurinol vs. placebo added on to antipsychotics in patients with schizophrenia or schizoaffective disorder," *Schizophrenia Research*, vol. 138, no. 1, pp. 35–38, 2012.

[389] L. A. Adler, E. Peselow, J. Rotrosen et al., "Vitamin E treatment of tardive dyskinesia," *The American Journal of Psychiatry*, vol. 150, no. 9, pp. 1405–1407, 1993.

[390] L. A. Adler, J. Rotrosen, R. Edson, P. Lavori, J. Lohr, R. Hitzemann et al., "Vitamin E treatment for tardive dyskinesia," *Archives of General Psychiatry*, vol. 56, no. 9, pp. 836–841, 1999.

[391] A. Dorevitch, M. Kalian, M. Shlafman, and V. Lerner, "Treatment long-term tardive dyskinesia with vitamin E," *Biological Psychiatry*, vol. 41, no. 1, pp. 114–116, 1997.

[392] J. B. Lohr and M. P. Caligiuri, "A double-blind placebo-controlled study of vitamin E treatment of tardive dyskinesia," *The Journal of Clinical Psychiatry*, vol. 57, no. 4, pp. 167–173, 1996.

[393] X. Y. Zhang, D. F. Zhou, L. Y. Cao, C. Q. Xu, D. C. Chen, and G. Y. Wu, "The effect of vitamin E treatment on tardive dyskinesia and blood superoxide dismutase: a double-blind placebo-controlled trial," *Journal of clinical psychopharmacology*, vol. 24, no. 1, pp. 83–86, 2004.

[394] S. H. A. Sajjad, "Vitamin E in the treatment of tardive dyskinesia," *International Clinical Psychopharmacology*, vol. 13, no. 4, pp. 147–156, 1998.

[395] K. Soares-Weiser, N. Maayan, and H. Bergman, "Vitamin E for antipsychotic-induced tardive dyskinesia," *Cochrane Database of Systematic Reviews*, no. article CD000209, 2018.

[396] G. N. Dakhale, S. D. Khanzode, S. S. Khanzode, and A. Saoji, "Supplementation of vitamin C with atypical antipsychotics reduces oxidative stress and improves the outcome of schizophrenia," *Psychopharmacology*, vol. 182, no. 4, pp. 494–498, 2005.

[397] N. Michael, H. Sourgens, V. Arolt, and A. Erfurth, "Severe tardive dyskinesia in affective disorders: treatment with vitamin E and C," *Neuropsychobiology*, vol. 46, no. 1, pp. 28–30, 2003.

[398] M. Arvindakshan, M. Ghate, P. K. Ranjekar, D. R. Evans, and S. P. Mahadik, "Supplementation with a combination of ω-3 fatty acids and antioxidants (vitamins E and C) improves the outcome of schizophrenia," *Schizophrenia Research*, vol. 62, no. 3, pp. 195–204, 2003.

[399] E. Y. Sivrioglu, S. Kirli, D. Sipahioglu, B. Gursoy, and E. Sarandöl, "The impact of ω-3 fatty acids, vitamins E and C supplementation on treatment outcome and side effects in schizophrenia patients treated with haloperidol: An open-label pilot study," *Progress in Neuro-Psychopharmacology and Biological Psychiatry*, vol. 31, no. 7, pp. 1493–1499, 2007.

[400] R. Emsley, C. Myburgh, P. Oosthuizen, and S. J. van Rensburg, "Randomized, placebo-controlled study of ethyl-eicosapentaenoic acid as supplemental treatment in schizophrenia," *American Journal of Psychiatry*, vol. 159, no. 9, pp. 1596–1598, 2002.

[401] M. Peet, J. Brind, C. N. Ramchand, S. Shah, and G. K. Vankar, "Two double-blind placebo-controlled pilot studies of eicosapentaenoic acid in the treatment of schizophrenia," *Schizophrenia Research*, vol. 49, no. 3, pp. 243–251, 2001.

[402] M. Peet, D. F. Horrobin, and E-E Multicentre Study Group, "A dose-ranging exploratory study of the effects of ethyl-eicosapentaenoate in patients with persistent schizophrenic symptoms," *Journal of Psychiatric Research*, vol. 36, no. 1, pp. 7–18, 2002.

[403] G. P. Amminger, M. R. Schäfer, K. Papageorgiou et al., "Long-chain ω-3 fatty acids for indicated prevention of psychotic Disorders," *Archives of general psychiatry*, vol. 67, no. 2, pp. 146–154, 2010.

[404] R. Emsley, D. J. Niehaus, L. Koen et al., "The effects of eicosapentaenoic acid in tardive dyskinesia: a randomized, placebo-controlled trial," *Schizophrenia Research*, vol. 84, no. 1, pp. 112–120, 2006.

[405] W. S. Fenton, F. Dickerson, J. Boronow, J. R. Hibbeln, and M. Knable, "A placebo-controlled trial of omega-3 fatty acid (ethyl eicosapentaenoic acid) supplementation for residual symptoms and cognitive impairment in schizophrenia," *American Journal of Psychiatry*, vol. 158, no. 12, pp. 2071–2074, 2001.

[406] T. W. Sedlak, L. G. Nucifora, M. Koga et al., "Sulforaphane augments glutathione and influences brain metabolites in human subjects: a clinical pilot study," *Molecular Neuropsychiatry*, vol. 3, no. 4, pp. 214–222, 2018.

[407] A. Shiina, N. Kanahara, T. Sasaki et al., "An open study of sulforaphane-rich broccoli sprout extract in patients with schizophrenia," *Clinical Psychopharmacology and Neuroscience*, vol. 13, no. 1, pp. 62–67, 2015.

[408] Y. Shirai, Y. Fujita, R. Hashimoto et al., "Dietary intake of sulforaphane-rich broccoli sprout extracts during juvenile and adolescence can prevent phencyclidine-induced cognitive deficits at adulthood," *PLoS One*, vol. 10, no. 6, article e0127244, 2015.

[409] L. L. Xu, Y. F. Wu, F. Yan et al., "5-(3,4-Difluorophenyl)-3-(6-methylpyridin-3-yl)-1,2,4-oxadiazole (DDO-7263), a novel Nrf2 activator targeting brain tissue, protects against MPTP-induced subacute Parkinson's disease in mice by inhibiting the NLRP3 inflammasome and protects PC12 cells against oxidative stress," *Free Radical Biology and Medicine*, vol. 134, pp. 288–303, 2019.

[410] C. Miodownik, V. Lerner, N. Kudkaeva et al., "Curcumin as add-on to antipsychotic treatment in patients with chronic schizophrenia: a randomized, double-blind, placebo-controlled study," *Clinical Neuropharmacology*, vol. 42, no. 4, pp. 117–122, 2019.

[411] K. Zortea, V. C. Franco, L. P. Francesconi, K. M. Cereser, M. I. R. Lobato, and P. S. Belmonte-de-Abreu, "Resveratrol supplementation in schizophrenia patients: a randomized clinical trial evaluating serum glucose and cardiovascular risk factors," *Nutrients*, vol. 8, no. 2, p. 73, 2016.

[412] K. Zortea, V. C. Franco, P. Guimarães, and P. S. Belmonte-de-Abreu, "Resveratrol supplementation did not improve cognition in patients with schizophrenia: results from a randomized clinical trial," *Frontiers in psychiatry*, vol. 7, no. 159, 2016.

[413] M. G. Magaji, L. O. Iniaghe, M. Abolarin, O. I. Abdullahi, and R. A. Magaji, "Neurobehavioural evaluation of resveratrol in murine models of anxiety and schizophrenia," *Metabolic Brain Disease*, vol. 32, no. 2, pp. 437–442, 2017.

[414] Q. Huang, X. Ye, L. Wang, and J. Pan, "Salvianolic acid B abolished chronic mild stress-induced depression through suppressing oxidative stress and neuro-inflammation via regulating NLRP3 inflammasome activation," *Journal of Food Biochemistry*, vol. 43, no. 3, article e12742, 2019.

[415] L. Yu, C. An, L. Jia et al., "Combination therapy of salvianolic acid and fluoxetine improves the cognitive function of rats with chronic stress-induced depression," *World Neurosurgery*, vol. 86, pp. 173–180, 2016.

[416] W. L. Jiang, D. B. Cai, F. Yin et al., "Adjunctive metformin for antipsychotic-induced dyslipidemia: a meta-analysis of randomized, double-blind, placebo-controlled trials," *Translational Psychiatry*, vol. 10, no. 1, article 117, 2020.

[417] A. Cuadrado, A. I. Rojo, G. Wells et al., "Therapeutic targeting of the NRF2 and KEAP1 partnership in chronic diseases," *Nature Reviews Drug Discovery*, vol. 18, no. 4, pp. 295–317, 2019.

[418] D. Moretti, S. Tambone, M. Cerretani et al., "NRF2 activation by reversible KEAP1 binding induces the antioxidant response in primary neurons and astrocytes of a Huntington's disease mouse model," *Free Radical Biology and Medicine*, 2020.

[419] B. Cautain, F. Castillo, L. Musso et al., "Discovery of a novel, isothiazolonaphthoquinone-based small molecule activator of FOXO nuclear-cytoplasmic shuttling," *PLoS One*, vol. 11, no. 12, article e0167491, 2016.

[420] F. Zanella, A. Rosado, B. García, A. Carnero, and W. Link, "Chemical genetic analysis of FOXO nuclear–cytoplasmic shuttling by using image-based cell screening," *Chembiochem*, vol. 9, no. 14, pp. 2229–2237, 2008.

[421] M. Bulut, H. A. Savas, A. Altindag, O. Virit, and A. Dalkilic, "Beneficial effects of *N*-acetylcysteine in treatment resistant schizophrenia," *The World Journal of Biological Psychiatry*, vol. 10, no. 4-2, pp. 626–628, 2009.

[422] I. Pérez-Torres, V. Guarner-Lans, and M. E. Rubio-Ruiz, "Reductive stress in inflammation-associated diseases and the pro-oxidant effect of antioxidant agents," *International Journal of Molecular Sciences*, vol. 18, no. 10, article 2098, 2017.

Hindawi
Oxidative Medicine and Cellular Longevity
Volume 2020, Article ID 1974265, 21 pages
https://doi.org/10.1155/2020/1974265

Research Article

NAMPT/SIRT1 Attenuate Ang II-Induced Vascular Remodeling and Vulnerability to Hypertension by Inhibiting the ROS/MAPK Pathway

Lei Zhou,[1] **Sheng Zhang**,[2] **Enkhbat Bolor-Erdene**,[1] **Lingwei Wang**,[3] **Ding Tian**,[4] **and Yunqing Mei**[1]

[1]*Department of Cardiothoracic Surgery, Tongji Hospital, School of Medicine, Tongji University, Shanghai 200065, China*
[2]*Department of Cardiology, East Hospital, School of Medicine, Tongji University, 310000, China*
[3]*Department of Thoracic Surgery, East Hospital, School of Medicine, Tongji University, Shanghai 310000, China*
[4]*Department of Cardiology, Xinhua Hospital, School of Medicine, Shanghai Jiao Tong University, Shanghai 200092, China*

Correspondence should be addressed to Ding Tian; tianding@outlook.com and Yunqing Mei; drmeiyq2004@tongji.edu.cn

Received 4 July 2020; Revised 24 November 2020; Accepted 7 December 2020; Published 31 December 2020

Academic Editor: Karolina Szewczyk-Golec

Copyright © 2020 Lei Zhou et al. This is an open access article distributed under the Creative Commons Attribution License, which permits unrestricted use, distribution, and reproduction in any medium, provided the original work is properly cited.

Hypertension is characterized by endothelial dysfunction, vascular remodeling, and rearrangement of the extracellular matrix. Besides, the pathogenesis of hypertension is closely related to excess generation of reactive oxygen species (ROS). Nicotinamide phosphoribosyltransferase (NAMPT) is a rate-limiting enzyme in nicotinamide adenine dinucleotide (NAD) biosynthesis that influences the activity of NAD-dependent enzymes, such as sirtuins, which possess NAD-dependent protein deacetylase activity and cleave NAD during the deacetylation cycle. Recently, NAMPT has been shown to play a crucial role in various diseases associated with oxidative stress. However, the function and regulation of NAMPT in hypertension have not been extensively explored. In the present study, we identified NAMPT as a crucial regulator of hypertension, because NAMPT expression was significantly downregulated in both patients with hypertension and experimental animals. NAMPT knockout (NAMPT+/-) mice exhibited a significantly higher blood pressure and ROS levels after stimulation with angiotensin II (Ang II) than wild-type mice, and the administration of recombinant human NAMPT (rhNAMPT) reversed this effect. In vivo, overexpression of NAMPT protected against angiotensin II- (Ang II-) induced hypertension by inhibiting ROS production via sirtuin 1 in mouse aortic endothelial cells (MAECs) and mouse aortic vascular smooth muscle cells (MOVAs). In turn, NAMPT alleviated the ROS-induced mitogen-activated protein kinase (MAPK) pathway. In conclusion, NAMPT might be a novel biomarker and a therapeutic target in hypertension.

1. Introduction

As an important and independent risk factor for cardiovascular disease (CVD), hypertension affects 30% of adults and has been the leading risk factor for heart attack and stroke [1]. Angiotensin II (Ang II), the initial effector molecule of the renin-angiotensin system (RAS), has been shown to induce NAD(P)H oxidase (NOX) activity and increase local reactive oxygen species (ROS) production by binding to AT1R [2]. ROS are novel intracellular second messengers in signal transduction pathways. ROS-induced endothelial dysfunction appears to be the key early step in the development of hypertension [3]. The stimulation of vascular smooth muscle cell (VSMC) proliferation and rearrangement of extracellular matrix (ECM) formation are the major adaptive mechanisms involved in vascular alterations [4]. The ROS-sensitive mitogen-activated protein kinase (MAPK) cascade is also presumed to play a crucial role in endothelial cell (EC) dysfunction, the proliferation and migration of VSMCs, and formation of ECM through Ang II and ROS [5, 6].

Nicotinamide phosphoribosyltransferase (NAMPT) is one of the regulators of the intracellular nicotinamide adenine dinucleotide (NAD) pool through its NAD biosynthesis activity [8]. NAMPT influences the activity of NAD-

dependent enzymes, such as sirtuins [7], poly(ADP-ribose) polymerases (PARPs) [9], and CD38 [10], thereby regulating cellular metabolism, mitochondrial biogenesis, and adaptive responses to inflammation and oxidation. NAMPT is expressed in nearly all examined organs, tissues and cells [11] and has dual intracellular (mainly in the cytoplasm and nucleus) and extracellular roles [12]. NAMPT has been reported to be involved in various diseases and conditions, such as obesity, nonalcoholic fatty liver disease (NAFLD), type 2 diabetes mellitus (T2DM), cancer, and aging [11]. In the cardiovascular system, NAMPT promotes atherosclerosis development by exacerbating atherosclerotic inflammation [13]. NAMPT inhibits myocardial injury by regulating NAD and ATP levels [14]. NAMPT was recently suggested to play a role in pulmonary vascular remodeling, and NAMPT inhibition might be a potential therapeutic strategy for pulmonary arterial hypertension [15]. However, up to date, the molecular mechanism of NAMPT and its function in hypertension associated with oxidative stress have not been well studied.

In the present study, we identified NAMPT as a crucial regulator of hypertension, because the expression of NAMPT was significantly downregulated in both patients with hypertension and experimental animals. NAMPT knockout (NAMPT+/-) mice displayed significantly higher blood pressure and ROS levels than wild-type (WT) mouse littermates. Moreover, the administration of recombinant human NAMPT (rhNAMPT) reversed this effect in vivo. Overexpression of NAMPT protected against Ang II-induced increases in ROS levels through sirtuin 1 (SIRT1) and NAD+. In turn, NAMPT alleviated the ROS-induced MAPK pathway. These results confirm that approaches targeting or using NAMPT as a therapeutic option are potential strategies for the treatment of hypertension.

2. Results

2.1. NAMPT Expression Is Reduced in Tissues from Individuals with Hypertension, Mouse Aortic Vascular Smooth Muscle Cells (MOVAs), and Mouse Aortic Endothelial Cells (MAECs) Exposed to Ang II. Aortic wall samples were obtained from patients undergoing aortic replacement surgery due to acute aortic dissection to explore whether NAMPT is involved in the development of hypertension. The clinical characteristics of patients with hypertension and normal controls undergoing aortic replacement are shown in Table 1. Immunochemical staining and Western blotting revealed a slight decrease in NAMPT levels in patients with hypertension (Figures 1(a) and 1(c)). Ang II-induced hypertensive rats were used as a hypertension model in this study. The rats were continually stimulated with Ang II through osmotic minipumps for 4 weeks, and fresh aortic wall tissues were collected; immunochemical staining and Western blotting revealed a significant reduction in Ang II-induced hypertension in rats (Figures 1(b) and 1(d)). MOVAs and MAECs were treated with Ang II for 48 hours to further investigate the role of NAMPT in vitro. The Western blot analysis revealed a marked decrease in the level of the NAMPT protein in both of these cell lines after exposure to Ang II (Figures 1(e) and 1(f)).

2.2. NAMPT Haplodeficiency Exacerbates Increases in Blood Pressure and Promotes the Expression of Remodeling-Related Molecules after Ang II Stimulation. We generated NAMPT haplodeficient (NAMPT+/-) mice to determine the effects of NAMPT on Ang II-induced hypertension. 32.16% decrease in the expression of the NAMPT mRNA and a 30.11% decrease in the level of the NAMPT protein were observed in the aortic walls of NAMPT+/- mice compared to their WT littermates. Moreover, a 40.46% decrease in the expression of the NAMPT mRNA and a 50.37% decrease in the aortic walls of NAMPT+/- mice were observed after Ang II stimulation (Figures 2(a) and 2(b)). Hematoxylin and eosin (H&E) staining was performed to further analyze morphological changes in mice with Ang II-induced hypertension (Figure 2(b)). We determined the media thickness (M), lumen diameter (L), and the ratio of media thickness to lumen diameter (M/L) in the different groups of mice to evaluate the remodeling of the aortic wall. Compared with control mice, Ang II-stimulated NAMPT+/- mice displayed significantly increased aortic M and M/L. However, statistically significant changes in L were not observed between groups (Figure 2(d)). Then, we measured the blood pressure of NAMPT+/- mice and age-matched control mice after Ang II stimulation for 28 days. The NAMPT+/- mice showed a slight increase in systolic blood pressure (SBP), mean blood pressure (MBP), and diastolic blood pressure (DBP) beginning at the third week (Figure 2(e)). A detailed description of the blood pressure parameters is provided in Table S2. We examined the mRNA levels of remodeling-related molecules in the aortic wall to further determine the pathological consequences. The qRT-PCR analysis revealed the downregulation of the Ang II-induced expression of remodeling markers, including connective tissue growth factor (CTGF), collagen I, and collagen III, in NAMPT+/- mice compared to WT mice after Ang II stimulation (Figure 2(f)), as well as the picrosirius red staining (PSR). Based on these results, NAMPT haplodeficiency significantly exacerbates Ang II-induced hypertension.

2.3. Ang II-Induced Endothelial Dysfunction and Proliferation and Migration of MOVAs Were Ameliorated by the Overexpression of NAMPT. NAMPT was overexpressed through plasmid transfection, and cells were stimulated with Ang II for 48 hours to investigate the precise biological function of NAMPT in regulating Ang II-induced endothelial dysfunction. NAMPT expression in MAECs was substantially upregulated at 48 hours after transfection with the NAMPT plasmids, as measured by qRT-PCR and Western blotting (Fig. S1A and B). Moreover, the protein levels of apoptosis markers (Caspase 3 and Bcl-2) were significantly reduced in NAMPT-overexpressing cells stimulated with Ang II (Figure 3(a)), which was also assessed using double PI/Annexin V staining and flow cytometry (Figure 3(c)). Similar results were obtained at the level of endothelial nitric oxide synthase (P-eNOS/eNOS) (Figure 3(a)). Next, immunofluorescence staining further clarified that the

Table 1: Clinical characteristics of patients with hypertension and normal undergoing aortic replacement.

	Normal group ($n = 6$)	Hypertension group ($n = 6$)	p value
Age (years, mean ± SD)	56.33 ± 7.68	68.25 ± 5.63	0.32
Male (n, %)	2 (33.3%)	3 (50%)	0.599
Systolic BP (mmHg, mean ± SD)	130.51 ± 4.38	174.50 + 8.65	0.002
Diastolic BP (mmHg, mean ± SD)	83.67 ± 5.39	101.17 + 9.46	0.008
Mean BP (mmHg, mean ± SD)	99.11 ± 4.12	125.44 + 8.64	0.006
Risk factors			
Smoking (n, %)	3 (50%)	2 (33.3%)	0.599
Hypercholesterolemia (n, %)	3 (50%)	4 (66.7)	0.609
Total cholesterol (mmol/L, mean ± SD)	5.09 ± 1.12	4.75 ± 0.84	0.507
BMI (kg/m^2, mean ± SD)	25.97 ± 2.16	26.82 ± 3.05	0.493
LVEF (%)	55.33 ± 5.63	50.5 ± 8.35	0.344
Main medication			
Diuretics (n, %)	2 (33.3%)	3 (50%)	0.599
ACEI/ARB (n, %)	3 (50%)	4 (66.7)	0.609
β blockers (n, %)	5 (83.3%)	6 (100%)	0.341
Calcium antagonist (n, %)	2 (33.3%)	3 (50%)	0.599
Aldosterone antagonist (n, %)	3 (50%)	4 (66.7)	0.609
HMG CoA inhibitors (n, %)	2 (33.3%)	4 (66.7%)	0.29

BP: blood pressure; BMI: body mass index; ACEI: angiotensin-converting enzyme inhibitor; ARB: angiotensin receptor blocker; HMG-CoA: 3-hydroxy-3-methyl glutaryl coenzyme A.

dysregulation of ZO-1 protein (an EC cell permeability marker) was rescued by overexpression of NAMPT (Figure 3(b)). The transfection efficiency of NAMPT plasmids was determined using qRT-PCR and Western blotting (Fig. S1C and D. The increased protein levels of proliferation markers (proliferating cell nuclear antigen (PCNA) and cyclin D1) after stimulation were significantly blunted by the overexpression of NAMPT in MOVAs (Figure 3(d)). Moreover, in vitro scratch-wound assays and transwell migration assays revealed that Ang II-induced increases in cellular migration were significantly alleviated by NAMPT overexpression in MOVAs (Figures 3(e) and 3(f)). To further determine the role of NAMPT in ECM synthesis, levels of the fibronectin and matrix metalloproteinase (MMP-2 and MMP-9) were evaluated and were significantly reduced in Ang II-stimulated MOVAs that were transfected with the NAMPT plasmid (Figure 3(d)).

2.4. NAMPT Regulated SIRT1 Expression and the NAD Concentration In Vivo and In Vitro. Because NAMPT mainly regulates the SIRT family in the cardiovascular system, we used qRT-PCR to examine SIRT1-7 expression in MAECs and MOVAs transfected with the NAMPT plasmid and stimulated with Ang II to determine which SIRTs play the most important role in the development of hypertension. Interestingly, we found the SIRT1 mRNA was expressed at higher levels both in MAECs (Figure 4(a)) and MOVAs (Figure 4(c)) than the other SIRT family members. Next, Western blot analysis was performed to verify the level of the Sirt1 protein and showed increased levels in both MAECs (Figure 4(b)) and MOVAs (Figure 4(d)) transfected with the NAMPT plasmid and stimulated with Ang II. Immunohistochemical staining further confirmed a robust decrease in the level of SIRT1 in the aortic walls of Ang II-induced NAMPT +/- mice and control mice (Figure 4(e)).

2.5. NAMPT Alleviated Ang II-Induced Endothelial Injury and the Proliferation and Migration in MOVAs by Targeting NAD/SIRT1 Signaling. We designed a SIRT1-specific siRNA and transfected it into MAECs and MOVAs, followed by overexpression of NAMPT and Ang-II stimulation for 48 hours to further study the relationship between NAMPT and SIRT1. The expression of the SIRT1 mRNA was decreased in both cell lines (Fig. S2A and C). 48.26% decrease and 45.67% decrease in SIRT1 protein levels were observed in MAECs and MOVAs, respectively. Moreover, a 56.13% decrease and 58.11% decrease were observed after Ang II stimulation of these cells, respectively (Fig. S2B and D). Moreover, knockdown of SIRT1 rescued the expression of apoptosis markers (Caspase 3 and Bcl-2), which was also verified by PI/AnnexinV double staining and flow cytometry (Figure 5(c)). Similar results were obtained for the level of endothelial nitric oxide synthase (P-eNOS/eNOS) (Figure 5(a)). Immunofluorescence staining showed the restoration of the expression of the ZO-1 protein (an EC permeability marker) in SIRT1-silenced MAECs that overexpressed NAMPT and were stimulated with Ang II for 48 hours (Figure 5(b)). Moreover, the protein levels of proliferation markers (PCNA and cyclin D1) were also restored after SIRT1 silencing and NAMPT overexpression in cells stimulated with Ang II for 48 hours (Figure 5(d)). Scratch-wound and transwell migration assays revealed that cellular

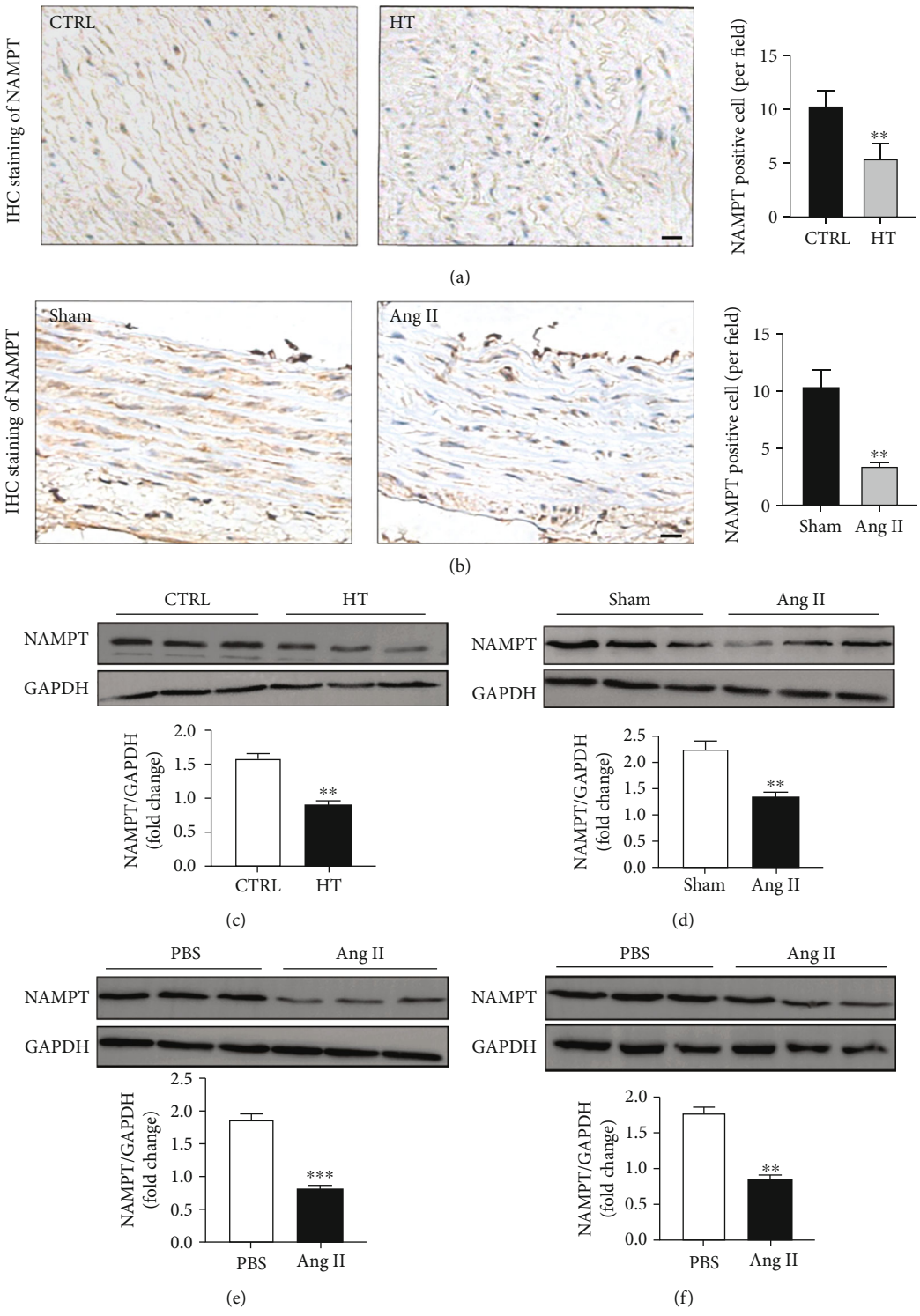

Figure 1: NAMPT expression is reduced in tissues from patients with hypertension and MOVAs and MAECs exposed to Ang II. (a) Immunohistochemical staining for NAMPT in tissues from patients with hypertension and control patients (scale bar = 20 μm) and quantification of NAMPT-positive cells ($n = 6$ in each group, ≥40 fields per group). Data are presented as means ± SEM. $^{**}p < 0.01$ compared with the group. (b) Immunohistochemical staining for NAMPT in tissues from the Ang II-infused rats and sham rats (scale bar = 20 μm) and quantification of NAMPT-positive cells ($n = 6$ in each group, ≥40 fields per group). Data are presented as means ± SEM. $^{**}p < 0.01$ compared with the group. (c) Representative Western blots and quantification showing NAMPT levels in the patients with hypertension and control patients ($n = 6$ in each group). (d) Representative Western blots and quantification showing NAMPT levels in the Ang II-infused rats and sham rats ($n = 6$ in each group). Representative Western blots and quantification showing NAMPT levels in MAECs (e) and MOVAs (f) after Ang II stimulation for 48 hours. Data are presented as means ± SEM and $^{***}p < 0.001$ compared with the sham or PBS groups.

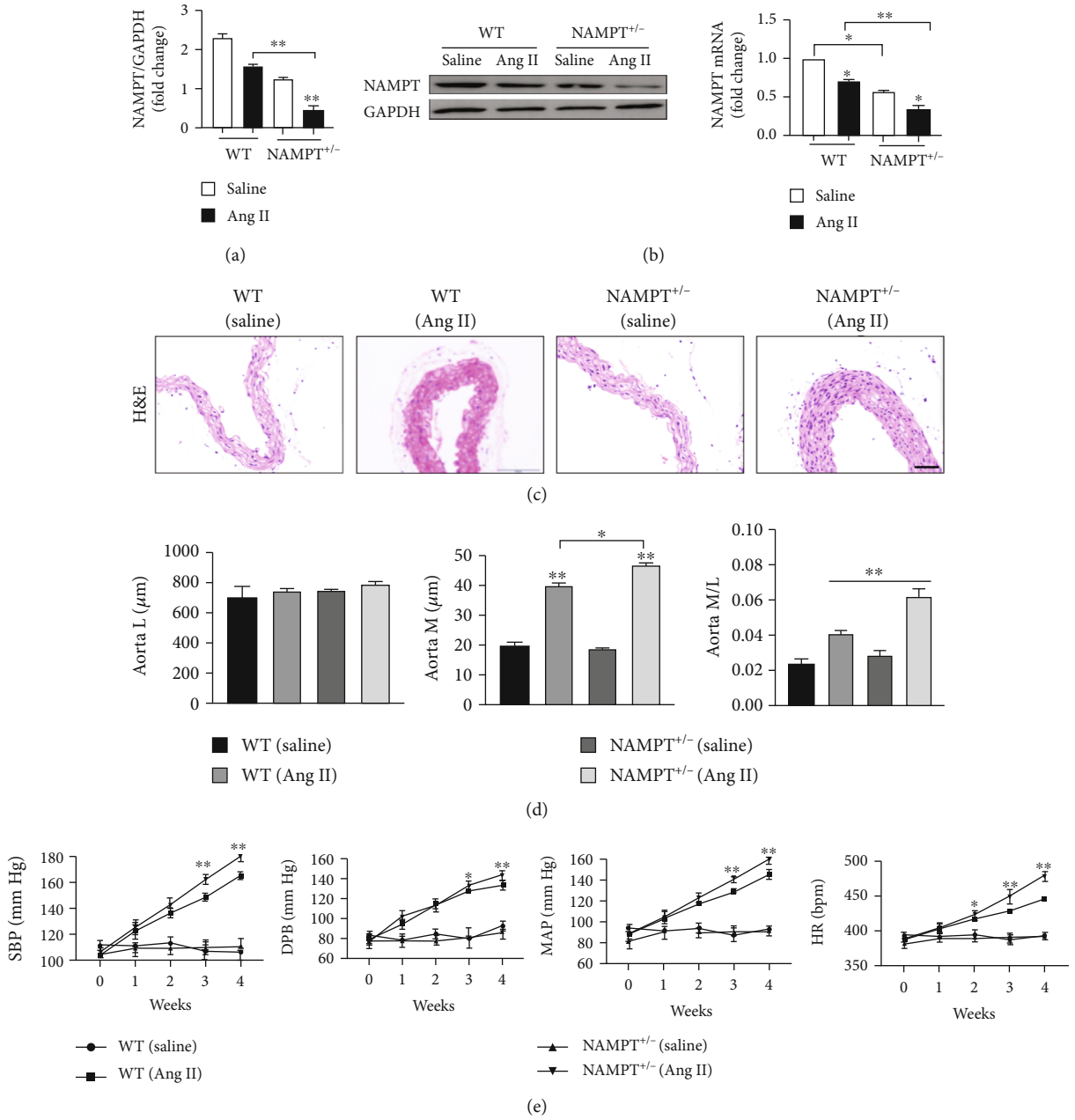

Figure 2: Continued.

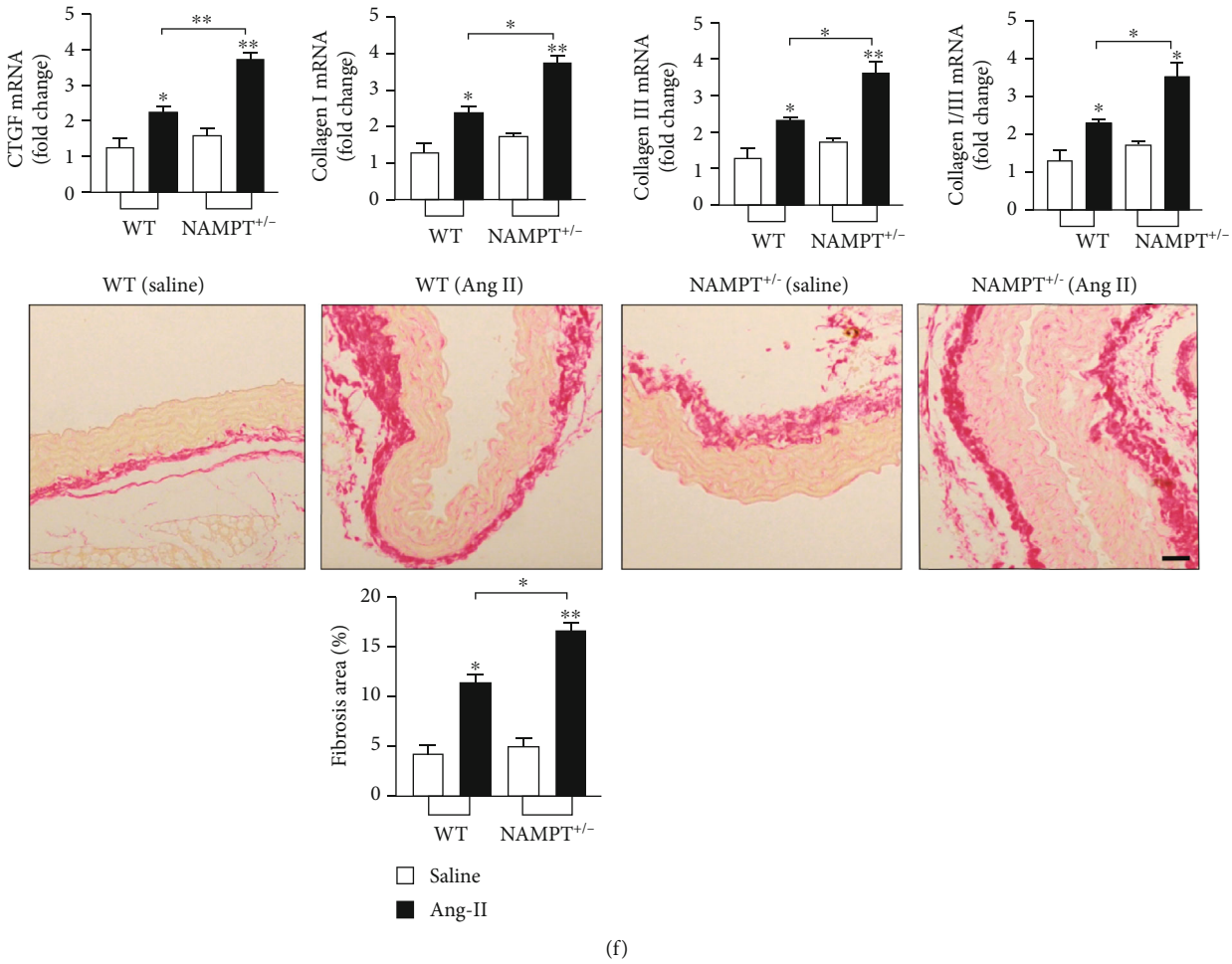

Figure 2: NAMPT haplodeficiency exacerbates changes in blood pressure and promotes the expression of remodeling-related molecules after Ang II stimulation. (a) The levels of the NAMPT mRNA and protein in the aortic wall tissues obtained from WT and NAMPT+/- mice treated with saline or Ang II ($n = 6$ in each group). (b) Representative images of H&E staining showing the remodeling of arteries (scale bar = 50 μm, $n = 5$ in each group, ≥40 fields per group). (c) M, L, and their ratio in the aorta. (d) The SBP, MAP, DBP, and HR were measured with a noninvasive computerized tail-cuff system in conscious mice. (e) Relative mRNA levels of CTGF, collagen I, and collagen III and the ratio of collagen type I and type III in WT littermates and NAMPT+/- mice treated with saline or Ang II treatment ($n = 6$ animals per group), as well as the picrosirius red staining (PSR). Data are presented as means ± SEM. $^{*}p < 0.05$ and $^{**}p < 0.01$ compared with the corresponding saline group; NS: not significant.

migration was also restored by SIRT1 knockdown (Figures 5(e) and 5(f)). The levels of the MMP-2 and MMP-9 mRNAs were also restored by silencing SIRT1 in MOVAs transfected with the NAMPT plasmid and stimulated with Ang II (Figure 5(d)). The intracellular and extracellular NAD levels were increased in MAECs and MOVAs transfected with the NAMPT plasmid and stimulated with Ang II (Fig. S3A-B).

2.6. NAMPT Reduced Intracellular ROS Levels through SIRT1 Signaling In Vivo and In Vitro. According to previous studies, NAMPT mainly reduces oxidative stress. Dihydroethidium (DHE) fluorescent probes were used to detect the intracellular ROS levels and verify whether NAMPT alleviates oxidative stress induced by Ang II. After the overexpression of NAMPT and Ang II stimulation of MAECs for 48 hours, the ROS level was significantly reduced (Figure 6(a)). Moreover, the ROS level was significantly reduced by NAMPT overexpression in MOVAs stimulated with Ang II (Figure 6(b)). We subsequently knocked down SIRT1 using the SIRT1-specific siRNA to verify the effects of NAMPT/-SIRT1 signaling. SIRT1 silencing restored the normal intracellular ROS level in MAECs (Figure 6(a)) and MOVAs (Figure 6(b)). Moreover, in vivo DHE staining showed an apparent increase in ROS levels in fresh aortic walls from NAMPT+/- mice compared with WT mice after Ang II stimulation (Figure 6(c)).

2.7. The MAPK Signaling Pathway Was Responsible for the Antihypertensive Effects of NAMPT/SIRT1. NAMPT has been shown to reduce oxidative stress caused by Ang II through SIRT1. Therefore, we examined the levels of the phosphorylated and total proteins for the kinases involved in the MAPK signaling pathway, specifically extracellular

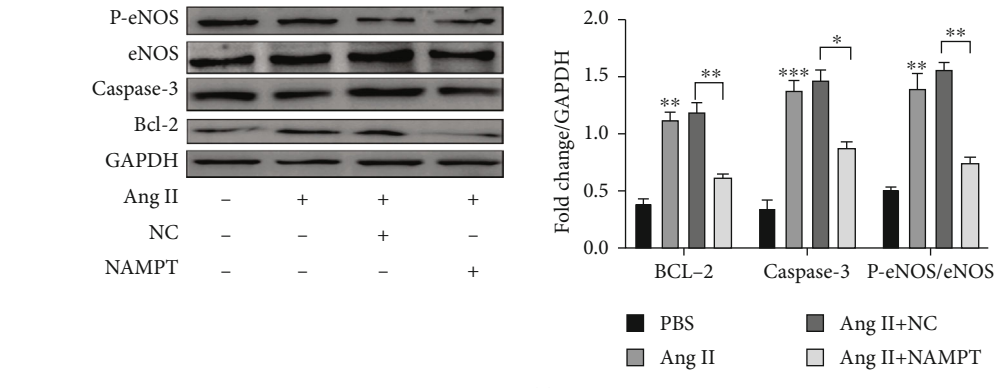

(a)

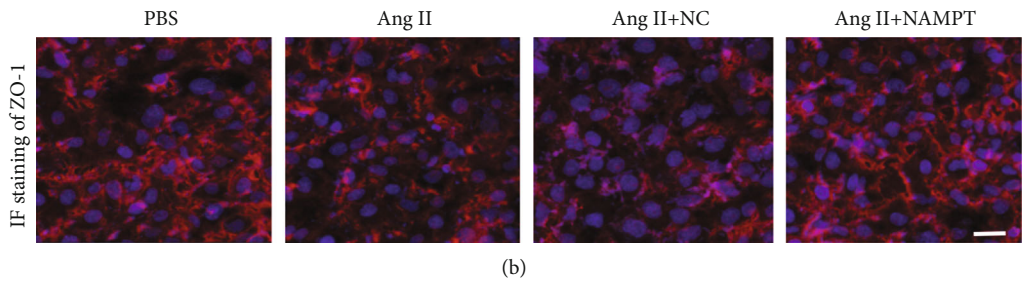

(b)

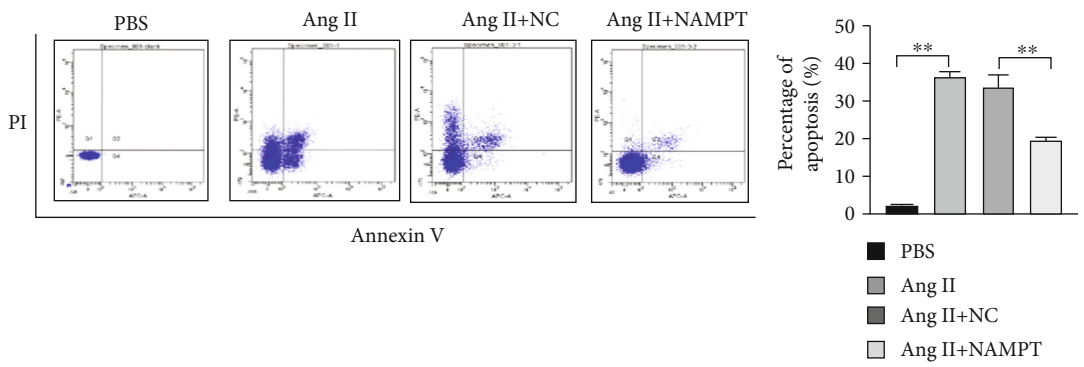

(c)

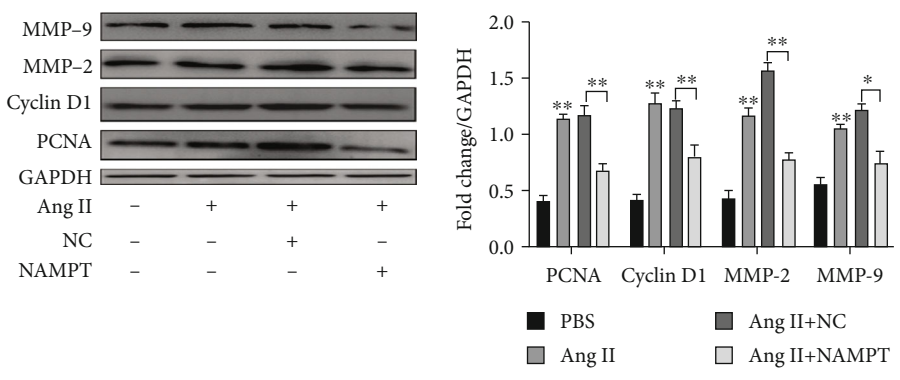

(d)

Figure 3: Continued.

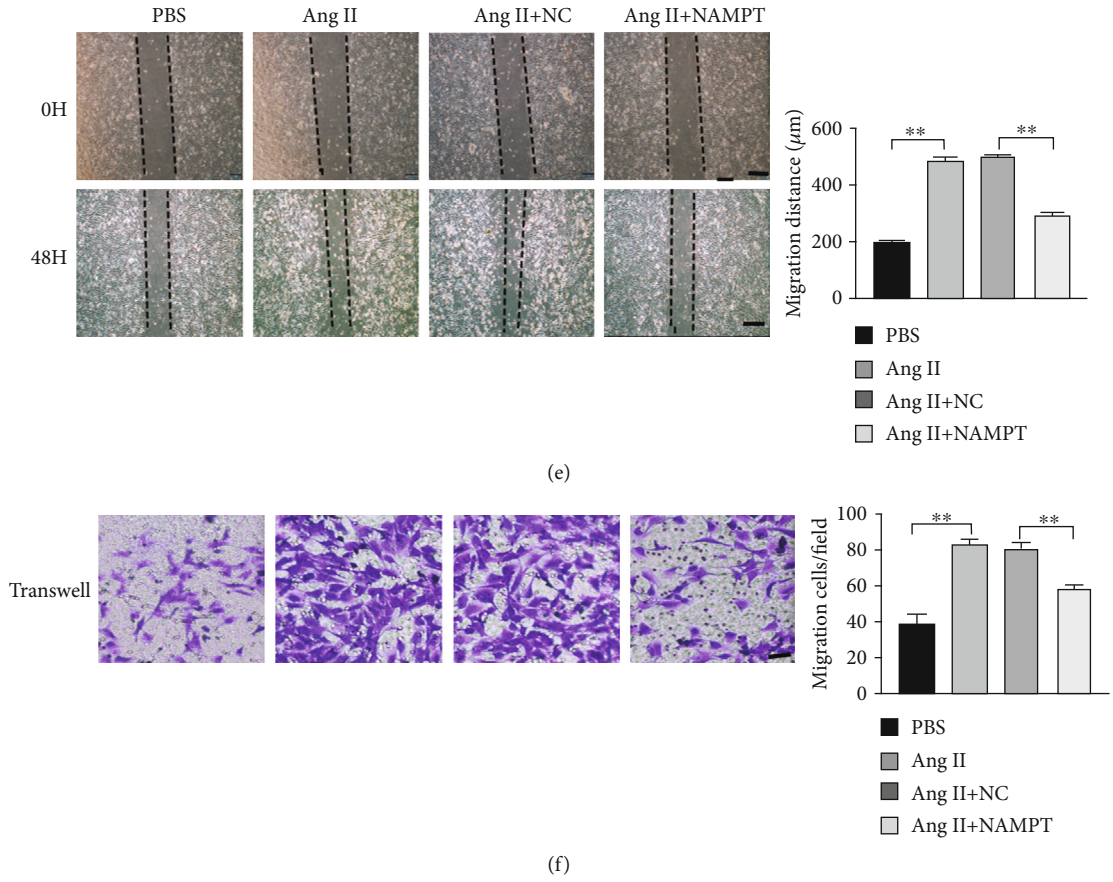

Figure 3: Ang II-induced endothelial dysfunction and changes in the proliferation and migration of MOVAs are ameliorated by the overexpression of NAMPT. (a) The protein levels and densitometric quantification of apoptosis markers (Caspase 3 and Bcl-2) and P-eNOS/eNOS were determined in cells transfected with the NAMPT plasmid and treated with Ang II for 48 h using Western blot analyses. (b) The expression of the endothelial cell permeability marker ZO-1 in MAECs was determined using immunofluorescence staining (ZO-1: red; nuclei (DAPI): blue). Scale bar = 500 μm. (c) MAECs subjected to different treatments were stained with Annexin V and propidium iodide (PI) and analyzed using flow cytometry to evaluate the effect of NAMPT on cell apoptosis after the Ang II treatment. Quantification of cell apoptosis is showed in the right panel. (d) Relative levels of proliferation-related proteins (PCNA and cyclin D1) and extracellular matrix synthesis-related proteins (MMP-2 and MMP-9) in cultured MOVAs from the indicated groups. (e, f). Representative images of scratch-wound assays and transwell assays and quantification of migrated MOVAs ($n = 4$ in each group; scale bar = 200 μm). Data are presented as means ± SEM.$^{*}p < 0.05$, $^{**}p < 0.01$, and $^{***}p < 0.001$ compared with the Ctrl or between the two indicated groups.

signal-regulated kinase 1/2 (ERK1/2), c-Jun N-terminal kinase 1/2 (JNK1/2), and P38, to investigate which downstream signaling pathways are modulated by ROS in vivo and in vitro. In MAECs, overexpression of NAMPT significantly reduced the levels of phosphorylated JNK and P38, but not ERK1/2. SIRT1 silencing rescued the levels of phosphorylated JNK1/2 and P38 in cells transfected with the NAMPT plasmid and stimulated with Ang II for 48 hours (Figure 7(a)). In MOVAs, the levels of phosphorylated ERK1/2, P38, and JNK1/2 were all decreased after transfection with NAMPT plasmids; moreover, SIRT1 silencing restored the levels of phosphorylated MAPK in cells transfected with the NAMPT plasmid and stimulated with Ang II for 48 hours (Figure 7(b)). We obtained fresh aortic walls from NAMPT+/- mice and WT mice after Ang II stimulation. The levels of phosphorylated MAPK pathway proteins, including ERK1/2, P38, and JNK1/2, were much higher in WT mice (Figure 7(c)).

2.8. Therapeutic Potential of rhNAMPT. An intraperitoneal injection of rhNAMPT (2 μg/100 g) was administered every 3 days from 1 week before surgically implanting the Ang II micropump to 4 weeks after surgery to investigate the therapeutic potential of rhNAMPT in vivo. The process continued until 4 weeks after surgery. H&E staining showed a slight decrease in the aortic M of NAMPT+/- mice after rhNAMPT administration, but the differences in L and M/L were not statistically significant in the different groups of mice during rhNAMPT treatment (Figures 8(a) and 8(b)). DHE staining was performed and suggested a significant alleviation of ROS levels in the aortic wall during rhNAMPT treatment compared with saline administration in NAMPT+/- and WT mice (Figure 7(b)). The ROS level in NAMPT+/- mice was obviously decreased compared with WT mice (Figure 8(c)). SBP, MBP, DBP, and HR were tested weekly to determine whether hypertension was ameliorated by rhNAMPT administration; a detailed description of blood

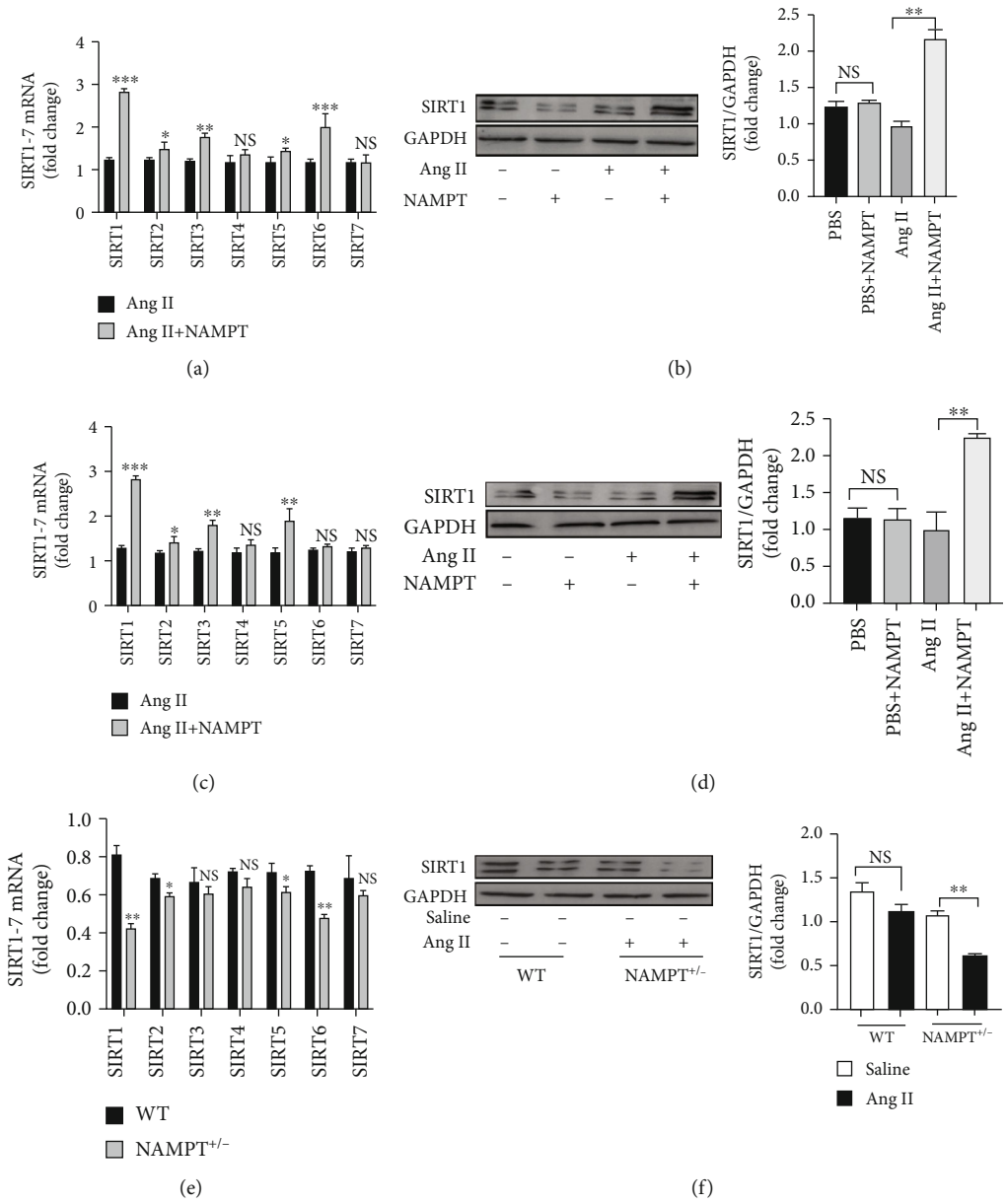

Figure 4: Continued.

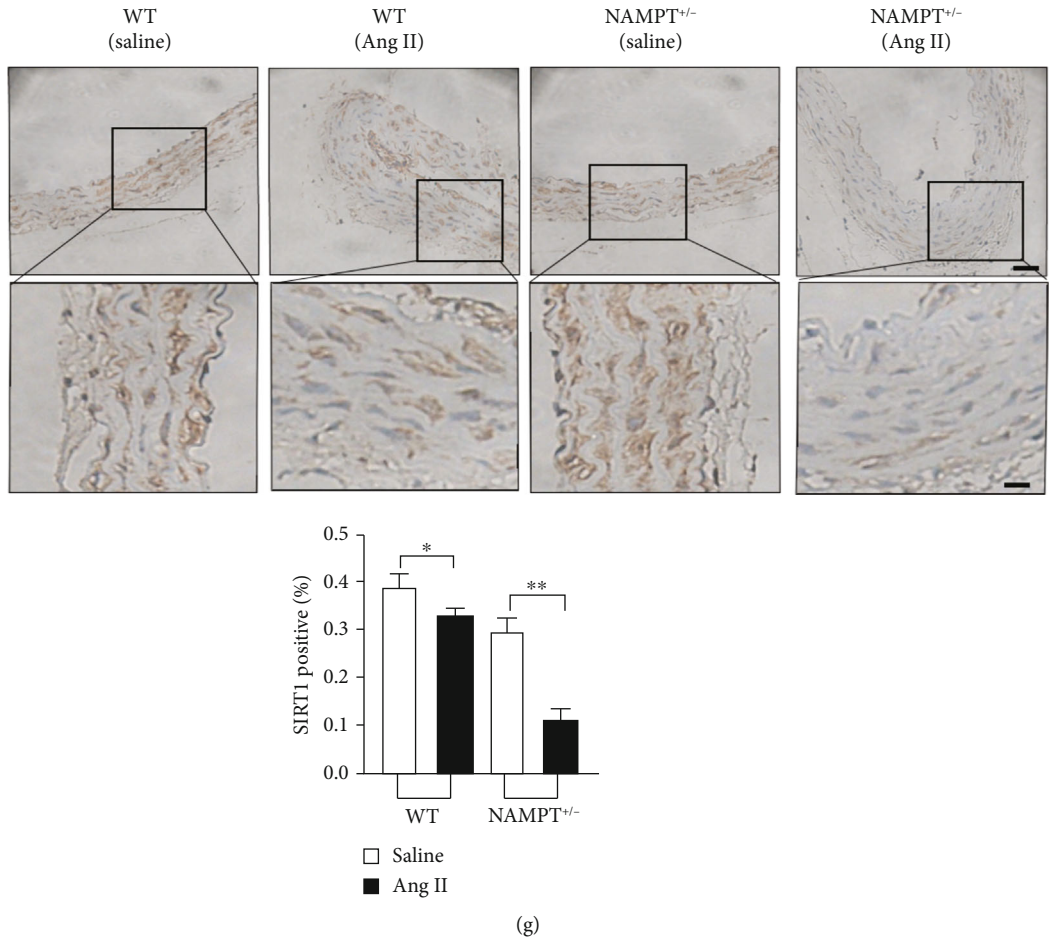

Figure 4: NAMPT regulates SIRT1 expression in vivo and in vitro. Representative qRT-PCR results and summarized data showing the expression of SIRT1-7 in MAECs (a) and MOVAs (c) transfected with NAMPT and stimulated with Ang II. Representative Western blot and summarized data showing the levels of SIRT1 in MAECs (b) and MOVAs (d) transfected with NAMPT plasmids and stimulated with Ang II. (e) Representative qRT-PCR and summarized data showing the expression of SIRT1-7 from NAMPT haplodeficient (NAMPT+/-) mice and their littermate control mice after Ang II stimulation ($n = 4$ in each group). (f) Representative Western blot and quantitative analysis of SIRT-1 levels among the different groups. (g) Immunohistochemical staining showing the level of SIRT1 in Ang II-treated NAMPT haplodeficient (NAMPT+/-) mice and their littermate control mice ($n = 4$ in each group; scale bar 50 μm). Data are presented as means ± SEM. $^{*}p < 0.05$, $^{**}p < 0.01$, and $^{***}p < 0.001$, and NS indicates no significant difference between the 2 indicated groups.

pressure parameters is provided in Table S3. Ang II-induced changes in SBP and DBP were slightly alleviated by rhNAMPT administration to NAMPT+/- mice and WT mice. No significant differences in DBP or HR were observed (Figure 8(d)). Additionally, the qRT-PCR analysis revealed the downregulation of the Ang II-induced increase in the expression of remodeling markers, including CTGF, collagen I, and collagen III, in NAMPT+/- mice compared to WT mice (Figure 8(e)), as well as the picrosirius red staining (PSR). Moreover, NAD levels were also increased in plasma and aortic wall tissues from WT and NAMPT+/- mice treated with rhNAMPT (Fig. S3C).

3. Discussion

Based on our results, the expression of NAMPT was significantly downregulated in both patients with hypertension and experimental animals. In addition, NAMPT+/- mice exhibited significantly higher blood pressure and ROS levels than WT littermates following Ang II stimulation. Moreover, overexpression of NAMPT alleviated the Ang II-induced increase in ROS levels through SIRT1/NAD signaling in vivo and in vitro. Finally, the administration of rhNAMPT alleviated vascular remodeling in NAMPT+/- mice by modulating the oxidative stress response. Considering its antioxidant function, NAMPT may be a useful treatment for hypertension.

NAMPT was identified as an enzyme involved in NAD biosynthesis [7] and is also named pre-B cell colony-enhancing factor (PBEF) and visfatin [16]. NAMPT exerts both intracellular and extracellular effects on immunity, inflammation, metabolism, and stress responses under physiological and pathophysiological conditions [17, 18]. NAMPT modulates processes involved in the pathogenesis of obesity and related disorders by influencing the oxidative stress response [12], is often overexpressed in tumor tissues,

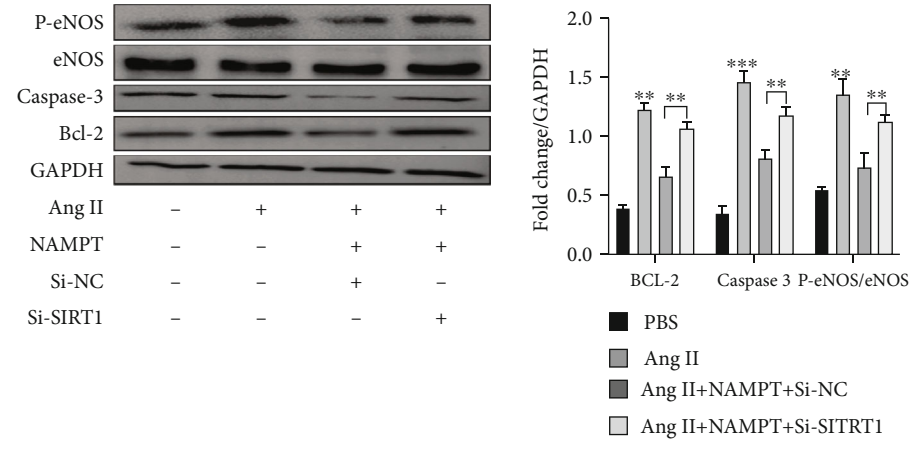

(a)

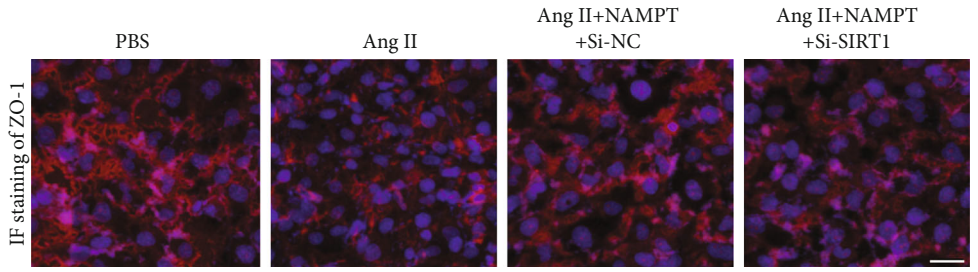

(b)

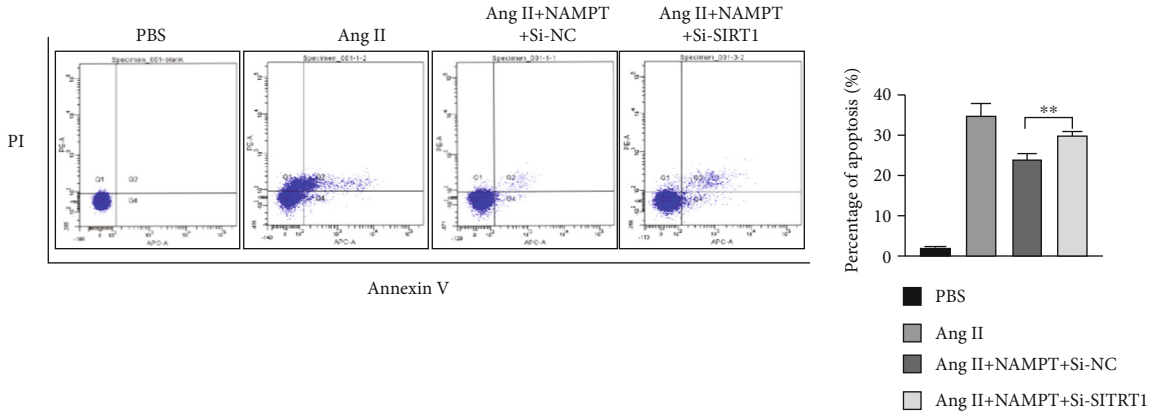

(c)

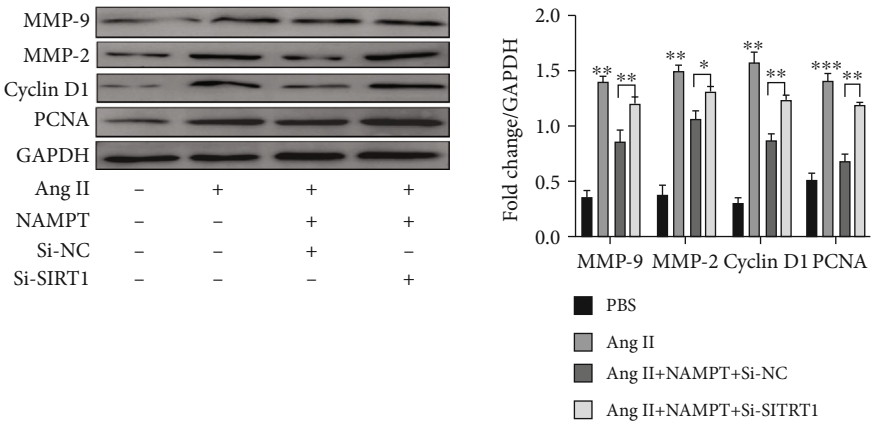

(d)

Figure 5: Continued.

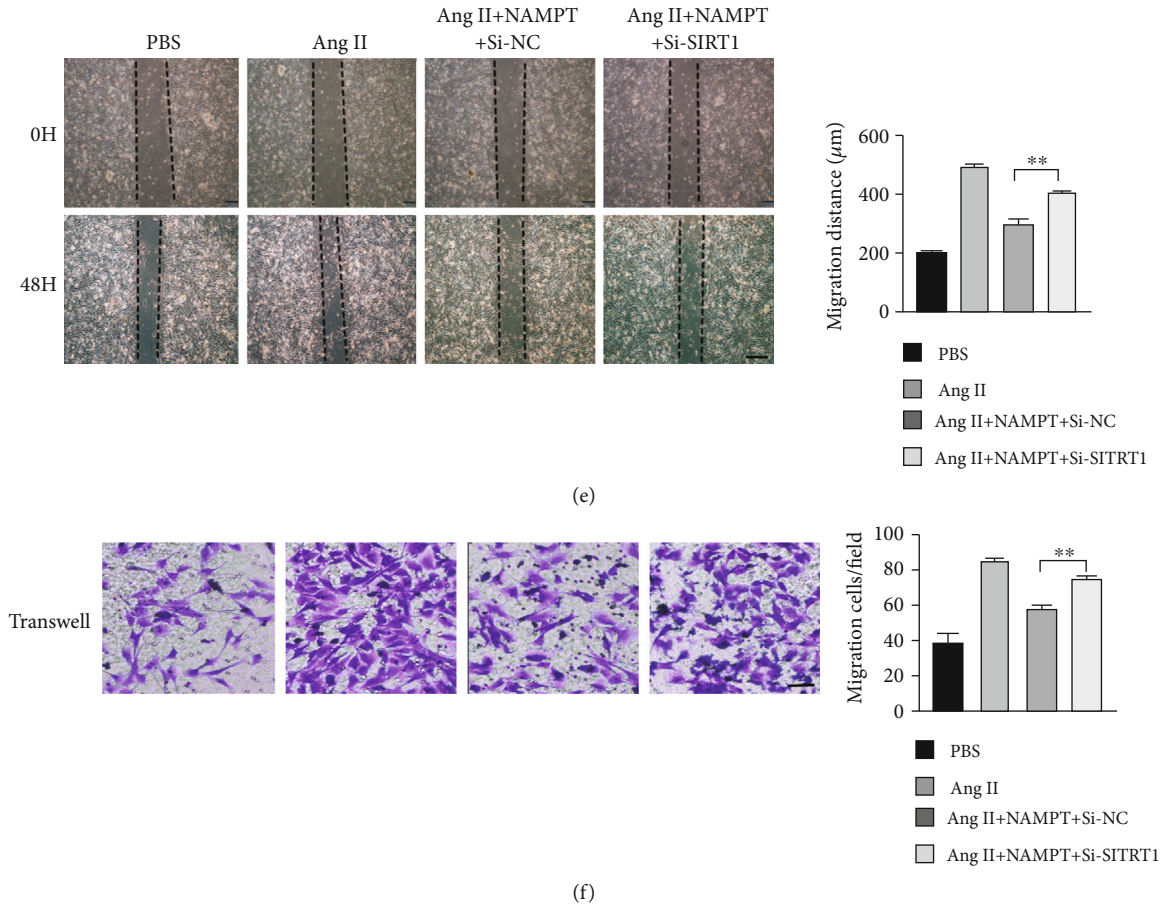

Figure 5: NAMPT alleviates Ang II-induced endothelial injury and changes in the proliferation and migration of MOVAs by targeting NAD/SIRT1 signaling. (a) The protein levels of apoptosis markers (Caspase 3 and Bcl-2) and P-eNOS/eNOS in NAMPT-overexpressing cells transfected with SIRT1-specific siRNA and stimulated with Ang II for 48 h were determined using Western blot analysis; the densitometric quantification is also shown. (b) The expression of the endothelial cell permeability marker ZO-1 in MAECs was determined using immunofluorescence staining (ZO-1: red; nuclei (DAPI): blue). Scale bar = 500 μm. (c) MAECs subjected to different treatments were stained with Annexin V and PI and analyzed using flow cytometry to evaluate the effect of NAMPT on cell apoptosis after the Ang II treatment. Quantification of the cell apoptosis rate is shown in the right panel. (d) Relative levels of proliferation-related proteins (PCNA and cyclin D1) and extracellular matrix synthesis-related proteins (MMP-2 and MMP-9) in cultured MOVAs from the indicated groups. (e, f) Representative images of scratch-wound assays and transwell assays and quantification of migrated MOVAs ($n = 4$ in each group; scale bar = 200 μm). Data are presented as means ± SEM.$^{*}p < 0.05$, $^{**}p < 0.01$, and $^{***}p < 0.001$ compared with the Ctrl or between the 2 indicated groups.

and potentially contributes to the ability of cancer cells to resist oxidative stress [19]. The levels of NAMPT decrease with aging due to chronic inflammation, oxidative stress, and DNA damage [20]. In the cardiovascular system, NAMPT exacerbates atherosclerotic inflammation and promotes atherosclerosis development in ApoE mice [13]. NAMPT promotes pulmonary vascular remodeling, and its inhibition potentially represents a therapeutic strategy for pulmonary arterial hypertension (PAH) [14]. NAMPT inhibits myocardial injury in response to myocardial ischemia and reperfusion by regulating NAD and ATP levels [21]. Therefore, visfatin/NAMPT might be a novel therapeutic target in various disorders [22]. However, the molecular mechanism of NAMPT and its function in hypertension are not well understood. In the present study, the expression of NAMPT was significantly downregulated in both patients with hypertension and experimental animals. Moreover, the level of NAMPT was reduced in both MAECs and MOVAs after Ang II stimulation. Thus, we hypothesize that decreased NAMPT expression is associated with hypertension and may serve as a biomarker of hypertension.

As the initial effector molecule of the RAS, Ang II activation exerts an important effect on hypertension1 and has been shown to induce NOX activity and increase local ROS production by binding to AT1R [2]. ROS function as novel intracellular second messengers in signal transduction pathways that originate from a variety of membrane receptors. ROS promote endothelial dysfunction, which is an early event in the pathogenesis of hypertension [3]. Then, the proliferation and migration of VSMCs are critically involved in vascular remodeling processes [4]. These processes are also related to increased collagen decomposition, activation of MMPs, and ECM reorganization [23, 24]. In addition, the correlation between NAMPT-associated signaling and ROS

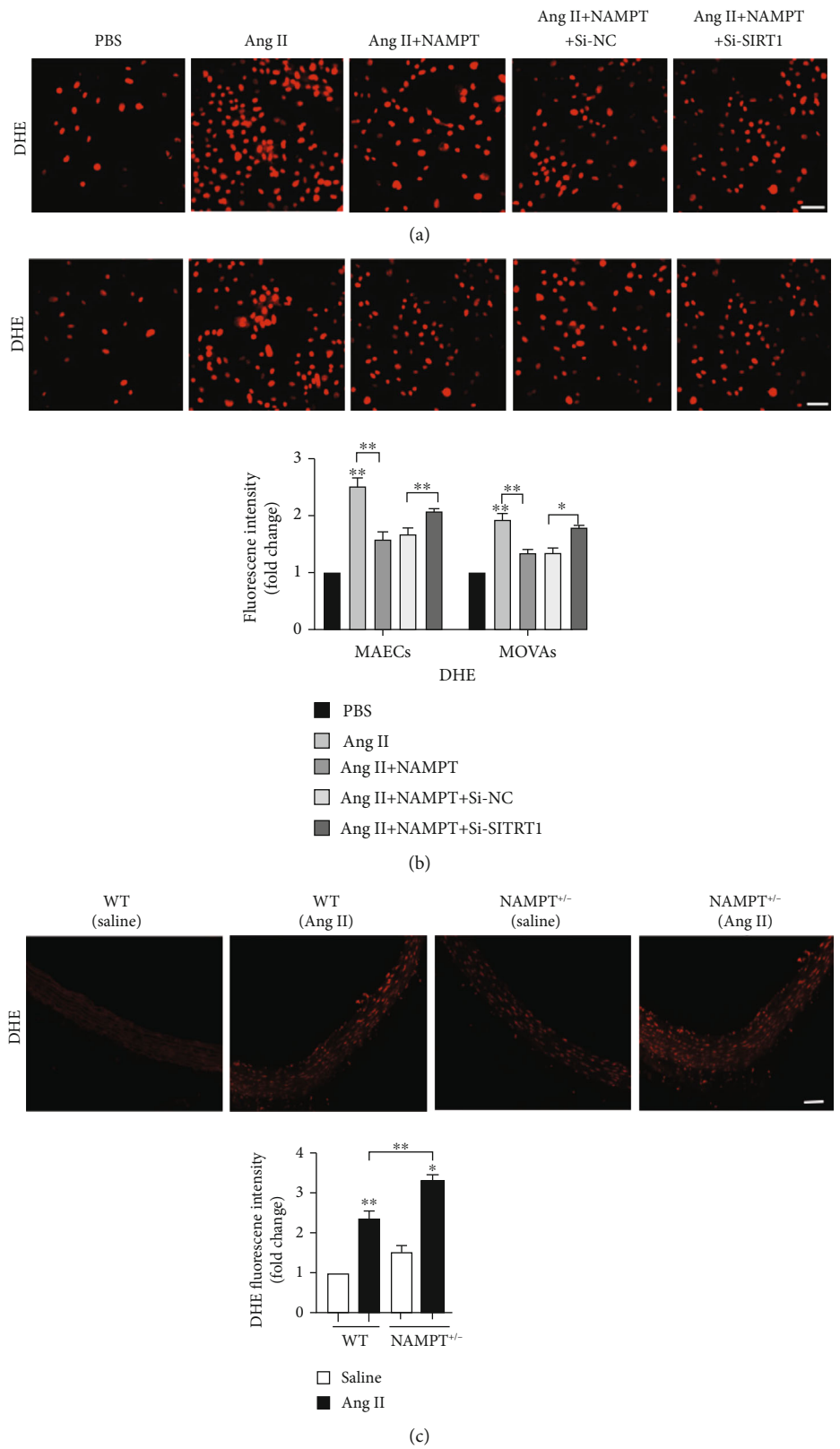

Figure 6: NAMPT reduces intracellular ROS levels through SIRT1 signaling in vivo and in vitro. DHE fluorescent probes and DCFH-DA were used to detect the level of ROS in MAECs (a) and MOVAs (b) with Sirt1 silencing, NAMPT overexpression, and Ang II stimulation. DHE (red) and DCF-DA (green). Scale bar = 500 μm. (c) DHE staining of fresh aortic wall tissues from NAMPT+/- and WT stimulated with Ang II ($n = 6$ in each group). DHE (red). Scale bar = 50 μm. Data are presented as means ± SEM. $^{*}p < 0.05$ and $^{**}p < 0.01$ compared with the corresponding saline group or between the 2 indicated groups.

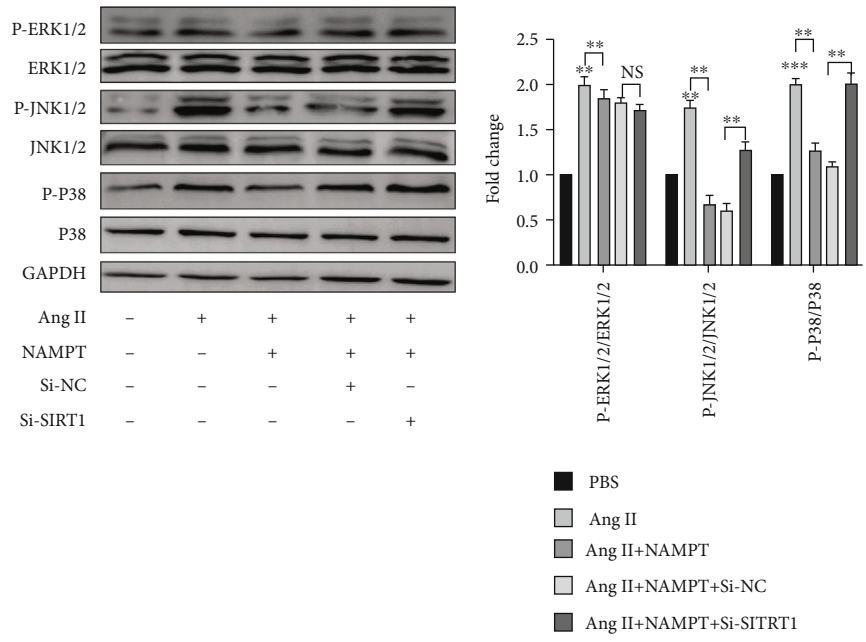

(a)

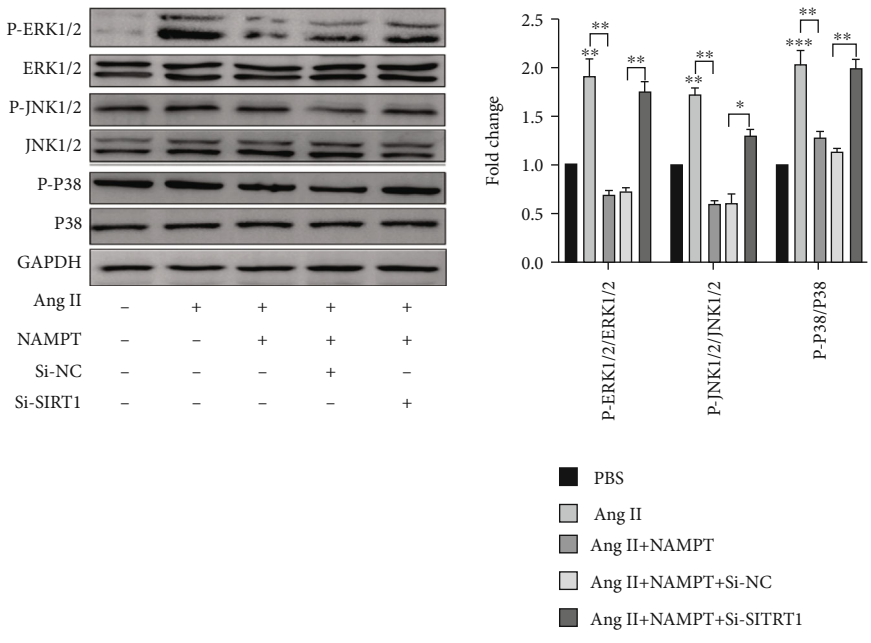

(b)

Figure 7: Continued.

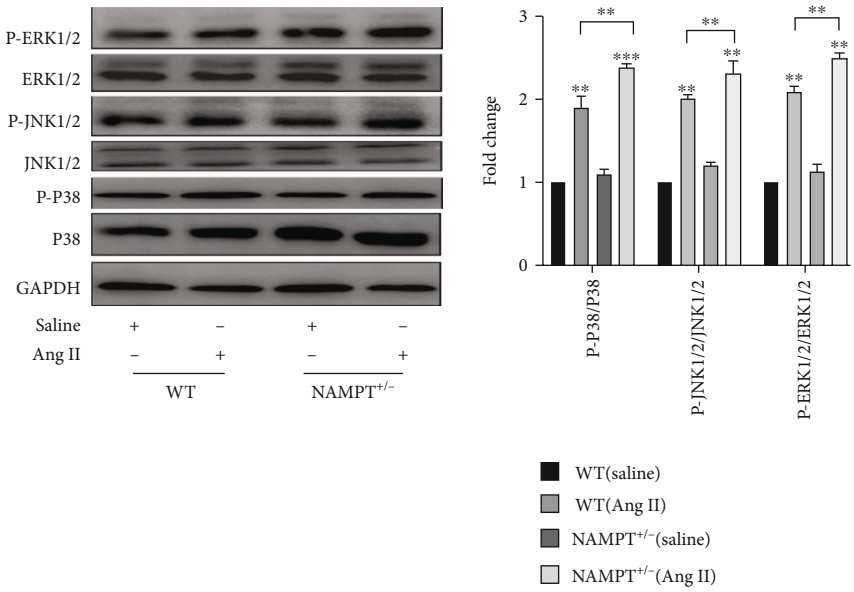

(c)

Figure 7: The MAPK signaling pathway is responsible for the antihypertensive effects of NAMPT/SIRT1. Western blots showing the levels of P-ERK1/2, P-JNK1/2, and P-P38 and quantification relative to the total ERK1/2, JNK1/2, and P38 levels in the MAECs (a) and MOVAs (b) transfected with the SIRT1-specific siRNA and NAMPT overexpression plasmid and stimulated with Ang II for 48 h. (c) Representative Western blots and quantitative analyses of the levels of the P-ERK1/2/ERK1/2, P-JNK1/2/JNK1/2, and P-P38/P38 proteins in fresh aortic wall tissues obtained from NAMPT+/- and WT mice after Ang II stimulation ($n = 6$ in each group). Data are presented as means ± SEM. $^{*}p < 0.05$, $^{**}p < 0.01$, $^{***}p < 0.001$, and NS indicates no significant difference between the 2 indicated groups.

has been detected in diverse diseases. NAMPT alleviates hypothalamic neuronal injury by reducing ROS production [25] and protects against ROS-induced inflammatory activation and DNA damage, which provides an integrated explanation for the dependence of inflammatory macrophages on the NAD salvage pathway [26]. NAMPT suppresses glucose deprivation-induced oxidative stress by increasing NADPH levels in breast cancer [27] and protects against myocardial injury in response to myocardial ischemia and reperfusion by regulating NAD+ and ATP levels [28]. Based on these findings, NAMPT plays an important role in ROS-associated injury [29]. However, the role of NAMPT in ROS-associated vascular remodeling remains unknown. Our study revealed a critical role for NAMPT in regulating Ang II-induced hypertension. NAMPT+/- mice exhibited significantly higher blood pressure and ROS levels than WT littermates after an Ang II infusion for 4 weeks. Moreover, the administration of rhNAMPT reduced the ROS level in NAMPT+/- mice, but the reduction in blood pressure was not obvious. NAMPT overexpression alleviated ROS-associated endothelial dysfunction, VSMC proliferation and migration, and ECM reorganization. Therefore, NAMPT may be employed in the clinic to prevent and potentially treat hypertension.

NAMPT modulates the activity of NAD-dependent enzymes, such as sirtuins [8], PARPs [9] and CD38 [10], thereby regulating cellular metabolism, mitochondrial biogenesis, and adaptive responses to inflammation, oxidation, and genotoxic stress [17, 18]. Sirtuins are a conserved family of enzymes present in diverse organisms. They possess NAD-dependent protein deacetylase activity, cleaving NAD during each deacetylation cycle [30]. Mammals express seven sirtuin homologs (SIRT1 to 7), of which SIRT1 is located in the nucleus and cytosol and, along with histone deacetylation, modulates transcription factors such as P53, nuclear factor kappa-light-chain-enhancer of activated B cells (NF-κB), FOXOs, and PARP1. SIRT2 is a cytosolic sirtuin [31], while SIRT3, 4, and 5 are located in the mitochondria and have roles in oxidative stress and lipid metabolism. SIRT6 and 7 are nuclear sirtuins with roles in gene expression and DNA repair [30, 31]. We transfected both MOVAs and MAECs with NAMPT-overexpressing plasmids and stimulated them with Ang II to verify which sirtuins were involved. Interestingly, the expression of the SIRT1 mRNA was significantly increased compared to other SIRTs mRNAs in MOVAs and MAECs. The level of the SIRT1 protein was increased in vivo and in vitro. Moreover, NAMPT increased both extracellular and intracellular NAD concentrations. Importantly, the regulation of SIRT1 depended on NAMPT activity, which has been implicated in aging, metabolism, and tolerance to oxidative stress [32]. NAMPT promotes colorectal cancer cell growth via the SIRT1/P53 signaling pathway and is a prognostic marker in colorectal cancer [33]. The suppression of the NLRP3 inflammasome improves longevity and prevents cardiac aging in male mice through NAMPT/-SIRT1 [34]. In cultured cardiomyocytes, NAMPT and SIRT1 cooperatively suppress the activity of mitochondrial proteins and ATP production, thereby promoting mitochondrial dysfunction [21]. Intracellular NAMPT has been recognized as the key enzyme involved in cellular NAD production.

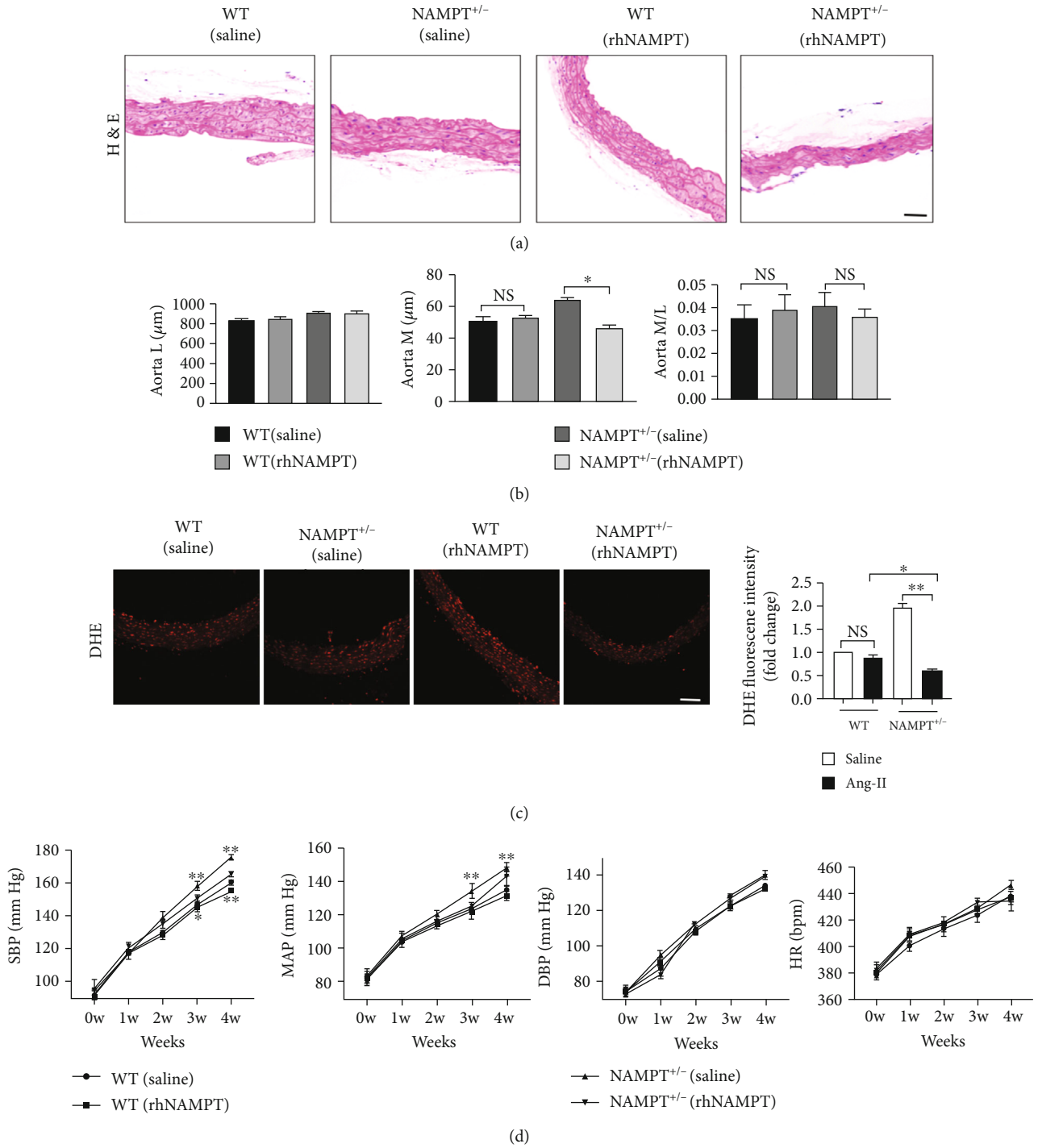

Figure 8: Continued.

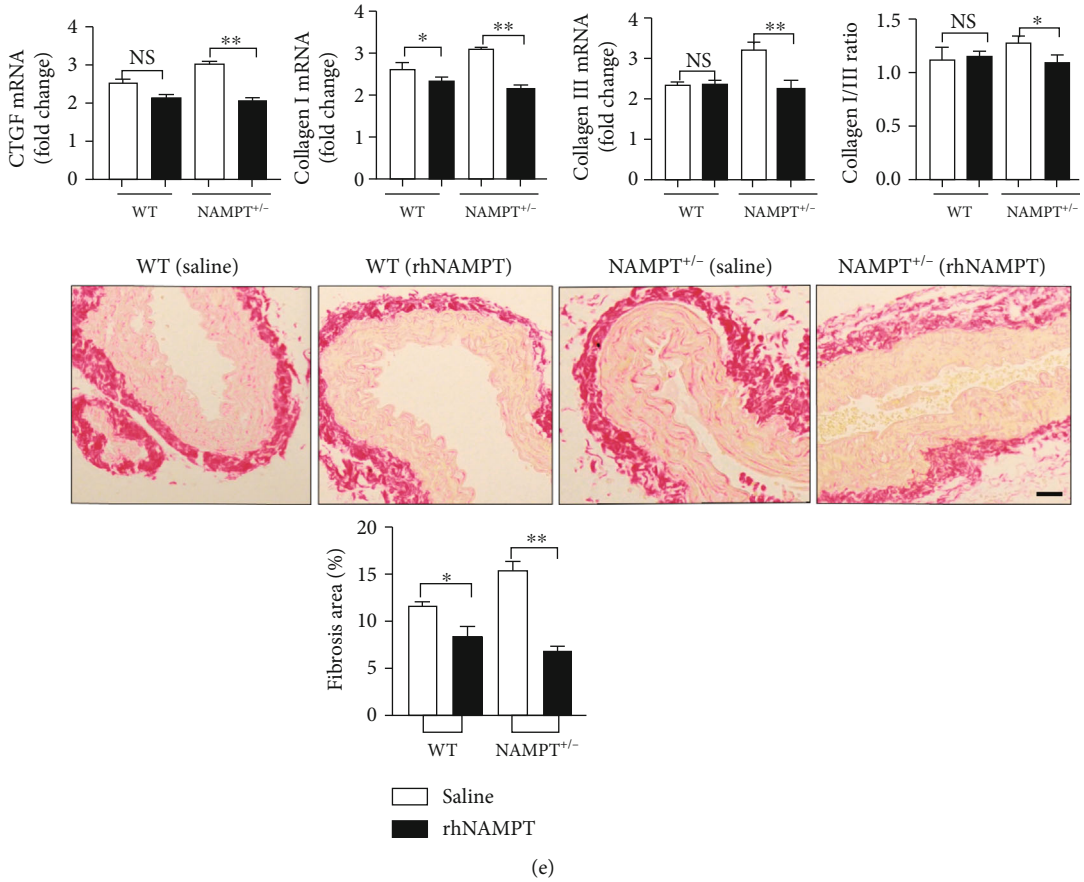

Figure 8: Therapeutic potential of rhNAMPT. (a) Representative images of H&E staining showing the remodeling of arteries (scale bar = 50 μm, $n = 5$ in each group, ≥40 fields per group). (b) M, L, and their ratio in the aorta. (c) DHE staining of fresh aortic wall tissues from NAMPT +/- and WT mice after Ang II stimulation and rhNAMPT administration (DHE (red); $n = 6$ in each group, scale bar = 500 μm). (d) The SBP, MAP, DBP, and HR were measured with a noninvasive computerized tail-cuff system in conscious mice. (e) Relative mRNA levels of CTGF, collagen I, and collagen III and the ratio of collagen type I and type III in WT littermates and NAMPT+/- mice treated with saline or Ang II treatment and injected with rhNAMPT ($n = 6$ in each group), as well as the picrosirius red staining (PSR). Data are presented as means ± SEM . $^{*}p < 0.05$ and $^{**}p < 0.01$ compared with the corresponding saline group; NS: not significant.

However, the biological functions of extracellular NAMPT are not clearly understood, and its receptor has not been identified. Researchers are still debating whether NAMPT has enzymatic activity outside the cell [11]. The intracellular NAMPT-NAD-SIRT1 cascade improves postischemic vascular repair by modulating Notch signaling in endothelial progenitors [35]. Meanwhile, extracellular NAMPT/visfatin causes P53 deacetylation via NAD production and SIRT1 activation in breast cancer cells [36]. Taken together, the role of the NAMPT/SIRT1 axis in the cardiovascular system remains controversial. In the present study, SIRT1 knockdown with a SIRT1-specific siRNA significantly exacerbated the Ang II-induced increases in the proliferation and migration of MOVAs and the apoptosis and endothelial nitric oxide synthase activity of MAECs after NAMPT overexpression, in addition to the ECM reorganization.

In turn, ROS activate a variety of protein tyrosine and serine/threonine kinases, many of which are known to promote multiple cellular responses, including growth, differentiation, apoptosis, and inflammation in diverse tissues and cells. Ang II-mediated ROS production activates the ERK signaling in ECs through the Ras/Raf/MEK pathway [37] and also induces JNK and P38-related signaling through apoptosis signaling kinase 1 (ASK1) [37, 38]. ROS promote the expression of vascular cell adhesion molecule-1 (VCAM1) and interstitial cell adhesion molecule-1 (ICAM1) and reduce intracellular nitric oxide synthase levels and eliminate endothelial NO, thereby decreasing EC viability [38, 39]. Ang II activates MAPK in VSMCs, promotes VSMC proliferation through ROS, and activates the expression of related proliferation genes such as AP-1, which further triggers the proliferation, migration, and secretion of ECM by VSMCs [40, 41]. Ang II activates JNK through c-Src and calcium ion-dependent protein kinase and promotes the proliferation of VSMCs [42]. In addition, c-Src activates ERK to promote migration. Furthermore, P38 MAPK plays an important role in activating heat shock protein 27- (HSP-27-) induced migration [40, 42], indicating that MAPK plays an important role in Ang II-mediated ROS-induced vascular remodeling. As shown in the present study, NAMPT overexpression alleviated the activation of ERK, P38

MAPK, and JNK induced by Ang II-mediated ROS production through SIRT1 in vivo and in vitro, but ERK activation in MAECs was not affected.

Collectively, this study is the first to show that NAMPT prevents Ang II-induced hypertension by inhibiting excess ROS accumulation, at least in part through the regulation of SIRT1 expression and the NAD concentration. Overall, NAMPT may be an innovative marker and therapeutic target for the intervention of hypertension and related vascular diseases.

The present study has several limitations. Firstly, due to laboratory conditions, we were unable to assess endothelium-dependent relaxation responses induced by acetylcholine (ACh) [43], which is a direct indicator of vascular endothelial function. Secondly, since NAMPT is expressed in almost all tissues in the body [11, 44], the effect of NAMPT knockout on the cardiovascular system is unknown. More experiments need to be performed, and conditional knockout mice should be created in sufficient numbers to obtain more powerful results in subsequent studies. Additionally, other signaling pathways may be associated with ROS, such as the PI3K/AKT, NF-κB, and JAK/STAT pathways [45–47]. Further studies are needed to determine whether NAMPT regulates ROS activity through these signaling pathways.

4. Materials and Methods

4.1. Human Aortic Wall Tissue. All studies were approved by the local ethics committee of Tongji Hospital Affiliated to Tongji University and adhered to the principles of the Declaration of Helsinki. Aortic wall samples were obtained from the patients receiving aortic replacement surgery due to acute aortic dissection at Tongji Hospital from January 2018 to October 2019. Patients with chronic heart failure, chronic obstructive pulmonary disease, chronic kidney disease, and diabetes were excluded. Based on the presence or absence of hypertension, patients were divided into the hypertension group ($n = 6$) and the normal group ($n = 6$). No differences in the risk factors and medications were observed between the two groups (Table 1).

4.2. Animal Studies and Generation of NAMPT Haplodeficient Mice. Animal studies were approved by the Animal Care and Use Committee of Tongji Hospital Affiliated to Tongji University. The NAMPT haplodeficient mice (NAMPT+/-) were generated using CRISPR-Cas9 technology, as described previously [18]. The disruption of NAMPT by homologous recombination results in early embryonic lethality because of its dysfunction in egg cylinder organization and gastrulation. At the age of 8 weeks, male NAMPT +/- mice and their littermate wild-type (WT) mice were subcutaneously implanted with osmotic minipumps (model 2004; Alzet) to permit an infusion of Ang II (Sigma-Aldrich, Cat. no. A9525, 0.7 mg/kg per day) or saline for 4 weeks under inhalation anesthesia with 2% *v*/*v* isoflurane/oxygen, as described previously [44]. Blood pressure was measured weekly with a tail-cuff system using a heated scanner unit (BP-2010A, Softron) after surgery. The blood pressure of each mouse was detected at least five times until reaching a steady state, and the final value was calculated from an average of three proximal repeats.

4.3. Cell Culture and Treatment. MAECs and MOVAs were purchased from American Type Culture Collection (Manassas, VA, USA) and cultured in high-glucose DMEM supplemented with 10% fetal bovine serum and 1% penicillin/streptomycin. Moreover, MOVAs were incubated with 2 mmol/L L-glutamine. Cells were cultured in a 37°C, 5% CO_2 incubator. Ang II was purchased from Sigma-Aldrich (Cat. no. A9525) and dissolved in sterile ultrapure water. Cells were exposed to Ang II at a final concentration of 10-6 mol/L and incubated for 24 or 48 hours.

4.4. Small Interfering RNA Transfection. The siRNA targeting mouse SIRT1 (5′-GCAGGTTGCAGGAATCCAAAG-3′) were synthesized by RiboBio Biotechnology Company (Guangzhou, China). For transfection, 50 nM SIRT1-siRNA and scrambled-siRNA were delivered into cells using the Lipofectamine™ 2000 transfection reagent (Invitrogen, Carlsbad, CA, USA) according to the manufacturer's instructions.

4.5. Transfection of pcDNA3.1-GFP-NAMPT Plasmids. After reaching 90% confluence, MOVAs and MAECs were transfected with 4 μg of pcDNA3.1-GFP-NAMPT plasmids (Hanbio, Shanghai, China) using Lipofectamine™ 2000 (Invitrogen, Carlsbad, CA, USA) according to the manufacturer's instructions.

4.6. Quantitative Reverse Transcription PCR (qRT-PCR). Total RNA was extracted from the aortic wall samples of rats, and MOVAs and MAECs were cultured using TRIzol (Takara). Total RNA (1ug) was reverse transcribed into cDNAs with the PrimeScript™ RT Reagent Kit (Takara). qRT-PCR was performed using SYBR Green (Takara), and the results were normalized to GAPDH expression. All primer sequences are shown in Table S1.

4.7. Western Blot Analysis. Proteins from the human aortic wall tissue of patients, aortic wall of mice, and cultured MOVAs and MAECs were extracted with RIPA lysis buffer (Thermo Fisher Scientific Inc.) supplemented with a protease and phosphatase inhibitor cocktail. Western blotting was performed using antibodies against NAMPT (Abcam, ab236874), P16 (Abcam, ab118459), P21 (Abcam, Ab109520), eNOS (Abcam, ab199956), P-eNOS (Abcam, ab32419), SIRT1 (Abcam, ab110304), MMP-2 (Abcam, ab97779), MMP-9 (Abcam, ab38898), AKT (CST, 4685S), P-AKT (CST, 4060S), P38 (CST, 8690S), P-P38 (CST, 4511S), ERK1/2 (Abcam, ab17942), P-ERK1/2 (Abcam, ab214362), JNK (Abcam, Ab179461), P-JNK (Abcam, Ab124956), and GAPDH (Abcam, ab8245), followed by an incubation with horseradish peroxidase-conjugated secondary antibodies (Santa Cruz Biotechnology) for 1 hour at room temperature. A gel imaging system (Tanon) and AlphaView software were used to image and analyze the Western blots.

4.8. Transwell Migration Assay and Scratch-Wound Assay. The transwell migration assay and scratch-wound assay were performed as previously described [26].

4.9. Histology, Immunohistochemical Staining, Immunofluorescence Staining, and Picrosirius Red Staining (PSR). Aortic wall samples from the patients and mouse aortic wall tissues were fixed with 4% paraformaldehyde for 24 hours and then embedded in paraffin and sliced into 4 μm sections. The morphology and fibrosis of the aortic wall were determined using H&E staining and picrosirius red staining (PSR) according to the manufacturer's instructions. Immunohistochemical staining was performed with antibodies against NAMPT (Abcam, ab236874) and SIRT1 (Abcam, ab110304). Immunofluorescence staining was performed using antibodies against CD31 (Abcam, ab28364), NAMPT (Abcam, ab236874), and ZO-1 (Abcam, ab190085) using previously described methods. Images were acquired and analyzed using Image-Pro Plus 6.0 software as previously described [25].

4.10. NAD Measurement. Intracellular and extracellular NAD levels were measured using an NAD/NADH analysis kit (Beyotime Biotechnology, Shanghai, China) according to the manufacturer's instructions. Briefly, cells or tissues were lysed, and the lysates were deproteinized with perchloric acid. Both the standard solution and samples were reacted with the developer in triplicate in a 96-well plate. After adding the specific enzyme, the plate was incubated at 37°C in the dark for 0.5 h. The absorbance of the resulting colored compound was measured at 450 nm.

4.11. Determination of ROS Levels. The MAECs, MOVAs, and fresh frozen vascular tissues were also stained with the DHE fluorescent probe (BestBio, Shanghai, China) diluted (1 : 1000 in cells and 1 : 500 in tissues) in serum-free medium to a final concentration of 5 μM for cells and 10 μM for tissues. Cells and tissues were incubated with the appropriate concentrations of DHE for 0.5 h at 37°C. The mean fluorescence intensity of DHE in the nuclei was measured. Finally, samples were detected using an excitation wavelength of 535 nm and an emission wavelength of 610 nm.

4.12. Data Analysis. Results are presented as means ± SEM. Two-tailed Student's tests were used for comparisons between two groups, and ANOVA followed by Tukey's post hoc test was used for comparisons of multiple groups. A p value less than 0.05 was considered statistically significant. GraphPad Prism 8.0 and SPSS 22.0 statistical software were used to analyze the data.

Abbreviations

NAMPT: Nicotinamide phosphoribosyltransferase
SIRT1: Sirtuin 1
ROS: Reactive oxygen species
Ang II: Angiotensin II
MMP-2: Matrix metalloproteinase 2
MMP-9: Matrix metalloproteinase 9
ECM: Extracellular matrix
eNOS: Endothelial nitric oxide synthase
CTGF: Connective tissue growth factor
NAD: Nicotinamide adenine dinucleotide
MAECs: Mouse aortic endothelial cells
MOVAs: Mouse aortic vascular smooth muscle cells.

Data Availability

The data used to support the findings of this study are included within the article and the supplementary information file.

Conflicts of Interest

The authors have no conflicts of interest to declare.

Authors' Contributions

Yunqing Mei helped to formulate the hypothesis. Ding Tian conceived the project, supervised all experiments, and edited the manuscript. Lei Zhou and Sheng Zhang contributed equally to this study.

Acknowledgments

We extend our thanks to the enrolled patients for their participation in the study. This study was supported by the National Natural Science Foundation of China (No. 8177020618) and Shanghai Science and Technology Commission Project (No. 16441907800).

Supplementary Materials

Supplementary 1. Figure S1: verification of overexpression plasmids in vitro. MAECs and MOVAs were transfected with NAMPT plasmids and then subjected to Ang II treatment for 48 h. Relative mRNA and protein expression of NAMPT was determined by qPCR and Western blot, respectively (A–D). The general structure of pcDNA3.1-GFP-NAMPT plasmids (E). Data were presented as mean ± SEM. $^{*}p < 0.05$ and $^{**}p < 0.01$ vs. the corresponding WT group or control.

Supplementary 2. Figure S2: verification of SIRT1-specific small interference RNA in vitro. MAECs and MOVAs were transfected with Si-SIRT1 and Si-NC, then subjected to Ang II treatment for 48 h. Relative mRNA and protein expression of SIRT1 was determined by qPCR (A)and Western blot (B) in MAECs, respectively, Moreover, relative mRNA and protein expression of SIRT1 was determined by qPCR (C) and Western blot (D) in MOVAs. Data were presented as mean ± SEM. $^{**}p < 0.01$ and $^{***}p < 0.001$ vs. control.

Supplementary 3. Figure S3: determination of NAD expression level in vivo and in vitro. Cells were transfected by sirt1-specific siRNA, followed by overexpression of NAMPT after Ang II stimulation for 48 hours; the intracellular and extracellular NAD levels of MAECs (A) and MOVAs (B). Representative NAD levels of plasma (C) and aortic wall from WT littermates and NAMPT+/- mice under saline or Ang-II treatment and rhNAMPT administration ($n = 6$ in

each group). Data were presented as mean ± SEM. $^{**}p < 0.01$ and $^{***}p < 0.001$, and NS indicates no significance between the 2 indicated groups.

Supplementary 4. Table S1: the primer sequence for qRT-PCR.

Supplementary 5. Table S2: the SBP, MAP, and DBP of WT and NAMPT+/- mouse after Ang II infusion.

Supplementary 6. Table S3: the SBP, MAP, and DBP of WT and NAMPT+/- mouse after rhNAMPT and Ang II infusion.

References

[1] M. H. Forouzanfar, P. Liu, G. A. Roth et al., "Global burden of hypertension and systolic blood pressure of at least 110 to 115 mm Hg, 1990-2015," *The Journal of the American Medical Association*, vol. 317, no. 2, pp. 165–182, 2017.

[2] V. Adams, A. Linke, N. Kränkel et al., "Impact of regular physical activity on the NAD(P)H oxidase and angiotensin receptor system in patients with coronary artery disease," *Circulation*, vol. 111, no. 5, pp. 555–562, 2005.

[3] S. Costantino, F. Paneni, A. Virdis et al., "Interplay among H3K9-editing enzymes SUV39H1, JMJD2C and SRC-1 drives p66Shc transcription and vascular oxidative stress in obesity," *European Heart Journal*, vol. 40, no. 4, pp. 383–391, 2019.

[4] M. Kuntic, M. Oelze, S. Steven et al., "Short-term e-cigarette vapour exposure causes vascular oxidative stress and dysfunction: evidence for a close connection to brain damage and a key role of the phagocytic NADPH oxidase (NOX-2)," *European Heart Journal*, vol. 41, no. 26, pp. 2472–2483, 2020.

[5] D. Nagata, R. Takeda, M. Sata et al., "AMP-activated protein kinase inhibits angiotensin II-stimulated vascular smooth muscle cell proliferation," *Circulation*, vol. 110, no. 4, pp. 444–451, 2004.

[6] F. Tabet, E. L. Schiffrin, G. E. Callera et al., "Redox-sensitive signaling by angiotensin II involves oxidative inactivation and blunted phosphorylation of protein tyrosine phosphatase SHP-2 in vascular smooth muscle cells from SHR," *Circulation Research*, vol. 103, no. 2, pp. 149–158, 2008.

[7] A. Rongvaux, R. J. Shea, M. H. Mulks et al., "Pre-B-cell colony-enhancing factor, whose expression is up-regulated in activated lymphocytes, is a nicotinamide phosphoribosyltransferase, a cytosolic enzyme involved in NAD biosynthesis," *European Journal of Immunology*, vol. 32, no. 11, pp. 3225–3234, 2002.

[8] S. C. Bowlby, M. J. Thomas, R. B. D'Agostino, and S. J. Kridel, "Nicotinamide phosphoribosyl transferase (Nampt) is required for de novo lipogenesis in tumor cells," *PLoS One*, vol. 7, no. 6, article e40195, 2012.

[9] F. Van Gool, M. Gallí, C. Gueydan et al., "Intracellular NAD levels regulate tumor necrosis factor protein synthesis in a sirtuin-dependent manner," *Nature Medicine*, vol. 15, no. 2, pp. 206–210, 2009.

[10] J. B. Pillai, A. Isbatan, S. Imai, and M. P. Gupta, "Poly(ADP-ribose) polymerase-1-dependent cardiac myocyte cell death during heart failure is mediated by NAD+depletion and reduced Sir2α deacetylase activity," *The Journal of Biological Chemistry*, vol. 280, no. 52, pp. 43121–43130, 2005.

[11] A. Garten, S. Schuster, M. Penke, T. Gorski, T. de Giorgis, and W. Kiess, "Physiological and pathophysiological roles of NAMPT and NAD metabolism," *Nature Reviews Endocrinology*, vol. 11, no. 9, pp. 535–546, 2015.

[12] H. O. El-Mesallamy, D. H. Kassem, E. El-Demerdash, and A. I. Amin, "Vaspin and visfatin/Nampt are interesting interrelated adipokines playing a role in the pathogenesis of type 2 diabetes mellitus," *Metabolism*, vol. 60, no. 1, pp. 63–70, 2011.

[13] Y.-y. Kong, G.-q. Li, W.-j. Zhang et al., "Nicotinamide phosphoribosyltransferase aggravates inflammation and promotes atherosclerosis in ApoE knockout mice," *Acta Pharmacologica Sinica*, vol. 40, no. 9, pp. 1184–1192, 2019.

[14] J. Chen, J. R. Sysol, S. Singla et al., "Nicotinamide phosphoribosyltransferase promotes pulmonary vascular remodeling and is a therapeutic target in pulmonary arterial hypertension," *Circulation*, vol. 135, no. 16, pp. 1532–1546, 2017.

[15] T. B. Dahl, S. Holm, P. Aukrust, and B. Halvorsen, "Visfatin/-NAMPT: a multifaceted molecule with diverse roles in physiology and pathophysiology," *Annual Review of Nutrition*, vol. 32, pp. 229–243, 2012.

[16] C. Hug and H. F. Lodish, "Medicine: Visfatin: a new adipokine," *Science*, vol. 307, pp. 366-367, 2005.

[17] S. J. Yang, J. M. Choi, L. Kim et al., "Nicotinamide improves glucose metabolism and affects the hepatic NAD-sirtuin pathway in a rodent model of obesity and type 2 diabetes," *The Journal of Nutritional Biochemistry*, vol. 25, no. 1, pp. 66–72, 2014.

[18] X. Guan, P. Lin, E. Knoll, and R. Chakrabarti, "Mechanism of inhibition of the human sirtuin enzyme SIRT3 by nicotinamide: computational and experimental studies," *PLoS One*, vol. 9, no. 9, article e107729, 2014.

[19] K. J. Bitterman, R. M. Anderson, H. Y. Cohen, M. Latorre-Esteves, and D. A. Sinclair, "Inhibition of silencing and accelerated aging by nicotinamide, a putative negative regulator of yeast sir2 and human SIRT1," *The Journal of Biological Chemistry*, vol. 277, no. 47, pp. 45099–45107, 2002.

[20] I. Shats, J. G. Williams, J. Liu et al., "Bacteria boost mammalian host NAD metabolism by engaging the deamidated biosynthesis pathway," *Cell Metabolism*, vol. 31, pp. 564–579.e7, 2020.

[21] J. Byun, S.-i. Oka, N. Imai et al., "Both gain and loss of Nampt function promote pressure overload-induced heart failure," *American Journal of Physiology-Heart and Circulatory Physiology*, vol. 317, no. 4, pp. H711–H725, 2019.

[22] W. Liu, B. Wang, T. Wang et al., "Ursodeoxycholic acid attenuates acute aortic dissection formation in angiotensin II-infused apolipoprotein E-deficient mice associated with reduced ROS and increased Nrf2 levels," *Cellular Physiology and Biochemistry*, vol. 38, no. 4, pp. 1391–1405, 2016.

[23] Z. S. Galis and J. J. Khatri, "Matrix metalloproteinases in vascular remodeling and atherogenesis: the good, the bad, and the ugly," *Circulation Research*, vol. 90, no. 3, pp. 251–262, 2002.

[24] K. Grote, I. Flach, M. Luchtefeld et al., "Mechanical stretch enhances mRNA expression and proenzyme release of matrix metalloproteinase-2 (MMP-2) via NAD(P)H oxidase-derived reactive oxygen species," *Circulation Research*, vol. 92, pp. e80–e86, 2003.

[25] R. M. Guia, A. S. Hassing, L. J. Skov et al., "Fasting- and ghrelin-induced food intake is regulated by NAMPT in the hypothalamus," *Acta Physiologica*, vol. 228, article e13437, 2020.

[26] A. M. Cameron, A. Castoldi, D. E. Sanin et al., "Inflammatory macrophage dependence on NAD^+ salvage is a consequence of reactive oxygen species-mediated DNA damage," *Nature Immunology*, vol. 20, no. 4, pp. 420–432, 2019.

[27] S. M. Hong, C. W. Park, S. W. Kim et al., "NAMPT suppresses glucose deprivation-induced oxidative stress by increasing NADPH levels in breast cancer," *Oncogene*, vol. 35, no. 27, pp. 3544–3554, 2016.

[28] C.-P. Hsu, S. Oka, D. Shao, N. Hariharan, and J. Sadoshima, "Nicotinamide phosphoribosyltransferase regulates cell survival through NAD+ synthesis in cardiac myocytes," *Circulation Research*, vol. 105, no. 5, pp. 481–491, 2009.

[29] L. Bordone, M. C. Motta, F. Picard et al., "Sirt1 regulates insulin secretion by repressing UCP2 in pancreatic β cells," *PLoS Biology*, vol. 4, article e31, 2006.

[30] S.-i. Imai and L. Guarente, "NAD^+ and sirtuins in aging and disease," *Trends in Cell Biology*, vol. 24, no. 8, pp. 464–471, 2014.

[31] X. Wu, X. Kong, D. Chen et al., "SIRT1 links CIITA deacetylation to MHC II activation," *Nucleic Acids Research*, vol. 39, no. 22, pp. 9549–9558, 2011.

[32] E. Katsyuba, A. Mottis, M. Zietak et al., "De novo NAD synthesis enhances mitochondrial function and improves health," *Nature*, vol. 563, pp. 354–359, 2018.

[33] R. Ma, Y. Wu, Y. Zhai et al., "Exogenous pyruvate represses histone gene expression and inhibits cancer cell proliferation via the NAMPT-NAD+-SIRT1 pathway," *Nucleic Acids Research*, vol. 47, no. 21, pp. 11132–11150, 2019.

[34] F. Marín-Aguilar, A. V. Lechuga-Vieco, E. Alcocer-Gómez et al., "NLRP3 inflammasome suppression improves longevity and prevents cardiac aging in male mice," *Aging Cell*, vol. 19, article e13050, 2019.

[35] P. Wang, H. Du, C.-C. Zhou et al., "Intracellular NAMPT-NAD+-SIRT1 cascade improves post-ischaemic vascular repair by modulating notch signalling in endothelial progenitors," *Cardiovascular Research*, vol. 104, no. 3, pp. 477–488, 2014.

[36] K. Behrouzfar, M. Alaee, M. Nourbakhsh, Z. Gholinejad, and A. Golestani, "Extracellular NAMPT/visfatin causes p53 deacetylation via NAD production and SIRT1 activation in breast cancer cells," *Cell Biochemistry and Function*, vol. 35, no. 6, pp. 327–333, 2017.

[37] T. F. Luscher, "Endothelial dysfunction: the role and impact of the renin-angiotensin system," *Heart*, vol. 84, no. 90001, pp. 20i–222, 2000.

[38] R. K. Stewart, A. Dangi, C. Huang et al., "A novel mouse model of depletion of stellate cells clarifies their role in ischemia/reperfusion- and endotoxin-induced acute liver injury," *Journal of Hepatology*, vol. 60, no. 2, pp. 298–305, 2014.

[39] A. Costanzo, F. Moretti, V. L. Burgio et al., "Endothelial activation by angiotensin II through NFkappaB and p 38 pathways: involvement of NFkappaB-inducible kinase (NIK), free oxygen radicals, and selective inhibition by aspirin," *Journal of Cellular Physiology*, vol. 195, no. 3, pp. 402–410, 2003.

[40] B. Su, S. Mitra, H. Gregg et al., "Redox regulation of vascular smooth muscle cell differentiation," *Circulation Research*, vol. 89, no. 1, pp. 39–46, 2001.

[41] S. Eguchi, G. D. Frank, M. Mifune, and T. Inagami, "Metalloprotease-dependent ErbB ligand shedding in mediating EGFR transactivation and vascular remodelling," *Biochemical Society Transactions*, vol. 31, no. 6, pp. 1198–1202, 2003.

[42] M. Ushio-Fukai, R. W. Alexander, M. Akers et al., "Reactive oxygen species mediate the activation of Akt/protein kinase B by angiotensin II in vascular smooth muscle cells," *Journal of Biological Chemistry*, vol. 274, no. 32, pp. 22699–22704, 1999.

[43] T. D. Paula, B. R. Silva, M. D. Grando, H. C. D. Souza, and L. M. Bendhack, "Activation of TP receptors induces high release of PGI_2 in coronary arteries of renal hypertensive rats," *Journal of Molecular and Cellular Cardiology*, vol. 122, pp. 125–133, 2018.

[44] J. Yoshino, J. A. Baur, and S.-i. Imai, "NAD intermediates: the biology and therapeutic potential of NMN and NR," *Cell Metabolism*, vol. 27, no. 3, pp. 513–528, 2018.

[45] E. Ko, H.-W. Seo, and G. Jung, "Telomere length and reactive oxygen species levels are positively associated with a high risk of mortality and recurrence in hepatocellular carcinoma," *Hepatology*, vol. 67, no. 4, pp. 1378–1391, 2018.

[46] C. G. Pham, C. Bubici, F. Zazzeroni et al., "Ferritin heavy chain upregulation by NF-κB inhibits TNFα-induced apoptosis by suppressing reactive oxygen species," *Cell*, vol. 119, no. 4, pp. 529–542, 2004.

[47] N. R. Madamanchi, S. Li, C. Patterson, and M. S. Runge, "Reactive oxygen species regulate heat-shock protein 70 via the JAK/STAT pathway," *Arteriosclerosis, Thrombosis, and Vascular Biology*, vol. 21, no. 3, pp. 321–326, 2001.

Hindawi
Oxidative Medicine and Cellular Longevity
Volume 2020, Article ID 1936580, 15 pages
https://doi.org/10.1155/2020/1936580

Research Article

HSF1 Attenuates LPS-Induced Acute Lung Injury in Mice by Suppressing Macrophage Infiltration

Tao Li,[1,2] Gui Xiao,[1,3] Sipin Tan,[1] Xueyan Shi,[1] Leijing Yin,[1] Chuyi Tan,[1] Jia Gu,[1] Yanjuan Liu,[1] Huafei Deng,[1] Ke Liu,[1] Meidong Liu,[1] Huali Zhang ,[1] and Xianzhong Xiao [1]

[1]*Key Laboratory of Sepsis Translational Medicine of Hunan, Department of Pathophysiology, Xiangya School of Medicine, Central South University, Changsha, Hunan 410008, China*
[2]*Department of Pathophysiology, Medical College of Jiaying University, Meizhou, Guangdong 514031, China*
[3]*Department of Nursing, Hainan Medical University, Haikou, Hainan 571199, China*

Correspondence should be addressed to Huali Zhang; zhanghuali@csu.edu.cn and Xianzhong Xiao; xiaoxianzhong@csu.edu.cn

Received 2 April 2020; Revised 21 June 2020; Accepted 1 December 2020; Published 18 December 2020

Academic Editor: Manjit Singh Rana

Copyright © 2020 Tao Li et al. This is an open access article distributed under the Creative Commons Attribution License, which permits unrestricted use, distribution, and reproduction in any medium, provided the original work is properly cited.

Heat shock factor 1 (HSF1) is a transcription factor involved in the heat shock response and other biological processes. We have unveiled here an important role of HSF1 in acute lung injury (ALI). *HSF1* knockout mice were used as a model of lipopolysaccharide- (LPS-) induced ALI. Lung damage was aggravated, and macrophage infiltration increased significantly in the bronchoalveolar lavage fluid (BALF) and lung tissue of $HSF^{-/-}$ mice compared with the damage observed in $HSF1^{+/+}$ mice. Upon LPS stimulation, $HSF^{-/-}$ mice showed higher levels of monocyte chemoattractant protein-1 (MCP-1) in the serum, BALF, and lung tissue and increased the expression of MCP-1 and chemokine (C-C motif) receptor 2 (CCR2) on the surface of macrophages compared with those in $HSF1^{+/+}$. Electrophoretic mobility shift assays (EMSA) and dual luciferase reporter assays revealed that HSF1 could directly bind to heat shock elements (HSE) in the promoter regions of *MCP-1* and its receptor *CCR2*, thereby inhibiting the expression of both genes. We concluded that HSF1 attenuated LPS-induced ALI in mice by directly suppressing the transcription of MCP-1/CCR2, which in turn reduced macrophage infiltration.

1. Introduction

Acute lung injury is a type of acute and progressive hypoxic respiratory failure, where noncardiac pathogenic factors inside and outside the lungs cause damage to the alveolar and capillary endothelia, increasing the permeability of alveolar-capillary membrane. If the condition is not controlled, it will progress to acute respiratory distress syndrome (ARDS) (1) eventually leading to death. The pathogenesis of ALI is complex and has not been fully elucidated yet. Current studies indicate that inflammation is an important mechanism of ALI (2).

HSF1 is a transcription factor implicated in the heat shock response; it regulates the transcription of heat shock proteins such as Hsp27, Hsp60, and Hsp70, which play an important cytoprotective role in lung inflammation and injury (3–6). Our previous studies showed that HSF1 has a protective effect on LPS-induced multiorgan dysfunction syndrome (7, 8). Furthermore, HSF1 reduced leukocyte infiltration into the lungs and decreased the production of several inflammatory mediators, thereby attenuating inflammatory responses and exhibiting a protective effect on endotoxemia caused by LPS. However, the underlying mechanisms by which HSF1 alleviates ALI need to be further explored.

Macrophages are important effector cells in the pathogenesis of ALI. It has been reported that macrophage activation and migration are closely related to the severity of ALI (9). However, the effect of HSF1 on macrophages in ALI remains unclear. This study is aimed at exploring the effect of HSF1 on macrophages in ALI, by assessing the role of HSF1 in regulating chemokine expression. To the best of our knowledge, this is the first report showing that HSF1

alleviates LPS-induced macrophage infiltration and ALI in mice, by downregulating macrophage-related chemokines.

2. Materials and Methods

2.1. Animals. HSF1 knockout ($HSF1^{-/-}$) and wild-type ($HSF1^{+/+}$) mice were gifts from Dr. Ivor J. Benjamin (Medical College of Wisconsin, Milwaukee city, Wisconsin, USA) and have been described elsewhere (10). HSF1 mice were created using homologous recombination with a gene-targeting vector in embryonic stem cells as described by McMillan et al. (11). After mating HSF1 heterozygous female mice (♀$HSF1^{+/-}$) with HSF1 heterozygous male mice (♂$HSF1^{+/-}$), offspring with three genotypes was obtained: wild type, heterozygous type, and homozygous type. 3 weeks after birth, young mice were weaned and kept in separate cages. At the fourth week, mouse were genotyped using DNA from tail to identify qualified HSF1 knockout homozygous ($HSF1^{-/-}$) and wild-type ($HSF1^{+/+}$) mice for the experiments. Protocols for animal breeding and experiments were previously approved by the Institutional Animal Care and Use Committee of Central South University (Hunan, China) under license number 2018sydw0378 (approval date: 25 Nov., 2018).

2.2. Acute Lung Injury Model. Age- and sex-matched $HSF1^{-/-}$ and $HSF1^{+/+}$ mice (males, 4-5 months old, 20-25 g) were randomly divided into the $HSF1^{+/+}$+normal saline (NS) group, $HSF1^{+/+}$+LPS (E. coli 0111:B4, Sigma, USA) group, $HSF1^{-/-}$ + NS group, and $HSF1^{-/-}$ + LPS group. Mice were anesthetized with 5% chloral hydrate (0.01 ml/g, intraperitoneally) and 2% isoflurane (inhalation). Then, LPS (1 mg/ml) was instilled into the trachea at a dose of 3 mg/kg (12) in $HSF1^{+/+}$+LPS and $HSF1^{-/-}$ + LPS groups. $HSF1^{+/+}$+NS and $HSF1^{-/-}$ + NS groups were instilled with normal saline using the same dose and procedure as for LPS. Treatments were evaluated after 12 h, 24 h, and 36 h. In this experiment, pain and distress assessment of mice was conducted from postoperative to euthanasia. The method is as follows: mice were placed in a small transparent observation room ($10 \times 10 \times 10$ cm) for monitoring, and each mouse was observed for 3-4 minutes. According to GAP scores (13), pain indicators such as activity, posture, breathing pattern, coat condition, and relation to other mice were recorded, respectively. A blind observer assessed each mouse at 1, 6, 12, 24, and 36 h after the operation according to the time of sample collection. Mice were assigned a score of 0 (normal) or 1 (abnormal) for each parameter. Scores were recorded based on changes in pain indicators and then aggregated to get a composite score for each mouse. Mice in the LPS-treated group showed symptoms such as deeper breathing, decrease in movement, hair erect, back arch, reduced consumption of feed and water, and increased body temperature after using LPS. Therefore, in order to exclude the interference caused by LPS, we strictly observed differences between the LPS-treated group and the saline group and then scored the mice in the LPS-treated group.

2.3. Lung Wet/Dry Weight (W/D) Ratio. Pulmonary edema in treated groups was assessed using the lung wet/dry weight ratio. Mice were killed, and the lungs were removed and weighed (wet weight). Lungs were heated at 80°C for 24 h to obtain the dry weight and calculate the W/D ratio.

2.4. Extraction of Bronchoalveolar Lavage Fluid. BALF was collected as previously described (14). Mice were sacrificed by cervical dislocation. The skin of the neck was cut off to expose the trachea, and a small oblique incision was made at the telecentric end of the trachea using ophthalmic scissors. Then, a trocar was inserted into the trachea to wash mice lungs thrice by flushing 1 ml of cold sterile phosphate-buffered saline (PBS) per wash. The collected lavage fluid was centrifuged at 250× *g* for 15 minutes at 4°C. The cell pellet was resuspended in PBS for flow cytometry detection. The supernatant was stored at −80°C until further use.

2.5. Enzyme-Linked Immunosorbent Assay (ELISA). Supernatants from lung tissue homogenate, BALF, and serum were collected to measure the levels of MCP-1 using an ELISA kit (MJE00B, RD, USA) according to the manufacturer's instructions.

2.6. Immunofluorescence. Immunofluorescence analysis was performed as previously published (15). Briefly, ALI model mice were sacrificed at different time points. The left lung was removed immediately after death and fixed in 4% paraformaldehyde for 24 h. After embedding in paraffin, the lung tissue was cut into 4 μm thick sections. For antigen retrieval, sections were placed in sodium citrate buffer and heated in a microwave at 100°C for 15 min, then incubated with 10% bovine serum albumin (BSA) in PBS for 2 h at room temperature to block nonspecific binding sites. Subsequently, sections were incubated with murine macrophage-monocyte specific monoclonal antibody(anti-F4/80) (1 : 200, Santa Cruz, USA) and C-C chemokine receptor type 2 monoclonal antibody (anti-CCR2) (1 : 100, Abcam, USA) overnight at 4°C, followed by incubation with horseradish peroxidase secondary antibodies (1 : 50, ABclonal, Wuhan) for 1 h at 37°C under darkness. After washing 4 times with PBS, samples were treated with sealing liquid. Images were obtained using Panoramic 250/MIDI (Hungary).

2.7. Flow Cytometry. Cells collected from BALF and prepared for flow cytometric analysis as previously reported (16). Cells were suspended in 1 ml of 1× red blood cell lysis buffer (BD Biosciences, USA) for 5 minutes, then centrifuged at 250× *g* for 5 min. The supernatant containing BALF cells was resuspended in 100 μl PBS, then blocked with 0.5 μl of purified rat anti-mouse CD16/CD32 antibody (BD Biosciences, USA) for 10 min at 4°C. BALF cells were stained with fluorescent-conjugated antibodies: PerCP-Cy™ 5.5 rat anti-mouse CD45 antibody (0.5 μl, BD Biosciences, USA), PE anti-mouse F4/80 antibody (0.5 μl, BD Biosciences, USA), and Alexa Fluor 647 anti-mouse CCR2 (0.5 μl, Biolegend, USA) for 20 min at 4°C under darkness, then centrifuged at 250× *g* for 5 min. The supernatant was fixed with 100 μl of 2% paraformaldehyde at 4°C for 10 min under darkness. After washing twice with PBS, samples were resuspended in 200 μl PBS, then analyzed by flow cytometry (BD

Biosciences) using FlowJo analysis software (FlowJo, LLC, Ashland, Ore.).

2.8. Real-Time Quantitative Reverse Transcription PCR (qRT-PCR). Total RNA extraction and qRT-PCR were performed as previously described (17).Total RNA was extracted from the lung tissue using TRIzol® reagent (Invitrogen, USA) according to the manufacturer's instructions, then retrotranscribed into cDNA using PrimeScript reverse transcriptase (TaKaRa, Kyoto, Japan) and random primers. qRT-PCR was performed using TB Green™ Premix ExTaq™ (TaKaRa, Kyoto, Japan) on a 7500 Real-Time PCR System (Applied Biosystems, USA). The primer sequences used for qRT-PCR were MCP-1 forward: 5′–TTA AAA ACC TGG ATC GGA ACC AA–3′ and reverse: 5′–GCA TTA GCT TCA GAT TTA CGG GT–3′; CCR-2 forward: 5′–ATC CAC GGC ATA CTA TCA ACA TC–3′ and reverse: 5′–CAA GGC TCA CCA TCA TCG TAG–3′; β-actin forward: 5′–TGC TGG AAG GTG GAC AGT GAG G–3′ and reverse: 5′–CAT TGC TGA CAG GAT GCA GAA GG–3′.The $2^{-\Delta\Delta CT}$ method was applied to determine relative mRNA expression levels.

2.9. Electrophoretic Mobility Shift Assay (EMSA). EMSA was performed using the RAW 264.7 mouse macrophage cell line. Cells were treated at 43°C for 60 min in a 10 cm cell culture dish (11). After heating, nuclear extracts were prepared using nuclear and cytoplasmic protein extraction reagents (20126ES50, Yeasen, China). Oligonucleotide probes were synthesized and labeled with biotin by Sangon Biotech, which based on the sequence covering the HSE sequence (18, 19) from the promoter regions of *MCP-1* and *CCR2* (Table 1). The following oligonucleotide probes were used (for the sake of clarity, they are shown single-stranded, but double-stranded were used): MCP-1.1: 5′-aggtgagttttatata-***GAA****A T****TTC***ttctgcaccatgagct-3′ (HSE1, −613 to −606 bp); MCP-1.2: 5′-atctcaggtccagggaagc a***TTC****TG****GAA***gcaccagcccca-3′ (HSE2, −1475 to −1468 bp); CCR2.1: 5′-agcatttaccta ***GAA****TT****TTC***cataacag-3′ (HSE1, −754 to −747 bp); CCR2.2: 5′-gtttacat***TTC****TA****GAA***cc ttatactgtg-3′ (HSE2: −1095 to −1088 bp). EMSA was performed using the LightShift® Chemiluminescent EMSA Kit (20148, Thermo Scientific, USA), according to the manufacturer's instructions. The binding reaction was performed as previously described (20). Briefly, biotin-labeled oligonucleotide containing the HSE sequence was incubated with 5 μg of nuclear extract for 20 min at room temperature in binding buffer (10× binding buffer, 1 μg Poly (dI-dC), 50% glycerol, 1% NP-40, 100 mM $MgCl_2$, 100 mM EDTA). This reaction was then subjected to gel electrophoresis on a 5% native polyacrylamide gel and transferred to a nylon membrane. Biotin-labeled DNA was detected by chemiluminescence. For supershift assays, 2 μl of anti-HSF1 antibody (ab2923, Abcam, USA) was added to the binding reaction. 200-fold molar excess of the unlabeled competitor oligonucleotides (competitive probe) and the unlabeled mutant oligonucleotides (mutant probe) were used for competition assays.

2.10. Dual-Luciferase Reporter Assay. The constitutively activated HSF1 plasmid pcDNA3.1 (+)/HSF1 (+) (mHSF1) and empty vector plasmid pcDNA3.1 (+)/HSF1-wt were kindly provided by Dr. Richard Voellmy at HSF Pharmaceuticals S.A., Switzerland. Generation of the *MCP-1* promoter luciferase reporter constructs (the full-length pGL3-MCP-1-wt (−1600 to −1 bp)), pGL3-MCP-1-Mut1 (mutations of HSE1, −613 to −606 bp), pGL3-MCP-1-Mut2 (mutations of HSE2, −1475 to −1468 bp), and pGL3-MCP-1-Mut3 (mutations of HSE1 and HSE2)), and the *CCR2* promoter luciferase reporter constructs (the full-length pGL3-CCR2-wt (−1162 to −1 bp), pGL3-CCR2-Mut1 (mutations of HSE1, −754 to −747 bp), pGL3-MCP-1-Mut2 (mutations of HSE2, −1095 to −1088 bp), and pGL3-MCP-1-Mut3 (mutations of HSE1 and HSE2), was performed by PCR and cloned into a luciferase vector pGL3-Basic. The authenticity of the synthesized sequence was verified by sequencing. Plasmids were extracted (D6950-01, Omega, USA) and stored at -20°C for subsequent experiments. RAW 264.7 cells were incubated in a 24-well plate and grown to 70-90% confluence, then transfected with 500 ng of the MCP-1 or CCR2 promoter luciferase reporter plasmid, 20 ng of pRL-TK, and 500 ng of mHSF1 plasmid or empty vector plasmid using the Lipofectamine™ 3000 transfection reagent (L3000015, Invitrogen™, USA). After 48 h of transfection, the cell lysate was extracted and tested using a dual-luciferase reporter assay kit (E1910, Promega, USA). Luminescence was measured using a Synergy^{HI} Microplate Reader (BioTek, USA).

2.11. Statistical Analysis. All data were analyzed using GraphPad Prism 7.0 (GraphPad Software, USA) and SPSS 21.0 (SPSS, USA). Data were expressed as mean ± standard deviation. Student's *t*-test was performed for comparing two groups and one-way analysis of variance (ANOVA) for comparing multiple groups, followed by a multiple comparison test (Bonferroni post hoc test). The Kaplan-Meier analysis was used to compare differences of survival rates between groups. $p < 0.05$ was considered statistically significant.

3. Results

3.1. HSF1 Alleviated Lung Tissue Damage and Improved Vascular Permeability in LPS-Induced ALI. A dark red congestion was observed on the surface of the lungs from LPS-instillated mice, which was more obvious in the HSF1$^{-/-}$+LPS group than that in the HSF1$^{+/+}$+LPS group (Figure 1(a)). Pathological histomorphology of the lungs revealed increased pulmonary edema, infiltration of inflammatory cells, alveolar hemorrhage, and destruction of the epithelial and endothelial cell structure in the HSF1$^{-/-}$+LPS group compared with the symptoms observed in the LPS-treated HSF1$^{+/+}$ group (Figure 1(b)). The lung W/D ratio in the HSF1$^{-/-}$+LPS group was significantly higher (33%) than that in the HSF1$^{+/+}$+LPS group ($p < 0.01$) (Figure 1(c)). The BALF total protein content at 12, 24, and 36 h after LPS instillation increases significantly in LPS-stimulated mice, showing a significant difference between HSF1$^{-/-}$+LPS and HSF1$^{+/+}$+LPS groups ($p < 0.01$) (Figure 1(d)). Moreover, we found that the survival rate of the HSF1$^{-/-}$+LPS group was

Table 1: List of MCP-1 and CCR2 probe sequences.

Probe	Probe sequence(5′-3′)
MCP-1.1:labeled probe F:	Biotin-AGGTGAGTTTTATATAGAAATTTCTTCTGCACCATGAGCT
MCP-1.1: labeled probe R:	Biotin-AGCTCATGGTGCAGAAGAAATTTCTATATAAAACTCACCT
MCP-1.1: competitive probe F:	AGGTGAGTTTTATATAGAAATTTCTTCTGCACCATGAGCT
MCP-1.1:competitive probe R:	AGCTCATGGTGCAGAAGAAATTTCTATATAAAACTCACCT
MCP-1.1: mutant probe F:	ATGTGAGTGCTATCTAGCACTGTATGCTGCACAATGAGGT
MCP-1.1: mutant probe R:	ACCTCATTGTGCAGCATACAGTGCTAGATAGCACTCACAT
MCP-1.2: labeled probe F:	Biotin-ATCTCAGGTCCAGGGAAGCATTCTGGAAGCACCAGCCCCA
MCP-1.2: labeled probe R:	Biotin-TGGGGCTGGTGCTTCCAGAATGCTTCCCTGGACCTGAGAT
MCP-1.2: competitive probe F:	ATCTCAGGTCCAGGGAAGCATTCTGGAAGCACCAGCCCCA
MCP-1.2:competitive probe R:	TGGGGCTGGTGCTTCCAGAATGCTTCCCTGGACCTGAGAT
MCP-1.2: mutant probe F:	ATATCAGATCCATGGCAGCAGTCTGTACGTACTAGACTCA
MCP-1.2: mutant probe R:	TGAGTCTAGTACGTACAGACTGCTGCCATGGATCTGATAT
CCR2.1:labeled probe F:	Biotin-AGCATTTACCTAGAATTTTCCATAACAG
CCR2.1: labeled probe R:	Biotin-CTGTTATGGAAAATTCTAGGTAAATGCT
CCR2.1:competitive probe F:	AGCATTTACCTAGAATTTTCCATAACAG
CCR2.1:competitive probe R:	CTGTTATGGAAAATTCTAGGTAAATGCT
CCR2.1: mutant probe F:	AGCACTGATCTATGATTAATCATGACAG
CCR2.1: mutant probe R:	CTGTCATGATTAATCATAGATCAGTGCT
CCR2.2: labeled probe F:	Biotin-GTTTACATTTCTAGAACCTTATACTGTG
CCR2.2: labeled probe R:	Biotin-CACAGTATAAGGTTCTAGAAATGTAAAC
CCR2.2: competitive probe F:	GTTTACATTTCTAGAACCTTATACTGTG
CCR2.2:competitive probe R:	CACAGTATAAGGTTCTAGAAATGTAAAC
CCR2.2:mutant probe F:	GTCTATAGGTCTATCACTCTATGCTGTG
CCR2.2:mutant probe R:	CACAGCATAGAGTGATAGACCTATAGAC

significantly lower than that of the $HSF1^{+/+}$+LPS group ($p < 0.05$) (Figure 1(e)). These results showed that lung tissue injury was more severe in the $HSF1^{-/-}$ group after LPS treatment, indicating that HSF1 alleviated lung tissue damage and improved vascular permeability and survival of LPS-induced ALI mice.

3.2. HSF1 Attenuated Macrophage Infiltration into BALF and Lung Tissue from LPS-Induced ALI Mice. Macrophages are important effector cells in ALI pathogenesis and are closely related to disease severity. To evaluate the macrophage infiltration and exudation in the lung tissue from LPS-treated $HSF1^{+/+}$ and $HSF1^{-/-}$ mice, we measured the change in percentage of macrophages in BALF at different time points using flow cytometry. The results showed that at 12 h, 24 h, and 36 h after LPS instillation, the macrophage content in BALF from $HSF1^{-/-}$ mice was significantly higher than that in $HSF1^{+/+}$ mice ($p < 0.01$) (Figures 2(a)–(d)). Additionally, the tissue immunofluorescence assay results showed that the $HSF1^{-/-}$ + LPS group had a significantly higher macrophage infiltration into the lung tissue than that observed in the $HSF1^{+/+}$+LPS group (Figure 2(e)). These results suggested that HSF1 could attenuate macrophage infiltration into the lung tissue from LPS-induced ALI mice.

3.3. HSF1 Reduced the MCP-1 Expression in Serum, Lung Tissue, and BALF from LPS-Induced ALI Mice. Macrophage infiltration is regulated by MCP-1/CCR2 chemokines (21–24). MCP-1 levels were measured at different time points in serum, lung tissue, and BALF. At 12 h, 24 h, and 36 h after LPS treatment, the MCP-1 levels in serum from the $HSF1^{-/-}$ + LPS group peaked at 36 h and were significantly higher than those observed in the $HSF1^{+/+}$+LPS group ($p < 0.05$), ($p < 0.01$) (Figure 3(a)). Similar changes were observed in the lung tissue and BALF (Figures 3(b) and 3(c)). Additionally, we found that MCP-1 mRNA levels in the lung tissue were significantly higher in the $HSF1^{-/-}$ + LPS group than those found in the $HSF1^{+/+}$ + LPS group ($p < 0.05$) (Figure 3(d)). Combined with the relative mRNA expression level of HSF1 (Figure 3(e)), these results indicated that HSF1 played a protective role in LPS-induced ALI mice by reducing the MCP-1 expression, thus inhibiting macrophage infiltration.

3.4. HSF1 Reduced the CCR2 Expression in Macrophages from LPS-Induced ALI Mice. Our next question was whether HSF1 affects the expression of CCR2 on the surface of macrophages. The CCR2 expression in mice BALF was detected using flow cytometry. We found that the CCR2 expression increased after 24 h and 36 h of LPS treatment, and the difference was more significant after 36 h ($p < 0.01$) (Figures 4(a)–(d)). Additionally, a tissue immunofluorescence assay was carried out to detect the expression of CCR2 in macrophages from the lung tissue. No significant

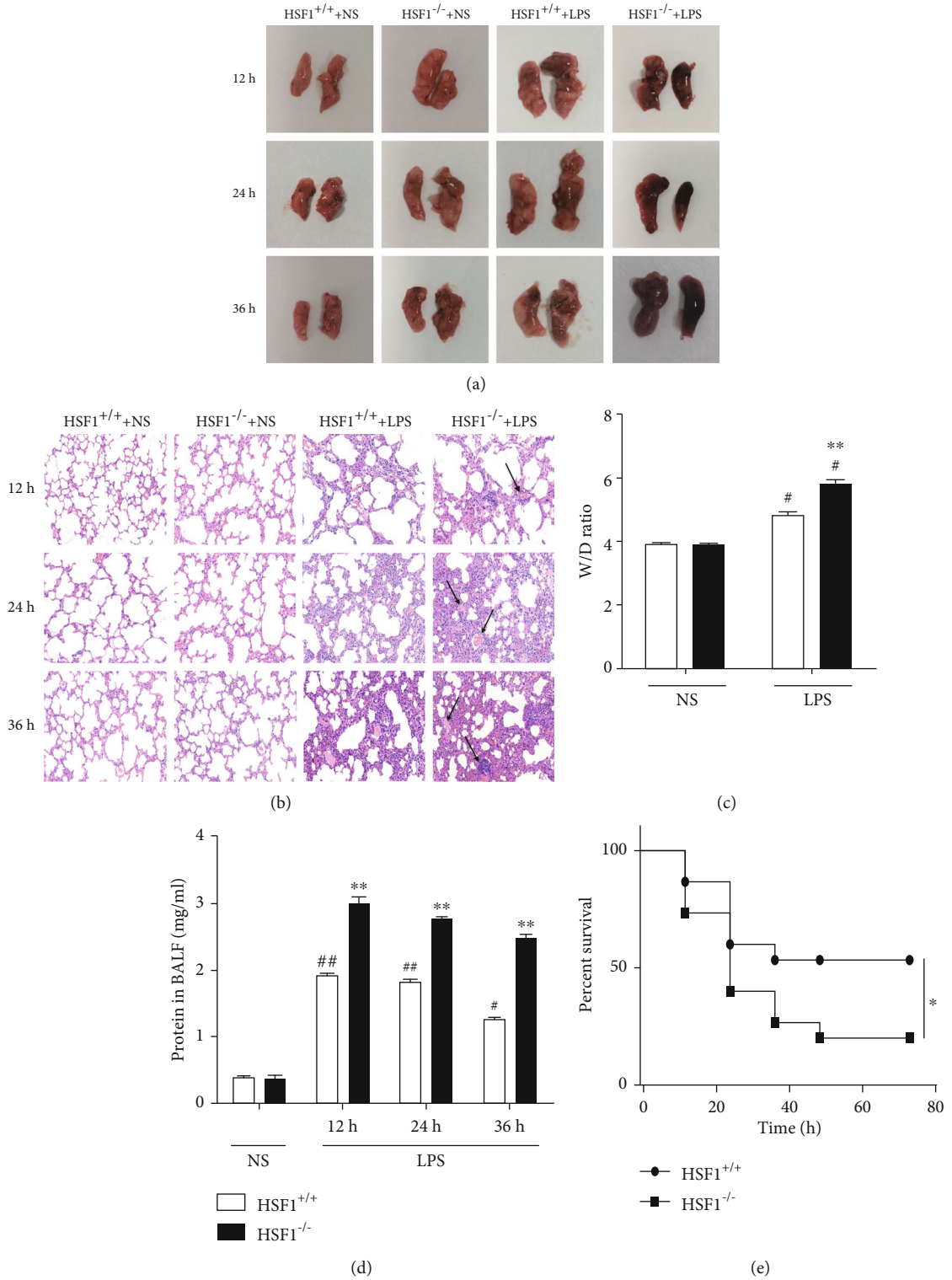

FIGURE 1: HSF1 reduced lung tissue injury and improved the outcome of LPS-induced ALI mice. (a) Effect of HSF1 on macroscopic changes at 12 h, 24 h, and 36 h after LPS treatment of ALI mice. (b) Representative morphological changes of the lung tissue from LPS-induced ALI mice. Arrows show pulmonary edema, inflammatory cell infiltration, and alveolar hemorrhage (HE staining, ×20 magnification). (c) The lung W/D ratio after 24 h of LPS treatment of ALI mice. (d) The total protein content in BALF from LPS-induced ALI mice; $^{\#}p < 0.05$, $^{\#\#}p < 0.01$, versus HSF1$^{+/+}$+NS group; $^{**}p < 0.01$, versus HSF1$^{+/+}$+LPS group; $n = 6$ mice per group. (e) The survival rate of LPS-induced ALI mice expressed as a percentage. The survival rate was significantly lower in the HSF1$^{-/-}$ group than in wild-type mice (20.0% versus 53.3%) after 72 h of LPS treatment; $n = 15$ mice per group; $^{*}p < 0.05$, versus HSF1$^{+/+}$ group. p values were determined using two-tailed Student's t-test for comparing two groups and one-way ANOVA for comparing multiple groups.

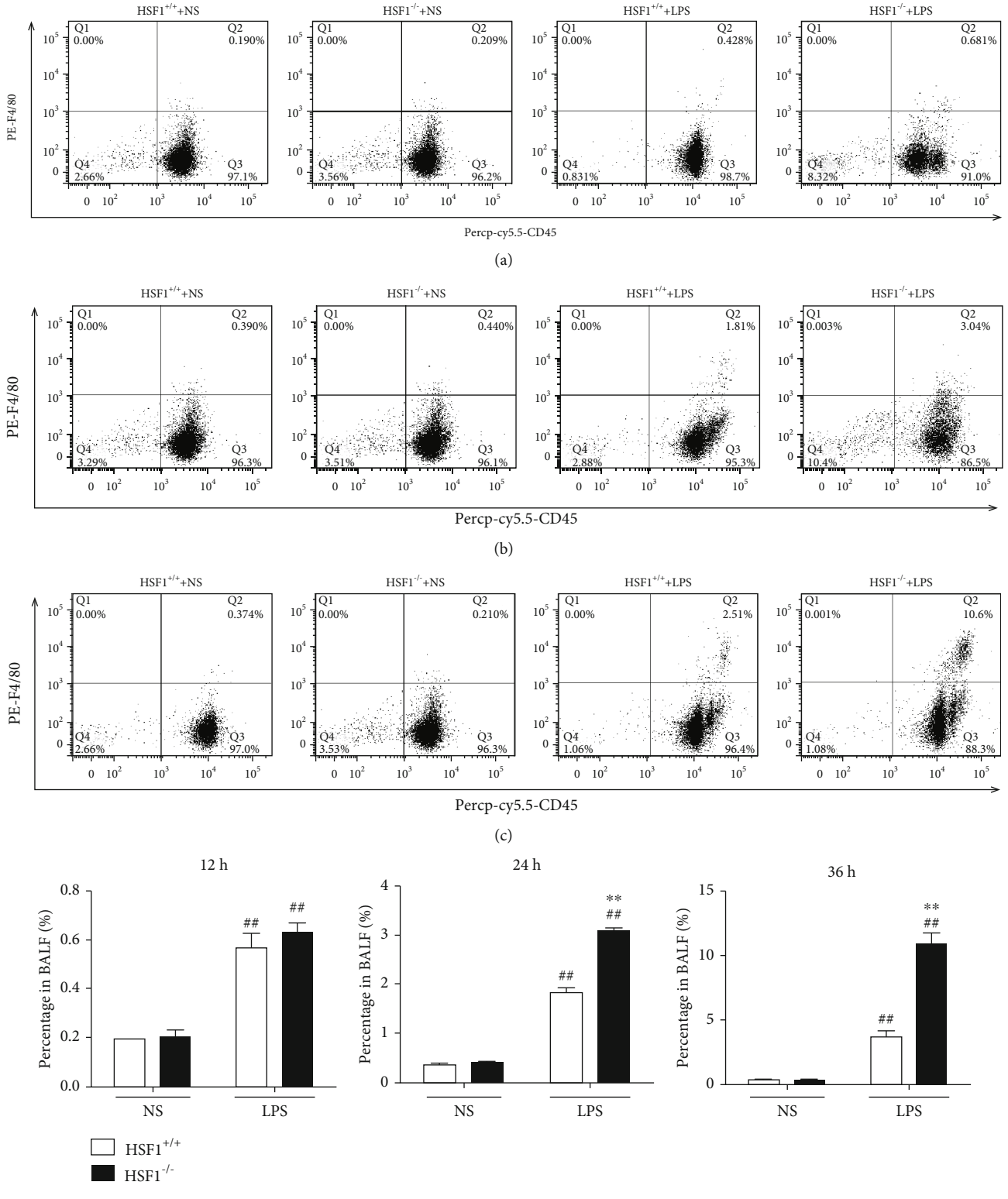

Figure 2: Continued.

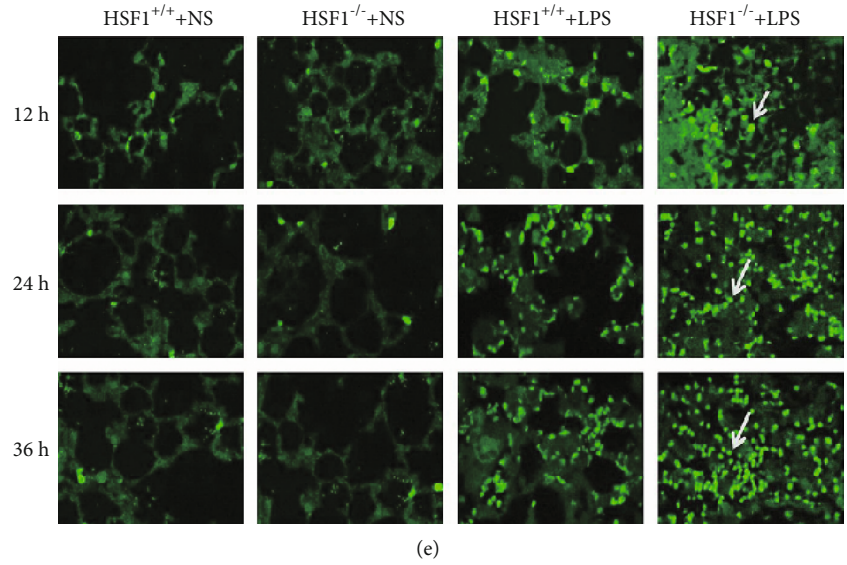

FIGURE 2: HSF1 reduced macrophage infiltration into the lung tissue from LPS-induced ALI mice. (a)–(d) BALF weas harvested and analyzed for macrophage accumulation using flow cytometry to detect $CD45^+$ and $F4/80^+$ cells at 12 h (a), 24 h (b), and 36 h (c) after LPS treatment. (d) Statistical analysis of (a), (b), (c), respectively. (e) Effect of HSF1 on macrophage infiltration into the lung tissue at 12 h, 24 h, and 36 h after LPS treatment in ALI mice (F4/80, green; white arrowheads indicate individual macrophages; immunofluorescence staining, ×40 magnification); $^{\#}p < 0.05$, $^{\#\#}p < 0.01$, versus $HSF1^{+/+}$+NS group; $^{*}p < 0.05$, $^{**}p < 0.01$, versus $HSF1^{+/+}$+LPS group; $n = 6$ mice per group. p values were determined using two-tailed Student's t-test for comparing two groups and one-way ANOVA for comparing multiple groups.

difference was found between the expression levels of CCR2 in macrophages from $HSF1^{+/+}$ and $HSF1^{-/-}$ mice after 12 h of LPS treatment (Figure 4(e)). However, at 24 h and 36 h after LPS treatment (Figures 4(f) and 4(g)), the CCR2 expression in $HSF1^{-/-}$ mice peaked and was higher than that in $HSF1^{+/+}$ mice. Similarly, CCR2 mRNA levels in the lung tissue increased gradually after LPS stimulation, its value being significantly higher in $HSF1^{-/-}$ mice than that in $HSF1^{+/+}$ mice ($p < 0.01$) (Figure 4(h)). These results indicated that in the LPS-induced ALI model, HSF1 inhibited macrophage infiltration by reducing the expression of CCR2. On the other hand, we proved that by modifying the CCR2 expression, the macrophage infiltration increased significantly in the lung tissue from LPS-treated $HSF1^{-/-}$ mice.

3.5. HSF1 Inhibited Monocyte/Macrophage Chemotaxis by Directly Regulating the Transcription of MCP-1/CCR2. In previous studies, we prepared an endotoxemia model using $HSF1^{-/-}$ and $HSF1^{+/+}$ mice. We prepared a microarray containing 384 inflammatory factor genes for screening HSF1-regulated inflammation-associated genes. It was found that HSF1 inhibited the expression of MCP-1 and its receptor CCR2 (25). A further bioinformatic analysis identified two HSE (HSE1 and HSE2) in the promoters of *MCP-1* and *CCR2*. To conduct the EMSA, we designed probes recognizing the identified HSE sites. Our results showed that HSF1 specifically bound in vitro to HSE1 in both promoters and to HSE2 in the promoter of *MCP-1* (Figures 5(a), (b), and (d)). To investigate whether HSF1 regulates the *MCP-1* and *CCR2* expression at the transcriptional level, we performed luciferase assays using reporter constructs containing a DNA fragment with HSE (wt) or with mutant HSE of the *MCP-1* and *CCR2* promoters, both separately and together (Figures 5(c) and 5(e)). As shown in Figure 5(c), the HSF1 overexpression resulted in significantly inhibited the promoter activity of MCP-1-wt compared with that observed for the empty vector ($p < 0.01$). The promoter activity of *MCP-1* was still suppressed by the single HSE1 or HSE2 mutant reporter structure ($p < 0.05$). However, HSF1 did not alter the promoter activity when both two sites were mutated simultaneously. Combined with EMSA results, these findings suggested that the HSF1-binding sites at −613 to −606 bp (HSE1) and−1475 to −1468 bp (HSE2) played a major role in regulating the *MCP-1* promoter activity by HSF1. On the other hand, the luciferase activity of the CCR2-wt reporter was repressed in cells cotransfected with mHSF1 plasmid compared with that observed in the empty vector (Figure 5(e)). However, the repression could be removed when HSE1 was mutated, but not the mutations of HSE2. Combined with EMSA results, these findings suggest that the HSE1 (−754 to −747 bp) played a major role in regulating the *CCR2* promoter activity by HSF1. Overall, these results indicated that HSF1 could downregulate the transcription of *MCP-1* and *CCR2*, by binding to HSE in their promoter regions.

4. Discussion

ALI, or its more severe phenotype acute respiratory distress syndrome (ARDS), can be caused by factors such as severe trauma or infection (26). ARDS affects approximately 200,000 patients every year, resulting in nearly 75,000 deaths in the USA (27). The pathogenesis of ALI is complex and has not been fully elucidated yet. Therefore, further understanding of its pathogenesis has potential therapeutic significance. Based on an ALI model induced by intratracheal instillation

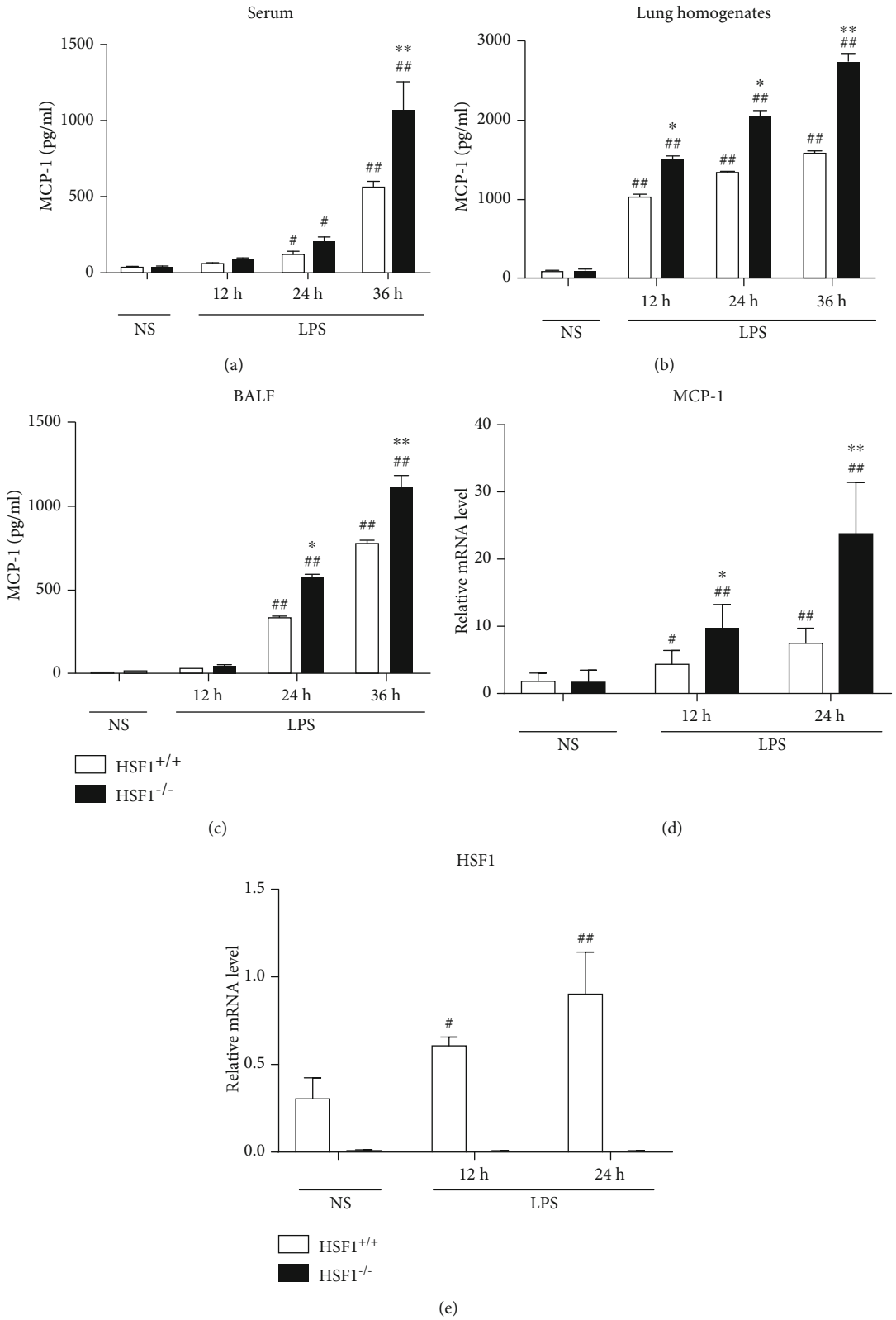

Figure 3: HSF1 attenuates the MCP-1 expression in serum, lung tissue, and BALF from LPS-induced ALI mice. MCP-1 levels were measured in (a) serum, (b) lung tissue, and (c) BALF at 12 h, 24 h, and 36 h after LPS treatment. (d) MCP-1 mRNA levels in the lung tissue from LPS-induced ALI mice using qRT-PCR. (e) HSF1 mRNA levels in the lung tissue from LPS-induced ALI mice using qRT-PCR. $^{\#}p < 0.05$, $^{\#\#}p < 0.01$, versus HSF1$^{+/+}$+NS group; $^{*}p < 0.05$, $^{**}p < 0.01$, versus HSF1$^{+/+}$+LPS group; $n = 6$ mice per group. p values were determined using two-tailed Student's t-test for comparing two groups and one-way ANOVA for comparing multiple groups.

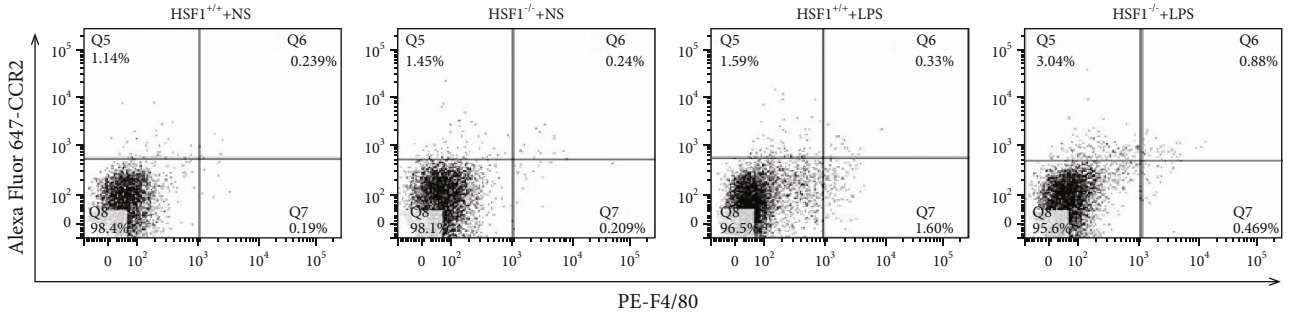

(a)

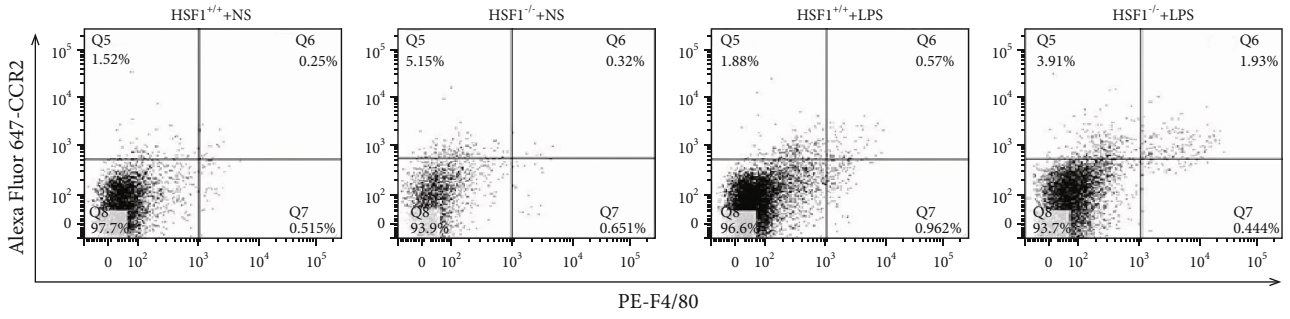

(b)

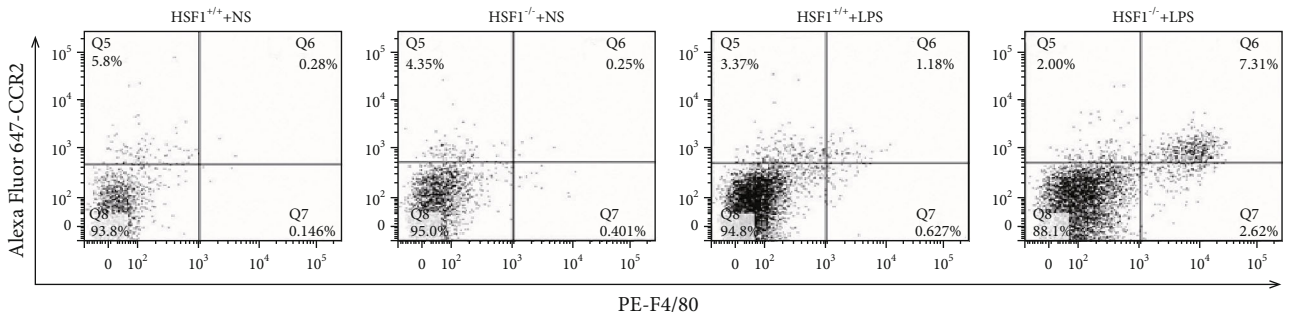

(c)

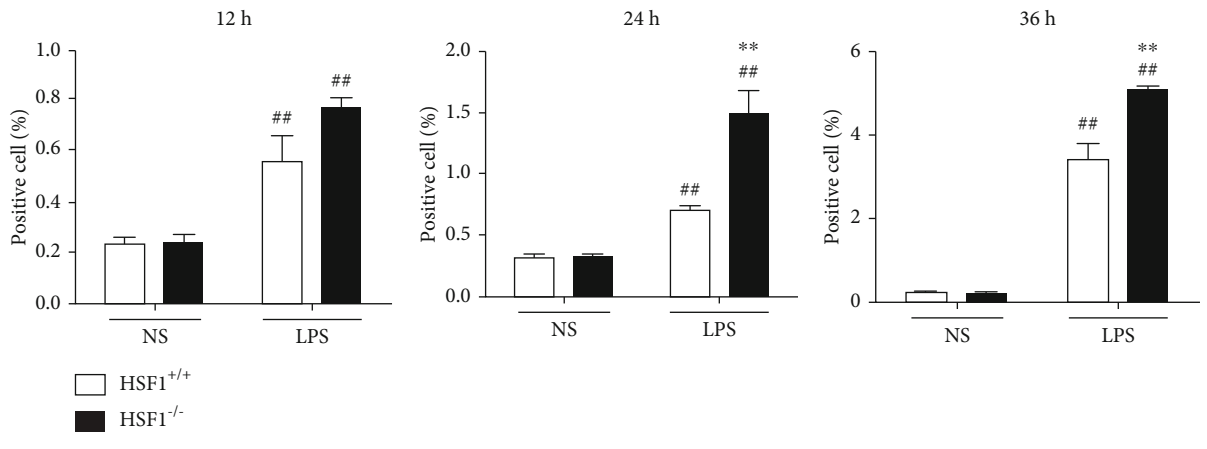

(d)

Figure 4: Continued.

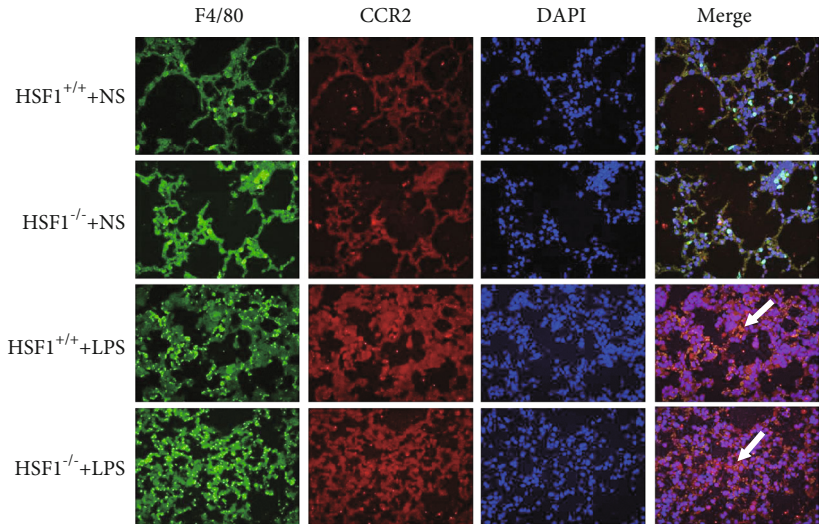

(e)

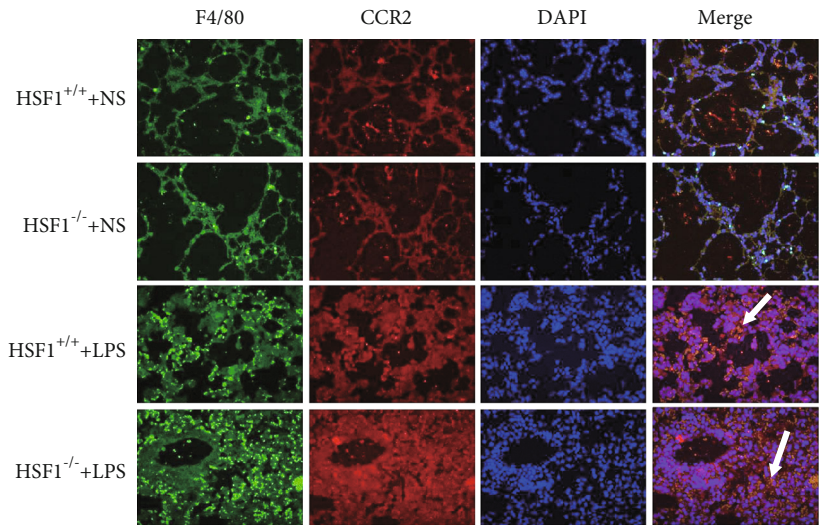

(f)

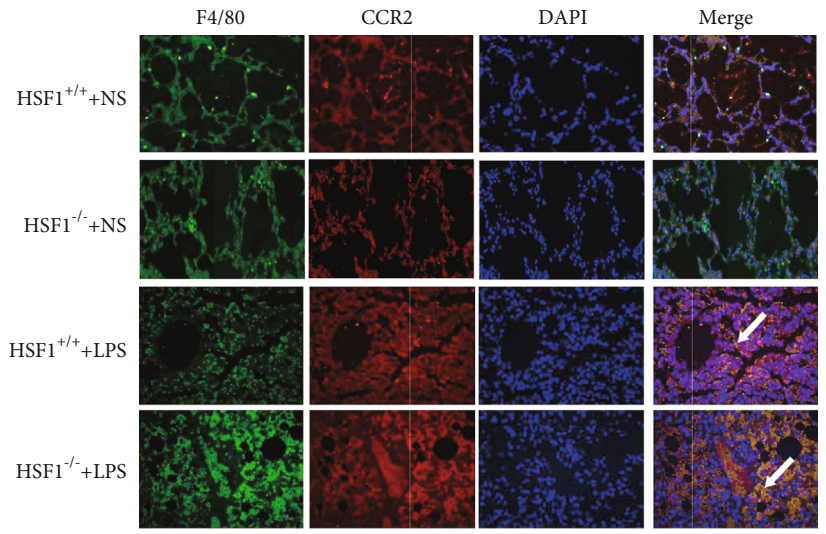

(g)

Figure 4: Continued.

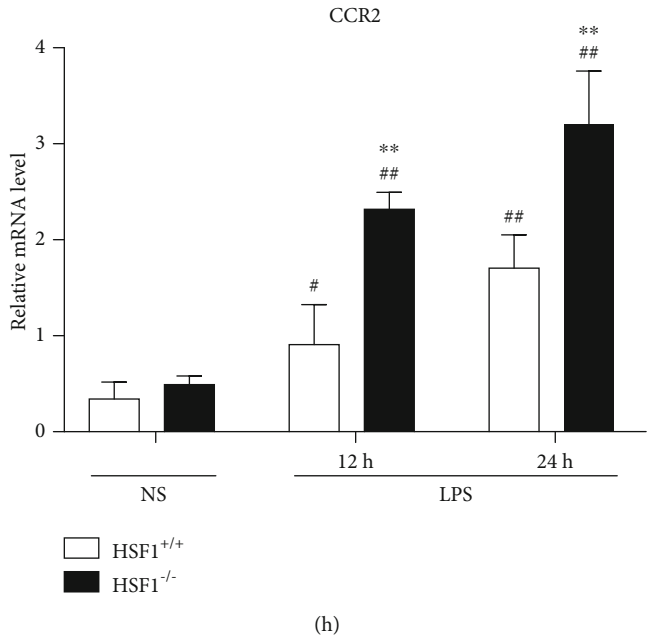

(h)

Figure 4: HSF1 reduced the CCR2 expression in macrophages from LPS-induced ALI mice. (a)–(d) BALF samples were analyzed using flow cytometry to measure the CCR2 expression in macrophages ($CD45^+$, $F4/80^+$, $CCR2^+$) at 12 h (a), 24 h (b), and 36 h (c) after LPS treatment. (d) Statistical analysis of (a), (b), and (c). (e)–(g) Immunofluorescence staining of the CCR2 expression (red) in macrophages (green) from the lung tissue at 12 h (e), 24 h (f), and 36 h (g) after LPS treatment (F4/80, green; CCR2, red; DAPI, blue; yellow dots indicated by white arrowheads represent the CCR2 expression in macrophages; immunofluorescence staining, ×40 magnification). (h) CCR2 mRNA levels in the lung tissue from LPS-induced ALI mice using qRT-PCR. $^{\#}p < 0.05$, $^{\#\#}p < 0.01$, versus $HSF1^{+/+}$+NS group; $^{*}p < 0.05$, $^{**}p < 0.01$, versus $HSF1^{+/+}$+LPS group; $n = 6$ mice per group. p values were determined using two-tailed Student's t-test for comparing two groups and one-way ANOVA for comparing multiple groups.

of LPS in HSF1 knockout mice, this study showed that HSF1 had a protective effect on ALI mice. To the best of our knowledge, we demonstrated for the first time that the protective effect of HSF1 is due to the downregulation of *MCP-1* and *CCR2*, owing to the binding of HSF1 to HSE in the promoters of both genes. Consequently, macrophage infiltration was suppressed.

Our previous work showed that HSF1 alleviated multiple organ damages by inhibiting the release of inflammatory factors and leukocyte infiltration into the tissue of endotoxemia mice (7, 8). To determine the protective role of HSF1 in LPS-induced ALI, we used HSF1 knockout mice to prepare an ALI model. We found that after LPS stimulation, the lung tissue damage in $HSF\text{-}1^{-/-}$ mice was significantly more severe than that observed in wild-type mice. Furthermore, HSF1 alleviated pulmonary edema, macrophage infiltration, alveolar hemorrhage, reduced protein leakage, and improved the survival of ALI mice. These observations are consistent with those from other studies using LPS-induced ALI models (28, 29). Altogether, these results demonstrated that HSF1 could alleviate lung damage, improved the survival rate, and had a protective effect against LPS-induced ALI.

The inflammatory response is a crucial element in the pathogeneses of ALI; its pathophysiological features are inflammatory exudation and an imbalance between proinflammatory and anti-inflammatory responses, which may eventually lead to respiratory failure (30). The evidence suggests that macrophages are key cells in the pathogenesis of ALI/ARDS (31, 32). Macrophage recruitment into the damaged tissue is an important process leading to inflammatory damage. Some studies show that MCP-1 and its receptor CCR2 play important roles in macrophage migration (21–24). MCP-1 (also known as CCL2) is a member of the C-C chemokine family and binds to CCR2 (33). MCP-1 is usually secreted by macrophages in response to pathogen infection (34) and is the most potent inducer of the signal transduction pathways leading to monocyte transmigration (35). The high affinity of MCP-1 for CCR2 is an important factor in promoting monocyte/macrophage activation, chemotaxis, and inflammatory responses, resulting in important biological consequences (21, 22). To confirm the effect of HSF1 on macrophage infiltration, we analyzed serum, lung tissue homogenates, and BALF from ALI mice to quantify the concentration of MCP-1. Further, we analyzed the expression of CCR2 on the surface of macrophages in BALF and lung tissue using flow cytometry and immunofluorescence assay, respectively. The results showed that the expression of MCP-1 in serum, lung tissue, and BALF from LPS-stimulated $HSF1^{-/-}$ mice gradually increased after stimulation and was significantly higher than that observed in wild-type mice. The expression of CCR2 on the surface of macrophages was concomitant with the MCP-1 expression.

The results suggested that HSF1 inhibited macrophage migration by downregulating both MCP-1 and CCR2. However, the downregulating mechanism is unclear. It has been proved that HSF1 plays a role in several diseases by regulating gene transcription (36–38). The binding of HSF1 to a

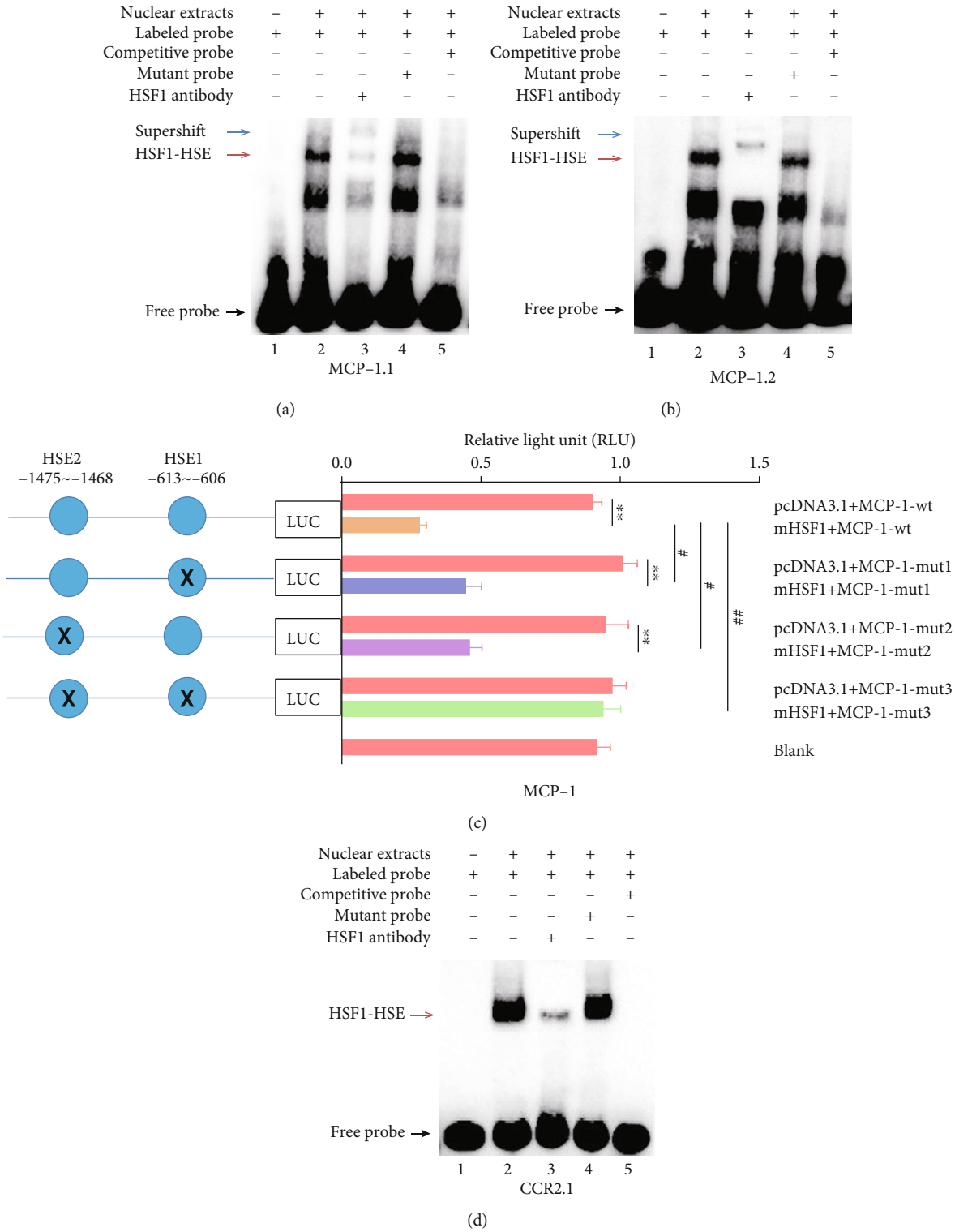

Figure 5: Continued.

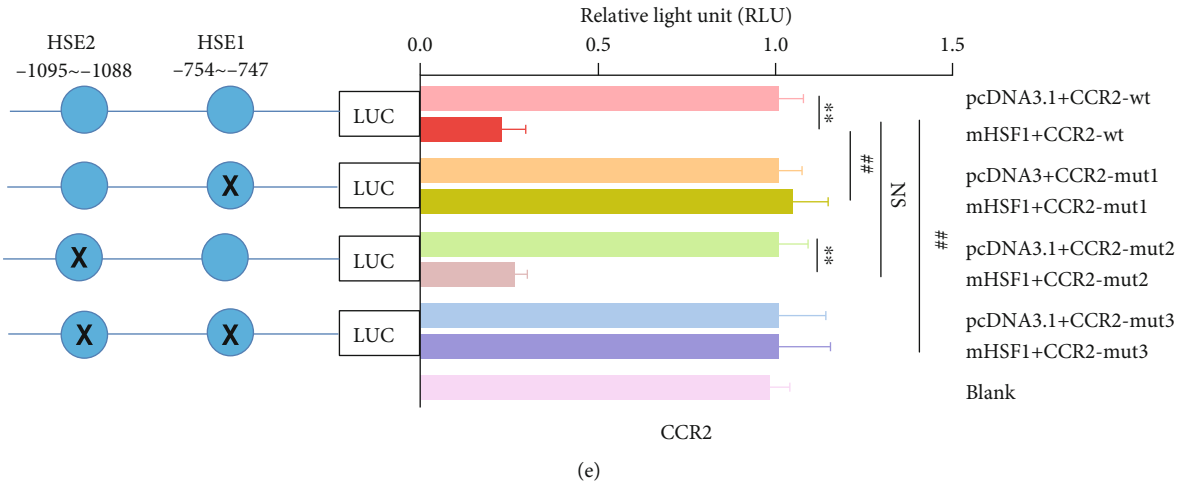

(e)

Figure 5: HSF1 downregulated the transcription of *MCP-1*/*CCR2*. (a, b, d) The binding of HSF1 to HSE in *MCP-1* and *CCR2* promoters was assessed using EMSA. (a, b) EMSA was used to detect the binding of the HSF1 protein with HSE1 (a) and HSE2 (b) in the *MCP-1* promoter region in vitro. The biotin probe specific for HSE1 or HSE2 was bound by nuclear extracts of RAW 264.7 cells, which could be blocked by an HSF1 antibody. (d) EMSA was used to detect the binding of the HSF1 protein with HSE1 in the *CCR2* promoter region in vitro. The biotin probe specific for HSE1 was bound by nuclear extracts, which could be blocked by an HSF1 antibody. Lane 1: negative control; lane 2: biotin-labeled HSE probe preincubated with nucleoproteins (HSF1-HSE complexes); lane 3: supershift analysis using anti-HSF1 antibodies; lane 4: competition using a 200-fold excess of the unlabeled competitive probe; lane 5: competition using a 200-fold excess of the unlabeled mutant probe. The HSF1/HSE complex is indicated by red arrowheads, the supershift band is indicated by blue arrowheads, and unbound HSE probe is indicated by black arrowheads. (c, e) Luciferase reporter assay analysis of HSF1 regulation on the promoter transcription activity of *MCP-1* (c) and *CCR2* (e) in RAW 264.7 cells transfected with the HSF1 overexpression vector (mHSF1) or empty expression vector pcDNA3.1. After 48 h of transfection, the cell lysate was extracted, and the firefly luciferase activity was measured and normalized to the Renilla luciferase activity. $^{**}p < 0.01$, pcDNA3.1 versus mHSF1 (intragroup comparison); $^{\#}p < 0.05$, versus mHSF1 + MCP-1-wt (or mHSF1 + CCR2-wt); $^{\#\#}p < 0.01$, versus mHSF1 + MCP-1-wt (or mHSF1 + CCR2-wt). Data are representative of at least three independent experiments. p values were determined using two-tailed Student's t-test for comparing two groups and one-way ANOVA for comparing multiple groups.

gene promoter is a key step to activate gene transcription. Under stress conditions, HSF1 forms homotrimers that upon phosphorylation bind to the promoter of heat shock genes to regulate their transcription (39–41). HSF1 can regulate the expression of other genes, including inflammatory cytokines (37, 42, 43). To explore the effect of HSF1 on inflammation, in previous studies, we screened for inflammation-associated genes potentially regulated by HSF1, using a microarray containing inflammatory cytokine genes. We found that HSF1 regulated the expression of several genes including *MCP-1*/*CCR2* (25). Further, bioinformatic analysis showed that there were several HSE in the promoters of *MCP-1*/*CCR2*. Combined with the results from the JASPAR core database, we proposed a hypothesis on how HSF1 may affect the course of inflammation by directly regulating the expression of *MCP-1*/*CCR2*. In this study, we tested such hypothesis by using EMSA and dual luciferase reporter assay experiments and found that HSF1 could directly downregulate *MCP-1*/*CCR2*. Therefore, the protective effect of HSF1 on ALI mice would be explained by the inhibition of macrophage migration and infiltration, owing to the downregulation of *MCP-1*/*CCR2*.

5. Conclusion

In summary, HSF1 attenuated LPS-induced ALI in mice by suppressing macrophage infiltration owing to the downregulation of *MCP-1*/*CCR2*.

Abbreviations

ALI: Acute lung injury
ARDS: Acute respiratory distress syndrome
BALF: Bronchoalveolar lavage fluids
BSA: Bovine serum albumin
CCR2: Chemokine (C-C motif) receptor 2
ELISA: Enzyme-linked immunosorbent assay
EMSA: Electrophoretic mobility shift assay
HSE: Heat shock element
HSF1: Heat shock factor 1
LPS: Lipopolysaccharide
MODS: Multiorgan dysfunction syndrome
MCP-1: Monocyte chemoattractant protein-1
NS: Normal saline
PBS: Phosphate-buffered saline
qRT-PCR: Real-time quantitative reverse transcription PCR
W/D: Wet/dry weight.

Data Availability

The data used to support the findings of this study are available from the corresponding author upon request.

Conflicts of Interest

The authors declare no conflict of interest, and the work described here has not been published previously and not

under consideration for publication elsewhere, in whole or in part.

Acknowledgments

This study is supported by the Hainan Provincial Natural Science Foundation of China, Grant No. 819QN229; Training Program of the Hainan Medical University, Grant No. HY2018-33; the National Natural Science Fund of China, Grant No. 81671895, 81871610, 81471897, and 81870071; Natural Science Foundation of Hunan Province, China, Grant No. 2019JJ40393.

References

[1] P. Arthur and G. R. B. Wheeler, "Acute lung injury and the acute respiratory distress syndrome: a clinical review," *The Lancet*, vol. 369, no. 9572, pp. 1553–1564, 2007.

[2] L. B. Ware, "Pathophysiology of acute lung injury and the acute respiratory distress syndrome," *Seminars in Respiratory and Critical Care Medicine*, vol. 27, no. 4, pp. 337–349, 2006.

[3] J. Villar, J. D. Edelson, M. Post, J. B. Mullen, and A. S. Slutsky, "Induction of heat stress proteins is associated with decreased mortality in an animal model of acute lung injury," *The American Review of Respiratory Disease*, vol. 147, no. 1, pp. 177–181, 1993.

[4] J. Villar, S. P. Ribeiro, J. B. Mullen, M. Kuliszewski, M. Post, and A. S. Slutsky, "Induction of the heat shock response reduces mortality rate and organ damage in a sepsis-induced acute lung injury model," *Critical Care Medicine*, vol. 22, no. 6, pp. 914–921, 1994.

[5] M. Pespeni, R. C. Mackersie, H. Lee et al., "Serum levels of Hsp60 correlate with the development of acute lung injury after Trauma1," *The Journal of Surgical Research*, vol. 126, no. 1, pp. 41–47, 2005.

[6] D. S. Wheeler and H. R. Wong, "The heat shock response and acute lung injury," *Free Radical Biology and Medicine*, vol. 42, no. 1, pp. 1–14, 2007.

[7] S. Chen, X. Zuo, M. Yang et al., "Severe multiple organ injury in HSF1 knockout mice induced by lipopolysaccharide is associated with an increase in neutrophil infiltration and surface expression of adhesion molecules," *Journal of Leukocyte Biology*, vol. 92, no. 4, pp. 851–857, 2012.

[8] B. J. Zhongyi Tong and L. Zhang, "HSF-1 is involved in attenuating the release of inflammatory cytokines induced by LPS through regulating autophagy," *SHOCK*, vol. 41, no. 5, p. 449Y453, 2014.

[9] A. E. Williams and R. C. Chambers, "The mercurial nature of neutrophils: still an enigma in ARDS?," *American Journal of Physiology-Lung Cellular and Molecular Physiology*, vol. 306, no. 3, pp. L217–L230, 2014.

[10] X. Xiao, "HSF1 is required for extra-embryonic development, postnatal growth and protection during inflammatory responses in mice," *The EMBO Journal*, vol. 18, no. 21, pp. 5943–5952, 1999.

[11] D. R. McMillan, X. Xiao, L. Shao, K. Graves, and I. J. Benjamin, "Targeted disruption of heat shock transcription factor 1 abolishes thermotolerance and protection against heat-inducible apoptosis," *The Journal of Biological Chemistry*, vol. 273, no. 13, pp. 7523–7528, 1998.

[12] L. Jiang, L. Zhang, K. Kang et al., "Resveratrol ameliorates LPS-induced acute lung injury via NLRP3 inflammasome modulation," *Biomedicine & pharmacotherapy*, vol. 84, pp. 130–138, 2016.

[13] A. M. Wolfe, L. H. Kennedy, J. J. Na, and J. A. Nemzek-Hamlin, "Efficacy of tramadol as a sole analgesic for postoperative pain in male and female mice," *Journal of the American Association for Laboratory Animal Science*, vol. 54, no. 4, pp. 411–419, 2015.

[14] G. Dos Santos, M. R. Rogel, M. A. Baker et al., "Vimentin regulates activation of the NLRP3 inflammasome," *Nature communications*, vol. 12, no. 1, pp. 1–13, 2015.

[15] L. S. de Aragão-França, L. S. Aragão-França, V. C. J. Rocha et al., "Tolerogenic dendritic cells reduce airway inflammation in a model of dust mite triggered allergic inflammation," *Allergy, Asthma & Immunology Research*, vol. 10, no. 4, pp. 406–419, 2018.

[16] A. Pierre, F. Lemaire, A. Meghraoui-Kheddar, S. Audonnet, S. Héry-Huynh, and R. Le Naour, "Impact of aging on inflammatory and immune responses during elastin peptide-induced murine emphysema," *American Journal of Physiology. Lung Cellular and Molecular Physiology*, vol. 316, no. 4, pp. L608–L620, 2019.

[17] J. Hu, W. Zhang, Y. Liu et al., "LDK378 inhibits the recruitment of myeloid-derived suppressor cells to spleen via the p38-GRK2-CCR2 pathway in mice with sepsis," *Immunology and Cell Biology*, vol. 97, no. 10, pp. 902–915, 2019.

[18] C. J. Goldenberg, Y. Luo, M. Fenna, R. Baler, R. Weinmann, and R. Voellmy, "Purified human factor activates heat shock promoter in a HeLa cell-free transcription system," *The Journal of Biological Chemistry*, vol. 263, no. 36, pp. 19734–19739, 1988.

[19] H. S. Choi, Z. Lin, B. S. Li, and A. Y. Liu, "Age-dependent decrease in the heat-inducible DNA sequence-specific binding activity in human diploid fibroblasts," *The Journal of Biological Chemistry*, vol. 265, no. 29, pp. 18005–18011, 1990.

[20] L. Zhang, M. Yang, Q. Wang et al., "HSF1 regulates expression of G-CSF through the binding element for NF-IL6/CCAAT enhancer binding protein beta," *Molecular and Cellular Biochemistry*, vol. 352, no. 1-2, pp. 11–17, 2011.

[21] S. Bose and J. Cho, "Role of chemokine CCL2 and its receptor CCR2 in neurodegenerative diseases," *Archives of Pharmacal Research*, vol. 36, no. 9, pp. 1039–1050, 2013.

[22] J. C. Lima-Junior, R. N. Rodrigues-da-Silva, V. A. Pereira et al., "Cells and mediators of inflammation (C-reactive protein, nitric oxide, platelets and neutrophils) in the acute and convalescent phases of uncomplicated plasmodium vivax and plasmodium falciparum infection," *Memórias do Instituto Oswaldo Cruz*, vol. 107, no. 8, pp. 1035–1041, 2012.

[23] T. Okuma, Y. Terasaki, N. Sakashita et al., "MCP-1/CCR2 signalling pathway regulates hyperoxia-induced acute lung injury via nitric oxide production," *International Journal of Experimental Pathology*, vol. 87, no. 6, pp. 475–483, 2006.

[24] B. Z. Qian, J. Li, H. Zhang et al., "CCL2 recruits inflammatory monocytes to facilitate breast-tumour metastasis," *Nature*, vol. 475, no. 7355, pp. 222–225, 2011.

[25] F. X. Yu, H. L. Zhang, G. W. Chen et al., "Screen of inflammatory genes regulated by heat shock factor 1 and corroboration w ith SOCS3 gene," *Journal of Central South University. Medical sciences*, vol. 31, no. 2, pp. 167–173, 2006.

[26] A. S. Slutsky, J. Villar, and A. Pesenti, "Happy 50th birthday ARDS!," *Intensive Care Medicine*, vol. 42, no. 5, pp. 637–639, 2016.

[27] G. D. Rubenfeld, E. Caldwell, E. Peabody et al., "Incidence and outcomes of acute lung injury," *The New England Journal of Medicine*, vol. 353, no. 16, pp. 1685–1693, 2005.

[28] A. Pfalzgraff, L. Heinbockel, Q. Su, T. Gutsmann, K. Brandenburg, and G. Weindl, "Synthetic antimicrobial and LPS-neutralising peptides suppress inflammatory and immune responses in skin cells and promote keratinocyte migration," *Scientific Reports*, vol. 6, no. 31577, pp. 1–12, 2016.

[29] Z. Zhang, J. Zhou, D. Song, Y. Sun, C. Liao, and X. Jiang, "Gastrodin protects against LPS-induced acute lung injury by activating Nrf2 signaling pathway," *Oncotarget*, vol. 8, no. 19, pp. 32147–32156, 2017.

[30] F. Gerin, U. Sener, H. Erman et al., "The effects of quercetin on acute lung injury and biomarkers of inflammation and oxidative stress in the rat model of sepsis," *Inflammation*, vol. 39, no. 2, pp. 700–705, 2016.

[31] J. Lomas-Neira, C. S. Chung, M. Perl, S. Gregory, W. Biffl, and A. Ayala, "Role of alveolar macrophage and migrating neutrophils in hemorrhage-induced priming for ALI subsequent to septic challenge," *American Journal of Physiology-Lung Cellular and Molecular Physiology*, vol. 290, no. 1, pp. L51–L58, 2006.

[32] L. K. Johnston, C. R. Rims, S. E. Gill, J. K. McGuire, and A. M. Manicone, "Pulmonary macrophage subpopulations in the induction and resolution of acute lung injury," *American Journal of Respiratory Cell and Molecular Biology*, vol. 47, no. 4, pp. 417–426, 2012.

[33] P. E. Kolattukudy and J. Niu, "Inflammation, endoplasmic reticulum stress, autophagy, and the monocyte chemoattractant protein-1/CCR2 pathway," *Circulation Research*, vol. 110, no. 1, pp. 174–189, 2012.

[34] G. H. Tesch, "MCP-1/CCL2: a new diagnostic marker and therapeutic target for progressive renal injury in diabetic nephropathy," *American Journal of Physiology. Renal Physiology*, vol. 294, no. 4, pp. F697–F701, 2008.

[35] S. Sozzani, D. Zhou, M. Locati et al., "Receptors and transduction pathways for monocyte chemotactic protein-2 and monocyte chemotactic protein-3. Similarities and differences with MCP-1," *Journal of Immunology*, vol. 152, no. 7, pp. 3615–3622, 1994.

[36] C. M. Cahill, W. R. Waterman, Y. Xie, P. E. Auron, and S. K. Calderwood, "Transcriptional repression of the prointerleukin 1beta gene by heat shock factor 1," *The Journal of Biological Chemistry*, vol. 271, no. 40, pp. 24874–24879, 1996.

[37] Y. Xie, C. Chen, M. A. Stevenson, P. E. Auron, and S. K. Calderwood, "Heat shock factor 1 represses transcription of theIL-1βGene through physical interaction with the nuclear factor of interleukin 6," *The Journal of Biological Chemistry*, vol. 277, no. 14, pp. 11802–11810, 2002.

[38] I. S. Singh, R. M. Viscardi, I. Kalvakolanu, S. Calderwood, and J. D. Hasday, "Inhibition of tumor necrosis factor-alpha transcription in macrophages exposed to febrile range temperature. A possible role for heat shock factor-1 as a negative transcriptional regulator," *Journal of Biological Chemistry*, vol. 275, no. 13, pp. 9841–9848, 2000.

[39] Y. Zhang, L. Huang, J. Zhang, D. Moskophidis, and N. F. Mivechi, "Targeted disruption ofhsf1 leads to lack of thermotolerance and defines tissue-specific regulation for stress-inducible Hsp molecular chaperones," *Journal of Cellular Biochemistry*, vol. 86, no. 2, pp. 376–393, 2002.

[40] E. S. Christians, L. J. Yan, and I. J. Benjamin, "Heat shock factor 1 and heat shock proteins: critical partners in protection against acute cell injury," *Critical Care Medicine*, vol. 30, Suppl., pp. S43–S50, 2002.

[41] S. G. Ahn and D. J. Thiele, "Redox regulation of mammalian heat shock factor 1 is essential for Hsp gene activation and protection from stress," *Genes & Development*, vol. 17, no. 4, pp. 516–528, 2003.

[42] P. A. Mercier, N. A. Winegarden, and J. T. Westwood, "Human heat shock factor 1 is predominantly a nuclear protein before and after heat stress," *Journal of cell science*, vol. 112, no. 16, pp. 2765–2774, 1999.

[43] M. Vujanac, A. Fenaroli, and V. Zimarino, "Constitutive nuclear import and stress-regulated nucleocytoplasmic shuttling of mammalian heat-shock factor 1," *Traffic*, vol. 6, no. 3, pp. 214–229, 2005.

Hindawi
Oxidative Medicine and Cellular Longevity
Volume 2020, Article ID 8815655, 8 pages
https://doi.org/10.1155/2020/8815655

Research Article

Early Enteral Nutrition Preserves Intestinal Barrier Function through Reducing the Formation of Neutrophil Extracellular Traps (NETs) in Critically Ill Surgical Patients

Qiongyuan Hu,[1,2] Huajian Ren,[1] Zhiwu Hong,[1] Chenyang Wang,[1] Tao Zheng,[1] Yanhan Ren,[3] Kai Chen,[2] Song Liu,[2] Gefei Wang,[1] Guosheng Gu,[1] Xiuwen Wu,[1] and Jianan Ren[1]

[1]*Research Institute of General Surgery, Jinling Hospital, Medical School of Nanjing University, Nanjing 210002, China*
[2]*Department of Gastrointestinal Surgery, Nanjing Drum Tower Hospital, The Affiliated Hospital of Nanjing University Medical School, 210008, China*
[3]*Rosalind Franklin University of Medicine and Sciences, North Chicago, IL, USA*

Correspondence should be addressed to Jianan Ren; jiananr@gmail.com

Received 29 August 2020; Revised 20 October 2020; Accepted 5 November 2020; Published 21 November 2020

Academic Editor: Joanna Lecka

Copyright © 2020 Qiongyuan Hu et al. This is an open access article distributed under the Creative Commons Attribution License, which permits unrestricted use, distribution, and reproduction in any medium, provided the original work is properly cited.

Background. The gut was suggested as the driver of critical illness and organ injury. Recently, excessive formation of neutrophil extracellular traps (NETs) was associated with mucosal inflammation. Direct investigation of intestinal mucosa is essential to illuminate the potential mechanism of gut barrier in critically ill patients. We hypothesized that early enteral nutrition (EN) could decrease intestinal NETs and maintain the gut barrier. *Methods*. Intestinal biopsies were obtained using biopsy forceps from critically ill surgical patients complicated with enterocutaneous fistula. Expressions of tight junction (TJ) proteins, mucosal inflammation, and apoptosis were evaluated. Moreover, NET-associated proteins were evaluated in intestinal specimens of patients by Western blot and immunofluorescence analysis. *Results*. The intestinal barrier was significantly impaired in critically ill patients receiving early total parenteral nutrition (TPN), evidenced by intestinal villi atrophy, inflammatory infiltration, increased enterocyte apoptosis, and abnormal TJ expressions. Early EN significantly alleviated these intestinal injuries. In addition, we observed increased formation of the NET structure and elevated expressions of NET-associated proteins in intestines of critically ill surgical patients. Early EN was associated with the diminished presence of NETs and reduced expression of NET-associated proteins. Mechanically, analysis of the TLR4 pathway showed a significant increase in TLR4, NFκB, and MAPK signaling in patients receiving TPN when compared to those receiving early EN. *Conclusion*. The intestinal barrier is disrupted in the human gut during critical illness. Our data suggests that an increased NET structure was showed in the gut of critically ill surgical patients, and early EN treatment was associated with the reduction of NET formation and the preservation of mucosal immunity.

1. Background

Critical illness disrupts gut integrity by increasing inflammatory response and epithelial apoptosis. The gut has long been suggested as the "engine" of multiple organ dysfunction (MOD) for critically ill patients [1]. However, the original evidence for this theory has only been supported by experimental or retrospective data. Direct investigation of human intestinal mucosa in critically ill patients is required to confirm this theory. Increasing evidence also suggested that an advanced approach to target the human gut would be the most effective way of demonstrating the gut's role as the driver of critical illness [1, 2].

Nutritional support is the cornerstone of therapy for critical illness. In the absence of enteral nutrition (EN), disruption of mucosal integrity contributes to an impaired gut barrier [3, 4]. Increasing evidence based on animal models demonstrated that total parenteral nutrition (TPN) contributes to increased infection incidence due to mucosal injury [5]. However, changes in the gut barrier and mucosal

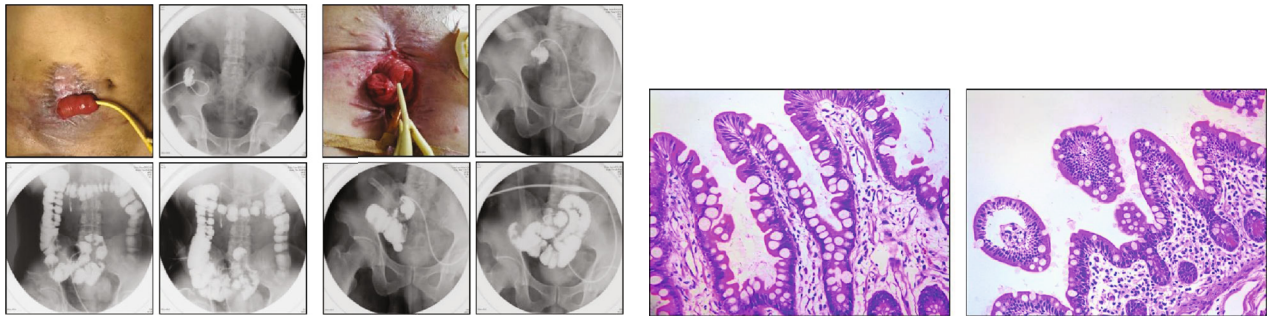

Figure 1: The effect of early EN on mucosal morphology in critical illness. (a) Abdominal manifestations and fistula radiography for critically ill surgical patients. (b) H&E staining for intestinal histology in critical illness receiving different types of nutrition.

morphology of critically ill patients receiving TPN or EN are scarcely documented and poorly understood. Piton et al. [6] recently investigated the impact of early EN on intestinal mucosa in shock patients by measuring plasma biomarkers of enterocyte damage. However, the precise mechanism of the impact of nutrition on the intestinal barrier of critically ill patients still remains undetermined. Therefore, direct evaluation of the intestine in critically ill patients is essential to deeply understand the potential mechanisms of gut dysfunction.

Accumulated neutrophils at the subepithelial space can disrupt the local immunological milieu and impair the epithelial barrier. In 2004, a new mechanical action was described in neutrophils: activated neutrophil can erupt web-like chromatin filaments to form neutrophil extracellular traps (NETs) in response to various states of inflammation [7]. A recent study demonstrated that NETs are implicated in the inflammatory cascade of ulcerative colitis patients [8]. Increased inflammatory response in the gut is very crucial in the progression of patients with sepsis and MOD [9]. The contribution of NETs to intestinal inflammation and gut barrier dysfunction remains to be elucidated. Therefore, we compared the effects of the formation of NET structures in critically ill patients receiving either EN and TPN.

The primary objective of our study was to investigate changes in intestinal mucosa during critical illness among patients receiving EN or TPN. The secondary objective is aimed at evaluating the formation of the NET structure in the gut among critically ill patients and comparing the impact of different routes of nutrition on NET formation.

2. Materials and Methods

2.1. Ethics Statement and Human Tissues. Our study was performed based on the Recommendations of Guidelines for Clinical Trials by the Ethics Committee of Jinling Hospital. All patients provided written informed consent before performance of any study-related procedure.

Recently, the evaluation of gut barrier function by measuring circulating biomarkers for critically ill patients has been limited and indirect. In addition, there is no consensus on the appropriate cutoff points for plasma biomarkers [10]. In our study, we presented an ideal model (enterocutaneous fistula (ECF)) to directly observe the morphology and investigate the intestines during critical illness. Abdominal manifestations and fistula radiography for ECF patients are shown in Figure 1(a). Intestinal mucosa specimens were percutaneously obtained using biopsy through the fistula. Informed consent was obtained from all participants that received this procedure.

Our prospective study cohort enrolled 20 ECF patients who were admitted to the surgical intensive care unit (SICU) at Jinling Hospital from October 2018 to Jun 2019. The SICU, which belongs to the Department of General Surgery, receives abdominal trauma and perioperative patients. For critical illness, although early EN is preferred, the TPN group is still used in some specific circumstance, including (a) inability to tolerate adequate caloric intake, (b) continued vomiting, (c) increasing abdominal distension, (d) evidence of intestinal obstruction, (e) intra-abdominal infections complicated with other undefined fistula, and (f) high-output fistula. Feeding routes were determined by chart review and discussion with the family and the surgical team. In our study, the groups were divided according to the routes of nutrition: one group received early TPN (TPN group, $n = 10$), whereas the other group received early full enteral nutrition (early EN group, $n = 10$) for seven days. On day 7, intestinal samples were obtained. The baseline characteristics of the enrolled patients are shown in Supplementary Table 1. At baseline, there was no difference between the early EN and TPN groups.

2.2. Histology, Immunohistochemistry, and Immunofluorescence. Human intestine biopsies were fixed in formalin and embedded in paraffin. Hematoxylin and eosin (H&E) staining was then performed, and Chiu's scoring system was used to evaluate intestinal injuries. To evaluate the density of goblet cells, periodic acid-Schiff (PAS) staining and Alcian blue-PAS staining were performed, as previously described [11].

For immunohistochemistry (IHC) staining, slides were incubated with anti-IL-1β antibody (Servicebio, GB11113, Wuhan), anti-IL-6 antibody (Servicebio, GB11117-1,

Wuhan), anti-TNF-α antibody (Servicebio, GB11188, Wuhan), anti-Bax antibody (Servicebio, GB11007-1, Wuhan), and anti-Bcl-2 antibody (Servicebio, GB12318, Wuhan) after antigen retrieval (with citrate buffer) and organization background closing (with goat serum). Then, the slides were incubated with a biotin-linked second antibody (goat-anti-rabbit) for 20 min, with streptavidin labeled with horseradish-peroxidase (S-A/HRP) for 20 min and with DAB (Servicebio, K5007, Wuhan) for 5 min [12]. The sections were stained with hematoxylin and then dehydrated. Finally, the staining was observed under a microscope.

The localization and expression of tight junction (TJ) proteins and NET-associated proteins were detected by immunofluorescent staining using antibodies against ZO-1 (ab96587; Abcam), occludin (ab216327, Abcam), claudin-1 (ab180158, Abcam), mouse anti-human MPO (ab25989, Abcam), rabbit anti-human NE (ab131260, Abcam), and rabbit anti-human citH3 (ab5103, Abcam). DAPI was used to counterstain DNA. Images were acquired using a Leica DMI 4000 B fluorescence microscope.

2.3. Western Blot. For this assay, 0.1 g of intestinal samples was homogenized and ultrasonicated and then treated with lysis buffer. All protein samples were boiled after being mixed with the commensurable buffer. The expression level of proteins from intestines was detected and separated via SDS-PAGE gels. The total protein from gels was then transferred to PVDF membranes. The membranes were blocked with milk and then incubated with primary antibodies against the protein of interest at 4°C overnight. Next, the membranes were incubated with HRP-labeled secondary antibodies. The expression of protein was quantified in optical density units using Image Lab software (Bio-Rad, CA, USA) and was normalized to the corresponding sample expression of GAPDH (P.R.C. KeyGEN Biotech).

2.4. Apoptosis Evaluation. The detection of apoptosis in the intestinal tissues used TUNEL (terminal deoxynucleotidyl transferase dUTP nick end labeling) staining according to the manufacturer's instruction, as previously described [13].

2.5. Statistical Analysis. Statistical analyses were performed using SPSS software. Results are expressed as means ± SD unless otherwise specified. A comparison between two groups used the unpaired, one-tailed Student t-test. For the expression of protein and cytokines, a paired Student t-test was used. All p values < 0.05 were considered significant.

3. Results

3.1. The Effect of Early EN on Mucosal Morphology and Biochemical Barrier in Critical Illness. Morphologically, villus atrophy and decline in villus height were shown in the TPN group, and early EN improved villus morphology (Figure 1(b)). Furthermore, H&E staining of intestines showed significant intestinal mucosal injury, evidenced by tissue destruction and infiltration of inflammatory cells in patients receiving TPN (Figure 1(b)). However, early EN significantly alleviated these injuries. Additionally, using PAS and Alcian blue-PAS staining, our results showed a significant increase in the number of goblet cells in the early EN group compared with that of the TPN group (Supplementary Figure 1).

3.2. Early Enteral Nutrition Improves the Immunological Milieu in the Gut. A dense network of immune cells that cooperate with the gastrointestinal epithelium maintains inflammatory balance in the gut [5]. IHC staining showed that proinflammatory factors, including IL-1β, IL-6, and TNF-α, were significantly increased in the TPN group compared with the early EN group (Figures 2(a)–2(c)). The anti-inflammatory cytokine IL-10, mainly derived from intraepithelial lymphocytes, is a vital factor for the intestinal epithelial barrier. Figure 2(d) showed that IL-10 expression was markedly decreased in the TPN group compared with the EN group.

3.3. Early EN Restores Intestinal Physical Barrier for Critically Ill Patients. Impaired TJ integrity is the key factor for increased intestinal epithelial permeability [12]. Our results showed that the expressions of ZO-1, occludin, and claudin-1 were significantly increased in the intestinal mucosa in the early EN group compared with those of the TPN group (Figure 3). The presence of impaired intestinal villi was further verified through microscopy. As shown in Supplementary Figure 2, the ultrastructural morphology of TJ and desmosomes in the intestines was disrupted in the TPN group. However, the TJ and desmosomes were nearly intact in patients receiving EN.

Enterocyte apoptosis is one of the important accelerants of disrupted TJ [13]. An increased number of TUNEL-positive cells were shown in the gut mucosa in the TPN group, while early EN treatment significantly attenuated apoptosis of enterocytes (Figure 4(a)). Moreover, the expression of the proapoptotic protein Bax and antiapoptotic protein Bcl-2 was assessed to check the apoptosis level in the gut. IHC staining and Western blot results showed increased expression of Bax and decreased expression of Bcl-2 in the TPN group as compared to the early EN group (Figures 4(b) and 4(c)).

3.4. NET-Associated Proteins Are Upregulated in the Gut of Critically Ill Patients and Could Be Diminished following Early EN Treatment. Increased formation of NETs is associated with gut damage. However, the clinical plasma biomarkers of NETs are unstable and subject to enzymatic degradation [14]. Better detection of local formation of the NET structure is required to investigate the potential mechanisms. Microscopic analysis detected positive staining for citH3 and MPO (Figure 5(a)) and NE and MPO (Figure 5(b)), overlapping with diffuse DNA scaffolds and confirming the increased formation of the NET structure in the gut during critical illness. Figure 5 also showed that early EN is associated with the diminished presence of NETs in the intestinal mucosa. PAD4 acts as a driver of NET formation, and Western blot demonstrated a significant decrease in the gut in the early EN group as compared to the TPN group (Supplementary Figure 3). We next evaluated the other three components of NETs, including the expression of NE,

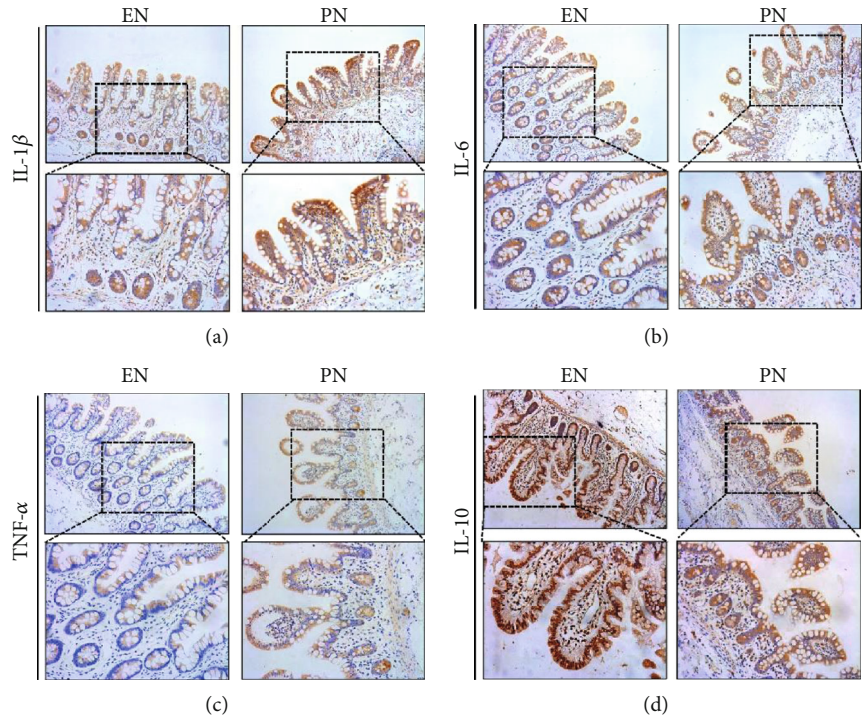

Figure 2: Early enteral nutrition improves the immunological milieu in the gut. Representative immunohistochemical images showing the inflammatory factors, IL-1β, IL-6, TNF-α, and IL-10, in intestinal samples taken during critical illness.

MPO, and citH3. The expression of these NET-associated proteins was decreased in the intestines of patients receiving early EN.

3.5. Effects of Early EN on the TLR4 Pathway. The expression of TLR4 protein in the gut was assessed in our patients. The results showed that early EN was associated with decreased TLR4 expression in the intestines compared with that of the TPN group. The NFκB pathway activated by TLR4 could initiate the transcription of inflammatory genes. Supplementary Figure 4A showed that p-IKKβ, p-IκBα, and p-p65 proteins were greatly reduced in the early EN group compared with those of the TPN group. MAPKs are another vital pathway activated by TLR4. The p38, ERK, and JNK signaling was evaluated using Western blot. Our results indicated that the levels of p-p38 and p-ERK were significantly decreased in the gut in the early EN group (Supplementary Figure 4B). Interestingly, the expression of p-JNK protein showed no significant differences between the two groups.

4. Discussion

The gut has long been suggested to be the driver of critical illness [1]. Under normal physiological conditions, the gut plays an important role in health maintenance. However, multiple elements of the gut are damaged in critically ill patients, potentially worsening MOD. Our study examined potential mechanisms for these changes and provided solid proof for the importance of the gut in human critical illness. We investigated the changes in the intestinal barrier in critically ill patients receiving different types of early nutrition. Our results demonstrated that the patients receiving TPN showed an injured mucus barrier, increased inflammatory response, abnormal TJ proteins, and increased apoptosis in the intestinal specimens compared with the enterally fed gut. This finding correlated with increased formation of the NET structure in the gut. Excessive formation of NETs was recently suggested to contribute to mucosal injury [15, 16]. Immunofluorescence images demonstrated that the intensity and distribution of the NET structure were significantly increased in the gut of critically ill patients receiving TPN. Therefore, the dysfunction of the gut barrier may be associated with increased NET-associated proteins and NET structure.

In the present study, atrophic mucosa was also shown in the patients with TPN treatment; early EN treatment significantly helped to restore the mucosal morphology. These findings indicate that an interaction between intestinal epithelial cells and nutrients plays an important role in keeping cellular function and metabolism active. In one study of rats with brain injury, unfed rats, compared to those with delayed EN, showed a significant atrophic mucosa and faster apoptosis of epithelial cells. Additionally, restarting EN was suggested to awake dormant intestinal mucosal cells, which can induce epithelial cells to enhance protein synthesis [17]. Mucin secreted by goblets also plays an important role to protect the gut epithelium against bacteria invasion. In the present study, early EN treatment helped to maintain the number of goblets in the human gut during critical illness.

Results from studies of mice and cell culture suggested that impaired TJ proteins were associated with the increased production of proinflammatory cytokines and were elevated following TPN treatment. Our previous study suggested that

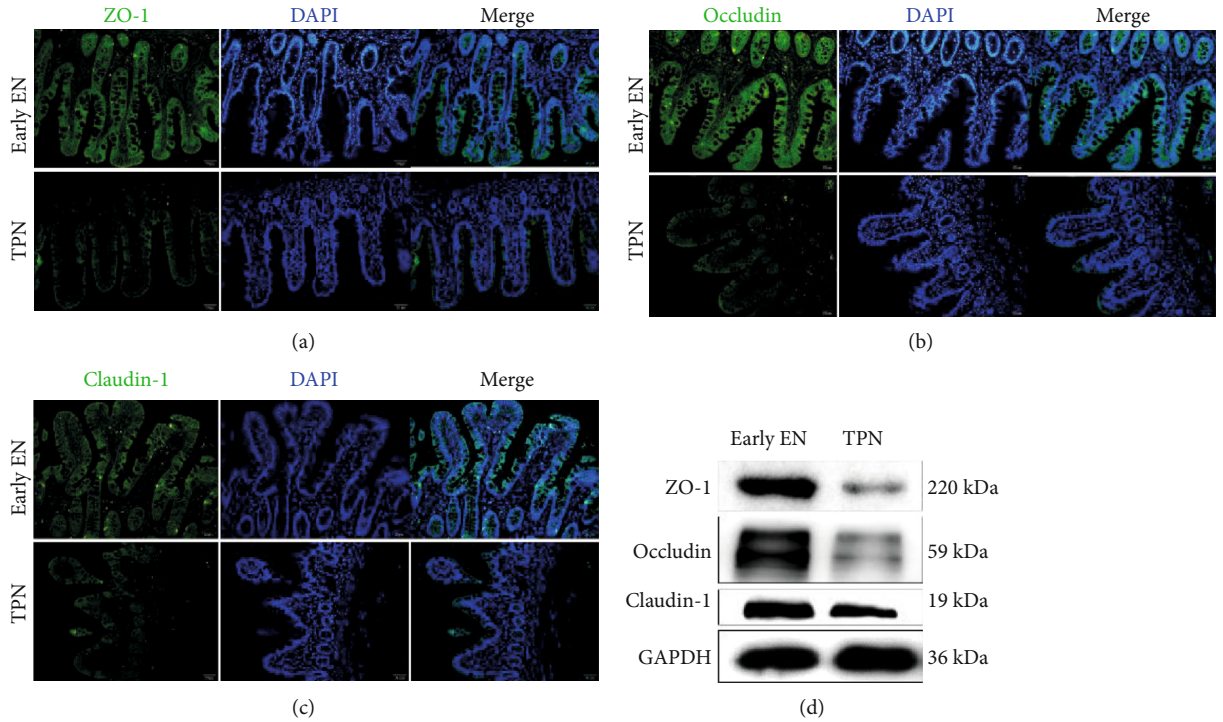

Figure 3: Effect of early enteral nutrition on the intestinal mechanical barrier. (a) Location and expression of tight junction protein within intestinal mucosa in critically ill patients, comparing TPN and early EN groups. (b) Protein levels of ZO-1, occludin, and claudin-1 were determined using Western blotting.

increased production of proinflammatory cytokines contributes to increased epithelial cell apoptosis [13]. In the present study, we confirmed that increased local proinflammatory factors in the human gut were associated with alternant expression of TJ proteins and increased apoptosis in patients receiving TPN. These significant changes in the production of proinflammatory factors initiate a chain effect leading to a profound impairment of the cellular mechanisms that preserve the intestinal epithelial barrier under physiological conditions [18]. Anti-inflammatory responses that are regulated by IL-10 are important in maintaining the epithelial barrier. Evidence obtained from in vivo studies of mice indicated that IL-10 expression is markedly decreased during TPN, which is associated with injured TJs and increased epithelial permeability. Sun et al. [19] showed that the exogenous administration of IL-10 markedly alleviated the TPN-associated decrease in TJ protein expression. In our study, EN deprivation was associated with decreased levels of IL-10, and early EN treatment significantly increased IL-10 expression in the gut of critically ill patients.

Recent studies investigated that excessive formation of NET structures was suggested to lead to the progression of sepsis or MODS [20]. Elevated levels of NET biomarkers have been reported in critically ill patients, but currently, methods to detect NET formation are limited to indirect measurement in the circulation [21, 22]. Moreover, circulating levels of NET markers are unstable and subject to enzymatic degradation. Therefore, detection of local NET formation is urgently necessary for the study of critical illness. Recently, NETs were suggested to directly induce epithelial cell death [23], which can aggravate gut barrier dysfunction. Lang et al. [24] reported that the degradation of NETs could reverse intestinal inflammation and injury in nonobese diabetic mice. Additionally, Dinallo et al. [8] showed that NETs were released in colonic mucosal tissue and suggested that excessive induction of NETs contributes to the amplification of intestinal inflammatory cascade. Li et al. [16] recently demonstrated that NET degradation by DNase may be protective in DSS-induced experimental colitis, and DNase treatment prevented the increase in serum inflammatory cytokines. In the present study, we discovered that the gut of critically ill patients showed increased protein levels of NE and MPO, two main components of NETs. Our IF images further showed that NE and MPO colocalize with DNA and citH3, indicating that the NET structure occurs in the gut of critically ill patients. Accordingly, a diminished presence of the NET structure was shown in early EN-treated patients. Further investigation is required to delineate the potential mechanisms involved in the clearance of intestinal NETs.

TLR4 signaling is an important pathway by which the intestinal mucosa senses change in the luminal environment. Our study found that the expression of TLR4 was significantly increased in the gut of critically ill patients receiving early TPN as compared with early EN. There is an emerging theory that altered microbial populations in patients receiving TPN induce intestinal barrier dysfunction, including an increase in many Gram-negative organisms. Nutrients play an important role in regulating intestinal bacteria-mucosal immune crosstalk [25, 26]. An expansion of Gram-negative

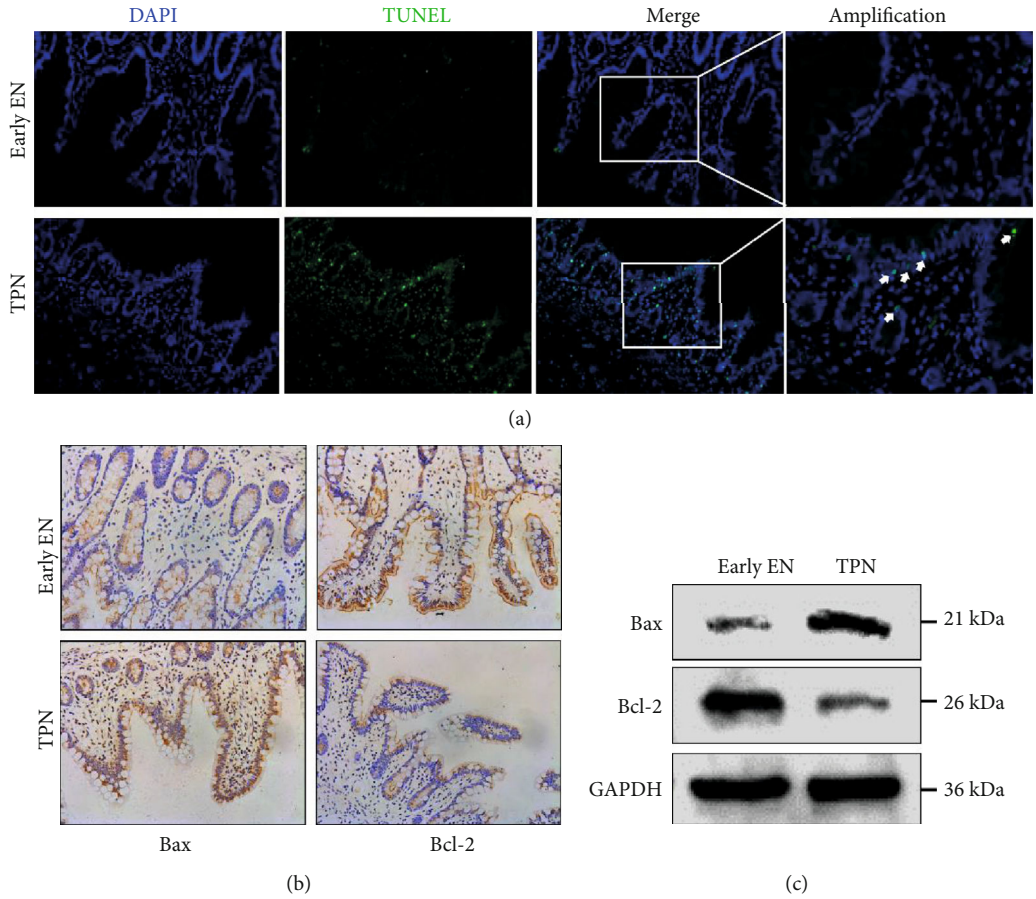

Figure 4: The effect of early nutrition on intestinal apoptosis. (a) Representative images of TUNEL staining in the gut of critically ill patients. (b) Representative immunohistochemical images showing the Bax and Bcl-2 expression in the intestinal samples of critically ill patients. (c) The expression of Bax and Bcl-2 was determined by Western blotting. GAPDH was used as control.

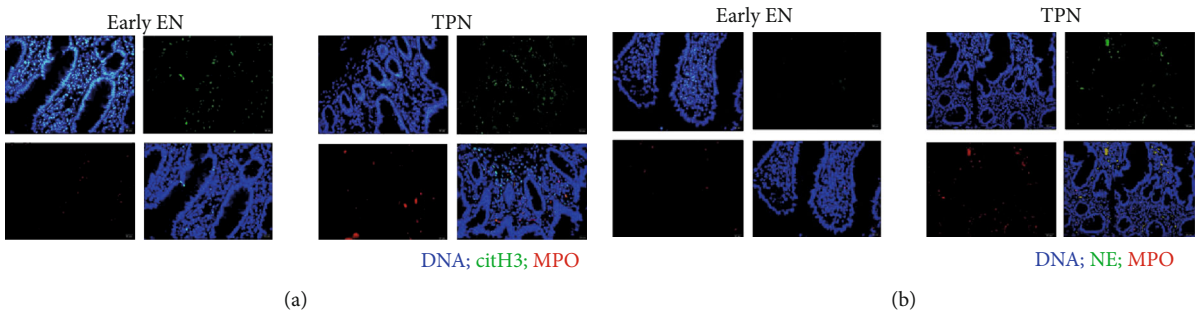

Figure 5: Early enteral nutrition reduces the intestinal presence of NETs. (a) Representative images of double immunofluorescence staining of intestinal samples in critically ill patients for citrullinated histone H3 (citH3, green) and myeloperoxidase (MPO, red). (b) Double immunofluorescence staining for neutrophil elastase (NE, green) and myeloperoxidase (MPO, red). Colocalizations of citH3 and MPO or NE and MPO are indicative of NET structure.

bacteria has been suggested to activate the TLR4 signaling pathway [27]. Although we did not report microbial data, the findings of increased TLR4 expression would be consistent with previous publications. Recent studies indicated that the TLR4 signaling pathway is associated with the increased formation of NET structures [28]. In this study, TLR4 signaling was likely involved in intestinal NET formation.

The main limitation of this study is that all patients suffered ECFs, and this affects enterohepatic circulation that also affects gut architecture. Additionally, all the patients were critically ill, and because of associated conditions/morbidity, there may have been an additional effect on the enterocytes. However, it is really difficult and dangerous to perform systematic digestive endoscopy in critically ill patients. We provide an advanced approach to evaluate the pathological changes in the gut using the ECF model.

The concept of the gut as the driver of critical illness has been established for more than 30 years. The dysregulation of

the intestinal microenvironment can drive the progression of sepsis and induce distant organ injury. However, no current therapy exists to target the gut barrier or permeability at the bedside of critically ill patients. The clinical model (ECF) in our study helps to investigate the impact of selected pharmacologic therapies on the local intestinal mucosa, while further studies are urgently required to determine how to target mucosa during critical illness.

Data Availability

The data used to support the findings of this study are included within the article.

Conflicts of Interest

All authors declare no conflicts of interest.

Authors' Contributions

Qiongyuan Hu, Huajian Ren, and Zhiwu Hong equally contributed to the paper.

Acknowledgments

This work was supported by the National Natural Science Foundation of China (81772052) and the Postgraduate Research & Practice Innovation Program of Jiangsu Province (KYCX19_0052).

Supplementary Materials

Supplementary Table 1: demographic and clinical variables of patients in surgical ICU. Supplementary Figure 1: effect of early nutrition on the biochemical barrier in the gut. (A) PAS staining and AB-PAS staining were performed to determine the numbers of intestinal goblets in the gut. Supplementary Figure 2: critical illness damaged the morphology of tight junctions in the gut. (A) In the intestinal samples in patients receiving TPN, the TJ ultrastructure was injured. The TJs were nearly intact in the gut of the early EN group. Supplementary Figure 3: expression of NET-associated proteins was determined in the gut of critically ill patients. Western blot showing PAD4, NE, MPO, and citH3 expression in the intestinal samples, comparing the TPN and early EN groups. Supplementary Figure 4: effect of early enteral nutrition on the expression level of TLR4 signaling. (A) The levels of TLR4, IKKβ, IκBα, and p65 protein were analyzed in the gut in critically ill patients receiving different types of nutrition. (B) Effect of nutrition on MAPK signaling, including p38, ERK, and JNK, in the human intestine during critical illness. *(Supplementary Materials)*

References

[1] R. Mittal and C. M. Coopersmith, "Redefining the gut as the motor of critical illness," *Trends in Molecular Medicine*, vol. 20, no. 4, pp. 214–223, 2014.

[2] S. Otani and C. M. Coopersmith, "Gut integrity in critical illness," *Journal of Intensive Care*, vol. 7, no. 1, p. 17, 2019.

[3] J. Wu, N. Ma, L. J. Johnston, and X. Ma, "Dietary nutrients mediate intestinal host defense peptide expression," *Advances in nutrition*, vol. 11, no. 1, pp. 92–102, 2020.

[4] N. Ma, P. Guo, J. Zhang et al., "Nutrients mediate intestinal bacteria-mucosal immune crosstalk," *Frontiers in Immunology*, vol. 9, p. 5, 2018.

[5] M. Schorghuber and S. Fruhwald, "Effects of enteral nutrition on gastrointestinal function in patients who are critically ill," *The Lancet Gastroenterology & Hepatology*, vol. 3, no. 4, pp. 281–287, 2018.

[6] G. Piton, A. Le Gouge, N. Brule et al., "Impact of the route of nutrition on gut mucosa in ventilated adults with shock: an ancillary of the NUTRIREA-2 trial," *Intensive Care Medicine*, vol. 45, no. 7, pp. 948–956, 2019.

[7] V. Brinkmann, U. Reichard, C. Goosmann et al., "Neutrophil extracellular traps kill bacteria," *Science*, vol. 303, no. 5663, pp. 1532–1535, 2004.

[8] V. Dinallo, I. Marafini, D. Di Fusco et al., "Neutrophil extracellular traps sustain inflammatory signals in ulcerative colitis," *Journal of Crohn's & Colitis*, vol. 13, no. 6, pp. 772–784, 2019.

[9] N. J. Klingensmith and C. M. Coopersmith, "The gut as the motor of multiple organ dysfunction in critical illness," *Critical Care Clinics*, vol. 32, no. 2, pp. 203–212, 2016.

[10] G. Piton and G. Capellier, "Biomarkers of gut barrier failure in the ICU," *Current Opinion in Critical Care*, vol. 22, no. 2, pp. 152–160, 2016.

[11] Y. Zhao, Y. Sun, G. Wang, S. Ge, and H. Liu, "Dendrobium officinale polysaccharides protect against MNNG-induced PLGC in rats via activating the NRF2 and antioxidant enzymes HO-1 and NQO-1," *Oxidative Medicine and Cellular Longevity*, vol. 2019, Article ID 9310245, 11 pages, 2019.

[12] Q. Hu, J. Ren, G. Li et al., "The mitochondrially targeted antioxidant MitoQ protects the intestinal barrier by ameliorating mitochondrial DNA damage via the Nrf2/ARE signaling pathway," *Cell Death & Disease*, vol. 9, no. 3, p. 403, 2018.

[13] Q. Hu, H. Ren, G. Li et al., "STING-mediated intestinal barrier dysfunction contributes to lethal sepsis," *eBioMedicine*, vol. 41, pp. 497–508, 2019.

[14] S. T. Abrams, N. Zhang, J. Manson et al., "Circulating histones are mediators of trauma-associated lung injury," *American Journal of Respiratory and Critical Care Medicine*, vol. 187, no. 2, pp. 160–169, 2013.

[15] Y. Liang, X. Wang, D. He et al., "Ameliorating gut microenvironment through staphylococcal nuclease-mediated intestinal NETs degradation for prevention of type 1 diabetes in NOD mice," *Life Sciences*, vol. 221, pp. 301–310, 2019.

[16] T. Li, C. Wang, Y. Liu et al., "Neutrophil extracellular traps induce intestinal damage and thrombotic tendency in inflammatory bowel disease," *Journal of Crohn's & Colitis*, vol. 14, no. 2, pp. 240–253, 2020.

[17] T. A. Winter, S. J. O'Keefe, M. Callanan, and T. Marks, "Effect of severe undernutrition and subsequent refeeding on gut mucosal protein fractional synthesis in human subjects," *Nutrition*, vol. 23, no. 1, pp. 29–35, 2007.

[18] T. Ikeda, K. Hiromatsu, M. Hotokezaka, and K. Chijiiwa, "Up-regulation of intestinal Toll-Like receptors and cytokines expressions change after TPN administration and a lack of enteral feeding," *The Journal of Surgical Research*, vol. 160, no. 2, pp. 244–252, 2010.

[19] X. Sun, H. Yang, K. Nose et al., "Decline in intestinal mucosal IL-10 expression and decreased intestinal barrier function in a

mouse model of total parenteral nutrition," *American journal of physiology Gastrointestinal and liver physiology*, vol. 294, no. 1, pp. G139–G147, 2008.

[20] N. L. Denning, M. Aziz, S. D. Gurien, and P. Wang, "DAMPs and NETs in Sepsis," *Frontiers in Immunology*, vol. 10, p. 2536, 2019.

[21] Y. Maruchi, M. Tsuda, H. Mori et al., "Plasma myeloperoxidase-conjugated DNA level predicts outcomes and organ dysfunction in patients with septic shock," *Critical care*, vol. 22, no. 1, p. 176, 2018.

[22] S. T. Abrams, B. Morton, Y. Alhamdi et al., "A novel assay for neutrophil extracellular trap formation independently predicts disseminated intravascular coagulation and mortality in critically ill patients," *American Journal of Respiratory and Critical Care Medicine*, vol. 200, no. 7, pp. 869–880, 2019.

[23] M. Saffarzadeh, C. Juenemann, M. A. Queisser et al., "Neutrophil extracellular traps directly induce epithelial and endothelial cell death: a predominant role of histones," *PLoS One*, vol. 7, no. 2, article e32366, 2012.

[24] J. Lang, X. Wang, K. Liu et al., "Oral delivery of staphylococcal nuclease by Lactococcus lactis prevents type 1 diabetes mellitus in NOD mice," *Applied Microbiology and Biotechnology*, vol. 101, no. 20, pp. 7653–7662, 2017.

[25] N. Ma and X. Ma, "Dietary amino acids and the gut-microbiome-immune axis: physiological metabolism and therapeutic prospects," *Comprehensive Reviews in Food Science and Food Safety*, vol. 18, no. 1, pp. 221–242, 2019.

[26] Y. J. Jang, W. K. Kim, D. H. Han, K. Lee, and G. Ko, "Lactobacillus fermentum species ameliorate dextran sulfate sodium-induced colitis by regulating the immune response and altering gut microbiota," *Gut Microbes*, vol. 10, no. 6, pp. 696–711, 2019.

[27] M. W. Ralls, E. Miyasaka, and D. H. Teitelbaum, "Intestinal microbial diversity and perioperative complications," *JPEN Journal of Parenteral and Enteral Nutrition*, vol. 38, no. 3, pp. 392–399, 2014.

[28] H. Li, P. Pan, X. Su et al., "Neutrophil extracellular traps are pathogenic in ventilator-induced lung injury and partially dependent on TLR4," *BioMed Research International*, vol. 2017, Article ID 8272504, 13 pages, 2017.

Hindawi
Oxidative Medicine and Cellular Longevity
Volume 2020, Article ID 3912173, 15 pages
https://doi.org/10.1155/2020/3912173

Research Article

Oxymatrine Ameliorates Memory Impairment in Diabetic Rats by Regulating Oxidative Stress and Apoptosis: Involvement of NOX2/NOX4

Yongpan Huang,[1,2] **Xinliang Li**,[2] **Xi Zhang**,[3] **and Jiayu Tang**[3]

[1]*Department of Clinic, Medicine School, Changsha Social Work College, Changsha, Hunan, China*
[2]*Institute of Chinese Medicine, Hunan Academy of Chinese Medicine, Changsha, China*
[3]*Department of Neurology, Brain Hospital of Hunan Province, Changsha, China*

Correspondence should be addressed to Jiayu Tang; tangjiayu1978@163.com

Received 22 February 2020; Revised 11 August 2020; Accepted 28 October 2020; Published 16 November 2020

Academic Editor: Manjit Singh Rana

Copyright © 2020 Yongpan Huang et al. This is an open access article distributed under the Creative Commons Attribution License, which permits unrestricted use, distribution, and reproduction in any medium, provided the original work is properly cited.

Oxymatrine (OMT) is the major quinolizidine alkaloid extracted from the root of *Sophora flavescens Ait* and has been shown to exhibit a diverse range of pharmacological properties. The aim of the present study was to investigate the role of OMT in diabetic brain injury *in vivo* and *in vitro*. Diabetic rats were induced by intraperitoneal injection of a single dose of 65 mg/kg streptozotocin (STZ) and fed a high-fat and high-cholesterol diet. Memory function was assessed using a Morris water maze test. A SH-SY5Y cell injury model was induced by incubation with glucose (30 mM/l) to simulate damage *in vitro*. The serum fasting blood glucose, insulin, serum S100B, malondialdehyde (MDA), and superoxide dismutase (SOD) levels were analyzed using commercial kits. Morphological changes were observed using Nissl staining and electron microscopy. Cell apoptosis was assessed using Hoechst staining and TUNEL staining. NADPH oxidase (NOX) and caspase-3 activities were determined. The effects of NOX2 and NOX4 knockdown were assessed using small interfering RNA. The expression levels of NOX1, NOX2, and NOX4 were detected using reverse transcription-quantitative PCR and western blotting, and the levels of caspase-3 were detected using western blotting. The diabetic rats exhibited significantly increased plasma glucose, insulin, reactive oxygen species (ROS), S-100B, and MDA levels and decreased SOD levels. Memory function was determined by assessing the percentage of time spent in the target quadrant, the number of times the platform was crossed, escape latency, and mean path length and was found to be significantly reduced in the diabetic rats. Hyperglycemia resulted in notable brain injury, including histological changes and apoptosis in the cortex and hippocampus. The expression levels of NOX2 and NOX4 were significantly upregulated at the protein and mRNA levels, and NOX1 expression was not altered in the diabetic rats. NOX and caspase-3 activities were increased, and caspase-3 expression was upregulated in the brain tissue of diabetic rats. OMT treatment dose-dependently reversed behavioral, biochemical, and molecular changes in the diabetic rats. *In vitro*, high glucose resulted in increases in reactive oxygen species (ROS), MDA levels, apoptosis, and the expressions of NOX2, NOX4, and caspase-3. siRNA-mediated knockdown of NOX2 and NOX4 decreased NOX2 and NOX4 expression levels, respectively, and reduced ROS levels and apoptosis. The results of the present study suggest that OMT alleviates diabetes-associated cognitive decline, oxidative stress, and apoptosis via NOX2 and NOX4 inhibition.

1. Introduction

Diabetes mellitus (DM) is a common metabolic disorder associated with chronic complications, including nephropathy, angiopathy, retinopathy, and peripheral neuropathy [1]. It is widely accepted that diabetes can lead to cognitive impairment to some extent [2]. An increasing amount of evidence, including experimental and clinical studies, has demonstrated the alterations in cognitive deterioration, in particular cognitive dysfunction as a result of diabetes [3]. Oxidative stress has emerged as a critical pathogenic factor involved in the initiation and development of diabetic

complications [4]. Diabetes is accompanied by overproduction of reactive oxygen species (ROS) in various organs and tissues, including the brain, retina, kidney, and heart [5]. ROS production in diabetes is predominantly mediated by various NADPH oxidases (NOXs). NOXs are a major source of ROS in nonphagocytic cells and are critical mediators in brains afflicted by the diabetic milieu. The NOX family of proteins contains seven members, including NOX1-5, DUOX1, and DUOX2 [6]. Among these, NOX2 and NOX4 have been shown to be the primary sources of ROS in multiple types of brain disease, including ischemic stroke and traumatic brain injury [7–9]. Increasing evidence has now demonstrated that NOXs serve a variety of essential roles requiring deliberate ROS generation in the brain [10]. The deleterious role of NOX-derived ROS in the pathogenesis of diabetes may result in the initiation of neuronal damage [11, 12]. However, the mechanisms underlying NOX-mediated neuronal dysfunction in diabetic brain injury remain largely unknown and still require further study.

Oxymatrine (OMT) is a major component extracted from *Sophora flavescens Ait*. OMT possesses multiple pharmacological properties, including anti-inflammatory [13], antiviral [14], antioxidative, antifibrotic [15, 16], and antiapoptotic activity [14, 17]. To date, the majority of studies have focused on the anti-inflammatory and antifibrotic properties of OMT, which have been shown to be mediated by modulation of the NF-κB, JAK/STAT, and TLR4 signaling pathways. Recently, numerous studies showed the neuroprotective effects of OMT against diabetes. Our previous study demonstrated that endothelial dysfunction following diabetes was due to upregulated expression of NOX4 in the thoracic aorta, which resulted in increased oxidative stress in diabetes [18]. Thus, it was hypothesized that OMT inhibited diabetic brain injury through regulation of NOX2/NOX4. To test this hypothesis, a rat model of diabetes and an *in vitro* high-glucose model were used. The aim of the present study was to assess the neuroprotective effects of OMT on diabetic brain injury via inhibition of NOX2/NOX4 activation *in vitro* and *in vivo*.

2. Materials and Methods

2.1. Animal Experiments. Male Sprague-Dawley rats weighing 250-300 g were purchased from Hunan SJA Laboratory Animal Co., Ltd. (Xiang 2018-00A1). Animals were housed in the following conditions: 12 h light/dark cycle, at 22-25°C and 50-65% humidity. All animals were given *ad libitum* access to food and water. The study was performed in accordance with the guidelines described in the *Guide for the Care and Use of Laboratory Animals* (NIH Publication No. 85-23, revised 1996), and the experiments were approved by the Hunan Academy of Chinese Medicine Animal Care and Use Committee.

2.2. Induction and Assessment of Diabetes. To simulate type 2 diabetes, first, all the rats were fed a high-fat and high-cholesterol diet. After 4 weeks, diabetes was induced in the rats by intraperitoneal injection of a single dose of 65 mg/kg streptozotocin (STZ) that was freshly dissolved in citrate buffer (pH 4.4, 0.1 mol/l). Control rats were treated with citrate buffer only. A total of 48 h after STZ injection, blood samples were collected and plasma glucose levels were measured using an enzymatic glucose oxidase peroxidase diagnostic kit. Rats with fasting plasma glucose levels > 250 mg/dl were defined as diabetic and used for further experiments. Animals in each experiment were randomly assigned to one of six groups ($n = 10$ per group): (i) control group, normal rats that received a saline injection intraperitoneally (physiological saline 0.1 ml/100 g); (ii) model diabetes mellitus (DM) group, diabetic rats that received a saline injection intraperitoneally (saline 0.1 ml/100 g); DM+OMT groups (iii) 30, (iv) 60, and (v) 120 mg/kg, and (vi) a vehicle group (DM) ($n = 10$). The OMT dosage and dosing frequency were selected based on previous studies [15, 17]. The rats were intragastrically administered saline or OMT for 7 weeks and then intraperitoneally injected with normal saline.

After 10 weeks, learning and memory functions were evaluated for 5 consecutive days in a Morris water maze.

2.3. Morris Water Maze Test. The Morris water maze test was performed as described previously [19, 20]. The Morris water maze pool was 160 cm in diameter, 50 cm high, and 29 cm deep. The platform had a diameter of 12 cm and a height of 27 cm and was fixed at 2 cm below the water surface of the southeast quadrant (target quadrant). The camera lens was placed at the center of the pool, 2 cm from the bottom of the pool to record the movements of the rat. The water temperature was maintained at 22 ± 1°C. The experiments lasted for 5 days, including the hidden platform tests and space exploration experiments. On the first 4 days, the hidden platform tests were performed, and on the last day, space exploration experiments were performed.

The pool was placed in the center of a large room containing various visual cues and divided into four equal quadrants, north (N), south (S), east (E), and west (W). The cues remained constant throughout the study. A translucent acrylic platform was submerged ~1 cm below the water surface (for the navigation test) or removed from the tank (for the spatial probe test). The water maze task was used for 5 consecutive days.

2.4. Learning Test. The experiments lasted for 4 days. During the test, the platform position was fixed in the target quadrant (SE quadrant), and the water was inserted into the water from the four quadrants. During the training, the animals were gently placed in the water and the amount of time it took for the animals to find the platform was recorded. Once the animals had found the platform, they were left on for 10 sec. If the platform was not found within 90 sec, the time was recorded as 90 sec and the animal was placed on the platform for 10 sec. At the end of the training, the rats were returned to the cage and kept warm. Rats were trained at each of the four water intake points once a day, and for the final experimental trials, an average of four repeats was used. The order of water entry per animal per day was consistent, but the order of different animals in the same cage was different to exclude the possibility of exchange of animal information within the group.

2.5. Measurement of Blood Glucose and Serum Insulin Levels. After fasting the rats for 12 h overnight, they were anesthetized and sacrificed. Blood samples were collected from the abdominal aorta, allowed to clot for 30 min at 4°C, and centrifuged (3,500 × g, 10 min, 4°C), and the supernatant was used for measurement of glucose and insulin. Blood glucose was estimated using a commercially available glucose kit based on the glucose oxidase method. Insulin was measured by a radioimmunoassay method [18].

2.6. Determination of S-100B Levels in Plasma. Commercially available ELISA kits (BioSource) were used to determine the levels of S-100B proteins in plasma/brain homogenates. Analyses of all samples, standards, and controls were run in duplicate, according to the manufacturer's protocol.

2.7. Nissl Staining. Nissl staining was performed using a 0.1% cresyl violet solution (Sigma-Aldrich; Merck KGaA) using a standard protocol to evaluate the injury of diabetic rats [18]. In total, 6 coronal sections between the anterior edge and posterior edge of the brain were collected and processed for Nissl staining. The peri-impact area was defined as the region in the cortex. Every sixth coronal tissue section was chosen at random to quantify cell survival. Brain sections were examined using a light microscope (×200). Neuronal survival in the brain was quantified using ImageJ (National Institutes of Health).

2.8. Cell Culture. SH-SY5Y cells were obtained from American Type Culture Collection. The SH-SY5Y cells were authenticated by Short Tandem Repeat identification. SH-SY5Y cells were cultured in DMEM supplemented with 10% FBS, 100 m/ml penicillin, and 100 m/ml streptomycin and maintained in a humidified atmosphere of 5% CO_2 at 37°C. The medium was changed every 2 days. Cells were incubated with OMT (8 μm/l) for 1 h, after which, cells were treated with glucose (30 mmol/l) for 48 h. All assays consisting of appropriate controls were performed in triplicate and repeated on three separately initiated cultures.

2.9. Measurement of ROS. The total ROS level was measured using a reactive oxygen species assay kit. According to the manufacturer's protocol, intracellular ROS levels were determined by measuring the oxidative conversion of cell permeable 2V,7V-dichlorofluorescein diacetate (DCFH-DA) to fluorescent dichlorofluorescein (DCF) using a fluorospectrophotometer (F4000). Briefly, tissues or cells were incubated with control media or 10 Ag/ml LPC for 4 h in the absence or presence of DPI (100 or 300 AM) or allopurinol (100 AM) followed by washing with D-Hank's and incubating with DCFHDA at 37°C for 20 min. Then, DCF fluorescence distribution was detected using fluorospectrophotometer analysis at an excitation wavelength of 488 nm and at an emission wavelength of 535 nm.

2.10. Determination of Apoptosis Using Hoechst 33258 Staining. For detection of apoptosis, Hoechst 33258 staining was performed as previously described [21, 22]. After treatment with glucose, SH-SY5Y cells were fixed with fixing solution for 5 min. Subsequently, SH-SY5Y cells were washed with PBS three times and incubated in Hoechst 33258 solution (0.5 ml) for 5 min, then washed with PBS three times. Apoptosis of SH-SY5Y cells was examined under a fluorescence microscope.

2.11. Small Interference (si)RNA Transfection. The SH-SY5Y cells were inoculated in 6-well plates and transfected with 20 nM control siRNA or validated NOX2 siRNA (cat. no. sc-35503) or NOX4 siRNA (cat. no. sc-36149) from Santa Cruz Biotechnology, Inc., using RPMI 1640 media. Briefly, 5 μl NOX2 and NOX4 siRNA (20 μM) were mixed with RPMI 1640 media. Separately, Lipofectamine 2000 (Invitrogen; Thermo Fisher Scientific, Inc.) was mixed with RPMI 1640 media, and the mixtures were then combined for 20 min at room temperature. The Lipofectamine-siRNA mixture was then added to each well containing cells and medium and incubated for 6 h. The medium was subsequently replaced with antibiotic-free ECM supplemented with 5% FBS for 24 h. The cells were harvested 48 h after transfection.

2.12. Determination of Apoptosis in Brain Tissue. Tissue apoptosis was determined using TUNEL staining. Briefly, brain tissues were excised and fixed in 4% paraformaldehyde in PBS at room temperature for 24 h. Fixed tissues were embedded in paraffin and stained using a TUNEL kit (Roche Diagnostics). The apoptotic index (percentage of TUNEL-positive nuclei/total number of nuclei) was determined.

2.13. Ultrastructural Studies. Electron transmission microscopic examination was performed as previously described [23]. Hippocampal tissues (diameter = 1 mm) were fixed in 4% glutaraldehyde for 24 h, rinsed with 0.1 M phosphate buffer, fixed with 2% acid, dehydrated with acetone, soaked with epoxy resin embedding agent, pure acetone, embedded into a block, and cut into a semithin section (2 μm). Ultrathin sections were stained with uranyl acetate and lead bismuth citrate and observed using a Zeiss Libra 120 transmission electron microscope (Carl Zeiss AG).

2.14. Caspase-3 Activity Assay. Caspase-3 activity was measured according to the manufacturer's protocol (Beyotime Institute of Biotechnology). Briefly, 10 μl brain tissue homogenates or SH-SY5Y cell lysates were mixed with 90 μl reaction solution containing caspase-3 substrate (Ac-DEVD-pNA) and incubated at 37°C for 60 min. The absorbance at 450 nm was recorded. Enzyme activity is presented as U/g protein and 1 U of enzyme and is defined as the amount of enzyme required to cleave 1.0 nmol AcDEVD-pNA per hour at 37°C.

2.15. Determination of NOX Activity. NOX activity was determined as previously described [24, 25]. The assay was based on detecting the reduction of ferrocytochrome c by the superoxide anion formed by NOX in the presence of NADPH. NOX activity was evaluated after exposure of brain tissue and SH-SY5Y cell homogenates to GD for 15, 30, and 60 min. The homogenates were incubated with SDS (100 μM) and ferrocytochrome c (100 μM; Sigma-Aldrich; Merck KGaA) for 5 min at 37°C. The reaction

was initiated by the addition of NADPH (250 μM), and the reduction of ferrocytochrome c was measured spectrophotometrically at 550 nm for 5 min. In order to test the specificity of the reaction for NOX and to discard an effect of XaO or cPLA2 inhibitors on NOX activity, cells exposed to GD for 30 min were homogenized and enzyme activity was measured in the presence of apocynin, AEBSF, allopurinol, or AACOCF3, which were added to the reaction buffer. Results are expressed as nmol/h/mg protein.

2.16. Reverse Transcription-Quantitative (RT-q)PCR. Gene expression levels (mRNA) in cartilage were determined using RT-qPCR. Total RNA was extracted (Takara, China) and purified with 75% ethanol, and its concentration was determined by spectrophotometry. The purified total RNA (200 ng per sample) was added to a transcription kit (cat. no. DRR037A; Takara Bio, Inc.) and mixed to generate the first strand template (reverse transcription reaction). The sequences of the primers used for qPCR were the following: NOX1 forward, 5′-ATA TTT TGG AAT TGC AGA TGA ACA-3′ and reverse, 5′-ATA TTG AGG AAG AGA CGG TAG-3′; NOX2 forward, 5′-GGA GAA TTA ACC CCT GCC A-3′ and reverse, 5′-GGC TAG CTG GAG AAG ACC AC-3′; NOX4 forward, 5′-TGT TGG ATG ACT GGA AAC CA-3′ and reverse, 5′-TGG GTC CAC AAC AGA AAA CA-3′; and GADPH forward, 5′-CAA CAG CCT CAA GAT CAT CAG CA-3′ and reverse, 5′-TGG CAT GGT CTG TCA TGA GT-3′. qPCR was performed using a real-time PCR system (ABI 7300). Expression levels were determined quantitatively using SYBR Premix ExTaq (Takara Bio, Inc.).

2.17. Western Blot Analysis. For western blotting analysis, 40 μg protein per sample was loaded on a 10% gel and resolved using SDS-PAGE. The proteins were transferred to a PVDF membrane; the membranes were blocked using 5% milk and subsequently incubated with rabbit anti-NOX2, NOX4, full-length caspase-3, cleaved caspase-3, and β-actin antibodies (Santa Cruz Biotechnology, Inc.) at 4°C overnight. Subsequently, the membrane was washed and incubated with secondary antibodies (horseradish peroxidase-conjugated) at 4°C, and the protein bands were visualized using an enhanced chemiluminescence kit (Amersham Biosciences). Finally, the expression levels of protein were calculated using a Molecular Imager Chemi-Doc XRS system (Bio-Rad Laboratories, Inc.). β-Actin was used as the loading control.

2.18. Statistical Analysis. SPSS version 21.0 was used for statistical analysis. Data are presented as the mean ± standard deviation or standard error of the mean. The differences between groups of data were analyzed using a one-way ANOVA. $P < 0.05$ was considered to indicate a statistically significant difference.

3. Results

3.1. OMT Improves Blood Glucose and Insulin Levels and Diabetes-Induced Cognitive Deficits in Diabetic Rats. To determine whether STZ injection-induced diabetes and to assess the protective effects of OMT against diabetic brain injury, blood glucose and insulin levels were assessed. A diabetic rat model was constructed, and the rats exhibited higher fasting blood glucose levels compared with the control. As shown in Figure 1(a), diabetic rats had a blood glucose level > 11.1 mmol/l, which was significantly higher compared with the control group. OMT significantly decreased the blood glucose levels of diabetic rats in a dose-dependent manner. Plasma insulin levels were not significantly altered by OMT treatment (Figure 1(b)). These results suggest that OMT treatment may be a potential therapeutic strategy for the treatment of DM.

To assess the effects of OMT on the cognitive function in diabetic rats, a Morris water maze test (on the 10th week) was used. After 12 weeks of diabetes induction, the diabetic rats exhibited notable cognitive impairment. The mean escape latency for the trained animals was reduced from 60 sec to 20 sec over the course of the 20 learning trials. There were no significant differences between the groups on the first day of testing in the Morris water maze. On the second day, the transfer latency was notably different longer in diabetic rats (52.21 ± 1.35 sec) and the control group (32.15 ± 1.27 sec) ($P < 0.05$). OMT (30, 60, and 120 mg/kg) dose-dependently decreased the mean escape latency ($P < 0.05$).

As shown in Figure 2(a), diabetic rats spent more time finding the platform and learning its location during the training session. OMT reversed the poorer performance in a concentration-dependent manner, as indicated by the decrease in latency from the 2nd training day ($P < 0.05$). The results of mean path length, shown in Figure 2(b), also demonstrated a significant increase in the diabetic rats for 4 consecutive days of training ($P < 0.05$).

To investigate how the animals learned and consolidated the platform location during the experiments, the probe trial was assessed. The results first exhibited a significant difference ($P < 0.05$) during the 4th training day. As shown in Figure 2(c), there was a decline in the time spent in the target quadrant in diabetic rats compared with the control rats ($P < 0.05$). Compared with the diabetic rats, as indicated in Figure 2(d), OMT increased the time spent in the target quadrant significantly ($P < 0.05$) and decreased the number of times the animals crossed the former platform location ($P < 0.05$). OMT improved this index significantly in diabetic rats ($P < 0.05$).

3.2. OMT Decreases Oxidative Stress Injury in the Brain Tissues of Diabetic Rats. Oxidative stress is an important cause of brain injury. To investigate whether OMT exhibited protective effects on oxidative stress-related brain injury in diabetic rats, the total ROS levels were determined. As shown in Figure 3(a), the ROS levels in the brain tissues were significantly increased in the diabetic rats compared with the control group, and OMT dose-dependently decreased the ROS levels of brain tissues.

Nissl staining showed that the neurons exhibited notable morphological alterations in diabetic rats compared with the control and OMT dose-dependently protected

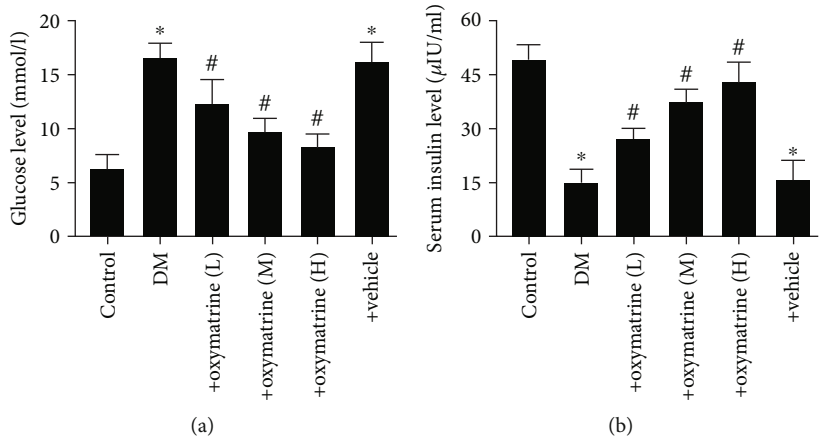

Figure 1: OMT improves blood glucose and insulin levels in diabetic rats. (a) Blood glucose and (b) serum insulin levels. Data are presented as the mean ± standard deviation. $^{*}P < 0.05$ vs. control; $^{\#}P < 0.05$ vs. DM. DM: diabetes mellitus; DM+oxymatrine (L): DM+ 30 mg/kg OMT; DM+oxymatrine (M): DM+OMT 60 mg/kg; DM+oxymatrine (H): DM+oxymatrine+120 mg/kg OMT. OMT: oxymatrine.

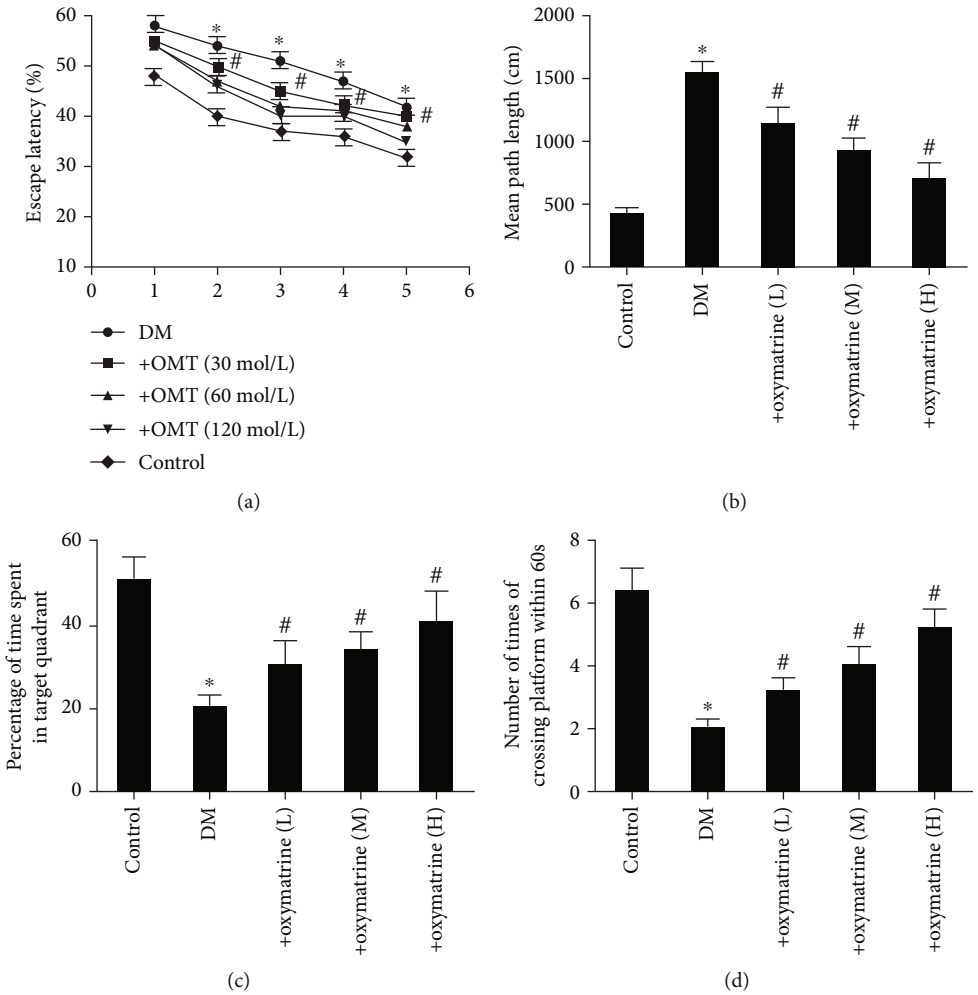

Figure 2: Effects of OMT on the cognitive function in diabetic rats. (a) Mean percentage of time spent in the target quadrant, (b) mean path length, and (c) spatial memory acquisition phase in control and diabetic rats. (d) Number of platform crosses. $n = 10$. Data are presented as the mean ± standard deviation. $^{*}P < 0.05$ vs. control; $^{\#}P < 0.05$ vs. DM. DM: diabetes mellitus; OMT: oxymatrine.

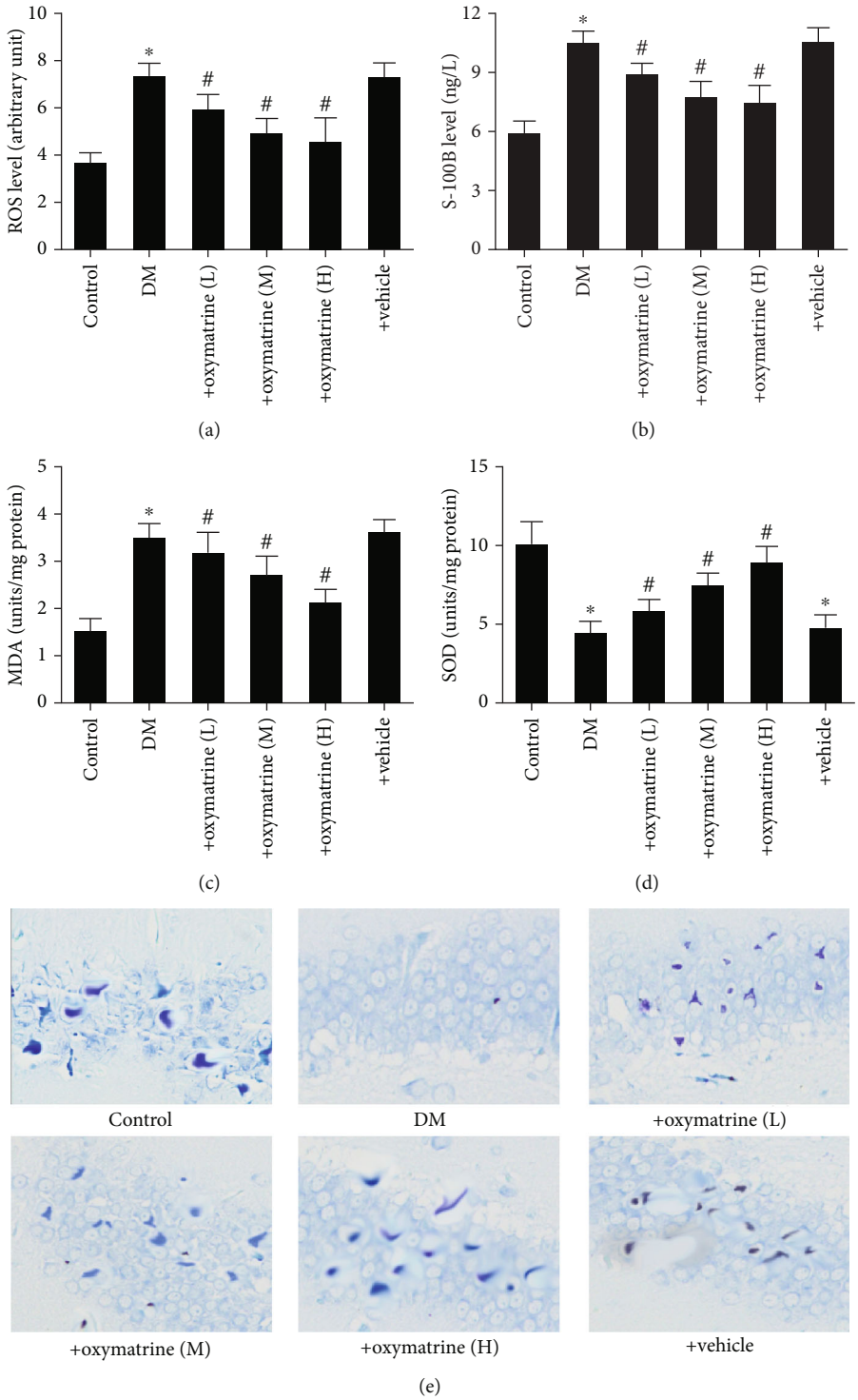

Figure 3: OMT decreases oxidative stress injury of brain hippocampal tissue in diabetic rats. (a) ROS, (b) S-100B, (c) SOD, and (d) MDA levels. (e) Nissl staining. Data are presented as the mean ± the standard error of the mean. $^{*}P < 0.05$ vs. control; $^{\#}P < 0.05$, $^{\#\sim}P < 0.001$ vs. DM. DM: diabetes mellitus; OMT: oxymatrine; ROS: reactive oxygen species; MDA: malondialdehyde; SOD: superoxide dismutase.

diabetic rats from morphological alterations of the Nissl body (Figure 3(b)). Consistently, the plasma S-100B levels were significantly increased in diabetic rats; OMT significantly decreased the plasma S-100B levels in a dose-dependent manner (Figure 3(c)). These results suggest that OMT ameliorated oxidative stress in diabetic rats.

Furthermore, the antioxidative index including SOD and MDA levels was assessed. The results showed that the activity

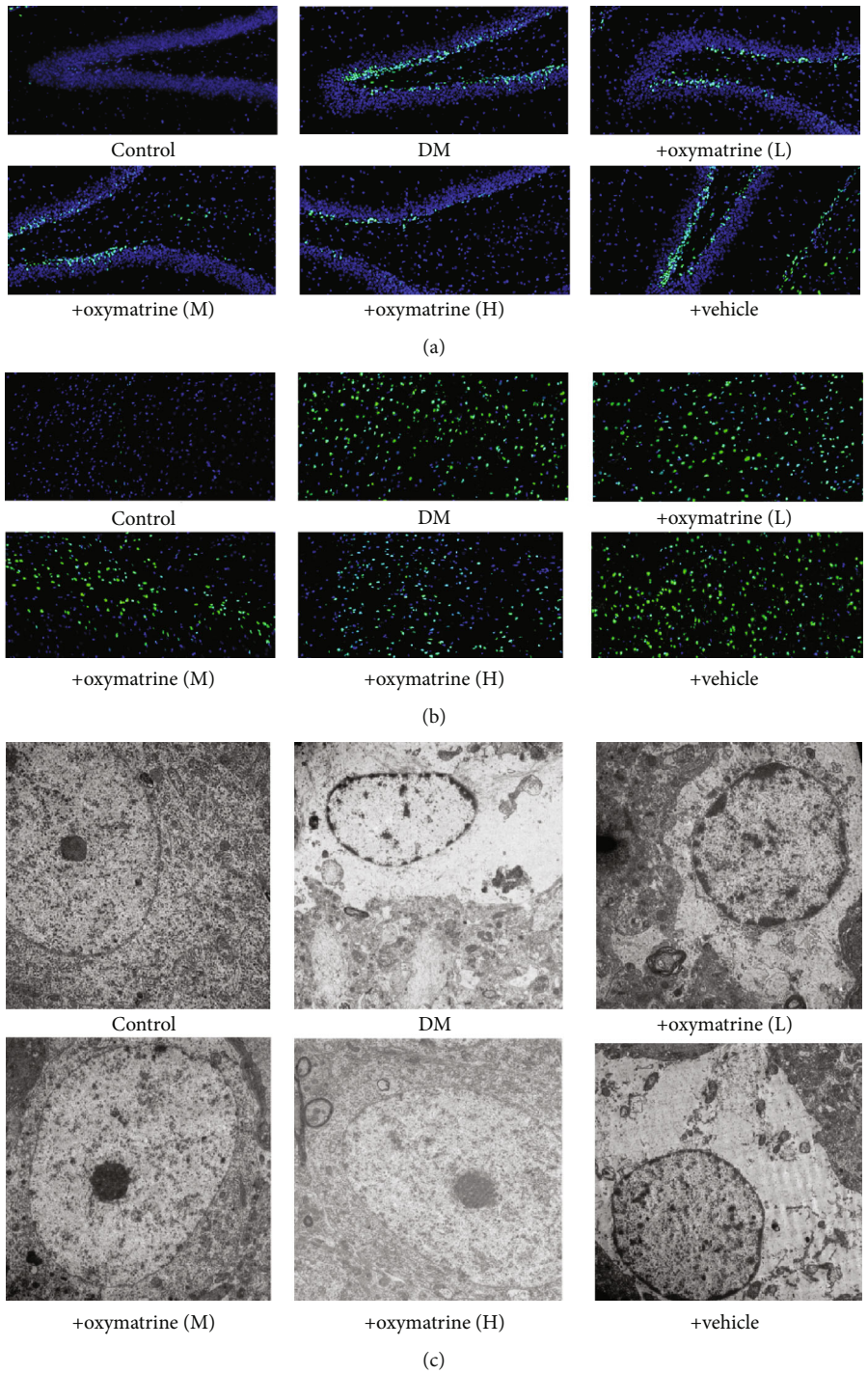

Figure 4: Effects of OMT on the apoptosis of brain tissue in diabetic rats. (a) TUNEL staining of hippocampal tissue. (b) TUNEL staining in the cortex. Magnification, ×200. (c) Electron micrograph of hippocampal tissue. OMT: oxymatrine.

of SOD decreased whereas MDA content increased. Additionally, OMT reversed these effects (Figures 3(d) and 3(e)).

3.3. OMT Ameliorates Oxidative Stress-Related Apoptosis in Diabetic Rats. As shown in Figures 4(a) and 4(b), there were no TUNEL-positive cells in the control group. Induction of diabetes significantly increased the number of TUNEL-positive cells, and this increase was significantly reduced by OMT. The vehicle did not show any effects on apoptosis. Electron microscopy was used to investigate the protective effects of OMT on ultrastructural changes. As shown in Figure 4(c), serious heterogeneous subcellular and extracellular space abnormalities were observed in the hippocampal tissues, which were attenuated by OMT.

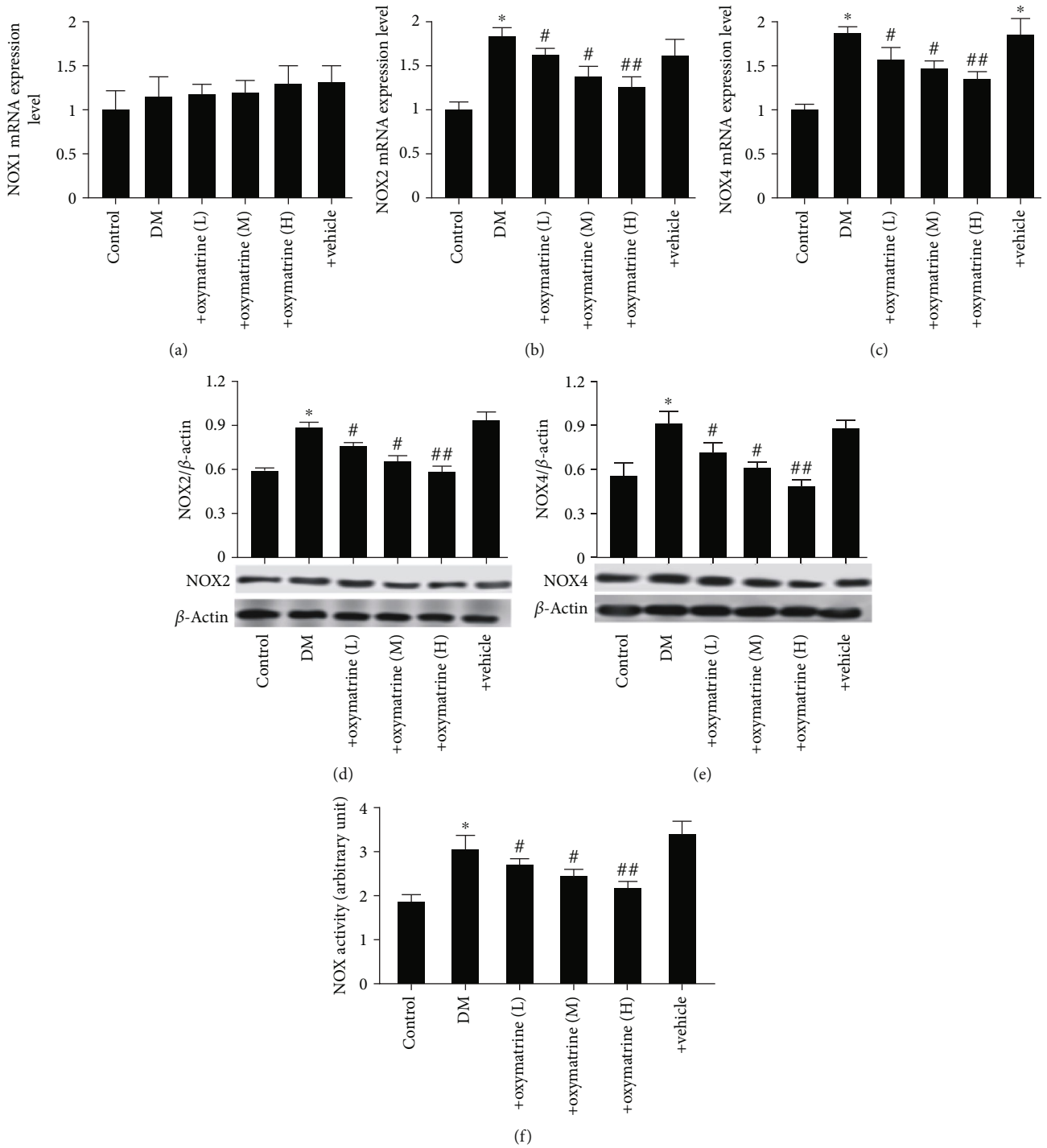

Figure 5: Effects of OMT on the expression of NOX in the brain tissues of diabetic rats. (a) NOX1, (b) NOX2, and (c) NOX4 mRNA expression levels. (d) NOX2 and (e) NOX4 protein expression levels. (f) NOX activity. Data are presented as the mean ± standard deviation. $^{*}P < 0.05$ vs. control; $^{\#\#}P < 0.01$ vs. DM. DM: diabetes mellitus; OMT: oxymatrine; NOX: NADPH oxidase.

3.4. OMT Decreases the Expression of NOX in Brain Tissues of Diabetic Rats. Whether OMT mediated protection against protected diabetes-related brain injury associated with NOX expression was next determined. As shown in Figure 5(a), there were no significant changes in NOX1 expression in the diabetic rat brains compared with the control group, whereas diabetes significantly elevated NOX2 and NOX4 expression levels in the brain tissues compared with the control group. OMT significantly decreased NOX2 and NOX4 expression levels in the brain tissues of type 2 diabetes rats in a dose-dependent manner (Figures 5(b)–5(e)). Consistently, total NOX enzyme activity was significantly increased in brain tissues, and OMT treatment dose-dependently decreased the total

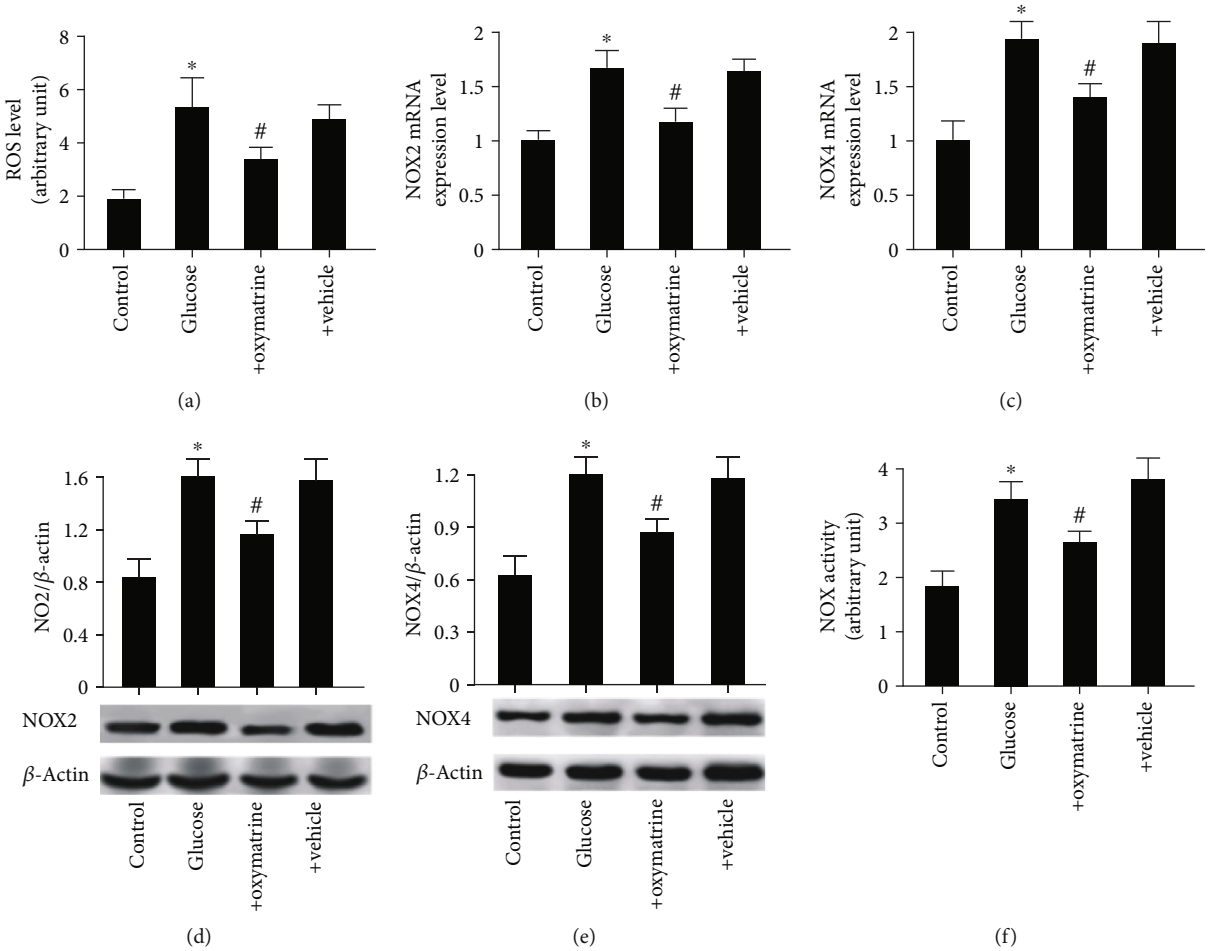

Figure 6: OMT decreases oxidative stress in SH-SY5Y cells treated with high glucose: (a) ROS levels; (b) NOX2 and (c) NOX4 mRNA expression levels; (d) NOX2 and (e) NOX4 protein expression levels; (f) NOX activity. Data are presented as the mean ± standard deviation. $^{*}P < 0.05$ vs. control; $^{\#}P < 0.05$, $^{\#\#}P < 0.01$ vs. glucose. Glucose: 30 mM/l glucose; glucose+oxymatrine: 30 mM/l glucose+8 μM OMT; glucose+vehicle: glucose+DMSO. OMT: oxymatrine; NOX: NADPH oxidase.

NOX enzyme activity of hippocampal tissues (Figure 5(f)). These results suggest that OMT attenuated diabetic brain injury through the downregulation of NOX2 and NOX4 expression, but not NOX1.

3.5. OMT Decreases Oxidative Stress and Apoptosis of SH-SY5Y Cells Treated with High Glucose. To further verify the results regarding OMT using an *in vitro* model of diabetes, a nerve cell (SH-SY5Y) model of high glucose was utilized to mimic the *in vivo* conditions. As shown in Figure 6(a), ROS levels were significantly increased in the SH-SY5Y cells treated with high glucose compared with the control group, and the increase in ROS levels was abolished by OMT. Consistent with the animal results, the expression levels of NOX2 and NOX4 and the total NOX enzyme activity were significantly increased in SH-SY5Y cells treated with high glucose. OMT significantly decreased NOX2 and NOX4 expression levels and the total NOX enzyme activity in SH-SY5Y cells treated with high glucose (Figures 6(b)–6(f)). Additionally, apoptosis was significantly increased in SH-SY5Y cells treated with high glucose compared with the control group, whereas OMT treatment significantly reduced this (Figures 7(a) and 7(b)). Similarly, the expression levels of cleaved caspase-3 and caspase-3 enzyme activity were significantly increased in SH-SY5Y cells treated with high glucose. The results showed increases in the proportion of apoptotic and necrotic cells in cells treated with high glucose compared with the control group. These alterations were reversed by OMT treatment in a dose-dependent manner (Figures 7(c)–7(f)).

3.6. Knockdown of NOX2 and NOX4 Decreases the Oxidative Stress and Apoptosis of SH-SY5Y Cells Treated with High Glucose. To further assess the contributions of NOX2 and NOX4 in the high-glucose conditions, NOX2 and NOX4 expression was knocked down using NOX2- and NOX4-specific siRNAs. The knockdown efficiency shown in Figures 8(a)–8(d) showed that NOX2 and NOX4 knockdown was successful. In addition, knockdown of NOX2 and NOX4 significantly reduced the overproduction of ROS when cells were subjected to high-glucose conditions (Figures 8(e) and 8(f)). Furthermore, flow cytometry analysis showed that NOX2 and NOX4 knockdown reduced high-glucose-induced apoptosis (Figures 9(a) and 9(b)).

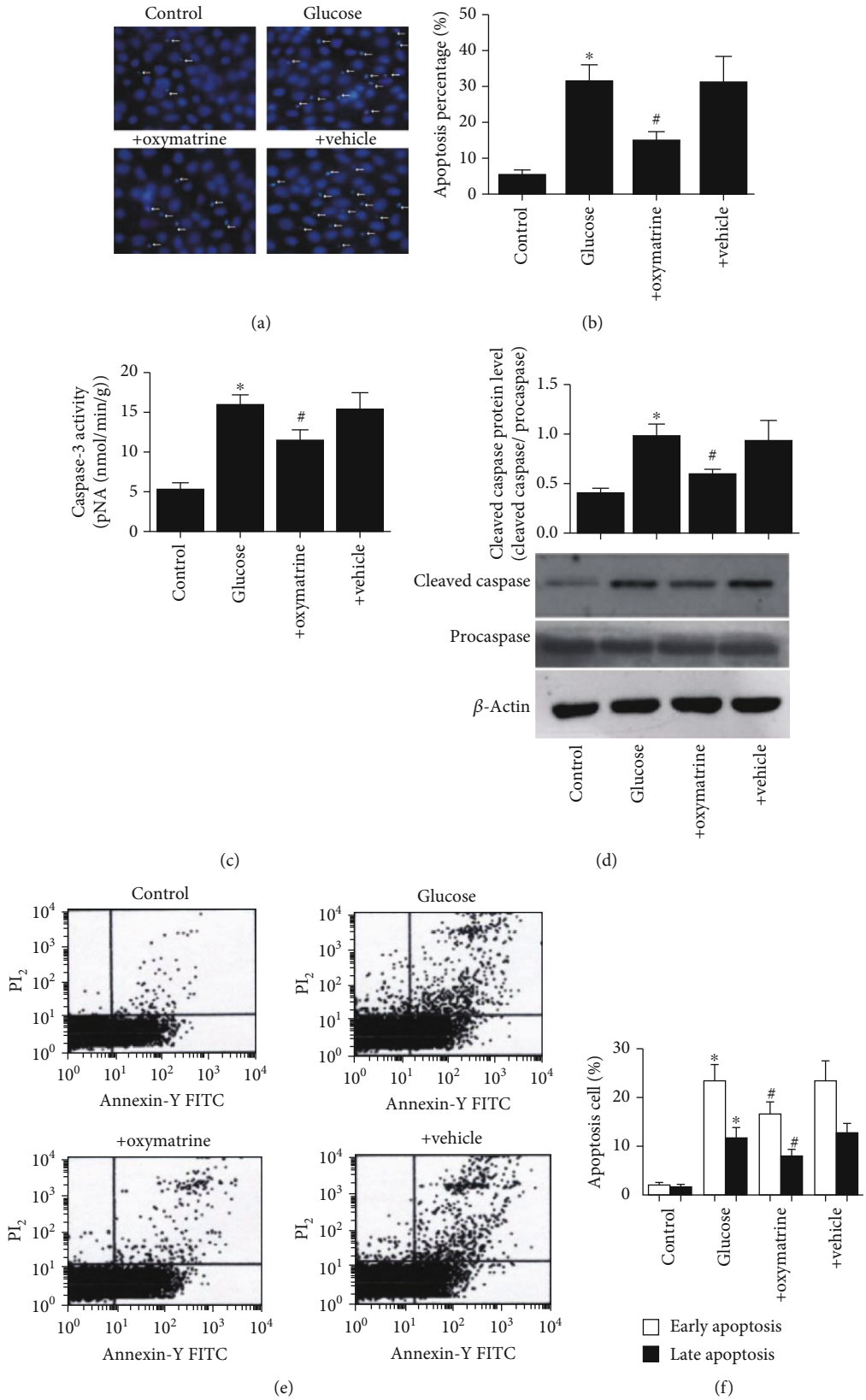

Figure 7: OMT inhibits oxidative stress and apoptosis in SH-SY5Y cells treated with high glucose. (a) Representative images of Hoechst staining. (b) Percentage of apoptotic cells. (c) Caspase-3 activity. (d) Caspase-3 protein expression levels. (e) Flow cytometry analysis of the annexin V-FITC/PI staining. (f) Quantification of annexin V-FITC/PI staining, showing the percentage of early (annexin V-FITC positive and PI negative) and late (annexin V-FITC positive and PI positive) apoptotic cells. Data are presented as the mean ± standard deviation. $^{*}P < 0.05$ vs. control; $^{\#}P < 0.05$ vs. glucose. OMT: oxymatrine.

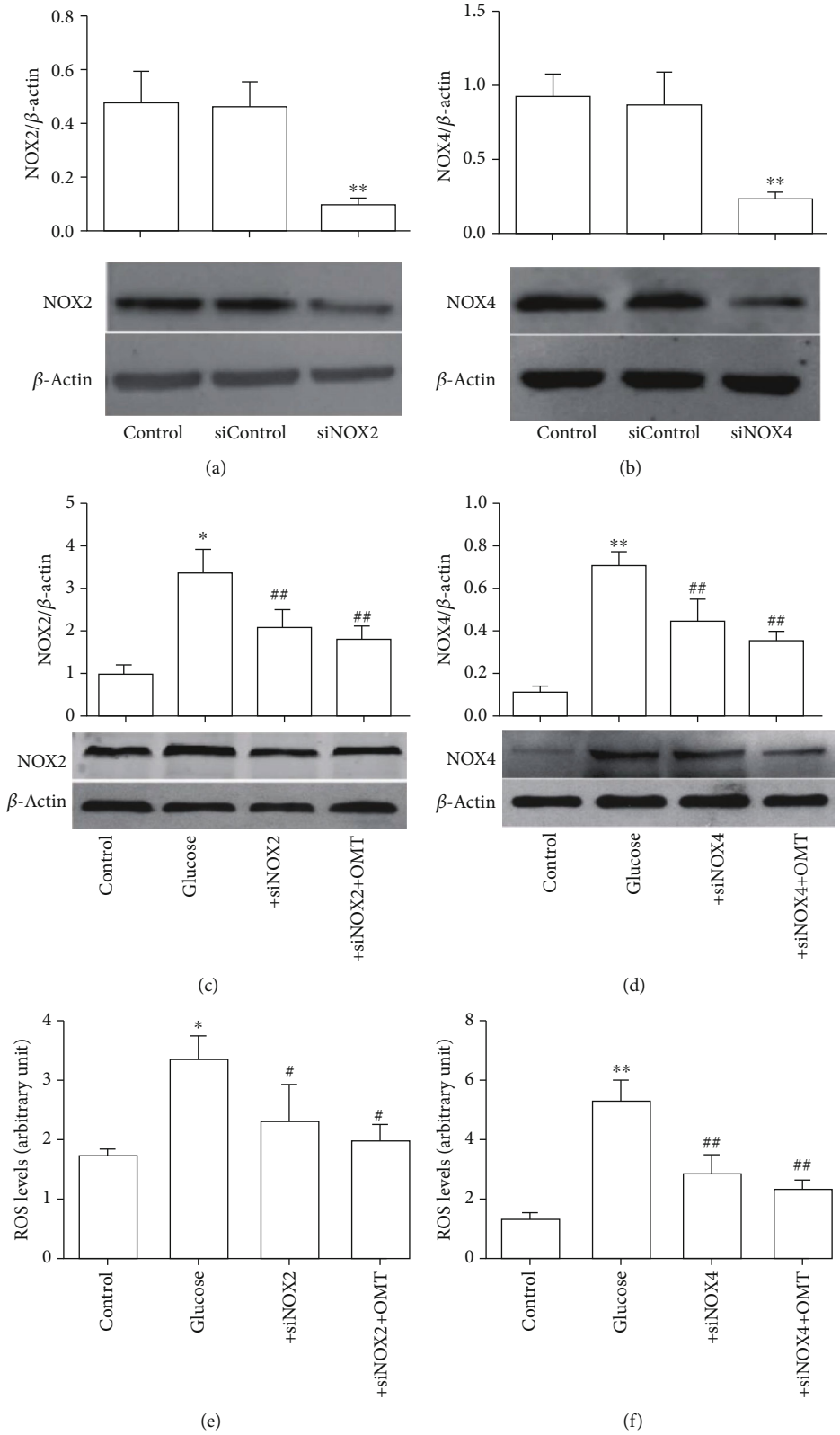

Figure 8: Knockdown of NOX2 and NOX4 reduced oxidative stress and apoptosis in SH-SY5Y cells treated with high glucose. (a, b) NOX2 and NOX4 siRNA transfection effectively reduced NOX2 and NOX4 expression levels. (c, d) NOX2 and NOX4 siRNA transfection effectively downregulated NOX2 and NOX4 expression levels in SH-SY5Y cells treated with high glucose and OMT. (e, f) NOX2 and NOX4 siRNA transfection effectively decreased ROS levels in SH-SY5Y cells treated with high glucose and OMT. Data are presented as the mean ± standard deviation. $^{*}P < 0.05$, $^{**}P < 0.01$ vs. control; $^{\#}P < 0.05$, $^{\#\#}P < 0.01$ vs. glucose. OMT: oxymatrine; NOX: NADPH oxidase; ROS: reactive oxygen species; siRNA: small interfering RNA.

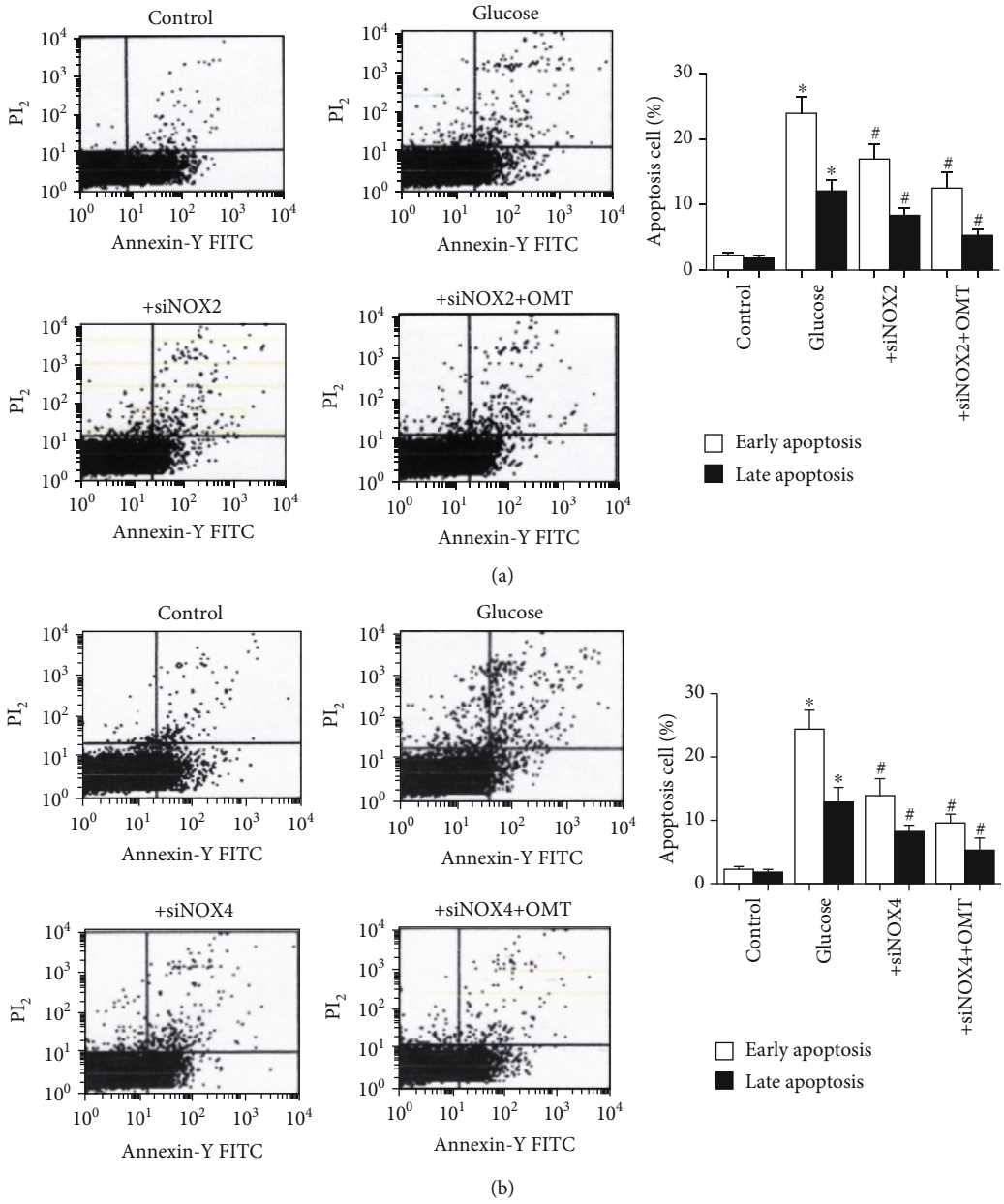

Figure 9: Knockdown of NOX2 and NOX4 reduced apoptosis in SH-SY5Y cells treated with high glucose. Flow cytometry analysis and quantitative analysis of annexin V-FITC/PI staining showing the percentages of early (annexin V-FITC positive and PI negative) and late (annexin V-FITC positive and PI positive) apoptotic cells. (a) NOX2 siRNA transfection effectively reduced apoptosis. (b) NOX2 siRNA transfection effectively reduced apoptosis. Data are presented as the mean ± standard deviation. $^{*}P < 0.05$ vs. control; $^{\#}P < 0.05$ vs. glucose. NOX: NADPH oxidase.

Taken together, these findings suggest that OMT ameliorates oxidative stress and apoptosis through the inhibition of NOX2 and NOX4 activity.

4. Discussion

The major novel finding of the present study was that diabetic brain injury response culminates in the production of ROS through NOX enzymes and the linking of OMT to the inhibition of NOX activity and reduction in caspase-3 levels. In the present study, using a rat model of diabetes, generated by feeding rats with high-fat and high-cholesterol diets and intraperitoneal injection of STZ, or a nerve cell model of high glucose, the results showed that OMT significantly reduced blood glucose and insulin levels, improved cognitive dysfunction and histological changes, inhibited oxidative stress, and suppressed neuronal apoptosis in diabetic rats and SH-SY5Y cells. Moreover, OMT downregulated the expression of NOX2, NOX4, and caspase-3 and decreased NOX and caspase-3 activity. These results suggest that OMT ameliorates diabetes-induced injuries related to inhibition of NOX2, NOX4, and apoptosis *in vivo* and *in vitro*.

There is growing evidence showing the long-term effects of diabetes on the brain and that it manifests at a structural, neurophysiological, and neuropsychological level, and multiple pathogenic factors appear to be involved in the pathogenesis of cerebral dysfunction in diabetes, such as episodes of hypoglycemia, cerebrovascular alterations, the role of insulin in the brain, and the involvement of hyperglycemia-induced impairments [26–28]. One of the causes of cerebral dysfunction in the diabetic brain relates to oxidative stress mediated by free radicals. Oxidative stress, one of the primary contributors to cerebral pathogenesis, accelerates brain aging and tissue damage in diabetes mellitus [29, 30]. A recent study showed that oxidative stress and changes in the antioxidative defense systems impaired learning and memory in rats. Wang and Jia [19] showed that decreased antioxidant status was an important mechanism underlying cognitive impairment in diabetic rats. Oxidative stress has been shown to cause diabetes-induced aortic endothelial dysfunction via NOX4 activation [31]. In addition, NOX4 activation, which serves as the predominant source of $O_2\cdot$ production, is observed in diabetes-induced vascular dysfunction. Therefore, NOX activation may be considered an important mechanism underlying increased oxidative stress in diabetes [32]. Studies have shown that NOX2 and NOX4 expression and activity were significantly upregulated under several conditions, including brain ischemia/reperfusion injury [33], hypertension [34], hypoxia-related diseases [35], and DOX-induced cardiomyopathy [36]. Based on these studies, it is reasonable to speculate that NOX-derived ROS accumulation may be responsible for the impairment of SH-SY5Y cell function when treated with high glucose. The present study showed that NOX2 and NOX4 expression and activity were significantly increased in SH-SY5Y cells treated with high glucose, accompanied by an increased NOX-derived ROS production as well as deteriorated function of cells. Knockdown of NOX2 and NOX4 partially inhibited the increase in oxidative stress and NOX2 and NOX4 expression and activity in SH-SY5Y cells treated with high glucose. Furthermore, numerous studies have demonstrated that NOX2 and NOX4 activation underlies the perturbation in cellular homeostasis in diabetes [37, 38]. It is well known that excessive production of ROS under diabetic circumstances contributes to reduced antioxidant capacity, leading to diabetic injuries, including neuropathy, nephropathy, vascular dysfunction, and retinopathy, and initiating mitochondrial oxidative damage, which accelerates cell apoptosis and/or necrosis. Studies in experimental models and in patients have demonstrated that oxidative stress is the primary contributor to diabetes-related complications [39, 40]. Several studies have confirmed that STZ-induced diabetic rats exhibit high levels of MDA, combined with increased glutathione disulfide reductase activity, a lower GSH/GSSG ratio, and lower ATP levels [41, 42]. These studies highlight the involvement of oxidative stress in diabetes-associated cerebral disturbances. In the present study, the results showed that oxidative stress not only accelerated the pathogenesis of cerebral dysfunction but also significantly increased the ROS levels and S-100B levels in diabetes. Furthermore, the levels of SOD and MDA were shown to be upregulated in the brain tissues of diabetic rats. These results support our hypothesis. In the *in vivo* and *in vitro* experiments, OMT suppressed the ROS levels and NOX2 and NOX4 expression. These results suggest that attenuation of diabetes-associated cerebral injury by OMT is associated with its antioxidant properties.

A common theory attempting to explain the pathogenesis of cerebral dysfunction in diabetes relates to neuronal cell death caused by oxidative stress, which is mediated by oxygen free radicals. The brain is particularly vulnerable to oxidative damage as a result of high oxygen consumption rates, abundant lipid content, and a lack of antioxidant enzymes. Neuronal cells are sensitive to oxidative insults. Numerous studies have demonstrated that accumulation of ROS in diabetes is a critical factor underlying brain damage [42, 43]. Oxidative stress is an important contributor to diabetic complications and exacerbates cellular damages. Excessive production of ROS contributes to the initiation of programmed cell death in diabetes, which increased neuronal apoptosis in diabetes [44, 45]. In view of the important role of oxidative stress, strategies for intervention of ROS-induced cell apoptosis may be of particular relevance. As the primary active ingredient of *Sophora flavescens*, OMT has a wide range of pharmacological properties, including treatment of cardiovascular and cerebrovascular diseases. Our previous study confirmed that OMT inhibited autophagy-activated cell apoptosis/death via a MIF/mTOR signaling pathway [46]. In the present study, OMT was shown to ameliorate diabetes-related complications; specifically, the significant increases in neuronal apoptosis and caspase activity in the cerebral cortex and hippocampus were attenuated by treatment with OMT.

A Morris water maze test is a widely accepted behavioral test used for evaluating brain function related to spatial learning and memory. The present study evaluated cognitive function of the *in viv*o diabetes rat model. The results showed that the diabetic rats exhibited learning and memory deficits, consistent with previous studies [19, 27]. These learning and memory deficits were prevented by OMT treatment, suggesting that the ameliorative effects of OMT on the learning and memory deficits are associated with decreased apoptosis in diabetic rats.

In conclusion, the present study demonstrated that OMT exhibits beneficial effects by lowering blood glucose levels, reducing learning and memory deficits, suppressing oxidative stress, and decreasing caspase-3 expression, possibly through inhibition of NOX2 and NOX4 activation *in vivo* and *in vitro*. These novel findings may provide a pharmacological foundation for the use of OMT as treatment in diabetic patients.

Data Availability

The datasets used and/or analyzed during the current study are available from the corresponding author on reasonable request.

Ethical Approval

The experiments were approved by the Animal Care and Use Committee, Hunan Academy of Chinese Medicine, and were performed in accordance with the *Guide for the Care and Use of Laboratory Animals*, published by the National Institutes of Health (NIH Publication No. 85-23, revised 1996).

Conflicts of Interest

All authors in this article declare no conflict of interest.

Authors' Contributions

YPH designed and undertook experiments and analyzed, interpreted, and presented results for group discussions. XZ and XLL provided methods, description of results, and figures for the manuscript. JYT and XLL provided rationale, background, framework, and feedback. All authors have gone through and approved the manuscript. All authors have agreed both to be personally accountable for the author's own contributions and to ensure that questions related to the accuracy or integrity of any part of the work.

Acknowledgments

This project was funded by the Scientific Research Projects of Education Department of Hunan Province (No. 19B042 to Yongpan Huang), Key R&D program of Hunan Province (2018SK1030 to Jiayu Tang), and Scientific Research Project of Health Commission of Hunan Province (20200853 to Jiayu Tang).

Supplementary Materials

The figure in the supplementary file represents the consequence of OMT on memory impairment. *(Supplementary Materials)*

References

[1] M. Blair, "Diabetes mellitus review," *Urologic Nursing*, vol. 36, no. 1, pp. 27–36, 2016.

[2] L. A. Zilliox, K. Chadrasekaran, J. Y. Kwan, and J. W. Russell, "Diabetes and cognitive impairment," *Current Diabetes Reports*, vol. 16, no. 9, p. 87, 2016.

[3] G. J. Biessels and F. Despa, "Cognitive decline and dementia in diabetes mellitus: mechanisms and clinical implications," *Nature Reviews. Endocrinology*, vol. 14, no. 10, pp. 591–604, 2018.

[4] B. S. Karam, A. Chavez-Moreno, W. Koh, J. G. Akar, and F. G. Akar, "Oxidative stress and inflammation as central mediators of atrial fibrillation in obesity and diabetes," *Cardiovascular Diabetology*, vol. 16, no. 1, p. 120, 2017.

[5] U. Asmat, K. Abad, and K. Ismail, "Diabetes mellitus and oxidative stress-a concise review," *Saudi Pharm J*, vol. 24, no. 5, pp. 547–553, 2016.

[6] A. Tarafdar and G. Pula, "The role of NADPH oxidases and oxidative stress in neurodegenerative disorders," *International Journal of Molecular Sciences*, vol. 19, no. 12, p. 3824, 2018.

[7] R. P. Brandes, N. Weissmann, and K. Schroder, "Nox family NADPH oxidases: molecular mechanisms of activation," *Free Radical Biology & Medicine*, vol. 76, pp. 208–226, 2014.

[8] H. Sumimoto, "Structure, regulation and evolution of Nox-family NADPH oxidases that produce reactive oxygen species," *The FEBS Journal*, vol. 275, no. 13, pp. 3249–3277, 2008.

[9] K. Bedard and K. H. Krause, "The NOX family of ROS-generating NADPH oxidases: physiology and pathophysiology," *Physiological Reviews*, vol. 87, no. 1, pp. 245–313, 2007.

[10] C. X. C. Santos, A. A. Nabeebaccus, A. M. Shah, L. L. Camargo, S. V. Filho, and L. R. Lopes, "Endoplasmic reticulum stress and Nox-mediated reactive oxygen species signaling in the peripheral vasculature: potential role in hypertension," *Antioxidants & Redox Signaling*, vol. 20, no. 1, pp. 121–134, 2014.

[11] G. R. Drummond and C. G. Sobey, "Endothelial NADPH oxidases: which NOX to target in vascular disease?," *Trends in Endocrinology and Metabolism*, vol. 25, no. 9, pp. 452–463, 2014.

[12] S. A. Manea, A. Constantin, G. Manda, S. Sasson, and A. Manea, "Regulation of Nox enzymes expression in vascular pathophysiology: focusing on transcription factors and epigenetic mechanisms," *Redox Biology*, vol. 5, pp. 358–366, 2015.

[13] M. I. Christodoulou, J. Tchoumtchoua, A. L. Skaltsounis, A. Scorilas, and M. Halabalaki, "Natural alkaloids intervening the insulin pathway: new hopes for anti-diabetic agents?," *Current Medicinal Chemistry*, vol. 26, no. 32, pp. 5982–6015, 2019.

[14] Y. Jiang, W. Sang, C. Wang et al., "Oxymatrine exerts protective effects on osteoarthritis via modulating chondrocyte homoeostasis and suppressing osteoclastogenesis," *Journal of Cellular and Molecular Medicine*, vol. 22, no. 8, pp. 3941–3954, 2018.

[15] Y. Y. Zhang, M. Yi, and Y. P. Huang, "Oxymatrine ameliorates doxorubicin-induced cardiotoxicity in rats," *Cellular Physiology and Biochemistry*, vol. 43, no. 2, pp. 626–635, 2017.

[16] L. Zhao, Y. Xu, L. Tao et al., "Oxymatrine inhibits transforming growth factor β1 (TGF-β1)-induced cardiac fibroblast-to-myofibroblast transformation (FMT) by mediating the notch signaling pathway in vitro," *Medical Science Monitor*, vol. 24, pp. 6280–6288, 2018.

[17] X. H. Ge, L. Shao, and G. J. Zhu, "Oxymatrine attenuates brain hypoxic-ischemic injury from apoptosis and oxidative stress: role of p-Akt/GSK3β/HO-1/Nrf-2 signaling pathway," *Metabolic Brain Disease*, vol. 33, no. 6, pp. 1869–1875, 2018.

[18] L. Wang, X. Li, Y. Zhang, Y. Huang, Y. Zhang, and Q. Ma, "Oxymatrine ameliorates diabetes-induced aortic endothelial dysfunction via the regulation of eNOS and NOX4," *Journal of Cellular Biochemistry*, vol. 120, no. 5, pp. 7323–7332, 2018.

[19] S. B. Wang and J. P. Jia, "Oxymatrine attenuates diabetes-associated cognitive deficits in rats," *Acta Pharmacologica Sinica*, vol. 35, no. 3, pp. 331–338, 2014.

[20] Z. B. Yang, X. J. Luo, K. D. Ren et al., "Beneficial effect of magnesium lithospermate B on cerebral ischemia-reperfusion injury in rats involves the regulation of miR-107/glutamate transporter 1 pathway," *European Journal of Pharmacology*, vol. 766, pp. 91–98, 2015.

[21] X. D. Han, Y. Y. Zhang, K. L. Wang, Y. P. Huang, Z. B. Yang, and Z. Liu, "The involvement of Nrf2 in the protective effects of (-)-Epigallocatechin-3-gallate (EGCG) on NaAsO2-induced hepatotoxicity," *Oncotarget*, vol. 8, no. 39, pp. 65302–65312, 2017.

[22] T. L. Sun, Z. Liu, Z. J. Qi, Y. P. Huang, X. Q. Gao, and Y. Y. Zhang, "(-)-Epigallocatechin-3-gallate (EGCG) attenuates arsenic-induced cardiotoxicity in rats," *Food and Chemical Toxicology*, vol. 93, pp. 102–110, 2016.

[23] Z. Q. Huang, G. G. Shi, J. H. Zheng, and B. Liu, "Effects of N-n-butyl haloperidol iodide on rat myocardial ischemia and reperfusion injury and L-type calcium current," *Acta Pharmacologica Sinica*, vol. 24, no. 8, pp. 757–763, 2003.

[24] L. Jiang, T. Wang, J. Xue, P. Yu, J. Zhang, and J. Wang, "Nano-sized carbon black exposure induces neural injury: effects on nicotinamide adenine dinucleotide phosphate oxidases and endoplasmic reticulum stress," *Journal of Applied Toxicology*, vol. 39, no. 8, pp. 1108–1117, 2019.

[25] M. Niocel, R. Appourchaux, X. N. Nguyen, M. Delpeuch, and A. Cimarelli, "The DNA damage induced by the cytosine deaminase APOBEC3A leads to the production of ROS," *Scientific Reports*, vol. 9, no. 1, p. 4714, 2019.

[26] L. Bordier, J. Doucet, J. Boudet, and B. Bauduceau, "Update on cognitive decline and dementia in elderly patients with diabetes," *Diabetes & Metabolism*, vol. 40, no. 5, pp. 331–337, 2014.

[27] N. M. Bornstein, M. Brainin, A. Guekht, I. Skoog, and A. D. Korczyn, "Diabetes and the brain: issues and unmet needs," *Neurological Sciences*, vol. 35, no. 7, pp. 995–1001, 2014.

[28] M. Lunetta, A. R. Damanti, G. Fabbri, M. Lombardo, M. Di Mauro, and L. Mughini, "Evidence by magnetic resonance imaging of cerebral alterations of atrophy type in young insulin-dependent diabetic patients," *Journal of Endocrinological Investigation*, vol. 17, no. 4, pp. 241–245, 1994.

[29] S. Kar, T. N. Kambis, and P. K. Mishra, "Hydrogen sulfide-mediated regulation of cell death signaling ameliorates adverse cardiac remodeling and diabetic cardiomyopathy," *American Journal of Physiology. Heart and Circulatory Physiology*, vol. 316, no. 6, pp. H1237–H1252, 2019.

[30] N. Sahin, C. Orhan, F. Erten et al., "Effects of allyl isothiocyanate on insulin resistance, oxidative stress status, and transcription factors in high-fat diet/streptozotocin-induced type 2 diabetes mellitus in rats," *Journal of Biochemical and Molecular Toxicology*, vol. 33, no. 7, article e22328, 2019.

[31] F. Rezende, F. Moll, M. Walter et al., "The NADPH organizers NoxO1 and p47phox are both mediators of diabetes-induced vascular dysfunction in mice," *Redox Biology*, vol. 15, pp. 12–21, 2018.

[32] J. Wang, Y. Liu, H. Shen, H. Li, Z. Wang, and G. Chen, "Nox2 and Nox4 participate in ROS-induced neuronal apoptosis and brain injury during ischemia-reperfusion in rats," *Acta Neurochirurgica. Supplement*, vol. 127, pp. 47–54, 2020.

[33] H. F. Zhang, T. B. Li, B. Liu et al., "Inhibition of myosin light chain kinase reduces NADPH oxidase-mediated oxidative injury in rat brain following cerebral ischemia/reperfusion," *Naunyn-Schmiedeberg's Archives of Pharmacology*, vol. 388, no. 9, pp. 953–963, 2015.

[34] J. M. Sasser, M. W. Cunningham Jr., and C. Baylis, "Serelaxin reduces oxidative stress and asymmetric dimethylarginine in angiotensin II-induced hypertension," *American Journal of Physiology. Renal Physiology*, vol. 307, no. 12, pp. F1355–F1362, 2014.

[35] B. Liu, K. D. Ren, J. J. Peng et al., "Suppression of NADPH oxidase attenuates hypoxia-induced dysfunctions of endothelial progenitor cells," *Biochemical and Biophysical Research Communications*, vol. 482, no. 4, pp. 1080–1087, 2017.

[36] J. Lin, L. Fang, H. Li et al., "Astragaloside IV alleviates doxorubicin induced cardiomyopathy by inhibiting NADPH oxidase derived oxidative stress," *European Journal of Pharmacology*, vol. 859, p. 172490, 2019.

[37] B. Steinhorn, J. L. Sartoretto, A. Sorrentino et al., "Insulin-dependent metabolic and inotropic responses in the heart are modulated by hydrogen peroxide from NADPH-oxidase isoforms NOX2 and NOX4," *Free Radical Biology & Medicine*, vol. 113, pp. 16–25, 2017.

[38] H. Wang and M. Hartnett, "Roles of nicotinamide adenine dinucleotide phosphate (NADPH) oxidase in angiogenesis: isoform-specific effects," *Antioxidants*, vol. 6, no. 2, p. 40, 2017.

[39] J. Smith-Palmer, M. Brandle, R. Trevisan, M. Orsini Federici, S. Liabat, and W. Valentine, "Assessment of the association between glycemic variability and diabetes-related complications in type 1 and type 2 diabetes," *Diabetes Research and Clinical Practice*, vol. 105, no. 3, pp. 273–284, 2014.

[40] H. Heidari, M. Kamalinejad, M. Noubarani et al., "Protective mechanisms of Cucumis sativus in diabetes-related modelsof oxidative stress and carbonyl stress," *BioImpacts: BI*, vol. 6, no. 1, pp. 33–39, 2016.

[41] N. F. Khedr, "Fish oil and wheat germ oil supplementation modulates brain injury in streptozotocin-induced diabetic rats," *Journal of Diabetes*, vol. 9, no. 11, pp. 1012–1022, 2017.

[42] D. Peña-Montes, M. Huerta-Cervantes, M. Ríos-Silva et al., "Protective effect of the hexanic extract of Eryngium carlinae inflorescences in vitro, in yeast, and in streptozotocin-induced diabetic male rats," *Antioxidants*, vol. 8, no. 3, p. 73, 2019.

[43] A. Arcambal, J. Taile, P. Rondeau, W. Viranaicken, O. Meilhac, and M. P. Gonthier, "Hyperglycemia modulates redox, inflammatory and vasoactive markers through specific signaling pathways in cerebral endothelial cells: insights on insulin protective action," *Free Radical Biology & Medicine*, vol. 130, pp. 59–70, 2019.

[44] A. M. Conteh, C. A. Reissaus, M. Hernandez-Perez et al., "Platelet-type 12-lipoxygenase deletion provokes a compensatory 12/15-lipoxygenase increase that exacerbates oxidative stress in mouse islet β cells," *The Journal of Biological Chemistry*, vol. 294, no. 16, pp. 6612–6620, 2019.

[45] H. Tanaka, J. L. Espinoza, R. Fujiwara et al., "Excessive reactive Iron impairs hematopoiesis by affecting both immature hematopoietic cells and stromal cells," *Cells*, vol. 8, no. 3, p. 226, 2019.

[46] Y. Zhang, Y. Zhang, J. Tang et al., "Oxymatrine inhibits homocysteine-mediated autophagy via MIF/mTOR signaling in human umbilical vein endothelial cells," *Cellular Physiology and Biochemistry*, vol. 45, no. 5, pp. 1893–1903, 2018.

Hindawi
Oxidative Medicine and Cellular Longevity
Volume 2020, Article ID 3216415, 12 pages
https://doi.org/10.1155/2020/3216415

Research Article

Natural Exogenous Antioxidant Defense against Changes in Human Skin Fibroblast Proteome Disturbed by UVA Radiation

Agnieszka Gęgotek,[1] **Pedro Domingues**,[2] **and Elżbieta Skrzydlewska**[1]

[1]*Department of Analytical Chemistry, Medical University of Bialystok, Mickiewicza 2D, 15-222 Bialystok, Poland*
[2]*Mass Spectrometry Center, Department of Chemistry, University of Aveiro, 3810-193 Aveiro, Portugal*

Correspondence should be addressed to Agnieszka Gęgotek; agnieszkagegotek@o2.pl

Received 25 May 2020; Accepted 15 October 2020; Published 5 November 2020

Academic Editor: Przemko Tylzanowski

Copyright © 2020 Agnieszka Gęgotek et al. This is an open access article distributed under the Creative Commons Attribution License, which permits unrestricted use, distribution, and reproduction in any medium, provided the original work is properly cited.

Daily exposure of the skin to UVA radiation causes oxidative modifications to cellular components and biomolecules. These include proteins involved in the metabolism and cytoprotection of fibroblasts, and their modification can contribute to the disruption of cell function and the development of skin disorders. Therefore, there remains a need for highly active cytoprotective compounds with antioxidant properties. The purpose of this study was to investigate the effect of ascorbic acid on the activity of rutin against UVA-induced changes in the proteome of human fibroblasts. All analyses were carried out on fibroblasts cultured in a three-dimensional system exposed to UVA radiation and incubated with rutin and ascorbic acid. Their proteomic profile was analyzed using nano-HPLC, which revealed 150 proteins whose expression was significantly altered between treatment conditions. UVA radiation led to changes in the expression of 82 proteins. However, some of these changes were mitigated by rutin and ascorbic acid separately (23 and 25 proteins, respectively) and rutin and ascorbic acid together (23 proteins). UVA radiation has led to the upregulation of proteins involved in gene expression, catalytic processes and antioxidant pathways, and downregulation of proteins with binding activity. Nevertheless, rutin and ascorbic acid used separately or together have countered these changes to varying degrees. Moreover, rutin and ascorbic acid stimulated fibroblasts irradiated by UVA to increase the expression of the signalling molecules responsible for the opening of the transmembrane channels. In the context of the results obtained, the observed cytoprotective effect of the cooperation of rutin and ascorbic acid results not only from the overlapping properties of the compounds. The effect of rutin alone is probably inhibited by its limited bioavailability. Therefore, its interaction with ascorbic acid increases membrane penetration and improves the cytoprotective effect on skin fibroblasts.

1. Introduction

Rutin is one of the phenolic compounds found in various plant species, where it contributes to the antibacterial properties of the plant [1]. As a glycoside combining the flavonol quercetin and the disaccharide rutinose, it has a chemical structure rich in double bonds and hydroxyl groups (Figure 1(a)) [2]. Rutin also exerts several cytoprotective actions on mammalian cells [3]. Its reported properties include strong antioxidant activities, linked to its ability to directly scavenge free radicals. Rutin can also interact with components of the intracellular antioxidant system, resulting in the restoration of the low-molecular-weight antioxidant pool, increased activity of antioxidant enzymes, and the initiation of expression of cytoprotective genes [4–6]. Studies have also shown that rutin reduces proinflammatory signalling. It does so by reducing the level of reactive oxygen species (ROS) and inhibiting the activity of cyclooxygenase/-lipoxygenase, preventing the oxidative metabolism of components of the cell membrane [7, 8].

The cytoprotective properties of rutin contribute to the protection of skin cells exposed to various types of radiation, considerably increasing cell viability [4, 9]. However, its cell-protection properties are limited due to the reduced penetration of the membrane, which increases under the oxidative stress induced by UV radiation [4]. Other factors can also

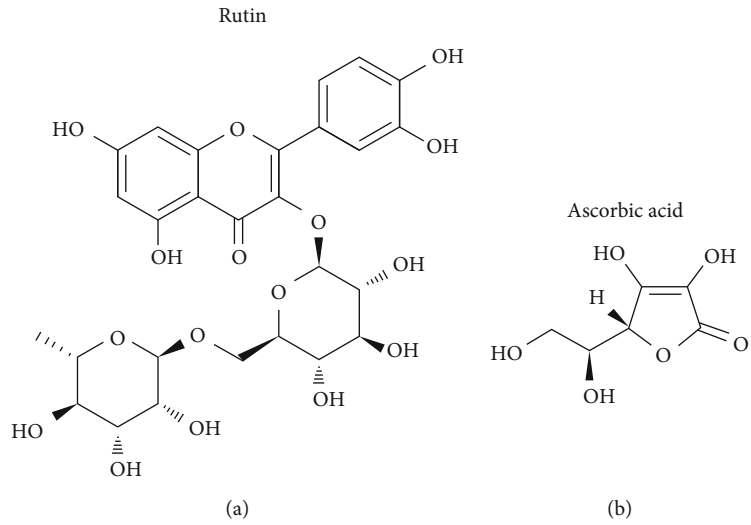

Figure 1: Chemical structure of rutin (a) and ascorbic acid (b).

stimulate cells to uptake rutin, including another natural antioxidant, ascorbic acid [10]. Ascorbic acid is a smaller molecule than rutin, and its chemical structure provides a wide antioxidant capacity (Figure 1(b)) [11]. The main intracellular antioxidant function of ascorbic acid is the recycling the lipid-soluble vitamin E by reducing the α-tocopheroxyl radicals in the membranes [12]. Ascorbic acid can also protect against inflammation caused by sunburn [13–15]. The synergistic effect between ascorbic acid and rutin has been widely demonstrated in studies analyzing the oral administration of the compounds. These findings were mainly related to their anti-inflammatory and vascular sealing actions [16]. Also, as ascorbic acid is essential for the biosynthesis of collagen [17] and has a direct effect on the absorption of rutin, the potential, synergistic effects of rutin and ascorbic acid in the protection of skin cells have also been described [18–20]. Compounds that exert protective effects on skin cells are of great importance as the cells in different layers of the skin are constantly exposed to harmful environmental factors, including UV radiation, mainly present in sunlight.

UV radiation can disturb various metabolic pathways in skin cells, a feature that has been widely documented in published reports [21, 22]. The main effect of UV radiation is the increased generation of ROS linked to a dysfunction of the antioxidant system [22]. UV radiation is also associated with irreversible oxidative modifications in intracellular molecules, including nucleic acids, phospholipids, and proteins. These modifications can cause metabolic changes, DNA mutations, and even the development of skin cancer [23, 24]. Moreover, ROS, as well as highly reactive lipid peroxidation products, modify the structure of proteins that has been shown for UVB-irradiated fibroblasts [20] and altered protein conformation, leading to a modification of their biological activity [25]. The prevention of this action in skin cells is crucial, mainly in the case of proteins with antioxidant and repairing properties not only in DNA but also in the molecules involved in the transduction of the anti-inflammatory or anti-apoptotic signal [25, 26].

While the surface layers of the skin disperse most of the long UV wavelengths, UVA radiation (320–400 nm) shows strong penetration deep into the skin, reaching the dermis, which is mainly composed of fibroblasts [27]. As a result, these fibroblasts have a well-developed cytoprotective system to maintain intracellular homeostasis [28]. However, these natural cellular defense systems are insufficient to cope with the damage associated with UV radiation, requiring the daily use of protective compounds for the skin. Also, the different penetration of these compounds through biological membranes and multilayer cell systems is an additional problem to be solved. So far, the cooperation of rutin and ascorbic acid protects protein structures of UVB-irradiated skin fibroblasts [20]. Therefore, this study was aimed at examining the effect of ascorbic acid on the cytoprotective action of rutin against UVA-induced changes in the proteomic profile of the human skin fibroblasts cultured in a three-dimensional (3D) system.

2. Materials and Methods

2.1. Cell Culture. The human skin fibroblasts (CRL-1474) were obtained from the American Type Culture Collection (ATCC) and cultured in a humidified atmosphere of 5% CO_2 at 37°C in a medium composed of Dulbecco's modified Eagle medium (DMEM) with 10% fetal bovine serum (FBS) according to the standard protocol for fibroblasts. To avoid bacterial contamination, medium was supplemented with penicillin (50 U/ml) and streptomycin (50 μg/ml). Following two passages, cells were seeded in 24-well plates (500,000 cells/well) with AlgiMatrix gel (Life Technologies, California, USA) to create a three-dimensional (3D) model. After four days of culturing, the cells were exposed to UVA radiation (Bio-Link Crosslinker BLX 365; Vilber Lourmat, Germany) at a total dose of 20 J/cm^2 (λ = 365 nm). Before irradiation, cells were washed with PBS (4°C). In this buffer, cells in plates put on ice were exposed to the irradiation from 6 lamps with an assembly of 6 W each, which corresponds to 4.2 mW/cm^2. The distance between cells and lamps was 15 cm. To analyze

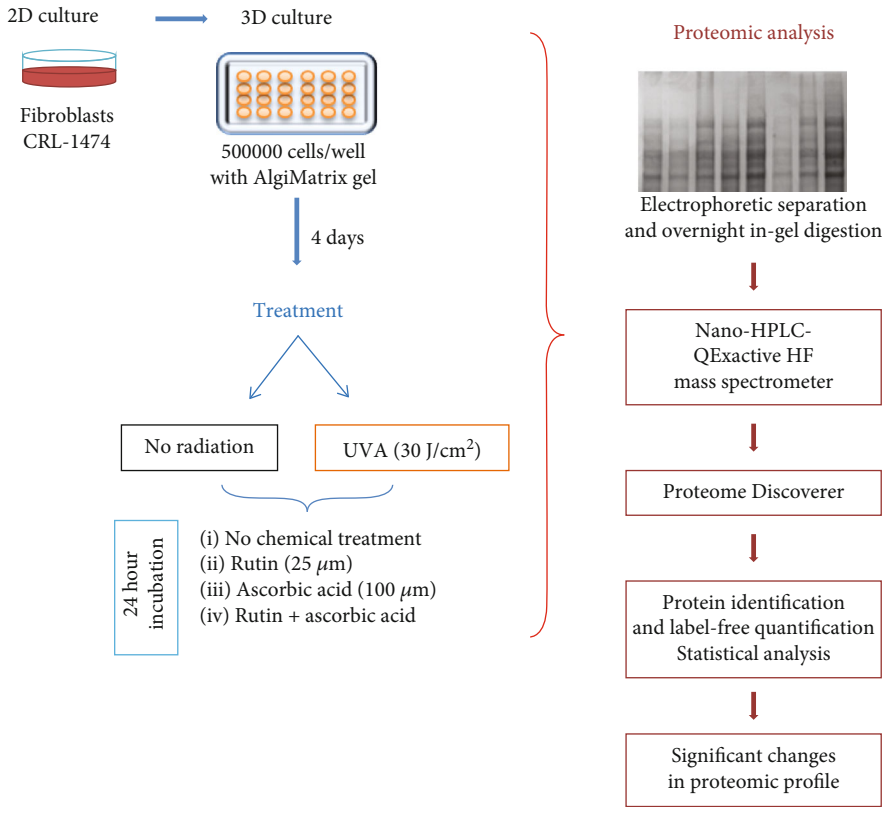

Figure 2: The design of the experiment including cells treatment, sample processing, and statistical data analysis.

the effect of rutin and ascorbic acid on UVA-radiated cells, we followed the corresponding methods of Gęgotek et al. [20] that were dedicated changes caused by UVB radiation. Following irradiation, cells were incubated for 24 h in medium containing 25 μM rutin or/and 100 μM ascorbic acid in 0.1% DMSO. Parallelly, control cells were cultured in medium containing 0.1% DMSO. The diagram showing the course of the experiment is shown in Figure 2.

Following incubation, using AlgiMatrix™ dissolving buffer (Life Technologies, California, USA), fibroblasts were collected from the 3D gel. Cells were washed with PBS and lysed by sonification. The total protein content in the lysate was measured using a Bradford assay [29].

2.2. Protein Separation and Analysis. Before proteomic analysis, proteins were denatured by mixing with Laemmli buffer that contained 5% 2-mercaptoethanol (1 : 1v/v) and heated 10 min at 95°C. Preliminary protein separation was prepared on 10% Tris-glycine SDS-PAGE gels. All bands were detected by overnight staining with Coomassie Brilliant Blue R-250. Proteins were sliced and in-gel digested overnight with trypsin (Promega, Madison, WI, USA). Obtained peptide mixture was dissolved in 5% acetonitrile (ACN) + 0.1% formic acid (FA) and separated on 150 mm × 75 mm PepMap RSLC capillary analytical C18 column (Dionex, LC Packings) using Ultimate 3000 HPLC (Dionex, Idstein, Germany). Eluted peptides were analyzed using a QExactive HF mass spectrometer (Thermo Fisher Scientific, Bremen, Germany) operated in a positive mode. Details of the analysis have been described previously [6, 20].

2.3. Protein Identification and Label-Free Quantification. Raw data were processed using Proteome Discoverer 2.0 (Thermo Fisher Scientific, Bremen, Germany) and searched against the UniProtKB-SwissProt database (taxonomy: Homo sapiens, release 2019-04). Peptide mass tolerance was set to 10 ppm, MS/MS mass tolerance was set to 0.02 Da, and up to two allowed missed cleavages were used for protein identification. Details of the protein identification have been described previously [6, 20]. Only proteins with at least three identified peptides longer than 6 amino acid residues and at least two unique peptides were selected for further analysis.

2.4. Statistical Analysis. Analyses of each sample were performed in three independent experiments. Missing values were estimated using half of the minimum value from the original data imputation. Results from individual protein label-free quantifications were log and Z-score transformed. Statistical analysis of data was performed using free available MetaboAnalyst 4.0 software (http://www.metaboanalyst.ca), RStudio software (R version 3.6.2 (2019-12-12)), and Perseus 1.6.10.43. Principal component analysis (PCA) was conducted for exploratory data analysis, with the R package MetaboAnalyst [30]. ANOVA test followed by the Fisher post hoc tests was performed with the R built-in function. Heatmaps were created using the R package pheatmap [31]

using "Euclidean" as clustering distance and "ward.D" as the clustering method.

3. Results

The proteomic data obtained in this study allowed us to create a list of proteins whose expression was significantly altered in fibroblasts cultured in 3D after irradiation with UVA followed by treatment with rutin and ascorbic acid (Supplementary Table S1). This list includes 150 proteins, 94 of which were identified in control cells and 128 in UVA-irradiated fibroblasts without rutin or ascorbic acid.

Treatment with rutin alone induced expression of 4 proteins not found in other treatment groups and 4 other proteins when used with ascorbic acid. The same behaviour was observed in cells treated with rutin/ascorbic acid following UVA irradiation. The number of all significantly altered proteins identified in cells treated with rutin or/and ascorbic acid but without UVA irradiation was generally higher than when cells were irradiated with UVA (46 proteins versus 94). In this case, the chemical treatment induced the expression of 18 proteins which were not found among the 128 proteins expressed in the cells treated only with UVA irradiation (Figure 3).

Using principal component analysis (PCA), we found that the changes in the proteomic profiles of skin fibroblast cells led to the clustering of the experimental groups (PC1 40.9% and PC2 28.6% for nonirradiated fibroblasts and PC1 37.5% and PC2 22.7% for UVA-irradiated fibroblasts) (Figure 4). In the case of nonirradiated fibroblasts, the control group clustered from the ascorbic acid and the rutin plus ascorbic acid groups, mainly in the lower quadrant. The samples treated with rutin assembled in the upper left quadrant (Figure 4(a)). Observations were different after UVA irradiation, where samples within the treatment groups clustered together mainly in the lower quadrant, and the group treated with ascorbic acid assembled in the upper right quadrant (Figure 4(b)).

The volcano plots comparing the effect of ascorbic acid and rutin on the cells irradiated by UVA also highlight the number of proteins which changed expression under experimental conditions (Figure 5). UVA radiation has caused significant changes in the expression of 82 proteins. However, these changes were attenuated by these cytoprotective compounds to 23 and 25 proteins, respectively, in the case of rutin and ascorbic acid used separately, and 23 proteins in cells treated with rutin plus ascorbic acid. The list of significant proteins and the fold changes (FC) is shown in Supplementary Table S2. The clustering and functions of these proteins can be visualized in the two-dimensional hierarchical clustering heat map (Figure 6). In all the experiments, the clustering of the individual proteins for their similarity in the changes of expression shows that they cluster into three main groups. In the control group, UVA radiation led to upregulation of proteins with mainly catalytic activity or transcription/translation regulatory properties and downregulation of proteins with binding to other molecule activity (Figure 6(a)). Similar observations were made in the case of cells treated with rutin (Figure 6(b)) or with ascorbic acid (Figure 6(c)) before the UVA irradiation. Treatment of cells with these compounds in combination before the UVA irradiation led to upregulation of proteins with antioxidant and transcription/translation activity, as well as regulators of protein degradation. (Figure 6(d)).

4. Discussion

Skin cells are exposed to sunlight, which often disrupts cell metabolism due to harmful UVA and UVB radiation [22]. Proteomic analysis of UVB-irradiated fibroblasts indicates that this harmful factor by oxidative stress induction can lead to ROS-dependent changes in protein structures and through enhanced lipid peroxidation products such as reactive aldehydes (4-hydroxynonenal, 4-oxynonenal, and malondialdehyde) cause aldehyde-protein adduct formation [20]. Moreover, UVB has been found as a stimulator of active heat shock protein 90 complex formation that is crucial for proper protein conformation [20]. On the other hand, UVA radiation at the dose used in this study also can modify protein structure, which has been showed as direct oxidation of amino acid residues and advanced glycation end-product creation [32, 33]. These effects involve simultaneous changes at many levels of cell function, including gene transcription, protein biosynthesis, intracellular metabolism, and intercellular signalling [6], without induction of necrosis. Therefore, this study is directly focused on changes in expression of proteins from fibroblasts exposed to UVA radiation in a dose that causes significant changes in cellular metabolism but allows cells to maintain the integrity of nucleus. Moreover, to describe the changes that occur in UVA-irradiated skin cells, it is necessary to understand homeostasis not only at the cell level but also at the tissue level. The use of a three-dimensional cell culture model facilitates the observation of different layers of processes in the skin tissue, including changes in intracellular metabolism and intercellular signalling [34–36].

Fibroblasts are one of the main types of cells that build human skin, but their location in the inner layer of the skin, the dermis, gives them partial protection against external factors by epidermal cells. As a result, fibroblasts are very sensitive to penetrating UVA radiation [37]. To support their self-defense mechanisms, cytoprotective substances (such as rutin) can be administered orally or topically. Many therapeutic properties of rutin as a pharmacological substance have been described [38–40]. However, previous research suggests that regardless of its content in the diet, the low concentrations of rutin in plasma limit its bioavailability to all cells in an organism [41, 42]. However, it has also been shown that rutin can effectively penetrate 3D cultures of skin cells and induce cytoprotective effects even in the deep layers [19]. Moreover, the membrane transport of rutin can be enhanced by ascorbic acid, significantly increasing its action [18].

The results obtained in this study corroborate the previously published data, clearly showing that UVA radiation induces large changes in the proteome of skin fibroblasts [34, 43]. The results also demonstrate that rutin and ascorbic acid exhibit cytoprotective effects, partially preventing UVA-

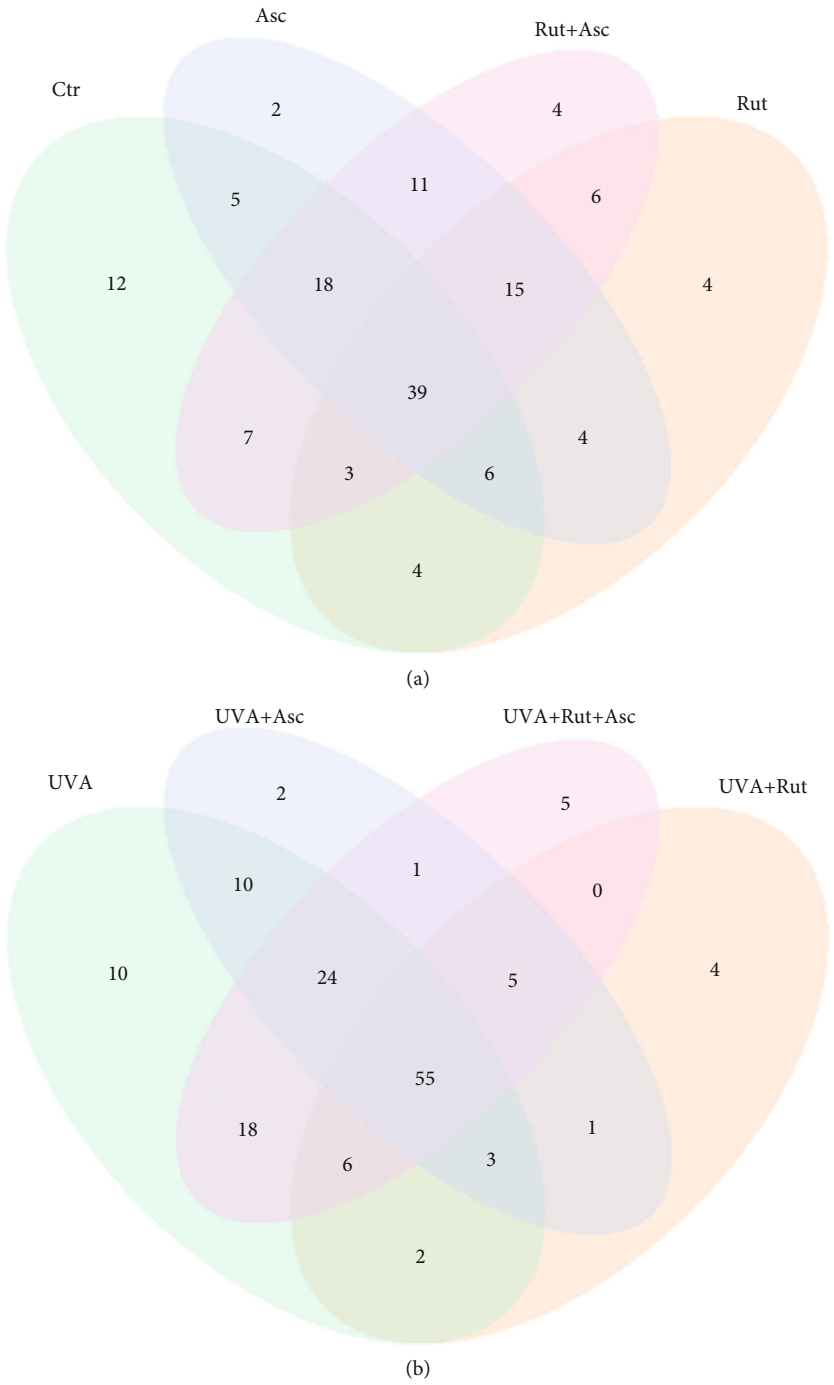

Figure 3: Venn diagram showing the distribution of the number of significantly changed proteins ($p < 0.05$) in the 3D cultured fibroblasts treated with rutin (25 μM) or/and ascorbic acid (100 μM) (a) and following exposure to UVA (20 J/cm^2) (b). Significant proteins are listed in Supplementary Table 1. Abbreviations: Asc: ascorbic acid; Ctr: control; Rut: rutin.

induced changes in the proteome of different cell types [5, 6, 15, 18, 19]. Moreover, recently, it has also been shown that cooperation of rutin and ascorbic acid prevents against UVB induced disturbances in protein structures [20].

The main proteins whose expression was sensitive to UVA radiation were those involved in protein biosynthesis; our data show that UVA radiation significantly upregulates the expression of proteins involved in mRNA transcription processes, including elongation factors (A8K9C4, P26641, and P49411), the translation initiation factor 2 (P41091), ribosomal proteins (A0A024R2P0), and ribonucleoproteins (P62318, Q7Z5A3). This cellular response is aimed at defending against radio-induced stress caused by UVA rays [44].

The cytoprotective action of rutin after UVA irradiation significantly prevents increased expression of translation-inducing proteins, which, in previously published data, has been suggested as a method of inhibiting carcinogenesis

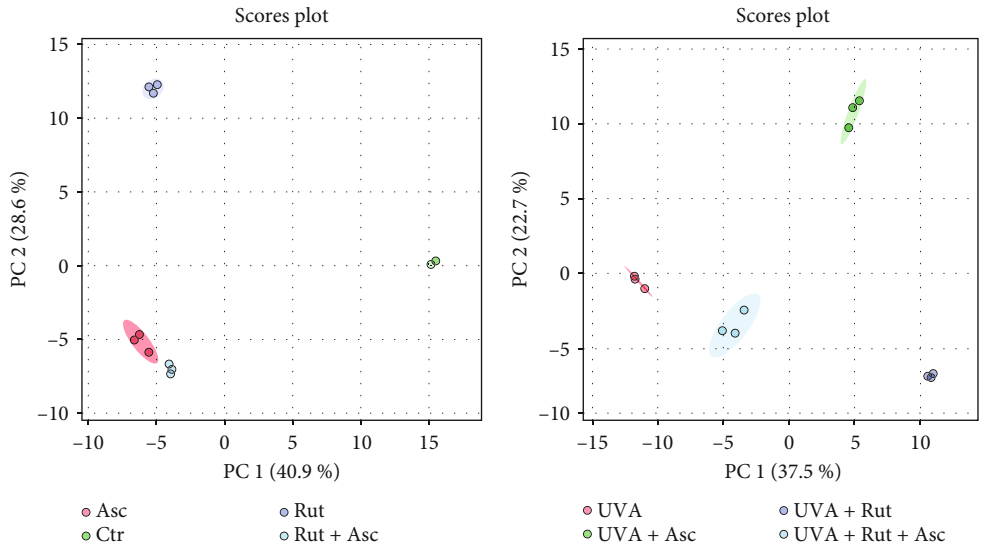

(a) Nonirradiated cells (b) UVA-irradiated cells

Figure 4: Principal component analysis (PCA) of proteins from the 3D cultured fibroblasts treated with rutin (25 μM) or/and ascorbic acid (100 μM) (a) and following exposure to UVA (20 J/cm^2) (b). Abbreviations: Asc: ascorbic acid; Ctr: control; Rut: rutin.

[39]. The action of ascorbic acid (separately and in conjunction with rutin) also promotes the expression of these proteins in response to UVA radiation. The changes are very visible not only for the elongation factors and the ribosomal proteins but also in the case of the amino acid-tRNA ligases (tryptophan and threonine-tRNA ligases, P23381 and P26639). These changes in expression lead to the formation of ribosomes, and it is well known that ascorbic acid promotes the increase of the hydroxylation of amino acids in the ribosome. Hydroxylation of amino acids is necessary for the formation of collagen chains, especially under stressful conditions, such as in the case of skin incision wounds [43–45]. Similar changes as those we have described have also been observed in the proteins responsible for the regulation of proteolysis. UVA radiation significantly increases the expression of proteins involved in degradation process, such as the proteasome subunits (A0A087WXQ8, P49720, P49721, and Q59EG8), which is linked to oxidative stress induced by UVA [46]. Rutin counteracts these changes, even causing a reduction in the level of ubiquitin carboxyl-terminal hydrolase (D6RF53) in cells, following exposure to UVA. The reduction of this protein limits the generation of ubiquitin monomers from protein adducts [47], thereby preventing labelling of proteins for degradation. Similar effects of proteasome inhibition by flavonoids have already been observed [48].

In our study, we have found that ascorbic acid also modestly reduced the expression of several proteins involved in degradation following UVA radiation. However, some of these proteins were more strongly upregulated than in fibroblasts without treatment with ascorbic acid. A similar complex and ambiguous effect of ascorbic acid on proteasomal activity has also been observed, mainly in cells with disturbed metabolism, such as cancer cells [49, 50]. The response of fibroblasts irradiated with UVA to the actions of rutin and ascorbic acid shows that these compounds, when administered together, significantly prevent the degradation of proteins in irradiated cells. This observation may be related to structural changes in proteins caused by UVA radiation. These modifications could make the proteins dysfunctional and be eliminated by degradation, as previously observed in keratinocytes or UVB-irradiated fibroblasts [20, 51]. However, the cytoprotective effect of rutin with ascorbic acid protects proteins from oxidative damage, and high levels of proteasomal subunits in the cytoplasm are not necessary.

Other groups of proteins highly upregulated by UVA radiation in 3D cultured skin fibroblasts were proteins with catalytic activity, in particular in glycolytic processes. Similar changes have been previously described also for UVB-irradiated fibroblasts [20]. Reducing stress induced by exposure to UV requires a lot of energy from the cells, which induces an additional consumption of glucose and is associated with accelerated cellular metabolism [52]. Rutin significantly limits the number of catalytic proteins participating in energy reactions following UVA radiation and has already been shown to impair energy processes in the mitochondria of stressed cells by inhibiting substrate oxidation, as well as acting as an uncoupler of oxidative phosphorylation [53]. Ascorbic acid also lowers the levels of proteins involved in glycogenolysis (glycogen phosphorylase, P06737) and interfering with glutaminolysis (phosphoserine aminotransferase, A0A024R280). The effect of ascorbic acid on ATP generation and energy metabolism is closely related to its concentration, as well as to the conditions in which the cells are found [54]. As has been shown for UVB-irradiated fibroblasts and other skin cells (keratinocytes), ascorbic acid, as well as rutin, also supports the production of aerobic energy by cells, especially under stress [19, 20]. However, in fibroblasts, these two processes overlap when cells were treated with rutin and ascorbic acid. This mechanism provides cells with a reduced intensity of electron flow in the mitochondrial respiratory chain and thus reduces the likelihood of generation of free radicals [55].

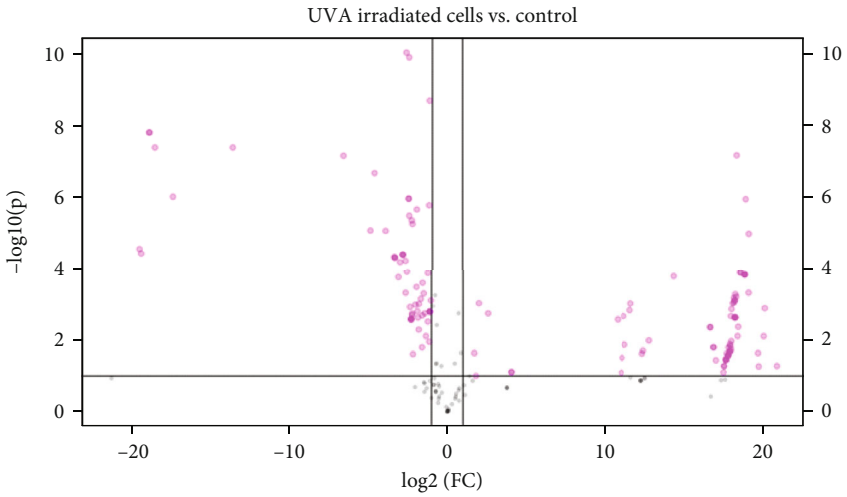

(a) UVA-irradiated cells vs. control

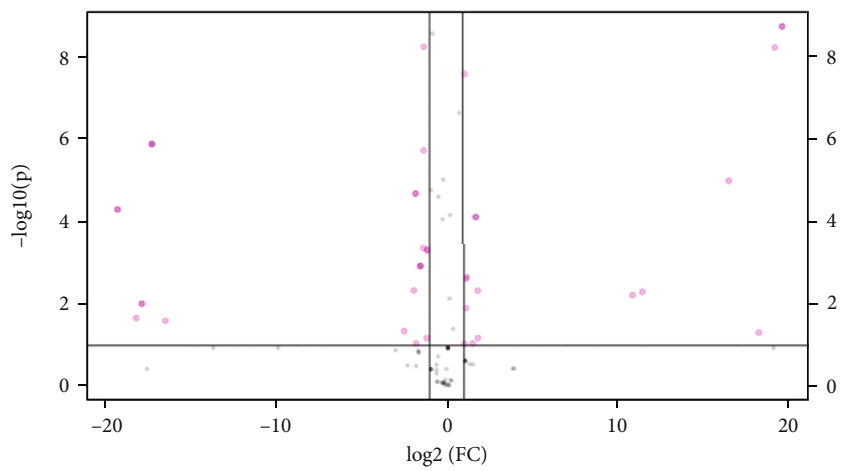

(b) UVA+Rut vs. Rut-treated cells

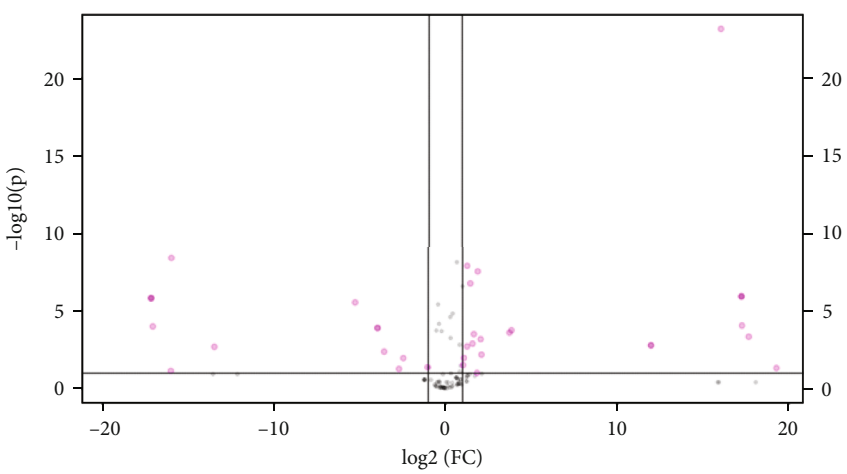

(c) UVA+Asc vs. Asc-treated cells

Figure 5: Continued.

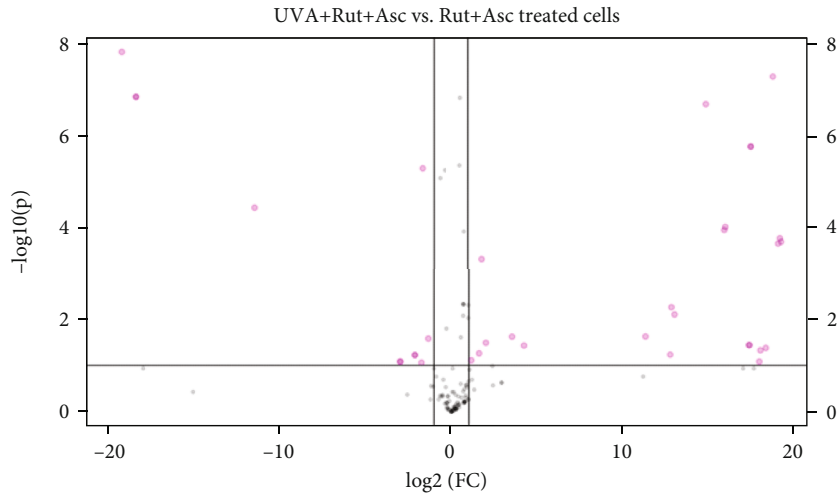

(d) UVA+Rut+Asc vs. Rut+Asc-treated cells

Figure 5: Volcano plots comparing the effect of rutin (25 μM) or/and ascorbic acid (100 μM) on UVA- (20 J/cm^2) irradiated fibroblasts cultured in a 3D model. Abbreviations: Asc: ascorbic acid; Ctr: control; Rut: rutin. The list of significant proteins, their p values, and fold change (FC) are shown in Supplementary Table 2.

The antioxidant action of rutin and ascorbic acid, which according to the literature is mainly based on their free radical scavenging activity [56], leads to a reduced expression of the proteins of the antioxidant system which are strongly activated by UVA radiation. An example of such an action is the effect on the thioredoxin system, previously observed also in the case of UVB-irradiated cells [20]. UVA radiation significantly changes the level and activity of proteins in this system [19, 57], including the thioredoxin-like protein 4B (Q9NX01), as found in this study. The antioxidant activity of this system is based on the reduction of NADPH-dependent protein disulfide. This is ensured by the structure of thioredoxin, which, as a small thiol-active polypeptide, is an essential electron donor for UV-oxidized proteins [58]. UVA radiation also induces the expression of cystathionine gamma-lyase (CTH, P32929), which catalyzes the biosynthesis of cysteine or thiocysteine. The increased activity of CTH is the response of cells to the increased demand for thiol groups under oxidative stress [59], an effect observed following UVA irradiation. Due to their effective antioxidant properties, rutin and ascorbic acid probably reduce free radicals so vigorously that they prevent the reduction of the thiol group pool, which occurs after UVA irradiation of fibroblasts.

A slightly different situation has been observed in keratinocytes cultured in a 3D model. In these cells, treatment with antioxidant compounds additionally supports the natural cellular antioxidant system [19]. Moreover, when used separately, rutin and ascorbic acid reduce the expression of other antioxidant proteins in skin fibroblasts after UVA irradiation, altering the level of reduced thiol groups such as glutathione S-transferase (P21266) and the protein disulfide-isomerase (Q15084). However, rutin and ascorbic acid used together not only prevent UVA-induced activation of the antioxidant system but also silence the machinery necessary for protein repair, observed by the decrease of the heat shock cognate protein (E9PS65). Similar effects of flavonoids on the level of heat shock proteins have already been observed in cancer cells, a mechanism that was important for removing mutated cells from the organism [60].

The additional cytoprotective mechanism of skin fibroblasts against UVA radiation is their ability to provide multilayer protection for skin cells [61]. In such a system, communication between cells by transmission signal factors is highly developed [62]. However, as previously shown, UV radiation also disturbs the functioning of the skin cell at this level [19, 63]. In the case of the epidermis, UV radiation substantially induces proinflammatory and proapoptotic signals, while rutin and ascorbic acid prevent these changes [19]. In this study focused on dermal fibroblasts, the main proteins with modified expression (from the top 50 significant proteins) after UVA irradiation are mainly associated with the functioning of intracellular membranes, including voltage-dependent anion channel 2 (VDAC, A0A024QZN9) and transmembrane emp24 domain-containing protein 9 (TMED, A0A024R7M0). VDAC is a major protein in the outer mitochondrial membrane (and, to a lesser extent, the cell membrane). It facilitates the flow of ions and small hydrophilic molecules through the membrane [64]. Ascorbic acid is an example of such a molecule, but, conversely, it is a potent inhibitor of other voltage-dependent channels in the mitochondrial membrane [65]. Moreover, rutin has also been shown to act as a VDAC inhibitor [66]. Therefore, in fibroblasts cultured in 3D, we observed a UV-induced increase in the expression of VDAC and the complete elimination of this effect following treatment of the cells with rutin and ascorbic acid. However, the role of TMED following UVA irradiation is still unclear; the downregulation of this protein by rutin and ascorbic acid may prevent metabolic dysfunctions [67].

Rutin, in combination with ascorbic acid, also causes UV-irradiated fibroblasts to upregulate the expression of Ras-related protein Rab-5C (P51148). This protein activity

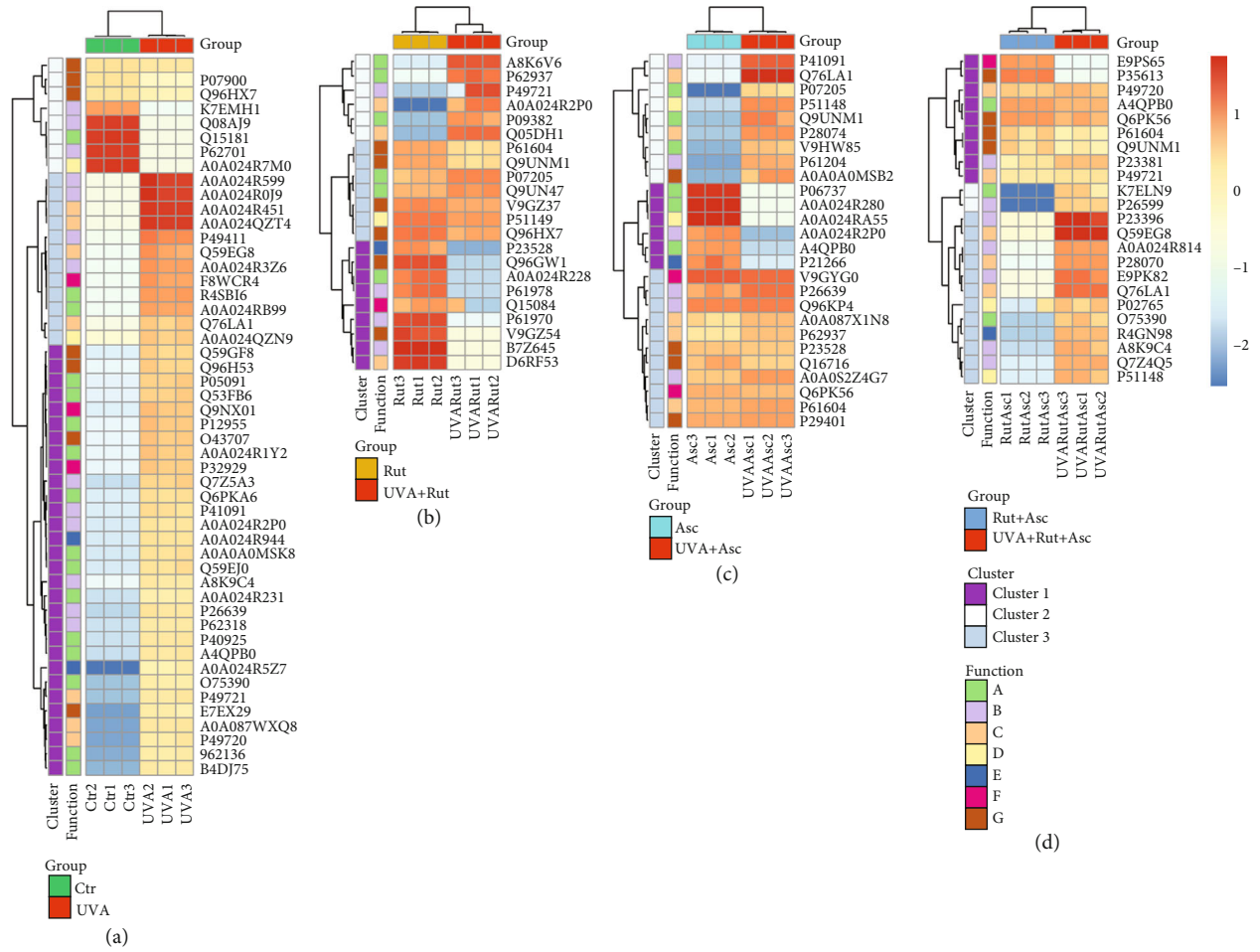

FIGURE 6: Two-dimensional hierarchical clustering heat map of the significantly different proteins (p value < 0.05) from the 3D cultured fibroblasts following exposure to UVA (20 J/cm^2) (a) and treated separately with rutin (25 μM) (b) or ascorbic acid (100 μM) (c) as well as both compounds together (d). For the creation of heat map A, only the top 50 of significant proteins were used, while all significant proteins were used in heat maps (b–d). Abbreviations: Asc: ascorbic acid; Ctr: control; Rut: rutin. Functions: (A) catalytic activity; (B) transcription/translation regulator; (C) protein degradation regulator; (D) signaling molecule; (E) inflammation regulator; (F) antioxidant activity; (G) binding activity.

is also closely linked to the membrane-bound proteins and GTP hydrolysis, which participates in the regulation of the secretion of extracellular signalling molecules [68]. Other polyphenols (e.g., resveratrol) can upregulate Ras-related protein, Rab [69, 70]. However, rutin has not been shown to have these properties. This study shows that it is only possible in association with ascorbic acid. Ascorbic acid promotes intercellular communication under oxidative stress and protects cells from the harmful effects of UVA radiation.

5. Conclusions

In conclusion, the strong antioxidant properties of rutin, as well as its effects on intracellular and intercellular signalling, are probably inhibited by its limited bioavailability. In the context of the results obtained in this study, this natural polyphenol requires to be administered with ascorbic acid not only to increase its membrane penetration but also to complement its cytoprotective effect on skin cells irradiated with UV. Analysis of the mechanisms of action of rutin and ascorbic acid in different types of skin cells, such as fibroblasts and keratinocytes [19], draws particular attention to the changes in the proteome. These changes mainly involved proteins associated with gene expression, signal transduction, and the antioxidant response. Thus, the coadministration of rutin and ascorbic acid can protect against the harmful effects induced by UVA rays and these findings can be useful for the prevention of skin diseases linked to irradiation and oxidation processes.

Data Availability

The mass spectrometry proteomics data have been deposited to the ProteomeXchange Consortium via the PRIDE [70] partner repository with the dataset identifier PXD018730.

Conflicts of Interest

The authors declare that there is no conflict of interest regarding the publication of this paper.

Acknowledgments

This study was financed by the National Science Centre, Poland (NCN), grant no. 2017/25/N/NZ7/00863. Cooperation between coauthors is financed by the Polish National Agency for Academic Exchange (NAWA) as part of the International Academic Partnerships (PPI/APM/2018/-00015/U/001). Thanks are also due for the financial support to QOPNA (FCT UID/QUI/00062/2019) and LAQV/REQUIMTE (UIDB/50006/2020).

Supplementary Materials

Supplementary Table 1: list of significant proteins indicated in the 3D cultured fibroblasts treated with rutin (25 μM) or/and ascorbic acid (100 μM) and following exposure to UVA (20 J/cm^2). Supplementary Table 2: list of significant proteins form volcano plots (Figure 5) comparing the effect of rutin (25 μM) or/and ascorbic acid (100 μM) on UVA-(20 J/cm^2) irradiated fibroblasts cultured in a 3D model. *(Supplementary materials)*

References

[1] A. Basile, S. Sorbo, S. Giordano et al., "Antibacterial and allelopathic activity of extract from Castanea sativa leaves," *Fitoterapia*, vol. 71, pp. S110–S116, 2000.

[2] M. Kessler, G. Ubeaud, and L. Jung, "Anti- and pro-oxidant activity of rutin and quercetin derivatives," *The Journal of Pharmacy and Pharmacology*, vol. 55, no. 1, pp. 131–142, 2003.

[3] K. Patel and D. K. Patel, *In Bioactive Food as Dietary Interventions for Arthritis and Related Inflammatory Diseases*, Elsevier, 2019.

[4] A. Gęgotek, K. Bielawska, M. Biernacki, I. Dobrzyńska, and E. Skrzydlewska, "Time-dependent effect of rutin on skin fibroblasts membrane disruption following UV radiation," *Redox Biology*, vol. 12, pp. 733–744, 2017.

[5] A. Gęgotek, P. Rybałtowska-Kawałko, and E. Skrzydlewska, "Rutin as a mediator of lipid metabolism and cellular signaling pathways interactions in fibroblasts altered by UVA and UVB radiation," *Oxidative Medicine and Cellular Longevity*, vol. 2017, Article ID 4721352, 20 pages, 2017.

[6] A. Gęgotek, P. Domingues, and E. Skrzydlewska, "Proteins involved in the antioxidant and inflammatory response in rutin-treated human skin fibroblasts exposed to UVA or UVB irradiation," *Journal of Dermatological Science*, vol. 90, no. 3, pp. 241–252, 2018.

[7] H. Bouriche, E. A. Miles, L. Selloum, and P. C. Calder, "Effect of Cleome arabica leaf extract, rutin and quercetin on soybean lipoxygenase activity and on generation of inflammatory eicosanoids by human neutrophils," *Prostaglandins, Leukotrienes and Essential Fatty Acids*, vol. 72, no. 3, pp. 195–201, 2005.

[8] I. Dobrzyńska, A. Gęgotek, E. Gajko, E. Skrzydlewska, and Z. A. Figaszewski, "Effects of rutin on the physicochemical properties of skin fibroblasts membrane disruption following UV radiation," *Chemico-Biological Interactions*, vol. 282, pp. 29–35, 2018.

[9] S. Sunada, H. Fujisawa, I. M. Cartwright et al., "Monoglucosyl-rutin as a potential radioprotector in mammalian cells," *Molecular Medicine Reports*, vol. 10, no. 1, pp. 10–14, 2014.

[10] J. Čvorović, L. Ziberna, S. Fornasaro, F. Tramer, and S. Passamonti, *In Polyphenols: Mechanisms of Action in Human Health and Disease*, Elsevier, 2018.

[11] A. Bendich, L. J. Machlin, O. Scandurra, G. W. Burton, and D. D. M. Wayner, "The antioxidant role of vitamin C," *Advances in Free Radical Biology & Medicine*, vol. 2, no. 2, pp. 419–444, 1986.

[12] M. G. Traber and J. F. Stevens, "Vitamins C and E: beneficial effects from a mechanistic perspective," *Free Radical Biology & Medicine*, vol. 51, no. 5, pp. 1000–1013, 2011.

[13] F. Al-Niaimi and N. Y. Z. Chiang, "Topical Vitamin C and the Skin: Mechanisms of Action and Clinical Applications," *The Journal of Clinical and Aesthetic Dermatology*, vol. 10, no. 7, pp. 14–17, 2017.

[14] J. Pullar, A. Carr, and M. Vissers, "The Roles of Vitamin C in Skin Health," *Nutrients*, vol. 9, no. 8, p. 866, 2017.

[15] A. Gęgotek, K. Bielawska, M. Biernacki, I. Zaręba, A. Surażyński, and E. Skrzydlewska, "Comparison of protective effect of ascorbic acid on redox and endocannabinoid systems interactions in in vitro cultured human skin fibroblasts exposed to UV radiation and hydrogen peroxide," *Archives of Dermatological Research*, vol. 309, no. 4, pp. 285–303, 2017.

[16] J. Milde, E. F. Elstner, and J. Graßmann, "Synergistic inhibition of low-density lipoprotein oxidation by rutin, γ-terpinene, and ascorbic acid," *Phytomedicine*, vol. 11, no. 2-3, pp. 105–113, 2004.

[17] R. S. Sharma, R. Poddar, P. Sen, and T. J. Rews, "Effect of vitamin C on collagen biosynthesis and degree of birefringence in polarization sensitive optical coherence tomography (PS-OCT)," *African Journal of Biotechnology*, vol. 7, pp. 2049–2054, 2008.

[18] A. Gęgotek, E. Ambrożewicz, A. Jastrząb, I. Jarocka-Karpowicz, and E. Skrzydlewska, "Rutin and ascorbic acid cooperation in antioxidant and antiapoptotic effect on human skin keratinocytes and fibroblasts exposed to UVA and UVB radiation," *Archives of Dermatological Research*, vol. 311, no. 3, pp. 203–219, 2019.

[19] A. Gęgotek, I. Jarocka-Karpowicz, and E. Skrzydlewska, "Synergistic Cytoprotective Effects of Rutin and Ascorbic Acid on the Proteomic Profile of 3D-Cultured Keratinocytes Exposed to UVA or UVB Radiation," *Nutrients*, vol. 11, no. 11, p. 2672, 2019.

[20] A. Gęgotek, I. Jarocka-Karpowicz, and E. Skrzydlewska, "Cytoprotective effect of ascorbic acid and rutin against oxidative changes in the proteome of skin fibroblasts cultured in a three-dimensional system," *Nutrients*, vol. 12, no. 4, p. 1074, 2020.

[21] J. D'Orazio, S. Jarrett, A. Amaro-Ortiz, and T. Scott, "UV Radiation and the Skin," *International Journal of Molecular Sciences*, vol. 14, no. 6, pp. 12222–12248, 2013.

[22] A. Gegotek, M. Biernacki, E. Ambrozewicz, A. Surazyński, A. Wroński, and E. Skrzydlewska, "The cross-talk between electrophiles, antioxidant defence and the endocannabinoid system in fibroblasts and keratinocytes after UVA and UVB irradiation," *Journal of Dermatological Science*, vol. 81, no. 2, pp. 107–117, 2016.

[23] J. Cadet and T. Douki, "Formation of UV-induced DNA damage contributing to skin cancer development," *Photochemical & Photobiological Sciences*, vol. 17, no. 12, pp. 1816–1841, 2018.

[24] E. McAdam, R. Brem, and P. Karran, "Oxidative stress-induced protein damage inhibits DNA repair and determines mutation risk and therapeutic efficacy," *Molecular Cancer Research*, vol. 14, no. 7, pp. 612–622, 2016.

[25] W. Łuczaj, A. Gęgotek, and E. Skrzydlewska, "Antioxidants and HNE in redox homeostasis," *Free Radical Biology & Medicine*, vol. 111, pp. 87–101, 2017.

[26] S. Anavi, Z. Ni, O. Tirosh, and M. Fedorova, "Steatosis-induced proteins adducts with lipid peroxidation products and nuclear electrophilic stress in hepatocytes," *Redox Biology*, vol. 4, pp. 158–168, 2015.

[27] F. Brugè, L. Tiano, P. Astolfi, M. Emanuelli, and E. Damiani, "Prevention of UVA-Induced Oxidative Damage in Human Dermal Fibroblasts by New UV Filters, Assessed Using a Novel In Vitro Experimental System," *PLoS ONE*, vol. 9, no. 1, p. e83401, 2014.

[28] H. Yang, X. Wang, X. Liu et al., "Antioxidant peptidomics reveals novel skin antioxidant system," *Molecular & Cellular Proteomics*, vol. 8, no. 3, pp. 571–583, 2009.

[29] M. Bradford, "A rapid and sensitive method for the quantitation of microgram quantities of protein utilizing the principle of protein-dye binding," *Analytical Biochemistry*, vol. 72, no. 1-2, pp. 248–254, 1976.

[30] J. Chong, D. S. Wishart, and J. Xia, "Using MetaboAnalyst 4.0 for Comprehensive and Integrative Metabolomics Data Analysis," *Current Protocols in Bioinformatics*, vol. 68, no. 1, p. e86, 2019.

[31] R. L. Barter and B. Yu, "Superheat: An R package for creating beautiful and extendable heatmaps for visualizing complex data," *Journal of Computational and Graphical Statistics*, vol. 27, no. 4, pp. 910–922, 2019.

[32] Y. Okano, H. Masaki, and H. Sakurai, "Pentosidine in advanced glycation end-products (AGEs) during UVA irradiation generates active oxygen species and impairs human dermal fibroblasts," *Journal of Dermatological Science*, vol. 27, pp. 11–18, 2001.

[33] C. S. Sander, H. Chang, S. Salzmann et al., "Photoaging is associated with protein oxidation in human skin in vivo," *The Journal of Investigative Dermatology*, vol. 118, no. 4, pp. 618–625, 2002.

[34] A. Gęgotek, S. Atalay, P. Domingues, and E. Skrzydlewska, "The differences in the proteome profile of cannabidiol-treated skin fibroblasts following UVA or UVB irradiation in 2D and 3D cell cultures," *Cells*, vol. 8, no. 9, p. 995, 2019.

[35] S. S. Htwe, H. Harrington, A. Knox et al., "Investigating NF-*K*B signaling in lung fibroblasts in 2D and 3D culture systems," *Respiratory Research*, vol. 16, no. 1, 2015.

[36] R. J. Petrie and K. M. Yamada, "Fibroblasts lead the way: a unified view of 3D cell motility," *Trends in Cell Biology*, vol. 25, no. 11, pp. 666–674, 2015.

[37] S. Hofer, M. Stonig, V. Wally et al., "Contradictory effects of chemical filters in UV/ROS-stressed human keratinocyte and fibroblast cells," *ALTEX*, vol. 36, no. 2, pp. 231–244, 2019.

[38] L. S. Chua, "A review on plant-based rutin extraction methods and its pharmacological activities," *Journal of Ethnopharmacology*, vol. 150, no. 3, pp. 805–817, 2013.

[39] A. Ganeshpurkar and A. K. Saluja, "The pharmacological potential of rutin," *Saudi Pharm. J.*, vol. 25, no. 2, pp. 149–164, 2017.

[40] S. Sharma, A. Ali, J. Ali, J. K. Sahni, and S. Baboota, "Rutin: therapeutic potential and recent advances in drug delivery," *Expert Opinion on Investigational Drugs*, vol. 22, no. 8, pp. 1063–1079, 2013.

[41] C. Manach, C. Morand, C. Demigné, O. Texier, F. Régérat, and C. Rémésy, "Bioavailability of rutin and quercetin in rats," *FEBS Letters*, vol. 409, no. 1, pp. 12–16, 1997.

[42] I. Erlund, T. Kosonen, G. Alfthan et al., "Pharmacokinetics of quercetin from quercetin aglycone and rutin in healthy volunteers," *European Journal of Clinical Pharmacology*, vol. 56, no. 8, pp. 545–553, 2000.

[43] P.-W. Wang, Y.-C. Hung, T.-Y. Lin et al., "Comparison of the biological impact of UVA and UVB upon the skin with functional proteomics and immunohistochemistry," *Antioxidants*, vol. 8, no. 12, p. 569, 2019.

[44] J. Deng, H. P. Harding, B. Raught et al., "Activation of gcn2 in uv-irradiated cells inhibits translation," *Current Biology*, vol. 12, no. 15, pp. 1279–1286, 2002.

[45] B. Kaplan, B. Gönül, S. Dinçer, F. N. D. Kaya, and A. Babül, "Relationships Between Tensile Strength, Ascorbic Acid, Hydroxyproline, and Zinc Levels of Rabbit Full-Thickness Incision Wound Healing," *Surgery Today*, vol. 34, no. 9, pp. 747–751, 2004.

[46] C. T. Aiken, R. M. Kaake, X. Wang, and L. Huang, "Oxidative stress-mediated regulation of proteasome complexes," *Molecular & Cellular Proteomics*, vol. 10, no. 5, p. R110.006924, 2011.

[47] C. M. Pickart and I. A. Rose, "Ubiquitin carboxyl-terminal hydrolase acts on ubiquitin carboxyl-terminal amides," *The Journal of Biological Chemistry*, vol. 260, no. 13, pp. 7903–7910, 1985.

[48] T. L. Chang, "Inhibitory effect of flavonoids on 26S proteasome activity," *Journal of Agricultural and Food Chemistry*, vol. 57, no. 20, pp. 9706–9715, 2009.

[49] G. Perrone, T. Hideshima, H. Ikeda et al., "Ascorbic acid inhibits antitumor activity of bortezomib in vivo," *Leukemia*, vol. 23, no. 9, pp. 1679–1686, 2009.

[50] W. Zou, P. Yue, N. Lin et al., "Vitamin C inactivates the proteasome inhibitor PS-341 in human cancer cells," *Clinical Cancer Research*, vol. 12, no. 1, pp. 273–280, 2006.

[51] Y. Zhao, C. F. Zhang, H. Rossiter et al., "Autophagy is induced by UVA and promotes removal of oxidized phospholipids and protein aggregates in epidermal keratinocytes," *The Journal of Investigative Dermatology*, vol. 133, no. 6, pp. 1629–1637, 2013.

[52] Y. Kamenisch, I. Ivanova, K. Drexler, and M. Berneburg, "UVA, metabolism and melanoma: UVA makes melanoma hungry for metastasis," *Experimental Dermatology*, vol. 27, no. 9, pp. 941–949, 2018.

[53] L. Takahashi, M. A. Sert, A. M. Kelmer-Bracht, A. Bracht, and E. L. Ishii-Iwamoto, "Effects of rutin and quercetin on mitochondrial metabolism and on ATP levels in germinating tissues of Glycine max," *Plant Physiology and Biochemistry*, vol. 36, no. 7, pp. 495–501, 1998.

[54] M. J. González, G. Rosario-Pérez, A. M. Guzmán et al., "Mitochondria, energy and Cancer: the relationship with ascorbic acid," *J. Orthomol. Med.*, vol. 25, no. 1, pp. 29–38, 2010.

[55] H. Nojiri, T. Shimizu, M. Funakoshi et al., "Oxidative stress causes heart failure with impaired mitochondrial respiration," *The Journal of Biological Chemistry*, vol. 281, no. 44, pp. 33789–33801, 2006.

[56] J. Yang, J. Guo, and J. Yuan, "In vitro antioxidant properties of rutin," *LWT - Food Science and Technology*, vol. 41, no. 6, pp. 1060–1066, 2008.

[57] S. Ciesielska, P. Bil, K. Gajda, A. Poterala-Hejmo, D. Hudy, and J. Rzeszowska-Wolny, "Cell type-specific differences in redox regulation and proliferation after low UVA doses," *PLoS One*, vol. 14, no. 1, p. e0205215, 2019.

[58] F. Mohammadi, A. Soltani, A. Ghahremanloo, H. Javid, and S. I. Hashemy, "The thioredoxin system and cancer therapy: a review," *Cancer Chemotherapy and Pharmacology*, vol. 84, no. 5, pp. 925–935, 2019.

[59] Y. Zhang, A. Ali, Z. Jin, Y. Pei, and G. Yang, "Induction of cystathionine gamma-lyase expression and metallothionein-1 S-sulfhydration alleviate cadmium-induced cell death in myoblast cells," *Ecotoxicology and Environmental Safety*, vol. 179, pp. 222–231, 2019.

[60] Z. Zhou, B. Luo, X. Liu et al., "Flavonoid-alkylphospholipid conjugates elicit dual inhibition of cancer cell growth and lipid accumulation," *Chemical Communications*, vol. 55, no. 61, pp. 8919–8922, 2019.

[61] T. Quan, E. Little, H. Quan, Z. Qin, J. J. Voorhees, and G. J. Fisher, "Elevated matrix metalloproteinases and collagen fragmentation in photodamaged human skin: impact of altered extracellular matrix microenvironment on dermal fibroblast function," *The Journal of Investigative Dermatology*, vol. 133, no. 5, pp. 1362–1366, 2013.

[62] B. Orzechowska, J. Pabijan, J. Wiltowska-Zuber, J. Zemła, and M. Lekka, "Fibroblasts change spreading capability and mechanical properties in a direct interaction with keratinocytes in conditions mimicking wound healing," *Journal of Biomechanics*, vol. 74, pp. 134–142, 2018.

[63] M. Biernacki, E. Ambrożewicz, A. Gęgotek, M. Toczek, and E. Skrzydlewska, "Long-term administration of fatty acid amide hydrolase inhibitor (URB597) to rats with spontaneous hypertension disturbs liver redox balance and phospholipid metabolism," *Advances in Medical Sciences*, vol. 64, no. 1, pp. 15–23, 2019.

[64] V. De Pinto, A. Messina, D. J. R. Lane, and A. Lawen, "Voltage-dependent anion-selective channel (VDAC) in the plasma membrane," *FEBS Letters*, vol. 584, no. 9, pp. 1793–1799, 2010.

[65] J. Hao, W.-W. Li, H. Du et al., "Role of Vitamin C in Cardioprotection of Ischemia/Reperfusion Injury by Activation of Mitochondrial KATP Channel," *Chemical and Pharmaceutical Bulletin*, vol. 64, no. 6, pp. 548–557, 2016.

[66] D. G. Mostafa, E. F. Khaleel, R. M. Badi, G. A. Abdel-Aleem, and H. M. Abdeen, "Rutin hydrate inhibits apoptosis in the brains of cadmium chloride-treated rats via preserving the mitochondrial integrity and inhibiting endoplasmic reticulum stress," *Neurological Research*, vol. 41, no. 7, pp. 594–608, 2019.

[67] R. Aber, W. Chan, S. Mugisha, and L. A. Jerome-Majewska, "Transmembrane emp24 domain proteins in development and disease," *Genet. Res. (Camb).*, vol. 101, 2019.

[68] F. Darchen and B. Goud, "Multiple aspects of Rab protein action in the secretory pathway: focus on Rab3 and Rab6," *Biochimie*, vol. 82, no. 4, pp. 375–384, 2000.

[69] H. Y. Choi, S. A. Chong, and M. J. Nam, "Resveratrol induces apoptosis in human SK-HEP-1 hepatic cancer cells," *Cancer Genomics Proteomics*, vol. 6, no. 5, pp. 263–268, 2009.

[70] Y. Perez-Riverol, A. Csordas, J. Bai et al., "The PRIDE database and related tools and resources in 2019: improving support for quantification data," *Nucleic Acids Research*, vol. 47, no. D1, pp. D442–D450, 2019.

Hindawi
Oxidative Medicine and Cellular Longevity
Volume 2020, Article ID 7178123, 14 pages
https://doi.org/10.1155/2020/7178123

Research Article

Protective Effect of Polydatin on Jejunal Mucosal Integrity, Redox Status, Inflammatory Response, and Mitochondrial Function in Intrauterine Growth-Retarded Weanling Piglets

Hao Zhang,[1,2,3] **Yanan Chen**,[1] **Yue Li**,[4] **and Tian Wang**[1]

[1]*College of Animal Science & Technology, Nanjing Agricultural University, Nanjing 210095, China*
[2]*Postdoctoral Research Station of Clinical Veterinary Medicine, College of Veterinary Medicine, Nanjing Agricultural University, Nanjing, Jiangsu, China 210095*
[3]*Shanghai Key Laboratory of Veterinary Biotechnology, Shanghai 200240, China*
[4]*Institute of Animal Science, Jiangsu Academy of Agricultural Sciences, Nanjing 210014, China*

Correspondence should be addressed to Tian Wang; tianwangnjau@163.com

Received 11 May 2020; Revised 23 August 2020; Accepted 25 September 2020; Published 12 October 2020

Academic Editor: Przemko Tylzanowski

Copyright © 2020 Hao Zhang et al. This is an open access article distributed under the Creative Commons Attribution License, which permits unrestricted use, distribution, and reproduction in any medium, provided the original work is properly cited.

Intrauterine growth retardation (IUGR) delays the gut development of neonates, but effective treatment strategies are still limited. This study used newborn piglets as a model to evaluate the protective effect of polydatin (PD) against IUGR-induced intestinal injury. In total, 36 IUGR piglets and an equal number of normal birth weight (NBW) littermates were fed either a basal diet or a PD-supplemented diet from 21 to 35 days of age. Compared with NBW, IUGR induced jejunal damage and barrier dysfunction of piglets, as indicated by observable bacterial translocation, enhanced apoptosis, oxidative and immunological damage, and mitochondrial dysfunction. PD treatment decreased bacterial translocation and inhibited the IUGR-induced increases in circulating diamine oxidase activity ($P = 0.039$) and D-lactate content ($P = 0.004$). The apoptotic rate ($P = 0.024$) was reduced by 35.2% in the PD-treated piglets, along with increases in villus height ($P = 0.033$) and in ratio of villus height to crypt depth ($P = 0.049$). PD treatment promoted superoxide dismutase ($P = 0.026$) and glutathione S-transferase activities ($P = 0.006$) and reduced malondialdehyde ($P = 0.015$) and 8-hydroxy-2′-deoxyguanosine accumulation ($P = 0.034$) in the jejunum. The PD-treated IUGR piglets showed decreased jejunal myeloperoxidase activity ($P = 0.029$) and tumor necrosis factor alpha content ($P = 0.035$) than those received a basal diet. PD stimulated nuclear sirtuin 1 ($P = 0.028$) and mitochondrial citrate synthase activities ($P = 0.020$) and facilitated adenosine triphosphate production ($P = 0.009$) in the jejunum of piglets. Furthermore, PD reversed the IUGR-induced declines in mitochondrial DNA content ($P = 0.048$), the phosphorylation of adenosine monophosphate-activated protein kinase alpha ($P = 0.027$), and proliferation-activated receptor gamma coactivator 1 alpha expression ($P = 0.033$). Altogether, the results indicate that PD may improve jejunal integrity, mitigate mucosal oxidative and immunological damage, and facilitate mitochondrial function in IUGR piglets.

1. Introduction

Intrauterine growth retardation (IUGR) refers to the failure of a fetus to achieve its genetic growth potential. This clinical problem affects approximately 5–10% of pregnancies and remains a predisposing factor for perinatal morbidity and mortality [1]. In most cases, IUGR results from uteroplacental insufficiency where a hemodynamic adaptation occurs with blood flow redistribution in the fetal body. This redistribution favors adequate perfusion to the vital organs like the brain and the heart to support the survival of fetus under adverse intrauterine circumstances, but it inevitably limits the supply of oxygen and nutrients to other organs including the small intestine [2]. Consequently, IUGR can delay the normal development of the small intestine in neonates [3–6].

The small intestine is the key location for nutrient digestion and absorption, but it also serves as a critical barrier against various infectious agents [7]. Previous studies have

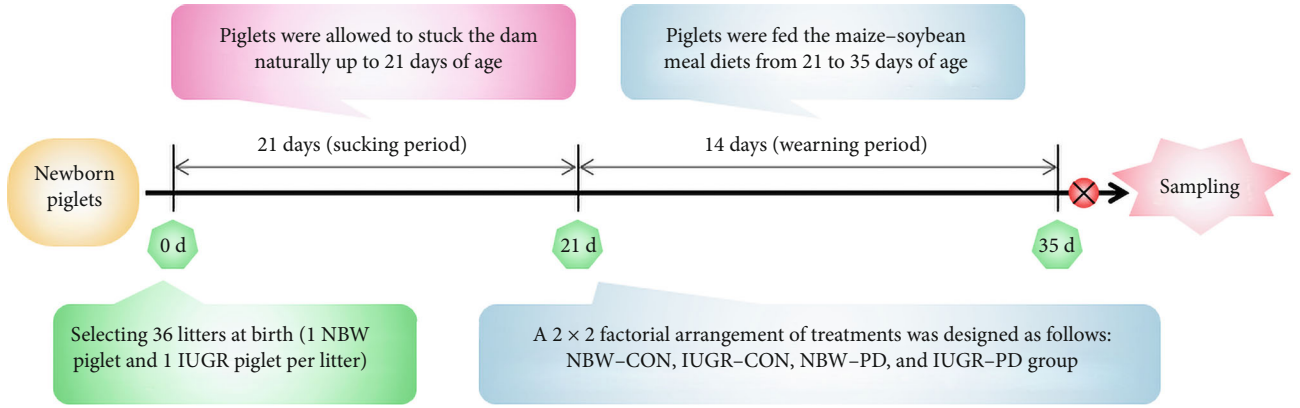

Figure 1: Schematic representation of the experimental procedures. IUGR: intrauterine growth retardation; IUGR-CON: intrauterine growth-retarded piglets fed a basal diet; IUGR-PD: intrauterine growth-retarded piglets fed a polydatin-supplemented diet; NBW: normal birth weight; NBW-CON: normal birth weight piglets fed a basal diet; NBW-PD: normal birth weight piglets fed a polydatin-supplemented diet.

demonstrated that IUGR impairs small intestinal morphology, disturbs redox and immune status, and induces enterocyte apoptosis and mucosal damage. The end result is a decrease in the ability of neonates to resist diseases and, ultimately, a compromised growth performance [4–6, 8, 9]. Finding appropriate ways to alleviate IUGR-induced damage to the small intestine of neonates is therefore critical.

Emerging evidence now indicates that polydatin (PD, also known as piceid) is a promising therapeutic treatment for intestinal injury [10–12]. This naturally occurring polyphenol has several health benefits, such as antioxidant and anti-inflammatory activities, and can be found in nonalcoholic grape juices and the traditional Chinese herb *Polygonum cuspidatum*. PD has potent bioactive properties, with antioxidant activities that can protect enterocytes against oxidative stress induced by hydrogen peroxide [11]. It may also serve as a protective substance to maintain mitochondrial function and facilitate the supply of energy in intestinal epithelial cells [11].

Recent studies have demonstrated that PD improves the features of intestinal damage in animal models [12–14]. In mice with acute colitis induced by dextran sulfate sodium, PD has been found to ameliorate the colitis symptoms and prevent oxidative stress and apoptosis in colon tissues [12]. In a mouse model of radiation-induced intestinal injury, PD effectively preserved mucosal morphology and inhibited the radiation-induced increase in intestinal endothelial apoptosis [13]. PD can also functionally regulate intestinal and systematic inflammatory responses [10, 14].

At present, however, little information is available regarding the use of PD as a nutritional supplement in IUGR offspring, and satisfactory strategies for the treatment of intestinal damage due to IUGR in neonates remain limited. Therefore, the present study was conducted using the piglet as a model to test the hypothesis that dietary supplementation with PD may have the potential to protect against small intestinal injury induced by IUGR. Notably, the spontaneous IUGR piglet is currently recognized as an ideal model for the research on IUGR in human infants, as increasing evidence now points to physiological and metabolic similarities between swine and humans [15]. In this regard, this study may help develop appropriate therapeutic approaches for treating intestinal disorders in the IUGR neonates.

2. Materials and Methods

2.1. Experimental Animals and Design. The animal experimentation and the corresponding protocols performed in this study (Permit number SYXK-2017-0027) were approved by the Nanjing Agricultural University Institutional Animal Care and Use Committee. Crossbred piglets (Duroc × [Landrace × Yorkshire]) were obtained from sows of the experimental herd of the Anyou Biotechnology Group Co., Ltd. (Taicang, Jiangsu, China). Piglets with a BW near the mean value of the herd (less than 0.5 SD) were identified as the normal BW (NBW) piglets, and the IUGR piglets were defined as having a 2 SD lower BW [4, 16, 17]. At birth, 36 female NBW piglets (1.56 ± 0.08) and an equal number of same-sex IUGR littermates (0.91 ± 0.10) were selected from 36 litters (one NBW piglet and one IUGR piglet per litter) from the herd, for a total of 72 neonatal piglets. All piglets were weaned at 21 days of age and then moved from the farrowing room to the weaner unit. A 2×2 factorial design was used with two levels of BW factors (i.e., NBW and IUGR) and two levels of diet factors (i.e., fed either a basal diet [CON] or a diet supplemented with PD at a dosage of 250 mg/kg [PD]). Each treatment had six replicates (pens) and each replicate had 6 piglets (Figure 1). The composition and nutrient levels of the basal diet are listed in Supplementary Table 1. The body weight and feed intake of piglets in each pen were recorded at 21 and 35 days of age to calculate their average daily gain (ADG), average daily feed intake (ADFI), and feed efficiency (FE) during the entire period of feeding trial.

2.2. Sample Collection. At 35 days of age, one piglet was randomly selected from each replicate of per treatment for blood sample collection after overnight fasting. Heparinized blood was collected from the precaval vein of piglets and its plasma

was obtained by centrifugation. The selected piglets were then euthanized by exsanguination after electrical stunning, and the small intestine was immediately collected. Two continuous sections (1.5 cm) were collected from the middle position of the whole jejunum. One sample was fixed in 4% paraformaldehyde (#G1101; Wuhan Servicebio Technology Co., Ltd., Wuhan, Hubei, China), and the other one was immersed in *in situ* hybridization fixing solution (#G1113; Wuhan Servicebio Technology Co., Ltd.). An additional jejunum section (approximately 20 cm) was cut from the adjacent position for the collection of mucosal samples. The plasma and mucosal samples were stored in −80°C freezers for subsequent biochemical analysis.

2.3. Plasma Parameters. Circulating diamine oxidase (DAO) activity was analyzed using a colorimetric assay kit (#A088-1-1; Nanjing Jiancheng Institute of Bioengineering, Nanjing, Jiangsu, China) based on the spectrophotometry method of Hosoda et al. [18]. The content of D-lactate in plasma was determined using a commercial kit (#AAT-13811) obtained from AAT Bioquest (Sunnyvale, CA, USA). All procedures were performed with strict adherence to the manufacturer's instructions.

2.4. Intestinal Morphology Observation. Jejunal segments were dehydrated and embedded in paraffin after fixation in paraformaldehyde solution for 24 h. Specimens were sliced into 5 μm thick sections and stained with hematoxylin and eosin for morphological evaluation. Twenty well-oriented and intact villi and adjacent crypts per slide were randomly selected for the evaluation of jejunal mucosal morphology. Villus height (VH) and crypt depth (CD) were determined by microscopy (Nikon 80i; Nikon, Tokyo, Japan) by an assessor blinded to the treatments.

2.5. Fluorescence In Situ Hybridization (FISH). Paraffin-embedded jejunal tissue slides (5 μm) were deparaffinized and hybridized to the universal eubacterial oligonucleotide probe EUB-338 (5′-GCTGCCTCCCGTAGGAGT-3′) or to a control probe NONEUB-338 (5′-CGACGGAGGGCATC CTCA-3′), according to the method described previously [19]. The 5-prime ends of the probes were labeled with Cy3 (EUB-338) or FAM (NONEUB-338). The Universal *In Situ* Hybridization Detection Kit III (#MK1031) was used for FISH in this study. All procedures were performed in accordance with the experimental protocols provided by the manufacturer (Boster, Wuhan, China). Stained bacteria were observed with a fluorescence microscope (Nikon 80i).

2.6. Terminal Deoxynucleotidyl Transferase-Mediated dUTP Nick End Labeling (TUNEL). The percentage of apoptotic cells was measured using a TUNEL assay kit (#A113-03), according to the manufacturer's guidelines (Vazyme, Nanjing, Jiangsu, China). Paraffin sections were deparaffinized and then pretreated with proteinase K (20 μg/mL dissolved in phosphate-buffered saline) at room temperature for 20 min. The slides were then incubated with the TUNEL reagents in the dark at 37°C for 1 h. The nuclei were identified by staining with 4′-6-diamidino-2-phenylindole (DAPI) dissolved in antifade mounting medium (#P0131; Beyotime, Shanghai, China). The number of TUNEL-labeled cells in fifteen randomly fields per section was quantified by a blinded observer using a fluorescence microscope.

2.7. Mucosal Redox and Immune Status. Approximately 300 mg of frozen jejunal mucosa samples was placed in 1 : 9 (wt/vol) saline solution and then homogenized with a high-speed benchtop homogenizer (Tekmar, Cincinnati, OH, USA). The resulting mucosal homogenate was centrifuged at 15,000 g for 10 min at 4°C, and the supernatant was used for the analysis of superoxide dismutase (SOD; #A001-1-2), glutathione peroxidase (GSH-Px; #A005-1-2), catalase (CAT; #A007-1-1), glutathione S-transferase (GST; #A004-1-1), glutathione reductase (GR; #A062-1-1), and myeloperoxidase (MPO; #A044-1-1) activities and reduced glutathione (GSH; #A006-1-1) and malondialdehyde (MDA; #A003-1-2) concentrations with colorimetric kits purchased from Nanjing Jiancheng Institute of Bioengineering. For the detection of 8-hydroxy-2′-deoxyguanosine (8-OHDG), total DNA of jejunal mucosa was extracted with a Genomic DNA Isolation Kit (#K281-50; BioVision, Milpitas, CA, USA) and the 8-OHDG content in the DNA samples was tested using a 8-OHDG Enzyme-Linked Immunosorbent Assay (ELISA) Detection Kit (#589320-96S) following the manufacturer's protocol (Cayman Chemical, Ann Arbor, MI, USA). The concentrations of tumor necrosis factor alpha (TNF-α; CSB-E16980p) and interleukin-10 (IL-10; CSB-E06779p) were determined by porcine-specific ELISA kits obtained from CUSABIO Biotech (Wuhan, China). The detection ranges were 0.047 to 3 ng/mL for TNF-α and 6.25 to 400 pg/mL for IL-10, respectively. The minimum detectable doses were less than 0.040 ng/mL for TNF-α and 1.56 pg/mL for IL-10. The inter- and intra-assay coefficients of variance of the assay kits were less than 8% and 10%, respectively.

Protein concentrations of the samples were determined according to the manufacturer's instructions using an Enhanced Bicinchoninic Acid (BCA) Protein Assay Kit (#P0010; Beyotime). The data of each sample were normalized using the protein content to allow intersample comparisons.

2.8. Transmission Electron Microscopy. Jejunum samples were fixed in 2.5% glutaraldehyde in 0.1 M sodium cacodylate buffer overnight at 4°C and then postfixed with 1% osmium tetroxide in 0.2 M phosphate-buffered saline for 2 h at 4°C. Following which, the sections were dehydrated with a graded series of ethanol solutions, rinsed in propylene oxide, and embedded in epoxy resin. Thin sections were cut with a Reichert Ultracut microtome (Leica, Deerfield, IL, USA) and observed and photographed using a transmission electron microscope (Hitachi H-7650, Tokyo, Japan).

2.9. Detection of Mitochondrial DNA (mtDNA) Content. After the isolation of total DNA as described above, the copy number of mtDNA in each DNA sample was measured by coamplifying the mitochondrial D-loop (mtD-loop) and beta actin (ACTB) genes by quantitative PCR using the QuantStudio 5 Real-Time PCR System and the SYBR Green reagent (#Q311-02; Vazyme). The following primer sequences were used: mtD-loop sense primer GATCGTACATAGCACA

Table 1: Primer sequences used for real-time PCR assay.

Name[1]	GenBank[2]	Sequence[3] (5′ → 3′)	Length (bp)
ZO1	XM_021098827.1	AGGCGTGTTTAACAGCAACG CCAAAGGACTCAGCAGGGTT	182
OCLN	NM_001163647.2	CAGGTGCACCCTCCAGATTG ATGTCGTTGCTGGGTGCATA	167
CLDN1	NM_001244539.1	ACAGGAGGGAAGCCATTTTCA TTTAAGGACCGCCCTCTCCC	82
CLDN2	NM_001161638.1	GGATCCTGCGGGACTTCTAC TGGAGCGATTTCCTTGCAGT	153
CLDN3	NM_001160075.1	GAGACCAGTCCACCCAGATG AGGTTTCATGGTCCGTGCTG	147
GAPDH	NM_001206359.1	CCAAGGAGTAAGAGCCCCTG AAGTCAGGAGATGCTCGGTG	125
ACTB	XM_003124280.5	TGGAACGGTGAAGGTGACAG CTTTTGGGAAGGCAGGGACT	176

[1]*ACTB*: beta actin; *CLDN1*: claudin 1; *CLDN2*: claudin 2; *CLDN3*: claudin 3; *GAPDH*: glyceraldehyde-3-phosphate dehydrogenase; *OCLN*: occludin; *ZO1*: zonula occludens 1. [2]GenBank accession number. [3]Shown as the forward primer followed by the reverse primer.

Table 2: Effect of dietary polydatin supplementation on the growth performance of weanling piglets with different birth weights from 21 to 35 days of age.

Items[1,2]	CON		PD		SEM	*P* value		
	NBW	IUGR	NBW	IUGR		BW	Diet	$B \times D$
Initial body weight (kg)	6.64[a]	4.83[b]	6.66[a]	4.81[b]	0.20	<0.001	0.983	0.916
Final body weight (kg)	9.45[a]	6.69[b]	9.39[a]	7.19[b]	0.28	<0.001	0.300	0.194
ADG (g/d)	200.20[a]	132.94[c]	195.24[ab]	169.84[b]	7.04	<0.001	0.101	0.035
ADFI (g/d)	286.11[a]	209.92[b]	280.36[a]	251.98[a]	8.66	0.001	0.171	0.076
FE (g/g)	0.70	0.63	0.70	0.68	0.01	0.120	0.373	0.465

[1]Data are presented as the means and SEM, $n = 6$. Mean values with different letters indicate a significant difference ($P < 0.05$). [2]ADG: average daily gain; ADFI: average daily feed intake; BW: birth weight; $B \times D$: the interaction effect of the main effects (BW and diet); CON: basal diet; FE: feed efficiency; IUGR: intrauterine growth retardation; NBW: normal birth weight; PD: polydatin-supplemented diet.

TATCATGTC and anti-sense primer GGTCCTGAAGT AAGAACCAGATG and ACTB sense primer CCCCTC CTCTCTTGCCTCTC and anti-sense primer AAAAGT CCTAGGAAAATGGCAGAAG. The $2^{-\Delta\Delta Ct}$ method was performed to calculate the copy number of mtDNA [20].

2.10. Measurement of Mitochondrial Enzyme Activities. Mitochondria were isolated from jejunum mucosa with the Tissue Mitochondria Isolation Kit (#C3606; Beyotime). After quantifying the protein content of the mitochondrial suspension, the activities of citrate synthase (CS; #BC1065), electron transport chain (ETC) complexes I (#BC0515), II (#BC3230), III (#BC3240), and IV (#BC0945), and adenosine triphosphate (ATP) synthase (#BC1445) were determined by colorimetric kits following the guidelines of the manufacturer (Solarbio, Beijing, China).

2.11. Determination of Mucosal ATP Content. Jejunal mucosa samples were weighed, ground, blended with boiling double-distilled H_2O, and boiled for 30 min. After centrifugation, the supernatant was collected to determine the ATP content of each sample with a commercial kit (#A095-1-1; Nanjing Jiancheng Institute of Bioengineering). The results were expressed as μmol/g wet weight.

2.12. Sirtuin 1 (SIRT1) Activity. Jejunal nuclear fractions were prepared based on a method described by Park et al. [21]. The deacetylase activity of SIRT1 in the jejunal mucosa was measured with a SIRT1 Activity Detection Kit (#50287.2) according to the recommended protocols of the manufacturer (Genmed, Shanghai, China).

2.13. Gene Expression. Total RNA was extracted from jejunal mucosa samples using the Total RNA Isolation Reagent (#R401-01; Vazyme). Determination of the yields, quality, and integrity of isolated RNA samples were performed based on the method reported by Li et al. [8]. After that, the first-strand complementary DNA (cDNA) was synthesized from total RNA with the High-Capacity cDNA Reverse Transcription Kit (#RR036A; Takara Biotechnology, Dalian, Liaoning, China). Real-time PCR reactions were performed following the recommended process of the manufacturer (Vazyme). Table 1 includes the details of the primer sequences used for the following target and reference genes: occludin (*OCLN*), zonula

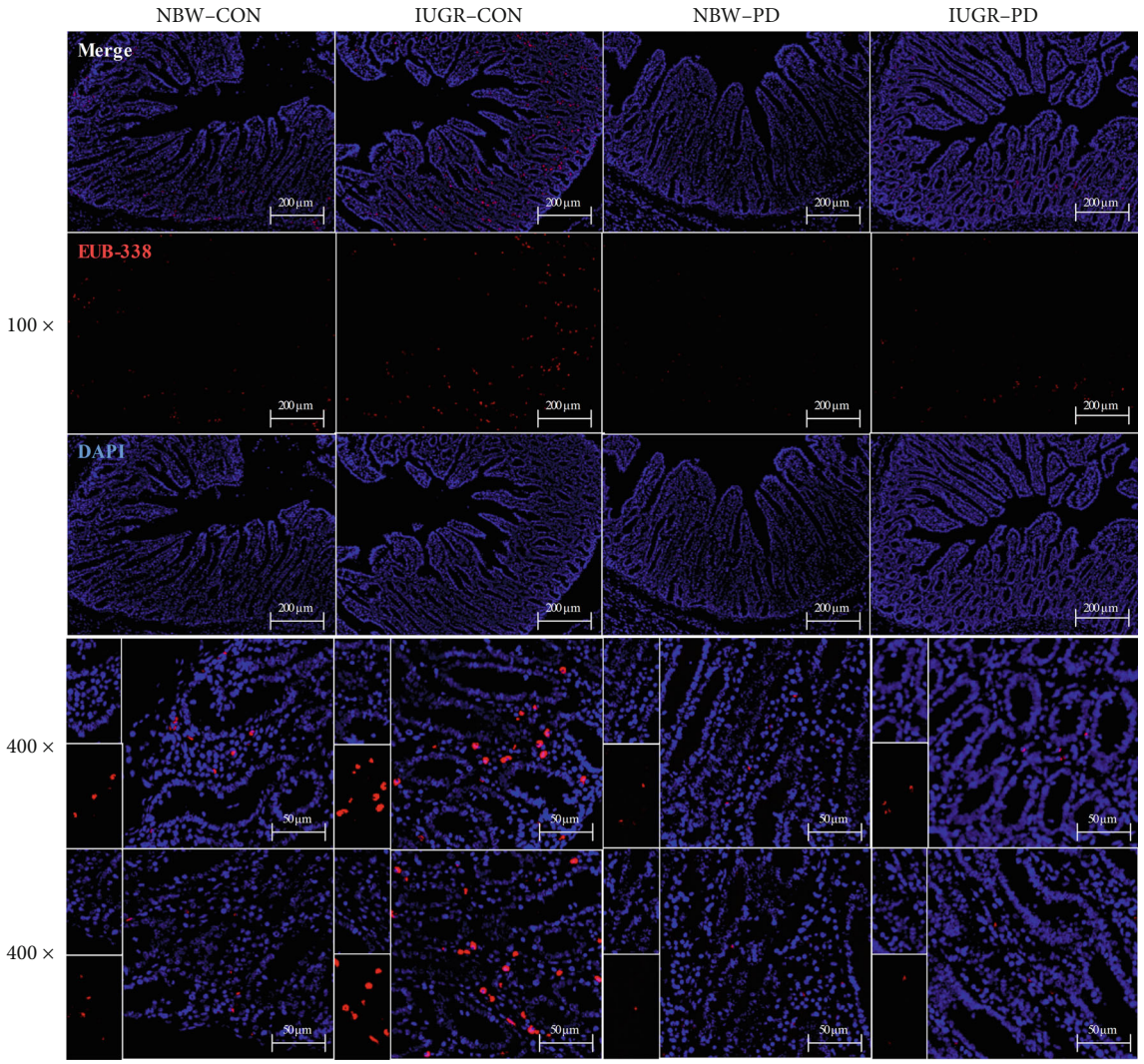

Figure 2: Representative micrographs of bacteria colonization detected by FISH using the Cy3-labeled oligonucleotide EUB-338. DAPI: 4′-6-diamidino-2-phenylindole; FISH: fluorescence *in situ* hybridization; IUGR-CON: intrauterine growth-retarded piglets fed a basal diet; IUGR-PD: intrauterine growth-retarded piglets fed a polydatin-supplemented diet; NBW-CON: normal birth weight piglets fed a basal diet; NBW-PD: normal birth weight piglets fed a polydatin-supplemented diet.

Table 3: Effect of dietary polydatin supplementation on the plasma diamine oxidase activity and D-lactate content of weanling piglets with different birth weights.

Items[1,2]	CON		PD		SEM	*P* value		
	NBW	IUGR	NBW	IUGR		BW	Diet	$B \times D$
DAO (U/mL)	26.95[b]	102.84[a]	36.67[b]	58.55[b]	8.35	0.001	0.174	0.039
D-Lactate (nmol/mL)	435.59[b]	891.20[a]	496.69[b]	564.18[b]	46.18	<0.001	0.039	0.004

[1]Data are presented as the means and SEM, $n = 6$. Mean values with different letters indicate a significant difference ($P < 0.05$). [2]BW: birth weight; $B \times D$: the interaction effect of the main effects (BW and diet); CON: basal diet; DAO: diamine oxidase; IUGR: intrauterine growth retardation; NBW: normal birth weight; PD: polydatin-supplemented diet.

occludens 1 (*ZO1*), claudin 1 (*CLDN1*), claudin 2 (*CLDN2*), claudin 3 (*CLDN3*), glyceraldehyde-3-phosphate dehydrogenase, and *ACTB*. The fold changes in the expression of specific mRNAs were calculated using the $2^{-\Delta\Delta Ct}$ method [20].

2.14. Western Blotting. Jejunal mucosa samples were lysed in ice-cold radioimmunoprecipitation assay reagent (#P0013B; Beyotime) containing protease inhibitors (#ST506; Beyotime) and phosphatase inhibitors (#P2850; Sigma-Aldrich, St. Louis, MO, USA). Protein solutions were obtained by centrifugation and then mixed with 5× sodium dodecyl sulfate sample buffer (#P0015; Beyotime). The mixture was boiled for 5 min. After determining protein content with the BCA detection kit, an equal amount of extracted

Table 4: Effect of dietary polydatin supplementation on the mRNA levels of jejunal tight junction complexes in weanling piglets with different birth weights.

Items[1,2]	CON		PD		SEM	*P* value		
	NBW	IUGR	NBW	IUGR		BW	Diet	$B \times D$
ZO1	1.00^{ab}	0.68^{b}	1.03^{a}	0.96^{ab}	0.06	0.090	0.171	0.279
OCLN	1.00^{b}	0.54^{c}	1.53^{a}	0.91^{bc}	0.10	0.001	0.004	0.579
CLDN1	1.00	1.13	1.04	0.59	0.11	0.456	0.259	0.187
CLDN2	1.00^{b}	1.60^{a}	1.26^{ab}	0.91^{b}	0.10	0.489	0.233	0.013
CLDN3	1.00	1.09	1.30	1.11	0.11	0.839	0.486	0.550

[1]Data are presented as the means and SEM, $n = 6$. Mean values with different letters indicate a significant difference ($P < 0.05$). [2]BW: birth weight; $B \times D$: the interaction effect of the main effects (BW and diet); *CLDN1*: claudin 1; *CLDN2*: claudin 2; *CLDN3*: claudin 3; CON: basal diet; IUGR: intrauterine growth retardation; NBW: normal birth weight; *OCLN*: occludin; PD: polydatin-supplemented diet; *ZO1*: zonula occludens 1.

Table 5: Effect of dietary polydatin supplementation on the jejunal morphology of weanling piglets with different birth weights.

Items[1,2]	CON		PD		SEM	*P* value		
	NBW	IUGR	NBW	IUGR		BW	Diet	$B \times D$
VH (μm)	451.63^{a}	359.04^{b}	479.05^{a}	422.55^{a}	13.14	0.001	0.033	0.376
CD (μm)	198.18	174.88	180.87	183.08	5.81	0.384	0.704	0.294
VH : CD (μm/μm)	2.31^{ab}	2.08^{b}	2.70^{a}	2.34^{ab}	0.09	0.071	0.049	0.677

[1]Data are presented as the means and SEM, $n = 6$. [2]BW: birth weight; $B \times D$: the interaction effect of the main effects (BW and diet); CD: crypt depth; CON: basal diet; IUGR: intrauterine growth retardation; NBW: normal birth weight; PD: polydatin-supplemented diet; VH: villus height; VH : CD: the ratio of villus height to crypt depth.

protein was separated by polyacrylamide gel electrophoresis in the presence of sodium dodecyl sulfate. The separated proteins were then transferred to an Immobilon-P transfer membrane (#IPVH00010; Millipore, Bedford, MA, USA). The membranes were blocked with 5% skimmed dry milk in Tris-buffered saline combined with 0.2% Tween-20 (TBST) at room temperature for 2 h. After three washes in TBST, the blots were incubated with the following primary antibodies at room temperature for 4 h: antiphosphorylated adenosine monophosphate-activated protein kinase alpha (AMPKα, phosphorylated at Thr^{172}) (#2535S; CST, Danvers, MA, USA; 1 : 1,000 dilution), anti-AMPKα (#2532S; CST; 1 : 1,000 dilution), anti-SIRT1 (#NBP2-27205; Novus Biologicals, Littleton, CO, USA; 1 : 750 dilution), antiperoxisome proliferation-activated receptor gamma coactivator 1 alpha (PGC-1α; #ab106814; Abcam, Cambridge, MA, USA; 1 : 1,000 dilution), and ACTB (#4970S; CST; 1 : 1,000 dilution). After incubation with appropriate secondary antibodies, the immunoreactive proteins were detected with an enhanced chemiluminescence HRP substrate (#WBKLS0100; Millipore, Bedford, MA, USA). The gray scale values of bands were measured using the Gel-Pro Analyzer program (version 4.0, Media Cybernetics, Inc., MD, USA).

2.15. Statistical Analysis. The Statistical Package for the Social Sciences (SPSS Inc., version 22.0; IBM Corporation, Armonk, NY, USA) was used for statistical analysis. The data were subjected to a two-way analysis of variance using the general linear model procedure to analyze the main effects of BW and diet and their interaction ($B \times D$). A *P* value of less than 0.05 was considered statistically significant. Duncan's post hoc test was used to explore all significant differences. All data are expressed as the mean and their pooled standard error (SEM).

3. Results

3.1. Growth Performance. Relative to the NBW piglets, IUGR decreased the initial ($P < 0.001$) and final body weights ($P < 0.001$) of piglets and reduced their ADG ($P < 0.001$) and ADFI ($P = 0.001$) during the first two weeks after weaning (Table 2). Supplementation with PD had no effect on body weights, ADG, ADFI, or FE of weanling piglets regardless of BW ($P > 0.05$). A significant interaction of BW and diet was observed for the ADG of piglets; the decrease in ADG in the IUGR piglets was not observed when IUGR piglets were supplemented with PD ($P = 0.035$).

3.2. Intestinal Barrier Function. The FISH analysis using the Cy3-labeled oligonucleotide EUB-338 revealed an increased bacterial colonization in the jejunal crypts of IUGR-CON piglets (Figure 2). Conversely, the jejunal sections from the IUGR-PD group showed decreased fluorescence signals for eubacterial staining to levels similar to those of their NBW counterparts. Monitoring of intestinal integrity by D-lactate concentration and DAO activity in the plasma revealed higher DAO activity ($P = 0.001$) and D-lactate concentration ($P < 0.001$) in the IUGR piglets than in their NBW littermates (Table 3). The PD-supplemented diet significantly reduced the content of circulating D-lactate ($P = 0.039$) when compared with the basal diet. In addition, the increments in DAO activity ($P = 0.039$) and D-lactate concentration ($P = 0.004$) in the IUGR piglets were reversed by supplementation with PD.

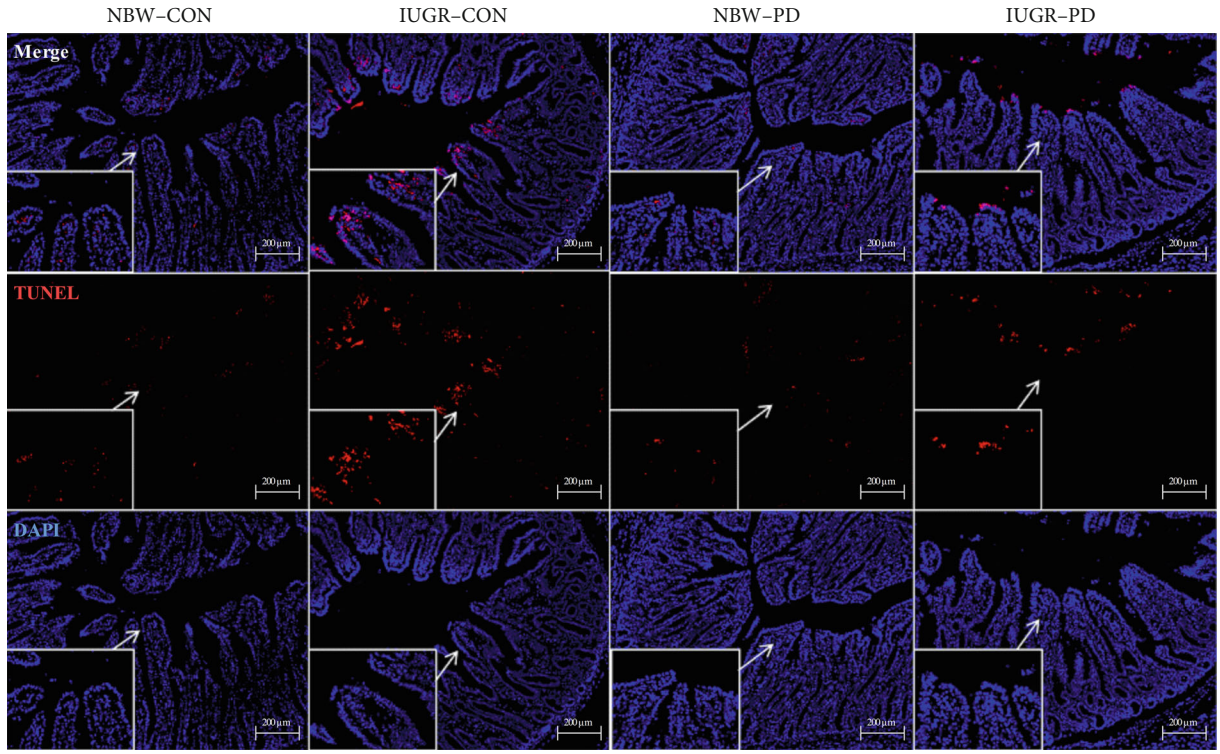

Figure 3: Representative micrographs of TUNEL staining carried out on paraformaldehyde-fixed jejunal sections of weanling piglets. DAPI: 4′-6-diamidino-2-phenylindole; IUGR-CON: intrauterine growth-retarded piglets fed a basal diet; IUGR-PD: intrauterine growth-retarded piglets fed a polydatin-supplemented diet; NBW-CON: normal birth weight piglets fed a basal diet; NBW-PD: normal birth weight piglets fed a polydatin-supplemented diet; TUNEL: terminal deoxynucleotidyl transferase-mediated dUTP nick end labeling.

Table 6: Effect of dietary polydatin supplementation on the jejunal apoptosis and caspase activities of weanling piglets with different birth weights.

Items[1,2]	CON		PD		SEM	*P* value		
	NBW	IUGR	NBW	IUGR		BW	Diet	$B \times D$
Apoptosis (%)	2.68^{b}	8.20^{a}	3.07^{b}	3.98^{b}	0.59	0.001	0.024	0.008
Caspase-3 (U/mg protein)	22.12^{b}	43.48^{a}	24.74^{b}	25.92^{b}	2.55	0.010	0.073	0.019
Caspase-8 (U/mg protein)	6.79	10.71	8.35	7.29	0.67	0.269	0.470	0.062
Caspase-9 (U/mg protein)	14.15^{ab}	18.79^{a}	9.59^{b}	13.99^{ab}	1.01	0.011	0.009	0.940

[1]Data are presented as the means and SEM, $n = 6$. Mean values with different letters indicate a significant difference ($P < 0.05$). [2]BW: birth weight; $B \times D$: the interaction effect of the main effects (BW and diet); CON: basal diet; IUGR: intrauterine growth retardation; NBW: normal birth weight; PD: polydatin-supplemented diet.

3.3. Jejunal Tight Junction Expression. The mRNA abundance of *OCLN* ($P = 0.001$) was significantly reduced by IUGR in the piglet jejunum (Table 4). By contrast, supplementation with PD increased the expression of jejunal *OCLN* ($P = 0.004$). PD supplementation also reversed the IUGR-induced increase in the mRNA level of *CLDN2* ($P = 0.013$). Neither BW nor diet affected the mRNA expression of jejunal *ZO1*, *CLDN1*, or *CLDN3* in the piglet jejunum ($P > 0.05$).

3.4. Jejunal Morphology. Relative to the NBW piglets, the IUGR piglets showed a decrease in jejunal VH ($P = 0.001$; Table 5). PD increased jejunal VH ($P = 0.033$) and the VH : CD ratio ($P = 0.049$) of piglets relative to those fed a basal diet. No difference was found in the jejunal CD of piglets among the groups ($P > 0.05$).

3.5. Jejunal Apoptotic Rate and Caspase Activities. An increased apoptotic rate ($P = 0.001$; Figure 3) was noted in the jejunum of IUGR piglets relative to their NBW counterparts (Table 6), along with increased caspase-3 ($P = 0.010$) and caspase-9 ($P = 0.011$) activities. Supplementation with PD reduced the percentage of jejunal apoptosis ($P = 0.024$) and the activity of caspase-9 ($P = 0.009$) in comparison with the basal diet. The IUGR piglets showed decreased apoptotic rate ($P = 0.008$) and caspase-3 activity ($P = 0.019$) when supplemented with PD.

3.6. Jejunal Redox Status. IUGR induced a decrease in the GSH content ($P = 0.001$) and increases in MDA ($P = 0.023$) and 8-OHDG formation ($P = 0.017$) in the jejunum of IUGR piglets when compared with their NBW counterparts

Table 7: Effect of dietary polydatin supplementation on the jejunal redox status of weanling piglets with different birth weights.

Items[1,2]	CON		PD		SEM	*P* value		
	NBW	IUGR	NBW	IUGR		BW	Diet	$B \times D$
SOD (U/mg protein)	62.85^{ab}	52.99^{b}	70.58^{a}	68.13^{a}	2.62	0.210	0.026	0.445
GSH-Px (U/mg protein)	60.97	57.82	65.95	51.20	3.18	0.177	0.899	0.376
CAT (U/mg protein)	7.77	8.14	8.39	6.87	0.26	0.267	0.526	0.075
GST (U/mg protein)	79.92^{ab}	70.71^{b}	97.09^{a}	97.48^{a}	4.08	0.541	0.006	0.506
GR (U/g protein)	42.27	37.59	45.80	40.36	1.69	0.149	0.361	0.911
GSH (μmol/mg wet weight)	0.45^{a}	0.31^{b}	0.47^{a}	0.38^{ab}	0.02	0.001	0.105	0.384
MDA (nmol/mg protein)	0.57^{b}	0.90^{a}	0.60^{b}	0.56^{b}	0.04	0.023	0.015	0.006
8-OHDG (ng/mg DNA)	0.85^{b}	1.35^{a}	0.75^{b}	0.89^{b}	0.07	0.017	0.034	0.158

[1]Data are presented as the means and SEM, $n = 6$. Mean values with different letters indicate a significant difference ($P < 0.05$). [2]BW: birth weight; $B \times D$: the interaction effect of the main effects (BW and diet); CAT: catalase; CON: basal diet; GSH: reduced glutathione; GSH-Px: glutathione peroxidase; GR: glutathione reductase; GST: glutathione S-transferase; IUGR: intrauterine growth retardation; MDA: malondialdehyde; NBW: normal birth weight; 8-OHDG: 8-hydroxy-2′-deoxyguanosine; PD: polydatin-supplemented diet; SOD: superoxide dismutase.

Table 8: Effect of dietary polydatin supplementation on the jejunal inflammatory responses of weanling piglets with different birth weights.

Items[1,2]	CON		PD		SEM	*P* value		
	NBW	IUGR	NBW	IUGR		BW	Diet	$B \times D$
MPO (U/g protein)	41.58^{b}	85.26^{a}	46.71^{b}	50.68^{b}	5.31	0.010	0.096	0.029
TNF-α (pg/mg protein)	47.90^{b}	94.52^{a}	38.15^{b}	47.00^{b}	6.02	0.003	0.003	0.035
IL-10 (pg/mg protein)	5.09	5.06	6.05	5.32	0.43	0.680	0.509	0.700

[1]Data are presented as the means and SEM, $n = 6$. Mean values with different letters indicate a significant difference ($P < 0.05$). [2]BW: birth weight; $B \times D$: the interaction effect of the main effects (BW and diet); CON: basal diet; IL-10: interleukin-10; IUGR: intrauterine growth retardation; MPO: myeloperoxidase; NBW: normal birth weight; PD: polydatin-supplemented diet; TNF-α: tumor necrosis factor alpha.

Table 9: Effect of dietary polydatin supplementation on the jejunal energy metabolism of weanling piglets with different birth weights.

Items[1,2]	CON		PD		SEM	*P* value		
	NBW	IUGR	NBW	IUGR		BW	Diet	$B \times D$
CS (U/mg protein)	15.11^{a}	10.79^{b}	17.36^{a}	15.13^{a}	0.78	0.021	0.020	0.432
Complex I (U/mg protein)	33.79^{ab}	18.07^{b}	41.31^{a}	31.15^{ab}	3.10	0.029	0.075	0.619
Complex II (U/mg protein)	19.38	19.42	13.34	16.97	1.47	0.540	0.165	0.549
Complex III (U/mg protein)	20.11^{a}	7.65^{b}	19.28^{a}	19.88^{a}	1.76	0.058	0.068	0.039
Complex IV (U/mg protein)	98.74	91.26	95.83	98.95	3.16	0.746	0.722	0.434
ATP synthase (U/mg protein)	19.69^{a}	14.87^{b}	17.64^{ab}	21.54^{a}	0.84	0.751	0.119	0.006
ATP (μmol/g wet weight)	0.48^{a}	0.33^{b}	0.56^{a}	0.49^{a}	0.03	0.017	0.009	0.383

[1]Data are presented as the means and SEM, $n = 6$. Mean values with different letters indicate a significant difference ($P < 0.05$). [2]ATP: adenosine triphosphate; BW: birth weight; $B \times D$: the interaction effect of the main effects (BW and diet); CON: basal diet; CS: citrate synthase; IUGR: intrauterine growth retardation; NBW: normal birth weight; PD: polydatin-supplemented diet.

(Table 7). Dietary PD supplementation increased the activities of jejunal SOD ($P = 0.026$) and GST ($P = 0.006$) and inhibited the generation of MDA ($P = 0.015$) and 8-OHDG ($P = 0.034$). Two-way ANOVA showed an obvious interaction between BW and diet for the concentration of MDA ($P = 0.006$). IUGR significantly elevated the MDA concentration in piglets fed a basal diet, but this increase was suppressed by PD supplementation.

3.7. Jejunal Inflammatory Responses. The activity of jejunal MPO ($P = 0.010$) and the TNF-α content ($P = 0.003$) were substantially increased in the IUGR group compared with the NBW group (Table 8). Supplementation with PD decreased TNF-α concentration ($P = 0.003$) and inhibited the IUGR-induced increase in MPO activity ($P = 0.029$) in the jejunum. No difference was observed in the amount of jejunal IL-10 protein among the groups ($P > 0.05$).

3.8. Jejunal Energy Metabolism. When compared with NBW piglets, IUGR piglets showed inhibited CS ($P = 0.021$) and complex I ($P = 0.029$) activities in the jejunum, along with a reduction in ATP production ($P = 0.017$; Table 9). Dietary PD supplementation increased the CS activity ($P = 0.020$) and improved the ATP generation ($P = 0.009$) in the jejunum irrespective of BW. PD supplementation increased the activities of complex III ($P = 0.039$) and ATP synthase ($P = 0.006$) in the IUGR jejunum. Neither BW nor diet affected the activity of complex II or IV among the groups ($P > 0.05$).

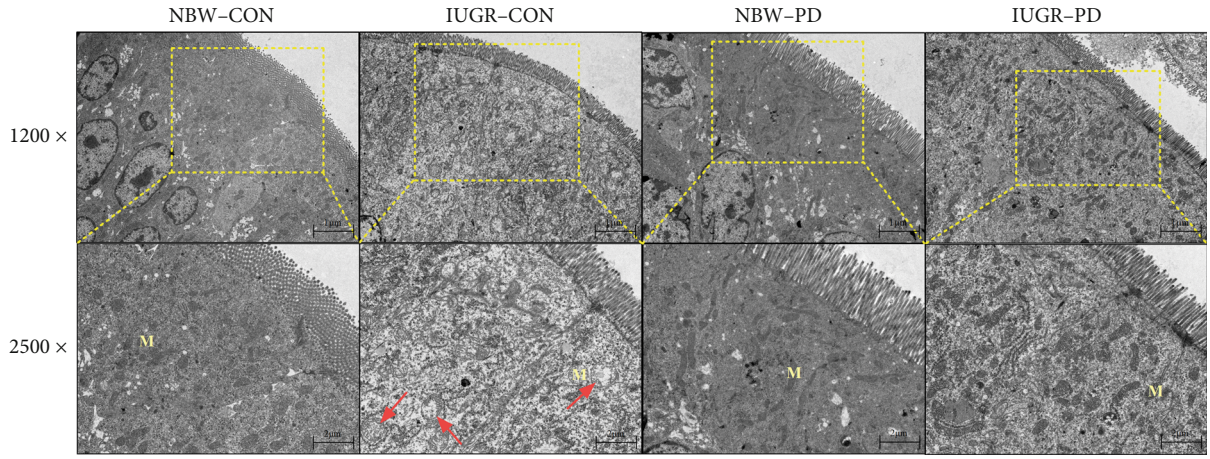

Figure 4: Effect of dietary polydatin supplementation on the jejunal mitochondrial ultrastructure of weanling piglets with different birth weights. Red arrows indicated the swelling of mitochondria. IUGR-CON: intrauterine growth-retarded piglets fed a basal diet; IUGR-PD: intrauterine growth-retarded piglets fed a polydatin-supplemented diet; M: mitochondrion; NBW-CON: normal birth weight piglets fed a basal diet; NBW-PD: normal birth weight piglets fed a polydatin-supplemented diet.

Table 10: Effect of dietary polydatin supplementation on the jejunal mitochondrial DNA content and sirtuin 1 activity of weanling piglets with different birth weights.

Items[1,2]	CON		PD		SEM	*P* value		
	NBW	IUGR	NBW	IUGR		BW	Diet	$B \times D$
mtDNA (fold to NBW-CON)	1.00^{a}	0.36^{b}	0.91^{a}	0.76^{a}	0.07	0.003	0.211	0.048
SIRT1 (nmol/min/mg protein)	183.56^{ab}	88.22^{b}	284.02^{a}	228.36^{ab}	27.96	0.152	0.028	0.700

[1]Data are presented as the means and SEM, $n = 6$. Mean values with different letters indicate a significant difference ($P < 0.05$). [2]ATP: adenosine triphosphate; BW: birth weight; $B \times D$: the interaction effect of the main effects (BW and diet); CON: basal diet; CS: citrate synthase; IUGR: intrauterine growth retardation; NBW: normal birth weight; PD: polydatin-supplemented diet.

3.9. Jejunal Mitochondrial Structure. The mitochondria of enterocytes in the NBW piglets were intact with dense matrix and regular cristae (Figure 4). By contrast, in the IUGR-CON piglets, quite a few mitochondria were markedly damaged with abnormal shape and disorganized cristae, probably due to oedema in the matrix of mitochondria. After a two-week administration of PD, the severity of mitochondrial swelling in enterocytes was effectively improved.

3.10. Jejunal Mitochondrial Biogenesis and the Associated Signaling Pathway. Piglets in the IUGR group exhibited significantly decreased mtDNA copy number ($P = 0.003$; Table 10) and PGC-1α protein expression ($P = 0.004$; Figure 5) in the jejunum compared with their NBW littermates. However, IUGR had no effect on SIRT1 activity, the expression levels of phosphorylated AMPKα (p-AMPKα), total AMPKα (t-AMPKα), and SIRT1, or the ratio of p-AMPKα to t-AMPKα ($P > 0.05$). PD supplementation promoted SIRT1 activity ($P = 0.028$), increased the relative phosphorylation level of AMPKα ($P = 0.034$), and upregulated the protein amount of PGC-1α ($P = 0.032$) in comparison with the basal diet. PD supplementation also reversed the IUGR-induced reductions in jejunal mtDNA copy number ($P = 0.048$) and the protein contents of phosphorylated AMPKα ($P = 0.027$) and PGC-1α ($P = 0.033$).

4. Discussion

The present findings demonstrated that IUGR was detrimental to the jejunal barrier function of weanling piglets, as evidenced by a greater intestinal permeability, increased bacterial translocation, and disturbed expression patterns of tight junction genes. Disruption of the jejunal barrier function increases the exposure risk of young piglets to exogenous pathogens, antigens, and other noxious factors, which may in turn promote mucosal injury and systemic inflammation [7]. This impaired barrier function may account for the increases in jejunal 8-OHDG and MDA contents, MPO activity, and TNF-α secretion observed in the IUGR piglets. These changes in the jejunum of the IUGR piglets were signs of oxidative stress and inflammation that can promote the occurrence and development of small intestinal injury [22].

The decreased mtDNA content and the lower efficiency of ATP production noted in the jejunum of IUGR piglets could also possibly reflect a disturbance in mitochondrial biogenesis and oxidative metabolism. Mitochondrial dysfunction limits the availability of ATP for both nutrient absorption and the renewal of the intestinal epithelium, resulting in malabsorption and intestinal disorders [23]. Collectively, these effects of IUGR act in concert to incite the small intestinal injury observed in the IUGR piglets and may therefore be part of potential mechanisms that explain

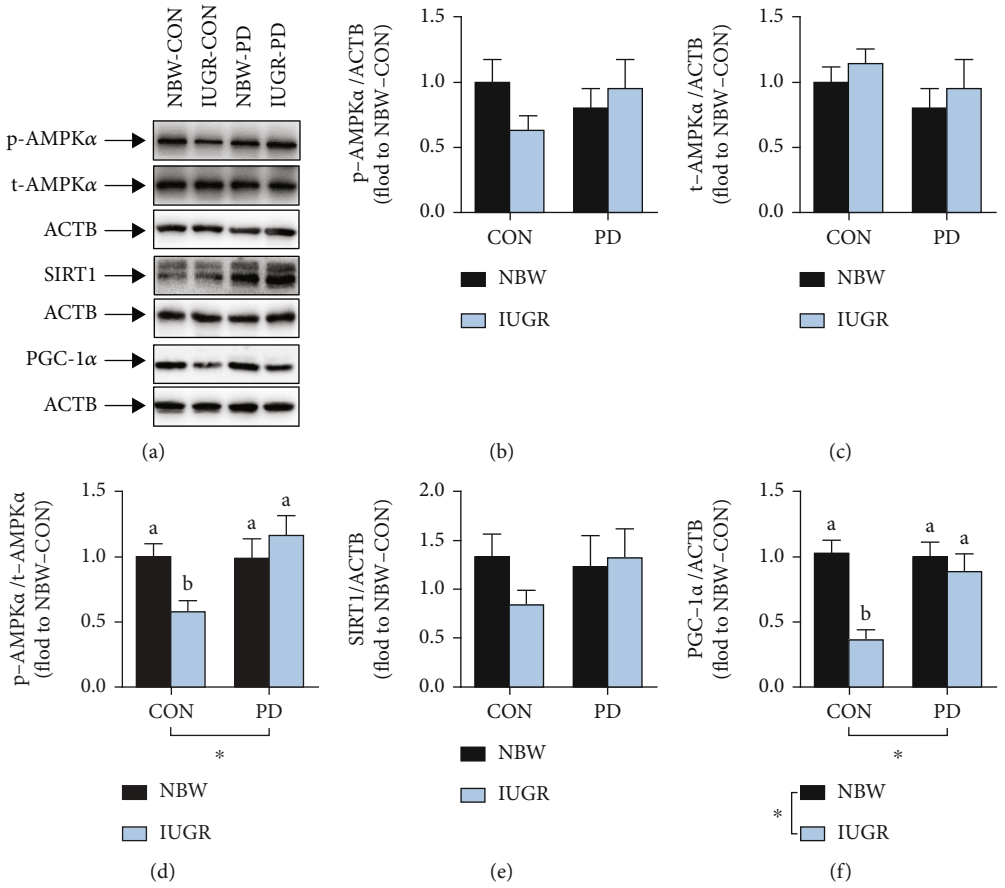

Figure 5: Effect of dietary polydatin supplementation on the protein expression of jejunal total AMPKα (b), phosphorylated AMPKα (c), SIRT1 (e), and PGC-1α (f) and the relative phosphorylation of AMPKα (d) in weanling piglets with different birth weights. Data are presented as the means and SEM, $n = 6$. $^*P < 0.05$. Different letters above the bar indicate a significant difference ($P < 0.05$). ACTB: beta actin; CON: basal diet; IUGR: intrauterine growth retardation; mtDNA: mitochondrial DNA; NBW: normal birth weight; p-AMPKα: phosphorylated adenosine monophosphate-activated protein kinase alpha; PD: polydatin-supplemented diet; PGC-1α: peroxisome proliferation-activated receptor gamma coactivator 1 alpha; SIRT1: sirtuin 1; t-AMPKα: total adenosine monophosphate-activated protein kinase alpha.

the inferior growth performance of the IUGR piglets during the early period after weaning.

After the two-week feeding trial, PD supplementation was found to increase the ADG and FE of piglets, which may be associated with the beneficial roles of PD in restoring jejunal mucosal damage and barrier dysfunction. In the current study, PD supplementation showed potential to inhibit the excessive apoptosis of villus cells due to IUGR. Similarly, rodent studies have indicated that PD is effective in alleviating different harmful stimuli-induced apoptosis in the small intestine [14], the liver [24], and the heart [25]. Under stressful circumstances, PD can inhibit the overactivation of the apoptotic signaling pathway by stabilizing caspase cascades and the expression of proapoptotic and antiapoptotic regulators [26, 27]. Consistently, in the present study, supplementation of IUGR piglets with PD resulted in lower activity of jejunal caspase-9, which is an initiator caspase in the mitochondrial-dependent apoptotic pathway [28]. These results implied that PD may alleviate the IUGR-induced enterocyte apoptosis, probably through its protective action that blocks the overactivation of apoptosis signals associated with mitochondrial dysfunction. Our findings therefore confirm the previous findings reported on a rodent model regarding small intestinal damage, where PD was proposed to protect mitochondria and to counteract the higher apoptosis of enterocytes due to hemorrhagic shock [11].

Excessive apoptosis of the epithelial cells not only induces mucosal villus atrophy but it also causes the formation of "bare areas" in the epithelial layer that would provide attachments and penetration sites for bacteria on the lamina propria [29]. In the present study, a decrease in apoptosis of epithelial cells in IUGR-PD piglets appeared to alleviate the jejunal barrier dysfunction and mucosal damage, as indicated by the lower DAO activity and D-lactate concentration in the plasma. DAO is an intracellular enzyme that is particularly abundant in the villi of the small intestine and it is released into the circulation when mucosal epithelial cells and intestinal integrity are impaired [30]. Similarly, D-lactate is a byproduct of bacterial metabolism and its accumulation in the blood circulation can reflect the severity of intestinal barrier dysfunction [31]. Furthermore, the beneficial effect of PD on the mucosal

barrier function was also confirmed by FISH analysis, which showed a reduced expression of bacterial rRNA in the jejunal crypts of the IUGR piglets supplemented with PD.

Treatment with PD increased the expression of *OCLN* in the jejunum of piglets, which may provide another line of evidence for the maintenance of jejunal barrier function. OCLN is an important extracellular component of the tight junction and serves to restrict permeability to low-molecular-mass molecules while increasing the electrical resistance of epithelial barrier [32]. Ruan et al. [33] have shown that PD also protects the blood-brain barrier after stroke by upregulating the expression of ZO1 and OCLN. Moreover, PD treatment inhibited the upregulation of jejunal *CLDN2* in the IUGR piglets. CLDNs are mainly responsible for controlling paracellular transport through the distinct charge and size selectivity. Some members act by plugging the paracellular pathway, whereas others function as paracellular channels [34]. Among them, CLDN2 increases the permeability of epithelial barrier by promoting the expression of cation-selective pores, and its upregulation is frequently observed in the leaky epithelium [35]. Therefore, in addition to alleviating enterocyte apoptosis, the role of PD in regulating the *OCLN* and *CLDN2* expression may also promote the recovery of jejunal barrier function in the IUGR piglets.

In the present study, supplementation with PD reversed the increased activity of jejunal MPO observed in the IUGR piglets, suggesting that PD may alleviate the inflammation caused by the MPO system of neutrophils. Bacteria that enter the intestinal mucosa can trigger mucosal inflammation by stimulating neutrophil infiltration and MPO reactions. The MPO system of neutrophils plays a crucial role in host defense against bacterial pathogens by generating hypochlorous acid [36]. However, hypochlorous acid is a highly destructive and nonselective oxidant that reacts avidly with cellular macromolecules such as DNA and lipids. Consequently, prolonged MPO activation is implicated in the development of inflammation and oxidative stress in normal tissue and can lead to an eventual injury outcome in the small intestine [37].

In addition, PD may act as a potent anti-inflammatory agent by inhibiting the overproduction of jejunal TNF-α. Xu et al. [27] have shown that PD suppresses the secretion of proinflammatory cytokines, including TNF-α, IL-1β, and IL-6, into the circulation. The available literature has indicated that the anti-inflammatory effects of PD may be attributed to its ability to prevent the overactivation of nuclear factor-kappa B (NF-κB) signals, as this signaling pathway is responsible for regulating the transcription of proinflammatory mediators during immunological stress [10, 38, 39]. Support for an inhibitory effect of PD on NF-κB signals has been provided by Wu et al. [24], who observed that PD decreased the DNA binding ability of NF-κB p65 during intestinal inflammation. Similarly, Ye et al. [38] demonstrated that PD inhibited the translocation of p65 protein from the cytoplasm to the nucleus, therefore preventing the overactivation of NF-κB signals.

The antioxidant potency of PD is another key factor that promotes resistance to oxidative stress and the recovery of small intestinal damage. PD acts as a scavenger for free radicals as it contains hydroxyl groups. Among which, the 4′-hydroxyl group is the preferred reaction site as a result of the resonance effects that occur between the two aromatic rings [40–42]. Therefore, PD can quench a variety of free radicals produced both *in vitro* and *in vivo*, including 2,2-diphenyl-1-picryl-hydrazyl, 2,2-azobis (2-amidino-propane) dihydrochloride, superoxide anion, hydrogen peroxide, and hydroxyl radicals [27, 43, 44]. Notably, Fabris et al. [45] showed that PD is a suitable compound for the prevention and control of the lipid peroxidation because of its lipophilicity. These antioxidant effects of PD may decrease the risk of development of oxidative stress in the intestine and could parallel the decline in MDA and 8-OHDG levels observed in the jejunum of IUGR piglets supplemented with PD.

The present study also demonstrated that PT had the ability to facilitate enzymatic antioxidant mechanism with evidence of the increases in SOD and GST activities in the jejunum of piglets supplemented with PD. SOD serves as the first-line player in the antioxidant defense system and is responsible for eliminating superoxide anion, the precursor of other free radicals with high reactivity. Consistent with our findings, previous studies have also reported that PD can stimulate cellular antioxidant defenses by activating SOD, GSH-Px, GST, and CAT [46–48]. Moreover, the IUGR-induced reduction in jejunal GST activity was largely recovered by supplementation with PD. GST is an important cellular enzyme that can detoxify both exogenous and endogenous toxins by mediating the reaction between electrophiles and GSH [49]. Recently, PD has been demonstrated to function as an activator of nuclear factor erythroid 2-related factor 2 (NRF2), the master regulator that can activate the transcription of intracellular antioxidants and phase II detoxifying enzymes to control the cellular redox balance [50]. This finding may offer a further explanation for the ability of PD to stimulate SOD and GST activities, as both these enzymes are downstream of NRF2 signals [51]. Collectively, the anti-inflammatory and antioxidant properties of PD may assist in the mitigation of small intestinal inflammation and oxidative damage in the IUGR piglets.

Apart from its anti-inflammatory and antioxidant activities, PD may also alleviate IUGR-induced jejunal damage by a mechanism that promotes the efficiency of mitochondrial oxidative metabolism. The mitochondria are the major source of ATP in most eukaryotic cells, so they are vital organelles for energy homeostasis and cell survival. In the intestine, enterocytes have a high energy requirement as their roles are rapid renewal of epithelium and the active transport of nutrients. In this study, dietary PD supplementation was effective in increasing ATP generation and CS activity in the jejunum. CS is a critical enzyme that functions as the entry gate for acetyl CoA into the tricarboxylic acid cycle, thereby determining subsequent ATP formation [52]. The IUGR piglets showed decreased ETC complex III and ATP synthase activities, but dietary PD supplementation significantly restored their activities, suggesting the promotion of a higher flux through the ETC and an increase in intracellular ATP levels as a result.

Previous studies have consistently reported that PD can reverse the broad myocardial infarction-induced decreases in the activities of mitochondrial oxidative metabolic enzymes, such as CS, and in the functioning of the ETC

complexes [25]. A recent study of *Musca domestica* larvae confirmed that PD could also restore mitochondrial membrane potential, increase oxidative phosphorylation efficiency, and facilitate ATP production in response to cadmium-induced heavy metal stress [53]. In the present study, the numbers of swollen mitochondria were substantially reduced by PD supplementation, further confirming previous findings that PD ameliorates mitochondrial ultrastructural injury *in vitro* [25, 54, 55]. Therefore, the beneficial responses may aid in the recovery of the intestinal epithelium from stress-associated damage in the IUGR neonates.

The induction of AMPKα phosphorylation after PD treatment may contribute to the improved mitochondrial function and ATP supply in the small intestine of IUGR piglets. AMPK functions as a regulator of the metabolic adaptations in response to energy deprivation by acting in coordination with another metabolic sensor SIRT1, a nicotinamide adenine dinucleotide- (NAD^+-) dependent deacetylase [56]. The activation of AMPK stimulates the activity of SIRT1 by enhancing the cellular NAD^+ concentration [56]. This effect may explain the increase in jejunal SIRT1 activity observed in the piglets after supplementation with PD.

Similarly, in a rat model of acute hemorrhagic shock, PD has been demonstrated to prevent the decreases in SIRT1 expression and activity [55]. SIRT1 can improve mitochondrial function by activating several transcriptional regulators, including PGC-1α, which synergistically facilitates mitochondrial biogenesis and respiration rates and increases substrate availability for ATP generation [56]. In this regard, we infer that the AMPK/SIRT1 signaling pathway and its downstream PGC-1α may be part of the mechanism by which PD activates mitochondrial CS, complex III, and ATP synthase to increase ATP generation in the jejunum of IUGR piglets. In agreement with this idea, Chen and Lan [57] have shown that PD is capable of promoting AMPK phosphorylation and increasing SIRT1 expression.

PD also has the potential to improve glucose and lipid metabolisms in insulin-resistant HepG2 cells by activating AMPK signals [58]. Zeng et al. [14] have demonstrated that PD is a potent SIRT1 activator and stimulates the SIRT1/PGC-1α/SOD2 axis to alleviate small intestine injury following severe hemorrhagic shock. Thus, the benefits of PD in mitigating jejunal damage may be mediated at least in part by the combined actions of AMPK, SIRT1, and PGC-1α, which form an orchestrated network to maintain mitochondrial function and cellular energy homeostasis in the small intestine.

5. Conclusions

The data obtained from the present study indicates that PD supplementation confers protection against IUGR-induced jejunal injury and barrier dysfunction, probably by mitigating oxidative damage and inflammatory responses, restoring the expression of tight junction complexes, and facilitating mitochondrial biogenesis and oxidative metabolism. This study provides important support for using PD as a nutritional supplement to alleviate the small intestinal damage observed in IUGR neonates.

Data Availability

The datasets used and analyzed during the current study are available from the corresponding author on reasonable request.

Conflicts of Interest

The authors declare no conflict of interest.

Acknowledgments

The authors would like to thank Liqi Zhang for the help in the measurements of H&E and immunofluorescence assays in this trial. This research was supported by the Natural Science Foundation of Jiangsu Province (grant number BK20180531), the National Natural Science Foundation of China (grant numbers 31802094 and 31902197), the Postdoctoral Research Foundation of China (grant numbers 2018M632320 and 2019T120436), and the Foundation of Key Laboratory of Veterinary Biotechnology, Shanghai, China (grant number klab201710).

Supplementary Materials

Supplementary Table 1: the composition and nutrient levels of diet. *(Supplementary Materials)*

References

[1] J. A. Wixey, K. K. Chand, P. B. Colditz, and S. T. Bjorkman, "Review: Neuroinflammation in intrauterine growth restriction," *Placenta*, vol. 54, pp. 117–124, 2017.

[2] C. N. Hales and D. J. Barker, "The thrifty phenotype hypothesis," *British Medical Bulletin*, vol. 60, no. 1, pp. 5–20, 2001.

[3] D. R. Shanklin and R. J. Cooke, "Effects of intrauterine growth on intestinal length in the human fetus," *Neonatology*, vol. 64, no. 2–3, pp. 76–81, 2004.

[4] R. D'Inca, C. Gras-Le Guen, L. Che, P. T. Sangild, and I. Le Huerou-Luron, "Intrauterine growth restriction delays feeding-induced gut adaptation in term newborn pigs," *Neonatology*, vol. 99, no. 3, pp. 208–216, 2011.

[5] Q. He, P. Ren, X. Kong et al., "Intrauterine growth restriction alters the metabonome of the serum and jejunum in piglets," *Molecular BioSystems*, vol. 7, no. 7, pp. 2147–2155, 2011.

[6] L. Che, L. Hu, Y. Liu et al., "Dietary nucleotides supplementation improves the intestinal development and immune function of neonates with intra-uterine growth restriction in a pig model," *Plos One*, vol. 11, no. 6, article e0157314, 2016.

[7] J. R. Turner, "Intestinal mucosal barrier function in health and disease," *Nature Reviews Immunology*, vol. 9, no. 11, pp. 799–809, 2009.

[8] Y. Li, H. Zhang, W. Su et al., "Effects of dietary Bacillus amyloliquefaciens supplementation on growth performance, intestinal morphology, inflammatory response, and microbiota of intra-uterine growth retarded weanling piglets," *Journal of Animal Science and Biotechnology*, vol. 9, no. 11, article 22, 2018.

[9] H. Zhang, Y. Li, Y. Chen, L. Zhang, and T. Wang, "N-Acetylcysteine protects against intrauterine growth retardation-induced intestinal injury via restoring redox status and

mitochondrial function in neonatal piglets," *European Journal of Nutrition*, vol. 58, no. 8, pp. 3335–3347, 2019.

[10] J. Yao, J. Y. Wang, L. Liu et al., "Polydatin ameliorates DSS-induced colitis in mice through inhibition of nuclear factor-kappaB activation," *Planta Medica*, vol. 77, no. 5, pp. 421–427, 2011.

[11] Z. Zeng, Y. Yang, X. Dai et al., "Polydatin ameliorates injury to the small intestine induced by hemorrhagic shock via SIRT3 activation-mediated mitochondrial protection," *Expert Opinion on Therapeutic Targets*, vol. 20, no. 6, pp. 645–652, 2016.

[12] T. Lv, L. Shen, L. Yang et al., "Polydatin ameliorates dextran sulfate sodium-induced colitis by decreasing oxidative stress and apoptosis partially via Sonic hedgehog signaling pathway," *International Immunopharmacology*, vol. 64, pp. 256–263, 2018.

[13] L. Li, K. Zhang, J. Zhang et al., "Protective effect of polydatin on radiation-induced injury of intestinal epithelial and endothelial cells," *Bioscience Reports*, vol. 38, no. 6, article BSR20180868, 2018.

[14] Z. Zeng, Z. Chen, S. Xu, R. Song, H. Yang, and K. S. Zhao, "Polydatin alleviates small intestine injury during hemorrhagic shock as a SIRT1 activator," *Oxidative Medicine and Cellular Longevity*, vol. 2015, Article ID 965961, 12 pages, 2015.

[15] C. A. Merrifield, M. Lewis, S. P. Claus et al., "A metabolic system-wide characterisation of the pig: a model for human physiology," *Molecular BioSystems*, vol. 7, no. 9, pp. 2577–2588, 2011.

[16] T. Wang, Y. J. Huo, F. X. Shi, R. J. Xu, and R. J. Hutz, "Effects of intrauterine growth retardation on development of the gastrointestinal tract in neonatal pigs," *Neonatology*, vol. 88, no. 1, pp. 66–72, 2005.

[17] H. Zhang, Y. Li, W. P. Su et al., "Resveratrol attenuates mitochondrial dysfunction in the liver of intrauterine growth retarded suckling piglets by improving mitochondrial biogenesis and redox status," *Molecular Nutrition & Food Research*, vol. 61, no. 5, article 1600653, 2017.

[18] N. Hosoda, M. Nishi, M. Nakagawa, Y. Hiramatsu, K. Hioki, and M. Yamamoto, "Structural and functional alterations in the gut of parenterally or enterally fed rats," *Journal of Surgical Research*, vol. 47, no. 2, pp. 129–133, 1989.

[19] S. I. Grivennikov, K. Wang, D. Mucida et al., "Adenoma-linked barrier defects and microbial products drive IL-23/IL-17-mediated tumour growth," *Nature*, vol. 491, no. 7423, pp. 254–258, 2012.

[20] K. J. Livak and T. D. Schmittgen, "Analysis of relative gene expression data using real-time quantitative PCR and the 2 $-\Delta\Delta$CT method," *Methods*, vol. 25, no. 4, pp. 402–408, 2001.

[21] C. H. Park, J. S. Noh, N. Yamabe, K. S. Kang, T. Tanaka, and T. Yokozawa, "Beneficial effect of 7-O-galloyl-D-sedoheptulose on oxidative stress and hepatic and renal changes in type 2 diabetic db/db mice," *European Journal of Pharmacology*, vol. 640, no. 1–3, pp. 233–242, 2010.

[22] M. L. Circu and T. Y. Aw, "Intestinal redox biology and oxidative stress," *Seminars in Cell & Developmental Biology*, vol. 23, no. 7, pp. 729–737, 2012.

[23] V. Kolli, K. Natarajan, B. Isaac, D. Selvakumar, and P. Abraham, "Mitochondrial dysfunction and respiratory chain defects in a rodent model of methotrexate-induced enteritis," *Human & Experimental Toxicology*, vol. 33, no. 10, pp. 1–15, 2013.

[24] M. Wu, X. Gong, R. Jiang, L. Zhang, X. H. Li, and J. Y. Wan, "Polydatin protects against lipopolysaccharide-induced fulminant hepatic failure in D-galactosamine-sensitized mice," *International Journal of Immunopathology and Pharmacology*, vol. 25, no. 4, pp. 923–934, 2012.

[25] M. Zhang, Z. Zhao, M. Shen et al., "Polydatin protects cardiomyocytes against myocardial infarction injury by activating Sirt3," *Biochimica et Biophysica Acta (BBA)-Molecular Basis of Disease*, vol. 1863, no. 8, pp. 1962–1972, 2017.

[26] T. Li, Y. Liu, G. Li et al., "Polydatin attenuates ipopolysaccharide-induced acute lung injury in rats," *International Journal of Clinical and Experimental Pathology*, vol. 7, no. 12, pp. 8401–8410, 2014.

[27] L. Q. Xu, Y. L. Xie, S. H. Gui et al., "Polydatin attenuates d-galactose-induced liver and brain damage through its anti-oxidative, anti-inflammatory and anti-apoptotic effects in mice," *Food & Function*, vol. 7, no. 11, pp. 4545–4555, 2016.

[28] M. Brentnall, L. Rodriguez-Menocal, R. L. De Guevara, E. Cepero, and L. H. Boise, "Caspase-9, caspase-3 and caspase-7 have distinct roles during intrinsic apoptosis," *BMC Cell Biology*, vol. 14, no. 1, article 32, 2013.

[29] L. Montagne, G. Boudry, C. Favier, I. Le Huërou-Luron, J. P. Lalles, and B. Seve, "Main intestinal markers associated with the changes in gut architecture and function in piglets after weaning," *British Journal of Nutrition*, vol. 97, no. 1, pp. 45–57, 2007.

[30] I. Fukudome, M. Kobayashi, K. Dabanaka et al., "Diamine oxidase as a marker of intestinal mucosal injury and the effect of soluble dietary fiber on gastrointestinal tract toxicity after intravenous 5-fluorouracil treatment in rats," *Medical Molecular Morphology*, vol. 47, no. 2, pp. 100–107, 2014.

[31] L. Szalay, F. Umar, A. Khadem et al., "Increased plasma D-lactate is associated with the severity of hemorrhagic/traumatic shock in rats," *Shock*, vol. 20, no. 3, pp. 245–250, 2003.

[32] G. J. Feldman, J. M. Mullin, and M. P. Ryan, "Occludin: structure, function and regulation," *Advanced Drug Delivery Reviews*, vol. 57, no. 6, pp. 883–917, 2005.

[33] W. Ruan, J. Li, Y. Xu et al., "MALAT1 up-regulator polydatin protects brain microvascular integrity and ameliorates stroke through C/EBPβ/MALAT1/CREB/PGC-1α/PPARγ pathway," *Cellular and Molecular Neurobiology*, vol. 39, no. 2, pp. 265–286, 2019.

[34] Z. Lu, L. Ding, Q. Lu, and Y. H. Chen, "Claudins in intestines: distribution and functional significance in health and diseases," *Tissue Barriers*, vol. 1, no. 3, article e24978, 2014.

[35] C. M. Van Itallie and J. M. Anderson, "Claudins and epithelial paracellular transport," *Annual Review of Physiology*, vol. 68, no. 1, pp. 403–429, 2006.

[36] M. B. Hampton, A. J. Kettle, and C. C. Winterbourn, "Inside the neutrophil phagosome: oxidants, myeloperoxidase, and bacterial killing," *Blood*, vol. 92, no. 9, pp. 3007–3017, 1998.

[37] J. A. Smith, "Neutrophils, host defense, and inflammation: a double-edged sword," *Journal of Leukocyte Biology*, vol. 56, no. 6, pp. 672–686, 1994.

[38] J. Ye, H. Piao, J. Jiang et al., "Polydatin inhibits mast cell-mediated allergic inflammation by targeting PI3K/Akt, MAPK, NF-κB and Nrf2/HO-1 pathways," *Scientific Reports*, vol. 7, no. 1, pp. 11895–11895, 2017.

[39] B. Liu, S. Li, X. Sui et al., "Root extract of Polygonum cuspidatum Siebold & Zucc. ameliorates DSS-induced ulcerative colitis by affecting NF-kappaB signaling pathway in a

mouse model via synergistic effects of polydatin, resveratrol, and emodin," *Frontiers in Pharmacology*, vol. 9, article 347, 2018.

[40] L. A. Stivala, M. Savio, F. Carafoli et al., "Specific structural determinants are responsible for the antioxidant activity and the cell cycle effects of resveratrol," *Journal of Biological Chemistry*, vol. 276, no. 25, pp. 22586–22594, 2001.

[41] J. C. Cheng, J. G. Fang, W. F. Chen, B. Zhou, L. Yang, and Z. L. Liu, "Structure–activity relationship studies of resveratrol and its analogues by the reaction kinetics of low density lipoprotein peroxidation," *Bioorganic Chemistry*, vol. 34, no. 3, pp. 142–157, 2006.

[42] C. Iuga, J. R. Alvarez-Idaboy, and N. Russo, "Antioxidant activity of trans-resveratrol toward hydroxyl and hydroperoxyl radicals: a quantum chemical and computational kinetics study," *Journal of Organic Chemistry*, vol. 77, no. 8, pp. 3868–3877, 2012.

[43] D. Su, Y. Cheng, M. Liu et al., "Comparision of piceid and resveratrol in antioxidation and antiproliferation activities in vitro," *PloS One*, vol. 8, no. 1, article e54505, 2013.

[44] J. Jin, Y. Li, X. Zhang, T. Chen, Y. Wang, and Z. Wang, "Evaluation of both free radical scavenging capacity and antioxidative damage effect of polydatin," *Oxygen Transport to Tissue XXXVIII*, vol. 923, pp. 57–62, 2016.

[45] S. Fabris, F. Momo, G. Ravagnan, and R. Stevanato, "Antioxidant properties of resveratrol and piceid on lipid peroxidation in micelles and monolamellar liposomes," *Biophysical Chemistry*, vol. 135, no. 1–3, pp. 76–83, 2008.

[46] H. L. Wang, J. P. Gao, Y. L. Han et al., "Comparative studies of polydatin and resveratrol on mutual transformation and antioxidative effect in vivo," *Phytomedicine*, vol. 22, no. 5, pp. 553–559, 2015.

[47] H. B. Liu, Q. H. Meng, C. Huang, J. B. Wang, and X. W. Liu, "Nephroprotective effects of polydatin against ischemia/reperfusion injury: a role for the PI3K/Akt signal pathway," *Oxidative Medicine and Cellular Longevity*, vol. 2015, Article ID 362158, 13 pages, 2015.

[48] X. J. Zhao, H. W. Yu, Y. Z. Yang et al., "Polydatin prevents fructose-induced liver inflammation and lipid deposition through increasing miR-200a to regulate Keap1/Nrf2 pathway," *Redox Biology*, vol. 18, pp. 124–137, 2018.

[49] B. Leiers, A. Kampkötter, C. G. Grevelding, C. D. Link, T. E. Johnson, and K. Henkle-Dührsen, "A stress-responsive glutathione S-transferase confers resistance to oxidative stress in Caenorhabditis elegans," *Free Radical Biology and Medicine*, vol. 34, no. 11, pp. 1405–1415, 2003.

[50] H. Zeng, Y. Wang, Y. Gu et al., "Polydatin attenuates reactive oxygen species-induced airway remodeling by promoting Nrf2-mediated antioxidant signaling in asthma mouse model," *Life Sciences*, vol. 218, pp. 25–30, 2019.

[51] J. Li, T. Ichikawa, J. S. Janicki, and T. Cui, "Targeting the Nrf2 pathway against cardiovascular disease," *Expert Opinion on Therapeutic Targets*, vol. 13, no. 7, pp. 785–794, 2009.

[52] M. Warren, K. Subramani, R. Schwartz, and R. Raju, "Mitochondrial dysfunction in rat splenocytes following hemorrhagic shock," *Biochimica et Biophysica Acta Molecular Basis of Disease*, vol. 1863, no. 10, pp. 2526–2533, 2017.

[53] Y. Zhang, Y. Li, Q. Feng, M. Shao, F. Yuan, and F. Liu, "Polydatin attenuates cadmium-induced oxidative stress via stimulating sod activity and regulating mitochondrial function in Musca domestica larvae," *Chemosphere*, vol. 248, article 126009, 2020.

[54] Y. Gao, Z. Zeng, T. Li et al., "Polydatin inhibits mitochondrial dysfunction in the renal tubular epithelial cells of a rat model of sepsis-induced acute kidney injury," *Anesth Analgesia*, vol. 121, no. 5, pp. 1251–1260, 2015.

[55] P. Li, X. Wang, M. Zhao, R. Song, and K. Zhao, "Polydatin protects hepatocytes against mitochondrial injury in acute severe hemorrhagic shock via SIRT1-SOD2 pathway," *Expert Opinion on Therapeutic Targets*, vol. 19, no. 7, pp. 997–1010, 2015.

[56] C. Cantó, Z. Gerhart-Hines, J. N. Feige et al., "AMPK regulates energy expenditure by modulating NAD^+ metabolism and SIRT1 activity," *Nature*, vol. 458, no. 7241, pp. 1056–1060, 2009.

[57] L. Chen and Z. Lan, "Polydatin attenuates potassium oxonate-induced hyperuricemia and kidney inflammation by inhibiting NF-κB/NLRP3 inflammasome activation via the AMPK/-SIRT1 pathway," *Food & Function*, vol. 8, no. 5, pp. 1785–1792, 2017.

[58] J. Hao, K. Huang, C. Chen et al., "Polydatin improves glucose and lipid metabolisms in insulin-resistant HepG2 cells through the AMPK pathway," *Biological & Pharmaceutical Bulletin*, vol. 41, no. 6, pp. 891–898, 2018.

Hindawi
Oxidative Medicine and Cellular Longevity
Volume 2020, Article ID 3732718, 15 pages
https://doi.org/10.1155/2020/3732718

Research Article

Bakuchiol Alleviates Hyperglycemia-Induced Diabetic Cardiomyopathy by Reducing Myocardial Oxidative Stress via Activating the SIRT1/Nrf2 Signaling Pathway

Wenshuai Ma, Wangang Guo, Fujun Shang, Yan Li, Wei Li, Jing Liu, Chao Ma, and Jiwei Teng

Department of Cardiology, Second Affiliated Hospital, The Air Force Medical University, 1 Xinsi Road, Xi'an 710038, China

Correspondence should be addressed to Jiwei Teng; tengjiwei@sina.com

Received 20 March 2020; Revised 3 August 2020; Accepted 5 September 2020; Published 30 September 2020

Academic Editor: Joanna Lecka

Copyright © 2020 Wenshuai Ma et al. This is an open access article distributed under the Creative Commons Attribution License, which permits unrestricted use, distribution, and reproduction in any medium, provided the original work is properly cited.

Bakuchiol (BAK), a monoterpene phenol reported to have exerted a variety of pharmacological effects, has been related to multiple diseases, including myocardial ischemia reperfusion injury, pressure overload-induced cardiac hypertrophy, diabetes, liver fibrosis, and cancer. However, the effects of BAK on hyperglycemia-caused diabetic cardiomyopathy and its underlying mechanisms remain unclear. In this study, streptozotocin-induced mouse model and high-glucose-treated cell model were conducted to investigate the protective roles of BAK on diabetic cardiomyopathy, in either the presence or absence of SIRT1-specific inhibitor EX527, SIRT1 siRNA, or Nrf2 siRNA. Our data demonstrated for the first time that BAK could significantly abate diabetic cardiomyopathy by alleviating the cardiac dysfunction, ameliorating the myocardial fibrosis, mitigating the cardiac hypertrophy, and reducing the cardiomyocyte apoptosis. Furthermore, BAK achieved its antifibrotic and antihypertrophic actions by inhibiting the TGF-β1/Smad3 pathway, as well as decreasing the expressions of fibrosis- and hypertrophy-related markers. Intriguingly, these above effects of BAK were largely attributed to the remarkable activation of SIRT1/Nrf2 signaling, which eventually strengthened cardiac antioxidative capacity by elevating the antioxidant production and reducing the reactive oxygen species generation. However, all the beneficial results were markedly abolished with the administration of EX527, SIRT1 siRNA, or Nrf2 siRNA. In summary, these novel findings indicate that BAK exhibits its therapeutic properties against hyperglycemia-caused diabetic cardiomyopathy by attenuating myocardial oxidative damage via activating the SIRT1/Nrf2 signaling.

1. Introduction

Diabetes mellitus (DM), a chronic endocrine metabolic disorder characterized by long-standing hyperglycemia, has become more prevalent in recent years and seriously threatens the human health [1, 2]. In people with DM, the existence of abnormal myocardial structure and performance has led to the descriptive terminology diabetic cardiomyopathy [3]. These diabetes-associated changes, featured by the presence of myocardial fibrosis, pathological remodeling, and associated cardiac dysfunction, occur independent of conventional cardiovascular risk factors, such as coronary artery disease, valvular disease, hypertension, and dyslipidemia [4, 5]. Until now, no efficacious approaches have been applicated in clinical trials that can definitely alleviate this specific form of heart disease. Therefore, it is of great significance to search for a therapeutic substance for treating diabetic cardiomyopathy.

Oxidative stress, induced by glycometabolism disorder, is widely accepted to be one of the key pathophysiological mechanisms in the development of diabetic cardiomyopathy [6, 7]. Simultaneously, under the condition of prolonged hyperglycemia, reactive oxygen species (ROS) are excessively produced in the myocardium due to impaired mitochondrial oxidative phosphorylation which, in turn, intensifies myocardial oxidative stress, aggravates mitochondrial dysfunction, and accelerates the progression of myocardial fibrosis and hypertrophy [8–10]. Thus, finding agents that alleviate oxidative stress and inhibit ROS generation may represent as a practicable therapy for diabetic cardiomyopathy.

Bakuchiol (BAK), a bioactive monoterpene phenol, can be vastly extracted from the seeds of *Psoralea corylifolia*. Previous literatures have demonstrated that BAK exerts extensive pharmacological properties, including antioxidant, antibacterial, anti-inflammatory, antiaging, and estrogen-like effects [11, 12]. Given its wide spectrum of biological activities, especially the antioxidative capability, BAK has been verified to exhibit protective roles against multiple diseases in various organs or tissues [13–16]. Additionally, experimental evidence revealed that BAK also possessed promising potency on substance metabolism in diabetic animal models [17, 18]. However, whether BAK treatment could prevent the occurrence and progression of cardiomyopathy in diabetic hearts and the underlying mechanisms remain ambiguous.

Silent information regulator 1 (SIRT1), one of the sirtuin family distinguished by holding a highly conserved nicotinamide adenine dinucleotide- (NAD^+-) binding catalytic domain, is deemed to be responsible for the beneficial effects in the development and treatment of cardiovascular diseases [19, 20]. Intriguingly, in recent years, SIRT1 has attracted widespread attentions as a protein modulator and stress adaptor related to hyperglycemia attenuating cardiac dysfunction and improving diabetic cardiomyopathy [21, 22]. Moreover, nuclear factor-erythroid 2-related factor 2 (Nrf2), an important transcription factor that binds to antioxidant-responsive elements (AREs), shows an outstanding performance in attenuating oxidative damage to consolidate the cellular defense system against diabetic cardiomyopathy [23, 24]. Numerous studies have also clearly indicated that SIRT1 could manifest its antioxidative effects via the activation of Nrf2 [25, 26]. Therefore, it is of great interest to probe whether SIRT1/Nrf2 signaling plays a vital role in the amelioration actions of BAK against diabetic cardiomyopathy.

Herein, this study was carried out aimed at exploring the pharmacological effects of BAK in the setting of hyperglycemia-induced diabetic cardiomyopathy and elucidate whether SIRT1/Nrf2 signaling is involved in its protective molecular mechanisms both *in vivo* and *in vitro*.

2. Materials and Methods

2.1. Reagents. BAK (purity ≥ 98%) was purchased from Winherb Medical Co. (Shanghai, China). Streptozotocin (STZ) and EX527 were purchased from Sigma-Aldrich (St. Louis, MO, USA). The *In Situ* Cell Death Detection Kit was purchased from Roche Biochemicals (Mannheim, Germany) to detect the cell apoptosis. Kits for determining glutathione peroxidase (GSH-Px), superoxide dismutase (SOD) activities, and malondialdehyde (MDA) content were obtained from Nanjing Jiancheng Bioengineering Institute (Nanjing, China). The fluorescent probe 2′,7′-dichlorofluorescein diacetate (DCFH-DA) was purchased from Beyotime Institute of Biotechnology (Shanghai, China) to detect intracellular ROS generation. Dihydroethidium (DHE) was purchased from Invitrogen (Carlsbad, CA, USA) for detecting ROS generation in the myocardium. Primary antibodies against p-Smad3, t-Smad3, and β-actin were purchased from Cell Signaling Technology (Boston, MA, USA). Primary antibodies against SIRT1, Nrf2, transforming growth factor-$\beta1$ (TGF-$\beta1$), α-smooth muscle actin (α-SMA), and Histone H3 were purchased from Abcam (Cambridge, MA, USA). The rabbit anti-goat and goat anti-mouse secondary antibodies were obtained from Zhongshan Company (Beijing, China).

2.2. Animals and In Vivo Protocols. Healthy C57BL/6 male mice (weighing 20-25 g at the age of 8 weeks) were obtained from the Experimental Animal Center of the Air Force Medical University. Animals were housed at 22-24°C under a specific pathogen-free environment with a 12/12 h light/dark cycle and had free access to food and water. All of the animal care and experimental procedures conformed to the Guidelines for the Care and Use of Laboratory Animals published by the United States National Institutes of Health (NIH Publication, revised 2011). All procedures were reviewed and approved by the Air Force Medical University Committee on Animal Care.

After being fed with high-fat diet (HFD) for 4 weeks, diabetes was induced by intraperitoneal injection of STZ (dissolved in 0.1 mM sodium citrate (pH 4.5), 60 mg/kg) for 3 consecutive days. The age-matched control mice received the same volume of vehicle injection (sodium citrate). Two weeks after the final STZ injection, mice with fasting blood glucose above 11.1 mM were defined as diabetic, which were continued to be fed with HFD in the following experiments. Animals were randomly divided into 4 groups ($n = 15$): (1) control group, (2) diabetic mouse (DM) group, (3) DM +BAK group, and (4) DM+BAK+EX527 group. Groups (3) and (4) were orally administrated with BAK (60 mg/kg/d, first dissolved in ethanol and then diluted in sterile saline) for 12 weeks, while groups (1) and (2) received the same volume of vehicle alone. EX527 (5 mg/kg/d, first dissolved in ethanol and then diluted in sterile saline) was intraperitoneally administered twice a week for 12 weeks.

2.3. Cell Culture and Treatment. H9c2 cardiomyoblast cell line was purchased from the American Type Culture Collection (ATCC). Cells were maintained in Dulbecco's modified Eagle's medium (DMEM, Gibco, Grand Island, NY, USA), supplemented with 10% heat-inactivated bovine calf serum (FBS, Gibco, Grand Island, NY, USA) and 1% Penicillin-Streptomycin Solution at 37°C with 5% CO_2.

In the high-glucose (HG) group, cells were cultured in DMEM containing 33 mM D-glucose to mimic the plasma level of glucose from diabetic mice, while cells in the control group were incubated in normal glucose medium containing 5.5 mM glucose, supplemented with 27.5 mM mannitol to achieve the osmotic pressure at 33 mM. At the same time, cells in the BAK-treated groups were cultured in a high-glucose medium with additional 2, 5, and 10 μM of BAK.

2.4. Echocardiography. As described previously [27], transthoracic echocardiography was performed with a VisualSonics Vevo 770 ultrasound system (Toronto, Ontario, Canada) to evaluate cardiac function. Animals were anesthetized with 1.0% isoflurane and placed on a thermostabilized pad, while the heart rates should be maintained at 400-500

beats per minute during the whole process. Motion- (M-) mode echocardiographic images were recorded at the level of the papillary muscles to calculate the left ventricular end-systolic volumes (LVESV), left ventricular end-diastolic volumes (LVEDV), left ventricular ejection fraction (LVEF), and left ventricular fractional shortening (LVFS).

2.5. HMI, LVMI, and HW/TL Assessment. After the body weight was measured, the animals were euthanized, and their hearts and right lower extremity tibias were immediately harvested and rinsed with phosphate-buffered saline (PBS). After being placed on filter paper to blot moisture, the total heart mass, left ventricular mass, and tibial length of each mouse were measured. The total heart mass index (HMI, total heart mass/body mass), left ventricular mass index (LVMI, left ventricular mass/body mass), and heart weight/-tibial length (HW/TL) ratio were calculated to evaluate the cardiac hypertrophy.

2.6. Histological and Immunohistochemistry Staining. Tissues were fixed in 4% paraformaldehyde solution, embedded in paraffin, and sectioned at 5 μm thickness. Hematoxylin-eosin (HE), wheat germ agglutinin (WGA), or Masson trichrome staining was used to examine the cross-sectional area of cardiomyocyte and extracellular collagen deposition, respectively. Six random fields in each sample were captured to assess the quantitative difference in the cross-sectional area and collagen content with the ImageJ software (NIH, Bethesda, MD, USA). For immunohistochemistry staining, heart sections were deparaffinized in xylene and rehydrated. After antigen retrieval was achieved with citrate (pH = 6), the slides were washed in PBS. Primary antibodies (collagen I (1 : 50) and collagen III (1 : 50)) were applied overnight at 4°C in PBS containing 2% bovine serum albumin (BSA). The sections were then washed in PBS followed by incubation with anti-mouse or rabbit secondary antibodies labeled with horse radish peroxidase. Staining was achieved by completing the DAB (3,3′-diaminobenzidine tetrahydrochloride) and hematoxylin counterstain process. All images were obtained by the bright field microscope (Olympus CX41, Olympus, Tokyo, Japan).

2.7. Cell Viability. Cell counting kit (CCK-8 kit, Dojindo, Kumamoto, Japan) was used to evaluate cell viability. Procedures were carried out according to the manufacturer's protocol. Cells of different groups were counted, adjusted the density to 1×10^5 cells per well, and seeded in a 96-well plate. CCK-8 (10 μL) solution was added in each well, and the plate was incubated darkly for 2 h. The absorbance at 450 nm was detected using a microplate reader. All data were normalized to the control well, which contained no cells but normal culture media.

2.8. Assessment of SOD Activity, GSH-Px Activity, and MDA Content. The activities for SOD and GSH-Px and content of MDA in heart tissues and cultured cells were analyzed spectrophotometrically with a SpectraMax M5 device, following the instructions of the special commercial kits.

2.9. TUNEL Assay. Cell apoptosis was analyzed via TUNEL staining using the *In Situ* Cell Death Detection Kit according to the manufacturer's protocol. All the cells exhibited blue nuclear after DAPI (4′,6-diamidino-2-phenylindole) staining, while the TUNEL-positive cells exhibited green nuclear staining. Five randomly selected fields were observed using an Olympus FV10C-W3 laser confocal microscope (Olympus, Tokyo, Japan). The apoptotic index was calculated to reflect the degree of apoptosis and expressed as the number of apoptotic positive cells/total cells.

2.10. ROS Detection. As previously described [28], the frozen tissue sections were stained with DHE reaction mixture to detect ROS generation in the myocardium. Each sample was examined with an Olympus FV10C-W3 laser confocal microscope, and the fluorescent intensity in different groups was determined by the ImageJ software. Intracellular ROS production was measured after H9c2 cells in each group were treated with DCFH-DA reaction mixture [29]. A microplate reader (SpectraMax M5) was used to measure fluorescent intensity at an emission of 535 nm (excitation at 485 nm). The amount of emitted fluorescence was correlated with the quantity of ROS volume.

2.11. siRNA Transfection. To knock down the SIRT1 and Nrf2 expressions, predesigned and validated siRNAs along with corresponding negative control (GenePharma, Suzhou, China) were transfected into H9c2 cells for 24 h by Lipofectamine™ 3000 transfection reagent (Invitrogen, Carlsbad, CA, USA). The sense and antisense sequences of SIRT1 siRNA and Nrf2 siRNA are listed in Table 1, and the siRNAs were transiently transfected into H9c2 cells with Lipofectamine 3000 according to the manufacturer's instructions for 24 h in OPTI-MEM medium (Gibco, Carlsbad, CA, USA).

2.12. RT-PCR and Western Blot. As previously described [30, 31], real-time polymerase chain reaction (RT-PCR) was performed with the CFX96 system-C1000 Thermal Cycler (Bio-Rad Laboratories, Hercules, CA, USA) and western blotting was analyzed by Image Lab 5.2.1 (Bio-Rad Laboratories, Hercules, CA, USA). The primer sequences used are listed in Table 2, and the concentrations of antibodies are SIRT1 (1 : 1000), Nrf2 (1 : 1000), TGF-$\beta 1$ (1 : 1000), α-SMA (1 : 1000), p-Smad3 (1 : 1000), t-Smad3 (1 : 1000), H3 (1 : 1000), and β-actin (1 : 5000).

2.13. Statistical Analysis. Data were presented as mean ± standard error of the mean (SEM). The statistical significance of differences was determined using two-tailed Student's t test and one-way ANOVA, followed by a Bonferroni multiple-comparison test, using GraphPad Prism 5 (GraphPad Software, San Diego, CA, USA). $P < 0.05$ was considered to indicate significant differences.

3. Results

3.1. BAK Upregulated the Expressions of SIRT1 and Nrf2 in Diabetic Myocardium. To explore the protective roles of BAK on hyperglycemia-induced cardiac damages in diabetic mice, as well as the underlying molecular mechanisms,

Table 1: Transfection siRNAs used in the present study.

siRNA	Sense	Antisense
SIRT1	5′-CCA GUA GCA CUA AUU CCA ATT-3′	5′-UUG GAA UUA GUG CCA CUG GTT-3′
Nrf2	5′-GAG GAU GGG AAA CCU UAC UTT-3′	5′-AGU AAG GUU UCC CAU CCU CTT-3′
Negative control	5′-UUC UCC GAA CGU GUC ACG UTT-3′	5′-ACG UGA CAC GUU CGG AGA ATT-3′

SIRT1: silent information regulator 1; Nrf2: nuclear factor-erythroid 2-related factor 2.

Table 2: Real-time quantitative RT-PCR primers used in the present study.

Gene	Forward	Reverse
ANP	5′-ACCTGCTAGACCACCTGGAG-3′	5′-CCTTGGCTGTTATCTTCGGTACCGG-3′
BNP	5′-GAGGTCACTCCTATCCTCTGG-3′	5′-GCCATTTCCTCCGACTTTTCTC-3′
α-MHC	5′-TGCACTACGGAAACATGAAGTT-3′	5′-CGATGGAATAGTACACTTGCTGT-3′
β-MHC	5′-ACTGTCAACACTAAGAGGGTCA-3′	5′-TTGGATGATTTGATCTTCCAGGG-3′
GAPDH	5′-AGAACATCATCCCTGCATCC-3′	5′-AGTTGCTGTTGAAGTCGC-3′

ANP: atrial natriuretic polypeptide; BNP: brain natriuretic peptide; α-MHC: α-myosin heavy chain; β-MHC: β-myosin heavy chain; GAPDH: glyceraldehyde-3-phosphate dehydrogenase.

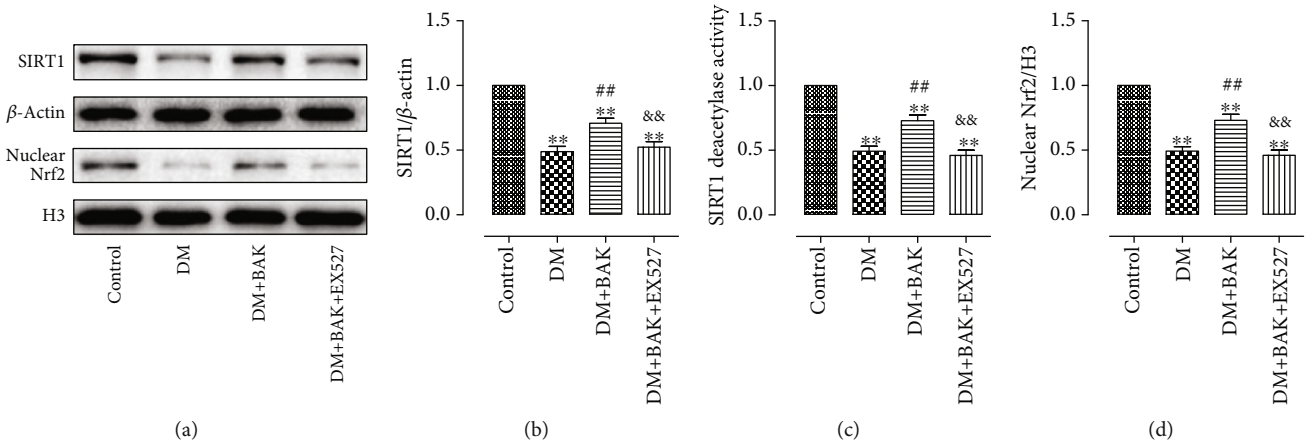

Figure 1: BAK treatment increased the expression and activity of SIRT1 and nuclear accumulation of Nrf2 in diabetic hearts. (a) Representative blots. (b) SIRT1 expression. (c) Relative SIRT1 activity. (d) Nrf2 nuclear translocation. Data are presented as the mean ± SEM ($n = 6$ in each group). $^{*/**}P < 0.05/0.01$ vs. the control group, $^{\#/\#\#}P < 0.05/0.01$ vs. the DM group, and $^{\&/\&\&}P < 0.05/0.01$ vs. the DM +BAK group.

SIRT1-specific inhibitor EX527 was employed in our *in vivo* experiments. As shown in Figure 1, the expression and activity of SIRT1 were notably decreased in the diabetic myocardium compared with the control group, accompanied by the prominently reduced nuclear translocation of Nrf2, while treatment with BAK markedly restored SIRT1 expression and deacetylation activity and Nrf2 nuclear accumulation. Simultaneously, as exhibited in Figure S1, BAK alone could not increase the expression and deacetylation activity of SIRT1 or promote the nuclear accumulation of Nrf2 under a normal condition, indicating that the upregulation of SIRT1 and Nrf2 is a secondary outcome of the BAK treatment in a pathological state. Taken together, the results suggested that SIRT1 and Nrf2 signaling might mediate the cardioprotective action of BAK in diabetic hearts.

3.2. EX527 Abolished BAK-Induced Alleviation of Myocardial Dysfunction in Diabetic Mice. As echocardiography recorded in Figure 2(a), cardiac functions were markedly impaired in the DM group, as confirmed by decreased LVEF and LVFS, while BAK treatment significantly increased both LVEF and LVFS in the DM+BAK group. Moreover, cardiac dysfunction was markedly alleviated with BAK supplementation, as evidenced by reduced LVESV and LVEDV compared with the DM group (Figures 2(d) and 2(e)). Nevertheless, these cardioprotective activities were all blunted by EX527

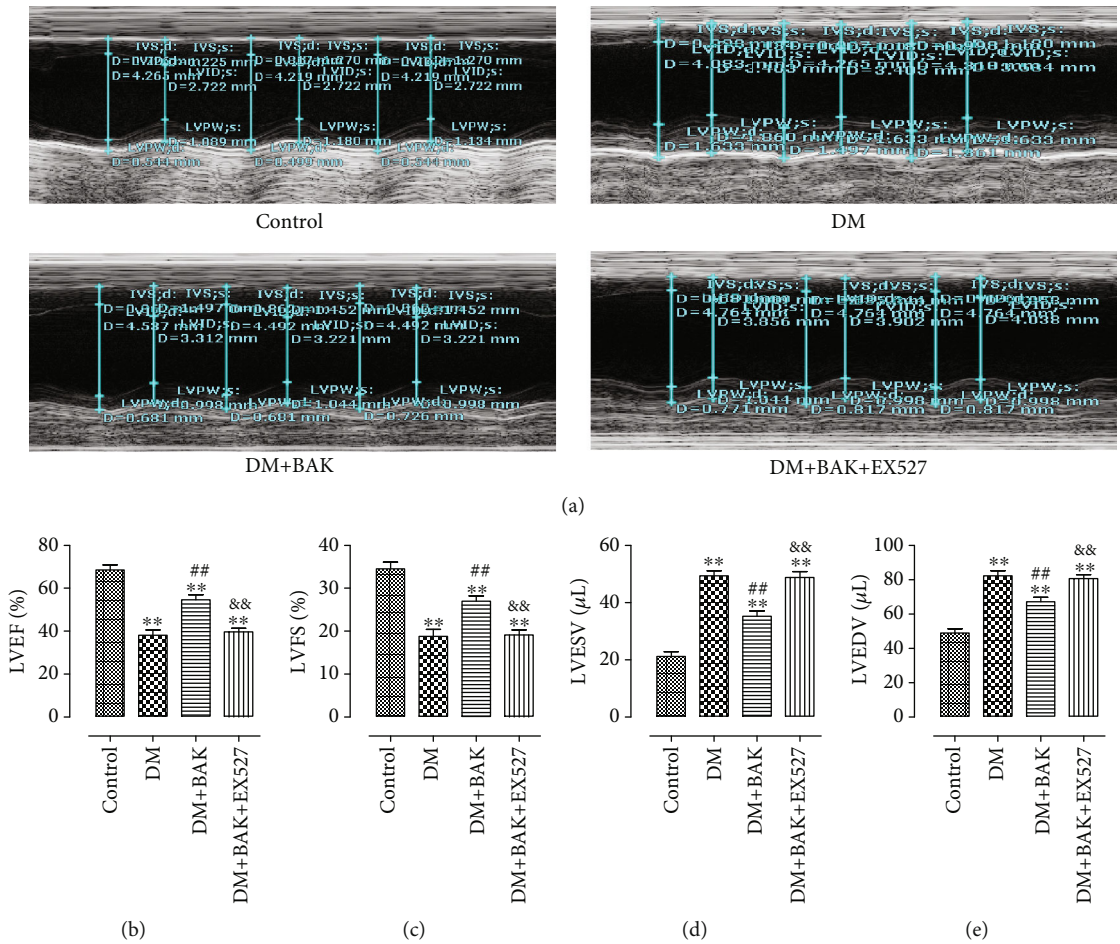

Figure 2: EX527 abolished BAK-induced cardioprotective effects in diabetic mice. (a) Representative M-mode images by echocardiography. (b) Left ventricular ejection fraction (LVEF). (c) Left ventricular fractional shortening (LVFS). (d) Left ventricular end-systolic volume (LVESV). (e) Left ventricular end-diastolic volume (LVEDV). Data are presented as the mean ± SEM ($n = 6$ in each group). $^{*/**}P < 0.05/0.01$ vs. the control group, $^{\#/\#\#}P < 0.05/0.01$ vs. the DM group, and $^{\&/\&\&}P < 0.05/0.01$ vs. the DM+BAK group.

administration, suggesting that SIRT1 signaling played a vital role in the amelioration effects of BAK on cardiac dysfunction in diabetic mice.

3.3. EX527 Blocked BAK-Induced Mitigation of Cardiac Hypertrophy in Diabetic Mice. Cardiac hypertrophy is a prominent characteristic of diabetic hearts induced by prolonged hyperglycemia. Consistent with the findings from other papers [6, 32], mice in the DM group showed remarkable increased HMI, LVMI, and enhanced HW/TL ratio (Figures 3(a)–3(c)), while BAK treatment markedly mitigated these changes, as evidenced by the obviously decreased HMI and LVMI and declined HW/TL ratio. However, EX527 administration reversed the favorable ameliorative effects of BAK. As shown in Figures 3(e) and 3(f), HE staining and WGA staining of the cross-sections of the left ventricle are more intuitive ways to assess the cardiac hypertrophic response in each group. Compared with the DM group, BAK treatment greatly reduced the mean cross-sectional area of the left ventricular myocytes. Consistently, EX527 administration abolished the outstanding curative effect of BAK on delaying the progression of cardiac hypertrophy (Figure 3(d)).

Myosin heavy chain (MHC) is the basic unit of myosin and plays an important role in ensuring the normal function of muscle cells. The two isoforms of myosin heavy chain, α-MHC and β-MHC, will undergo canonical MHC changes from α-MHC to β-MHC in the hypertrophic hearts [33]. In accordance with previous studies [6, 34], α-MHC was downregulated and β-MHC was upregulated in mRNA levels in the hearts of the DM group, while BAK administration reversed this transformation in MHC expression (Figures 4(a) and 4(b)). Moreover, the accurate biomarkers for myocardial expansion-caused cardiac insufficiency, ANP and BNP, were markedly raised in mRNA levels in the DM group as well. Similarly, BAK treatment inhibited the alteration (Figures 4(d) and 4(e)). However, the above BAK-induced suppression on activation of hypertrophy-related genes was significantly invalidated by EX527.

These data indicated that BAK mitigated cardiac hypertrophy in diabetic mice in a SIRT1-dependent manner.

3.4. EX527 Blunted BAK-Induced Amelioration of Myocardial Fibrosis and Collagen Deposition in Diabetic Myocardium. Cardiac fibrosis is a critical hallmark in the process of cardiac remodeling caused by diabetic cardiomyopathy, which

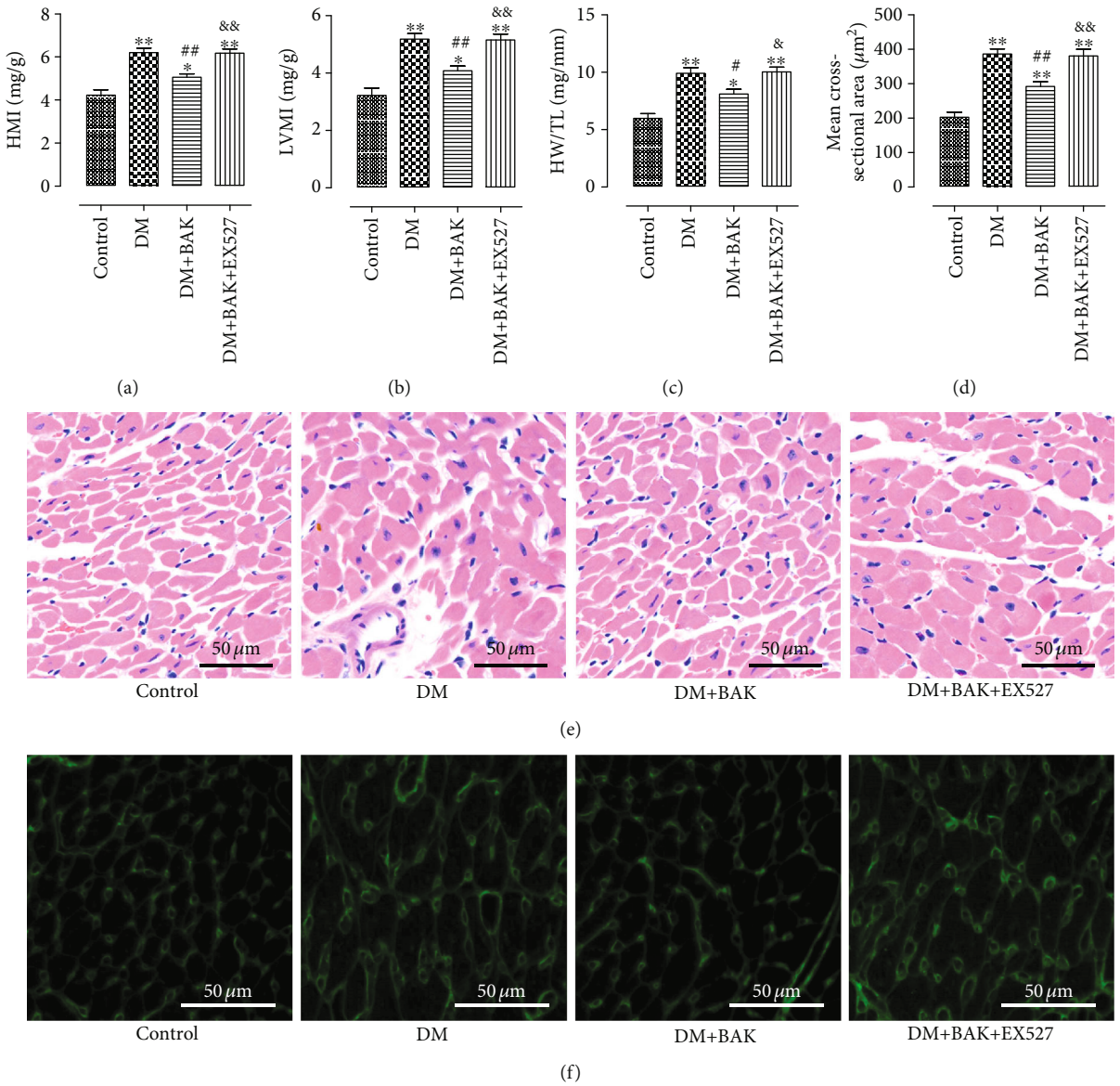

Figure 3: EX527 blocked BAK-induced mitigation of cardiac hypertrophy in diabetic mice. (a) Heart mass index (HMI). (b) Left ventricular mass index (LVMI). (c) Heart weight/tibia length (HW/TL) ratio. (d) Mean cross-sectional area of individual cardiomyocyte. (e) Representative images of HE staining of myocardial tissue (scale bar = 50 μm). (f) Representative images of WGA staining of myocardial tissue (scale bar = 50 μm). Data are presented as the mean ± SEM ($n = 6$ in each group). $^{*/**}P < 0.05/0.01$ vs. the control group, $^{\#/\#\#}P < 0.05/0.01$ vs. the DM group, and $^{\&/\&\&}P < 0.05/0.01$ vs. the DM+BAK group.

further contributes to worsening of the already compromised cardiac functions [35, 36]. To investigate the antifibrotic properties of BAK treatment in diabetic hearts, we detected the level of collagen deposition in myocardium tissue by Masson staining. Representative images of Masson staining for the interstitial and perivascular areas are shown in Figure 5(a), respectively. Markedly, compared to the DM group, BAK administration significantly attenuated collagen accumulation both in the interstitial and perivascular areas in the DM+BAK group (Figures 5(b) and 5(c)). Of note, these antifibrotic effects of BAK were markedly reversed by EX527.

Immunohistochemical staining of collagen I and collagen III was also conducted to further determine the alleviative effect of BAK treatment on cardiac fibrosis. A similar trend consistent with Masson staining is shown in Figure 6, revealing that BAK treatment could restrain the deposition of collagen I and collagen III, compared to the DM group. Intriguingly, the amelioration of BAK on this pathologic characteristic was blunted with the administration of EX527 as well.

Collectively, these data demonstrated that BAK displayed its protective properties against myocardial fibrosis and collagen deposition in diabetic myocardium via SIRT1 signaling.

3.5. EX527 Counteracted BAK-Induced Inhibition of Synthesis of Fibrosis-Associated Proteins in Diabetic Myocardium. As shown in Figures 7(a) and 7(b), the antifibrotic effectiveness

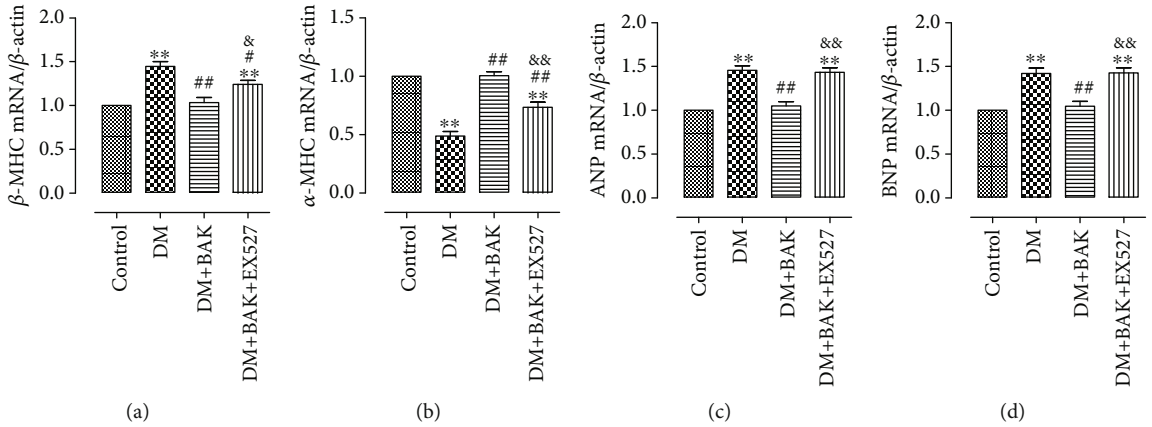

Figure 4: EX527 blunted BAK-induced suppression on activation of hypertrophy-related genes in diabetic myocardium. (a) β-MHC mRNA level. (b) α-MHC mRNA level. (c) ANP mRNA level (8W). (d) BNP mRNA level. Data are presented as the mean ± SEM ($n = 6$ in each group). $^{*/**}P < 0.05/0.01$ vs. the control group, $^{\#/\#\#}P < 0.05/0.01$ vs. the DM group, and $^{\&/\&\&}P < 0.05/0.01$ vs. the DM+BAK group.

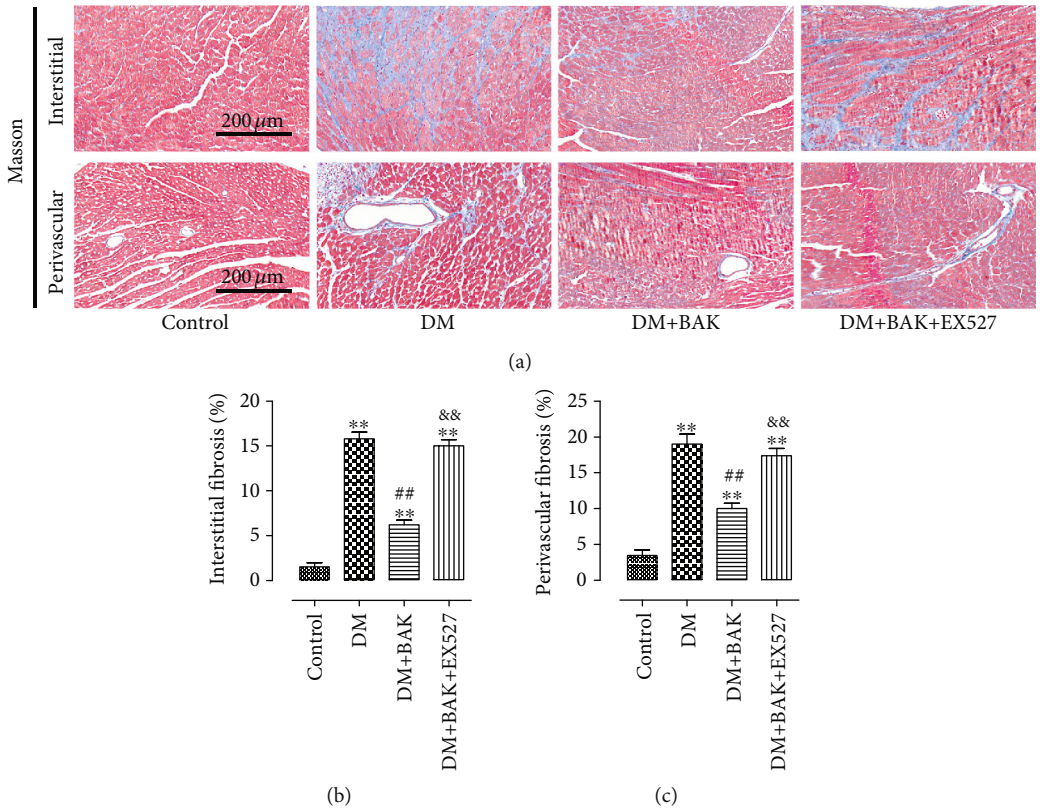

Figure 5: EX527 inhibited BAK-induced amelioration of myocardial fibrosis in diabetic myocardium. (a) Representative images of Masson's trichrome staining of the cardiac interstitial and perivascular areas (scale bar = 200 μm). (b) Mean cardiac interstitial fibrosis. (c) Mean cardiac perivascular fibrosis. Data are presented as the mean ± SEM ($n = 6$ in each group). $^{*/**}P < 0.05/0.01$ vs. the control group, $^{\#/\#\#}P < 0.05/0.01$ vs. the DM group, and $^{\&/\&\&}P < 0.05/0.01$ vs. the DM+BAK group.

of BAK was further verified by inhibiting the expression level of the cardiac fibrotic marker α-SMA, which was dramatically elevated in the DM group and could be significantly reversed by EX527 treatment. Moreover, the TGF-$\beta 1$/Smad3 signaling pathway, playing a key role in mediating ROS generation to pathologic fibrosis, was further measured in our research. As shown in Figures 7(a), 7(c), and 7(d), the TGF-$\beta 1$/Smad3 pathway was evidently inhibited after BAK treatment compared with the DM group. Consistently, this phenomenon was prominently blunted by EX527 administration, indicating that expressive suppression of the TGF-$\beta 1$/Smad3 signaling was involved in the noteworthy benefit

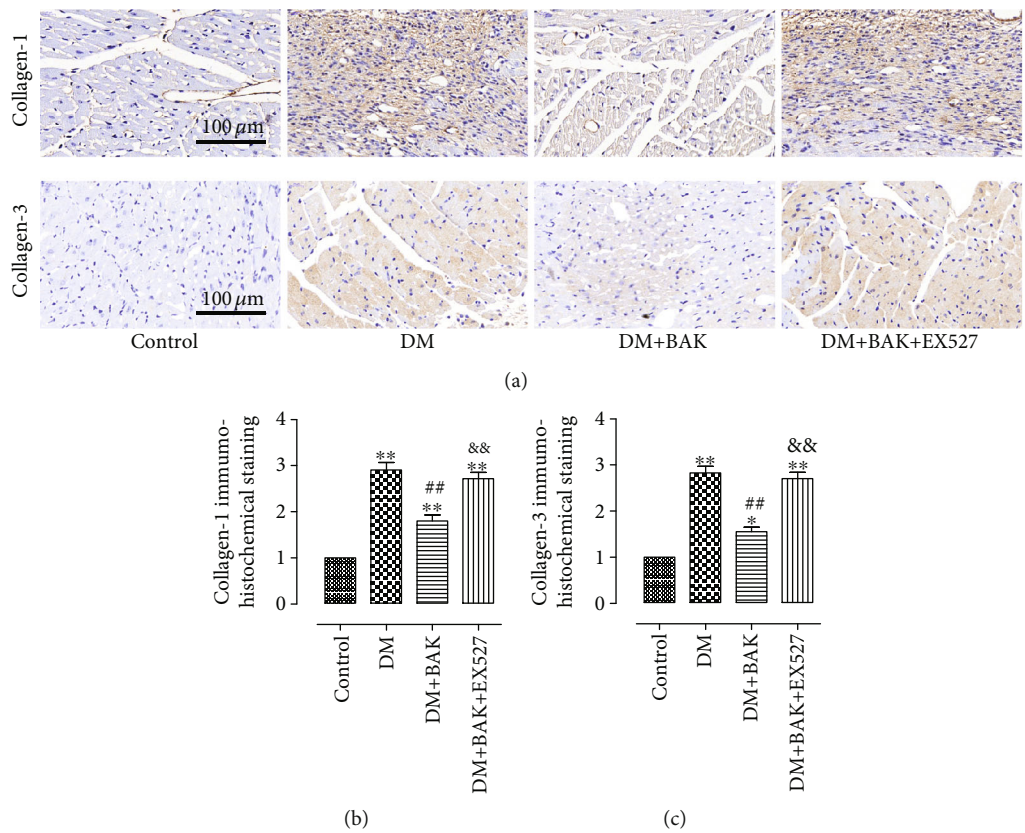

Figure 6: EX527 blunted BAK-induced amelioration of collagen deposition in diabetic myocardium. (a) Representative images of immunohistochemistry of collagen I/III (scale bar = 100 μm). (b) Collagen I immunohistochemical expression. (c) Collagen III immunohistochemical expression. Data are presented as the mean ± SEM ($n = 6$ in each group). $^{*/**}P < 0.05/0.01$ vs. the control group, $^{\#/\#\#}P < 0.05/0.01$ vs. the DM group, and $^{\&/\&\&}P < 0.05/0.01$ vs. the DM+BAK group.

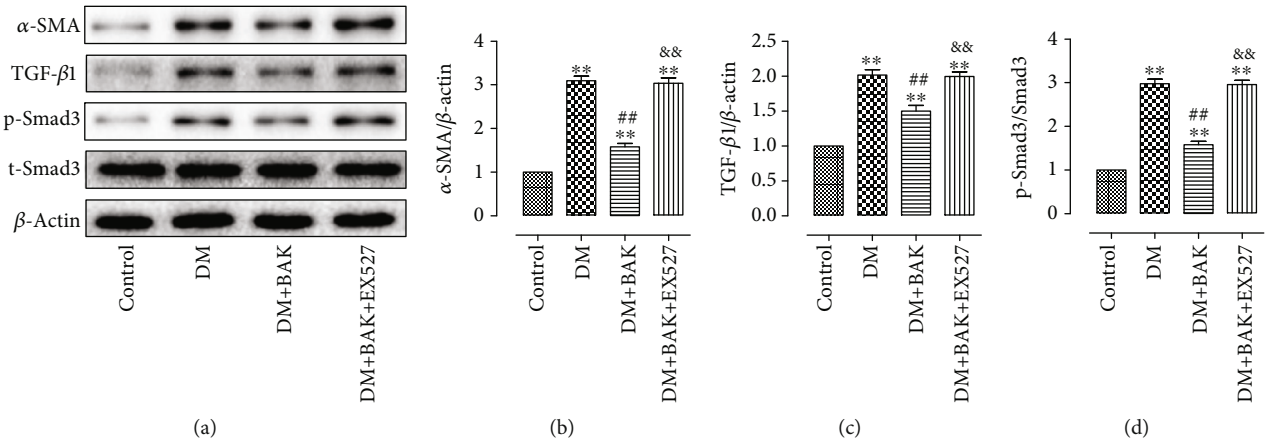

Figure 7: EX527 attenuated BAK-induced restrained stimulation of the TGF-$\beta 1$/Smad3 pathway in diabetic myocardium. (a) Representative blots. (b) α-SMA expression. (c) TGF-$\beta 1$ expression. (d) p-Smad3 expression. Data are presented as the mean ± SEM ($n = 6$ in each group). $^{*/**}P < 0.05/0.01$ vs. the control group, $^{\#/\#\#}P < 0.05/0.01$ vs. the DM group, and $^{\&/\&\&}P < 0.05/0.01$ vs. the DM+BAK group.

of BAK to alleviate cardiac fibrosis in diabetic hearts via SIRT1-induced inhibition of ROS generation.

3.6. EX527 Attenuated BAK-Induced Suppression of the Oxidative Stress in Diabetic Myocardium. As shown in Figures 8(a)–8(c), BAK exhibited its antioxidative capabilities by markedly increasing the enzymatic activities of SOD and GSH-Px in myocardial tissues in the DM+BAK group, together with observably decreased MDA content. However, all these effects were significantly reversed by EX527 administration. Furthermore, compared with the DM group, BAK also verified its antioxidant capacity by inhibiting ROS

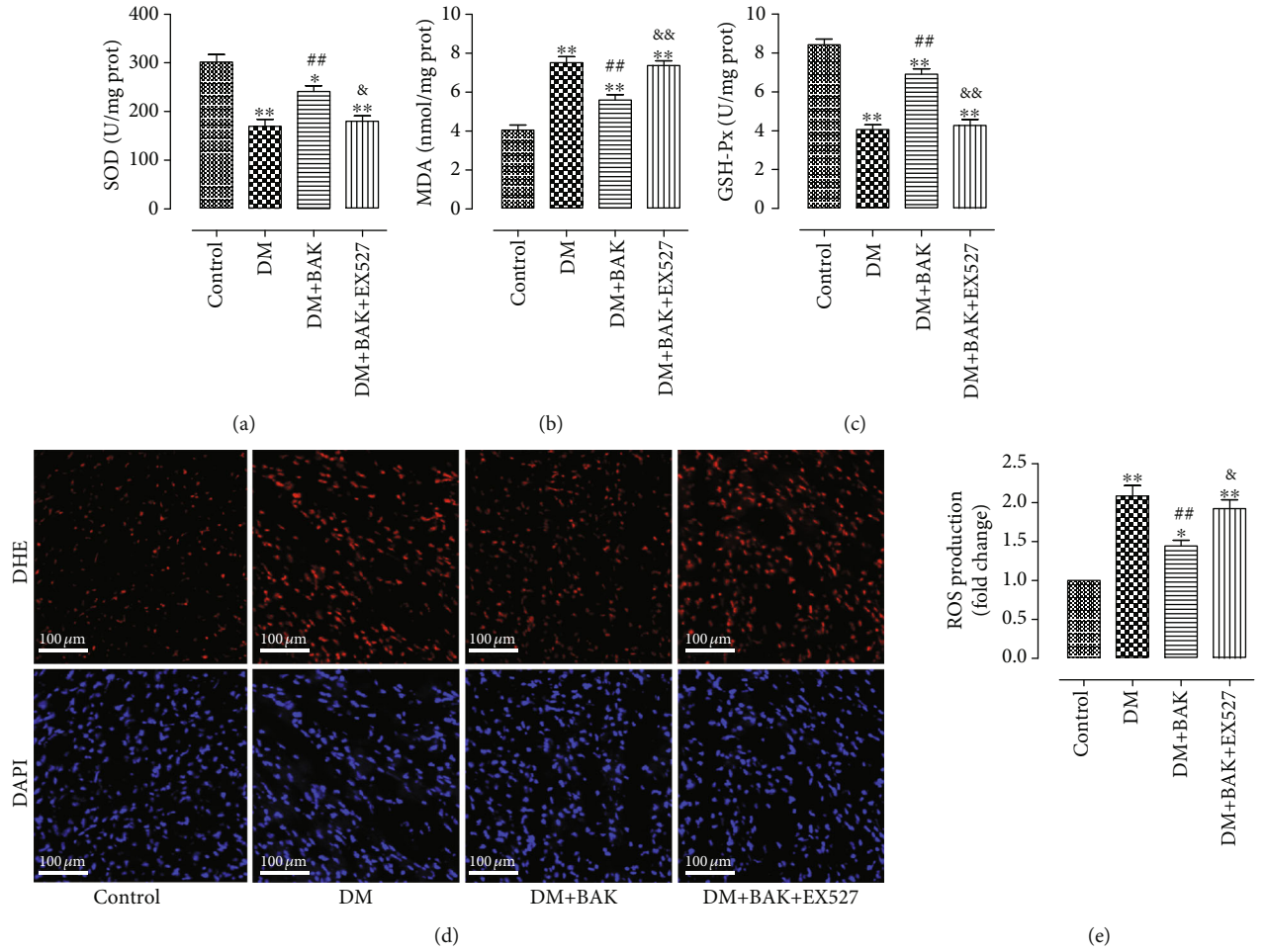

Figure 8: EX527 blunted BAK-induced suppression on oxidative stress level in diabetic myocardium. (a) Myocardial SOD activity. (b) Myocardial MDA contents. (c) Myocardial GSH-Px activity. (d) Representative images of DHE staining (scale bar = 100 μm). (e) DHE intensity. Data are presented as the mean ± SEM ($n = 6$ in each group). $^{*/**}P < 0.05/0.01$ vs. the control group, $^{\#/\#\#}P < 0.05/0.01$ vs. the DM group, and $^{\&/\&\&}P < 0.05/0.01$ vs. the DM+BAK group.

production in the diabetic hearts, which was shown by the declined intensity of DHE fluorescence (Figures 8(d) and 8(e)). Nonetheless, EX527 administration dramatically abolished this effect. Those results confirmed that SIRT1 signaling participated in the ameliorative effects of BAK against myocardial oxidative stress *in vivo*.

3.7. BAK Markedly Enhanced the Expressions of SIRT1 and Nrf2 in HG-Treated H9c2 Cells. To further verify the positive effects of BAK against HG-induced damages on cardiomyocytes and illuminate the molecular mechanisms, we used cardiomyoblast-derived H9c2 cells and employed the SIRT1 siRNA and Nrf2 siRNA to conduct the *in vitro* experiments. As shown in Figures 9(a) and 9(b), we first investigated that BAK treatment alone had no toxic effect on cell survival when H9c2 cells were incubated with normal glucose, while it could significantly increase cell viability following HG treatment dose dependently. This protective effect of BAK was most obvious at the concentration of 10 μM, which was selected for further studies.

Next, as results exhibited in Figures 9(c)–9(f), compared with the control group, we also observed that the expression and activity of SIRT1 were significantly decreased after HG incubation, along with the markedly decreased translocation of nuclear Nrf2. Simultaneously, treatment with BAK prominently restored SIRT1 expression and deacetylation activity and increased Nrf2 nuclear accumulation, which further indicated that BAK might exert its protective capabilities by upregulating the SIRT1 and Nrf2 signaling *in vitro*. Additionally, in accordance with our *in vivo* data, the results in Figure S2 confirmed that the changes of intracellular SIRT1 expression and activity and Nrf2 nuclear accumulation were a secondary outcome of the BAK treatment as well.

3.8. SIRT1 siRNA and Nrf2 siRNA Abolished BAK-Induced Prevention on Cardiomyocyte Death and Oxidative Stress in HG-Treated H9c2 Cells. As shown in Figures 10(a) and 10(b), BAK significantly prevented HG-induced cardiomyocyte apoptosis by decreasing TUNEL-positive nuclei and apoptotic ratio compared with the HG group. Moreover, cell viability in the HG+BAK group was markedly elevated with BAK supplementation (Figure 10(c)). However, these beneficial effects of BAK were notably blunted by SIRT1 siRNA and Nrf2 siRNA administration.

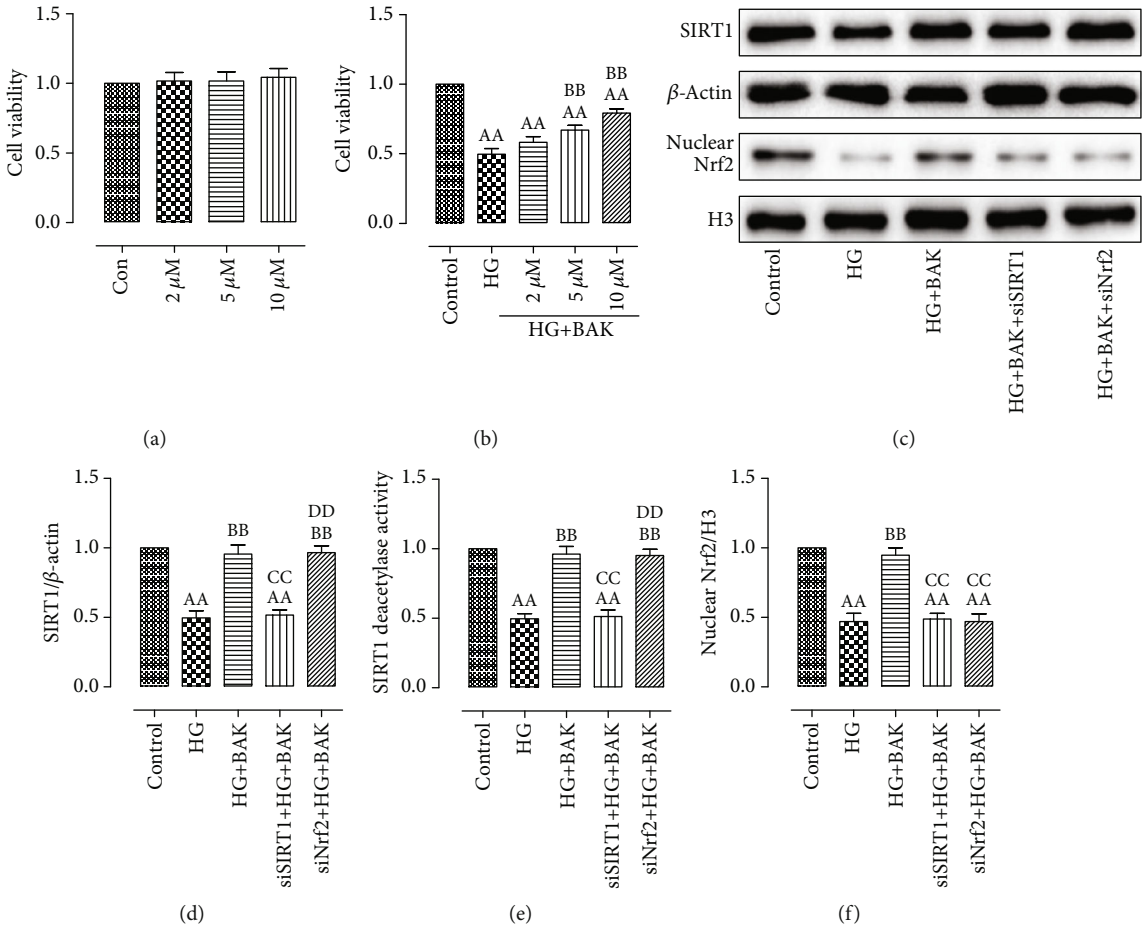

Figure 9: BAK treatment increased cell viability, raised intracellular SIRT1 expression and activity, and enhanced Nrf2 nuclear accumulation in HG-treated H9c2 cells. (a) BAK treatment (2 μM, 5 μM, and 10 μM) had no toxic effect on the cell viability of control H9c2 cells. (b) BAK treatment dose dependently increased the cell viability in HG-treated H9c2 cells. (c) Representative blots. (d) SIRT1 expression. (e) Relative SIRT1 activity. (f) Nrf2 nuclear translocation. Data are presented as the mean ± SEM ($n = 6$ in each group). $^{aa}P < 0.01$ vs. the control group, $^{bb}P < 0.01$ vs. the HG group, $^{cc}P < 0.01$ vs. the HG+BAK group, and $^{dd}P < 0.01$ vs. the siSIRT1+HG+BAK group.

In accordance with our *in vivo* results, BAK also improved SOD and GSH-Px activities and reduced MDA content in HG-treated H9c2 cells, whereas SIRT1 siRNA and Nrf2 siRNA abolished these effects (Figures 11(a)–11(c)). In addition, DCFH-DA fluorescence, used to detect intracellular ROS generation, has shown that BAK treatment significantly inhibited HG-triggered ROS production in the HG+BAK group. Consistently, SIRT1 siRNA and Nrf2 siRNA transfection blunted this antioxidative effect (Figures 11(d) and 11(e)).

Taken together, these data indicated that BAK could attenuate cellular death and oxidative damage in HG-cultured H9c2 cells via SIRT1 and Nrf2 signaling.

3.9. Nrf2 Acted as a Downstream Target of SIRT1 in Mediating the Cardioprotective Effects of BAK. And lastly, we investigated the regulatory relationship between SIRT1 and Nrf2. Results from both *in vivo* and *in vitro* research showed that EX527 or SIRT1 siRNA not only markedly suppressed BAK-induced promotion in expression and activity of SIRT1 but also abolished BAK-induced nuclear accumulation of Nrf2 (Figures 1 and 9(c)–9(f)). In the meantime, notwithstanding the remarkably inhibition of BAK-induced nuclear localization of Nrf2 by Nrf2 siRNA, it had little effect on SIRT1 expression or activity (Figures 9(c)–9(f)). In summary, these data indicated that Nrf2 might function downstream of SIRT1 signaling in mediating the cardioprotective actions of BAK against diabetic cardiomyopathy.

4. Discussion

The present study revealed that in the setting of diabetic cardiomyopathy, BAK reversed the adverse effects of hyperglycemia-induced oxidative stress in diabetic hearts, as demonstrated by improvement of cardiac function, mitigation of pathological cardiac hypertrophy, prevention of myocardial fibrosis, and elevation of cardiomyocyte survival rate. Mechanistically, the above protective capabilities of BAK were in part mediated by SIRT1/Nrf2-related antioxidative activities, including increased production of antioxidants, decreased generation of ROS, and suppressed expressions of fibrosis- and hypertrophy-associated molecules. So far as we know, it is the first research concerning

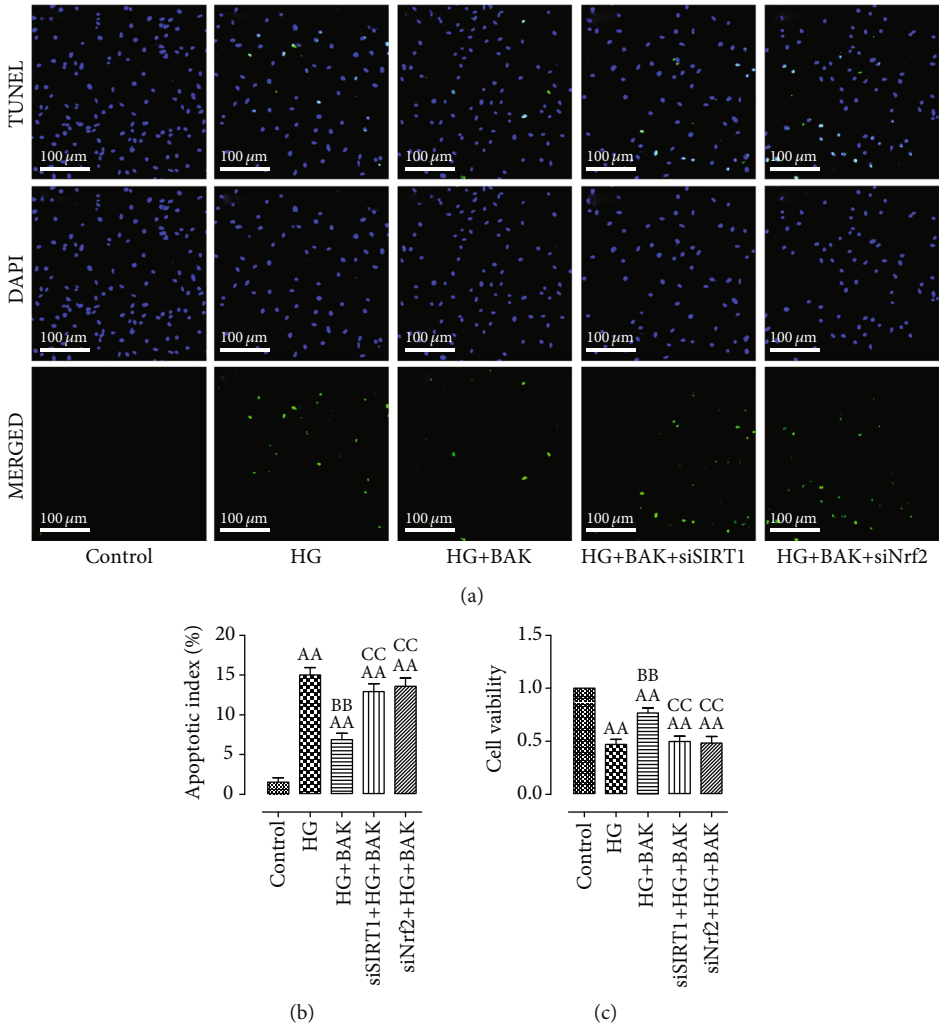

Figure 10: SIRT1 siRNA and Nrf2 siRNA transfection blunted BAK-induced antiapoptotic effect in HG-treated H9c2 cells. (a) Representative images of TUNEL staining (scale bar = 100 μm). The apoptotic cells were detected by TUNEL (green), and the nuclei were detected by DAPI (blue). (b) Cellular apoptotic index. (c) Cell viability. Data are presented as the mean ± SEM ($n = 6$ in each group). $^{aa}P < 0.01$ vs. the control group, $^{bb}P < 0.01$ vs. the HG group, and $^{cc}P < 0.01$ vs. the HG+BAK group.

the cardioprotective effects and potential underlying mechanisms of BAK against diabetic cardiomyopathy.

The incidence of DM is rising at an alarming rate, making it one of the most prevalent disorders that threaten the world health [37]. Clinical evidence obtained from population-based observational studies has indicated that structural and functional abnormalities in diabetic hearts adversely affect the prognosis of diabetic patients [38, 39]. These cardiac pathophysiological changes, induced by the metabolic alterations in DM, were defined as a distinct clinical entity named diabetic cardiomyopathy, which is initially characterized by myocardial fibrosis and cardiac remodeling, later by diastolic and systolic dysfunctions, and eventually by clinical heart failure [5]. As yet, due to the severe consequences of diabetes-associated hyperglycemia, diabetic cardiomyopathy has become a leading cause responsible for the greater risk of morbidity and mortality in diabetic patients [34]. Considering that conventional antidiabetic drugs cannot completely prevent the occurrence and progression of this cardiovascular complication [40, 41], searching for a novel agent targeting the pathophysiology and molecular mechanisms involved in diabetic cardiomyopathy could be a promising candidate therapy.

Bakuchiol (BAK), a bioactive natural meroterpene isolated from the seeds of *Psoralea corylifolia*, has long been used as a traditional Chinese medicine [11]. Crucially, previous studies have observed the favorable effects of BAK in the setting of diabetes. Seo et al. noted that BAK significantly reduces blood glucose levels, improves glucose tolerance, and increases serum insulin levels in streptozotocin-induced diabetic mice [17]. Krenisky et al. confirmed that the oral administration of BAK reduces blood glucose levels in db/db mice with type 2 diabetes [18]. Moreover, growing attention has also been paid to its protective actions on cardiovascular performance. Wang et al. demonstrated that BAK protects against pathological cardiac hypertrophy by blocking the NF-κB signaling pathway [42]. Feng et al. reported that BAK attenuates myocardial ischemia reperfusion injury by maintaining mitochondrial function [15]. Additionally, Kassahun et al. found that BAK induces

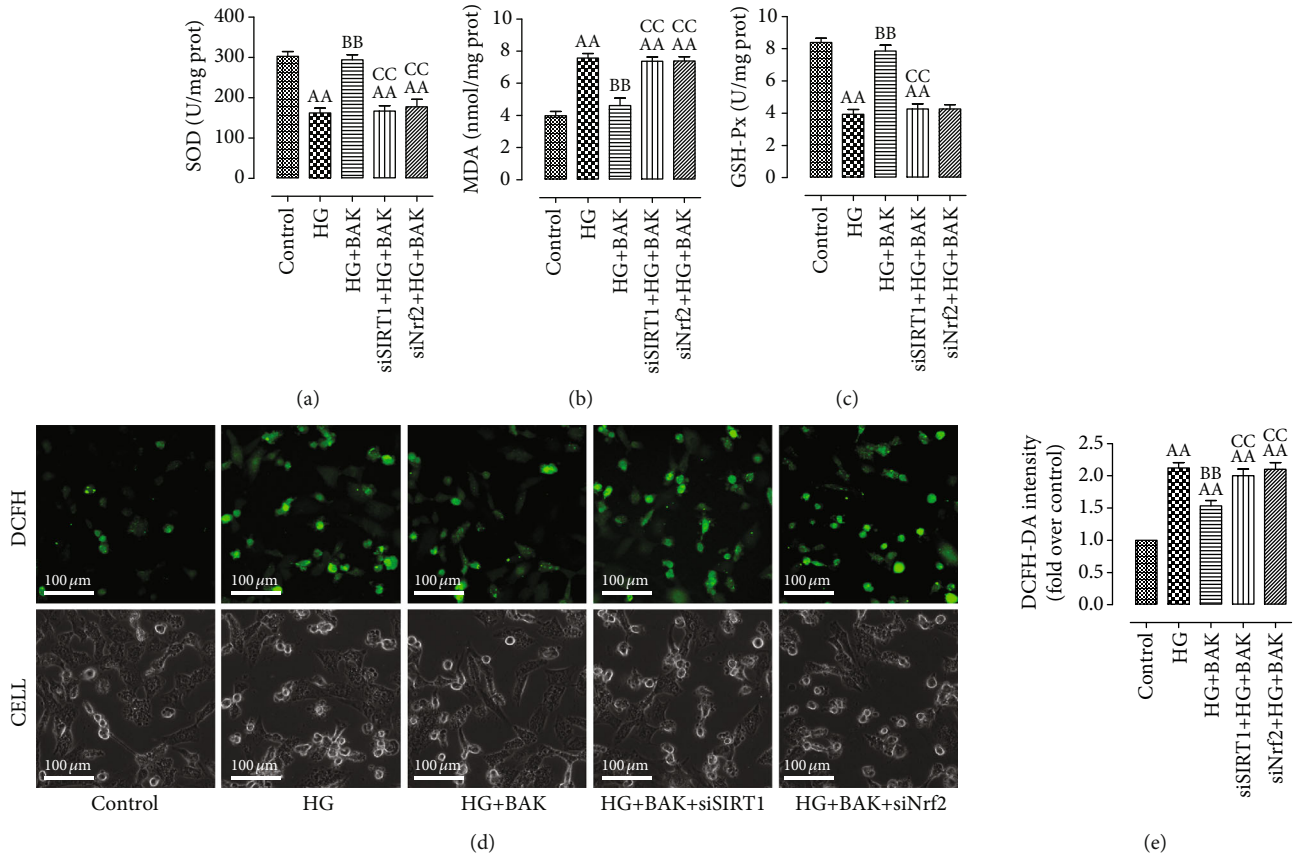

FIGURE 11: SIRT1 siRNA and Nrf2 siRNA transfection inhibited BAK-induced suppression on oxidative stress in HG-treated H9c2 cells. (a) Intracellular SOD activity. (b) Intracellular MDA content. (c) Intracellular GSH-Px activity. (d) Representative images of DCFH-DA staining (scale bar = 100 μm). (e) DCFH-DA intensity. Data are presented as the mean ± SEM ($n = 6$ in each group). $^{aa}P < 0.01$ vs. the control group, $^{bb}P < 0.01$ vs. the HG group, and $^{cc}P < 0.01$ vs. the HG+BAK group.

vasodilation in rat arteries through both endothelium-dependent and endothelium-independent mechanisms [43]. However, the relationship between BAK and diabetic cardiomyopathy has not been clarified thus far. In this study, we first observed that BAK treatment could significantly increase cell viability and prevent cell apoptosis in HG-cultured H9c2 cells. Then, the *in vivo* study further verified that BAK supplementation not only blocked myocardial hypertrophic response and alterations in left ventricular mass but also attenuated interstitial and perivascular fibrosis and collagen deposition. And the improvement of above structural abnormalities ultimately alleviated the cardiac dysfunction in the BAK-treated mice. Therefore, the administration of BAK may be a potential approach for the intervention of diabetic cardiomyopathy.

Evidence has shown that the oxidative stress in human diabetic hearts was overwhelming, which has been proven to be one of the pivotal roles in the development and progression of diabetic cardiomyopathy [5, 7, 44]. The metabolic milieu associated with DM, such as hyperglycemia, hyperlipidemia, and hyperinsulinemia, unduly increased ROS generation from mitochondrial and extramitochondrial sources [7, 45]. And the overly stimulated ROS production further triggered the oxidative stress in the diabetic myocardium, accompanied by immoderately exhausted endogenous antioxidants and excessively accumulated prooxidative damage products [6, 46]. At the same time, continuously boosted state of oxidative stress altered multiple molecular pathways within the cardiomyocytes, finally leading to the myocyte apoptosis or necrosis [9, 47]. More importantly, the pathogenies of diabetes-associated cardiac fibrosis and hypertrophy were proven to be closely connected with increased oxidative stress. On the one hand, overproduction of ROS could induce TGF-$\beta 1$/Smad3 signaling activation, which promoted the expressions of several fibrotic markers, causing the proliferation of cardiac fibroblasts and collagen synthesis [48, 49]. On the other hand, increased oxidative stress could lead to the switch in the hypertrophy-related gene MHC expression from the α-MHC isoform to the β-MHC isoform, which marked the progression of cardiac hypertrophy [7, 50]. Hence, to inhibit ROS generation and relive the oxidative stress will be a very promising treatment strategy for diabetic cardiomyopathy. Intriguingly, numerous studies have provided supports for the use of BAK as an effective antioxidant. Haraguchi et al. found that BAK showed broad antioxidative activities in rat liver microsomes and mitochondria [51]. Adhikari et al. revealed the importance of the terpenoid moiety of BAK in controlling its antioxidant action via radical scavenging [52]. Moreover, thanks to its highly efficient antioxidative capacity, BAK has been certified to exhibit

protective roles against multiple diseases in various organs or tissues [13–16], which greatly prompts us to confirm this effect in diabetic cardiomyopathy. As expected, data collected in our study showed that BAK treatment markedly improved SOD and GSH-Px activities and reduced MDA content, as well as inhibited hyperglycemia-triggered ROS production, thus alleviating myocardial oxidative stress both *in vivo* and *in vitro*. Furthermore, from the fibrosis-related protein and hypertrophy-related gene levels, BAK administration remarkably inhibited the expression of α-SMA and suppressed the activation of TGF-$\beta 1$/Smad3 signaling. Meanwhile, mRNA levels of ANP and BNP were significantly decreased, and gene MHC expression underwent canonical changes from β-MHC to α-MHC.

To further unravel the molecular mechanisms implicated in the antioxidative effects of BAK against diabetic cardiomyopathy, we have focused on the SIRT1/Nrf2 signaling pathway. SIRT1, a protein widely expressed in mammalian cells, is highly sensitive to the cellular redox states and has recently been intensively investigated in the cardiovascular system [53]. Immense amounts of concrete research have demonstrated that endogenous SIRT1 is tightly linked to the cardioprotection of various cardiovascular diseases for its pivotal role in increasing resistance to oxidative damage [19, 54]. As for Nrf2, another vital antioxidant sensor, it confers maintenance of cellular defense system by promoting the expressions of antioxidant molecules when its position shifts from the cytoplasm to the nucleus where it binds to AREs [55, 56]. Many previous studies have already revealed the two redox-sensitive proteins closely implicated in the therapeutic effects on diabetic cardiomyopathy [21, 46, 57, 58]. More importantly, SIRT1 is involved in the regulation and control of oxidative stress that are associated with diverse stimulus, which appears to be exerted by activating Nrf2, indicating that Nrf2 serves as an important downstream target of SIRT1 signaling [25, 26, 31, 59]. Additionally, novel observations have suggested that BAK inhibits ROS generation in cardiomyocytes via SIRT1. And Shoji et al. found that BAK is a phenolic isoprenoid with novel enantiomer-selective anti-influenza A virus activity involving Nrf2 activation [60]. Therefore, the above findings strongly intrigued us to test the connection between the SIRT1/Nrf2 signaling and BAK protective effects in this diabetic complication. Within expectation, our results showed that BAK treatment reversed the downward trends of SIRT1 expression and Nrf2 nuclear translocation caused by hyperglycemia, while EX527, SIRT1 siRNA, or Nrf2 siRNA abolished this effect, finally nullifying the antioxidative actions of BAK. In the meantime, EX527 and SIRT1 siRNA not only blocked the BAK-induced increase in SIRT1 expression and activity but also inhibited the Nrf2 nuclear accumulation, but Nrf2 siRNA had little effect on SIRT1 expression or activity, suggesting that SIRT1 functioned upstream of Nrf2 signaling. Consequently, we concluded that BAK ameliorated diabetic cardiomyopathy by reducing myocardial oxidative damage in a SIRT1/Nrf2 signaling-dependent pathway.

In conclusion, we have demonstrated for the first time that BAK treatment can effectively retard the progression of pathological cardiac hypertrophy and inhibit the development of cardiac fibrosis against diabetic cardiomyopathy, which ultimately alleviate the impairment of the cardiac function. These effects were primarily ascribed to the activation of SIRT1/Nrf2 signaling and its followed attenuation of myocardial oxidative stress, as SIRT1/Nrf2 signaling played an important role in elevating the antioxidant production and reducing the ROS generation in diabetic myocardium. Our study strongly suggested that long-term BAK supplement may be chosen as a therapeutic intervention for treating diabetics with cardiac abnormalities. In the future, experiments concerning other upstream and (or) downstream signals of SIRT1 should be warranted to establish a more comprehensive molecular mechanisms of BAK protective actions, and additional trials using larger animal models must be operated before enabling its application towards clinical practice.

Data Availability

The data used to support the findings of this study are available from the corresponding author upon request.

Conflicts of Interest

The authors declare that they have no conflicts of interest in the studies described.

Authors' Contributions

Wenshuai Ma and Wangang Guo contributed equally to this study.

Acknowledgments

This work was supported by grants from the Basic Research Program of Natural Science of Shaanxi Province (2016JM8062).

Supplementary Materials

Figure S1: the effects of BAK on the expression and activity of SIRT1 and nuclear accumulation of Nrf2 in normal hearts. (a) Representative blots. (b) SIRT1 expression. (c) Relative SIRT1 activity. (d) Nrf2 nuclear translocation. Data are presented as the mean ± SEM ($n = 6$ in each group). Figure S2: the effects of BAK on intracellular SIRT1 expression and activity and Nrf2 nuclear accumulation in normal H9c2 cells. (a) Representative blots. (b) SIRT1 expression. (c) Relative SIRT1 activity. (d) Nrf2 nuclear translocation. Data are presented as the mean ± SEM ($n = 6$ in each group). *(Supplementary Materials)*

References

[1] "Diabetes: a dynamic disease," *The Lancet*, vol. 389, no. 10085, article 2163, 2017.

[2] "Diagnosis and classification of diabetes mellitus," in *Diabetes Care*, vol. 37, Supplement 1pp. S81–S90, American Diabetes Association, 2013.

[3] W. H. Dillmann, "Diabetic cardiomyopathy," *Circulation Research*, vol. 124, no. 8, pp. 1160–1162, 2019.

[4] G. Jia, A. Whaley-Connell, and J. R. Sowers, "Diabetic cardiomyopathy: a hyperglycaemia- and insulin-resistance-induced heart disease," *Diabetologia*, vol. 61, no. 1, pp. 21–28, 2018.

[5] G. Jia, M. A. Hill, and J. R. Sowers, "Diabetic cardiomyopathy: an update of mechanisms contributing to this clinical entity," *Circulation Research*, vol. 122, no. 4, pp. 624–638, 2018.

[6] E. Liang, X. Liu, Z. du, R. Yang, and Y. Zhao, "Andrographolide ameliorates diabetic cardiomyopathy in mice by blockage of oxidative damage and NF-κB-mediated inflammation," *Oxidative Medicine and Cellular Longevity*, vol. 2018, Article ID 9086747, 13 pages, 2018.

[7] H. Bugger and E. D. Abel, "Molecular mechanisms of diabetic cardiomyopathy," *Diabetologia*, vol. 57, no. 4, pp. 660–671, 2014.

[8] N. Kaludercic and F. Di Lisa, "Mitochondrial ROS formation in the pathogenesis of diabetic cardiomyopathy," *Frontiers in Cardiovascular Medicine*, vol. 7, p. 12, 2020.

[9] R. Ni, T. Cao, S. Xiong et al., "Therapeutic inhibition of mitochondrial reactive oxygen species with Mito-TEMPO reduces diabetic cardiomyopathy," *Free Radical Biology & Medicine*, vol. 90, pp. 12–23, 2016.

[10] A. J. Wilson, E. K. Gill, R. A. Abudalo, K. S. Edgar, C. J. Watson, and D. J. Grieve, "Reactive oxygen species signalling in the diabetic heart: emerging prospect for therapeutic targeting," *Heart*, vol. 104, no. 4, pp. 293–299, 2018.

[11] Z. Xin, X. Wu, T. Ji et al., "Bakuchiol: a newly discovered warrior against organ damage," *Pharmacological Research*, vol. 141, pp. 208–213, 2019.

[12] H. S. Lim, Y. J. Kim, B. Y. Kim, and S. J. Jeong, "Bakuchiol suppresses inflammatory responses via the downregulation of the p 38 MAPK/ERK signaling pathway," *International Journal of Molecular Sciences*, vol. 20, no. 14, p. 3574, 2019.

[13] K. A. Kim, S. H. Shim, H. R. Ahn, and S. H. Jung, "Protective effects of the compounds isolated from the seed of *Psoralea corylifolia* on oxidative stress-induced retinal damage," *Toxicology and Applied Pharmacology*, vol. 269, no. 2, pp. 109–120, 2013.

[14] E. Seo, Y. S. Oh, D. Kim, M. Y. Lee, S. Chae, and H. S. Jun, "Protective role of *Psoralea corylifolia* L. seed extract against hepatic mitochondrial dysfunction induced by oxidative stress or aging," *Evidence-based Complementary and Alternative Medicine*, vol. 2013, Article ID 678028, 9 pages, 2013.

[15] J. Feng, Y. Yang, Y. Zhou et al., "Bakuchiol attenuates myocardial ischemia reperfusion injury by maintaining mitochondrial function: the role of silent information regulator 1," *Apoptosis*, vol. 21, no. 5, pp. 532–545, 2016.

[16] X. Zhang, N. Chang, Y. Zhang et al., "Bakuchiol protects against acute lung injury in septic mice," *Inflammation*, vol. 40, no. 2, pp. 351–359, 2017.

[17] E. Seo, E. K. Lee, C. S. Lee, K. H. Chun, M. Y. Lee, and H. S. Jun, "*Psoralea corylifolia* L. seed extract ameliorates streptozotocin-induced diabetes in mice by inhibition of oxidative stress," *Oxidative Medicine and Cellular Longevity*, vol. 2014, Article ID 897296, 9 pages, 2014.

[18] J. M. Krenisky, J. Luo, M. J. Reed, and J. R. Carney, "Isolation and antihyperglycemic activity of bakuchiol from *Otholobium pubescens* (Fabaceae), a Peruvian medicinal plant used for the treatment of diabetes," *Biological & Pharmaceutical Bulletin*, vol. 22, no. 10, pp. 1137–1140, 1999.

[19] A. E. Kane and D. A. Sinclair, "Sirtuins and $NAD^{(+)}$ in the development and treatment of metabolic and cardiovascular diseases," *Circulation Research*, vol. 123, no. 7, pp. 868–885, 2018.

[20] N. D'Onofrio, L. Servillo, and M. L. Balestrieri, "SIRT1 and SIRT6 signaling pathways in cardiovascular disease protection," *Antioxidants & Redox Signaling*, vol. 28, no. 8, pp. 711–732, 2018.

[21] H. Karbasforooshan and G. Karimi, "The role of SIRT1 in diabetic cardiomyopathy," *Biomedicine & Pharmacotherapy*, vol. 90, pp. 386–392, 2017.

[22] M. Waldman, K. Cohen, D. Yadin et al., "Regulation of diabetic cardiomyopathy by caloric restriction is mediated by intracellular signaling pathways involving 'SIRT1 and PGC-1α'," *Cardiovascular Diabetology*, vol. 17, no. 1, p. 111, 2018.

[23] V. V. Sathibabu Uddandrao, P. Brahmanaidu, P. R. Nivedha, S. Vadivukkarasi, and G. Saravanan, "Beneficial role of some natural products to attenuate the diabetic cardiomyopathy through Nrf 2 pathway in cell culture and animal models," *Cardiovascular Toxicology*, vol. 18, no. 3, pp. 199–205, 2018.

[24] J. Gu, Y. Cheng, H. Wu et al., "Metallothionein is downstream of Nrf 2 and partially mediates sulforaphane prevention of diabetic cardiomyopathy," *Diabetes*, vol. 66, no. 2, pp. 529–542, 2017.

[25] F. Samimi, M. Baazm, E. Eftekhar, S. Rajabi, M. T. Goodarzi, and F. Jalali Mashayekhi, "Possible antioxidant mechanism of coenzyme Q10 in diabetes: impact on Sirt 1/Nrf 2 signaling pathways," *Research in Pharmaceutical Sciences*, vol. 14, no. 6, pp. 524–533, 2019.

[26] G. Wang, X. Xie, L. Yuan et al., "Resveratrol ameliorates rheumatoid arthritis via activation of SIRT1-Nrf 2 signaling pathway," *BioFactors*, vol. 46, no. 3, pp. 441–453, 2020.

[27] S. Li, H. Wu, D. Han et al., "A novel mechanism of mesenchymal stromal cell-mediated protection against sepsis: restricting inflammasome activation in macrophages by increasing mitophagy and decreasing mitochondrial ROS," *Oxidative Medicine and Cellular Longevity*, vol. 2018, Article ID 3537609, 15 pages, 2018.

[28] R. Li, Y. Liu, J. Xie et al., "Sirt 3 mediates the protective effect of hydrogen in inhibiting ROS-induced retinal senescence," *Free Radical Biology & Medicine*, vol. 135, pp. 116–124, 2019.

[29] R. Ding, C. Zhang, X. Zhu et al., "ROS-AKT-mTOR axis mediates autophagy of human umbilical vein endothelial cells induced by cooking oil fumes-derived fine particulate matters in vitro," *Free Radical Biology & Medicine*, vol. 113, pp. 452–460, 2017.

[30] P. D. Tatman, K. C. Woulfe, A. Karimpour-Fard et al., "Pediatric dilated cardiomyopathy hearts display a unique gene expression profile," *JCI Insight*, vol. 2, no. 14, 2017.

[31] B. Zhang, M. Zhai, B. Li et al., "Honokiol ameliorates myocardial ischemia/reperfusion injury in type 1 diabetic rats by reducing oxidative stress and apoptosis through activating the SIRT1-Nrf 2 signaling pathway," *Oxidative Medicine and Cellular Longevity*, vol. 2018, Article ID 3159801, 16 pages, 2018.

[32] S. Dong, S. Zhang, Z. Chen et al., "Berberine could ameliorate cardiac dysfunction via interfering myocardial lipidomic profiles in the rat model of diabetic cardiomyopathy," *Frontiers in Physiology*, vol. 9, article 1042, 2018.

[33] M. Zhai, Z. Liu, B. Zhang et al., "Melatonin protects against the pathological cardiac hypertrophy induced by transverse aortic

constriction through activating PGC-1β: in vivo and in vitro studies," *Journal of Pineal Research*, vol. 63, no. 3, 2017.

[34] X. Palomer, J. Pizarro-Delgado, and M. Vazquez-Carrera, "Emerging actors in diabetic cardiomyopathy: heartbreaker biomarkers or therapeutic targets?," *Trends in Pharmacological Sciences*, vol. 39, no. 5, pp. 452–467, 2018.

[35] J. Asbun and F. J. Villarreal, "The pathogenesis of myocardial fibrosis in the setting of diabetic cardiomyopathy," *Journal of the American College of Cardiology*, vol. 47, no. 4, pp. 693–700, 2006.

[36] I. Russo and N. G. Frangogiannis, "Diabetes-associated cardiac fibrosis: cellular effectors, molecular mechanisms and therapeutic opportunities," *Journal of Molecular and Cellular Cardiology*, vol. 90, pp. 84–93, 2016.

[37] P. Zimmet, K. G. Alberti, D. J. Magliano, and P. H. Bennett, "Diabetes mellitus statistics on prevalence and mortality: facts and fallacies," *Nature Reviews. Endocrinology*, vol. 12, no. 10, pp. 616–622, 2016.

[38] A. Lorenzo-Almorós, J. Tuñón, M. Orejas, M. Cortés, J. Egido, and Ó. Lorenzo, "Diagnostic approaches for diabetic cardiomyopathy," *Cardiovascular Diabetology*, vol. 16, no. 1, p. 28, 2017.

[39] G. Murtaza, H. U. H. Virk, M. Khalid et al., "Diabetic cardiomyopathy - a comprehensive updated review," *Progress in Cardiovascular Diseases*, vol. 62, no. 4, pp. 315–326, 2019.

[40] R. E. Gilbert and H. Krum, "Heart failure in diabetes: effects of anti-hyperglycaemic drug therapy," *The Lancet*, vol. 385, no. 9982, pp. 2107–2117, 2015.

[41] D. D. Huang, G. Shi, Y. Jiang, C. Yao, and C. Zhu, "A review on the potential of resveratrol in prevention and therapy of diabetes and diabetic complications," *Biomedicine & Pharmacotherapy*, vol. 125, article 109767, 2020.

[42] Z. Wang, L. Gao, L. Xiao et al., "Bakuchiol protects against pathological cardiac hypertrophy by blocking NF-κB signaling pathway," *Bioscience Reports*, vol. 38, no. 5, 2018.

[43] A. Kassahun Gebremeskel, T. D. Wijerathne, J. H. Kim et al., "*Psoralea corylifolia* extract induces vasodilation in rat arteries through both endothelium-dependent and -independent mechanisms involving inhibition of TRPC3 channel activity and elaboration of prostaglandin," *Pharmaceutical Biology*, vol. 55, no. 1, pp. 2136–2144, 2017.

[44] A. Faria and S. J. Persaud, "Cardiac oxidative stress in diabetes: mechanisms and therapeutic potential," *Pharmacology & Therapeutics*, vol. 172, pp. 50–62, 2017.

[45] P. M. Seferovic and W. J. Paulus, "Clinical diabetic cardiomyopathy: a two-faced disease with restrictive and dilated phenotypes," *European Heart Journal*, vol. 36, no. 27, pp. 1718–1727, 2015.

[46] K. Li, M. Zhai, L. Jiang et al., "Tetrahydrocurcumin ameliorates diabetic cardiomyopathy by attenuating high glucose-induced oxidative stress and fibrosis via activating the SIRT1 pathway," *Oxidative Medicine and Cellular Longevity*, vol. 2019, Article ID 6746907, 15 pages, 2019.

[47] K. Huynh, H. Kiriazis, X. J. du et al., "Targeting the upregulation of reactive oxygen species subsequent to hyperglycemia prevents type 1 diabetic cardiomyopathy in mice," *Free Radical Biology & Medicine*, vol. 60, pp. 307–317, 2013.

[48] H. H. Liao, J. X. Zhu, H. Feng et al., "Myricetin possesses potential protective effects on diabetic cardiomyopathy through inhibiting IκBα/NFκB and enhancing Nrf2/HO-1," *Oxidative Medicine and Cellular Longevity*, vol. 2017, Article ID 8370593, 14 pages, 2017.

[49] A. Biernacka, M. Cavalera, J. Wang et al., "Smad 3 signaling promotes fibrosis while preserving cardiac and aortic geometry in obese diabetic mice," *Circulation. Heart Failure*, vol. 8, no. 4, pp. 788–798, 2015.

[50] M. Aragno, R. Mastrocola, C. Medana et al., "Oxidative stress-dependent impairment of cardiac-specific transcription factors in experimental diabetes," *Endocrinology*, vol. 147, no. 12, pp. 5967–5974, 2006.

[51] H. Haraguchi, J. Inoue, Y. Tamura, and K. Mizutani, "Antioxidative components of *Psoralea corylifolia* (Leguminosae)," *Phytotherapy Research*, vol. 16, no. 6, pp. 539–544, 2002.

[52] S. Adhikari, R. Joshi, B. S. Patro et al., "Antioxidant activity of bakuchiol: experimental evidences and theoretical treatments on the possible involvement of the terpenoid chain," *Chemical Research in Toxicology*, vol. 16, no. 9, pp. 1062–1069, 2003.

[53] S. Winnik, J. Auwerx, D. A. Sinclair, and C. M. Matter, "Protective effects of sirtuins in cardiovascular diseases: from bench to bedside," *European Heart Journal*, vol. 36, no. 48, pp. 3404–3412, 2015.

[54] S. Matsushima and J. Sadoshima, "The role of sirtuins in cardiac disease," *American Journal of Physiology. Heart and Circulatory Physiology*, vol. 309, no. 9, pp. H1375–H1389, 2015.

[55] Q. M. Chen and A. J. Maltagliati, "Nrf 2 at the heart of oxidative stress and cardiac protection," *Physiological Genomics*, vol. 50, no. 2, pp. 77–97, 2018.

[56] R. M. da Costa, D. Rodrigues, C. A. Pereira et al., "Nrf 2 as a potential mediator of cardiovascular risk in metabolic diseases," *Frontiers in Pharmacology*, vol. 10, p. 382, 2019.

[57] S. Wang, B. Wang, Y. Wang et al., "Zinc prevents the development of diabetic cardiomyopathy in db/db mice," *International Journal of Molecular Sciences*, vol. 18, no. 3, p. 580, 2017.

[58] R. Li, Y. Liu, Y. G. Shan, L. Gao, F. Wang, and C. G. Qiu, "Baicalin protects against diabetic cardiomyopathy through Keap 1/Nrf 2/AMPK-mediated antioxidative and lipid-lowering effects," *Oxidative Medicine and Cellular Longevity*, vol. 2019, Article ID 3206542, 15 pages, 2019.

[59] L. Yu, S. Li, X. Tang et al., "Diallyl trisulfide ameliorates myocardial ischemia-reperfusion injury by reducing oxidative stress and endoplasmic reticulum stress-mediated apoptosis in type 1 diabetic rats: role of SIRT1 activation," *Apoptosis*, vol. 22, no. 7, pp. 942–954, 2017.

[60] M. Shoji, Y. Arakaki, T. Esumi et al., "Bakuchiol is a phenolic isoprenoid with novel enantiomer-selective anti-influenza a virus activity involving Nrf 2 activation," *The Journal of Biological Chemistry*, vol. 290, no. 46, pp. 28001–28017, 2015.

Hindawi
Oxidative Medicine and Cellular Longevity
Volume 2020, Article ID 9792836, 10 pages
https://doi.org/10.1155/2020/9792836

Research Article

The Impact of Modern Therapeutic Methods on the Oxidant-Antioxidant Equilibrium and Activities of Selected Lysosomal Enzymes and Serine Protease Inhibitor in Amateur Athletes

Łukasz Sielski,[1,2] Paweł Sutkowy,[3] Katarzyna Pawlak-Osińska,[1] Alina Woźniak,[3] Agnieszka Skopowska,[2,4] Bartosz Woźniak,[5] and Jolanta Czuczejko[6]

[1]*Department of Pathophysiology of Hearing and Balance, Ludwik Rydygier Collegium Medicum in Bydgoszcz, Nicolaus Copernicus University, Toruń, Poland*
[2]*Multidisciplinary City Hospital, Rehabilitation Center, Bydgoszcz, Poland*
[3]*Department of Medical Biology and Biochemistry, Ludwik Rydygier Collegium Medicum in Bydgoszcz, Nicolaus Copernicus University, Toruń, Poland*
[4]*Department of Laser Therapy and Physiotherapy, Ludwik Rydygier Collegium Medicum in Bydgoszcz, Nicolaus Copernicus University, Toruń, Poland*
[5]*Department of Neurosurgery, Stanisław Staszic Specialist Hospital, Piła, Poland*
[6]*Department of Psychiatry, Ludwik Rydygier Collegium Medicum in Bydgoszcz, Nicolaus Copernicus University, Toruń, Poland*

Correspondence should be addressed to Paweł Sutkowy; p.sutkowy@cm.umk.pl

Received 8 May 2020; Accepted 22 July 2020; Published 20 August 2020

Guest Editor: Manjit Singh Rana

Copyright © 2020 Łukasz Sielski et al. This is an open access article distributed under the Creative Commons Attribution License, which permits unrestricted use, distribution, and reproduction in any medium, provided the original work is properly cited.

Deep electromagnetic stimulation (DEMS) and low-frequency ultrasound (US) are new physical therapy methods used in the rehabilitation of the musculoskeletal system and wound healing. They are applied locally to treat the injured tissues. The beneficial effects of these methods in supportive care have been documented, but accurate biochemical effects are not known. The goal was to assess the effect of single DEMS and US sessions on the oxidant-antioxidant equilibrium, as well as the activities of lysosomal hydrolases and α_1-antitrypsin (AAT) in peripheral blood of juvenile injured amateur athletes. In the athletes with low back pain (DEMS treated, $N = 16$) and pain in the shoulder or ankle joint (US treated, $N = 14$), as well as in healthy control amateur athletes (DEMS treated, $N = 14$; US treated, $N = 17$), before the sessions and 30 minutes and 24 hours after them, the levels of the following parameters were determined: thiobarbituric acid reactive substances (TBARS) in erythrocytes and plasma, superoxide dismutase (SOD), glutathione peroxidase (GPx), and catalase (CAT) in erythrocytes, as well as acid phosphatase (AcP), arylsulfatase (ASA), cathepsin D (CTS D), and α_1-antitrypsin (AAT) in serum. After both procedures, the levels of parameters changed in a negligible manner, excluding the cathepsin D activity, which was statistically significantly lower 30 min and 24 h after US in the control athletes compared to the baseline activity determined directly before the procedure (47.5% and 55.7% differences, respectively). Similar tendency was observed after DEMS ($p > 0.05$). The procedures, especially low-frequency US, decrease lysosomal proteolytic activity and do not significantly disrupt the oxidant-antioxidant and lysosomal equilibriums in the peripheral blood both of healthy and injured athletes. No systemic acute-phase response of AAT was also detected in the athletes after both procedures. This trial is registered with CTRI/2018/01/011344.

1. Introduction

Technical advances in the development of medical devices have a significant effect on the improvement in treatment of sports injuries, diseases, and wounds characterized by acute or chronic pain and inflammation. The new methods allow to limit the amount of the administered medicines. Such methods are deep electromagnetic stimulation (DEMS) and low-frequency ultrasound (US). DEMS is used in order to alleviate pain in the treatment of musculoskeletal disorders

and spine problems, as well as in diseases such as rheumatoid arthritis (no reports on inflammation and other phenomena). The method involves variable/pulsed magnetic field with the induction of up to 2.5 Tesla (T) in the frequency range from 1 to 50 Hertz (Hz). Tissues are stimulated locally to the penetration depth of the field, i.e., approx. 10 cm, passing through clothing and tissues, including bones [1–3]. Low-frequency US has similar depth of action but is used with a gel (neutral for health; direct contact of device with the patient's skin) in continuous or pulsed mode. Traditional therapeutic US uses high frequencies, typically ranging between 1 and 3 megahertz (MHz). However, low-frequency US (22–40 kilohertz, kHz) was shown to be more effective (deeper impact and better results). Ultrasound induces similar results to DEMS, but is much better examined. US triggers thermal (an increase of temperature), if applied in a continuous manner, and nonthermal effects (acoustic cavitation and microstreaming) [4]. Low-frequency US in pulsed mode stimulates fracture healing, probably promoting proliferation and differentiation of chondrocytes, which is mediated by TGF-β1 [5]. In turn, the effects of ultrasound on wound healing, chronic ulcers, fracture healing, and osteoradionecrosis may be explained by the enhancement of angiogenesis mediated by IL-8, bFGF, and VEGF [6]. Chronic, difficult to heal wounds (e.g., pressure ulcers, surgical wounds, and diabetic foot ulcers) are especially effectively treated using low-frequency US without contact with the patient's skin [4]. US properties to tendon recovery after sports injury, in turn, probably may be explained by upregulation of proliferating cell nuclear antigen (PCNA; *in vitro* study of the Achilles tendon in a rat) [7]. The treatment stimulates fibroblasts to collagen synthesis at the second stage of healing (proliferation phase) and provides an antiedematous "drainage" action in the case of post-traumatic articular effusions with the effects visible to the naked eye already after one session. Therapeutic US seems to have a slightly proinflammatory effect that optimizes the effectiveness of damaged tissue repair. The healing process is extremely complicated, particularly when it occurs in multiple tissue types simultaneously. It progresses at different levels and requires revascularization. In the case of partly tendon rupture or excessive stretch, a small amount of effusion, tenderness, joint instability, and discomfort during effort can occur. Tissue damage and the accompanying inflammation initiate the regeneration processes. The last stage of healing (matrix-remodelling phase) includes collagen synthesis and scar formation [8]. What is crucial in this process is the adequate response of the body systems and tissues to the injury, as an insufficient or, more frequently, excessive inflammatory reaction leads to problematic healing which results in a reduction of tissue/organ functionality [9]. An important role is also played by the oxidant-antioxidant equilibrium, as oxidants (reactive oxygen species (ROS) and/or reactive nitrogen species (RNS)) mediate virtually all relevant cell functions. Oxidants are also mediators of the response to the disturbance of homoeostasis. When the oxidant-antioxidant equilibrium is disrupted, usually in association with oxidative stress (excessive generation of ROS/RNS), a change in the properties or dysfunction of cellular biomolecules occurs due to oxidative damage, which is accompanied by, e.g., inflammation and increased activity of lysosomal enzymes [10, 11]. Among the consequences of imbalance in the oxidation/reduction processes may be DNA mutations, denaturation, or aggregation of proteins, as well as increased lipid peroxidation which, depending on the intensity or duration of the disrupting factor, leads to necrosis, apoptosis, or inflammation [11]. Many studies have proven that prolonged inflammation is accompanied by chronic oxidative stress. Therefore, a vicious circle occurs which can result in severe chronic diseases, including cancer, diabetes mellitus, neurodegenerative disorders (e.g., Alzheimer's and Parkinson's diseases), rheumatoid arthritis, and cardiovascular and lung diseases. Among other consequences of chronic inflammation and oxidative stress are atherosclerosis, hypertension, ischaemia-reperfusion injury, or increased rate of aging [11, 12]. However, necrosis, apoptosis, and inflammation are not the only types of the organism response to the elevated ROS/RNS concentrations. Instead, an increase in the antioxidant capacity can occur as a result of adaptation of the body to a short-term or low-level stimulus. Increased antioxidant capacity is observed, e.g., during adaptation to high ROS concentrations induced by physical effort [13] or in tumour cells, which can result in acquired tumour radioresistance [12]. The crucial elements of the antioxidant system are antioxidant enzymes, especially superoxide dismutase (SOD), glutathione peroxidase (GPx), and catalase (CAT) [11], while among many markers of oxidative stress lipid peroxidation products are particularly known (e.g., thiobarbituric acid reactive substances (TBARS) including malondialdehyde (MDA)) [14]. Redox balance is also related to the activities of lysosomal enzymes, since they are associated with inflammation [15]. Lysosomal enzymes are also associated with the serine protease inhibitors [16]. Accordingly, the aim of the study was to assess the effect of single DEMS and US sessions on the concentration of TBARS and the activities of SOD, GPx, and CAT, as well as the activities of selected lysosomal enzymes (acid phosphatase (AcP), arylsulfatase (ASA), and cathepsin D (CTS D)) and the activity of the serine protease inhibitor, α_1-antitrypsin (AAT), in the peripheral blood of amateur athletes who had an injury in the lumbosacral segment of the spine, shoulder, or ankle joint.

2. Material and Methods

2.1. Subject. The study involved 30 amateur athletes (22 females and 8 males) subjected to DEMS procedure and 31 amateur athletes (17 females, 14 males) subjected to US procedure. The athletes attended sports clubs in Bydgoszcz, Poland (characteristics in Table 1). They practised indoor volleyball or canoeing. The participants were informed in detail about the aim and course of the experiment and signed their consent to participate in the study (parents in the case of minor ones). The participants were requested not to change their nutritional and sports-related habits throughout the study. They were examined by a sports physician at the beginning of the sports season and were permitted to continue practising their sport disciplines. The study excluded athletes with a history of surgical interventions, a viral or

Table 1: Characteristics of the study participants (mean ± SD).

	$DEMS_{healthy\ controls}$	$DEMS_{injured\ athletes}$	$US_{healthy\ controls}$	$US_{injured\ athletes}$
Number	14	16	17	14
Age (years)	17.9 ± 5.6	16.4 ± 2.6	22.3 ± 8.3	16.8 ± 4.0
Body mass (kg)	69.8 ± 12.1	61.8 ± 7.3	67.5 ± 13.2	69.6 ± 13.6
Body height (m)	1.8 ± 0.1	1.7 ± 0.1	1.7 ± 0.07	1.8 ± 0.1
Body mass index (kg/m^2)	21.5 ± 3.4	21.4 ± 2.1	23.3 ± 3.3	21.5 ± 2.5
Training experience (years)	4.5	4.4	2.2	3.8

bacterial infection, with fever or other inflammatory sign, and those with injuries other than those considered in the study, as well as the athletes which were taking any medications (e.g., painkillers) and dietary supplements that could affect the redox balance in the organism. The study was approved by the Bioethics Committee of the Nicolaus Copernicus University in Toruń, Collegium Medicum in Bydgoszcz, Poland (consent no. KB 395/2013). The study was also registered in the public web-based clinical study database (Clinical Trial Registry-India, no. CTRI/2018/01/011344).

2.2. Protocol. Four groups were distinguished among the study participants—two control and two study groups (Table 1). One study group included athletes with pain in the lumbosacral segment of the spine (low back pain (LBP)) caused by disturbances in the musculofascial tonus. They were treated with one DEMS procedure. The other one included athletes with pain in the shoulder or ankle joint with features of tendinopathy. These athletes were subjected to a single session of low-frequency US. Immediately before the procedure, DEMS-treated injured athletes assessed their pain at 3.4 ± 1.5, while US-treated injured athletes at 4.2 ± 1.9 points on the visual analogue scale (VAS) (0 = no pain, 5 = moderate pain, and 10 = the most intense pain imaginable). All athletes also subjectively assessed their overall health status on a scale of 0 to 10 (0 = the worst possible, 10 = perfect). The healthy (control) individuals identified the status at 8.0 ± 1.1 (DEMS) and 9.2 ± 0.9 points (US), while the injured ones at 7.4 ± 1.4 and 6.8 ± 1.2 points, respectively. DEMS was conducted using the Salus Talent device. The following parameters of the procedure were used: magnetic induction 1.3 T (approx. 50% of maximum value, i.e., 2.5 T), electromagnetic field frequency 50 Hz (max. value), and treatment duration 20 minutes. The disc-shaped transducer emitting electromagnetic field was applied to the lumbosacral segment of the spine. US was conducted with frequency 38 Hz in continuous mode using US device and USG gel (neutral for health; without medicines). The energy supplied to the subject's skin amounted 1.5 W/cm^2 (50% of maximum value of the device). The applied treatments were clearly felt by the participants deep in their tissues and were set to induce analgesic effect. After the sessions, the injured sportsmen evaluated their pain at 3.2 ± 1.4 (DEMS treated) and 3.8 ± 1.6 (US treated) on the VAS, whereas their health status at 7.5 ± 1.5 and 7.0 ± 1.3, respectively. The control individuals assessed their health status at 8.1 ± 1.1 after DEMS and 9.0 ± 1.1 after US.

2.3. Material. The study was based on laboratory analyses of venous blood taken from the basilic vein before the procedure and 30 minutes and 24 hours thereafter (2 vacuum tubes/individual: 1 with potassium versenate for blood plasma, vol. 4 mL, and 1 with coagulation activator and separation gel for serum, vol. 5 mL).

2.4. Methods. All biochemical methods used in the study were based on the spectrophotometric measurements of absorbance in the tested solutions.

In order to determine the concentration of TBARS in plasma and erythrocytes (TBARSpl and TBARSer, respectively), thiobarbituric acid (TBA) at 0.375%, trichloroacetic acid (TCA) at 15%, and hydrochloric acid (HCl) at 0.25 mol/L were added to tubes with plasma or erythrocyte suspension (50% *v*/*v* in PBS). The mixtures were incubated for 20 min at 100°C, cooled down to 4°C, and centrifuged for 15 min. Subsequently, supernatant was collected, and its absorbance at a wavelength of 532 nm was measured [17, 18]. Moreover, the activities of superoxide dismutase (SOD; EC 1.15.1.1), glutathione peroxidase (GPx; EC 1.11.1.9), and catalase (CAT; EC 1.11.1.6) were measured in the erythrocyte suspension. The method of determination of the SOD activity involved measuring the absorbance of a mixture of erythrocyte suspension and adrenaline at pH > 7. In such conditions, the enzyme inhibits adrenaline autoxidation to adrenochrome, as manifested by the change in the absorbance of the solution which corresponds to the activity of the enzyme [19]. Similarly, the erythrocyte activity of GPx was measured. Absorbance was measured after the reaction that occurred in the solution between the enzyme, hydrogen peroxide, and glutathione, a cofactor in the reaction [20]. The CAT activity was determined in a similar way. Changes in the absorbance of mixtures of hydrogen peroxide with the tested erythrocyte suspensions were measured [21].

In the peripheral blood serum of the study participants, the activity of the following enzymes was determined: AcP (EC 3.1.3.2), ASA (EC 3.1.6.1), CTS D (EC 3.4.23.5), and AAT. The measure of the AcP activity was the amount of p-nitrophenol generated during hydrolytic decomposition of p-nitrophenylphosphate. The reaction was buffered using 0.5 mol/L citrate-tartrate-formaldehyde buffer at pH 4.9. Absorbance was measured at a wavelength of 405 nm [22]. The ASA activity was determined by adding 0.01 mol/L 4-nitrocatechol sulphate and 0.5 mol/L acetate buffer at pH 5.6 to the tested serum. 4-Nitrocatechol sulphate was decomposed by the enzyme to 4-nitrocatechol. Absorbance was

measured at a wavelength of 510 nm [23]. The CTS D activity measurement was based on the hydrolysis of 2% denatured bovine haemoglobin by the enzyme present in the tested serum at 37°C. The reaction was terminated using an aqueous solution of sodium hydroxide (NaOH) at 0.1 mol/L, and a phenolic reagent was added which bound the hydrolysed haemoglobin and stained the solution blue. Absorbance was measured at a wavelength of 660 nm [24]. The AAT activity was directly proportional to the reduction of the enzymatic activity of trypsin after incubation with the tested blood serum (10 min, 25°C). The reaction was inhibited using 30% acetic acid, and the absorbance of the solution was measured at a wavelength of 410 nm. Finally, the AAT activity was read from a calibration curve generated using soybean trypsin inhibitor [25].

2.5. Statistical Analysis. Compatibility with the normal distribution was analysed using the Kolmogorov–Smirnov test, while the homogeneity of variances was established using Levene's test. The main analysis was based on the ANOVA test with Tukey's HSD (honestly significant difference) test for different N as post hoc analysis. If the results did not meet the criteria for parametric tests, the Kruskal–Wallis test with multiple comparisons was performed. Additionally, Pearson's correlation coefficients were determined. The results are shown as arithmetic means ± standard deviations. Differences between the means were considered as statistically significant at $p < 0.05$.

3. Results

As regards DEMS, the greatest difference was demonstrated in the activity of CTS D in the injured (LBP) athletes 24 hours after the treatment in relation to the baseline assay, before the session. The activity was over 2 times lower after the treatment (54.5% difference, $p = 0.052$, Table 2). The enzyme activity in these athletes was also clearly (23.2%) lower 30 minutes after DEMS compared to the baseline ($p > 0.05$). The same trend in the changes of the CTS D activity was also observed in the other study groups, and after the US treatment, the enzyme activity in the injured athletes was also the lowest at the 24-hour study time point (52.1% difference, $p = 0.086$). However, in the US-treated healthy controls, the decrease of the CTS D activity after the session was statistically significant, both at the 30 min ($p < 0.05$) and 24 h time points ($p < 0.01$) (47.5% and 55.7% differences, respectively), whereas in the control athletes after DEMS it was statistically insignificant. There were also no statistically significant differences in the CTS D activity between the control and injured athletes in both procedures, as well as between the procedures.

In all study groups, exactly the same character in the changes of SOD activity after the treatment was also noted. However, the differences were statistically insignificant, similarly as regards the other parameters. The SOD activity was higher 30 minutes after the given treatment compared to the baseline, but 24 hours thereafter practically returned to the initial state (before the treatment). It can also be stated that the CAT activity was slightly greater after the treatments in relation to the baseline assays (30 min and/or 24 h after them); however, it is difficult to find any other tendencies. The levels of other parameters changed in different ways.

Moreover, the study revealed many statistically significant linear relationships between the parameters. Before the DEMS session and 24 h after it, the AcP activity in the LBP athletes positively correlated with the CTS D activity ($r = 0.71$ and $p < 0.01$ and $r = 0.51$ and $p < 0.05$, respectively; Figure 1). Similar linear relationship was also found 24 h after US, both in the healthy control and injured athletes ($r = 0.54$ and $p < 0.05$ and $r = 0.79$ and $p = 0.001$, respectively; Figure 2). The ASA activity measured 30 minutes after DEMS was negatively correlated with the CTS D activity in the noninjured and injured athletes ($r = -0.67$ and $p < 0.05$ and $r = -0.63$ and $p < 0.01$, respectively; Figure 3) and positively before US in the healthy controls ($r = 0.75$, $p < 0.001$). In turn, 24 hours after the US treatment in the healthy controls, the ASA activity negatively correlated with the AAT activity ($r = -0.49$, $p < 0.05$). 30 minutes after US, a positive linear correlation between the TBARSer concentration and the GPx activity was also revealed in the injured athletes ($r = 0.63$, $p < 0.05$), similarly as the SOD and GPx activities before and 24 h after the procedure ($r = 0.73$ and $r = 0.70$, $p < 0.01$; Figure 4), whereas at 24 h time point in the US-treated healthy controls the TBARSer concentration was negatively correlated with the SOD activity ($r = -0.55$, $p < 0.05$). Furthermore, a number of statistically significant Pearson's linear correlations between redox balance parameters and lysosomal enzymes (Table 3) as well as between the AAT and GPx activities 30 min after DEMS ($r = -0.89$, $p < 0.001$) and between the AAT activity and the TBARSer concentration 24 h after US ($r = -0.63$, $p < 0.01$) in the control participants were also found.

4. Discussion

The study showed single DEMS and US sessions did not disturb the oxidant-antioxidant equilibrium in the healthy and injured juvenile amateur sportsmen, since no statistically significant differences in measurements of the TBARS concentration and antioxidant enzyme activities (SOD, GPx, and CAT) were demonstrated. The TBARSpl level tended to increase after the procedures in the groups of control and injured athletes, while there was no clear trend in the changes of TBARSer concentration. The SOD activity changed as a result of the treatment in a similar manner in both procedures ($p > 0.05$). TBARS are mainly malondialdehyde (MDA), which belongs to the specific markers of oxidative stress as a secondary product of lipoperoxidation induced by free radicals (nonenzymatic lipid peroxidation) [14]. The antioxidant enzymes analysed in the study are also reliable indicators for the evaluation of ratio between the oxidation and reduction reactions. These enzymes "scavenge" ROS and RNS: superoxide anion ($O_2^{\cdot-}$) (SOD), as well as hydrogen peroxide (H_2O_2) and organic peroxides (GPx and CAT) [26]. CAT demonstrates peroxidase activity at low concentration of H_2O_2 and oxidizes ethanol, methanol, phenols, formates or nitrites, and mentioned organic peroxides. The role of an H_2O_2 scavenger is then played almost completely by GPx

Table 2: Oxidative stress parameters together with lysosomal and antiprotease activities in the peripheral blood of juvenile athletes subjected to single DEMS and low-frequency ultrasound (US) sessions.

	$DEMS_{healthy\ controls}$ ($N = 14$)			$DEMS_{injured\ athletes}$ ($N = 16$)			$US_{healthy\ controls}$ ($N = 18$)			$US_{injured\ athletes}$ ($N = 14$)		
	I	II	III	I	II	III	I	II	III	I	II	III
TBARSpl	4.0 ± 0.6	4.1 ± 0.4	4.2 ± 0.8	4.2 ± 0.8	4.2 ± 0.7	4.5 ± 0.7	4.1 ± 0.6	3.9 ± 0.6	4.2 ± 0.7	3.8 ± 0.9	3.6 ± 0.5	4.0 ± 0.6
TBARSer	23.5 ± 6.1	23.7 ± 7.9	23.9 ± 8.0	21.5 ± 5.8	21.8 ± 6.1	21.3 ± 3.3	24.1 ± 8.0	21.8 ± 5.0	26.8 ± 12.3	24.3 ± 4.0	27.8 ± 9.8	24.6 ± 11.0
SOD	77.3 ± 9.8	81.4 ± 12.6	77.1 ± 9.7	74.0 ± 12.7	78.0 ± 10.2	76.5 ± 13.1	69.6 ± 6.3	71.0 ± 4.0	67.3 ± 3.2	73.1 ± 6.5	76.8 ± 9.6	71.1 ± 8.2
GPx	7.0 ± 5.4	7.1 ± 5.2	8.8 ± 3.6	8.6 ± 7.1	7.2 ± 3.7	7.0 ± 4.6	9.3 ± 7.9	5.6 ± 5.0	8.0 ± 5.3	8.2 ± 6.3	7.5 ± 5.6	8.5 ± 5.9
CAT	60.8 ± 7.3	60.5 ± 6.8	62.3 ± 10.6	59.5 ± 8.9	60.6 ± 9.7	61.9 ± 11.6	59.9 ± 6.8	59.7 ± 4.7	64.1 ± 8.6	61.2 ± 10.9	58.5 ± 9.0	61.5 ± 10.1
AcP	1.6 ± 0.5	1.6 ± 0.7	1.4 ± 0.5	2.0 ± 1.2	1.9 ± 1.0	1.7 ± 0.8	1.8 ± 0.8	1.7 ± 0.9	1.9 ± 1.0	2.1 ± 1.0	2.1 ± 0.9	2.0 ± 1.1
ASA	0.8 ± 0.3	1.0 ± 0.3	1.0 ± 0.4	0.7 ± 0.2	0.9 ± 0.2	0.8 ± 0.3	0.9 ± 0.3	0.8 ± 0.2	0.8 ± 0.2	0.7 ± 0.2	0.7 ± 0.1	0.7 ± 0.2
CTS D	10.5 ± 2.0	9.1 ± 5.5	7.7 ± 4.2	11.2 ± 0.3	8.6 ± 5.4	5.1 ± 3.0	12.2 ± 3.8	6.4 ± 4.1*	5.4 ± 4.4**	11.7 ± 3.1	8.3 ± 5.2	5.6 ± 3.7
AAT	8.3 ± 1.4	7.7 ± 1.3	8.3 ± 1.4	8.9 ± 1.8	8.2 ± 1.4	8.7 ± 1.0	7.8 ± 1.4	7.7 ± 1.2	7.6 ± 1.0	7.8 ± 1.6	7.3 ± 1.4	8.1 ± 1.2

Values are means ± SD. Statistically significant differences were revealed in relation to measurement I in the US-treated healthy controls (*$p < 0.05$, **$p < 0.01$). Measurement I: before the treatment; measurement II: 30 min after the treatment; measurement III: 24 hours after the treatment; TBARSpl/er: thiobarbituric acid reactive substances in plasma (10^{-1} nmol MDA/mL plasma)/erythrocytes (nmol MDA/g Hb); MDA: malondialdehyde; Hb: haemoglobin; SOD: superoxide dismutase (10 U/g Hb); GPx: glutathione peroxidase (U/g Hb); CAT: catalase (IU/g Hb); AcP: acid phosphatase (10^{-3} nmol 4-NP/mg protein/min); 4-NP: 4-nitrophenol; ASA: arylsulfatase (10^{-3} nmol 4-NC/mg protein/min); 4-NC: 4-nitrocatechol; CTS D: cathepsin D (10^{-2} nmol TYR/mg protein/min); TYR: tyrosine; AAT: α_1-antitrypsin (10^{-1} mg TR/mL serum); TR: trypsin.

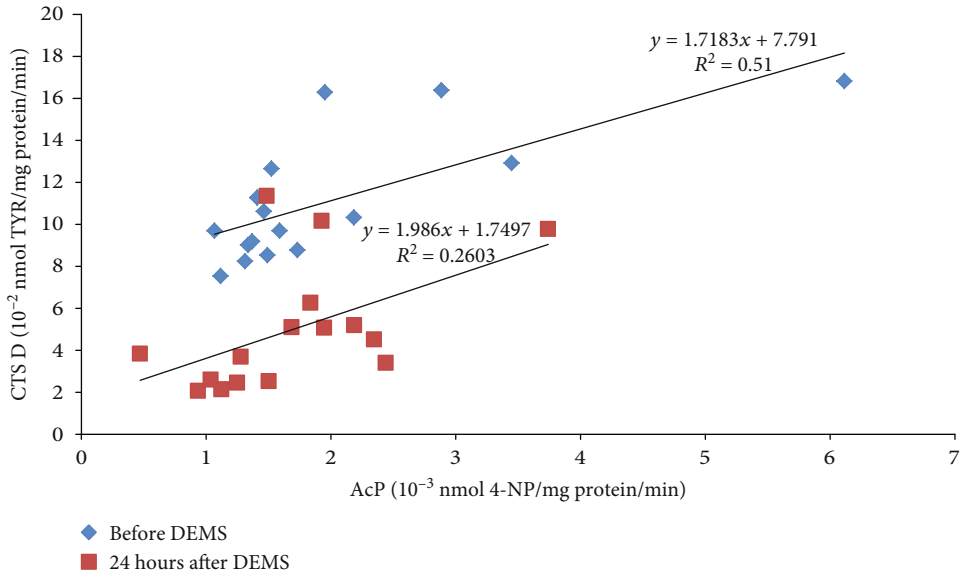

Figure 1: Positive linear correlations between the serum AcP and CTS D activities before and 24 h after the DEMS procedure in the injured sportsmen: $r = 0.71$ ($p < 0.01$) and $r = 0.51$ ($p < 0.05$), respectively. DEMS: deep electromagnetic stimulation; 4-NP: 4-nitrophenol; TYR: tyrosine.

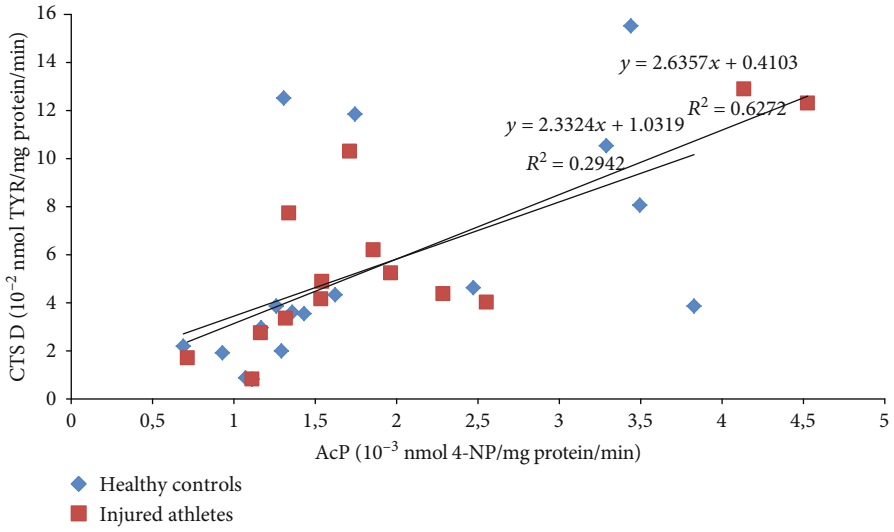

Figure 2: Linear regressions of the serum AcP and CTS D activities 24 h after the US procedure in the healthy and injured sportsmen ($r = 0.54$, $p < 0.05$, and $r = 0.79$, $p = 0.001$, respectively). US: ultrasound; 4-NP: 4-nitrophenol; TYR: tyrosine.

[27]. The enzymes prevent the generation of other dangerous free radicals as well—primarily the hydroxyl radical ($HO^{\cdot}$) and peroxynitrite ($ONOO^{-}$) [11]. Moreover, linear relationships found in the US procedure in the context of no differences between the results suggest rather the proper functioning of the antioxidant barrier or at most slightly increased production of ROS. 30 min after the treatment, strong positive linear correlations between the TBARSer concentration and the GPx activity ($r = 0.63$, $p < 0.05$) as well as between the SOD and GPx activities before and 24 h after the procedure ($r = 0.73$ and $r = 0.70$, $p < 0.01$; Figure 4) were shown in the injured athletes, whereas at 24 h study time point in the US healthy controls the TBARSer concentration was negatively correlated with the SOD activity ($r = -0.55$, $p < 0.05$), which can suggest that the likely increase in ROS production was rather a result of the injury, not the procedure.

The study also showed practically no impact on the lysosomal balance. Basically, there were no statistically significant changes in the activity of lysosomal enzymes. It seems only that the US session and probably also DEMS decrease lysosomal proteolytic activity in the blood serum, since the main proteolytic enzyme in lysosomes is CTS D [28], and its activity was meaningfully lower after the procedures both in the noninjured and injured sportsmen (reference time point—the baseline assay). After US, it was statistically significant difference. Lysosomal enzymes are acid hydrolases. Thanks to their ability to decompose biomolecules and their

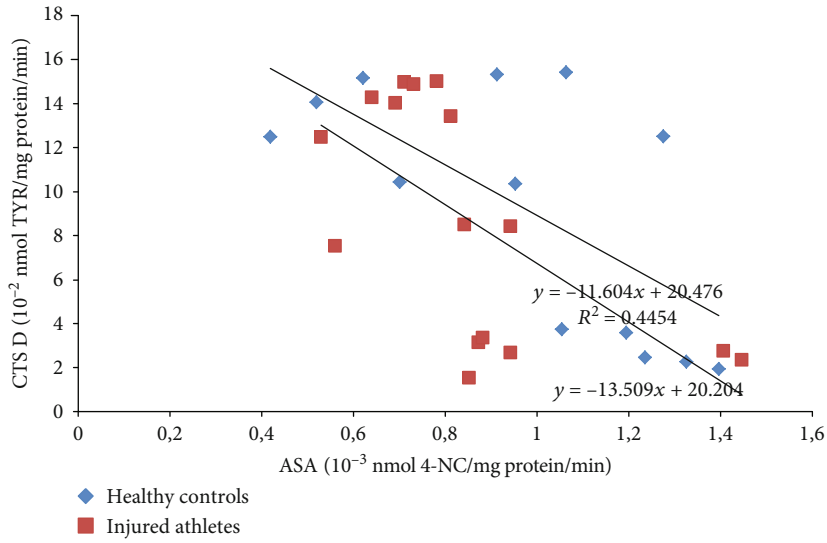

Figure 3: Negative linear correlations between the serum ASA and CTS D activities 30 min after the single DEMS procedure in the healthy and injured sportsmen ($r = -0.67$, $p < 0.05$, and $r = -0.63$, $p < 0.01$, respectively). DEMS: deep electromagnetic stimulation; ASA: arylsulfatase; 4-NC: 4-nitrocatechol; CTS D: cathepsin D; TYR: tyrosine.

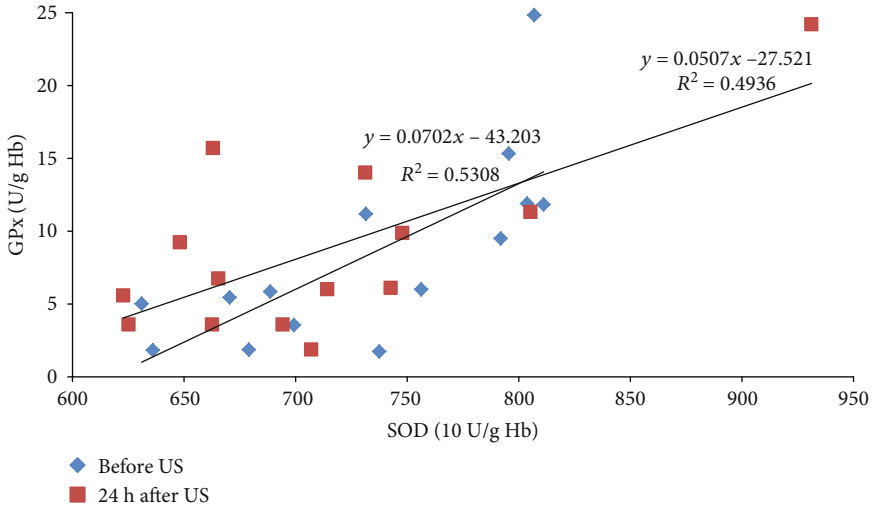

Figure 4: Linear relationships between the erythrocyte SOD and GPx activities before and 24 h after US in the injured athletes ($r = 0.73$ and $r = 0.70$, $p < 0.01$, respectively). US: ultrasound; SOD: superoxide dismutase; GPx: glutathione peroxidase; Hb: haemoglobin.

abundance (more than 60 types), cells are able to regulate many different processes, such as apoptosis, necrosis, phagocytosis, exocytosis, or removal of waste and dysfunctional proteins [15, 29]. Due to the aforementioned, lysosomes are also involved in the positive and negative regulation of inflammation [30]. Increased permeability of lysosomal membranes and thus higher activity of lysosomal hydrolases in the cytosol and/or intercellular space and blood plasma/-serum can occur in response to damaging factors (biological, chemical, and physical) based on the free radical mechanism. ROS/RNS can oxidize the protein-lipid lysosomal membrane and increase its permeability, as in the case of other biological membranes, including the cell membrane [15, 31]. Lysosomal enzymes can also be a source of ROS/RNS *per se*, e.g., AcP in Fenton reaction due to the presence of $Fe^{2+/3+}$ in the active site. In such a way, overactive AcP might carry out the fragmentation of collagen within osteoclasts in skeletal disorders involving the excessive activity of these cells. In this type of disorders, increased AcP activity has been shown in the patients' blood serum [32]. The enzyme can also be overproduced by macrophages and dendritic cells in the course of cancer [33] and rheumatoid arthritis [34], and its free radical activity occurs in macrophages during antigen presentation [35]; however, the basic function of this enzyme is removal of a phosphate group from phosphoric (V) acid monoesters [34]. Overexpression and the presence in peripheral blood have also been observed in the case of CTS D during tumour progression, similarly in the course of Alzheimer's disease. In general, high activity of the enzyme appears in damaged tissues and

Table 3: Pearson's linear correlations between parameters of redox balance and lysosomal enzymes.

Before DEMS in the injured athletes	SOD vs. CTS D	$r = 0.55$, $p < 0.05$
24 h after DEMS in the injured athletes	SOD vs. ASA	$r = 0.58$, $p < 0.05$
Before US in the controls	TBARSer vs. ASA	$r = 0.58$, $p < 0.05$
30 min after US in the controls	CAT vs. CTS D	$r = 0.49$, $p < 0.05$
24 h after US in the controls	TBARSer vs. ASA	$r = 0.51$, $p < 0.05$
	SOD vs. CTS D	$r = 0.62$, $p < 0.01$
	CAT vs. CTS D	$r = 0.66$, $p < 0.01$
Before US in the injured athletes	SOD vs. AcP	$r = 0.59$, $p < 0.05$
	GPx vs. AcP	$r = 0.65$, $p < 0.05$
30 min after US in the injured athletes	GPx vs. AcP	$r = 0.66$, $p < 0.05$
24 h after US in the injured athletes	TBARSer vs. ASA	$r = 0.65$, $p < 0.05$

DEMS: deep electromagnetic stimulation; SOD: superoxide dismutase; CTS D: cathepsin D; ASA: arylsulfatase; US: ultrasound; TBARSer: thiobarbituric acid reactive substances in erythrocytes; CAT: catalase; AcP: acid phosphatase; GPx: glutathione peroxidase.

sites of intense inflammation [28]. It has also been proven that this protein is released from lysosomes into the cytoplasm during apoptosis induced by oxidative stress [15]. In turn, mutations in the ASA gene resulting in a total loss or severe reduction of the enzyme activity can lead to neurodegenerative disorders [36]. It has been demonstrated that a single dose of human ASA administered into the damaged spinal cord in mice causes a significant improvement of their locomotor function [37]. ASA hydrolyses esters of sulfuric acid, which is important in, e.g., the processing of glycosphingolipids of the myelin sheath of neurons [36]. In the sportsmen's blood serum, in both procedures of the study, the character in changes of the CTS D and AcP activities was similar (Figures 1 and 2). However, relationships between the CTS D and ASA activities were opposite, comparing the DEMS and US treatments. The ASA activity measured 30 min after DEMS was negatively correlated with the CTS D activity in the injured and noninjured athletes (Figure 3) and positively before US in the healthy controls ($r = 0.75$, $p < 0.001$). Possibly, it was caused by selective release of enzymes from lysosomes due to their random aggregation after pH increase inside the lysosome [38]. The positive relationship described here between ROS and lysosomal activity is confirmed by numerous statistically significant linear correlations obtained in the study (Table 3). Thus, these proper relations (correlations) between the parameters may confirm the maintenance of the redox and lysosomal equilibriums in the healthy and injured subjects.

Differences in the serum activity of AAT in response to single DEMS and US procedures were statistically insignificant as well. AAT is a sialoglycoprotein, which belongs to *ser*ine *p*rotease *in*hibitors (SERPINS) and is classified as a positive acute-phase protein (APP), along with C-reactive protein, fibrinogen, and α_1-acid glycoprotein, because its activity in blood increases in response to damage and inflammation [16]. Therefore, many APPs are considered as classic biomarkers of inflammation (especially C-reactive protein, fibrinogen, and complement factors) [9]. The main function of these proteins is to protect the organism against further damages, help to restore the homoeostasis, and adapt to the harmful stimulus. AAT as a serpin inhibits neutrophilic proteases: elastase, cathepsin G, and proteinase 3. It is secreted mainly by hepatocytes, but can also be abundantly produced by macrophages, as well as intestinal and bronchial epithelial cells. Moreover, it has been discovered that AAT inhibits aggregation of certain proteins (e.g., alcohol dehydrogenase, aldolase, carbonic anhydrase, and catalase) induced by high temperature or chemical compounds; hence, AAT is also considered as an extracellular chaperone [16]. It has been also demonstrated in this study that the activity of AAT can negatively correlate in healthy men's blood serum with the ASA activity (the US-treated healthy controls, 24 h after the procedure: $r = -0.49$, $p < 0.05$), which confirms again no apparent disturbance of lysosomal balance. Similarly, correlations between AAT and parameters of oxidant-antioxidant balance in the healthy controls suggest no disturbances in the balance (AAT vs. GPx 30 min after DEMS: $r = -0.89$, $p < 0.001$; AAT vs. TBARSer 24 h after US: $r = -0.63$, $p < 0.01$).

In conclusion, no significant differences were demonstrated comparing the healthy and injured athletes, as well as both procedures. In general, the observed trends in the changes of the analysed parameters in the study were also similar in nature in both procedures. Therefore, the obtained results suggest that the conducted DEMS and US sessions did not have significant effect on the described physiological functions, except for lysosomal proteolytic activity in blood serum.

5. Conclusions

Single sessions of deep electromagnetic stimulation and low-frequency ultrasound do not significantly disturb the oxidant-antioxidant and lysosomal equilibriums, nor do they have impact on acute-phase response of the α_1-antitrypsin in the venous blood of amateur juvenile athletes. However, it seems that the US treatment significantly decreases proteolytic activity of cathepsin D in the healthy athletes' blood serum, as well as probably also in the injured athletes and after the DEMS treatment.

Data Availability

The data used to support the findings of this study are included within the article.

Disclosure

The study was conducted as part of regular employment of the authors by the Ludwik Rydygier Collegium Medicum in Bydgoszcz, Nicolaus Copernicus University, Toruń, Poland.

Conflicts of Interest

The authors declare that they have no competing interests.

Authors' Contributions

Łukasz Sielski and Paweł Sutkowy contributed equally to this work.

References

[1] N. Tomska, A. Turoń-Skrzypińska, A. Szylińska et al., "Deep electromagnetic stimulation and radial shock wave therapy in back pain," *Ortopedia, Traumatologia, Rehabilitacja*, vol. 20, no. 3, pp. 189–195, 2018.

[2] A. Przedborska, M. Misztal, and J. W. Raczkowski, "Impact of the deep electromagnetic stimulation on the level of the pain sensation in patients with the rheumatoid arthritis," *Fizjoterapia Polska*, vol. 16, no. 1, pp. 74–81, 2016.

[3] A. Przedborska, M. Misztal, and J. W. Raczkowski, "Assessment of the therapeutic effectiveness of deep electromagnetic stimulation in patients with chronic low back pain," *Ortopedia, Traumatologia, Rehabilitacja*, vol. 17, no. 5, pp. 531–541, 2015.

[4] E. K. Smith, A. Craven, and A. M. Wilson, "Effect of noncontact low-frequency ultrasound on wound Healing," *Journal of Acute Care Physical Therapy*, vol. 5, no. 1, pp. 36–44, 2014.

[5] S. Mukai, H. Ito, Y. Nakagawa, H. Akiyama, M. Miyamoto, and T. Nakamura, "Transforming growth factor-β_1 mediates the effects of low-intensity pulsed ultrasound in chondrocytes," *Ultrasound in Medicine and Biology*, vol. 31, no. 12, pp. 1713–1721, 2005.

[6] P. Reher, N. Doan, B. Bradnock, S. Meghji, and M. Harris, "Effect of ultrasound on the production of Il-8, basic FGF and VEGF," *Cytokine*, vol. 11, no. 6, pp. 416–423, 1999.

[7] W.-C. Tsai, C. C. Hsu, F. T. Tang, S. W. Chou, Y. J. Chen, and J. H. S. Pang, "Ultrasound stimulation of tendon cell proliferation and upregulation of proliferating cell nuclear antigen," *Journal of Orthopaedic Research*, vol. 23, no. 4, pp. 970–976, 2005.

[8] G. ter Haar, "Therapeutic ultrasound," *European Journal of Ultrasound*, vol. 9, no. 1, pp. 3–9, 1999.

[9] D. R. Germolec, R. P. Frawley, and E. Evans, "Markers of inflammation," *Methods in Molecular Biology*, vol. 598, pp. 53–73, 2010.

[10] S. Bolisetty and E. A. Jaimes, "Mitochondria and reactive oxygen species: physiology and pathophysiology," *International Journal of Molecular Sciences*, vol. 14, no. 3, pp. 6306–6344, 2013.

[11] M. Valko, D. Leibfritz, J. Moncol, M. T. D. Cronin, M. Mazur, and J. Telser, "Free radicals and antioxidants in normal physiological functions and human disease," *The International Journal of Biochemistry & Cell Biology*, vol. 39, no. 1, pp. 44–84, 2007.

[12] S. Reuter, S. C. Gupta, M. M. Chaturvedi, and B. B. Aggarwal, "Oxidative stress, inflammation, and cancer: how are they linked?," *Free Radical Biology and Medicine*, vol. 49, no. 11, pp. 1603–1616, 2010.

[13] T. T. Peternelj and J. S. Coombes, "Antioxidant supplementation during exercise training," *Sports Medicine*, vol. 41, no. 12, pp. 1043–1069, 2011.

[14] D. Grotto, L. S. Maria, J. Valentini et al., "Importance of the lipid peroxidation biomarkers and methodological aspects for malondialdehyde quantification," *Quimica Nova*, vol. 32, no. 1, pp. 169–174, 2009.

[15] A. C. Johansson, H. Appelqvist, C. Nilsson, K. Kågedal, K. Roberg, and K. Öllinger, "Regulation of apoptosis-associated lysosomal membrane permeabilization," *Apoptosis*, vol. 15, no. 5, pp. 527–540, 2010.

[16] F. Zsila, "Inhibition of heat- and chemical-induced aggregation of various proteins reveals chaperone-like activity of the acute-phase component and serine protease inhibitor human α_1-antitrypsin," *Biochemical and Biophysical Research Communications*, vol. 393, no. 2, pp. 242–247, 2010.

[17] J. A. Buege and S. D. Aust, "[30] Microsomal lipid peroxidation," *Methods in Enzymology*, vol. 52, pp. 302–310, 1978.

[18] H. Esterbauer and K. H. Cheeseman, "[42] Determination of aldehydic lipid peroxidation products: malonaldehyde and 4-hydroxynonenal," *Methods in Enzymology*, vol. 186, pp. 407–421, 1990.

[19] H. P. Misra and I. Fridovich, "The role of superoxide anion in the autoxidation of epinephrine and a simple assay for superoxide dismutase," *Journal of Biological Chemistry*, vol. 247, no. 10, pp. 3170–3175, 1972.

[20] D. E. Paglia and W. N. Valentine, "Studies on the quantitative and qualitative characterization of erythrocyte glutathione peroxidase," *The Journal of Laboratory and Clinical Medicine*, vol. 70, no. 1, pp. 158–169, 1967.

[21] R. F. Beers Jr. and I. W. Sizer, "A spectrophotometric method for measuring the breakdown of hydrogen peroxide by catalase," *The Journal of Biological Chemistry*, vol. 195, no. 1, pp. 133–140, 1952.

[22] J. Krawczyński, "Enzymatic diagnostics in practical medicine," in *Methods of Investigation*, Wydawnictwo lekarskie PZWL, Warszawa, Poland, 1972.

[23] W. Błeszyński and L. M. Działoszyński, "Purification of soluble arylsulphatases from ox brain," *Biochemical Journal*, vol. 97, no. 2, pp. 360–364, 1965.

[24] S. C. Colowick and N. C. Kaplan, *Methods in Enzymology*, Academic Press, New York, Europe, 2nd edition, 1993.

[25] S. Eriksson, "Studies in alpha 1-antitrypsin deficiency," *Acta Medica Scandinavica. Supplementum*, vol. 432, pp. 1–85, 1965.

[26] H. Kühn and A. Borchert, "Regulation of enzymatic lipid peroxidation: the interplay of peroxidizing and peroxide reducing enzymes," *Free Radical Biology & Medicine*, vol. 33, no. 2, pp. 154–172, 2002.

[27] D. Ścibior and H. Czeczot, "Catalase: structure, properties, functions," *Postępy Higieny i Medycyny Doświadczalnej*, vol. 60, pp. 170–180, 2006.

[28] T. Tsukuba, K. Okamoto, Y. Yasuda, W. Morikawa, H. Nakanishi, and K. Yamamoto, "New functional aspects of cathepsin D and cathepsin E," *Molecules and Cells*, vol. 10, no. 6, pp. 601–611, 2000.

[29] C. de Duve, "Lysosomes revisited," *European Journal of Biochemistry*, vol. 137, no. 3, pp. 391–397, 1983.

[30] W. Ge, D. Li, Y. Gao, and X. Cao, "The roles of lysosomes in inflammation and autoimmune diseases," *International Reviews of Immunology*, vol. 34, no. 5, pp. 415–431, 2015.

[31] S. V. Avery, "Molecular targets of oxidative stress," *Biochemical Journal*, vol. 434, no. 2, pp. 201–210, 2011.

[32] J. M. Halleen, S. Räisänen, J. J. Salo et al., "Intracellular fragmentation of bone resorption products by reactive oxygen species generated by osteoclastic tartrate-resistant acid phosphatase," *The Journal of Biological Chemistry*, vol. 274, no. 33, pp. 22907–22910, 1999.

[33] S. Muniyan, N. Chaturvedi, J. Dwyer, C. LaGrange, W. Chaney, and M. F. Lin, "Human prostatic acid phosphatase: structure, function and regulation," *International Journal of Molecular Sciences*, vol. 14, no. 5, pp. 10438–10464, 2013.

[34] A. J. Janckila, R. N. Parthasarathy, L. K. Parthasarathy et al., "Properties and expression of human tartrate-resistant acid phosphatase isoform 5a by monocyte-derived cells," *Journal of Leukocyte Biology*, vol. 77, no. 2, pp. 209–218, 2005.

[35] S. R. Räisänen, J. Halleen, V. Parikka, and H. K. Väänänen, "Tartrate-Resistant Acid Phosphatase Facilitates Hydroxyl Radical Formation and Colocalizes with Phagocytosed _Staphylococcus aureus_ in Alveolar Macrophages," *Biochemical and Biophysical Research Communications*, vol. 288, no. 1, pp. 142–150, 2001.

[36] Y. Echeverri, S. Diego, R.-L. Alexander, G. Janneth, J. Almeciga-Díaz, and B. Luis, "Understanding the metabolic consequences of human arylsulfatase A deficiency through a computational systems biology study," *Central Nervous System Agents in Medicinal Chemistry*, vol. 17, no. 1, pp. 72–77, 2017.

[37] M. Yoo, M. Khaled, K. M. Gibbs et al., "Arylsulfatase B improves locomotor function after mouse spinal cord injury," *PLoS One*, vol. 8, no. 3, article e57415, 2013.

[38] M. Tsuboi, K. Harasawa, T. Izawa, T. Komabayashi, H. Fujinami, and K. Suda, "Intralysosomal pH and release of lysosomal enzymes in the rat liver after exhaustive exercise," *Journal of Applied Physiology*, vol. 74, no. 4, pp. 1628–1634, 1993.

Hindawi
Oxidative Medicine and Cellular Longevity
Volume 2020, Article ID 7140496, 14 pages
https://doi.org/10.1155/2020/7140496

Review Article

Two Faces of Heme Catabolic Pathway in Newborns: A Potential Role of Bilirubin and Carbon Monoxide in Neonatal Inflammatory Diseases

Wiktoria Osiak,[1] **Sławomir Wątroba**,[2] **Lucyna Kapka-Skrzypczak**,[3] **and Jacek Kurzepa**[1]

[1]*Department of Medical Chemistry, Medical University of Lublin, 20-093, Poland*
[2]*Neonatal Department, Independent Public Health Care Facility, Puławy 24-100, Poland*
[3]*Department of Molecular Biology and Translational Research, Institute of Rural Health, Jaczewskiego 2, 20-090 Lublin, Poland*

Correspondence should be addressed to Wiktoria Osiak; wiktoria.osiak@gmail.com

Received 7 June 2020; Accepted 27 July 2020; Published 18 August 2020

Guest Editor: Jolanta Czuczejko

Copyright © 2020 Wiktoria Osiak et al. This is an open access article distributed under the Creative Commons Attribution License, which permits unrestricted use, distribution, and reproduction in any medium, provided the original work is properly cited.

In an infant's body, all the systems undergo significant changes in order to adapt to the new, extrauterine environment and challenges which it poses. Fragile homeostasis can be easily disrupted as the defensive mechanisms are yet imperfect. The activity of antioxidant enzymes, i.e., superoxide dismutase, catalase, and glutathione peroxidase, is low; therefore, neonates are especially vulnerable to oxidative stress. Free radical burden significantly contributes to neonatal illnesses such as sepsis, retinopathy of premature, necrotizing enterocolitis, bronchopulmonary dysplasia, or leukomalacia. However, newborns have an important ally—an inducible heme oxygenase-1 (HO-1) which expression rises rapidly in response to stress stimuli. HO-1 activity leads to production of carbon monoxide (CO), free iron ion, and biliverdin; the latter is promptly reduced to bilirubin. Although CO and bilirubin used to be considered noxious by-products, new interesting properties of those compounds are being revealed. Bilirubin proved to be an efficient free radicals scavenger and modulator of immune responses. CO affects a vast range of processes such as vasodilatation, platelet aggregation, and inflammatory reactions. Recently, developed nanoparticles consisting of PEGylated bilirubin as well as several kinds of molecules releasing CO have been successfully tested on animal models of inflammatory diseases. This paper focuses on the role of heme metabolites and their potential utility in prevention and treatment of neonatal diseases.

1. Introduction

A healthy infant is born with a concentration of bilirubin below 5 mg/dl [1]; then, serum bilirubin concentration rises quickly, up to 12 mg/dl within first 4-5 days. In pathological conditions, the growth is even more accelerated and serum bilirubin concentration, in the absence of appropriate treatment, may rise even above 40 mg/dl. The rapid increase in bilirubin appears at newborns due to both intense hemolysis and insufficiency of a liver enzyme, uridine 5′-diphospho-glucuronosyltransferase (UGT), involved in bilirubin catabolism. The increased hemolysis occurs as fetal hemoglobin (HbF), which is produced by erythroid precursor cells from 10-12 week of pregnancy till birth [2], switches to adult hemoglobin A (HbA) soon after the labor. Within the perinatal period, HbF is intensively eliminated and exchanged by HbA, leading to the low HbF concentration observed in adults (around 1% of total Hb) [3]. The increased hemoglobin catabolism is consistent with increased degradation of heme. Although this process is physiologically justified because unique properties of HbF only function during prenatal period, the mechanism of gene silencing responsible for the reduced synthesis of HbF is not fully understood [4].

Previously, some researchers have wondered whether the observed increase in bilirubin is only a side effect of the metabolic changes at newborn infants or such growth brings specific benefits [5]. Bilirubin is a compound with known antioxidant properties [6–8]; therefore, an increase in its concentration may be necessary to maintain a proper oxidative balance in the perinatal period or maybe not bilirubin but

another compound formed in the heme catabolic pathway—CO is the hero of the perinatal period? This review work explores both of these options.

2. Heme Functions and Its Catabolic Pathway

Heme moiety, consisting of an iron ion and porphyrin, plays a crucial role as a prosthetic group of apo-heme proteins, i.e., hemoglobin, myoglobin, catalase, guanylate cyclase, and cytochromes. All of them perform important functions participating in oxygen transportation, electron transfer reactions, and catalysis [9]. Heme is also a regulator of gene expression. Bach1 and Bach2 are transcriptional suppressors involved in heme metabolism, cell cycle, oxidative stress response, and immunity [10, 11]. Heme binding to Bach1 and Bach2 inhibits their DNA-binding activity, which results in inter alia, heme oxygenase 1 induction. Heme is also a ligand for nuclear hormone receptors, REV-ERBα and REV-ERBβ, involved in various biological processes including lipid and carbohydrate metabolism, cell differentiation, and circadian rhythms [12, 13]. Other target molecules for heme moiety are PAS domain of circadian factor period 2 (Per2) and neuronal PAS protein 2 (NPAS2)—transcription activator proteins associated with circadian rhythms [13]. Heme-regulated inhibitor kinase (HRI) is activated or inactivated depending on heme concentration. When heme is deficient, activated HRI phosphorylates eukaryotic translational initiation factor 2 (eIF2α) which leads to downregulation of α- and β-globin translation. This mechanism provides balanced synthesis of hemoglobin [14].

During intravascular hemolysis, a vast amount of hemoglobin is released into circulation. Haptoglobin (Hp), an acute phase protein, binds to hemoglobin and creates complexes which are subsequently taken up by hepatocytes and macrophages of the reticuloendothelial system via the CD163 receptor. Once binding capacity of Hp is saturated, free Hb is oxidized to methemoglobin and releases heme [15, 16]. In spite of many important biological functions mentioned above, a free heme molecule embodies a threat and acts in a destructive way [15]. Due to its lipophilic properties, heme intercalates in the membranes and modifies cellular structures [17]. Heme activates inflammatory reactions as it induces expression of adhesion molecules—intercellular adhesion molecule-1 (ICAM-1) and vascular cell adhesion molecule-1 (VCAM-1) through the signaling pathway of transcription factors nuclear factor-kappa beta (NF-κB) [18]—and stimulates neutrophils through protein kinase C [19]. Heme overload leads to intensified production of reactive oxygen species (ROS) and tumor necrosis factor (TNF) [19]. Hemin, an oxidized form of heme, also exerts proinflammatory and prooxidant effects [20]. In brief, free heme is too toxic to remain "at large" in plasma or cells. Indeed, free heme in plasma is promptly scavenged and neutralized by hemopexin [21]. Afterward, heme-hemopexin complexes are cleared from circulation by hepatocytes and macrophages via the CD91 receptor and undergo lysosomal degradation [15, 16, 21].

The intracellular enzyme, named heme oxygenase (HO), which initiates degradation of free heme was discovered in the 1970s. To date, two isoforms of HO were described: HO-1 and HO-2. Constitutively expressed HO-2 is synthesized mainly in the brain, testes, and vascular system [22–25]. Under normal conditions, HO-1 is expressed at high level in the spleen and reticuloendothelial cells involved in red blood cell degradation [25]. HO-1 has attracted researchers' attention as it is obviously upregulated in response to oxidative stress. The list of HO-1 inducers is long and includes, e.g., free heme molecules, hemin, metals, cytokines, vasoactive compounds, nephrotoxin, and endotoxin [26]. Enzymatic oxidative ring cleavage of heme molecule results in formation of CO, Fe^{2+}, $NADP^{+}$, and biliverdin according to the reaction presented below (Equation (1)):

$$\text{Heme} + \text{NADPH} + \text{H}^{+} + 3\text{O}_2 \longrightarrow \text{biliverdin} + \text{NADP}^{+} + \text{Fe}^{2+} + \text{CO} + \text{H}_2\text{O} \quad (1)$$

The carbon atom in the carbon monoxide molecule is detached directly from the heme ring during its cleavage. A free iron ion, which is released as one of the products of the reaction, is able to react with hydrogen peroxide and yield hydroxyl radicals; therefore, it can cause oxidative damage. However, it is noteworthy that induction of HO-1 is followed by upregulation of ferritin which binds free iron and neutralizes its cytotoxic effect [15].

There are several identified types of HO-1 gene polymorphisms, among which one is especially interesting in terms of potential clinical significance. The number of (GT)n dinucleotide repeats in 5-flanking regions of HO-1 gene varies between 12 and 40 [27, 28]. This polymorphism of the promoter region was found to affect the level of HO-1 expression in response to stimuli. In adults, shorter variant with fewer than 25 repeats was associated with higher HO-1 expression and better resistance to oxidative stress-related diseases according to some reports [27–29]. Obese children aged 6-17 with longer GT repeats in the HO-1 gene promoters were more susceptible to nonalcoholic fatty liver disease [30]. It might seem that fewer GT repeats in newborns should be associated with more severe jaundice and higher probability of phototherapy. Indeed, some researches confirm this hypothesis [31–33]. However, other published studies contradict the effect of HO-1 polymorphism on total serum bilirubin level [28, 34, 35]. One of the studies points out that polymorphism of HO-1 gene promoter can be an underlying cause of prolonged jaundice at breast-fed babies [28]. These discrepancies might be connected with different definitions of short length promoter variant and differences between various ethnic groups, then require further investigation [27].

The characteristic feature of HO-1 expression in newborns is that it rises for the first three days following labor and afterward it decreases [36]. On day 5, the expression is at the same level as at the moment of birth and then it continues to drop. HO-1 mRNA content is higher in premature newborns in comparison with term infants but with the same rise-drop pattern [36]. The changes in HO-1 expression at the early stage of life are reflected by bilirubin concentration which increases within first days of life and then it gradually declines.

3. Is Bilirubin Only a Toxic Waste Product?

At first, bilirubin was considered only a useless outcome of heme degradation. However, bilirubin is not the best candidate for pure waste end-product. It is toxic in high concentration and its synthesis by biliverdin reductase depends on nicotinamide adenine dinucleotide phosphate (NADPH). Furthermore, bilirubin neutralization and elimination is energy-consuming and requires additional processes such as glucuronidation (Figure 1). Nevertheless, most of the mammals and some other vertebrates excrete bilirubin as the main end-product of heme catabolism. Among the mammals, biliverdin is excreted as the only bile pigment by sloths and anteaters and as the principal end-product by, e.g., a nutria (90%) and a rabbit (60-70%) [37]. In spite of the lack of uniformity in the world of animals, it can be assumed that biliverdin reductase evolved because it brought some benefits to the organism.

In fact, thorough research focused on the compound brought to light interesting data. In 1954, Karl Bernhard published a report in which he declared that bilirubin possesses antioxidant properties which protect vitamin A and unsaturated fatty acids against oxidation [39]. Stocker et al. in 1987 proved that *in vitro* bilirubin's ability to scavenge peroxyl radicals is even more prominent than the ability of another powerful antioxidant—α-tocopherol [6]. To date, there were many studies examining bilirubin's activity *in vitro*, but also considerable effort has been made to confirm antioxidant properties of bilirubin *in vivo*. Nonetheless, the significance of neonatal hyperbilirubinemia is still not fully understood and requires further investigation because bilirubin might turn out to be a potent ally to newborns in their first days of life.

Pulmonary respiration after birth exposes newborns to significant oxidative stress resulting from a sharp increase of partial oxygen pressure in bodily tissues. Initially, neonatal antioxidant defense is not fully mature, especially in preterm infants. Apparently, activity of the most important antioxidant enzymes—superoxide dismutase (SOD), catalase (CAT), and glutathione peroxidase (GPx)—increases in the fetus at the last weeks of pregnancy [40] (it is significantly higher at term neonates). Lack of prooxidant/antioxidant balance results in overproduction of free radicals and damage to cellular proteins, lipids, and DNA. Malondialdehyde (MDA), a by-product of lipid peroxidation of polyunsaturated fatty acids, is an acknowledged marker of oxidative stress which was scrutinized in several researches over neonatal hyperbilirubinemia. Some studies reported lower concentration of MDA in babies with high bilirubin concentration of 20 mg/dl [41] or even 25 mg/dl [42]. Other studies declared contrary results, suggesting that this issue is still unsolved [43, 44]. Researches focusing on the influence of bilirubin on total plasma antioxidant capacity (TPAC) also give inconsistent outcomes [45]. It should be remembered that bilirubin is just one of many parameters affecting the amount of TPAC. However, in most studies concerning term neonates, TPAC seems to increase in the presence of high bilirubin concentration [7, 42, 46].

During cell culture studies, the researchers noted that a nanomolar bilirubin concentration was sufficient to control high oxidative stress caused by hydrogen peroxide [47]. There is a hypothesis saying that bilirubin turns back into biliverdin when is oxidized by hydrogen peroxide (Figure 1) [48]. At this reaction, there is probably no additional enzyme involved, unlike in glutathione cycle. Subsequently, the biliverdin reductase collaborates with its reducing cofactor, NADPH, to recoup a pool of bilirubin. Existence of bilirubin/biliverdin catabolic cycle might be a compromise which would allow to take an advantage of strong antioxidant properties of bilirubin while reducing the risk of cytotoxicity [49]. According to some researches, it would explain how such a little intracellular concentration of bilirubin (below 10 nM) could protect membrane lipids and membrane proteins against peroxidation [48]. However, a group of Czech scientists proposed and verified a model in which an efficient function of bilirubin oxidation cycle required serum albumins as the matrix for biochemical conversions [50]. Their studies support the theory of important antioxidant role of bilirubin/biliverdin cycle, but situate it in plasma rather than inside of cells.

Interestingly, the beneficial effect of bilirubin is not limited to antioxidant properties. There is evidence that bilirubin can decrease production of proinflammatory cytokines such as TNF and IL-1β as well as downregulate Toll-like receptors 4 (TLR4) and inhibit expression of MyD88 as an adapter in IL-1 signal transduction [51].

Endothelial cells are capable of expressing on their surface molecules of major histocompatibility complex class II (MHC-II) in response to stimulation. Bilirubin was found to inhibit MHC-II expression through interference with the activation of signal transduction dependent on the signal transducer and activator of transcription-1 (STAT-1). Later study revealed that bilirubin reduces MHC-II also in dendritic cells and macrophages [52].

Bilirubin suppresses T cell proliferative response in the concentration physiologic for neonates (1.2-8.8 mg/dl) [52]. Further increase of bilirubin concentration above 8.8 mg/dl leads to T cell apoptosis. Moreover, bilirubin prevents oxidant-induced leukocyte adhesion in microvessels [53].

Bilirubin metabolism is also associated with nitric oxide (NO) metabolism. NO is a multifunctional gaseous molecule with free radical properties, playing role in numerous signaling pathways. It is produced by three isoforms of NO synthases (NOS): neuronal NOS (nNOS), endothelial NOS (eNOS), and inducible NOS (iNOS). During endotoxemia, bilirubin inhibits the induction of iNOS by bacterial lipopolysaccharide (LPS) and therefore alleviates tissue injury [54].

Summarizing, bilirubin might bring to neonate multidimensional benefits which are still not fully understood. Considering previous studies, it seems very likely that the increase in bilirubin concentration in the blood in the perinatal period is not accidental and contributes to maintaining homeostasis.

4. Carbon Monoxide: Another Relevant Player

CO used to be another underestimated product of heme degradation. It is infamous for its ability to bind to Hb over 200

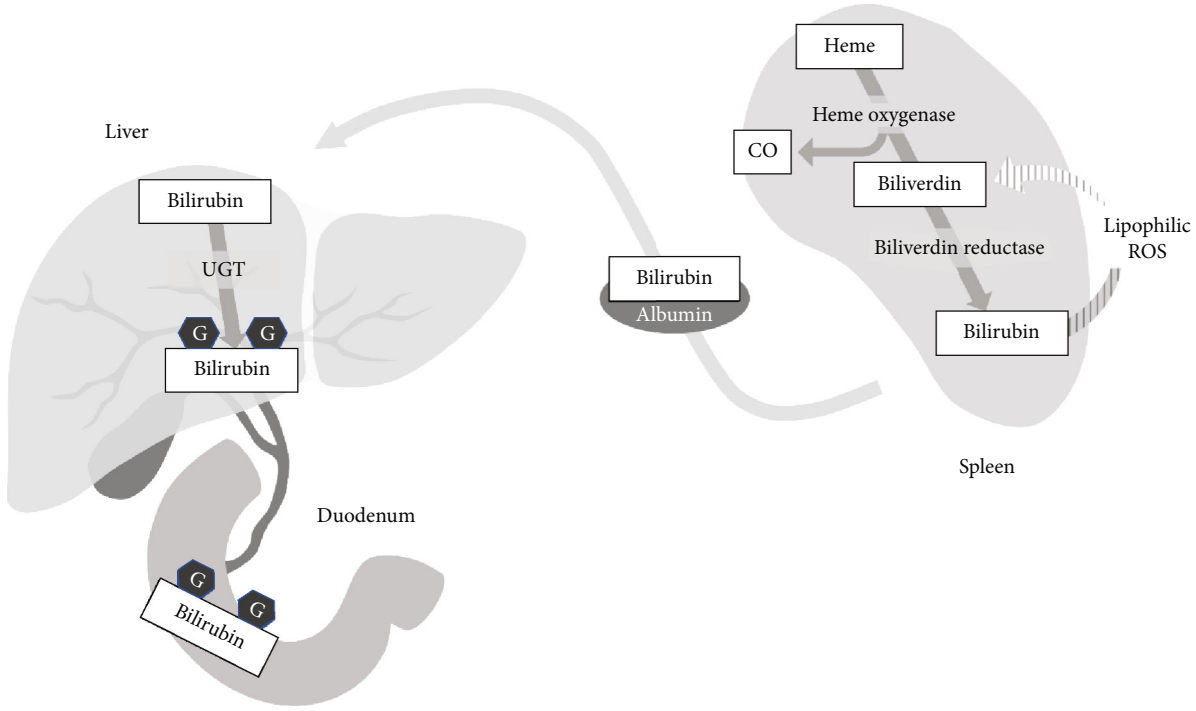

Figure 1: Bilirubin is formed during the degradation of heme by two forms of heme oxygenases (HO-1 and HO-2). HO-2 is constitutively expressed in various tissues. Under normal conditions HO-1 is expressed in selected organs, e.g., the spleen. The products of the reaction are green biliverdin and carbon monoxide (CO). Next, biliverdin undergoes reduction to yellow bilirubin. In the presence of lipophilic ROS, bilirubin can be reversely converted to biliverdin. Water-insoluble bilirubin is bound to serum albumin (1 g of albumin binds to 8 mg of bilirubin [38]) and transported to the liver, where glucuronidation takes place. Finally, conjugated bilirubin is excreted with the bile. G: glucuronide; UGT: 5′-diphospho-glucuronosyltransferase.

times tighter than oxygen and formation of carboxyhemoglobin (COHb). The association is reversible but it reduces amount of available Hb molecules and can cause an impaired oxygen delivery to tissues. At least 86% of endogenous CO production comes from heme metabolism and remaining 14% derives from other processes such as lipid oxidation and metabolism of xenobiotics [25, 55]. CO is produced locally and does not result in systemic intoxication. Under basal conditions, HO-1 expression is generally low, except for cells involved in degradation of erythrocytes, and HO-2 is the main source of CO in most other tissues. Stress stimulus upregulates inducible HO-1 and increases significantly the amount of CO [25]. Blood COHb is a parameter of reference to assess the amount of endogenous or externally derived CO. Normal concentration of COHb in umbilical cord blood of newborns of nonsmoking mothers was estimated as less 1.2% [56]. Higher concentration might indicate that the mother smoked during pregnancy. COHb value rises in a neonate's blood during the first days after delivery and partially correlates with total serum bilirubin concentration, especially for values below 15 mg/dl [57].

Apart from Hb, CO ligates with heme moiety of soluble guanylyl cyclase (sGC), cytochrome p-450 (CYP-450), cytochrome-*c* oxidase (CcO), inducible nitric oxide synthase (iNOS), NADPH oxidases (NOX), and other cytochromes [25]. Numerous studies revealed important putative functions of CO. In vascular tissue [58] and the brain [59], CO produced constitutively by HO-2 is an important activator of sGC. CO participates via cyclic guanosine monophosphate (cGMP) in neurotransmission, regulation of vascular tone, inhibition of vascular smooth muscle proliferation, and platelet aggregation [59–62].

CO relaxes vascular smooth muscles also by direct activation of large conductance calcium-activated potassium channels (BK_{Ca}) which is the most widely studied channel in the context of CO regulation [25, 63]. BK_{Ca} channels are found, i.e., in carotid bodies, where they play a central role in a response to hypoxia. Activity of several other channels was found to be modulated indirectly by CO by means of NO, cGMP, or ROS production [25]. ROS appears as a result of chemical asphyxiation of a cell when CO inhibits oxidase c (COX, complex IV of mitochondrium). CO binds to COX with high affinity, and a very little concentration of this gas is required to promote generation of ROS [25].

On the other hand, CO boosts antioxidative response as it activates a transcription factor NF-E2-related factor-2 (Nrf-2) [64]. Nrf-2 upregulates expression of HO-1, various ROS-detoxifying enzymes, and proteins, e.g., glutathione reductase (GR) GP-2, NADPH-quinone oxidoreductase (NQO), and light and heavy chains of ferritin complex [65].

Anti-inflammatory effect of CO is conferred through activation of the mitogen-activated protein kinase (p38 MAPK) pathway [66, 67], downregulation of the c-Jun N-terminal protein kinases (JNK) pathway [68], and the ERK1/2 extracellular signal-regulated kinases 1 and 2 (ERK1/2) [60]. Several studies focused on NOD, leucine-rich region, and pyrin

domain containing 3 (NLRP3) inflammasome which promote maturation and release of proinflammatory cytokines. Different CO-releasing molecules or exposure to inhaled CO suppressed NLRP3 inflammasome [69–71], possibly by inducing pyrin production which is its negative regulator [72]. As the consequence, activation of caspase-1 was inhibited, concentration of IL-10 was increased, and IL-1β and IL-18 were decreased.

A modulation of caveolin-1-TLR4 interactions at the plasma membrane results in downregulation of Toll-like receptor 4 (TLR4) [73]. Decreased expression of complex consisting of TLR4 and myeloid differentiation factor-2 (MD-2) on the surface of dendritic cells and neutrophils during an immune response to endotoxin was also accredited to CO treatment [74, 75]. CO-treated mice manifest increased systemic tolerance and are less susceptible to endotoxic shock. Moreover, there were studies on baboons indicating that inhaled CO can speed up resolution of inflammation by increasing of lipoxin and eicosapentaenoic acid- (EPA-) derived E-series resolvins (RvE) synthesis [75, 76].

Taking into account all above facts, we can presume that CO, which production in the perinatal period rises proportionally to the production of bilirubin, might be another important modulator of immune response as well as contribute to achievement of oxidant-antioxidant balance in newborns.

5. Neonatal Diseases Related to ROS and Intense Inflammation

Reactive species are free radicals and substances which readily lead to free radical formation. They play important role in physiological processes such as maturation, cell signaling, or immune reactions. However, due to impaired electrons on their outer shell, free radicals react easily with DNA, proteins, and phospholipids causing their modification and loss of original functions. When antioxidant defense is insufficient, oxygen (ROS) and nitrogen (RNS) reactive species cause oxidative and nitrosative stress and therefore induce significant damage in the organism. During labor, a newborn changes the environment from intrauterine to extrauterine, and at the same time, partial oxygen pressure in newborn's arterial blood rises rapidly from 25 mmHg to 100 mmHg. As a result of hyperoxia, a significant amount of free radicals is generated [77, 78]. Among procedures which are common in neonatal intensive care units (NICU), oxygen therapy [79] and parenteral nutrition [80] markedly promoted oxidative damage. Nowadays, ROS/RNS are considered an important contributory factor in pathogenesis of neonatological diseases, i.e., retinopathy of prematurity (ROP), respiratory distress syndrome (RDS), bronchopulmonary dysplasia (BPD), periventricular leukomalacia (PVL), necrotizing enterocolitis (NEC), patent ductus arteriosus (PDA), intrauterine growth restriction (IUGR), and some congenital malformations [81].

5.1. Brain Injury. Brain injuries which frequently affect newborns are hypoxic-ischemic encephalopathy (HIE), intraventricular hemorrhage (IVH), and periventricular leukomalacia (PVL). The still-developing nervous system is very sensitive to any disturbances. The complex processes such as neuronal cell differentiation, migration, formation of synapses, and myelination can be easily disrupted by insufficient energy supply or accumulation of noxious compounds. Inflammatory and infectious processes pose a significant threat to nervous tissue by activation of various biochemical cascades which disturb brain metabolism. Oxidative stress in neonates triggers degeneration of vulnerable oligodendrocyte precursor cells, which leads to PVL [82]. White matter of immature myelin is susceptible to free radical damage because of high concentration of polyunsaturated fatty acids which easily undergo peroxidation and themselves become a source of new free radicals [83]. Increased lipid peroxidation follows episodes of acute hypoxia. Two NO synthases are upregulated by hypoxia episode: nNOS and eNOS. eNOS seems to have protective properties while nNOS activity might be harmful [83]. Glutamate is an important neurotransmitter but in high concentration can impair glutathione production by competitive inhibition of cystine uptake and as the result causes oxidative stress-mediated neuronal death [84]. In the neonatal brain, a temporary upregulation of glutamate receptors has been observed and it can also contribute to brain damage (excitotoxicity) [83].

It is certain that severe hyperbilirubinemia is dangerous to the infant's nervous system. Unconjugated bilirubin (UCB), as a lipid-soluble compound, crosses easily blood-brain barrier (BBB). When neurotoxic effect of bilirubin cannot be longer compensated by neuroprotective mechanisms, bilirubin-induced neurologic dysfunction (BIND) occurs in various parts of the brain including the basal ganglia, central and peripheral auditory pathways, and hippocampus [85]. The intensity of bilirubin neurotoxicity depends on several factors, e.g., UCB level, duration of hyperbilirubinemia, concentration of serum albumin, plasma pH, and BBB permeability. Proposed mechanism of bilirubin-induced neurotoxicity includes excessive release of glutamate, energy failure, and proinflammatory cytokine induction [38]. Despite the negative effect of bilirubin on brain cells, in vitro studies have shown neuroprotective role of bilirubin formed from constitutive expressed HO-2 within hippocampal and cortical neuronal cultures, when bilirubin occurred in nanomolar concentration [47]. Additionally, HO-2-derived CO is required for physiological functions in neuronal population [86]. Normal expression of HO-1 in neurons is low and resistant to induction. In contrast, astrocytes were able to increase their HO-1 expression by 7-fold within 3 h after exposure to hydrogen peroxide and they were less vulnerable to oxidative stress [87].

5.2. Pulmonary Dysfunction. Respiratory distress syndrome (RDS) occurs in 4-7% of all neonates. In term newborns, RDS is mostly caused by transient tachypnea of the newborn and pneumonia, less frequently by meconium aspiration syndrome and congenital respiratory system defects [88]. Preterm infants develop RDS due to immature lungs and insufficient or dysfunctional surfactant. Without functional surfactant, alveoli collapse upon expiration. Mechanical

ventilation (MV) with increased mean airway pressure is often necessary to maintain adequate relationship of ventilation and perfusion, and to prevent respiratory failure. Therefore, preterm neonates are additionally exposed to hyperoxia, which activates NOX to intensive ROS production and promotes destruction of alveoli endothelial cells and release of proinflammatory cytokines [81, 89]. MV induces oxidative stress and leads to further lung injury [90].

A rising number of bronchopulmonary dysplasia (BPD) cases are recorded every year, although its definition has changed since it was first described in 1967. The clue of BPD pathogenesis is airways remodeling as the result of chronic inflammation and impairment of alveolar epithelial type II cells. Those important stem cells synthesize surfactant, control transepithelial movement of water, and regulate lung tissue development and regeneration. Hyperoxia induces death of alveolar epithelium and vascular endothelium. Loss of integrity of vascular cells results in edema and increased inflammatory cell migration to the lung tissue. Due to stromal cell proliferation and depleted vascularization of distal lung tissues, children with BPD may develop pulmonary hypertension [91].

Studies in mice confirmed that in the neonatal lung, HO-2 represents an important antioxidative mechanism. In HO-2 knockout mice, parameters of oxidative stress after hypoxia were higher and their ferritin level was insufficiently increased in relation to increased iron content, which led to accumulation of redox-active iron and exacerbation of oxidative stress injury [92].

Effects of HO-1 activity are complex and depend not only on its expression level but also on duration of HO-1 expression and its subcellular localization. This protein is the most abundant in the smooth endoplastic reticulum, anchored to its c-terminus, but it is also found in other cell compartments. Induction of mitochondrial HO-1 improves energy metabolism and prevents drop of ATP level [93]. Nuclear HO-1 upregulates genes protecting against oxidative stress and this action is independent from enzymatic activity [94].

In newborn rodents, HO-1 expression is higher than in adults but it is less susceptible to further induction, probably due to enhanced expression of Bach1 - nuclear repressor of HO-1 transcription-Bach1 [95]. HO-1-deficient mice presented disrupted alveolar growth [96]. However, HO-1 overexpression is also undesirable since it results in maladaptive proliferation of epithelial type II cells and impaired lung function [97].

Carbon monoxide—one of the products of HO reaction—plays an important role in defence against oxidative lung damage. The protective role of low doses of CO in hyperoxia-induced lung injury was discovered in a rodent model. CO at the concentration of 250 ppm (0.025%) prevented development of pulmonary injury manifestations (pleural infusion, protein accumulation, lung hemorrhage, edema, alveolar septal thickening, influx of inflammatory cells, and fibrin deposition) and prolonged the survival time of animals exposed to lethal hyperoxia [98]. In endothelial cells, CO exerts antiapoptotic activity through mechanism involving activation of the p38 MAPK and NF-κB pathways [67, 99, 100].

5.3. Retinopathy of Prematurity (ROP). The eye is an organ which at the early stage of life is highly susceptible to changes in oxygen concentration. Vascularization begins in a 16-17-week-old fetus and is stimulated by various hormonal factors as well as "physiological hypoxia" [101]. Intense exposure to oxygen causes loss of vessels at the first stage, followed by neovascularization at the next stage. Pathological vessels are sources of various ophthalmological problems including retinal hemorrhages, retinal detachment, and intravitreal neovascularization. Moreover, hyperoxia induces abundant retinal mitochondria to ROS overproduction, which further contributes to ROP progression. Results of multicenter trial with recombinant human superoxide dismutase (rhSOD) seem to confirm the role of oxidative stress in ROP pathology. Infants treated with rhSOD were less likely to suffer from severe ROP and they less frequently develop severe amblyopia or complete blindness [102]. Also, intramuscular injection of vitamin A, a recognized antioxidant, improves retinal function and decreases risk of eyesight loss [103].

The impact of bilirubin on ROP incidence and severity remains undetermined. Some studies claimed a reverse correlation between mean bilirubin level [104] and peak bilirubin level [105] in the first 2 weeks of life and the severity of ROP [104], while other studies denied protective effect of bilirubin on the development of ROP [106–108].

5.4. Necrotizing Enterocolitis. Like in the case of the previously described diseases, the main risk factor of NEC is prematurity. Feeding and bacterial colonization activate a defective immune response in the immature intestinal system leading to perfusion dysregulation and uncontrolled inflammation [109]. Large quantities of platelet-activating factor (PAF), TNF, and IL-6 are released and boost migration of leukocytes to the damaged tissue. Polymorphonuclear leukocytes are important producers of free radicals. Ischemia-reperfusion episodes also trigger increased ROS production resulting in mucosal injury [110]. An ischemia-reperfusion injury of gut tissue was induced in rats. Animals which were simultaneously treated with a continuous infusion of bilirubin presented less histopathologic and biochemical evidence of damage than the untreated group [111]. Moreover, in an experiment on a mouse model, heterozygous animals with partially deficient HO-1 (Hmox1(+/-)) were more susceptible to experimental NEC-like intestinal injury than a wild type [112], which additionally points out the important role of oxidative stress in NEC pathogenesis. In terms of human observational studies, significantly lower mean total serum bilirubin was found in preterm neonates with NEC in comparison with healthy newborns [104].

6. Clinical Opportunities regarding Elements of Heme Catabolism

Antioxidant and anti-inflammatory properties of bilirubin and CO as well as the beneficial effect of heme oxygenase (HO) upregulation have become a focus of interest for researchers looking for new ways of treatment. Earlier reports about amelioration of a disease course during jaundice, observational studies of patients with Gilbert syndrome,

and experiments on animal models provide us with some hints about in which illness heme-derived compounds can be effective. Based on the previous observations, it can be concluded that such a treatment would be able to improve endothelial function, reduce oxidative stress, and mitigate inflammatory response; therefore, it might be efficient in the case of cardiovascular diseases [113–115], diabetes mellitus 2 [116–119], inflammatory bowel diseases [51, 120–122], transplant rejection [123, 124], sepsis [64, 69, 70], rheumatic diseases [125, 126], wound healing [127, 128], ischemic-reperfusion injuries [129–131], and others.

One way to increase the quantity of heme catabolism products in an organism is upregulation of HO-1. This approach was adopted in numerous studies [23, 26, 47, 53]; upregulation of heme oxygenase can be obtained either by administration of HO inducers or gene transfer [26, 132].

Another way to increase the quantity of heme catabolism products is supplementation. A large part of our knowledge about bilirubin, biliverdin, and CO properties come from testing those substances on animal models, mainly via intravenous administration in the case of bilirubin and via inhalation in the case of CO. Bilirubin was also administrated to healthy human volunteers without causing evident adverse effects [133]. Many difficulties concerning the application of native substances may appear, including water insolubility and potential neurotoxicity of bilirubin or high affinity of CO to Hb. However, new technologies come in handy and enable us to overcome some of those limitations.

In 2016, a new bilirubin compound was synthetized. Bilirubin molecules with covalently attached polyethylene glycol (PEG) tend to aggregate spontaneously and form bilirubin nanoparticles (BRNPs). BRNPs have diameter of approximately 100 nm, dissolve in water, and display valuable properties of bilirubin without causing jaundice [134, 135]. BRNPs showed preferred accumulation at the inflamed tissue and longer circulation time, which positively influences its efficacy as a hydrogen peroxide scavenger [135]. The first study which tested newly invented BRNP indicated that BRNPs-treated mice were protected from dextran sodium sulfate-induced colitis [134]. Clinically, they manifested no intestinal bleeding or diarrhea; histologically, there was little immune cell infiltration in mucosa, submucosa, and muscle layers of the intestines compared to untreated mice. In the experiment on a mouse model of allergic asthma, BRNPs turned out to be clearly more active than unconjugated bilirubin and more effectively reduced population of activated Th2 cells as well as alleviated airway hyperresponsiveness [135]. Bilirubin nanoparticles were also found to enhance and prolong graft pancreatic islet survival and seem to be a very promising treatment against transplant rejections [136].

CO is another advantageous molecule which can be applied in treatment of various diseases. Delivery of gaseous CO to the target tissue is practically impossible because of the lack of specificity and high affinity to Hb. In order to make use of CO anti-inflammatory and cytoprotective properties, a nontoxic CO-releasing agent is required. Such a molecule should also be biocompatible and easy to mobilize. Most of CO-releasing molecules (CORMs) are organometallic compounds which include carbonyl complex with transient metal core. In recent years, some nonmetallic CORMs [137] have also been invented. Lower toxicity and easier modification may be in favor of the nonmetallic CORMs. Regardless of CORM type, two parts can be distinguished—a CORM and a drug sphere. The former is responsible for the mechanism of CO discharge and the number of released CO molecules; the latter determinates additional properties of CORM which gives it an advantage over inhaled CO, especially the ability to target the desired tissue [138].

Several different kinds of CO-releasing molecules have been already tested on animal models.

The list of potential therapeutic applications, including a vast range of diseases and pathological conditions, has been gathered in the table (Table 1).

Up to date, there were no studies focusing on the treatment of neonatal diseases with the use of either BRNPs or CORM technologies. In fact, none of these therapeutic strategies has been verified in clinical trials. However, reports concerning ameliorative activity of these substances in colitis, brain, or lung injuries in animal models seem promising. It should be considered that in spite of relatively high concentration of bilirubin in newborn's blood, which even put them in danger of kernicterus, neonates may still benefit from bilirubin or CO administration. At this group of patients' simple parenteral administration of bilirubin or induction of HO-1 would be undesirable, but there is definitely a need for antioxidant and anti-inflammatory treatment. In the case of preterm infants, the new molecules might be of great use as they display higher efficiency with lower toxicity. There is a good example of bilirubin nanoparticles which act as free radical scavengers and support antioxidant defense without generating jaundice.

7. Neonatal Jaundice: Different Therapeutic Approaches

Having discussed the role of heme catabolism in newborns, it is worth addressing again the subject of neonatal jaundice. This condition occurs in almost 2 out of 3 term infants as the result of disproportion between increased bilirubin production and less effective elimination of the pigment. Prematurity, hematomas, glucose intolerance in pregnancy, hemolysis, and mutations in a UGT gene are additional well-known factors which intensify bilirubin formation and boost the probability of jaundice-related complications [139]. In many cases, medical interventions are required to prevent bilirubin encephalopathy. A detailed description of the pathogenesis and consequences of neonatal jaundice is not the subject of this review. However, we would like to highlight a few aspects of jaundice treatment concerning safety of phototherapy and possible application of HO inhibition strategy.

Phototherapy of jaundiced neonates is a recognized and efficient method of serum bilirubin level reduction. The wavelength around 460 nm is considered safe and efficient because of good light penetration into the skin. Upon radiation exposure, a naturally occurring insoluble Z, Z-bilirubin changes into water-soluble configurational photoisomers Z, E-bilirubin and E, Z-bilirubin, and into structural

Table 1: Examples of CO-releasing molecules (CORMs) and their clinical applications. The table was based on Ismailova et al. [138].

Molecule	Clinical applications
CORM-2	Antibacterial activity (*E. coli* *, *H. pylori* *, *P. aeruginosa* *), neuroprotection**, cochlear inflammation**, neuropathic pain**, colitis**, bacterial LPS-induced inflammation**, TNF-α-induced inflammation*, inflammation-induced blood clotting*, abnormal platelet coagulation*, intestinal mucosa injury**, sepsis**, hyperglycemia**, obesity**, cancer (prolonged survival**, decreased angiogenesis**, and cell aggregation*), cardioprotection*, kidney transplantation**
CORM-3	Antibacterial effect* (*H. pylori* *, *S. typhimurium* *, *P. aeruginosa* **), neuroinflammation*, periodontal inflammation*, septic lung injury**, cardioprotection**, hemorrhagic shock*, cardiac transplantation**, renoprotection*, postoperative ileus**, increased intraocular pressure**, anticoagulation**, vascular inflammation*, pulmonary hypertension**
PhotoCORM/ TryptoCORM	Antibacterial effect against *E. coli* *, *N. gonorrhoeae* *
CORM-371	Antibacterial effect against *P. aeruginosa* *
CORM-A1	Antibacterial effect against *P. aeruginosa* *, improved neurodifferentiation*, diabetes (facilitated beta cell regeneration)**, obesity**, autoimmune uveoretinitis**, hemorrhagic shock**, liver injury**, anticoagulation**
ALF186, ALF492	Neuroprotection (ischemic insult*, malaria**)
CORM-401	Efficient vasodilator*
CO-Hbv	Colitis**

*In vitro studies (cell/tissue cultures). **In vivo studies (rodent models).

photoisomers Z- and E-lumirubin [140]. Only small amounts of lumirubin can be detected in an infant's body as it is quickly excreted into the urine and stool. The configurational isomers are eliminated more slowly and they can be reversed back to Z, Z-bilirubin. Importantly, bilirubin photoisomers can be removed from the organism without earlier glucuronidation. It is believed that Z, E- and E, Z-bilirubins are incapable of crossing the blood-brain barrier and therefore do not produce neurotoxic effects. However, more studies are desirable to confirm this hypothesis [141, 142]. There is also a need for thorough investigation of bilirubin photoisomers toxicity, especially in the context of aggressive phototherapy of very-low-body-weight infants [141, 143]. Moreover, Stevenson et al. raised question of oxidative stress resulting from bilirubin and riboflavin photosensitization [139].

Overheating, dehydration, hypocalcemia, conjunctivitis, and retinal damage are adverse effects observed after phototherapy [141, 144]. Additionally, neonates with porphyrinemia due to hepatic dysfunction or intensive hemolysis are in the risk of developing purpuric or bullous eruption and "bronze" baby syndrome. Brown skin pigmentation and purpuric eruptions are benign complications which resolve within few days after cessation of the phototherapy [144, 145].

Metalloporphyrins (Mps) are synthetic heme analogues which bring a promise of specific medical intervention for prevention and treatment of neonatal jaundice. Mps compete with heme for binding with the heme oxygenase; therefore, they decrease bilirubin production. Two kinds of Mps have been already studied in human clinical trials—tin protoporphyrin (SnPP) and tin mesoporphyrin (SnMP). SnPP was abandoned because of prominent photosensitizing properties [146]. SnMP proved efficient in reducing plasma peak bilirubin and the need for phototherapy [147, 148]. Nevertheless, some neonates still required phototherapy. In this group, a transient erythema was recorded as the only short-term side effect and occurred after exposure to white light. Some other Mps, such as chromium mesoporphyrin, zinc protoporphyrin, and zinc bis glycol, possess desirable properties. They are photoinert, can be administrated orally (SnMP requires intramuscular injections), and affect other heme-dependent enzymes in a lesser degree than SnMP [146, 149].

In the light of beneficial functions of bilirubin and CO, which are meticulously presented in this paper, additional questions might arise—What is the impact of phototherapy and Mps application on natural defensive strategies of a neonate against oxidative stress and inflammatory processes? Is the reduction of bilirubin encephalopathy occurrence the only goal to obtain or should we also take into account other aspects such as occurrence of ROS-related diseases in premature babies? The paper does not try to answer these questions and only points out at future challenges.

8. Conclusions

Summing up, the role of heme metabolism products is more multifaceted than it was assumed in the past. They modulate inflammation and ameliorate generation of noxious free radicals. As it was presented above, aggravated inflammatory reactions and increased oxidative stress are often implicated in the pathology of typical neonatal diseases. The more premature a newborn is, the higher is his susceptibility to oxidative stress and the greater risk of serious illnesses. Increased HO-1 activity and high bilirubin concentration are the response to stress stimuli faced by infants and constitute an important part of neonatal protection. In the case of jaundice of the newborn, its positive aspects should be taken into

account and bilirubin-lowering therapy should be based on clinical indications and careful risk assessment of hyperbilirubinemia complications. Newly developed bilirubin nanoparticles and CO-releasing molecules show good effects in the studies on animal models of inflammatory diseases. Moreover, they are characterized by lower toxicity and better controllability. There is a hope that in future some of those molecules can be employed in prevention and treatment of neonatal diseases connected with increased oxidative stress and an excessive inflammatory reaction.

Conflicts of Interest

The authors declare no conflict of interests.

Acknowledgments

This publication was funded by statutory funds of the Medical University of Lublin provided by the Polish Ministry of Science and Higher Education for Medical University of Lublin, Poland.

References

[1] C. Bandi, "Predictive value of total serum bilirubin within 6 hour of birth for the development of hyperbilirubinemia after 72 hours of birth," *Journal of Clinical and Diagnostic Research*, vol. 10, no. 9, 2016.

[2] S. R. Hansson, M. Gram, and B. Åkerström, "Fetal hemoglobin in preeclampsia: a new causative factor, a tool for prediction/diagnosis and a potential target for therapy," *Current Opinion in Obstetrics and Gynecology*, vol. 25, no. 6, pp. 448–455, 2013.

[3] D. P. Kaufman and S. L. Lappin, *Physiology, Fetal Hemoglobin*, StatPearls Publishing, Treasure Island, FL, USA, 2019, April 2020, http://www.ncbi.nlm.nih.gov/pubmed/29763187.

[4] X. Wang and S. L. Thein, "Switching from fetal to adult hemoglobin," *Nature Genetics*, vol. 50, no. 4, pp. 478–480, 2018.

[5] C. Hammerman, R. Goldstein, M. Kaplan et al., "Bilirubin in the premature: toxic waste or natural defense?," *Clinical Chemistry.*, vol. 44, no. 12, pp. 2551–2553, 1998.

[6] R. Stocker, Y. Yamamoto, A. F. McDonagh, A. N. Glazer, and B. N. Ames, "Bilirubin is an antioxidant of possible physiological importance," *Science*, vol. 235, no. 4792, pp. 1043–1046, 1987.

[7] V. Gopinathan, N. J. Miller, A. D. Milner, and C. A. Rice-Evans, "Bilirubin and ascorbate antioxidant activity in neonatal plasma," *FEBS Letters*, vol. 349, no. 2, pp. 197–200, 1994.

[8] G. L. Hatfield and L. R. C. Barclay, "Bilirubin as an antioxidant: kinetic studies of the reaction of bilirubin with peroxyl radicals in solution, micelles, and lipid bilayers," *Organic Letters*, vol. 6, no. 10, pp. 1539–1542, 2004.

[9] P. Ponka, "Cell biology of heme," *The American Journal of the Medical Sciences*, vol. 318, no. 4, pp. 241–256, 1999.

[10] X. Zhang, J. Guo, X. Wei et al., "Bach1: function, regulation, and involvement in disease," *Oxidative Medicine and Cellular Longevity*, vol. 2018, Article ID 1347969, 8 pages, 2018.

[11] Y. Zhou, H. Wu, M. Zhao, C. Chang, and Q. Lu, "The Bach family of transcription factors: a comprehensive review," *Clinical Reviews in Allergy and Immunology*, vol. 50, no. 3, pp. 345–356, 2016.

[12] T. P. Burris, "Nuclear hormone receptors for heme: REV-ERBα and REV-ERBβ are ligand-regulated components of the mammalian clock," *Molecular Endocrinology*, vol. 22, no. 7, pp. 1509–1520, 2008.

[13] K. Igarashi and M. Watanabe-Matsui, "Wearing red for signaling: the heme-bach axis in heme metabolism, oxidative stress response and iron immunology," *Tohoku Journal of Experimental Medicine*, vol. 232, no. 4, pp. 229–253, 2014.

[14] J.-J. Chen, "Regulation of protein synthesis by the heme-regulated eIF2α kinase: relevance to anemias," *Blood*, vol. 109, no. 7, pp. 2693–2699, 2006.

[15] B. Wu, Y. Wu, and W. Tang, "Heme catabolic pathway in inflammation and immune disorders," *Frontiers in Pharmacology*, vol. 10, 2019.

[16] T. Ganz, "Macrophages and systemic iron homeostasis," *Journal of Innate Immunity*, vol. 4, no. 5-6, pp. 446–453, 2012.

[17] G. Balla, G. Vercellotti, J. W. Eaton, and H. S. Jacob, "Heme uptake by endothelium synergizes polymorphonuclear granulocyte-mediated damage," *Transactions of the Association of American Physicians*, vol. 103, pp. 174–179, 1990.

[18] F. A. D. T. G. Wagener, E. Feldman, T. de Witte, and N. G. Abraham, "Heme induces the expression of adhesion molecules ICAM-1, VCAM-1, and E selectin in vascular endothelial cells," *Experimental Biology and Medicine*, vol. 216, no. 3, pp. 456–463, 1997.

[19] J. D. Belcher, C. Chen, J. Nguyen et al., "Heme triggers TLR4 signaling leading to endothelial cell activation and vaso-occlusion in murine sickle cell disease," *Blood*, vol. 123, no. 3, pp. 377–390, 2014.

[20] S. R. Robinson, T. N. Dang, R. Dringen, and G. M. Bishop, "Hemin toxicity: a preventable source of brain damage following hemorrhagic stroke," *Redox Report*, vol. 14, no. 6, pp. 228–235, 2013.

[21] E. Tolosano, S. Fagoonee, N. Morello, F. Vinchi, and V. Fiorito, "Heme scavenging and the other facets of hemopexin," *Antioxidants and Redox Signaling*, vol. 12, no. 2, pp. 305–320, 2010.

[22] M. D. Maines, "The heme oxygenase system and its functions in the brain," *Cellular and Molecular Biology*, vol. 46, no. 3, pp. 573–585, 2000.

[23] M. D. Maines, "Heme oxygenase: function, multiplicity, regulatory mechanisms, and clinical applications," *The FASEB Journal*, vol. 2, no. 10, pp. 2557–2568, 1988.

[24] G. Kikuchi, T. Yoshida, and M. Noguchi, "Heme oxygenase and heme degradation," *Biochemical and Biophysical Research Communications*, vol. 338, no. 1, pp. 558–567, 2005.

[25] S. W. Ryter, J. Alam, and A. M. K. Choi, "Heme oxygenase-1/carbon monoxide: from basic science to therapeutic applications," *Physiological Reviews*, vol. 86, no. 2, pp. 583–650, 2006.

[26] N. Abraham, A. Asija, G. Drummond, and S. Peterson, "Heme Oxygenase -1 gene therapy: recent advances and therapeutic applications," *Current Gene Therapy*, vol. 7, no. 2, pp. 89–108, 2007.

[27] M. Kaplan, R. J. Wong, and D. K. Stevenson, "Heme oxygenase-1 promoter polymorphisms: do they modulate neonatal hyperbilirubinemia?," *Journal of Perinatology*, vol. 37, no. 8, pp. 901–905, 2017.

[28] O. G. Bozkaya, A. Kumral, D. C. Yesilirmak et al., "Prolonged unconjugated hyperbilirubinaemia associated with the haem

oxygenase-1 gene promoter polymorphism," *Acta Paediatrica*, vol. 99, no. 5, pp. 679–683, 2010.

[29] Y. H. Chen, L. Y. Chau, J. W. Chen, and S. J. Lin, "Serum bilirubin and ferritin levels link heme oxygenase-1 gene promoter polymorphism and susceptibility to coronary artery disease in diabetic patients," *Diabetes Care*, vol. 31, no. 8, pp. 1615–1620, 2008.

[30] P. F. Chang, Y. C. Lin, K. Liu, S. J. Yeh, and Y. H. Ni, "Heme oxygenase-1 gene promoter polymorphism and the risk of pediatric nonalcoholic fatty liver disease," *International Journal of Obesity*, vol. 39, no. 8, pp. 1236–1240, 2015.

[31] Y. H. Weng, Y. W. Chiu, S. W. Cheng, and C. Y. Yang, "Risk assessment of gene variants for neonatal hyperbilirubinemia in Taiwan," *BMC Pediatrics*, vol. 16, no. 1, p. 144, 2016.

[32] Y. Katayama, T. Yokota, H. Zhao et al., "Association of HMOX1 gene promoter polymorphisms with hyperbilirubinemia in the early neonatal period," *Pediatrics International*, vol. 57, no. 4, pp. 645–649, 2015.

[33] P. K. Tiwari, A. Sethi, S. Basu, R. Raman, and A. Kumar, "Heme oxygenase-1 gene variants and hyperbilirubinemia risk in North Indian newborns," *European Journal of Pediatrics*, vol. 172, no. 12, pp. 1627–1632, 2013.

[34] M. Kaplan, P. Renbaum, C. Hammerman, H. J. Vreman, R. J. Wong, and D. K. Stevenson, "Heme Oxygenase-1 promoter polymorphisms and neonatal jaundice," *Neonatology*, vol. 106, no. 4, pp. 323–329, 2014.

[35] M. Kanai, K. Akaba, A. Sasaki et al., "Neonatal hyperbilirubinemia in Japanese neonates: analysis of the heme oxygenase-1 gene and fetal hemoglobin composition in cord blood," *Pediatric Research*, vol. 54, no. 2, pp. 165–171, 2003.

[36] Z. Maróti, M. Katona, H. Orvos, I. Németh, I. Farkas, and S. Túri, "Heme oxygenase-1 expression in premature and mature neonates during the first week of life," *European Journal of Pediatrics*, vol. 166, no. 10, pp. 1033–1038, 2007.

[37] C. E. Cornelius, "Biliverdin in biological systems," in *One Medicine*, pp. 321–334, 1984.

[38] R. Cayabyab and R. Ramanathan, "High unbound bilirubin for age: a neurotoxin with major effects on the developing brain," *Pediatric Research*, vol. 85, no. 2, pp. 183–190, 2019, https://pubmed.ncbi.nlm.nih.gov/.

[39] K. Bernhard, G. Ritzel, and K. U. Steiner, "Über eine biologische Bedeutung der Gallenfarbstoffe. Bilirubin und Biliverdin als Antioxydantien für das Vitamin A und die essentiellen Fettsäuren.," *Helvetica Chimica Acta*, vol. 37, no. 1, pp. 306–313, 1954.

[40] G. D. Georgeson, B. J. Szőny, K. Streitman et al., "Antioxidant enzyme activities are decreased in preterm infants and in neonates born via caesarean section," *European Journal of Obstetrics and Gynecology and Reproductive Biology.*, vol. 103, no. 2, pp. 136–139, 2002.

[41] M. S. Shahab, P. Kumar, N. Sharma, A. Narang, and R. Prasad, "Evaluation of oxidant and antioxidant status in term neonates: a plausible protective role of bilirubin," *Molecular and Cellular Biochemistry*, vol. 317, no. 1-2, pp. 51–59, 2008.

[42] A. Kumar, P. Pant, S. Basu, G. R. K. Rao, and H. D. Khanna, "Oxidative stress in neonatal hyperbilirubinemia," *Journal of Tropical Pediatrics*, vol. 53, no. 1, pp. 69–71, 2007.

[43] S. Basu, D. De, H. Dev Khanna, and A. Kumar, "Lipid peroxidation, DNA damage and total antioxidant status in neonatal hyperbilirubinemia," *Journal of Perinatology*, vol. 34, no. 7, pp. 519–523, 2014.

[44] M. Doğan, E. Peker, E. Kirimi et al., "Evaluation of oxidant and antioxidant status in infants with hyperbilirubinemia and kernicterus," *Human and Experimental Toxicology*, vol. 30, no. 11, pp. 1751–1760, 2011.

[45] C. Dani, C. Poggi, and S. Pratesi, "Bilirubin and oxidative stress in term and preterm infants," *Free Radical Research*, vol. 53, no. 1, pp. 2–7, 2019.

[46] S. Bélanger, J.-C. Lavoie, and P. Chessex, "Influence of bilirubin on the antioxidant capacity of plasma in newborn infants," *Neonatology*, vol. 71, no. 4, pp. 233–238, 2004.

[47] S. Dore, M. Takahashi, C. D. Ferris, L. D. Hester, D. Guastella, and S. H. Snyder, "Bilirubin, formed by activation of heme oxygenase-2, protects neurons against oxidative stress injury," in *Proceedings of the National Academy of Sciences of the United States of America*, vol. 96no. 5, pp. 2445–2450, 1999.

[48] D. E. Barañano, M. Rao, C. D. Ferris, and S. H. Snyder, "Biliverdin reductase: a major physiologic cytoprotectant," *Proceedings of the National Academy of Sciences of the United States of America*, vol. 99, no. 25, pp. 16093–16098, 2002.

[49] T. W. Sedlak and S. H. Snyder, "Bilirubin benefits: cellular protection by a biliverdin reductase antioxidant cycle," *Pediatrics*, vol. 113, no. 6, pp. 1776–1782, 2004.

[50] I. Goncharova, J. Jašprová, L. Vítek, and M. Urbanová, "Photo-isomerization and oxidation of bilirubin in mammals is dependent on albumin binding," *Analytical Biochemistry*, vol. 490, pp. 34–45, 2015.

[51] J.-D. Zheng, Y. He, H.-Y. Yu et al., "Unconjugated bilirubin alleviates experimental ulcerative colitis by regulating intestinal barrier function and immune inflammation," *Cellular and Molecular Biology*, vol. 25, no. 15, pp. 1865–1878, 2019.

[52] Y. Liu, P. Li, J. Lu et al., "Bilirubin possesses powerful immunomodulatory activity and suppresses experimental autoimmune encephalomyelitis," *The Journal of Immunology*, vol. 181, no. 3, pp. 1887–1897, 2008.

[53] S. Hayashi, R. Takamiya, T. Yamaguchi et al., "Induction of heme oxygenase-1 suppresses venular leukocyte adhesion elicited by oxidative stress: role of bilirubin generated by the enzyme," *Circulation Research*, vol. 85, no. 8, pp. 663–671, 1999.

[54] W. W. Wang, D. L. H. Smith, and S. D. Zucker, "Bilirubin inhibits iNOS expression and NO production in response to endotoxin in rats," *Hepatology*, vol. 40, no. 2, pp. 424–433, 2004.

[55] H. J. Vreman, R. J. Wong, C. A. Sanesi, P. A. Dennery, and D. K. Stevenson, "Simultaneous production of carbon monoxide and thiobarbituric acid reactive substances in rat tissue preparations by an iron-ascorbate system," *Canadian Journal of Physiology and Pharmacology*, vol. 76, no. 12, pp. 1057–1065, 1998.

[56] K. Hengstler, P. van 't Sant, and P. E. Jira, "Carboxyhemoglobin in umbilical cord blood and maternal smoking," *Journal of Perinatal Medicine*, vol. 47, no. 7, pp. 780–784, 2019.

[57] D. G. N. Bailey, H. Fuchs, and R. Hentschel, "Carboxyhemoglobin - the forgotten parameter of neonatal hyperbilirubinemia," *Journal of Perinatal Medicine*, vol. 45, no. 5, pp. 613–617, 2017.

[58] R. Zakhary, S. P. Gaine, J. L. Dinerman, M. Ruat, N. A. Flavahan, and S. H. Snyder, "Heme oxygenase 2: endothelial and

neuronal localization and role in endothelium-dependent relaxation," in *Proceedings of the National Academy of Sciences*, vol. 93no. 2, pp. 795–798, 1996.

[59] A. Verma, D. Hirsch, C. Glatt, G. Ronnett, and S. Snyder, "Carbon monoxide: a putative neural messenger," *Science*, vol. 259, no. 5093, pp. 381–384, 1993.

[60] L. Wu and R. Wang, "Carbon monoxide: endogenous production, physiological functions, and pharmacological applications," *Pharmacological Reviews*, vol. 57, no. 4, pp. 585–630, 2005.

[61] C. W. Leffler, H. Parfenova, and J. H. Jaggar, "Carbon monoxide as an endogenous vascular modulator," *American Journal of Physiology Heart and Circulatory Physiology*, vol. 301, no. 1, pp. H1–H11, 2011.

[62] R. Motterlini and R. Foresti, "Biological signaling by carbon monoxide and carbon monoxide-releasing molecules," *American Journal of Physiology - Cell Physiology*, vol. 312, no. 3, pp. C302–C313, 2017.

[63] C. Peers, J. P. Boyle, J. L. Scragg et al., "Diverse mechanisms underlying the regulation of ion channels by carbon monoxide," *British Journal of Pharmacology*, vol. 172, no. 6, pp. 1546–1556, 2015.

[64] S. Y. Qin, R. H. du, S. S. Yin, X. F. Liu, G. L. Xu, and W. Cao, "Nrf2 is essential for the anti-inflammatory effect of carbon monoxide in LPS-induced inflammation," *Inflammation Research*, vol. 64, no. 7, pp. 537–548, 2015.

[65] C. Gorrini, I. S. Harris, and T. W. Mak, "Modulation of oxidative stress as an anticancer strategy," *Nature Reviews Drug Discovery*, vol. 12, no. 12, pp. 931–947, 2013.

[66] L. E. Otterbein, F. H. Bach, J. Alam et al., "Carbon monoxide has anti-inflammatory effects involving the mitogen- activated protein kinase pathway," *Nature Medicine*, vol. 6, no. 4, pp. 422–428, 2000.

[67] S. Brouard, L. E. Otterbein, J. Anrather et al., "Carbon monoxide generated by heme oxygenase 1 suppresses endothelial cell apoptosis," *Journal of Experimental Medicine*, vol. 192, no. 7, pp. 1015–1026, 2000.

[68] D. Morse, S. E. Pischke, Z. Zhou et al., "Suppression of Inflammatory Cytokine Production by Carbon Monoxide Involves the JNK Pathway and AP-1," *Journal of Biological Chemistry*, vol. 278, no. 39, pp. 36993–36998, 2003.

[69] W. Zhang, A. Tao, T. Lan et al., "Carbon monoxide releasing molecule-3 improves myocardial function in mice with sepsis by inhibiting NLRP3 inflammasome activation in cardiac fibroblasts," *Basic Research in Cardiology*, vol. 112, no. 2, 2017.

[70] P. Wang, J. Huang, Y. Li et al., "Exogenous Carbon Monoxide Decreases Sepsis-Induced Acute Kidney Injury and Inhibits NLRP3 Inflammasome Activation in Rats," *International Journal of Molecular Sciences*, vol. 16, no. 9, pp. 20595–20608, 2015.

[71] S. S. Jung, J. S. Moon, J. F. Xu et al., "Carbon monoxide negatively regulates NLRP3 inflammasome activation in macrophages," *American Journal of Physiology - Lung Cellular and Molecular Physiology*, vol. 308, no. 10, pp. L1058–L1067, 2015.

[72] S. K. Kim, Y. Joe, Y. Chen et al., "Carbon monoxide decreases interleukin-1β levels in the lung through the induction of pyrin," *Cellular and Molecular Immunology*, vol. 14, no. 4, pp. 349–359, 2017.

[73] X. M. Wang, H. P. Kim, K. Nakahira, S. W. Ryter, and A. M. K. Choi, "The heme oxygenase-1/carbon monoxide pathway suppresses TLR4 signaling by regulating the interaction of TLR4 with caveolin-1," *The Journal of Immunology*, vol. 182, no. 6, pp. 3809–3818, 2009.

[74] S. A. Riquelme, S. M. Bueno, and A. M. Kalergis, "Carbon monoxide down-modulates Toll-like receptor 4/MD2 expression on innate immune cells and reduces endotoxic shock susceptibility," *Immunology*, vol. 144, no. 2, pp. 321–332, 2015.

[75] C. Chauveau, S. Rémy, P. J. Royer et al., "Heme oxygenase-1 expression inhibits dendritic cell maturation and proinflammatory function but conserves IL-10 expression," *Blood*, vol. 106, no. 5, pp. 1694–1702, 2005.

[76] J. Dalli, B. D. Kraft, R. A. Colas et al., "The regulation of proresolving lipid mediator profiles in baboon pneumonia by inhaled carbon monoxide," *American Journal of Respiratory Cell and Molecular Biology*, vol. 53, no. 3, pp. 314–325, 2015.

[77] C. Yzydorczyk, D. Mitanchez, C. Buffat et al., "Oxidative stress after preterm birth: Origins, biomarkers, and possible therapeutic approaches," *Archives de Pédiatrie*, vol. 22, no. 10, pp. 1047–1055, 2015.

[78] F. G. Coutinho, E. M. d. A. Diniz, I. Kandler, M. A. Cianciarullo, and N. R. d. Santos, "Assessment of oxidative damage and enzymatic antioxidant system activity on the umbilical cord blood and saliva from preterm newborns with risk factors for early-onset neonatal sepsis," *Revista da Associacao Medica Brasileira*, vol. 64, no. 10, pp. 888–895, 2018.

[79] M. Vento, M. Moro, R. Escrig et al., "Preterm Resuscitation With Low Oxygen Causes Less Oxidative Stress, Inflammation, and Chronic Lung Disease," *PEDIATRICS*, vol. 124, no. 3, pp. e439–e449, 2009.

[80] P. Chessex, C. Watson, G. W. Kaczala et al., "Determinants of oxidant stress in extremely low birth weight premature infants," *Free Radical Biology and Medicine*, vol. 49, no. 9, pp. 1380–1386, 2010.

[81] Y. Ozsurekci and K. Aykac, "Oxidative stress related diseases in newborns," *Oxidative Medicine and Cellular Longevity*, vol. 2016, 9 pages, 2016.

[82] S. A. Back, "White matter injury in the preterm infant: pathology and mechanisms," *Acta Neuropathologica*, vol. 134, no. 3, pp. 331–349, 2017.

[83] M. L. Tataranno, S. Perrone, and G. Buonocore, "Plasma biomarkers of oxidative stress in neonatal brain injury," *Clinics in Perinatology*, vol. 42, no. 3, pp. 529–539, 2015.

[84] K. Gupta, G. E. Hardingham, and S. Chandran, "NMDA receptor-dependent glutamate excitotoxicity in human embryonic stem cell- derived neurons," *Neuroscience Letters*, vol. 543, pp. 95–100, 2013.

[85] V. K. Bhutani, R. J. Wong, and D. K. Stevenson, "Hyperbilirubinemia in Preterm Neonates," *Clinics in Perinatology*, vol. 43, no. 2, pp. 215–232, 2016.

[86] J. Muñoz-Sánchez and M. E. Chánez-Cárdenas, "A Review on Hemeoxygenase-2: Focus on Cellular Protection and Oxygen Response," *Oxidative Medicine and Cellular Longevity*, vol. 2014, 16 pages, 2014.

[87] B. E. Dwyer, R. N. Nishimura, and S. Y. Lu, "Differential expression of heme oxygenase-1 in cultured cortical neurons and astrocytes determined by the aid of a new heme oxygenase antibody. Response to oxidative stress," *Molecular Brain Research*, vol. 30, no. 1, pp. 37–47, 1995.

[88] S. Sivanandan, R. Agarwal, and A. Sethi, "Respiratory distress in term neonates in low-resource settings," *Seminars*

in Fetal and Neonatal Medicine, vol. 22, no. 4, pp. 260–266, 2017.

[89] R. S. Frey, M. Ushio–Fukai, and A. B. Malik, "NADPH oxidase-dependent signaling in endothelial cells: role in physiology and pathophysiology," *Antioxidants and Redox Signaling*, vol. 11, no. 4, pp. 791–810, 2009.

[90] C. G. Carvalho, R. S. Procianoy, E. C. Neto, and R. C. Silveira, "Preterm Neonates with Respiratory Distress Syndrome: Ventilator-Induced Lung Injury and Oxidative Stress," *Journal of Immunology Research*, vol. 2018, Article ID 696375, 4 pages, 2018.

[91] G. Buonocore, S. Perrone, and M. Tataranno, "Oxidative stress and bronchopulmonary dysplasia," *Journal of Clinical Neonatology.*, vol. 1, no. 3, pp. 109–114, 2012.

[92] P. A. Dennery, D. R. Spitz, G. Yang et al., "Oxygen toxicity and iron accumulation in the lungs of mice lacking heme oxygenase-2," *Journal of Clinical Investigation*, vol. 101, no. 5, pp. 1001–1011, 1998, http://www.jci.org.

[93] A. Nikam, J. V. Patankar, C. Lackner et al., "Transition between acute and chronic hepatotoxicity in mice is associated with impaired energy metabolism and induction of mitochondrial heme oxygenase-1," *PLoS ONE*, M. Vinciguerra, Ed., vol. 8, no. 6, p. e66094, 2013.

[94] Q. Lin, S. Weis, G. Yang et al., "Heme oxygenase-1 protein localizes to the nucleus and activates transcription factors important in oxidative stress," *Journal of Biological Chemistry*, vol. 282, no. 28, pp. 20621–20633, 2007.

[95] S. Kassovska-Bratinova, G. Yang, K. Igarashi, and P. A. Dennery, "Bach1 Modulates Heme Oxygenase-1 Expression in the Neonatal Mouse Lung," *Pediatric Research*, vol. 65, no. 2, pp. 145–149, 2009.

[96] T. Zhuang, M. Zhang, H. Zhang, P. A. Dennery, and Q. S. Lin, "Disrupted postnatal lung development in heme oxygenase-1 deficient mice," *Respiratory Research*, vol. 11, no. 1, 2010.

[97] P. A. Dennery, "Heme Oxygenase in Neonatal Lung Injury and Repair," *Antioxidants & Redox Signaling*, vol. 21, no. 13, pp. 1881–1892, 2014.

[98] L. E. Otterbein, L. L. Mantell, and A. M. K. Choi, "Carbon monoxide provides protection against hyperoxic lung injury," *American Journal of Physiology - Lung Cellular and Molecular Physiology*, vol. 276, no. 4, pp. L688–L694, 1999.

[99] X. Zhang, P. Shan, L. E. Otterbein et al., "Carbon monoxide inhibition of apoptosis during ischemia-reperfusion lung injury is dependent on the p 38 mitogen-activated protein kinase pathway and involves caspase 3," *Journal of Biological Chemistry*, vol. 278, no. 2, pp. 1248–1258, 2003.

[100] S. Brouard, P. O. Berberat, E. Tobiasch, M. P. Seldon, F. H. Bach, and M. P. Soares, "Heme oxygenase-1-derived carbon monoxide requires the activation of transcription factor NF-κB to protect endothelial cells from tumor necrosis factor-α-mediated apoptosis," *Journal of Biological Chemistry*, vol. 277, no. 20, pp. 17950–17961, 2002.

[101] J. V. Aranda, J. Qu, G. B. Valencia, and K. D. Beharry, "Pharmacologic interventions for the prevention and treatment of retinopathy of prematurity," *Seminars in Perinatology*, vol. 43, no. 6, pp. 360–366, 2019.

[102] R. B. Parad, E. N. Allred, W. N. Rosenfeld, and J. M. Davis, "Reduction of retinopathy of prematurity in extremely low gestational age newborns treated with recombinant human Cu/Zn superoxide dismutase," *Neonatology*, vol. 102, no. 2, pp. 139–144, 2012.

[103] H. Mactier, D. L. McCulloch, R. Hamilton et al., "Vitamin A supplementation improves retinal function in infants at risk of retinopathy of prematurity," *Journal of Pediatrics*, vol. 160, no. 6, pp. 954–9.e1, 2012.

[104] S. M. Fereshtehnejad, K. P. B. Mir, A. P. B. Mir, and P. Mohagheghi, "Evaluation of the possible antioxidative role of bilirubin protecting from free radical related illnesses in neonates," *Acta Medica Iranica*, vol. 50, no. 3, pp. 153–163, 2012.

[105] K. L. Yeo, M. Perlman, Y. Hao, and P. Mullaney, "Outcomes of extremely premature infants related to their peak serum bilirubin concentrations and exposure to phototherapy," *Pediatrics*, vol. 102, no. 6, pp. 1426–1431, 1998.

[106] S. Hosono, T. Ohno, H. Kimoto et al., "No clinical correlation between bilirubin levels and severity of retinopathy of prematurity," *Journal of Pediatric Ophthalmology and Strabismus*, vol. 39, no. 3, pp. 151–156, 2002.

[107] D. D. Gaton, J. Gold, R. Axer-Siegel, E. Wielunsky, N. Naor, and I. Nissenkorn, "Evaluation of bilirubin as possible protective factor in the prevention of retinopathy of prematurity," *British Journal of Ophthalmology*, vol. 75, no. 9, pp. 532–534, 1991.

[108] B. R. Boynton and C. A. Boynton, "Retinopathy of prematurity and bilirubin," *New England Journal of Medicine*, vol. 321, no. 3, pp. 193-194, 1989.

[109] J. B. Sanchez and M. Kadrofske, "Necrotizing enterocolitis," *Neurogastroenterology & Motility*, vol. 31, no. 3, p. e13569, 2018.

[110] G. D'Angelo, S. Manti, S. Aversa et al., "Oxidative stress-mediated damage in newborns with necrotizing enterocolitis: a possible role of melatonin," *American Journal of Perinatology*, vol. 32, no. 10, pp. 905–909, 2015, https://www.thieme-connect.com/products/ejournals/abstract/10.1055/s-0035-1547328.

[111] C. Hammerman, D. Goldschmidt, M. S. Caplan et al., "Protective effect of bilirubin in ischemia-reperfusion injury in the rat intestine," *Journal of Pediatric Gastroenterology and Nutrition*, vol. 35, no. 3, pp. 344–349, 2002.

[112] S. Schulz, R. J. Wong, K. Y. Jang et al., "Heme oxygenase-1 deficiency promotes the development of necrotizing enterocolitis-like intestinal injury in a newborn mouse model," *American Journal of Physiology - Gastrointestinal and Liver Physiology*, vol. 304, no. 11, pp. G991–G1001, 2013.

[113] Y. Lan, H. Liu, J. Liu, H. Zhao, and H. Wang, "Is serum total bilirubin a predictor of prognosis in arteriosclerotic cardiovascular disease? A meta-analysis," *Medicine*, vol. 98, no. 42, p. e17544, 2019.

[114] T. Maruhashi, Y. Kihara, and Y. Higashi, "Bilirubin and endothelial function," *Journal of Atherosclerosis and Thrombosis*, vol. 26, no. 8, pp. 688–696, 2019.

[115] Y. Choi, S. J. Lee, W. Spiller et al., "Causal Associations Between Serum Bilirubin Levels and Decreased Stroke Risk," *Arteriosclerosis, Thrombosis, and Vascular Biology*, vol. 40, no. 2, pp. 437–445, 2020.

[116] D. Dekker, M. J. Dorresteijn, M. Pijnenburg et al., "The bilirubin-increasing drug atazanavir improves endothelial function in patients with type 2 diabetes mellitus," *Arteriosclerosis, Thrombosis, and Vascular Biology*, vol. 31, no. 2, pp. 458–463, 2011.

[117] N. Ikeda, T. Inoguchi, N. Sonoda et al., "Biliverdin protects against the deterioration of glucose tolerance in db/db mice," *Diabetologia*, vol. 54, no. 8, pp. 2183–2191, 2011.

[118] H. Dong, H. Huang, X. Yun et al., "Bilirubin increases insulin sensitivity in leptin-receptor deficient and diet-induced obese mice through suppression of ER stress and chronic inflammation," *Endocrinology*, vol. 155, no. 3, pp. 818–828, 2014.

[119] M. Yang, C. Ni, B. Chang et al., "Association between serum total bilirubin levels and the risk of type 2 diabetes mellitus," *Diabetes Research and Clinical Practice*, vol. 152, pp. 23–28, 2019.

[120] S. D. Zucker, M. E. Vogel, T. L. Kindel et al., "Bilirubin prevents acute DSS-induced colitis by inhibiting leukocyte infiltration and suppressing upregulation of inducible nitric oxide synthase," *American Journal of Physiology - Gastrointestinal and Liver Physiology*, vol. 309, no. 10, pp. G841–G854, 2015.

[121] X. Zhao, L. Li, X. Li, J. Li, D. Wang, and H. Zhang, "The relationship between serum bilirubin and inflammatory bowel disease," *Mediators of Inflammation*, vol. 2019, Article ID 5256460, 7 pages, 2019.

[122] M. Leníček, D. Ďuricová, O. Hradsky et al., "The relationship between serum bilirubin and Crohn's disease," *Inflammatory Bowel Diseases*, vol. 20, no. 3, pp. 481–487, 2014.

[123] C. A. Adin, Z. C. Vangundy, T. L. Papenfuss et al., "Physiologic doses of bilirubin contribute to tolerance of islet transplants by suppressing the innate immune response," *Cell Transplantation*, vol. 26, no. 1, pp. 11–21, 2017.

[124] S. A. Basdeo, N. K. Campbell, L. M. Sullivan et al., "Suppression of human alloreactive T cells by linear tetrapyrroles; relevance for transplantation," *Translational Research*, vol. 178, pp. 81–94.e2, 2016.

[125] P. S. Hench, "THE ANALGESIC EFFECT OF HEPATITIS AND JAUNDICE IN CHRONIC ARTHRITIS, FIBROSITIS AND SCIATIC PAIN," *Annals of Internal Medicine*, vol. 7, no. 10, p. 1278, 1934.

[126] M. Bonelli, A. Savitskaya, C.-W. Steiner et al., "Heme oxygenase-1 end-products carbon monoxide and biliverdin ameliorate murine collagen induced arthritis," *Clinical and Experimental Rheumatology*, vol. 30, no. 1, pp. 73–78, 2012.

[127] M. Ram, V. Singh, D. Kumar et al., "Antioxidant potential of bilirubin-accelerated wound healing in streptozotocin-induced diabetic rats," *Naunyn-Schmiedeberg's Archives of Pharmacology*, vol. 387, no. 10, pp. 955–961, 2014.

[128] M. Ram, V. Singh, S. Kumawat, V. Kant, S. K. Tandan, and D. Kumar, "Bilirubin modulated cytokines, growth factors and angiogenesis to improve cutaneous wound healing process in diabetic rats," *International Immunopharmacology*, vol. 30, pp. 137–149, 2016.

[129] W.-F. Tian, P. Weng, Q. Sheng et al., "Biliverdin Protects the Isolated Rat Lungs from Ischemia-reperfusion Injury via Antioxidative, Anti-inflammatory and Anti-apoptotic Effects," *Chinese Medical Journal*, vol. 130, no. 7, pp. 859–865, 2017.

[130] B. Bakrania, E. F. du Toit, K.-H. Wagner, J. P. Headrick, and A. C. Bulmer, "Pre- or post-ischemic bilirubin ditaurate treatment reduces oxidative tissue damage and improves cardiac function," *International Journal of Cardiology*, vol. 202, pp. 27–33, 2016.

[131] S. Y. Kim, D. K. Rah, Y. Chong, S. H. Lee, and T. H. Park, "Bilirubin provides perforator flap protection from ischaemia-reperfusion injury in a rat model: a preliminary result," *International Wound Journal*, vol. 13, no. 5, pp. 870–877, 2016.

[132] A. S. Pachori, L. G. Melo, L. Zhang, S. D. Solomon, and V. J. Dzau, "Chronic recurrent myocardial ischemic injury is significantly attenuated by pre-emptive adeno-associated virus heme oxygenase-1 gene delivery," *Journal of the American College of Cardiology*, vol. 47, no. 3, pp. 635–643, 2006.

[133] D. Dekker, M. J. Dorresteijn, M. E. B. Welzen et al., "Parenteral bilirubin in healthy volunteers: a reintroduction in translational research," *British Journal of Clinical Pharmacology*, vol. 84, no. 2, pp. 268–279, 2018.

[134] Y. Lee, H. Kim, S. Kang, J. Lee, J. Park, and S. Jon, "Bilirubin Nanoparticles as a Nanomedicine for Anti-inflammation Therapy," *Angewandte Chemie - International Edition*, vol. 55, no. 26, pp. 7460–7463, 2016.

[135] D. E. Kim, Y. Lee, M. G. Kim, S. Lee, S. Jon, and S. H. Lee, "Bilirubin nanoparticles ameliorate allergic lung inflammation in a mouse model of asthma," *Biomaterials*, vol. 140, pp. 37–44, 2017.

[136] M. J. Kim, Y. Lee, S. Jon, and D. Y. Lee, "PEGylated bilirubin nanoparticle as an anti-oxidative and anti-inflammatory demulcent in pancreatic islet xenotransplantation," *Biomaterials*, vol. 133, pp. 242–252, 2017.

[137] N. Abeyrathna, K. Washington, C. Bashur, and Y. Liao, "Nonmetallic carbon monoxide releasing molecules (CORMs)," *Organic and Biomolecular Chemistry*, vol. 15, no. 41, pp. 8692–8699, 2017.

[138] A. Ismailova, D. Kuter, D. S. Bohle, and I. S. Butler, "An overview of the potential therapeutic applications of CO-releasing molecules," *Bioinorganic Chemistry and Applications*, vol. 2018, Article ID 8547364, 23 pages, 2018.

[139] D. K. Stevenson, P. A. Dennery, and S. R. Hintz, "Understanding newborn jaundice," *Journal of Perinatology*, vol. 21, no. S1, pp. S21–S24, 2001.

[140] F. Ebbesen, P. H. Madsen, P. K. Vandborg, L. H. Jakobsen, T. Trydal, and H. J. Vreman, "Bilirubin isomer distribution in jaundiced neonates during phototherapy with LED light centered at 497 nm (turquoise) vs. 459 nm (blue)," *Pediatric Research*, vol. 80, no. 4, pp. 511–515, 2016.

[141] T. W. R. Hansen, M. J. Maisels, F. Ebbesen et al., "Sixty years of phototherapy for neonatal jaundice - from serendipitous observation to standardized treatment and rescue for millions," *Journal of Perinatology*, vol. 40, no. 2, pp. 180–193, 2020.

[142] T. W. R. Hansen, "Biology of bilirubin photoisomers," *Clinics in Perinatology*, vol. 43, no. 2, pp. 277–290, 2016.

[143] J. E. Tyson, for the Eunice Kennedy Shriver National Institute of Child Health, H. D. N. R. Network et al., "Does aggressive phototherapy increase mortality while decreasing profound impairment among the smallest and sickest newborns?," *Journal of Perinatology*, vol. 32, no. 9, pp. 677–684, 2012.

[144] J. LaRusso, J. Wilson, and R. Ceilley, "Phototherapy-induced Purpuric Eruption in a Neonate," *The Journal of Clinical and Aesthetic Dermatology*, vol. 8, no. 3, 2015.

[145] M. D. AF, "Bilirubin, copper-porphyrins, and the bronze-baby syndrome," *Journal of Pediatrics*, vol. 158, no. 1, pp. 160–164, 2011.

[146] D. K. Stevenson and R. J. Wong, "Metalloporphyrins in the management of neonatal hyperbilirubinemia," *Seminars in Fetal and Neonatal Medicine*, vol. 15, no. 3, pp. 164–168, 2010.

[147] P. A. Dennery, "Metalloporphyrins for the treatment of neonatal jaundice," *Current Opinion in Pediatrics*, vol. 17, no. 2, pp. 167–169, 2005.

[148] V. K. Bhutani, R. Poland, L. D. Meloy, T. Hegyi, A. A. Fanaroff, and M. J. Maisels, "Clinical trial of tin mesoporphyrin to prevent neonatal hyperbilirubinemia," *Journal of Perinatology*, vol. 36, no. 7, pp. 533–539, 2016.

[149] S. Schulz, R. J. Wong, H. J. Vreman, and D. K. Stevenson, "Metalloporphyrins - an update," *Frontiers in Pharmacology*, vol. 3, 2012.

Hindawi
Oxidative Medicine and Cellular Longevity
Volume 2020, Article ID 1720961, 11 pages
https://doi.org/10.1155/2020/1720961

Research Article

Neuregulin-1β Protects the Rat Diaphragm during Sepsis against Oxidative Stress and Inflammation by Activating the PI3K/Akt Pathway

Hua Liu,[1] **Xiao-jian Weng**,[2] **Jun-yan Yao**,[3] **Jun Zheng**,[4] **Xiang Lv**,[1] **Xu-hui Zhou**,[1] **Hong Jiang**,[1] **and Shi-tong Li**[3]

[1]*Department of Anesthesiology and Critical Care Medicine, Shanghai Ninth People's Hospital, Shanghai Jiao Tong University School of Medicine, Shanghai 200011, China*
[2]*Department of Anesthesiology and SICU, Xinhua Hospital, School of Medicine, Shanghai Jiao Tong University, Shanghai 200092, China*
[3]*Department of Anesthesiology, Shanghai General Hospital, Shanghai Jiao Tong University School of Medicine, Shanghai 200080, China*
[4]*Department of Pathology Center, Shanghai General Hospital, Shanghai Jiao Tong University School of Medicine, Shanghai 200080, China*

Correspondence should be addressed to Hong Jiang; jianghongjiuyuan@163.com and Shi-tong Li; lishitongs@yahoo.com

Received 26 April 2020; Revised 15 June 2020; Accepted 1 July 2020; Published 20 July 2020

Guest Editor: Jolanta Czuczejko

Copyright © 2020 Hua Liu et al. This is an open access article distributed under the Creative Commons Attribution License, which permits unrestricted use, distribution, and reproduction in any medium, provided the original work is properly cited.

Sepsis-induced diaphragm dysfunction (SIDD) which is mainly characterized by decrease in diaphragmatic contractility has been identified to cause great harms to patients. Therefore, there is an important and pressing need to find effective treatments for improving SIDD. In addition, acetylcholinesterase (AChE) activity is a vital property of the diaphragm, so we evaluated both diaphragmatic contractility and AChE activity. Though neuregulin-1β (NRG-1β) is known to exert organ-protective effects in some inflammatory diseases, little is known about the potential of NRG-1β therapy in the diaphragm during sepsis. Our study was aimed at exploring the effects of NRG-1β application on diaphragmatic contractility and AChE activity during sepsis. Proinflammatory cytokines, muscle injury biomarkers in serum, contractile force, AChE activity, proinflammatory cytokines, oxidative parameters, histological condition, terminal deoxynucleotidyl transferase-mediated dUTP nick end labeling (TUNEL) staining, and expression of phosphoinositide 3-kinase (PI3K)/protein kinase B (PKB/Akt) signaling proteins in the diaphragm were measured and compared between nonseptic and septic groups with or without NRG-1β treatment. In vitro, the effects of NRG-1β on reactive oxygen species (ROS) production in the lipopolysaccharide- (LPS-) stimulated L6 rat muscle skeletal cells with or without the Akt inhibitor MK-2206 were detected. NRG-1β inhibited proinflammatory cytokine release and muscle injury biomarkers soaring in serum and improved the sepsis-induced diaphragm dysfunction and AChE activity decrease significantly during sepsis. Meanwhile, the inflammatory response, oxidative stress, pathological impairment, and cell apoptosis in the diaphragm were mitigated by NRG-1β. And NRG-1β activated the PI3K/Akt signaling in the diaphragm of septic rats. Elevated ROS production in the LPS-stimulated L6 rat skeletal muscle cells was reduced after treatment with NRG-1β, while MK-2206 blocked these effects of NRG-1β. In conclusion, our findings underlined that NRG-1β could reduce circulating levels of proinflammatory cytokines in rats with sepsis, adjust diaphragmatic proinflammatory cytokine level, mitigate diaphragmatic oxidative injury, and lessen diaphragm cell apoptosis, thereby improving diaphragmatic function, and play a role in diaphragmatic protection by activating PI3K/Akt signaling.

1. Introduction

Sepsis is a series of clinical syndromes induced by severe infection, causing multiple organ dysfunctions [1]. It is often accompanied by acute respiratory failure, in which the weakness of respiratory muscles is an important factor [2]. Diaphragmatic dysfunction and weakness were identified during sepsis, leading to the specific definition of sepsis-induced diaphragm dysfunction (SIDD) [3, 4]. The diaphragm is the major respiratory muscle, and it is crucial for optimal respiration. SIDD can impair the ability of the respiratory pump, further leading to respiratory failure, weaning failure of mechanical ventilation, extended stay time in the intensive care unit (ICU), and even death [2, 5]. The common pathological events of diaphragmatic dysfunction during sepsis are complex, including inflammation, oxidative stress, metabolic imbalance, mitochondrial dysfunction, muscle apoptosis, and atrophy [6, 7]. The inflammation and oxidative stress are two main factors underlying diaphragmatic dysfunction during sepsis [8]. Inflammatory cytokine infiltration and recessive reactive oxygen species (ROS) generated from oxidative stress during sepsis could do damage to the skeletal muscle contractility-associated proteins such as sarco(endo)-plasmic reticulum calcium-ATPases (SERCA) and/or sarcomere, subsequently causing diaphragmatic weakness [9]. In addition, acetylcholinesterase (AChE) activity at the neuromuscular junction (NMJ) is another vital property of the diaphragm. Clinically, muscle relaxant antagonists are often needed to help restore the muscle contractile tension of patients after general anaesthesia [10, 11]. Muscle relaxant antagonists exert their therapeutic effect by inhibiting AChE activity, which causes more acetylcholine release and ultimately accelerates muscle function restoration [12]. Our previous study verified that AChE activity decreased at the NMJ in the diaphragm during sepsis and oxidative stress was a vital contributor [13]. Drugs could inhibit the inflammation, and/or oxidative stress is theoretically useful for maintaining diaphragmatic contractile function and AChE activity during sepsis.

Neuregulin-1 (NRG-1) belongs to the neuregulin family, which was first discovered and studied in neural and cancer cells [14]. Both peripheral nerves and skeletal muscle are assumed to synthesize and excrete NRG-1. NRG-1 contains an epidermal growth factor- (EGF-) like domain that can bind to and activate receptor tyrosine kinases of the ErbB family (ErbB2, ErbB3, and ErbB4), exerting its role in cell survival, proliferation, migration, and differentiation [15, 16]. All of the ErbB receptors are mainly present at the NMJ [17], and NRG-1 acts as a medium between terminal Schwann cells and motor axons, between motor axons and muscles, and between different muscle fibres [18, 19]. Previous studies have shown that sepsis can induce a reduction in NRG-1 in the skeletal muscle system [20, 21]. Both in vivo and in vitro studies have demonstrated that NRG-1 and its associated signaling pathway are protective against injury induced by inflammatory diseases in the cardiovascular and nervous systems and simultaneously improve organ function [22–25]. However, the effects of NRG-1β on diaphragmatic contractility and AChE activity during sepsis have yet been explored. These findings provide a theoretical basis for relieving diaphragmatic dysfunction by exogenously administering NRG-1β. Our present study was aimed at exploring the role of NRG-1β on diaphragmatic contractility and AChE activity and simultaneously analyzing its effects on proinflammatory cytokines (tumor necrosis factor-α (TNF-α), interleukin-1β (IL-1β), and IL-6) in serum and the diaphragm, oxidative parameters (thiobarbituric acid reactive species (TBARS), protein carbonyl contents, and myeloperoxidase (MPO) activity) in the diaphragm, nonspecific muscle injury parameters (aspartate transaminase (AST), lactate dehydrogenase (LDH), and creatine kinase (CK) activity and myohemoglobin (Myo) content) in serum, and specific diaphragm injury (hematoxylin-eosin (H&E) staining of diaphragm) and diaphragm cell apoptosis (terminal deoxynucleotidyl transferase-mediated dUTP nick end labeling (TUNEL) staining of the diaphragm) during sepsis. And we detected the phosphoinositide 3-kinase (PI3K)/protein kinase B (PKB/Akt) signaling proteins in the diaphragm using Western blotting. We further detected the effects of NRG-1β on reactive oxygen species (ROS) production in the lipopolysaccharide- (LPS-) stimulated L6 rat skeletal muscle cells with or without the Akt inhibitor MK-2206 in order to determine whether NRG-1β could protect rat skeletal muscle cells against oxidative stress during sepsis and whether this effect could be suppressed by the Akt inhibitor. Here, we provide evidence that NRG-1β was a therapeutic strategy for SIDD against oxidative stress and inflammation by activating the PI3K/Akt pathway.

2. Materials and Methods

2.1. Animals and Experimental Design. Our study was approved by the Animal Care and Use Committee of Shanghai General Hospital Affiliated with Shanghai Jiao Tong University (grant number 2017DW001). The experiment was performed using a total of 28 Sprague-Dawley rats weighing 220-260 g. All animals were allowed free access to food and water and were housed at a temperature of 24 ± 1°C under a 12 h light-dark cycle (lights on from 8 am to 8pm).

The rats were randomized into 3 groups: the sham group ($n = 6$), the sepsis group ($n = 11$), and the NRG group ($n = 11$). Sepsis was induced by caecal ligation and puncture (CLP) which was performed as described in our previous study [13, 26]. In brief, a 3 cm midline abdominal incision was made under aseptic conditions after the rats were anaesthetized with an intraperitoneal injection of pentobarbital (50 mg/kg). The caecum was ligated at a distance equal to 50% of the total length of the caecum below the ileocaecal valve and perforated once in the mesenteric-to-antimesenteric direction with an 18-gauge needle. Then, the caecum was pressed gently to produce droplets of faeces from the 2 puncture sites. Finally, the caecum was replaced into the peritoneal cavity, and the abdominal wall was closed in 2 layers with 3-0 silk sutures. The rats in the sham group underwent a similar procedure, but the caecum was neither ligated nor perforated. Shortly after the surgery, all rats received 10 ml prewarmed (37°C) normal saline subcutaneously.

Thirty minutes before surgery, the rats in the NRG group received tail vein injections of NRG-1β (10 μg/kg, PeproTech, Rocky Hill, NJ, USA), whereas the rats in the other two groups received an equal volume of normal saline.

Twenty-four hours after surgery, all surviving rats were euthanized by an intraperitoneal injection of pentobarbital (100 mg/kg), and then blood samples were collected from the inferior vena cava, centrifuged, and stored at -80°C until the assay. Then, the diaphragms were harvested for subsequent tests. A muscle strip (approximately 5 mm wide) was obtained from the midcoastal region of the left diaphragm to immediately measure the diaphragmatic contractile force. The remaining part of the left diaphragm was immediately stored at -80°C until it was assayed for Western blotting of p-PI3K, pan-PI3K, p-Akt, pan-Akt, and actin. The coastal region of the right hemidiaphragm was immediately removed for histological examination and TUNEL staining. Meanwhile, the remaining part was immediately stored at -80°C until it was assayed for proinflammatory cytokines, AChE activity, TBARS content, protein carbonyl content, and MPO activity.

2.2. Diaphragmatic Contractile Property Measurement. Diaphragmatic contractile properties were measured according to previous studies [27, 28]. The diaphragm strip was suspended vertically in a 37°C tissue bath filled with Krebs solution containing 137 mM NaCl, 4 mM KCl, 2 mM $CaCl_2$, 1 mM $MgCl_2$, 1 mM KH_2PO_3, 12 mM $NaHCO_3$, and 6.5 mM glucose (pH 7.40 ± 0.05). Additionally, 12 μM d-tubocurarine (Sigma-Aldrich, St. Louis, MO, USA) was added to the Krebs solution to prevent neuromuscular transmission, and the solution was bubbled with 95% O_2/5% CO_2. Two silver stimulating electrodes were placed parallel to the muscle strip and connected to an electrical stimulator (ALC-MPA2000-S; Alcott Biotech, Shanghai, China) that could be activated by a computer. After a 15 min thermoequilibration period, the optimal length (L_0) at which the muscle generated peak twitch force was determined. The stimulus intensity was then set to 120% of the voltage intensity, which was adjusted when the maximal twitch response was reached at the L_0 to ensure supramaximal stimulation. Each strip was stimulated with an ms train every 2 min at the following frequencies: 10, 20, 40, 60, 80, and 120 Hz.

Following the experiment, the muscle strip was blotted dry and weighed. Finally, the force was normalized to the muscle cross-sectional area (CSA), which was calculated by the following formula (assuming that muscle density was 1.056 g/cm^3): CSA = muscle weight (g)/[L_0 (cm) × 1.056 (g/cm^3)].

2.3. Biochemical Measurement of AChE Activity in the Diaphragm. The AChE activity was measured according to our previous research [13]. In brief, the AChE activity measurement was conducted using an AChE assay kit from the Nanjing Jiancheng Bioengineering Institute (A024, Nanjing, China) according to the manufacturer's instructions.

2.4. Enzyme-Linked Immunosorbent Assays for TNF-α, IL-1β, and IL-6 in Serum and the Diaphragm. The serum and diaphragmatic levels of TNF-α, IL-1β, and IL-6 were measured using enzyme-linked immunosorbent assay (ELISA) kits (Elabscience Biotechnology Co., Ltd., Wuhan, China) according to the manufacturer's instructions.

2.5. Measurement of AST, LDH, and CK Activity and Myo Content in Serum

2.5.1. Measurement of AST Activity. AST activity was measured using an Aspartate Aminotransferase Activity Assay kit (105135, Abcam, US) according to the manufacturer's instructions. Briefly, AST catalyses the reaction as follows:

$$\text{aspartate} + \alpha\text{-ketoglutarate} = \text{oxaloacetate} + \text{glutamate} \quad (1)$$

Glutamate was detected by the conversion of a nearly colourless probe to a coloured product that was detected at 450 nm. In detail, after freezing-thawing the serum samples, prepare test samples, standard, and positive control of up to 50 μl/well with assay buffer in a 96-well plate. Then, add 100 μl of the reaction mix to each well. After reaction, glutamate production was measured according to the glutamate standard curve and the corresponding optical density. One unit of AST was defined as the amount of AST required to generate 1.0 μmol of glutamate per minute at 37°C.

2.5.2. Measurement of LDH Activity. LDH activity was measured using a Lactate Dehydrogenase Assay kit (197000, Abcam, US) according to the manufacturer's instructions. LDH is a ubiquitous enzyme in vertebrate organisms that catalyses the reversible conversion of pyruvate to lactate and the concomitant conversion of NADH and NAD+. NADH converted a colourless probe to a coloured one. Then, the fluorescence (Ex/Em = 535/587 nm) was measured in a kinetic mode at 37°C for 10-30 min. In detail, after freezing-thawing the serum samples, set up a plate for diluted standard (50 μl), samples (50 μl), and positive control wells (50 μl). Then, add 50 μl of reaction mix to each well. Finally, LDH activity in the samples was expressed as U/l of sample. One unit of LDH was defined as the amount of enzyme required to generate 1.0 μmol of NADH per min at pH 8.8 and 37°C.

2.5.3. Measurement of CK Activity. CK activity was measured using a Creatine Kinase Assay kit (k777-100, Biovision, USA) according to the manufacturer's instructions. CK converts creatine into phosphocreatine and ADP. The generated phosphocreatine and ADP reacted with the CK Enzyme Mix to form an intermediate that converted a colourless probe to a coloured product with a strong absorbance at 450 nm. In detail, after freezing-thawing the serum samples, prepare test samples, standard, and positive control of up to 50 μl/well with assay buffer in a 96-well plate. Then, add 50 μl of reaction mix to each well. Finally, CK activity in the samples was expressed as U/l of sample. One unit of CK was defined as the amount of enzyme required to generate 1.0 μmol of NADH per min at pH 9.0 and 37°C.

2.5.4. Measurement of Myo Content. Myo content was measured using the Myoglobin Rat ELISA kit (157739, Abcam,

US) according to the manufacturer's instructions. Finally, the quantity of Myo in the serum was interpolated from the standard curve plotted from the standards and corrected for sample dilution.

2.6. Measurement of TBARS Contents in the Diaphragm. The formation of TBARS was determined by an acid-heating reaction, as previously described [29]. Specifically, prepare the homogenate after adding 100 μl H_2O_2 to 30 mg diaphragm tissue. Vortex and centrifuge the homogenate after adding 150 μl perchloric acid. Then, prepare the TBARS-TBA complex using the supernatant. Finally, add 200 μl TBARS-TBA complex to each well for the test. After the reaction, TBARS levels were finally determined based on malondialdehyde (MDA) equivalents per milligram of protein by measuring the absorbance at 535 nm.

2.7. Measurement of Protein Carbonyls in the Diaphragm. The levels of protein carbonyls were measured based on the reaction with dinitrophenyl hydrazine, as previously described [30]. Specifically, vortex and centrifuge the 10% diaphragm homogenate first. Then, drain the supernatant and dilute it at the ratio of 1 : 9 for further test. After the reaction, the levels of PC were determined as nmol of protein carbonyls per milligram of protein by reading the absorbance at 375 nm.

2.8. Assay of MPO Activity in the Diaphragm. MPO activity was determined by using a test kit from Nanjing Jiancheng Bioengineering Institute (A044, Nanjing, China). The activity was determined as units of MPO activity per gram of tissue wet weight by spectrophotometrically measuring the change in absorbance at 412 nm.

2.9. Histopathological Procedure and Semiquantitative Analysis of Diaphragm Damage Score (DDS). The harvested right hemidiaphragms were fixed in 4% formalin. After fixation, each tissue sample was routinely processed and embedded in paraffin. Then, 5 μm thick longitudinal sections were produced from the tissue blocks and stained with hematoxylin and eosin. The sections were dehydrated in a series of graded ethanol solutions and sealed with neutral resin. Then, these sections were photographed with a digital camera (Axioplan 2, Carl Zeiss, Oberkochen, Germany) for histopathological examination. The degree and severity of the diaphragm injury were assessed and graded according to the 5-point semiquantitative scale consisting of edema, neutrophil infiltration, haemorrhages, distribution of myofibrils, etc., described in the previous study [31] by a professional pathologist who was blinded to the experimental groups. A severity grade was finally expressed as the diaphragm damage score (DDS).

2.10. TUNEL Staining of Diaphragm Cells and Quantitative Analysis of Cell Apoptosis Percentages from TUNEL-Stained Images. TUNEL staining was performed using the Apoptosis Detection Kit (C1088, Beyotime, China) according to the manufacturer's instructions. Finally, the images were captured using the Axioplan 2 imaging system and software; then, the TUNEL-positive myonuclei were quantified by Image-Pro Plus software (six images in three rats were analyzed) and indicated as a percentage of all myonuclei.

2.11. Cell Culture and Treatment and Measurement of ROS Production in the L6 Skeletal Muscle Cells. L6 rat skeletal muscle cells were purchased from Shanghai Institutes for Biological Science (Shanghai, China) and regularly cultured and differentiated according to our previous study [32]. Thirty minutes before LPS (Sigma-Aldrich) treatment, cells were treated with PBS (control group (C group) and LPS group (L group)), NRG-1β (10 nM, PeproTech, PBS+NRG group (CN group) and LPS+NRG group (LN group)), or NRG-1β plus the Akt inhibitor MK-2206 (10 μM, Selleck, LPS+NRG+MK-2206 group (LNM group)) [33]. Then, except C and CN groups, cells of other groups were treated with LPS (1 μg/ml) [32] for 24 h. At the end of incubation, cells were collected for quantifying intracellular ROS with a Reactive Oxygen Species Assay Kit (S0033, Beyotime, China) according to the manufacturer's instructions. Briefly, cells were resuspended with a serum-free medium containing the fluorescent probe DCFH-DA (10 μM). Subsequently, cells were incubated at 37°C for 20 min in the dark. DCF fluorescence intensity was measured with a microplate absorbance reader.

2.12. Western Blotting Analysis. Firstly, the protein concentration of the diaphragm sample was determined using a bicinchoninic acid protein assay kit (Beyotime, Shanghai, China) after being homogenized in radioimmunoprecipitation lysis buffer (Beyotime) containing 1 mM phenylmethanesulfonyl fluoride (Amresco, LLC, Solon, OH, USA). Subsequently, 30 μg of the proteins was loaded on a 10% sodium dodecyl sulfate- (SDS-) polyacrylamide gel for electrophoresis. Then, the proteins were transferred to polyvinylidene difluoride membranes (Millipore, Billerica, MA, USA) which were blocked in Western blocking buffer (Beyotime) for 1.5 h at room temperature and incubated with primary antibodies at 4°C overnight for immunoblotting. The primary antibodies used were rabbit antibodies specific for p-PI3K (Tyr607) (1 : 1000; ab182651; Abcam), pan-PI3K (1 : 500; BS3678; Bioworld Technology, Nanjing, Jiangsu, China), p-Akt (Thr308) (1 : 1000; #2965; Cell Signaling Technology (CST), Boston, MA, USA), and pan-Akt (1 : 1000; #4691, CST) and a mouse antibody specific for actin (1 : 1000; AF0006; Beyotime). The blots were incubated for 1 h at room temperature with peroxidase-conjugated secondary antibodies after rinsing three times in Tris-buffered saline with Tween 20 (TBST). Finally, the membranes were washed with TBST and visualized using an electrochemiluminescence detection kit (Millipore). Densitometry was conducted using Image-Pro Plus software (version 6.0; Media Cybernetics, Inc.).

2.13. Statistical Analyses. Statistical analyses were conducted using SPSS (version 19.0; SPSS Inc., Chicago, Illinois, USA). The values are presented as the mean ± standard deviation (SD). The data were first tested for normality and equality of variance. Between-group comparisons for each dependent variable were assessed by analysis of variance (ANOVA) with

the least significant difference (LSD) test. $P < 0.05$ was considered to be statistically significant.

3. Results

3.1. Survival Rates within 24 h. Six of the 11 rats in the sepsis group and 9 of the 11 rats in the NRG group survived to 24 h after the CLP procedure, whereas all of the rats in the sham group survived. Additionally, the surviving rats that underwent CLP surgery developed varying degrees of septic symptoms, such as a loss of movement, hair erection, shortness of breath, subconjunctival exudation, and diarrhoea.

3.2. Diaphragm Force-Frequency Relationship. The data of the response of the diaphragm strips to stimuli of increasing frequencies are shown in Figure 1. A significant downward shift across all of the applied stimulation frequencies (10-120 Hz) was observed in the sepsis group ($P < 0.01$). NRG-1β treatment partially restored the downward shift ($P < 0.01$), which suggested that NRG-1β can improve the reduced diaphragmatic force generation during sepsis.

3.3. AChE Activity in the Diaphragm. Compared with the sham group, AChE activity decreased significantly in both the sepsis and the NRG groups 24 h after surgery ($P < 0.01$). However, AChE activity increased in the NRG group compared with the sepsis group ($P < 0.01$) (Figure 2).

3.4. Effects of NRG-1β on Serum and Diaphragmatic Proinflammatory Cytokines. As shown in Figure 3, the levels of serum TNF-α, IL-1β, and IL-6 were increased significantly in rats in the sepsis group compared to rats in the sham group 24 h after surgery ($P < 0.01$), while TNF-α, IL-1β, and IL-6 concentrations at 24 h after CLP were reduced after NRG-1β treatment ($P < 0.01$).

As shown in Figure 4, the levels of diaphragmatic TNF-α, IL-1β, and IL-6 were increased significantly in rats in the sepsis group compared to rats in the sham group 24 h after surgery ($P < 0.01$), while TNF-α, IL-1β, and IL-6 concentrations at 24 h after CLP were reduced after NRG-1β treatment ($P < 0.01$).

3.5. Effects of NRG-1β on Serum Biomarkers of Muscle Injury. As there is no specific biomarker for skeletal muscle injury, we detected the AST, LDH, and CK activity and the Myo content in serum to evaluate muscle injury generally. The AST, LDH, and CK activity and the Myo content in the serum rose significantly 24 h after CLP ($P < 0.01$), while the levels dropped significantly upon NRG-1β treatment ($P < 0.01$) (Figure 5).

3.6. Effects of NRG-1β on Oxidative Injury of the Diaphragm. As shown in Figure 6, the TBARS, protein carbonyl contents, and MPO activity in the diaphragm were increased significantly in rats in the sepsis group compared to rats in the sham group 24 h after surgery ($P < 0.01$), while the increase was partially restored after NRG-1β treatment ($P < 0.01$, $P < 0.05$).

3.7. Effects of NRG-1β on Histological Conditions in the Diaphragm. As shown in Figure 7, histological examinations

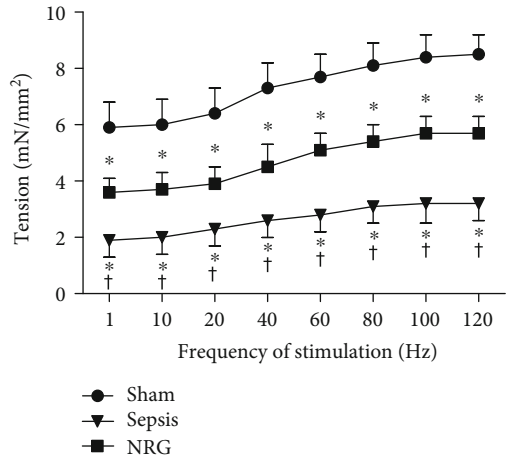

Figure 1: Force-frequency curves of the diaphragm strips. The data are presented as the mean ± SD. $^*P < 0.01$ vs. the sham group and $^\dagger P < 0.01$ vs. the sepsis group.

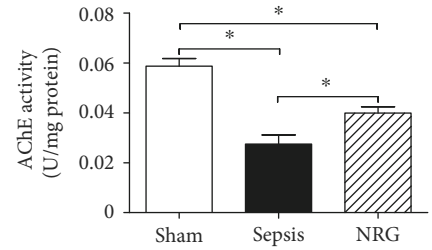

Figure 2: AChE activity in the three groups of the rat diaphragm. The data are presented as the mean ± SD. $^*P < 0.01$.

of the diaphragm were conducted in the three groups. H&E staining of diaphragms from the rats in the sham group revealed a normal structure of the diaphragm (polygonal pink fibres with several blue/purple cellular membranes and a neat and tight arrangement of muscle fibres). Twenty-four hours after the CLP procedure, obvious changes were noted in the diaphragms of the rats in the sepsis group; these diaphragms presented a disordered arrangement, more inflammatory cell infiltration, and widened intercellular spaces. The pathological changes were partially improved by NRG-1β treatment. The diaphragm fibre arrangement was more regular; intercellular edema and haemorrhages were alleviated. Additionally, the diaphragms of the rats in the NRG group exhibited lesser inflammatory infiltration. The semiquantitative analysis showed that the DDS was higher in the sepsis group than in the sham group, while NRG-1β treatment decreased the DDS significantly ($P < 0.01$).

3.8. Effects of NRG-1β on Cell Apoptosis of the Diaphragm. As shown in Figure 8, TUNEL staining was conducted to measure the apoptotic cells in the diaphragm. The TUNEL-positive myonuclei increased in the sepsis group compared with the sham group ($P < 0.01$). However, the TUNEL-positive myonuclei decreased significantly in the NRG group compared with the sepsis group ($P < 0.01$) although the

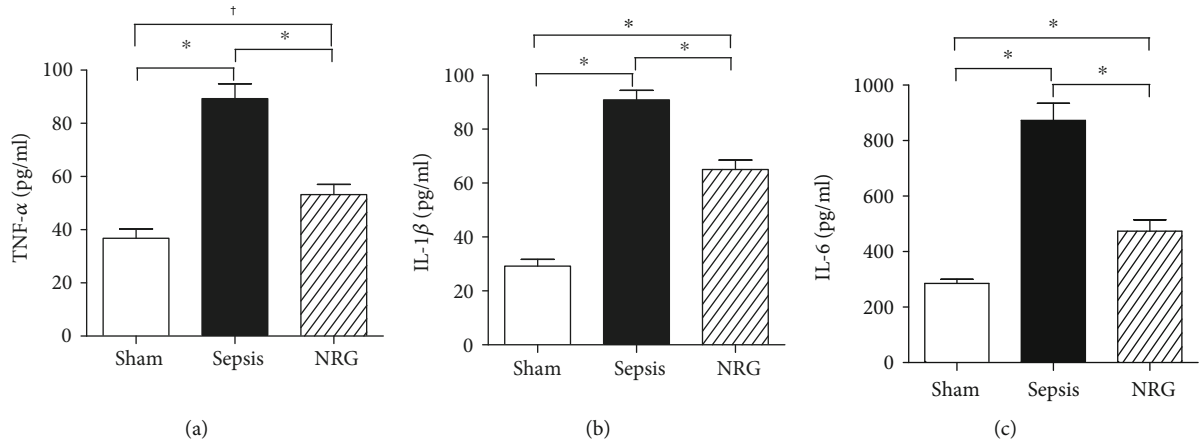

Figure 3: Levels of TNF-α, IL-1β, and IL-6 in the three groups of rat serum. The data are presented as the mean ± SD. $^{*}P < 0.01$, $^{\dagger}P < 0.05$.

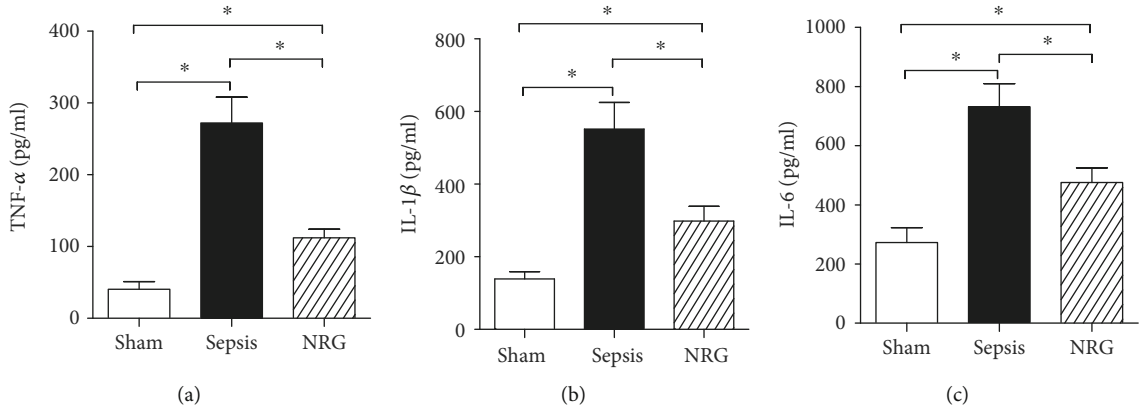

Figure 4: Levels of TNF-α, IL-1β, and IL-6 in the three groups of the rat diaphragm. The data are presented as the mean ± SD. $^{*}P < 0.01$.

TUNEL-positive myonuclei in the NRG group were still higher than those in the sham group ($P < 0.01$).

3.9. Effects of NRG-1β on the PI3K-Akt Signaling Pathway in the Diaphragm. As shown in Figure 9, the expressions of p-PI3K and p-Akt were reduced during sepsis ($P < 0.01$), while the expression of these proteins increased after NRG-1β treatment ($P < 0.05$).

3.10. Effects of NRG-1β on ROS Production in the L6 Rat Skeletal Muscle Cells. As shown in Figure 10, ROS production in the L group increased significantly compared with that in the C group and CN group ($P < 0.01$), while there is no significant difference in ROS production between the C group and CN group. Treatment with NRG-1β decreased the ROS production ($P < 0.01$), while the administration of MK-2206 blocked these effects of NRG-1β ($P < 0.01$).

4. Discussion

In the current study, we observed the effects of the NRG-1β on the diaphragm in a rat model of sepsis. Our study indicated that NRG-1β exerted diaphragm-protective functions, i.e., strengthening diaphragmatic contractile force and AChE activity, alleviating inflammatory infiltration, reducing oxidative and morphological injury, and lessening diaphragm cell apoptosis. Moreover, NRG-1β activated the PI3K/Akt signaling pathway in the diaphragm during sepsis. And NRG-1β protected LPS-stimulated L6 skeletal muscle cells against oxidative stress by activating the PI3K/Akt pathway, which was further confirmed.

These observations should be of clinical relevance, since SIDD causes great harms as mentioned before, which finally leads to a heavy social and financial burden. We firstly offered the evidence that NRG-1β may provide a therapeutic option for curing SIDD via suppressing oxidative stress and inflammation by activating the PI3K/Akt signaling pathway.

In this study, sepsis was established by CLP, as described in a previous study [26]. CLP is regarded as the gold standard model of sepsis [34]. Twenty-four hours after CLP, there were a significant increase in proinflammatory cytokines (TNF-α, IL-1β, and IL-6) in serum and an elevated death rate in rats, while the surviving rats developed septic syndrome; this demonstrated that our sepsis model was successfully established.

NRG-1 is a member of the neuregulin family, and it has two isoforms, namely, NRG-1α and NRG-1β, with different EGF-like domains. NRG-1β is 10-100 times more potent

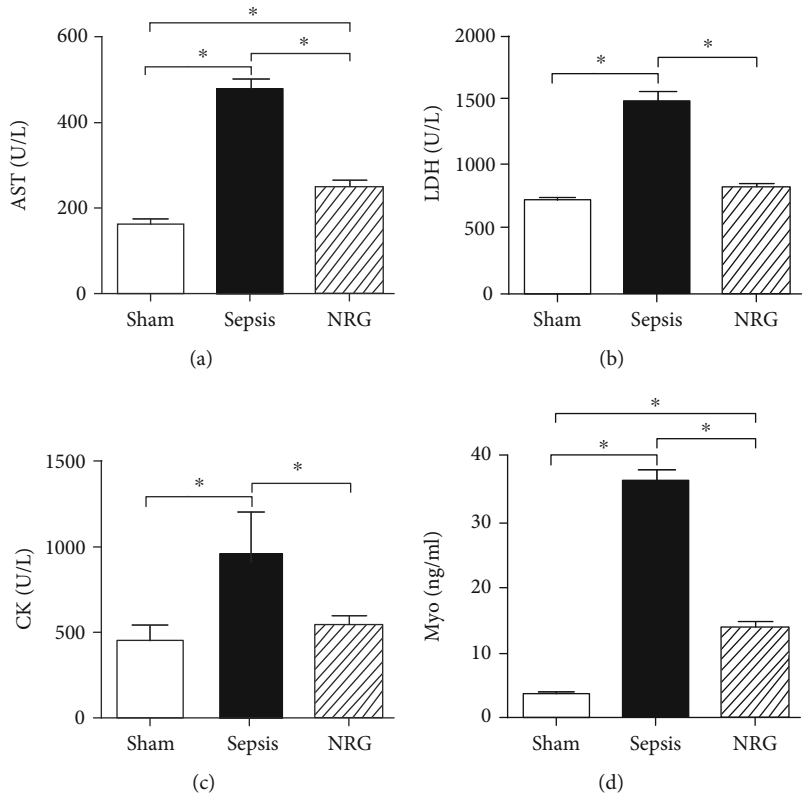

Figure 5: AST, LDH, and CK activity and Myo content in the three groups of the rat diaphragm. The data are presented as the mean ± SD. $^{*}P < 0.01$.

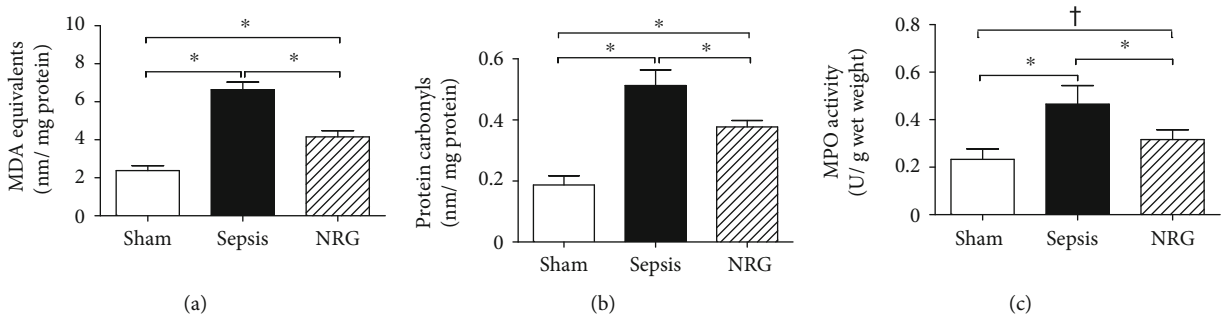

Figure 6: TBARS, protein carbonyl content, and MPO activity in the three groups of the rat diaphragm. The data are presented as the mean ± SD. $^{*}P < 0.01$, $^{\dagger}P < 0.05$.

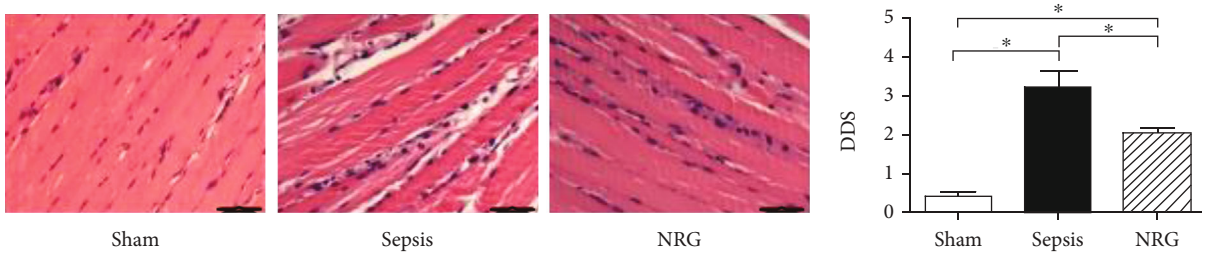

Figure 7: Histological conditions and DDS in the three groups of the rat diaphragm. The data are presented as the mean ± SD. $^{*}P < 0.01$. Bars = 50 μm.

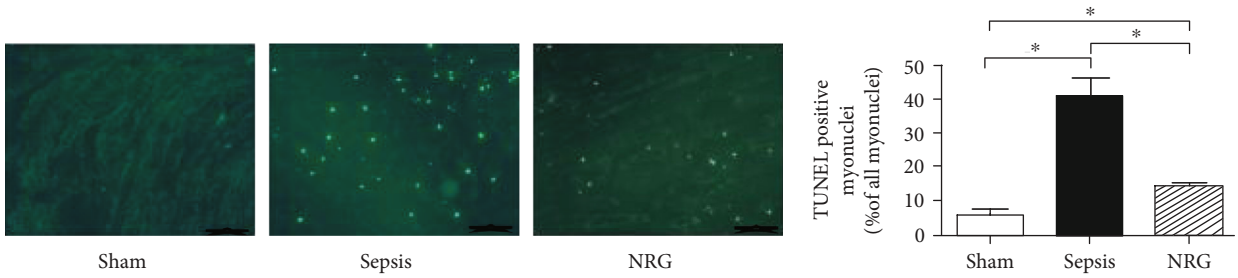

Figure 8: TUNEL staining and cell apoptosis percentages from TUNEL-stained images in the three groups of the rat diaphragm. The data are presented as the mean ± SD. $^{*}P < 0.01$. Bars = 50 μm.

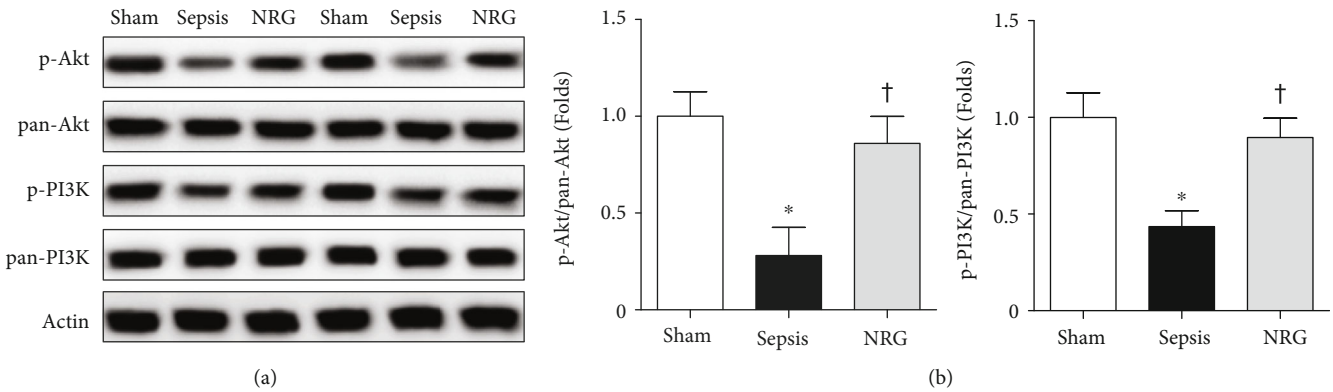

Figure 9: (a) Western blotting analyses of p-PI3K and p-Akt expressions in the three groups of the rat diaphragm. Representative blots from 2 of the 6 subjects in each group are displayed. (b) The corresponding bar graphs. Actin and pan-PI3K and Akt expressions serve as the internal control. Data are presented as the mean ± SD. $^{*}P < 0.01$ vs. the sham group; $^{\dagger}P < 0.05$ vs. the sepsis group.

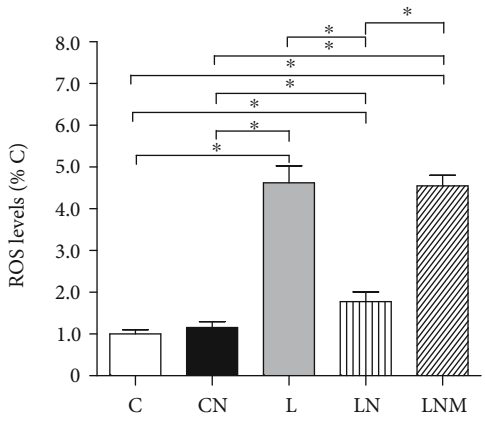

Figure 10: ROS levels in the L6 skeletal muscle cells of different groups (presented as percentages of the C group). Data are presented as the mean ± SD. $^{*}P < 0.01$. C: control group; CN: PBS +NRG group; L: LPS group; LN: LPS+NRG group; LNM: LPS +NRG+MK-2206 group.

than NRG-1α [15, 16]; thus, we chose to use NRG-1β in this study. Proinflammatory cytokines such as TNF-α, IL-1β, and IL-6 have been verified to participate in and promote sepsis in previous studies; similarly, our study suggested that sepsis-induced diaphragmatic dysfunction and AChE activity decrease were associated with an increased exposure of the diaphragm to proinflammatory cytokines. NRG-1β's anti-inflammatory roles on brains have been noted previously [22], but little is known whether it could also protect the diaphragm during sepsis via its anti-inflammatory effects. In this study, we clearly demonstrated that NRG-1β treatment substantially decreased the systemic and diaphragmatic proinflammatory cytokines. Meanwhile, inflammatory infiltration in the diaphragm during sepsis was also ameliorated after NRG-1β treatment.

Additionally, oxidative stress which is characterized by the excessive production of ROS [8, 35] has been proven to play an essential role in the onset and development of sepsis. ROS consist of active oxygen free radicals or molecules such as superoxide ($O_2^{\bullet -}$), hydrogen peroxide (H_2O_2), hydroxyl radicals (OH), and hypochlorous acid (HOCl) [36, 37], which can attack proteins, unsaturated lipids, nucleic acids, and carbohydrates, subsequently triggering injury in tissues and organisms. Malondialdehyde (MDA, detected by TBARS) and protein carbonyls are two typical markers of oxidative stress-induced injury to lipids and proteins, respectively [29, 30]. We measured TBARS and protein carbonyl levels to observe oxidative injury in the diaphragm of rats; simultaneously, we tested serum AST, LDH, and CK activity and Myo content to observe skeletal muscle injury indirectly, as in previous studies [38, 39]. Results from the current study

showed that sepsis induced severe oxidative injury in the diaphragm. Fortunately, NRG-1β treatment significantly reduced the serum AST, LDH, and CK activity and Myo content during sepsis. Moreover, NRG-1β administration could reduce TBARS and protein carbonyl levels in the diaphragm of rats with sepsis, which illustrated that sepsis-induced oxidative injury in the diaphragm was alleviated. These results were in line with its protective role against oxidative stress in the myocardium and neurons [22, 25]. Besides, AChE activity elevated after NRG-1β treatment as well, since our previous research suggested that oxidative stress played a vital role in AChE activity decrease in the diaphragm of rats with sepsis.

Interestingly, our study found that MPO activity of the diaphragm in the rats of the NRG group was significantly reduced compared to that of the sepsis group. MPO is synthesized and secreted by neutrophils and is regarded as a marker of inflammation and neutrophil infiltration in tissues [40]. Meanwhile, MPO can convert H_2O_2 into HOCl, which is a more active ROS than H_2O_2 [41]. Neutrophil infiltration, larger nuclei, and wider spacing of skeletal muscle fibres were observed in the diaphragms of rats with sepsis. After NRG-1β treatment, neutrophil infiltration was improved, which is consistent with the change in MPO activity. In addition, nuclear size, the spacing of skeletal muscle fibres, and DDS were diminished. These findings implied an interplay relationship of oxidative stress and inflammation in the development of SIDD while NRG-1β exerted its protective effects through alleviating both inflammatory and oxidative injuries in the diaphragm.

Our study showed that NRG-1β improved the inhibition of PI3K and Akt in the diaphragm of rats with sepsis, which is further verified in vitro since the protective effects of NRG-1β in the LPS-stimulated L6 skeletal muscle cells were blocked by the Akt inhibitor. Several previous studies have proven that NRG-1β could activate the PI3K/Akt signaling pathway and exert protective effects in cardiac myocytes subjected to a variety of pathological conditions [42, 43]. However, to the best of our knowledge, this study is the first to identify NRG-1β as an activator of a PI3K/Akt-mediated protective role against oxidative stress and inflammation in the diaphragm during sepsis. Both ErbB2 and ErbB3 receptors are verified to be expressed in the rat diaphragm [44]. NRG-1 could recruit and activate the PI3K through its EGF-like domain binding to the ErbB2/ErbB3 heterodimer [45]. Further studies are needed to detect the activation of the two ErbB receptors. The PI3K/Akt pathway is an important signal transduction pathway. Akt is the downstream target of PI3K and plays a pivotal role in several cellular processes, including cell proliferation, differentiation, apoptosis, migration, and transcription [46]. Akt inhibition is associated with an inflammatory response, while Akt activation reduces cellular oxidative stress and inhibits the release of proinflammatory cytokines [47, 48]. Several previous studies have reported that some drugs could prevent liver injury [49] or hepatic fibrosis [50] via regulating the PI3K/Akt pathway. These provide the theoretical foundation for our conclusions since we have proven that NRG-1β can activate the PI3K/Akt pathway in the diaphragm of rats with sepsis.

5. Conclusions

We consider that there were at least two highlights in the current study. First, our study found that NRG-1β could prevent diaphragmatic function and AChE activity during sepsis for the first time. Additionally, NRG-1β treatment also ameliorated the inflammatory infiltration, oxidative injury, and cell apoptosis in the diaphragm of the rats with sepsis. Second, the study showed that the PI3K/Akt pathway was responsible for NRG-1β's protective roles on the diaphragm against inflammation and oxidative stress during sepsis. In conclusion, the current study confirmed NRG-1β's diaphragm-protective role during sepsis and its related mechanisms, which would provide a new therapeutic vision of protecting SIDD in the future.

Data Availability

The Tiff. data used to support the findings of this study are included within the article.

Conflicts of Interest

The authors declare that they have no conflicts of interest.

Authors' Contributions

Hua Liu and Xiaojian Weng contributed equally to this work.

Acknowledgments

This study was supported by grants from the Shanghai Science and Technology Committee (Grant No. 19JC1413300) and the National Natural Science Foundation of China (Grant no. 81772121).

References

[1] M. Singer, C. S. Deutschman, C. W. Seymour et al., "The third international consensus definitions for sepsis and septic shock (sepsis-3)," *JAMA*, vol. 315, no. 8, pp. 801–810, 2016.

[2] D. Berger, S. Bloechlinger, S. von Haehling et al., "Dysfunction of respiratory muscles in critically ill patients on the intensive care unit," *Journal of Cachexia, Sarcopenia and Muscle*, vol. 7, no. 4, pp. 403–412, 2016.

[3] G. S. Supinski, P. E. Morris, S. Dhar, and L. A. Callahan, "Diaphragm dysfunction in critical illness," *Chest*, vol. 153, no. 4, pp. 1040–1051, 2018.

[4] J. Boczkowski, B. Dureuil, C. Branger et al., "Effects of sepsis on diaphragmatic function in rats," *The American Review of Respiratory Disease*, vol. 138, no. 2, pp. 260–265, 1988.

[5] M. Dres, E. C. Goligher, L. M. A. Heunks, and L. J. Brochard, "Critical illness-associated diaphragm weakness," *Intensive Care Medicine*, vol. 43, no. 10, pp. 1441–1452, 2017.

[6] R. C. Bone, C. J. Grodzin, and R. A. Balk, "Sepsis: a new hypothesis for pathogenesis of the disease process," *Chest*, vol. 112, no. 1, pp. 235–243, 1997.

[7] R. C. Bone, R. A. Balk, F. B. Cerra et al., "Definitions for sepsis and organ failure and guidelines for the use of innovative therapies in sepsis," *Chest*, vol. 101, no. 6, pp. 1644–1655, 1992.

[8] J. Duran-Bedolla, M. A. Montes de Oca-Sandoval, V. Saldaña-Navor, J. A. Villalobos-Silva, M. C. Rodriguez, and S. Rivas-Arancibia, "Sepsis, mitochondrial failure and multiple organ dysfunction," *Clinical and Investigative Medicine*, vol. 37, no. 2, pp. E58–E69, 2014.

[9] B. J. Petrof, "Diaphragm weakness in the critically ill: basic mechanisms reveal therapeutic opportunities," *Chest*, vol. 154, no. 6, pp. 1395–1403, 2018.

[10] S. J. Brull and G. S. Murphy, "Residual neuromuscular Block," *Anesthesia and Analgesia*, vol. 111, no. 1, pp. 129–140, 2010.

[11] J. U. Schreiber, "Management of neuromuscular blockade in ambulatory patients," *Current Opinion in Anaesthesiology*, vol. 27, no. 6, pp. 583–588, 2014.

[12] S. J. Brull and A. F. Kopman, "Current status of neuromuscular reversal and monitoring: challenges and opportunities," *Anesthesiology*, vol. 126, no. 1, pp. 173–190, 2017.

[13] H. Liu, J. Wu, J.-y. Yao, H. Wang, and S.-t. Li, "The role of oxidative stress in decreased acetylcholinesterase activity at the neuromuscular junction of the diaphragm during sepsis," *Oxidative Medicine and Cellular Longevity*, vol. 2017, Article ID 9718615, 6 pages, 2017.

[14] E. Peles, "Neu and its ligands: from an oncogene to neural factors," *Bioessays*, vol. 15, no. 12, pp. 815–824, 1993.

[15] D. L. Falls, "Neuregulins: functions, forms, and signaling strategies," *Experimental Cell Research*, vol. 284, no. 1, pp. 14–30, 2003.

[16] A. Gumà, V. Martínez-Redondo, I. López-Soldado, C. Cantó, and A. Zorzano, "Emerging role of neuregulin as a modulator of muscle metabolism," *American Journal of Physiology. Endocrinology and Metabolism*, vol. 298, no. 4, pp. E742–E750, 2010.

[17] M. Morano, G. Ronchi, V. Nicolò et al., "Modulation of the neuregulin 1/ErbB system after skeletal muscle denervation and reinnervation," *Scientific Reports*, vol. 8, no. 1, p. 5047, 2018.

[18] D. Kim, S. Chi, K. H. Lee et al., "Neuregulin stimulates myogenic differentiation in an autocrine manner," *The Journal of Biological Chemistry*, vol. 274, no. 22, pp. 15395–15400, 1999.

[19] G. Ennequin, F. Capel, K. Caillaud et al., "Neuregulin-1 improves complex 2-mediated mitochondrial respiration in skeletal muscle of healthy and diabetic mice," *Scientific Reports*, vol. 7, no. 1, p. 1742, 2017.

[20] F. Xie, S. Min, J. Chen, J. Yang, and X. Wang, "Ulinastatin inhibited sepsis-induced spinal inflammation to alleviate peripheral neuromuscular dysfunction in an experimental rat model of neuromyopathy," *Journal of Neurochemistry*, vol. 143, no. 2, pp. 225–235, 2017.

[21] L. Liu, F. Xie, K. Wei et al., "Sepsis induced denervation-like changes at the neuromuscular junction," *The Journal of Surgical Research*, vol. 200, no. 2, pp. 523–532, 2016.

[22] J. Xu, C. Hu, S. Chen et al., "Neuregulin-1 protects mouse cerebellum against oxidative stress and neuroinflammation," *Brain Research*, vol. 1670, pp. 32–43, 2017.

[23] J.-H. Lee, J.-Y. Yoo, H.-b. Kim et al., "Neuregulin1 attenuates H_2O_2-induced reductions in EAAC1 protein levels and reduces H_2O_2-induced oxidative stress," *Neurotoxicity Research*, vol. 35, no. 2, pp. 401–409, 2019.

[24] F. Timolati, D. Ott, L. Pentassuglia et al., "Neuregulin-1 beta attenuates doxorubicin-induced alterations of excitation-contraction coupling and reduces oxidative stress in adult rat cardiomyocytes," *Journal of Molecular and Cellular Cardiology*, vol. 41, no. 5, pp. 845–854, 2006.

[25] A. Siltanen, K. Nuutila, Y. Imanishi et al., "The paracrine effect of skeletal myoblasts is cardioprotective against oxidative stress and involves EGFR-ErbB4 signaling, cystathionase, and the unfolded protein response," *Cell Transplantation*, vol. 25, no. 1, pp. 55–69, 2016.

[26] D. Rittirsch, M. S. Huber-Lang, M. A. Flierl, and P. A. Ward, "Immunodesign of experimental sepsis by cecal ligation and puncture," *Nature Protocols*, vol. 4, no. 1, pp. 31–36, 2009.

[27] M. Yang, H. Wang, G. Han et al., "Phrenic nerve stimulation protects against mechanical ventilation-induced diaphragm dysfunction in rats," *Muscle & Nerve*, vol. 48, no. 6, pp. 958–962, 2013.

[28] J. Jiang, B. Yang, G. Han, M. Yang, and S. Li, "Early administration of cisatracurium attenuates sepsis-induced diaphragm dysfunction in rats," *Inflammation*, vol. 38, no. 1, pp. 305–311, 2015.

[29] H. H. Draper and M. Hadley, "[43] Malondialdehyde determination as index of lipid peroxidation," *Methods in Enzymology*, vol. 186, pp. 421–431, 1990.

[30] R. L. Levine, D. Garland, and C. N. Oliver, "[49] Determination of carbonyl content in oxidatively modified proteins," *Methods in Enzymology*, vol. 186, pp. 464–478, 1990.

[31] V. Jaćević, E. Nepovimova, and K. Kuča, "Toxic injury to muscle tissue of rats following acute oximes exposure," *Scientific Reports*, vol. 9, no. 1, p. 1457, 2019.

[32] J. Wu, H. Liu, T. Chu, P. Jiang, and S.-t. Li, "Neuregulin-1β attenuates sepsis-induced diaphragm atrophy by activating the PI3K/Akt signaling pathway," *Journal of Muscle Research and Cell Motility*, vol. 40, no. 1, pp. 43–51, 2019.

[33] F. Hu, N. Li, Z. Li et al., "Electrical pulse stimulation induces GLUT4 translocation in a Rac-Akt-dependent manner in C2C12 myotubes," *FEBS Lett Actions*, vol. 592, no. 4, pp. 644–654, 2018.

[34] L. Dejager, I. Pinheiro, E. Dejonckheere, and C. Libert, "Cecal ligation and puncture: the gold standard model for polymicrobial sepsis?," *Trends in Microbiology*, vol. 19, no. 4, pp. 198–208, 2011.

[35] P. Newsholme, V. F. Cruzat, K. N. Keane, R. Carlessi, and P. I. H. de Bittencourt Jr., "Molecular mechanisms of ROS production and oxidative stress in diabetes," *The Biochemical Journal*, vol. 473, no. 24, pp. 4527–4550, 2016.

[36] M. P. Fink, "Role of reactive oxygen and nitrogen species in acute respiratory distress syndrome," *Current Opinion in Critical Care*, vol. 8, no. 1, pp. 6–11, 2002.

[37] H. Bayir, "Reactive oxygen species," *Critical Care Medicine*, vol. 33, pp. S498–S501, 2005.

[38] E. Cavarretta, M. Peruzzi, R. del Vescovo et al., "Dark chocolate intake positively modulates redox status and markers of muscular damage in elite football athletes: a randomized controlled study," *Oxidative Medicine and Cellular Longevity*, vol. 2018, Article ID 4061901, 10 pages, 2018.

[39] S. O. El-Ganainy, A. El-Mallah, D. Abdallah, M. M. Khattab, M. M. M. El-Din, and A. S. El-Khatib, "Rosuvastatin safety: an experimental study of myotoxic effects and mitochondrial alterations in rats," *Toxicology Letters*, vol. 265, pp. 23–29, 2017.

[40] M. Faith, A. Sukumaran, A. B. Pulimood, and M. Jacob, "How reliable an indicator of inflammation is myeloperoxidase activity?," *Clinica Chimica Acta*, vol. 396, no. 1-2, pp. 23–25, 2008.

[41] J. P. Gaut, G. C. Yeh, H. D. Tran et al., "Neutrophils employ the myeloperoxidase system to generate antimicrobial

brominating and chlorinating oxidants during sepsis," *Proceedings of the National Academy of Sciences of the United States of America*, vol. 98, no. 21, pp. 11961–11966, 2001.

[42] M. X. Cai, X. C. Shi, T. Chen et al., "Exercise training activates neuregulin 1/ErbB signaling and promotes cardiac repair in a rat myocardial infarction model," *Life Sciences*, vol. 149, pp. 1–9, 2016.

[43] T. An, Y. Zhang, Y. Huang et al., "Neuregulin-1 protects against doxorubicin-induced apoptosis in cardiomyocytes through an Akt-dependent pathway," *Physiological Research*, vol. 62, no. 4, pp. 379–385, 2013.

[44] N. J. Hellyer, C. B. Mantilla, E. W. Park, W. Z. Zhan, and G. C. Sieck, "Neuregulin-dependent protein synthesis in C2C12 myotubes and rat diaphragm muscle," *American Journal of Physiology. Cell Physiology*, vol. 291, no. 5, pp. C1056–C1061, 2006.

[45] N. K. Lebrasseur, G. M. Coté, T. A. Miller, R. A. Fielding, and D. B. Sawyer, "Regulation of neuregulin/ErbB signaling by contractile activity in skeletal muscle," *American Journal of Physiology-Cell Physiology*, vol. 284, no. 5, pp. C1149–C1155, 2003.

[46] B. D. Manning and A. Toker, "AKT/PKB signaling: navigating the network," *Cell*, vol. 169, no. 3, pp. 381–405, 2017.

[47] L. Ma, X. P. Li, H. S. Ji, Y. F. Liu, and E. Z. Li, "Baicalein protects rats with diabetic cardiomyopathy against oxidative stress and inflammation injury via phosphatidylinositol 3-kinase (PI3K)/AKT pathway," *Medical Science Monitor*, vol. 24, pp. 5368–5375, 2018.

[48] D. Wang, M. Jin, X. Zhao et al., "FGF1$^{\Delta HBS}$ ameliorates chronic kidney disease via PI3K/AKT mediated suppression of oxidative stress and inflammation," *Cell Death & Disease*, vol. 10, no. 6, p. 464, 2019.

[49] S. Xu, L. Wu, Q. Zhang et al., "Pretreatment with propylene glycol alginate sodium sulfate ameliorated concanavalin A-induced liver injury by regulating the PI3K/Akt pathway in mice," *Life Sciences*, vol. 185, pp. 103–113, 2017.

[50] L. Wu, Q. Zhang, W. Mo et al., "Quercetin prevents hepatic fibrosis by inhibiting hepatic stellate cell activation and reducing autophagy via the TGF-β1/Smads and PI3K/Akt pathways," *Scientific Reports*, vol. 7, no. 1, p. 9289, 2017.

Hindawi
Oxidative Medicine and Cellular Longevity
Volume 2020, Article ID 5724024, 9 pages
https://doi.org/10.1155/2020/5724024

Research Article

Body Mass Index (BMI) and Its Influence on the Cardiovascular and Operative Risk Profile in Coronary Artery Bypass Grafting Patients: Impact of Inflammation and Leptin

Katja Buschmann,[1] **Julius Wrobel**,[1] **Ryan Chaban**,[1] **Romina Rösch**,[1] **Ahmed Ghazy**,[1] **Alina Hanf**,[2] **Katrin Schäfer**,[2,3] **Andreas Daiber**,[2,3] **Andres Beiras-Fernandez**,[1] **and Christian Friedrich Vahl**[1]

[1]*Department of Cardiothoracic and Vascular Surgery, University Medical Center of the Johannes Gutenberg-University Mainz, 55131 Mainz, Germany*
[2]*Center for Cardiology, Cardiology I, University Medical Center of the Johannes Gutenberg-University Mainz, 55131 Mainz, Germany*
[3]*German Center for Cardiovascular Research (DZHK), partner site Rhine-Main, Mainz, Germany*

Correspondence should be addressed to Katja Buschmann; katja.buschmann@unimedizin-mainz.de

Received 7 April 2020; Revised 29 May 2020; Accepted 3 June 2020; Published 24 June 2020

Guest Editor: Karolina Szewczyk-Golec

Copyright © 2020 Katja Buschmann et al. This is an open access article distributed under the Creative Commons Attribution License, which permits unrestricted use, distribution, and reproduction in any medium, provided the original work is properly cited.

Background. Obesity is related to coronary artery disease (CAD) and worse outcomes in coronary artery bypass graft (CABG) patients. Adipose tissue itself is an endocrine organ that secretes many humoral mediators, such as adipokines, which can induce or reduce inflammation and oxidative stress. *Objectives*. We investigate the relationship between the body mass index (BMI), inflammation, and oxidative stress by measuring serum levels of leptin, interleukin-6, and 3-nitrotyrosine in CABG patients and correlate their levels to the cardiovascular and operative risk profiles. *Methods and Results*. 45 men (<75 years) with a median BMI of 29 (21-51) kg/m^2, who were diagnosed with CAD and scheduled for elective CABG, were included after applying the following exclusion criteria: prior myocardial infarction, reoperation, female gender, and smoking. Patients' blood samples were taken preoperatively. Several markers were measured. We found significant correlations between leptin and BMI ($p < 0.0001$) as well as between leptin and 3-nitrotyrosine ($p = 0.006$). Interleukin-6 was correlated with C-reactive protein ($p < 0.0001$) and with the incidence of insulin-dependent diabetes mellitus ($p = 0.036$), arterial hypertension ($p = 0.044$), reduced left ventricular function ($p = 0.003$), and severe coronary calcification ($p = 0.015$). It was also associated with significantly longer extracorporeal bypass time ($p = 0.009$). Postoperative deep sternal wound infections could be predicted by a higher BMI ($p = 0.003$) and leptin level ($p = 0.001$). *Conclusions*. There seems to be a correlation between inflammatory processes and cardiovascular morbidity in our cohort. Further, the incidence of deep sternal wound infections is related to a higher BMI and leptin serum level.

1. Introduction

Adiposity is well-known as a cardiovascular risk factor. Obese coronary artery bypass graft (CABG) patients are associated with higher postoperative morbidity and worse long-term survival [1]. Nevertheless, the body mass index (BMI) itself does not play a role in preoperative risk adjustment scores for cardiac surgery so far [2]. In a former experimental study, we could prove a correlation of BMI with a negative inotropic effect in an isolated human myocardium [3]. The adipose tissue itself is the largest endocrine organ of the human body and secrets more than 150 adipokines with mostly proinflammatory and cardiovascular potent mediation [4–8].

Clinical studies in humans showed that obesity—defined by raised BMI—is associated with elevated serum levels of the

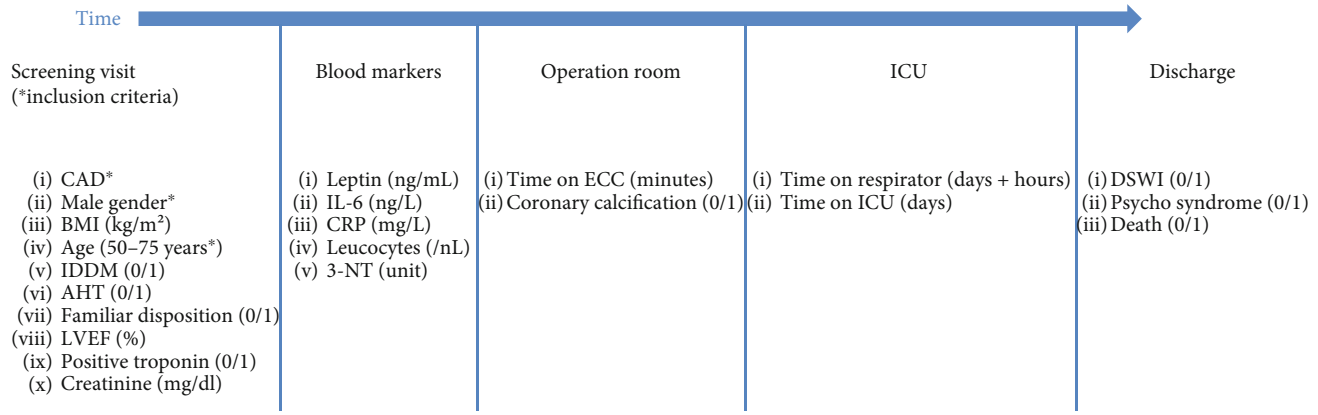

Figure 1: Flow chart of the time point of determination and documentation for each parameter/data ([0/1] = [No/yes]; 3-NT = 3-nitrotyrosine (rel. IOD, % of control normalized to loading control); AHT = arterial hypertension; BMI = body mass index; CRP=C-reactive protein; d = days; DSWI = deep sternal wound infection; ECC = extracorporeal circulation; h = hours; ICU = intensive care unit; IDDM = insulin-dependent diabetes mellitus II; IL-6 = interleukin 6; LVEF = left ventricular ejection fraction).

adipokine leptin [9]. Coronary artery disease (CAD) is also associated with increased serum leptin levels [10–12]. Leptin levels are identified as a malignant predictor of mortality and morbidity of patients with CAD [13]. Wallace et al. showed that women have significantly higher leptin levels than men [11]. Therefore, we decided to determine the serum leptin levels only in male CABG patients to avoid gender bias and to achieve more homogeneity in the measured leptin level. In addition, leptin has a direct proinflammatory effect on T cells and monocytes, leading to the release of cytokines such as tumor necrosis factor-α (TNF-α) and interleukin 6 (IL-6) [14–16]. Furthermore, leptin is associated with the inflammation marker C-reactive protein (CRP) [15], and high levels of these biomarkers (leptin, IL-6, and CRP) are predictive for worse outcome in patients with CAD [15]. Leptin also induces the formation and the intracellular accumulation of reactive oxygen species (ROS) [15]. In order to evaluate the referred association of inflammation and leptin, we planned to measure not only the standard serum CRP but also the IL-6 levels.

The aim of this study is to establish a correlation between the humoral expression of leptin and the inflammatory and oxidative status of obese patients undergoing CABG, as well as the clinical influence of these biomarkers.

2. Materials and Methods

2.1. Patients. This study was approved by the Institutional Review Board (processing number 837.051.15 (9819), 23 March 2015). A total of 45 consecutive elective isolated CABG patients with CAD and a median BMI of 29 [21-51] kg/m^2, male gender, and an age between 50 and 75 years (67 ± 8.4 years) were included. Exclusion criteria were prior myocardial infarction, reoperation, female gender, and smoking. Figure 1 shows the timing of the screening visit, the evaluation and documentation of preoperative characteristics, preoperative blood markers, and the final documentation of intraoperative and intensive care unit (ICU) data as well as the discharge data for the final recording of deep sternal wound infection (DSWI), as a postoperative complication. The observation period ended with the discharge of the patient. We interviewed the study patients for their age and the presence of cardiovascular risk factors as insulin-dependent diabetes mellitus (IDDM), familiar disposition, and arterial hypertension (AHT). Further comorbidities such as renal dysfunction, assessed by the creatinine serum level, and left ventricular ejection fraction (LVEF) were recorded. Blood samples were obtained simultaneously with the regular clinical blood sampling at administration, usually 24 hours before surgery. We measured leptin, IL-6, CRP, leukocytes, and 3-nitrotyrosine (3-NT). The duration of extracorporeal circulation (ECC) is relevant for postoperative outcome and therefore reported as well as the diagnosis of a severe coronary calcification, assessed by the cardiac surgeon in his operation report. The time on respirator and stay length on ICU were documented. Clinical assessments and documentations were used for the query of DSWI, a therapy relevant psychosyndrome and death.

2.2. Blood Biomarkers. Patients' blood samples were taken preoperatively each with 3 serum pipes. IL-6, CRP, and leukocytes were measured by the intern laboratory medicine. The other samples were frozen and collected for leptin enzyme-linked immunosorbent assay (ELISA) and oxidative stress level determination. Serum leptin levels were determined using a commercially available Human Leptin Quantikine ELISA Kit (R&D Systems), following the instructions of the manufacturer.

2.3. 3-Nitrotyrosine Levels (3-NT). Levels of 3-NT and 8-isoprostane, as markers of oxidative stress, were determined in human serum using a commercial ELISA kit (human immunoassay, 3-NT: #CSB-E14324h, Cusabio, Wuhan, Hubei Province 430206, China; 8-isoprostane: #MBS109360, San Diego, CA, USA) following the instructions of the vendor and previously [17]. Protein tyrosine nitration was also determined by dot blot analysis using a specific antibody for 3-NT (Millipore 05-233 Mouse mAb, 1 : 1000 in PBS/5% Milk) [17, 18]. Briefly, 100 μl (0.5 μg/μl protein based on Bradford analysis) of the ethylenediaminetetraacetic acid (EDTA) plasma

was transferred to a Protran BA85 (0.45 μm) nitrocellulose membrane (Schleicher & Schuell, Dassel, Germany) using a Minifold I vacuum Dot-Blot system (Schleicher & Schuell, Dassel, Germany). Each slot was washed twice with 200 μl phosphate-buffered saline (PBS) before and after protein transfer. The membrane was dried for 60 min at 60°C. Positive bands were detected by enhanced chemiluminescence after incubation with peroxidase-coupled anti-mouse or rabbit secondary antibodies for 3-NT-positive proteins or transferrin, respectively (goat-anti-mouse-peroxidase-labeled and goat-anti-rabbit-peroxidase-labeled, 1 : 10,000) (Vector Laboratories, CA, USA). All incubation and washing steps were performed according to the manufacturer's instructions. Densitometric quantification of the dots was performed using the SuperSignal-enhanced chemiluminescence kit from Thermo Scientific. The densitometric 3-NT signals were normalized to either Ponceau S staining or to the densitometric signals of the serum loading control transferrin (anti-transferrin antibody (Thermo Fisher PA3-913); rabbit pAb, 1 : 5,000 in PBS-T/5% BSA) staining (rel. IOD, % of control).

2.4. Statistical Analysis. Statistical description and analyses were performed using IBM SPSS 23 (IBM, USA). Quantitative variables were expressed as the mean ± standard deviation if they were normally distributed (skewness between -1 and 1) and as median with range if they were not normally distributed (skewness < −1 and>1). For nonparametric data, the Mann–Whitney U or the exact Fisher test were used; for parametric data Student's t-test. Linear regression was used for the assessment of correlation between metric parameters. An alpha-value of 0.05 was chosen for significance. The cut-off values were determined within an ROC analysis. As cut-off, the values with the smallest Euclidian distance to the upper left of the plot were taken.

3. Results

3.1. Blood Markers and Hospitalization Data. BMI and all measured blood markers showed a wide variation: BMI 29 (21-51) kg/m^2, leptin 9.157 (1.594-87.984) ng/mL, IL-6 16.5 (2-79) ng/L, CRP 5.3 (0.29-291) mg/L, leucocytes 8.2 (4.46-24.3) cells/nL, and 3-NT 53.24 (21.26-187.20) (rel. IOD, % of control). Time on ECC was 71.14 ± 20.77 minutes. Severe coronary calcifications were assessed in 21 CABG operations. The postoperative time on respirator was 10 (1-420) hours and stay on ICU was 2.54 ± 3.69 days. With the discharge of the patient to home or to rehabilitation 5 cases of DSWI, no psycho syndrome and no death were recorded.

3.2. Inflammation Markers and Preoperative Risk Profile. Parameters of inflammation showed a significant correlation as CRP was significantly correlated with IL-6 ($p < 0.0001$, $R^2 = 0.3$) and leukocytes ($p = 0.003$, $R^2 = 0.186$) (Figure 2). On the other hand, IL-6 serum levels were not affected by the BMI ($p = 0.821$, $R^2 = 0.001$) and did not correlate with serum leptin levels ($p = 0.608$, $R^2 = 0.007$). Leptin was significantly correlated with BMI ($p < 0.0001$, $R^2 = 0.6$) (Figure 3) and also with the oxidative stress marker 3-NT ($p = 0.0109$, $R^2 = 0.1628$ or $p = 0.0062$, $R^2 = 0.1857$, depending on the normalization method) (Figure 4). In a pilot experiment, we confirmed that patients with high leptin levels have higher oxidative stress parameters (3-NT and 8-isoprostane). The distribution pattern also varied to some extent in dependence of the normalization method, but the overall trend was reproducible in both measurements. 3-NT was not significantly correlated with IL-6 ($p = 0.7169$, $R^2 = 0.0038$) (Figure 5).

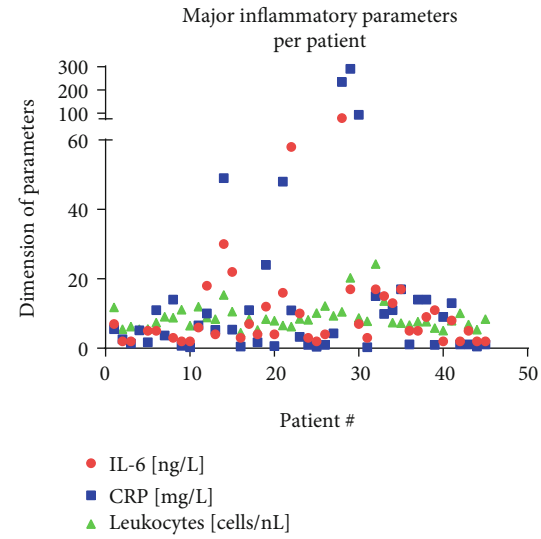

Figure 2: All 45 individual values for the measured parameters of inflammation are illustrated.

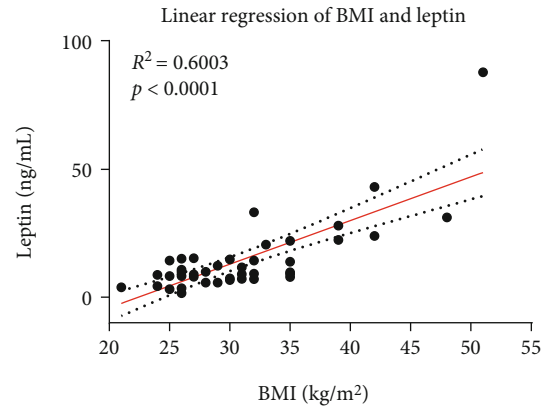

Figure 3: Significant correlation of BMI with leptin in 45 patients.

Preoperative left ventricular ejection fraction was inversely correlated with IL-6 ($p = 0.003$, $R^2 = 0.202$), CRP ($p = 0.005$, $R^2 = 0.171$), and leucocytes ($p = 0.005$, $R^2 = 0.170$), whereas patients with IDDM showed significantly higher level of IL-6 ($p = 0.036$) as well as patients with AHT ($p = 0.044$) (Figure 6). Furthermore, preoperative creatinine was proportional correlating with leptin ($p = 0.001$, $R^2 = 0.223$) and also significantly higher in patients with positive troponin ($p = 0.003$). Patients' age showed no statistical relation to IDDM, AHT, or familiar disposition.

3.3. Inflammation Markers and Coronary Sclerosis. Severe coronary sclerosis was assessed in 21 patients; these patients did not show a significantly higher blood level of leucocytes,

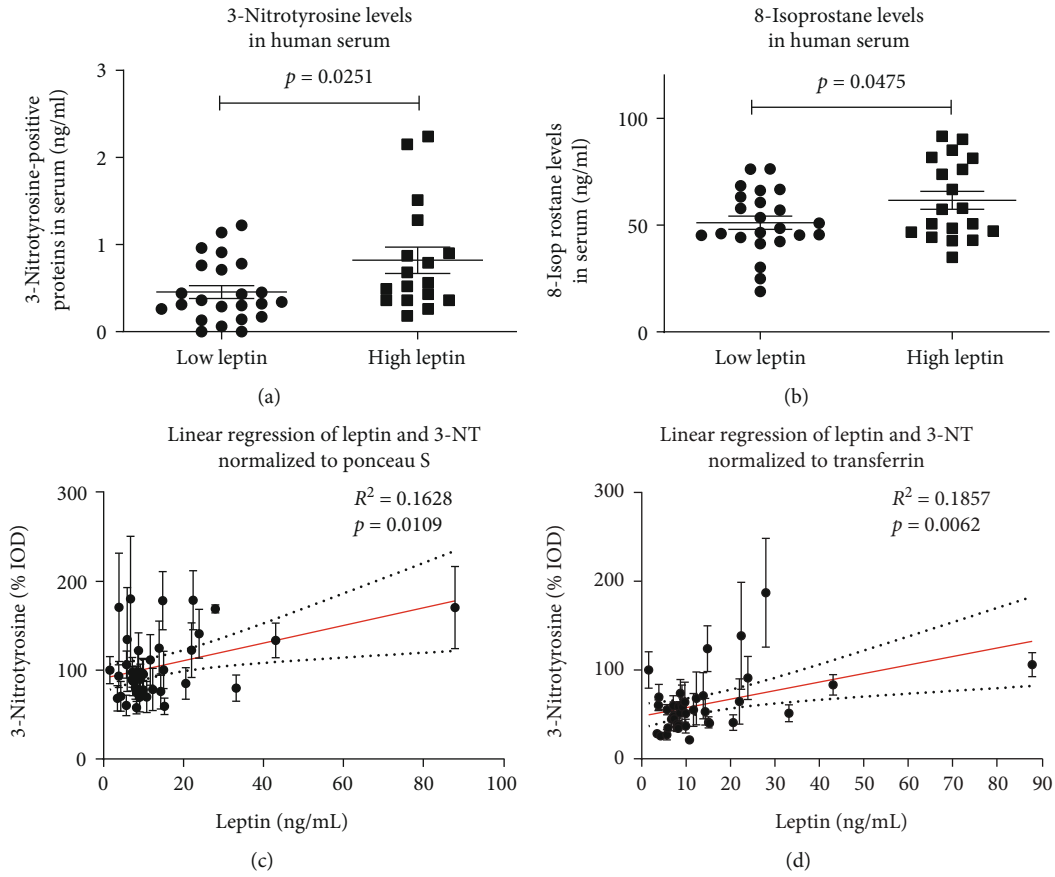

Figure 4: Determination of the oxidative stress parameters 3-nitrotyrosine (3-NT) (a) and 8-Isoprostane (b) by commercial ELISA assays of a proof of increased reactive oxygen and nitrogen species formation in patients with leptin levels higher than the median. Data are mean ± SEM. (c, d) Significant correlation of leptin and levels of the serum oxidative stress marker 3-NT in 40 patients (p values and correlation coefficients are provided in the graphs). Measured 3-NT staining was either normalized to Ponceau S staining (c) or transferrin content (d).

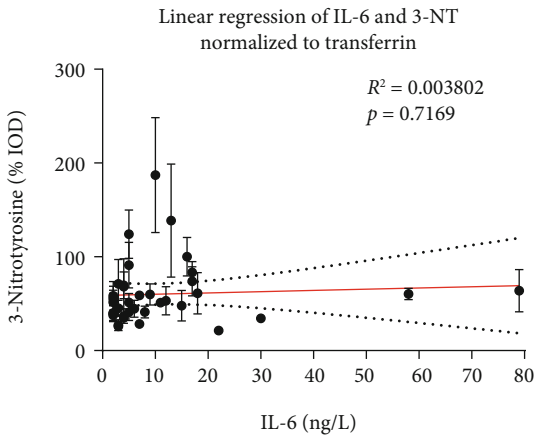

Figure 5: Correlation of IL-6 and levels of the serum oxidative stress marker 3-nitrotyrosine (3-NT) in 40 patients (correlation coefficient is provided in the graph).

but were outstanding with significantly higher blood levels of IL-6 ($p = 0.015$) (Figure 7). Patients' age, creatinine value, and LVEF were neither significant for the CVR profile nor for the severity of coronary calcification (Table 1). Patients with reduced LVEF did show the trend of a higher rate of severe coronary calcification ($p = 0.09$, Table 1) In addition to this, patients with severe coronary sclerosis had a significantly higher rate of IDDM ($p = 0.031$), and bypass grafting operation demanded significantly longer time on ECC (63.57 minutes versus 79.85 minutes, $p = 0.009$). The time on respirator was correlated with BMI ($p = 0.042$, $R^2 = 0.104$) and CRP ($p = 0.024$, $R^2 = 0.127$) and significantly longer in patients with IDDM ($p = 0.004$). Furthermore, patients with IDDM did show a prolonged stay on ICU ($p = 0.008$).

There were 5 cases of DSWI. Reliable DSWI markers were leptin ($p = 0.001$) and BMI ($p = 0.003$) (Figure 8). Patients with DSWI were significantly more often diabetic patients ($p = 0.021$) but did neither exceed in time on respirator nor on intensive care unit.

3.4. Analysis of Cut-Off Values. The inflammatory marker IL-6 delivers cut-off values for the cardiovascular and operative risk profile by significant correlation with IDDM, AHT, and severe coronary calcification whereas leptin and BMI are predictive for DSWI (Table 2).

4. Discussion

4.1. Main Findings and Clinical Relevance. This study investigated the association of the inflammatory marker IL-6 with

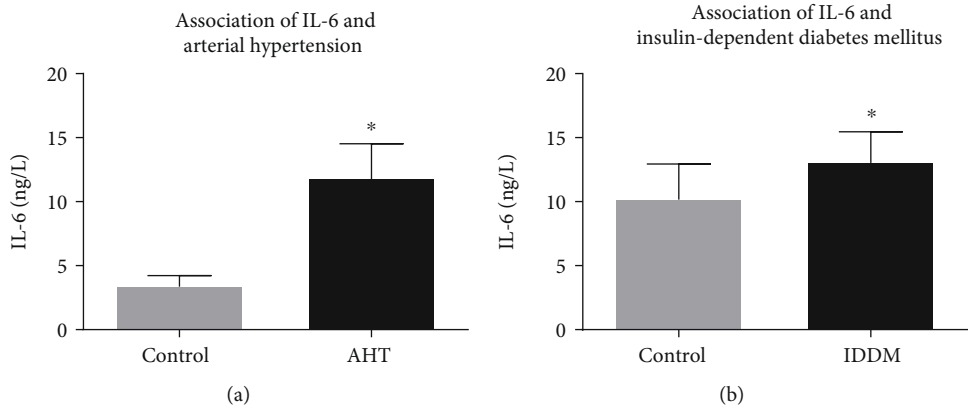

Figure 6: IL-6 levels in patients with (a) AHT ($n = 39$) and (b) IDDM ($n = 7$) compared to IL-6 levels in patients without arterial hypertension (no AHT/control (a), $n = 6$) and without IDDM (no IDDM/control (b), $n = 38$). IL-6 levels were significantly higher in patients with AHT (3.5 ± 0.7 vs 11.9 ± 2.6 ng/l) and with IDDM (10.3 ± 2.6 vs 13.2 ± 2.3 ng/l). Data are mean ± SEM.

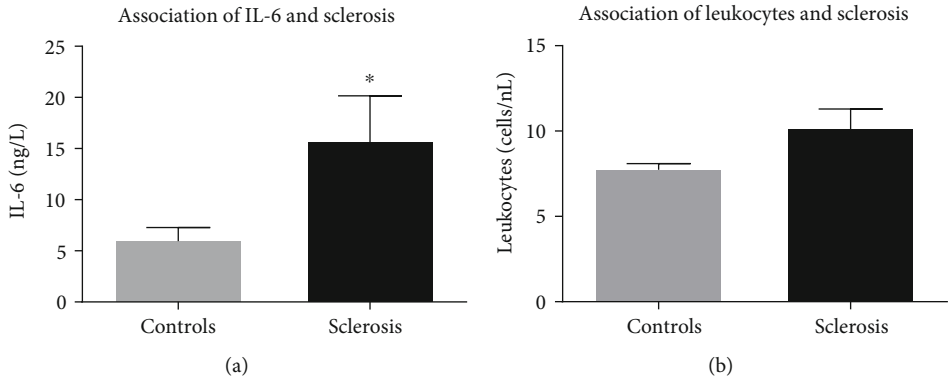

Figure 7: IL-6 levels (a) and leucocytes (b) compared in patients with intraoperative status of severe coronary calcification (sclerosis, black) or normal coronary sclerosis (control, grey). Patients with severe coronary calcification had significantly higher levels of IL-6 (6.1 ± 1.1 vs 15.8 ± 4.4 ng/l), whereas leucocytes were only increased by trend (7.7 ± 0.4 vs 10.2 ± 1.1 cells/ng, $p = 0.085$). Data are mean ± SEM, $n = 21 - 24$ patients.

Table 1: Patients' comorbidities (age, creatinine, and left ventricular function) are not significantly influencing the cardiovascular risk profile (IDDM, familiar disposition, and arterial hypertension) or significantly correlating with the intraoperative finding of a severe coronary calcification. However, there is a significant relation between the value of the left ventricular function (LVEF %) and severe coronary calcification.

	Insulin-dependent DM [0: $n = 38$, 1: $n = 7$]	Familiar disposition [0: $n = 33$, 1: $n = 12$]	Arterial hypertension [0: $n = 6$, 1: $n = 39$]	Severe coronary calcification [0: $n = 24$, 1: $n = 21$]
Age (years)	$p = 0.58$	$p = 0.97$	$p = 0.66$	$p = 0.89$
Creatinine (mg/dL)	$p = 0.95$	$p = 0.60$	$p = 0.79$	$p = 0.82$
LVEF (%)	$p = 0.87$	$p = 0.38$	$p = 0.71$	$p = 0.09$

the cardiovascular and operative risk profile of CABG patients. We found that IL-6 is associated with the cardiovascular (IDDM and AHT) as well as for the operative risk profile (inversely correlated with LVEF and severe coronary calcification). This finding is in accordance with the reported low-grade inflammatory phenotype of IDDM and AHT [19]. The clinical importance of IDDM and AHT is further supported by large epidemiological studies ranking them among the leading cardiovascular risk factors and causes of premature death at the global level [20]. AHT and its correlation with inflammation markers (CRP or IL-6) have been also described in literature [21]. Patients with reduced LVEF show the trend to have more often a severe coronary sclerosis. In the present study, the inflammation markers IL-6 and CRP and the number of leucocytes were significantly correlated. Moreover, we demonstrate a correlation between leptin and BMI and that both parameters are associated with DSWI as an operative complication risk.

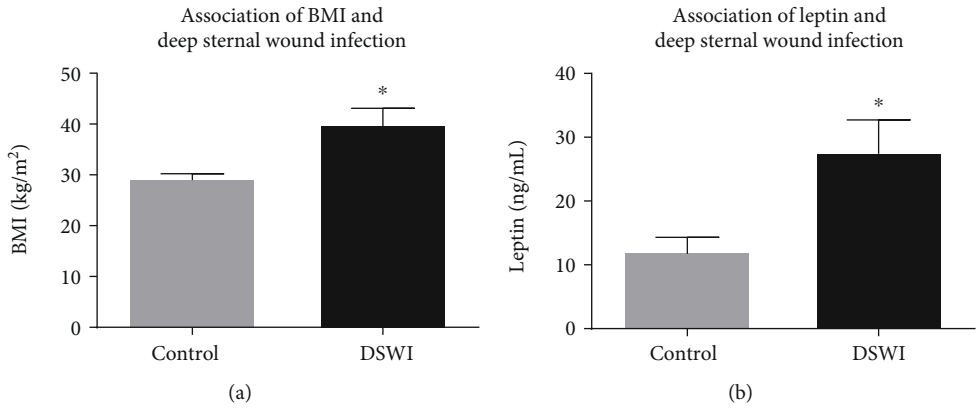

Figure 8: BMI (a) and leptin levels (b) in patients with deep sternal wound infection (black, DSWI, $n = 5$) versus the control (grey) group ($n = 40$). Patients with DSWI had significantly higher BMI (29.4 ± 0.9 vs $40.0 \pm 3.1\,kg/m^2$) and significantly raised levels of leptin (12.2 ± 2.2 vs 27.7 ± 5 ng/l). Data are mean ± SEM.

Table 2: Statistically tested cut-off values of markers of inflammation (IL-6) and adiposity (body mass index and leptin) for the presence of insulin-dependent diabetes as a cardiovascular risk factor, the intraoperatively finding of a severe coronary calcification as an operative risk profile, and the happening of a postoperatively deep sternal wound infection.

Cut-off values	Insulin-dependent DM	Arterial hypertension	Severe coronary calcification	Deep sternal wound infection
IL-6 (ng/L)	15.5	6.5	12.5	
BMI (kg/m^2)				37.0
Leptin (ng/mL)				23.17

4.2. CABG Surgery and Inflammation. Severe coronary calcification (reported by the surgeon itself) is accompanied by significantly longer time on ECC and thereby increasing operative risk. Also the leucocytes were significantly correlated with the status of severe coronary calcification in the present study, similar to the inflammation marker IL-6. Although, previous data do not support a significant correlation of coronary calcification and CRP levels in CABG patients, a subgroup analysis in statin-free patients found a clear correlation [22]. Another recent study has proven the association between fibrinogen level, an acute phase protein, and a parameter of inflammation, and the severity of coronary stenosis [23]. CRP is significantly correlated with the time on respirator [24]. Thus, elective CABG patients with preoperatively raised CRP values should firstly be searched for an infective pulmonary focus and optionally be treated with antibiotic therapy until surgery can be planned. Although higher preoperative CRP levels are mostly related to infections [25], also other conditions such as schizophrenia, cardiogenic shock, and autoimmune conditions, including rheumatoid arthritis, lupus, and certain types of inflammatory bowel disease, such as Crohn's disease and ulcerative colitis, may be associated with increased CRP levels.

4.3. CABG Surgery and Leptin. Our determination of leptin in this cohort of patients is completely coherent with the literature. Considine et al. describe leptin levels in obese with 31.3 ± 24.1 ng/mL and about 7.5 ± 9.3 ng/mL in normal-weighted humans [9], and Wolk et al. reported leptin levels with median 9.2 ng/mL [0.7-90.6 ng/mL] in patients with established CAD [12]. Both are similar to our results with median 9.157 (1.594-87.984) ng/mL. Furthermore, Wolk et al. reported that the leptin level is independent of other risk factors, e.g., lipid status and CRP. In this clinical study, the systemic leptin level was also not correlated with markers of inflammation. This can be caused by many other relevant effects of pro- and anti-inflammatory adipokines. Furthermore, we observed increased oxidative stress in patients with systemic higher levels of leptin. This can be explained by the fact that oxidative stress reduces the production of beneficial, anti-inflammatory adipokines [26]. In line with this notion, oxidative stress negatively affects the collagen turnover and supports the synthesis of collagen, for example, in the heart, resulting in worse LVEF by the remodeling process [27]. In a former experimental study, we found also signs of fibrotic remodeling in septic/inflammatory cardiomyopathy [28]. A more recent study proposed the leptin/adiponectin ratio as another parameter of prognostic importance besides markers of inflammation [29].

4.4. CABG Surgery and BMI. In our study, leptin is significantly correlated with the BMI. However, there are clear difficulties reported for the leptin level dependence on BMI [30]. In addition, the development of leptin resistance due to insulin resistance in diabetic and adipose patients may contribute to a rather reduced leptin effect [30, 31]. Regarding the here established significant correlation of BMI and leptin, it should be stressed that the preoperative BMI in CABG patients was associated with DSWI, a major complication in CABG surgery, and thereby may confer

some prognostic value to BMI as well as leptin levels (BMI > 37 kg/m^2 cut-off, Table 2). This is further supported by the significant correlation of leptin with the preoperative creatinine levels in our patient collective. This relation is also described by others [21, 31]. Also, previous studies reported on a higher risk for major complications among CABG patients with increasing BMI [32, 33].

4.5. Leptin, Inflammation, Arterial Hypertension, and Diabetes Mellitus. Tsai et al. showed a correlation between AHT and leptin predicting arterial stiffness in hypertensive patients [21]. In our results, we could not show any correlation between leptin and AHT. One explanation could be the bias of IDDM—at least seven patients in our study collective showing decreased leptin levels [30, 31]. Nevertheless, both of our study groups—with or without IDDM—show median leptin levels with 9.2/9.1 ng/mL. There is no effect of age (Table 1) upon the severity of coronary calcification. But patients with a preoperatively reduced LVEF showed the trend of a higher rate of severe coronary calcification—accompanied with and presumably caused by raised inflammation (marker IL-6). Nevertheless, inflammation markers in the blood seem to have more influence resulting in cardiovascular damage like AHT and coronary calcification.

The significance of the preoperative creatinine level was neither demonstrated in our study nor in another recent longitudinal study [34]. In our work, there was a significantly higher rate of severe coronary calcification in patients with IDDM. A recent study with the optical coronary tomography method [35] could exclude any impact of type 2 diabetes mellitus on coronary calcification but has proven the burden of a plaque rupture in type 2 diabetes mellitus. The definition of type 2 diabetes mellitus was Hba1c > 6.5% or intake of oral antidiabetic drugs. In our study. the criteria were stronger with the insulin-dependency. Thus, both different results are not comparable.

One explanation could be that there are pro- and anti-inflammatory adipokines that, depending on their expression profile, promote or suppress inflammation. In this study, we did only measure the proinflammatory leptin without measurement of an antagonist, e.g., the anti-inflammatory adiponectin. Instead, we concentrated on the consequences of inflammation by measurement of the oxidative stress marker 3-NT and its correlation with IL-6. To our surprise, we could not show a positive correlation between IL-6 and oxidative stress (Figure 5).

4.6. Limitations of the Study. A major limitation of our study is the small cohort size, thus limiting the power of our findings and resulting in small effect sizes. Previous studies were based on several hundreds of individuals, e.g., the investigation of risk factors for surgical wound infections and postoperative bacteremia for patients undergoing CABG surgery ($n = 693$) [36]. In addition, our observation period was quite short and ends with the discharge from hospital. Similar studies used longer follow-up periods of up to five years, e.g., investigation of impact of BMI and the associated biomarkers on clinical outcomes after CABG ($n = 234$) [32].

5. Conclusion

In our study, neither the BMI and nor the leptin level are as relevant as the systemic inflammation markers that are probably responsible for the worse prognosis and high cardiovascular event rate in obese CABG patients. Our observations are in good accordance with meta-analysis reporting pre- and perioperative inflammation to be major determinants of prognosis among CABG patients [37]. This may also explain why modern antidiabetic drugs with clearly characterized anti-inflammatory properties show beneficial effects on prognosis among CABG patients. Examples are the therapy with a sodium glucose cotransporter 2 inhibitor [38], glucagon-like peptide-1 [39], statins [40, 41], or even a specific anti-inflammatory, monoclonal-based drug [42].

Abbreviations

[0/1]:	No/yes
AHT:	Arterial hypertension
BMI:	Body mass index (body weight (kilogram)/body height (m)^2)
CABG:	Coronary artery bypass graft
CAD:	Coronary artery disease
CRP:	C-reactive protein
CVR:	Cardiovascular risk
ECC:	Extracorporeal circulation
ELISA:	Enzyme-linked immunosorbent assay
ICU:	Intensive care unit
IDDM:	Insulin-dependent diabetes mellitus (type II)
DSWI:	Deep sternal wound infection
IL-6:	Interleukin 6
LVEF:	Left ventricular ejection fraction
3-NT:	3-nitrotyrosine
SD (in Results):	Standard deviation
SEM (Figures 4-7):	Standard error of the mean.

Data Availability

The data used to support the findings of this study are available from the corresponding author upon request.

Conflicts of Interest

The authors have no conflict of interest.

Authors' Contributions

K.B., R.C., A.B.-F., and C.F.V. conceived and designed research; J.W., A.G., R.R., A.H., and K.S. carried out experiments; K.B., R.C., A.H., K.S., and A.D. performed data analysis; K.B. and A.D. drafted the manuscript. R.C. and C.F.V. made critical contribution to the discussion. K.B., A.D., R.C., and C.F.V. revised the manuscript. All authors read and approved the final manuscript.

Acknowledgments

A.D. was continuously supported by the DZHK (German Center for Cardiovascular Research), Partner Site Rhine-Main, Mainz, Germany. A.H. held a stipend from the International PhD Program on the "Dynamics of Gene Regulation, Epigenetics and DNA Damage Response" from the Institute of Molecular Biology gGmbH (Mainz, Germany) funded by the Boehringer Ingelheim Foundation.

References

[1] R. H. Habib, A. Zacharias, T. A. Schwann, C. J. Riordan, S. J. Durham, and A. Shah, "Effects of obesity and small body size on operative and long-term outcomes of coronary artery bypass surgery: a propensity-matched analysis," *The Annals of Thoracic Surgery*, vol. 79, no. 6, pp. 1976–1986, 2005.

[2] F. Roques, P. Michel, A. R. Goldstone, and S. A. M. Nashef, "The logistic EuroSCORE," *European Heart Journal*, vol. 24, no. 9, pp. 881-882, 2003.

[3] K. Denk, J. Albers, N. Kayhan et al., "Evidence for a negative inotropic effect of obesity in human myocardium?," *European Journal of Cardio-Thoracic Surgery*, vol. 36, no. 2, pp. 300–305, 2009.

[4] V. Lamounier-Zepter, M. Ehrhart-Bornstein, P. Karczewski, H. Haase, S. R. Bornstein, and I. Morano, "Human adipocytes attenuate cardiomyocyte contraction: characterization of an adipocyte-derived negative inotropic activity," *The FASEB Journal*, vol. 20, no. 10, pp. 1653–1659, 2006.

[5] M. Gnacińska, S. Małgorzewicz, M. Stojek, W. Łysiak-Szydłowska, and K. Sworczak, "Role of adipokines in complications related to obesity: a review," *Advances in Medical Sciences*, vol. 54, no. 2, pp. 150–157, 2009.

[6] A. Stofkova, "Leptin and adiponectin: from energy and metabolic dysbalance to inflammation and autoimmunity," *Endocrine Regulations*, vol. 43, pp. 157–168, 2009.

[7] E. Maury and S. M. Brichard, "Adipokine dysregulation, adipose tissue inflammation and metabolic syndrome," *Molecular and Cellular Endocrinology*, vol. 314, no. 1, pp. 1–16, 2010.

[8] S. Dhein, "Fat and the heart: a more and more complex interplay," *The Thoracic and Cardiovascular Surgeon*, vol. 62, no. 7, pp. 543–546, 2014.

[9] R. V. Considine, M. K. Sinha, M. L. Heiman et al., "Serum immunoreactive-leptin concentrations in normal-weight and obese humans," *The New England Journal of Medicine*, vol. 334, no. 5, pp. 292–295, 1996.

[10] A. Qasim, N. N. Mehta, M. G. Tadesse et al., "Adipokines, insulin resistance, and coronary artery calcification," *Journal of the American College of Cardiology*, vol. 52, no. 3, pp. 231–236, 2008.

[11] S. G. Wannamethee, J. Tchernova, P. Whincup et al., "Plasma leptin: associations with metabolic, inflammatory and haemostatic risk factors for cardiovascular disease," *Atherosclerosis*, vol. 191, no. 2, pp. 418–426, 2007.

[12] R. Wolk, P. Berger, R. J. Lennon, E. S. Brilakis, B. D. Johnson, and V. K. Somers, "Plasma leptin and prognosis in patients with established coronary atherosclerosis," *Journal of the American College of Cardiology*, vol. 44, no. 9, pp. 1819–1824, 2004.

[13] N. Sattar, G. Wannamethee, N. Sarwar et al., "Leptin and coronary heart disease: prospective study and systematic review," *Journal of the American College of Cardiology*, vol. 53, no. 2, pp. 167–175, 2009.

[14] K. Isozumi, "Obesity as a risk factor for cerebrovascular disease," *The Keio Journal of Medicine*, vol. 53, no. 1, pp. 7–11, 2004.

[15] P. C. Schulze and J. Kratzsch, "Leptin as a new diagnostic tool in chronic heart failure," *Clinica Chimica Acta*, vol. 362, no. 1-2, pp. 1–11, 2005.

[16] V. Abella, M. Scotece, J. Conde et al., "Leptin in the interplay of inflammation, metabolism and immune system disorders," *Nature Reviews Rheumatology*, vol. 13, no. 2, pp. 100–109, 2017.

[17] T. Münzel, A. Daiber, S. Steven et al., "Effects of noise on vascular function, oxidative stress, and inflammation: mechanistic insight from studies in mice," *European Heart Journal*, vol. 38, no. 37, pp. 2838–2849, 2017.

[18] S. Kröller-Schön, A. Daiber, S. Steven et al., "Crucial role for Nox2 and sleep deprivation in aircraft noise-induced vascular and cerebral oxidative stress, inflammation, and gene regulation," *European Heart Journal*, vol. 39, no. 38, pp. 3528–3539, 2018.

[19] S. Steven, K. Frenis, M. Oelze et al., "Vascular inflammation and oxidative stress: major triggers for cardiovascular disease," *Oxidative Medicine and Cellular Longevity*, vol. 2019, Article ID 7092151, 26 pages, 2019.

[20] A. J. Cohen, M. Brauer, R. Burnett et al., "Estimates and 25-year trends of the global burden of disease attributable to ambient air pollution: an analysis of data from the Global Burden of Diseases Study 2015," *The Lancet*, vol. 389, no. 10082, pp. 1907–1918, 2017.

[21] J. P. Tsai, B. G. Hsu, C. J. Lee, Y. H. Hsieh, Y. C. Chen, and J. H. Wang, "Serum leptin is a predictor for central arterial stiffness in hypertensive patients," *Nephrology (Carlton)*, vol. 22, no. 10, pp. 783–789, 2017.

[22] A. Hosseinsabet, A. Mohebbi, and A. Almasi, "C-reactive protein and coronary calcium score association in coronary artery disease," *Cardiology Journal*, vol. 15, no. 5, pp. 431–436, 2008.

[23] X. Y. Gao, B. Y. Zhou, M. Z. Zhang et al., "Association between fibrinogen level and the severity of coronary stenosis in 418 male patients with myocardial infarction younger than 35 years old," *Oncotarget*, vol. 8, no. 46, pp. 81361–81368, 2017.

[24] S. M. A. Lobo, F. R. M. Lobo, D. P. Bota et al., "C-Reactive Protein Levels Correlate With Mortality and Organ Failure in Critically Ill Patients[a]," *Chest*, vol. 123, no. 6, pp. 2043–2049, 2003.

[25] A. Landry, P. Docherty, S. Ouellette, and L. J. Cartier, "Causes and outcomes of markedly elevated C-reactive protein levels," *Canadian Family Physician*, vol. 63, pp. e316–e323, 2017.

[26] N. Netzer, H. Gatterer, M. Faulhaber, M. Burtscher, S. Pramsohler, and D. Pesta, "Hypoxia, oxidative stress and fat," *Biomolecules*, vol. 5, no. 2, pp. 1143–1150, 2015.

[27] E. Martínez-Martínez, R. Jurado-López, M. Valero-Muñoz et al., "Leptin induces cardiac fibrosis through galectin-3, mTOR and oxidative stress," *Journal of Hypertension*, vol. 32, no. 5, pp. 1104–1114, 2014.

[28] K. Buschmann, R. Chaban, A. L. Emrich et al., "Septic cardiomyopathy: evidence for a reduced force-generating capacity of

human atrial myocardium in acute infective endocarditis," *Innovative Surgical Sciences*, vol. 2, no. 2, pp. 81–87, 2017.

[29] C. Sardu, N. D'Onofrio, M. Torella et al., "Pericoronary fat inflammation and Major Adverse Cardiac Events (MACE) in prediabetic patients with acute myocardial infarction: effects of metformin," *Cardiovascular Diabetology*, vol. 18, no. 1, p. 126, 2019.

[30] I. A. Ku, R. Farzaneh-Far, E. Vittinghoff, M. H. Zhang, B. Na, and M. A. Whooley, "Association of low leptin with cardiovascular events and mortality in patients with stable coronary artery disease: the Heart and Soul Study," *Atherosclerosis*, vol. 217, no. 2, pp. 503–508, 2011.

[31] X. Gu, Z. Chen, and I. El Bayoumy, "Serum leptin levels in obese women with and without type 2 diabetes mellitus," *Minerva Endocrinologica*, vol. 39, no. 3, pp. 223–229, 2014.

[32] S. H. Sung, T. C. Wu, C. H. Huang, S. J. Lin, and J. W. Chen, "Prognostic impact of body mass index in patients undergoing coronary artery bypass surgery," *Heart*, vol. 97, no. 8, pp. 648–654, 2011.

[33] F. D. Ramirez, B. Hibbert, T. Simard et al., "Clinical outcomes among patients with extreme obesity undergoing elective coronary revascularization: Evaluation of major complications in contemporary practice," *International Journal of Cardiology*, vol. 186, pp. 266–272, 2015.

[34] C. Suh-Chiou, R. M. Moysés, M. S. Bittencourt, I. M. Bensenor, and P. A. Lotufo, "Chronic kidney disease and coronary artery calcification in the Brazilian Longitudinal Study of Adult Health (ELSA-Brasil)," *Clinical Cardiology*, vol. 40, no. 12, pp. 1309–1315, 2017.

[35] A. Milzi, M. Burgmaier, K. Burgmaier, M. Hellmich, N. Marx, and S. Reith, "Type 2 diabetes mellitus is associated with a lower fibrous cap thickness but has no impact on calcification morphology: an intracoronary optical coherence tomography study," *Cardiovascular Diabetology*, vol. 16, no. 1, p. 152, 2017.

[36] D. W. Spelman, P. Russo, G. Harrington et al., "Risk factors for surgical wound infection and bacteraemia following coronary artery bypass surgery," *The Australian and New Zealand Journal of Surgery*, vol. 70, no. 1, pp. 47–51, 2000.

[37] A. Weymann, A.-F. Popov, A. Sabashnikov et al., "Baseline and postoperative levels of C-reactive protein and interleukins as inflammatory predictors of atrial fibrillation following cardiac surgery: a systematic review and meta-analysis," *Kardiologia Polska*, vol. 76, pp. 440–451, 2017.

[38] S. Verma, C. D. Mazer, D. Fitchett et al., "Empagliflozin reduces cardiovascular events, mortality and renal events in participants with type 2 diabetes after coronary artery bypass graft surgery: subanalysis of the EMPA-REG OUTCOME® randomised trial," *Diabetologia*, vol. 61, no. 8, pp. 1712–1723, 2018.

[39] G. G. Sokos, H. Bolukoglu, J. German et al., "Effect of glucagon-like peptide-1 (GLP-1) on glycemic control and left ventricular function in patients undergoing coronary artery bypass grafting," *The American Journal of Cardiology*, vol. 100, no. 5, pp. 824–829, 2007.

[40] I. Singh, S. Rajagopalan, A. Srinivasan et al., "Preoperative statin therapy is associated with lower requirement of renal replacement therapy in patients undergoing cardiac surgery: a meta-analysis of observational studies," *Interactive Cardio-Vascular and Thoracic Surgery*, vol. 17, no. 2, pp. 345–352, 2013.

[41] C. N. Bang, A. M. Greve, J. Abdulla, L. Køber, G. H. Gislason, and K. Wachtell, "The preventive effect of statin therapy on new-onset and recurrent atrial fibrillation in patients not undergoing invasive cardiac interventions: a systematic review and meta-analysis," *International Journal of Cardiology*, vol. 167, no. 3, pp. 624–630, 2013.

[42] J. A. Patel and S. B. Ghatak, "Pexelizumab and its role in the treatment of myocardial infarction and in coronary artery bypass graft surgery: a review," *Recent Patents on Cardiovascular Drug Discovery*, vol. 3, no. 2, pp. 145–152, 2008.

Hindawi
Oxidative Medicine and Cellular Longevity
Volume 2020, Article ID 4751803, 9 pages
https://doi.org/10.1155/2020/4751803

Research Article

5α,6α-Epoxyphytosterols and 5α,6α-Epoxycholesterol Increase Nitrosative Stress and Inflammatory Cytokine Production in Rats on Low-Cholesterol Diet

Tomasz Wielkoszyński,[1,2] **Jolanta Zalejska-Fiolka**,[3] **Joanna K. Strzelczyk**,[4] **Aleksander J. Owczarek**,[5] **Armand Cholewka**,[6] **Katarzyna Kokoszczyk**,[2] **and Agata Stanek**[7]

[1]*Higher School of Strategic Planning in Dąbrowa Górnicza, Kościelna 6 St., 41-300 Dąbrowa Górnicza, Poland*
[2]*Wielkoszyński Medical Center and Laboratory, Piłsudskiego 10 St., 41-300 Dąbrowa Górnicza, Poland*
[3]*Medical University of Silesia, Faculty of Medical Sciences in Zabrze, Department of Biochemistry, Jordana 19 St., 41-808 Zabrze, Poland*
[4]*Medical University of Silesia, Faculty of Medical Sciences in Zabrze, Department of Medical and Molecular Biology, Jordana 19 St., 41-808 Zabrze, Poland*
[5]*Medical University of Silesia, Faculty of Pharmaceutical Sciences, Department of Statistics, Department of Instrumental Analysis, Ostrogórska 30 St., Sosnowiec 41-209, Poland*
[6]*University of Silesia, Faculty of Science and Technology, Katowice, Bankowa St., 40-007 Katowice, Poland*
[7]*Medical University of Silesia, Faculty of Medical Sciences in Zabrze, Department of Internal Medicine, Angiology and Physical Medicine, Batorego 15 St., 41-902 Bytom, Poland*

Correspondence should be addressed to Agata Stanek; astanek@tlen.pl

Received 7 April 2020; Accepted 26 May 2020; Published 8 June 2020

Guest Editor: Karolina Szewczyk-Golec

Copyright © 2020 Tomasz Wielkoszyński et al. This is an open access article distributed under the Creative Commons Attribution License, which permits unrestricted use, distribution, and reproduction in any medium, provided the original work is properly cited.

Objective. Oxidized cholesterol derivatives are compounds with proven atherogenic and mutagenic effects. However, little is known about the effect of oxidized plant sterol derivatives (oxyphytosterols), whose structure is similar to the one of oxycholesterols. Our previous studies indicate that they have a similar profile of action, e.g., both exacerbate disorder of lipid metabolism and oxidative stress in experimental animals. The aim of the present study was to assess the effect of epoxycholesterol and epoxyphytosterols (mainly sitosterol) on the severity of nitrosative stress and the concentration of selected proinflammatory cytokines in blood and liver tissue of rats on a low-cholesterol diet. *Material and Methods*. Forty-five male Wistar rats were fed with feed containing 5α,6α-epoxyphytosterols (ES group, *n*: 15), 5α,6α-epoxycholesterol (ECh group, *n*: 15), and oxysterol-free feed (C group, *n*: 15) for 90 days (daily dose of oxysterols: 10 mg/kg). At the end of the experiment, nitrotyrosine, TNF-α, IL-1β, IL-6, and lipid metabolism parameters were determined in blood serum. Furthermore, nitrotyrosine, TNF-α, cholesterol, and triglyceride content were determined in liver homogenates. *Results*. Serum nitrotyrosine, IL-1β, and TNF-α concentrations as well as TNF-α content in the liver were significantly higher in both groups exposed to oxysterols (ECh and ES groups) as compared to the C group. The serum IL-6 level and nitrotyrosine content in the liver were significantly higher in the ECh group, as compared to the C and ES groups. There was evidence to support the dyslipidemic effect of studied compounds. *Conclusions*. The results indicate that oxidized plant sterols have a similar toxicity profile to that of oxycholesterols, including nitrosative stress induction, proinflammatory effect, and impaired lipid metabolism.

1. Introduction

Oxysterols have been implicated in the underlying mechanisms of inflammation-mediated diseases, such as atherosclerosis, neurodegenerative disorders, and cancer [1–4]. Through upregulation of NADPH oxidase (NOX) family enzymes [2], which are the main source of cellular reactive oxygen species (ROS) [5], oxysterols may cause extensive ROS generation, causing oxidative and nitrosative stress. Reactive nitrogen species act together with ROS causing cellular damage. Nitrotyrosine is one of the nitrosative stress markers. The cytokine system plays the crucial role in triggering nitrosative stress [6].

Apart from endogenous production, oxycholesterols may also be sourced from nutrition, in particular from cholesterol-rich foods undergoing long-term thermal processing and exposed to gamma irradiation or long-term storage [7].

Thus, the aim of the research was to assess the effect of 5α,6α-epoxyphytosterols and 5α,6α-epoxycholesterol on nitrosative stress and cytokine system in experimental animals.

2. Material and Methods

2.1. Animals. The protocol was approved by the Bioethical Committee for Animal Experimentation of the Medical University of Silesia in Katowice, Poland (approval no. 27/2007, dated April 17, 2007). All animals received humane care in compliance with the 8th edition of the *Guide for the Care and Use of Laboratory Animals* published by the National Institutes of Health [8].

Male Wistar rats, with the body weight of 130-180 g at baseline, were sourced from the Center for Experimental Medicine, Medical University of Silesia, in Katowice. During the experiment, the rats were kept on wood shaving bedding in standard single rodent cages, at the temperature of 20-25°C, with artificial lighting (a 12 h/12 h day/night cycle). The feed was administered once a day, and tap water was available ad libitum. Prior to the commencement of the experiment, the animals were kept in the conditions described above for an acclimation period of 2 weeks to ensure reproducible results.

The rats were divided into 3 groups (15 animals each), to receive the following:

(i) Feed containing 5α,6α-epoxyphytosterol acetate at 100 mg per 1 kg of feed (ES group)

(ii) Feed containing 5α,6α-epoxycholesterol acetate at 100 mg per 1 kg of feed (ECh group)

(iii) Oxysterol-free feed (controls, C group)

Daily estimated sterol dose was 10 mg per 1 kg of animal body weight (assuming the feed intake equal to 10% of animal body weight). Labofeed B (Wytwórnia Pasz, Kcynia, Poland), a standard laboratory maintenance feed for rodents, was used during the study. The feed was administered for 90 days. The animals were weighted before and after the experiment. After 3 months, the rats were anaesthetised with the mixture of ketamine (50 mg/kg), droperidol (1 mg/kg), and fentanyl (0.1 mg/kg) administered i.m. and euthanized by cardiac exsanguination and cervical dislocation.

2.2. Synthesis of 5α,6α-Epoxycholesterol and 5α,6α-Epoxyphytosterol Acetate. 5α,6α-Epoxycholesterol acetate and 5α,6α-epoxyphytosterol acetate were synthetized from cholesterol and sitosterol (Sigma-Aldrich, USA), respectively, by acetylation and subsequent oxidation with m-chlorperoxybenzoic acid (Sigma-Aldrich, USA) as described by McCarthy [9]. Next, the oxidation mixture was purified by column chromatography on silica gel using chloroform-acetone (4 : 1, *v*/*v*) as a mobile phase. Fractions containing pure ester were controlled by TLC technique (silica gel plates, solvent as above), pooled, and dried under vacuum. As per manufacturer's data sheet, sitosterol contains about 90% β-sitosterol and ca. 10% other phytosterols and phytostanols. Thus, its oxidation products were termed 5α,6α-epoxyphytosterols.

2.3. Blood Sample Collection. Blood samples were collected into serum clot activator tubes (Sarstedt, S-Monovette). Directly after centrifugation (900g for 10 min. at 4°C), serum samples were separated and stored at –70°C, until biochemical analyses were performed [10–12].

2.4. Liver Homogenate Preparation. After the rats were euthanized, their livers were quickly excised, weighed, and homogenised in cooled (4°C) PBS at 1 : 10. The prepared 10% homogenates were frozen at -70°C for further analyses.

Full homogenates were used for lipid determination, whereas the supernatant obtained with centrifugation (10 min., 20 000 rpm, 4°C) of defrosted homogenates was used for nitrotyrosine and TNF-alpha determinations.

The total cholesterol, triglycerides, nitrotyrosine, and TNF-α concentrations were assayed both in serum samples and liver homogenates. Additionally, we determined serum IL-1, IL-6, and LDL- and HDL-cholesterol levels.

2.5. Biochemical Analyses

2.5.1. Serum Lipid Determination. Total cholesterol and triglyceride concentrations were assayed in serum samples using a standard enzymatic method (Emapol, Poland). HDL-cholesterol was determined using an enzymatic method after precipitation of other lipoproteins with phosphotungstic acid (Emapol, Poland). For the LDL-cholesterol assay, a Quantolip LDL kit (Technoclone, Austria) was used. Total phospholipids in serum were assayed with the use of an enzymatic method (DiaSys GmbH, Germany). All analyses were performed using the EM280 biochemical analyzer (Emapol, Poland). Interassay and intra-assay coefficients of variation (CV) were below 3% and 5%, respectively, for all parameters.

2.5.2. Cholesterol and Triglycerides in Liver Homogenates. Tissue lipids were extracted by mixing 1 volume of 10% liver homogenate prepared in phosphate-buffered solution (PBS), with 9 volumes of isopropyl alcohol. After 24 hours, the

supernatant was separated from the protein precipitate by centrifugation, and 1 mL of the clear supernatant was collected to two glass tubes.

In order to determine the *cholesterol* concentration, the solvent was dried under reduced pressure and the dry residue was dissolved in 0.1 mL of Triton X-100-methoxyethanol (2 : 8, *v*/*v*) mixture. After, 1 mL of cholesterol reagent (Human, Germany) was added, the samples were incubated in a water bath at 37°C for 30 minutes with continuous shaking, and the absorbance was measured at 510 nm against a blank. The calibration solution was cholesterol dissolved in the Triton X-100-methoxyethanol (2 : 8, *v*/*v*) mixture.

To determine *triglyceride* concentrations, the dry residue in the second tube was dissolved in 1 mL of Triton X100-methoxyethanol mixture (2 : 8, *v*/*v*) and the determination was performed on the Technicon RA-XT analyzer according to the standard serum processing procedure.

All results were expressed as mg/g (wet matter basis).

2.5.3. Determination of Inflammatory Cytokines. The concentration of TNF-α, IL-6, and IL-1β in rat serum and TNF-α in rat liver homogenates was determined by ELISA using Diaclone kits (France): rat TNF-α EliPair, cat. no. 872.010.010; murine IL-6 EliPair, cat. no. 861.020.010; and rat IL-1β ELISA kit, cat. no. 670.040.192 according to the manufacturer's instructions. The absorbance was measured using the PowerWave XS microplate reader (BioTek, USA), and data was processed using the KC Junior software bundle (BioTek, USA). The within-run coefficient of variation for the TNF-α, IL-1β, and IL-6 determination was 5.2%, 7.1%, and 4.8%, respectively.

The results of TNF-α concentration in liver homogenates were expressed as pg/mg total protein determined using the Lowry method [13]. Serum TNF-α, IL-1β, and IL-6 results were expressed as pg/mL.

2.5.4. Determination of Nitrotyrosine. Nitrotyrosine concentration was determined by ELISA using our own rabbit anti-nitrotyrosine polyclonal antibodies (Immunogen: peroxynitrite-modified keyhole limpet hemocyanin), which were coated on an ELISA plate after purification by affinity chromatography within the column with peroxynitrite-treated bovine serum albumin (BSA). After a 2-hour incubation with the specimens, the plate was washed and biotin-labelled murine anti-nitrotyrosine monoclonal antibody (Cayman Chemicals Company, cat. no. 10006966) was added. The dilution of the working solution was 1 : 1000. After another incubation with peroxidase-labelled streptavidin (DakoCytomation, Denmark), the 3,3′,5,5′-Tetramethylbenzidine (TMB) Liquid Substrate System for ELISA (TMB Supersenstive, Sigma-Aldrich, USA) was added. After 20-30 minutes, 0.5 M sulphuric acid solution was added as a stop solution. The absorbance was measured using the Power Wave XS microplate reader (BioTek, USA), and data was processed using the KC Junior software bundle (BioTek, USA). Peroxynitrite-treated rabbit serum albumin (RSA) was used as a standard. The nitrotyrosine content was determined using spectrophotometry based on the molar absorption coefficient of 4300 M^{-1} cm^{-1} [14]. Peroxynitrite was obtained as the product of the H_2O_2, $NaNO_2$, and HCl reaction with subsequent addition of NaOH solution [15]. The ELISA calibration curve was within the nitrated RSA concentration range of 0-1000 nmol/L, while the within-run coefficient of variation was 4.6%. The serum nitrotyrosine results were expressed in nmol/L; liver nitrotyrosine results were expressed in nmol/g protein.

2.6. Statistical Analyses. Statistical analyses were performed using STATISTICA 13 PL (Tibco Inc., Palo Alto, CA, USA), StataSE 12.0 (StataCorp LP, TX, U.S.), and R software (CRAN). The p value below 0.05 was considered significant for all comparisons. All tests were two-tailed. Imputations were not done for missing data. Nominal and ordinal data were expressed as percentages, while interval data were expressed as the mean value ± standard deviation if normally distributed, or as median/interquartile range if the distribution was skewed or nonnormal. Distribution of variables was evaluated by the Shapiro-Wilk test, and homogeneity of variances was assessed using Levene's test. One-way parametric ANOVA with the Tukey post hoc test was used for all comparisons.

3. Results

For rats exposed to epoxysterols and low-cholesterol feed, there was no effect of dietary intake on serum total cholesterol and LDL- and HDL-cholesterol levels. There was no significant between-group difference in the levels of the above markers. However, triglyceride concentrations were significantly higher in the ECh group than in controls. Serum total phospholipid levels were significantly lower in the ECh group than in controls. Furthermore, there was a significant difference between ECh and ES groups in total phospholipid levels (Table 1).

Liver homogenate analysis demonstrated significant differences in total cholesterol levels between the ES and C groups ($p < 0.05$). There were no significant between-group differences in triglyceride levels in liver homogenates (Table 2).

The analysis of serum inflammatory cytokine (IL-1β, IL-6, and TNF-α) levels demonstrated that exposure to epoxysterols induces their biosynthesis. A significant increase from baseline in serum IL-1β and TNF-α levels was shown in both ECh and ES groups. The IL-6 levels were significantly higher in the ECh group as compared to the ES group and controls. Furthermore, the evidence of increased liver production of TNF-α was demonstrated in both groups exposed to oxysterols (Table 3).

Serum nitrotyrosine levels were significantly higher in both oxysterol-exposed groups (ECh and ES) than in controls (C). However, only the ECh group had significantly higher nitrotyrosine levels in liver homogenate (Table 4).

4. Discussion

There is ample evidence to support extensive and multidirectional effect of oxycholesterol biological activity, whereas their mechanism of action has not been fully understood to

Table 1: Serum lipid levels (mean value ± standard deviation (SD)) in rats exposed to 5α,6α-epoxycholesterol (ECh group) and 5α,6α-epoxyphytosterols (ES group) vs. controls (C group).

	ECh group	ES group	C group	p
Total cholesterol (mg/dL)	51.6 ± 7.6	52.8 ± 7.5	47.1 ± 6.3	NS
Triglycerides (mg/dL)	58.3 ± 12.4	52.7 ± 10.0	44.9 ± 10.7	<0.01
Phospholipids (mg/dL)	78.6 ± 9.3*	88.5 ± 10.1	89.3 ± 9.2	<0.01
HDL-cholesterol (mg/dL)	22.2 ± 3.6	25.1 ± 4.3	25.0 ± 2.8	NS
HDL-cholesterol (%TCh)	44.0 ± 9.9	48.6 ± 12	53.5 ± 6.8	NS
LDL-cholesterol (mg/dL)	17.7 ± 7.9	17.2 ± 9.6	13.2 ± 5.3	NS

%TCh: total cholesterol; *$p < 0.05$ vs. ES group; NS: nonsignificant.

Table 2: Total cholesterol and triglyceride levels (mean value ± standard deviation (SD)) in liver homogenates of rats exposed to 5α,6α-epoxycholesterol (ECh group) and 5α,6α-epoxyphytosterols (ES group) vs. controls (C group).

	ECh group	ES group	C group	p
Total cholesterol (mg/g tissue)	2.46 ± 0.21	2.58 ± 0.33*	2.32 ± 0.17	<0.05
Triglycerides (mg/g tissue)	22.7 ± 3.0	20.6 ± 3.7	21.2 ± 3.2	NS

*$p < 0.05$ vs. controls (C); NS: nonsignificant.

Table 3: Inflammatory cytokine (TNF-α, IL-1β, and IL-6) levels (mean value ± standard deviation (SD)) in serum and liver homogenates of rats exposed to 5α,6α-epoxycholesterol (ECh group) and 5α,6α-epoxyphytosterols (ES group) vs. controls (C group).

	ECh group	ES group	C group	p
Serum TNF-α (pg/mL)	43.3 ± 10.6	36.4 ± 9.5	22.8 ± 5	<0.001
Serum IL-1β (pg/mL)	4.9 ± 2.7	4.4 ± 2	1.1 ± 1.4	<0.001
Serum IL-6 (pg/mL)	40.4 ± 9.5	26.9 ± 9.1	20.5 ± 6.1	<0.001
Liver TNF-α (pg/mg protein)	284.1 ± 45.2	288.2 ± 33.1	208.1 ± 23.3	<0.001

Table 4: Nitrotyrosine levels in serum and liver homogenates of rats exposed to 5α,6α-epoxycholesterol (ECh group) and 5α,6α-epoxyphytosterols (ES group) vs. controls (C group). The values were expressed as the mean ± standard deviation (SD).

	ECh group	ES group	C group	p
Serum nitrotyrosine (nmol/L)	60.5 ± 13.4	47.7 ± 11.5	34.3 ± 8.4	<0.001
Liver nitrotyrosine (nmol/g protein)	119.3 ± 24.1	94.9 ± 21.0	98.4 ± 8.4	<0.01

date. However, experimental studies in animals exposed to oxycholesterol-enriched feed provide contradictory data on the potential effect of oxycholesterols on the development of atherosclerosis [16–18], although most studies confirm atherogenic effect of oxidized cholesterol derivatives, in particular cholestantriol.

On the other hand, there are significantly fewer studies on the effect of oxyphytosterols on lipid metabolism and development of atherosclerosis in animals. The effect of oxidized phytosterols on lipid metabolism in experimental animals suggests that it is possible to regulate triglyceride and cholesterol concentrations on multiple levels, e.g., by regulating the endogenous lipid synthesis, mediating gastrointestinal lipid absorption, or altering lipid catabolism. For instance, the ability of 5-campestenone to activate β-oxidation pathway enzymes and simultaneously inhibit the enzymatic mediators of fatty acid synthesis, by activating the PPAR-α receptor and other mechanisms, has been demonstrated [19, 20]. It was capable of lowering serum triglyceride levels in rodent serum [21] and liver [19], which we did not confirm in our study. Bang et al. compared the effect of oxyphytosterols obtained by thermal oxidation of phytosterols and oxysterols (oxidized cholesterol derivatives) on serum and liver triglyceride levels in mice, finding a similar effect of both compounds on the above parameters. He demonstrated a reduction of the serum triglyceride level with no change of its liver content [21]. Similarly, hypolipidemic effect of 24-ethylcholest-4-en-3-one on experimental animals has also been reported [22]. Furthermore, meta-analyses concerning the effects of nonoxidized plant sterols and stanols on the lipid concentrations in human blood indicate their potential for lowering serum triglyceride levels [23, 24]. Considering the above, it is unclear whether the ability to reduce triglyceride levels is a common

characteristic shared by all oxidized and nonoxidized sterols or whether it results from contamination of sterol- and stanol-enriched food products with sterol and stanol oxidation products.

In our experiment, we observed different effects of oxysterols: in the ECh group, the serum triglyceride levels increased alongside decreased serum phospholipid levels, with no difference in triglyceride content in the liver. The liver cholesterol content was significantly higher only in the ES group. The observed changes can be partially explained by the dietary induction of acute phase reaction, which may be one of the causes for the increased production of triglyceride-rich lipoproteins in the liver and their elimination from plasma [25]. The concomitant decrease in serum phospholipid levels may additionally promote the development of atherosclerosis. Being relatively phospholipid-rich, lipoproteins such as the HDL are good cholesterol acceptors and the decrease in HDL phospholipid content may inhibit the reverse cholesterol transport from peripheral tissues back to the liver. A decreased phospholipid/cholesterol ratio was found in plasma lipoproteins, erythrocyte membranes, hepatocytes, and endothelial cells as a typical metabolic abnormality in atherosclerosis [26].

The excessive hepatic accumulation of cholesterol may also be explained by the effect of hyperhomocysteinemia on its endogenous biosynthesis, that is, an increased expression of HMG-CoA reductase in hepatocytes, activation of the mevalonate pathway, and resultant excessive cholesterol synthesis [27]. Additional exposure of animals to oxycholesterols or oxyphytosterols may exacerbate endothelial dysfunction, increasing homocysteinemia, which additionally intensifies the cholesterol biosynthesis in the liver.

The analysis of the effect of oxyphytosterols on the development of atherosclerosis in Apo E knockout mice [28] did not show any differences in serum and aortic tissue cholesterol levels between the group exposed to oxysterols and the group receiving only animal fat-rich feed. Additionally, in the group of mice fed with oxysterols, oxidative stress measured with 8-iso-prostaglandin F2α (8-iso-PGF2α) concentration was significantly increased.

Chronic inflammation of the arterial wall mediated by cytokines, oxidative-modified lipoproteins, and other endothelium-damaging factors is one of the most important mechanisms accelerating the development of atherosclerosis. The majority of proinflammatory cytokines show pleiotropic effects, affecting various cells, including those involved in the development of atherosclerosis and chronic systemic inflammatory response seen in atherosclerosis [29, 30]. Local cytokine production is responsible for extracellular matrix overproduction, growth and proliferation of vascular wall cells, recruitment of vascular luminal cells, endothelial dysfunction, and other processes, which ultimately determine the development of atherosclerosis and its progression rate [30].

The studies of animal models of atherosclerosis demonstrated a marked increase of IL-6 synthesis in response to dietary cholesterol intake [31–33]. Although the data on the effect of oxysterols on cytokine biosynthesis is quite fragmented, it seems to support the oxysterol capability to induce inflammation by causing imbalance between anti-inflammatory and proinflammatory cytokines [34, 35].

The analysis of IL-6 concentrations determined in our experiment indicates that its biosynthesis is mediated by exogenous oxycholesterols, whereas the effect was only significant in the ECh group. However, the elevated IL-6 levels in the ECh group did not affect the C-reactive protein (CRP) levels (unpublished data).

The *tumor necrosis factor* α (*TNF-*α) is a pleiotropic proinflammatory cytokine produced by various cell types, e.g., macrophages, leukocytes, vascular endothelial cells, adipocytes, smooth muscle cells, and cardiomyocytes [25, 36]. It affects the local immune activation by increasing the production of IL-1 and IL-6, thus stimulating endothelial cells to synthesize and release various adhesion molecules (ICAM-1, VCAM-1, and P- and E-selectins). Furthermore, it shows a procoagulant effect and, alongside IL-1 and IL-6, an antifibrinolytic effect [36]. Furthermore, TNF-α stimulates macrophages to release metalloproteinases, which leads to accelerated degradation and destabilization of the fibrous cover of atherosclerotic plaques, triggering dyslipidemia, insulin resistance, and endothelial dysfunction.

The analysis of changes in serum TNF-α levels in rats during exposure to epoxycholesterols and epoxyphytosterols indicates that it is one of the key variables to differentiate between the groups, as it increased significantly in both ECh and ES groups unlike in controls. Similarly, we observed a significant increase in TNF-α production in the liver in animals exposed to oxidized sterols (ECh and ES groups). In the light of the published data, the observed changes in TNF-α expression confirm the development of systemic and local inflammation (liver). It has been demonstrated that the diet activates a number of signalling pathways involved in lipid metabolism (SREBP-1) and inflammatory response (PPARγ), as well as TNF-α, INFγ, TGFβ1, and PDGF gene expression in Apo E/Leiden 3 transgenic mice fed with cholesterol-rich feed [37]. In line with the above, Ferre et al. demonstrated an increased expression of the IL-1α gene in the liver and decreased expression of TNF-α receptors (TNF-α receptor subfamily member 6) in Apo E-/- mice [38]. It was also shown that by activating liver X-receptor (LXR), 22(R)-hydroxycholesterol significantly increases TNF-α mRNA expression and TNF-α protein production in cytosol of human hepatocytes [39].

The increase in TNF-α production observed in animals exposed to oxysterols may be one of the factors, which exacerbate dyslipidemia, i.e., the increase in serum triglyceride levels in the ECh group and increase in liver cholesterol content. Its mechanism involves increased hepatic fatty acid biosynthesis by TNF-α and their release from the adipose tissue as well as impaired clearance of triglyceride-rich lipoproteins (mainly VLDL) from plasma [25]. The TNF-α stimulates lipolysis in adipose tissue by activating JNK and p44/42 kinases via increased expression of hormone-sensitive lipase (HSL) and adipose triglyceride lipase (ATGL), without altering their core activity or perlipin expression [25, 40, 41]. Another mechanism of TNF-α action seen in rodents involves inhibiting the expression of G protein-coupled receptors (GPCRs) present on the surface of adipocytes,

which in turn inhibits the antilipolytic effect of adenosine [42]. The associated increase in plasma-free fatty acid concentrations is considered one of the major contributors of insulin resistance and disorders of carbohydrate metabolism as well as hypertriglyceridemia and metabolic syndrome.

Increased liver biosynthesis of fatty acids mediated by TNF-α and other proinflammatory cytokines (e.g., IL-1 and IL-6) manifests as increased endogenous triglyceride-rich lipoprotein levels (mainly VLDL). Its mechanism involves upregulated hepatic synthesis of citrate, an allosteric carboxylase activator of Acetyl-CoA (acetyl-coenzyme A), which is the key enzyme in the fatty acid synthesis pathway [43].

The effect of TNF-α on cholesterol metabolism, on the other hand, differs significantly between primates and rodents. In rodents, a slow increase in serum cholesterol levels and its liver biosynthesis is observed (as shown in our experiment), whereas in humans and other primates, either no effect of TNF-α on plasma levels of total cholesterol and LDL-cholesterol or their reduced plasma levels have been seen. On the other hand, the mechanisms leading to increased TNF-α-mediated cholesterol levels in rodents include increased activity of HMG-CoA reductase and decreased activity of squalene monooxygenase in the liver [44, 45].

The proatherogenic effect of IL-1 includes T- and B-cell stimulation, increased proliferation and differentiation of neutrophils and monocytes, stimulating the expression of adhesive molecules (ICAM-1, VCAM-1), increased vascular endothelial permeability, stimulation of smooth muscle proliferation, and extracellular matrix synthesis [46]. The studies in animal models of atherosclerosis demonstrated an increased expression of IL-1α and IL-1β mRNAs in the aortas of animals fed with cholesterol. Similarly, their expression in the arterial wall was detectable in immunohistochemical studies [47]. The in vitro exposure of human macrophages or HUVEC cells to oxycholesterols led to an increased IL-1β production [48]. It is likely that a similar effect may also occur during the in vivo exposure to oxysterols, as seen in our experimental studies, where exposure to both epoxycholesterols and epoxyphytosterols resulted in a marked increase in serum IL-1β concentration, which was more pronounced in the ECh than ES group. The 3-nitrotyrosine, a product of interaction of tyrosine residues with peroxynitrite, plays a special role in oxidative stress-mediated protein damage. The formation of peroxynitrite, a highly reactive molecule, has been demonstrated in a number of chronic inflammatory conditions and cases of perfusion-reperfusion injury. The cells capable of releasing peroxynitrite include vascular endothelial cells, monocytes/macrophages, and neutrophils [49]. Peroxynitrite modifies both extracellular (e.g., plasma) and intracellular (e.g., antioxidant enzymes) proteins, especially the superoxide dismutase (SOD) [50]. Increased protein nitration, e.g., plasminogen or tPA, correlates with impaired coagulation and fibrinolysis, e.g., in diabetic patients [51], whereas an increased nitrotyrosine level may be an independent cardiovascular risk factor [52]. Immunohistochemical studies confirmed the presence of 3-nitrotyrosine residues in the vascular wall in atherosclerosis [53]. Other proteins particularly susceptible to in vivo nitration and chlorination are apolipoproteins, especially Apo A1, present in HDL particles [54]. It has been demonstrated that their exposure to peroxynitrite (also referred to as nitrosative stress) changes the properties of HDL leading to the loss of its antioxidant effect and capability of reverse cholesterol transport. An increased myeloperoxidase activity is an additional factor, which intensifies HDL nitration [54, 55].

The studies assessing changes in nitrated protein levels in animal models of atherosclerosis or hypercholesterolemia are very scarce and include mainly the results of nitrotyrosine determination in plasma and organ proteins of transgenic mice (Apo E-/-; iNOS-/-, or Apo E-/-). The iNOS gene deficiency very significantly inhibited the synthesis of nitrated proteins and slowed the progression of atherosclerosis [56]. Rat exposure to feed containing 2% of cholesterol led to an increase in serum 3-nitrotyrosine levels by over 100%, compared to animals receiving standard feed [57]. Similarly, experimentally induced hypercholesterolemia resulted in increased 3-nitrotyrosine synthesis in brains of rabbits [58]. Our experiment demonstrated that animal exposure to 5α,6α-epoxycholesterol or epoxyphytosterols in low-cholesterol feed leads to an increased 3-nitrotyrosine synthesis (increased serum nitrated proteins). Nevertheless, the 3-nitrotyrosine content in the liver tissue was significantly elevated only in the ECh group.

Comparing the results of most experimental animal studies with the oxysterol-associated risk in humans, it should be noted that the daily dietary intake of oxidized cholesterol derivatives by experimental animals in our experiment and in other studies reached 10 mg/kg body weight [59], which would translate into a daily intake of about 175-700 mg of oxysterols and represents at least 100% of the average daily cholesterol intake in an adult. Therefore, it is highly unlikely that a diet of a modern individual can comply with these assumptions. Another issue is interspecies differences between experimental animals (usually rabbits, rodents, or birds) and humans.

The limitations of the current study include a small sample size and the inability to monitor the dynamics of changes in the studied parameters, as the inflammatory response changes rapidly throughout the exposure to the studied compounds. Similarly, our results warrant further studies on the effect of other phytosterols and cholesterol derivatives in animal models.

5. Conclusion

Rat exposure to 5α,6α-epoxycholesterols or epoxyphytosterols increases nitrosative stress (increased production of 3-nitrotyrosine) and proinflammatory cytokine synthesis (TNF-α, IL-1β, and IL-6). This leads to secondary disorder of lipid metabolism in animals.

Data Availability

All data is included in the tables within the article.

Conflicts of Interest

The authors declare that there are no conflicts of interest regarding the publication of this paper.

Acknowledgments

This work was supported by the grants from the Medical University of Silesia (KNW-2-156/09).

References

[1] A. Attanzio, A. Frazzitta, A. Cilla, M. A. Livrea, L. Tesoriere, and M. Allegra, "7-Keto-cholesterol and cholestan-3beta, 5alpha, 6beta-triol induce eryptosis through distinct pathways leading to NADPH oxidase and nitric oxide synthase activation," *Cellular Physiology and Biochemistry*, vol. 53, no. 6, pp. 933–947, 2019.

[2] G. Poli, F. Biasi, and G. Leonarduzzi, "Oxysterols in the pathogenesis of major chronic diseases," *Redox Biology*, vol. 1, no. 1, pp. 125–130, 2013.

[3] B. Sottero, P. Gamba, S. Gargiulo, G. Leonarduzzi, and G. Poli, "Cholesterol oxidation products and disease: an emerging topic of interest in medicinal chemistry," *Current Medicinal Chemistry*, vol. 16, no. 6, pp. 685–705, 2009.

[4] T. Wielkoszyński, J. Zalejska-Fiolka, J. K. Strzelczyk et al., "Oxysterols increase inflammation, lipid marker levels and reflect accelerated endothelial dysfunction in experimental animals," *Mediators of Inflammation*, vol. 2018, Article ID 2784701, 9 pages, 2018.

[5] T. Wielkoszyński, J. Zalejska-Fiolka, J. K. Strzelczyk et al., "5α,6α-Epoxyphytosterols and 5α,6α-epoxycholesterol increase oxidative stress in rats on low-cholesterol diet," *Oxidative Medicine and Cellular Longevity*, vol. 2019, Article ID 1983975, 8 pages, 2019.

[6] A. Stanek, A. Gadowska-Cicha, K. Gawron et al., "Role of nitric oxide in physiology and pathology of the gastrointestinal tract," *Mini-Reviews in Medicinal Chemistry*, vol. 8, no. 14, pp. 1549–1560, 2008.

[7] D. Innosa, A. Ianni, F. Palazzo et al., "High temperature and heating effect on the oxidative stability of dietary cholesterol in different real food systems arising from eggs," *European Food Research and Technology*, vol. 245, no. 7, pp. 1533–1538, 2019.

[8] Guide for the Care and Use of Laboratory Animals, *National Research Council (US) Committee for the Update of the Guide for the Care and Use of Laboratory Animals*, National Academies Press (US), Washington (DC), 8th edition, 2011, http://www.ncbi.nlm.nih.gov/books/NBK54050/.

[9] F. O. McCarthy, J. Chopra, A. Ford et al., "Synthesis, isolation and characterisation of β-sitosterol and β-sitosterol oxide derivatives," *Organic and Biomolecular Chemistry*, vol. 3, no. 16, pp. 3059–3065, 2005.

[10] A. Stanek, A. Cholewka, T. Wielkoszyński, E. Romuk, K. Sieroń, and A. Sieroń, "Increased levels of oxidative stress markers, soluble CD40 ligand, and carotid intima-media thickness reflect acceleration of atherosclerosis in male patients with ankylosing spondylitis in active phase and without the classical cardiovascular risk factors," *Oxidative Medicine and Cellular Longevity*, vol. 2017, Article ID 9712536, 8 pages, 2017.

[11] A. Stanek, A. Cholewka, T. Wielkoszyński, E. Romuk, and A. Sieroń, "Whole-body cryotherapy decreases the levels of inflammatory, oxidative stress, and atherosclerosis plaque markers in male patients with active-phase ankylosing spondylitis in the absence of classical cardiovascular risk factors," *Mediators of Inflammation*, vol. 2018, Article ID 8592532, 11 pages, 2018.

[12] A. Stanek, K. Sieroń-Stołtny, E. Romuk et al., "Whole-body cryostimulation as an effective method of reducing oxidative stress in healthy men," *Advances in Clinical and Experimental Medicine*, vol. 25, no. 6, pp. 1281–1291, 2016.

[13] O. H. Lowry, N. J. Rosebrough, A. L. Farr, and R. J. Randall, "Protein measurement with the Folin phenol reagent," *The Journal of Biological Chemistry*, vol. 193, no. 1, pp. 265–275, 1951.

[14] A. M. M. Kahlf, "Analysis of Plant Sterols and Oxysterols in the Serum of Patients with Sitosterolemia under Different Drug Treatments," *Doctoral Dissertation*, Rheinischen Friedrich-Wilhelms-Universität Bonn, Bonn, 2007.

[15] J. S. Beckman, J. Chen, H. Ischiropoulos, and J. P. Crow, "[23] Oxidative chemistry of peroxynitrite," *Methods in Enzymology*, vol. 233, pp. 229–240, 1994.

[16] A. J. Brown and W. Jessup, "Oxysterols and atherosclerosis," *Atherosclerosis*, vol. 142, no. 1, pp. 1–28, 1999.

[17] D. A. Larsson, S. Baird, J. D. Nyhalah, X. M. Yuan, and W. Li, "Oxysterol mixtures, in atheroma-relevant proportions, display synergistic and proapoptotic effects," *Advances in Free Radical Biology and Medicine*, vol. 41, no. 6, pp. 902–910, 2006.

[18] L. L. Smith, "Review of progress in sterol oxidations: 1987-1995," *Lipids*, vol. 31, no. 5, pp. 453–487, 1996.

[19] I. Ikeda, R. Konno, T. Shimizu, T. Ide, N. Takahashi, and T. Kawada, "Campest-5-en-3-one, an oxidized derivative of campesterol, activates PPARα, promotes energy consumption and reduces visceral fat deposition in rats," *Biochimica et Biophysica Acta*, vol. 1760, no. 5, pp. 800–807, 2006.

[20] K. Suzuki, M. Tanaka, R. Konno, and Y. Kaneko, "Effects of 5-campestenone (24-methylcholest-5-en-3-one) on the type 2 diabetes mellitus model animal C57BL/KsJ-db/db mice," *Hormone and Metabolic Research*, vol. 34, no. 3, pp. 121–126, 2002.

[21] H. Bang, C. Arakawa, M. Takada, M. Sato, and K. Imaizumi, "A comparison of the potential unfarorable effects of oxycholesterol and oxyphytosterol in mice: different effects, on cerebral 24S-hydroxycholesterol and serum triacyloglycerols levels," *Bioscience, Biotechnology, and Biochemistry*, vol. 72, no. 12, pp. 3128–3133, 2014.

[22] K. Suzuki, T. Shimizu, and T. Nakata, "The cholesterol metabolite cholest-4-en-3-one and its 3-oxo derivatives suppress body weight gain, body fat accumulation and serum lipid concentration in mice," *Bioorganic and medicinal chemistry letters*, vol. 8, no. 16, pp. 2133–2138, 1998.

[23] E. Hovenkamp, I. Demonty, J. Plat, D. Lutjohann, R. P. Mensink, and E. A. Trautwein, "Biological effects of oxidized phytosterols: A review of the current knowledge," *Progress in lipid research*, vol. 47, no. 1, pp. 37–49, 2008.

[24] E. Naumann, J. Plat, A. D. Kester, and R. P. Mensink, "The baseline serum lipoprotein profile is related to plant stanol induced changes in serum lipoprotein cholesterol and triacylglycerol concentrations," *Journal of the American College of Nutrition*, vol. 27, no. 1, pp. 117–126, 2013.

[25] C. Popa, M. G. Netea, P. L. van Riel, J. W. van der Meer, and A. F. Stalenhoef, "The role of TNF-α in chronic inflammatory conditions, intermediary metabolism, and cardiovascular risk," *Journal of Lipid Research*, vol. 48, no. 4, pp. 751–762, 2007.

[26] J. Michalak, A. Kądziołka, R. Pruszkowska, A. Ledwożyw, and A. Madejczyk, "Compensatory mechanisms in erythrocyte

lipids in patients with atherosclerosis," *Lipids*, vol. 23, no. 5, pp. 476–480, 1988.

[27] N. Wu, L. K. Sarna, Y. L. Siow, and O. Karmin, "Regulation of hepatic cholesterol biosynthesis by berberine during hyperhomocysteinemia," *American journal of physiology, Regulatory, integrative and comparative physiology*, vol. 300, no. 3, pp. R635–R643, 2011.

[28] H. Tomoyori, Y. Kawata, T. Higuchi et al., "Phytosterol oxidation products are absorbed in the intestinal lymphatics in rats but do not accelerate atherosclerosis in apolipoprotein E-deficient mice," *The Journal of Nutrition*, vol. 134, no. 7, pp. 1690–1696, 2004.

[29] H. A. Lehr, T. A. Sagban, C. Ihling et al., "Immunopathogenesis of atherosclerosis: endotoxin accelerates atherosclerosis in rabbits on hypercholesterolemic diet," *Circulation*, vol. 104, no. 8, pp. 914–920, 2001.

[30] E. W. Raines and N. Ferri, "Thematic review series: the immune system and atherogenesis. Cytokines affecting endothelial and smooth muscle cells in vascular disease," *Journal of Lipid Research*, vol. 46, no. 6, pp. 1081–1092, 2005.

[31] M. Hongbao and C. Shen, "Relationship of inflammation/-thrombosis and C-reactive protein (CRP), plasminogen activator inhibitor 1 (PAI-1), inteleukin-6 (IL-6), inteleukin-1 (IL-1), tissue factor (TF), tumor necrosis factor-alpha (TNF-α), tTssue plasminogen activator (tPA), CD40," *Nature and Science*, vol. 5, no. 4, pp. 61–74, 2007.

[32] R. Largo, O. Sánchez-Pernaute, M. E. Marcos et al., "Chronic arthritis aggravates vascular lesions in rabbits with atherosclerosis: a novel model of atherosclerosis associated with chronic inflammation," *Arthritis and Rheumatism*, vol. 58, no. 9, pp. 2723–2734, 2008.

[33] R. Takeda, E. Suzuki, H. Satonaka et al., "Blockade of endogenous cytokines mitigates neointimal formation in obese Zucker rats," *Circulation*, vol. 111, no. 11, pp. 1398–1406, 2005.

[34] S. Lemaire-Ewing, A. Berthier, M. C. Royer et al., "7β-Hydroxycholesterol and 25-hydroxycholesterol-induced interleukin-8 secretion involves a calcium-dependent activation of c-fos via the ERK1/2 signaling pathway in THP-1 cells," *Cell Biology and Toxicology*, vol. 25, no. 2, pp. 127–139, 2009.

[35] P. Palozza, R. Simone, A. Catalano et al., "Lycopene prevents 7-ketocholesterol-induced oxidative stress, cell cycle arrest and apoptosis in human macrophages," *The Journal of Nutritional Biochemystry*, vol. 21, no. 1, pp. 34–46, 2010.

[36] N. Frangogiannis, "Targeting the inflammatory response in healing myocardial infarcts," *Current Medicinal Chemistry*, vol. 13, no. 16, pp. 1877–1893, 2006.

[37] R. Kleemann, L. Verschuren, M. J. van Erk et al., "Atherosclerosis and liver inflammation induced by increased dietary cholesterol intake: a combined transcriptomics and metabolomics analysis," *Genome Biology*, vol. 8, no. 9, p. R200, 2007.

[38] N. Ferré, M. Martínez-Clemente, M. López-Parra et al., "Increased susceptibility to exacerbated liver injury in hypercholesterolemic ApoE-deficient mice: potential involvement of oxysterols," *American journal of physiology Gastrointestinal and liver physiology*, vol. 296, no. 3, pp. G553–G562, 2009.

[39] M. S. Landis, H. V. Patel, and J. P. Capone, "Oxysterol activators of liver X receptor and 9-cis-retinoic acid promote sequential steps in the synthesis and secretion of tumor necrosis factor-alpha from human monocytes," *The Journal of Biolical Chemistry*, vol. 277, no. 7, pp. 4713–4721, 2002.

[40] S. Kralisch, J. Klein, U. Lossner et al., "Isoproterenol, TNFα, and insulin downregulate adipose triglyceride lipase in 3T3-L1 adipocytes," *Molecular and Cellular Endocrinology*, vol. 240, no. 1-2, pp. 43–49, 2005.

[41] M. Ryden, E. Arvidsson, L. Blomqvist, L. Perbeck, A. Dicker, and P. Arner, "Targets for TNF-α-induced lipolysis in human adipocytes," *Biochemical and biophysical research communications*, vol. 318, no. 1, pp. 168–175, 2004.

[42] S. Gasic, B. Tian, and A. Green, "Tumor necrosis factor α stimulates lipolysis in adipocytes by decreasing GiProtein concentrations," *The Journal of Biological Chemistry*, vol. 274, no. 10, pp. 6770–6775, 1999.

[43] C. Grunfeld, M. Soued, S. Adi, A. H. Moser, C. A. Dinarello, and K. R. Feingold, "Evidence for two classes of cytokines That stimulate hepatic lipogenesis: relationships among tumor necrosis factor, interleukin-1 and Interferon-Alpha," *Endocrinology*, vol. 127, no. 1, pp. 46–54, 1990.

[44] R. A. Memon, C. Grunfeld, A. H. Moser, and K. R. Feingold, "Tumor necrosis factor mediates the effects of endotoxin on cholesterol and triglyceride metabolism in mice," *Endocrinology*, vol. 132, no. 5, pp. 2246–2253, 1993.

[45] R. A. Memon, I. Shechter, A. H. Moser, K. Shigenaga, C. Grunfeld, and K. R. Feingold, "Endotoxin, tumor necrosis factor, and interleukin-1 decrease hepatic squalene synthase activity, protein, and mRNA levels in Syrian hamsters," *Journal of Lipid Research*, vol. 38, no. 8, pp. 1620–1629, 1997.

[46] R. R. Packard and P. Libby, "Inflammation in atherosclerosis: from vascular biology to biomarker discovery and risk prediction," *Clinical Chemistry*, vol. 54, no. 1, pp. 24–38, 2008.

[47] S. M. Rahman, A. M. Van Dam, M. Schultzberg, and M. Crisby, "High cholesterol diet results in increased expression of interleukin-6 and caspase-1 in the brain of apolipoprotein E knockout and wild type mice," *Journal of Neuroimmunology*, vol. 169, no. 1-2, pp. 59–67, 2005.

[48] T. Rosklint, B. G. Ohlsson, O. Wiklund, K. Norén, and L. M. Hultén, "Oxysterols induce interleukin-1beta production in human macrophages," *European Journal of Clinical Investigation*, vol. 32, no. 1, pp. 35–42, 2002.

[49] R. S. Ronson, M. Nakamura, and J. Vinten-Johansen, "The cardiovascular effects and implications of peroxynitrite," *Cardiovascular Research*, vol. 44, no. 1, pp. 47–59, 1999.

[50] C. Quijano, D. Hernandez-Saavedra, L. Castro, J. M. McCord, B. A. Freeman, and R. Radi, "Reaction of peroxynitrite with Mn-superoxide dismutase," *The Journal of Biological Chemistry*, vol. 276, no. 15, pp. 11631–11638, 2001.

[51] V. G. Nielsen, J. P. Crow, F. Zhou, and D. A. Parks, "Peroxynitrite inactivates tissue plasminogen activator," *Anesthesia and Analgesia*, vol. 98, no. 5, pp. 1312–1317, 2004.

[52] R. K. Upmacis, "Atherosclerosis: a link between lipid intake and protein tyrosine nitration," *Lipid Insights*, vol. 2008, no. 2, pp. 75–88, 2008.

[53] K. M. Cromheeke, M. M. Kock, G. R. de Meyer, and A. G. Herman, "Inducible nitric oxide synthase colocalizes with signs of lipid oxidation/peroxidation in human atherosclerotic plaques," *Cadiovascacular Research*, vol. 43, no. 3, pp. 744–754, 1999.

[54] B. Shao, C. Bergt, X. Fu et al., "Tyrosine 192 in apolipoprotein A-I is the major site of nitration and chlorination by myeloperoxidase, but only chlorination markedly impairs ABCA1-dependent cholesterol transport," *The Journal of Biological Chemistry*, vol. 280, no. 7, pp. 5983–5993, 2005.

[55] S. Pennathur, C. Bergt, B. Shao et al., "Human atherosclerotic intima and blood of patients with established coronary artery disease contain high density lipoprotein damaged by reactive nitrogen species," *The Journal of Biological Chemistry*, vol. 279, no. 41, pp. 42977–42983, 2004.

[56] R. K. Upmacis, M. J. Crabtree, R. S. Deeb et al., "Profound biopterin oxidation and protein tyrosine nitration in tissues of ApoE-null mice on an atherogenic diet: contribution of inducible nitric oxide synthase," *American journal of physiology Heart and circulatory physiology*, vol. 293, no. 5, pp. H2878–H2887, 2007.

[57] A. Onody, C. Csonka, Z. Giricz, and P. Ferdinandy, "Hyperlipidemia induced by a cholesterol-rich diet leads to enhanced peroxynitrite formation in rat hearts," *Cardiovasccular Research*, vol. 58, no. 3, pp. 663–670, 2003.

[58] N. Aytan, T. Jung, F. Tamtürk, T. Grune, and N. Kartal-Özer, "Oxidative stress related changes in the brain of hypercholesterolemic rabbits," *BioFactors*, vol. 33, no. 3, pp. 225–236, 2008.

[59] J. X. Rong, L. Shen, Y. H. Chang, A. Richters, H. N. Hodis, and A. Sevanian, "Cholesterol oxidation products induce vascular foam cell lesion formation in hypercholesterolemic New Zealand white rabbits," *Arteriosclerosis, Thrombosis and Vascular Biology*, vol. 19, no. 9, pp. 2179–2188, 1999.

Hindawi
Oxidative Medicine and Cellular Longevity
Volume 2020, Article ID 4858975, 12 pages
https://doi.org/10.1155/2020/4858975

Research Article

Effects of Early Resveratrol Intervention on Skeletal Muscle Mitochondrial Function and Redox Status in Neonatal Piglets with or without Intrauterine Growth Retardation

Kang Cheng, Ting Wang, Simian Li, Zhihua Song, Hao Zhang, Lili Zhang, and Tian Wang

College of Animal Science and Technology, Nanjing Agricultural University, Nanjing 210095, China

Correspondence should be addressed to Tian Wang; tianwangnjau@163.com

Received 27 March 2020; Accepted 29 April 2020; Published 22 May 2020

Guest Editor: Jolanta Czuczejko

Copyright © 2020 Kang Cheng et al. This is an open access article distributed under the Creative Commons Attribution License, which permits unrestricted use, distribution, and reproduction in any medium, provided the original work is properly cited.

Skeletal muscle mitochondrial malfunction of offspring induced by intrauterine growth retardation (IUGR) may be a contributor to growth restriction and metabolic disorder at various periods of life. This study explored the effects of IUGR and resveratrol (RSV) on mitochondrial function and redox status in the longissimus dorsi muscle (LM) of piglets during the sucking period. A total of 36 pairs of IUGR and normal birth weight male piglets were orally fed with either 80 mg RSV/kg body weight/d or 0.5% carboxymethylcellulose sodium during days 7-21 after birth. The results showed that RSV treatment improved anomalous mitochondrial morphology, increased adenosine triphosphate and glycogen contents, and enhanced nicotinamide adenine dinucleotide/reduced form of nicotinamide-adenine dinucleotide ratio in the LM of IUGR piglets. Moreover, the IUGR-induced increased malondialdehyde and protein carbonyl concentrations, abnormal mtDNA number, and suppressed genes expression of mitochondrial biogenesis such as nuclear respiratory factor 1, estrogen-related receptor alpha, and polymerase gamma in the LM were restored to some extent by RSV treatment. Additionally, RSV increased mitochondrial complex V activity in the LM of piglets. Collectively, RSV administration alleviated the LM mitochondrial dysfunction and oxidative damage of IUGR piglets.

1. Introduction

Offspring affected by a low birth weight (LBW) after suffering processes of intrauterine growth retardation (IUGR) is receiving increased attention in both human medicine and animals production, owing to the short-term (incremental morbidity and mortality of neonates) and long-term repercussions of LBW (decreased growth patterns, health status, and performance of individuals) [1]. The main reason for IUGR is the decrease of nutrients and oxygen to the fetus by the placenta [2]. In this case, the fetus preferentially shunts blood to the vital organs at the expense of nutrients and oxygen delivery to the periphery [3]. Compared with the brain and heart, skeletal muscle has a lower priority for nutrients redistribution, which makes it particularly susceptible to the nutritional deficiency in *utero* [4]. Epidemiological and animal studies have found that IUGR offspring exhibited impaired skeletal muscle growth and development as well as abnormal glucose metabolism [5–7], which may be associated with a mitochondrial malfunction in skeletal muscle. Mitochondria, "the powerhouse of the cell", generate energy (i.e., adenosine triphosphate (ATP)) via the efficient electron transport chain (ETC) system for muscular growth and glycogen storage. In addition, mitochondria are the primary site for reactive oxygen species production and are vulnerable to oxidative stress (OS). Several investigations in juvenile rats demonstrated that IUGR reduced mitochondrial nicotinamide adenine dinucleotide (NAD^+)/reduced form of nicotinamide-adenine dinucleotide (NADH) ratio and ATP synthesis in skeletal muscle, and altered skeletal muscle mitochondrial genes expression (e.g., NADH-ubiquinone-oxidoreductase subunit 4 L) [6, 8]. However, limited information about skeletal muscle mitochondrial redox status in IUGR offspring was available, which needs to be investigated in the present study. But maintaining optimal redox status is essential for mitochondrial function [9]. Therefore,

improving the mitochondrial function and redox status in skeletal muscle may be a potential strategy to alleviate the negative effects of IUGR on growth and metabolism.

Resveratrol (trans-3,4′,5-trihydroxystilbene, RSV), a polyphenol isolated from plants such as grapes, peanut, and polygonum cuspidatum, has been described as exhibiting pleiotropic functions including antioxidative and anti-inflammatory properties [10, 11], antiobesogenic [12, 13], antiatherosclerotic [14], and anticancer [15] activities. Previous studies conducted in rodents model demonstrated that RSV can govern glucose homeostasis under high-fat-diet-induced insulin resistance condition by improving mitochondrial ETC complexes activities and antioxidant function, and regulating the genes expression of mitochondrial biogenesis in skeletal muscle [16, 17]. In addition, a recent report showed that RSV improved muscle atrophy in streptozocin-induced diabetic mice evidenced by enhanced muscular mass and function as well as increased mitochondrial contents in part via increasing mitochondrial biogenesis [18]. However, the efficacy of RSV treatment in skeletal muscle mitochondrial dysfunction of IUGR offspring has not yet to be explored. Pigs have been selected as an ideal biomedical model for the study of the occurrence and consequence of IUGR in humans due to the similar morphology, physiology, metabolism, and proportional organ sizes between pigs and humans [19]. Therefore, in the present study, we investigated whether early RSV intervention could improve skeletal muscle mitochondrial function and redox status in neonates with IUGR using a piglet model.

2. Materials and Methods

The experiment performed in the present study was approved by the Animal Care and Use Committee of Nanjing Agricultural University. Resveratrol (purity 98%) was purchased from Zhejiang Yixin Pharmaceutical Co., Ltd. (Yixin, China). Carboxymethylcellulose sodium (CMC-Na) was purchased from Sinopharm Chemical Reagent Co., Ltd. (Shanghai, China).

2.1. Animals and Experimental Design. During the preparation, healthy sows (Landrace × Yorkshire) with the same parity of the third and similar expected days of farrowing (<3 d) were chosen. At birth, sows that had similar litter sizes (i.e., 11–13 piglets) and met the selection criteria for IUGR piglets were chosen. A total of 72 male newborn piglets (Duroc × (Landrace × Yorkshire)) were collected and tagged from 36 litters (1 normal birth weight (NBW) piglet and 1 IUGR piglet from each litter) for the experiment: 36 were NBW piglets (~1.72 kg) and the other 36 were naturally occurring IUGR littermates (~0.88 kg) according to their birth weight using our previous method [20]. An IUGR piglet was defined as having a birth weight was 2 SD below the mean BW of the total population, whereas a NBW littermate had a birth weight within 0.5 SD unit of the mean birth weight of the whole litter. The NBW and IUGR piglets were cross-fostered after birth by 24 four-parity sows (standardized litter size: 3 experimental piglets and 8 same type nonexperimental piglets). During the sucking period, all piglets remained with sows housed in lactation crates in environmentally controlled rooms. Sows were fed a commercial diet and provided water *ad libitum*. The sucking piglets had no access to the sow's diet. At 7 days of age, the NBW and IUGR piglets were orally fed with 80 mg RSV/kg body weight/d (diluted in 0.5% CMC-Na) or the same volume of 0.5% CMC-Na (diluted in 0.86% saline) for a period of 14 days, respectively. Therefore, all piglets were assigned into 4 groups (six replicates (pens or litters) per group, three piglets per replicate): NBW-CON, NBW-RSV, IUGR-CON, and IUGR-RSV.

2.2. Sample Collection. At the end of this experiment, six piglets per group (i.e., one piglet per replicate) were killed according to a previous study [21] and followed by a quick dissection of longissimus dorsi muscle (LM). The LM samples from the left half of the carcass were rapidly collected at the level of the twelfth/thirteenth ribs and cooled using liquid nitrogen and stored at −80°C until subsequent analysis. The remaining half and the contralateral LM samples were collected for the analysis of ultrastructure and mitochondrial parameters.

2.3. Transmission Electron Microscopy. For ultrastructural analysis, fresh LM was cut into small pieces and fixed in 2.5% glutaraldehyde (pH 7.4, 0.1 mol/L sodium cacodylate buffer) and 1% osmium tetroxide, dehydrated, and embedded in epoxy resin. The ultrastructure of LM was examined with a transmission electron microscope (Hitachi H-7650). Considering the costs and aim of the experiment, samples from NBW-CON, IUGR-CON, and IUGR-RSV groups were treated and analysed.

2.4. Analysis of Skeletal Muscle Metabolites. Glycogen contents in the LM were measured by a commercial kit (Nanjing Jiancheng Institute of Bioengineering, Nanjing, China) according to the anthracenone method. Amounts of ATP in the LM were determined through an ATP Content Assay Kit (Solarbio, Beijing, China) following the manufacturer's instructions. The concentrations of NAD^+ and NADH in the LM were determined using commercial kits according to the manufacturer's instructions (SinoBestBio, Shanghai, China). The relative intracellular glycogen, ATP, NAD^+, and NADH levels were calculated based on the quantified concentrations normalized to the weight of the sample.

2.5. Mitochondrial Redox Status. The activities of manganese superoxide dismutase (Mn-SOD), glutathione peroxidase (GPX), glutathione reductase (GR) and the concentrations of glutathione (GSH), malondialdehyde (MDA), and protein carbonyl (PC) in the LM mitochondria were determined using commercial kits (Nanjing Jiancheng Institute of Bioengineering, Nanjing, China). All the results were normalized against protein content in each sample for intersample comparison.

2.6. Mitochondrial ETC Complexes Activities. The activities of ETC complexes I, II, III, IV, and V were determined with commercially available kits obtained from SinoBestBio (Shanghai, China) following the guidelines of the manufacturer.

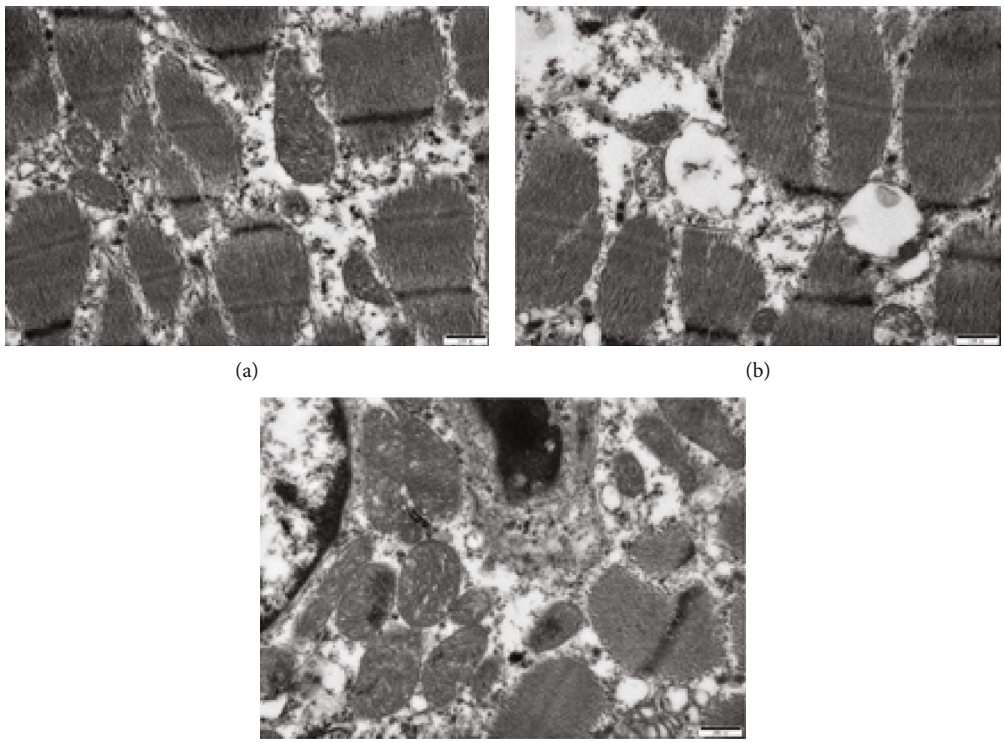

Figure 1: The ultrastructure of longissimus dorsi muscle in piglets at 21 days of age. (a) NBW-CON: normal birth weight piglets were orally fed with 0.5% carboxymethylcellulose sodium. (b) IUGR-CON: intrauterine growth-retarded piglets were orally fed with 0.5% carboxymethylcellulose sodium. (c) IUGR-RSV: intrauterine growth-retarded piglets were orally fed with 80 mg resveratrol/kg body weight/d. Scale bars, 500 nm.

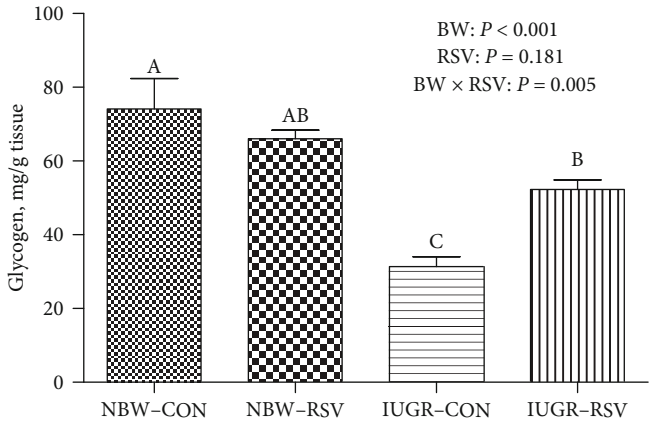

Figure 2: The glycogen content of longissimus dorsi muscle in piglets at 21 days of age. BW: birth weight; RSV: resveratrol; NBW-CON: normal birth weight piglets were orally fed with 0.5% carboxymethylcellulose sodium; NBW-RSV: normal birth weight piglets were orally fed with 80 mg resveratrol/kg body weight/d; IUGR-CON: intrauterine growth-retarded piglets were orally fed with 0.5% carboxymethylcellulose sodium; IUGR-RSV: intrauterine growth-retarded piglets were orally fed with 80 mg resveratrol/kg body weight/d. Results are expressed as mean ± standard error, $n = 6$. Mean Values with unlike superscript were significantly different ($P < 0.05$).

2.7. Total RNA Isolation and qRT-PCR Assays. Total RNA isolation and qRT-PCR analysis were conducted as described previously [10–13, 22]. Briefly, RNA was isolated from LM samples using Trizol reagent (TaKaRa Biotechnology Co. Ltd., Dalian, China). The quality of RNA was measured by checking its integrity using agarose gel electrophoresis and by conforming that the A260 nm/A280 nm absorbance ratio was between 1.8 and 2.0. After quantified, total RNA (1 μg) was reverse-transcribed into complementary DNA (cDNA) using the PrimeScript™ RT Reagent Kit (TaKaRa Biotechnology Co. Ltd., Dalian, China). The cDNA was amplified via qRT-PCR using ChamQ SYBR qPCR Master Mix Kit

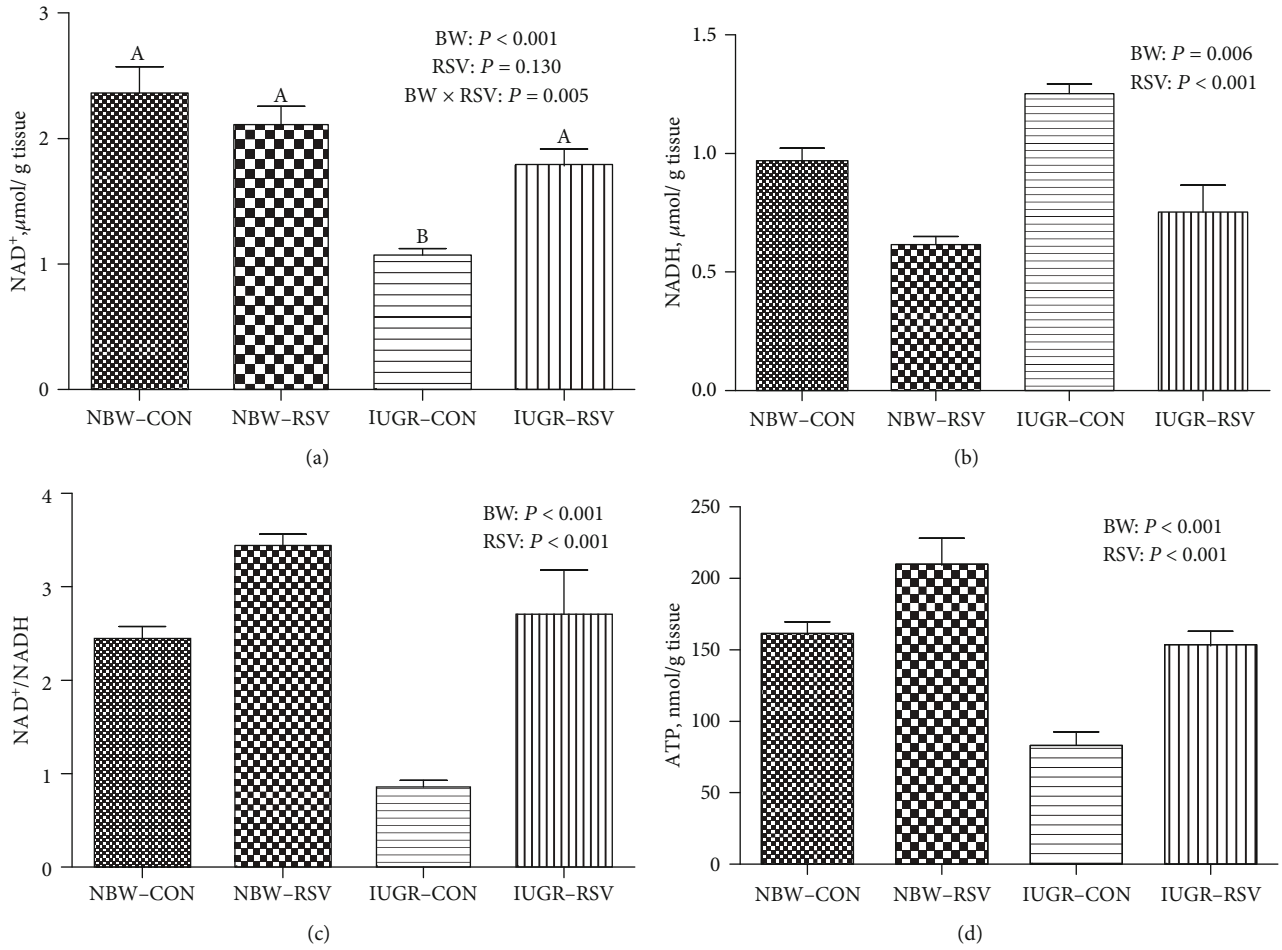

Figure 3: The contents of oxidized form of nicotinamide adenine dinucleotide (NAD^+, a), reduced form of nicotinamide-adenine dinucleotide (NADH, b) and adenosine triphosphate (ATP, d), and NAD^+/NADH (c) of longissimus dorsi muscle in piglets at 21 days of age. BW: birth weight; RSV: resveratrol; NBW-CON: normal birth weight piglets were orally fed with 0.5% carboxymethylcellulose sodium; NBW-RSV: normal birth weight piglets were orally fed with 80 mg resveratrol/kg body weight/d; IUGR-CON: intrauterine growth-retarded piglets were orally fed with 0.5% carboxymethylcellulose sodium; IUGR-RSV: intrauterine growth-retarded piglets were orally fed with 80 mg resveratrol/kg body weight/d. Results are expressed as mean ± standard error, $n = 6$. Mean Values with unlike superscript were significantly different ($P < 0.05$).

(Vazyme, Nanjing, China) and the QuantStudio®5real-time PCR Design & Analysis system (Applied Biosystems, USA). The reaction mixture was prepared using 2 μL of cDNA, 0.4 μL of forward primer, 0.4 μL of reverse primer, 10 μL of ChamQ SYBR qPCR Master Mix (Vazyme, Nanjing, China), 0.4 μL of ROX Reference Dye (Vazyme, Nanjing, China), and 6.8 μL of double-distilled water. The PCR consisted of a prerun at 95°C for 30 s and 40 cycles of denaturation at 95°C for 5 s, followed by a 60°C annealing step for 30 s. The conditions of the melting curve analysis were as follows: one cycle of denaturation at 95°C for 10 s, followed by an increase in temperature from 65 to 95°C at a rate of 0.5°C/s. Melting curve analysis was performed to validate the specificity of the PCR-amplified product. All primers for qRT-PCR were presented in Supplementary Table 1. The relative levels of mRNA expression were calculated using the $2^{-\Delta\Delta Ct}$ method normalizing against the reference gene β-actin expression [23]. The values of the NBW-CON group were used as a calibrator.

2.8. Analysis of Skeletal Muscle Mitochondrial DNA (mtDNA) Copy Number. Total genomic DNA was extracted from snap-frozen LM using a universal Genomic DNA Extraction Kit (TSINKE, Beijing, China). The concentration of DNA was quantified and diluted to the same concentration for further analysis. The relative mtDNA content was measured by coamplifying the mt D-loop and the nuclear-encoded β-actin gene using qRT-PCR assay. Primer sequences are presented in Supplementary Table 1. The PCR amplification was performed under the same condition as described above. The relative quantification values were calculated according to the $2^{-\Delta\Delta Ct}$ method [23].

2.9. Statistical Analysis. Data were analysed by ANOVA using a 2 × 2 factorial arrangement of treatments with the general linear model procedure (SPSS 22.0; IBM-SPSS Inc., Chicago, IL, USA) and GraphPad Prism (version 5.0, GraphPad Software Inc., San Diego, CA, USA), with the individual piglet as the experimental unit. The statistical model included

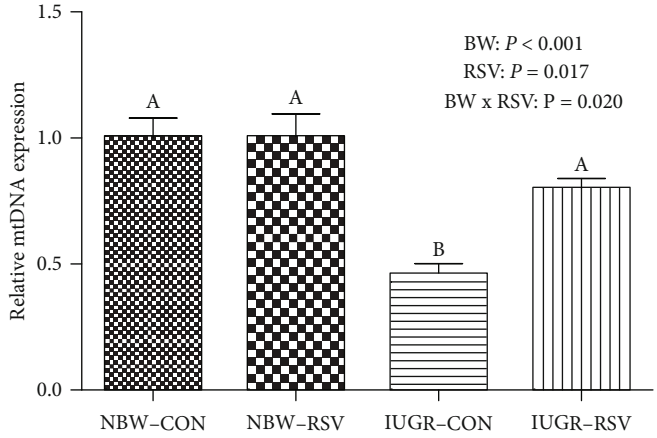

Figure 4: The mitochondrial DNA (mtDNA) content of longissimus dorsi muscle in piglets at 21 days of age. BW: birth weight; RSV: resveratrol; NBW-CON: normal birth weight piglets were orally fed with 0.5% carboxymethylcellulose sodium; NBW-RSV: normal birth weight piglets were orally fed with 80 mg resveratrol/kg body weight/d; IUGR-CON: intrauterine growth-retarded piglets were orally fed with 0.5% carboxymethylcellulose sodium; IUGR-RSV: intrauterine growth-retarded piglets were orally fed with 80 mg resveratrol/kg body weight/d. Results are expressed as mean ± standard error, $n = 6$. Mean Values with unlike superscript were significantly different ($P < 0.05$).

the effects of BW and RSV and their interaction. When the interaction was significant, the data were reanalysed by one-way analysis of variance and Tukey's post hoc test. The statistical results were presented by mean values and the standard error. Differences were considered significant if $P < 0.05$, and $0.05 < P < 0.10$ was considered a trend.

3. Results

3.1. Skeletal Muscle Mitochondrial Ultrastructure. As shown in Figure 1, piglets of the IUGR-CON group exhibited swollen mitochondria with disorganized and fragmented cristae in the LM relative to the NBW-CON group. Expectedly, RSV conferred substantial rescue of the mitochondrial morphological defects in the LM of IUGR-CON piglets.

3.2. Skeletal Muscle Metabolites. Compared with the NBW, IUGR pups had lower glycogen level in the LM ($P < 0.05$, Figure 2). Additionally, piglets suffering from IUGR exhibited the diminished levels of ATP and NAD^+, reduced NAD^+/NADH ratio, and increased NADH content in the LM ($P < 0.05$, Figure 3). As expected, the amount of ATP and NAD^+/NADH ratio were significantly increased, and the NADH level was obviously reduced in the LM of piglets due to oral RSV administration ($P < 0.05$). A noticeable interaction between BW and RSV treatment was observed in the levels of glycogen and NAD^+ ($P < 0.05$); the IUGR-induced decreased glycogen and NAD^+ concentrations in the LM of piglets were restored by RSV supplementation ($P < 0.05$).

3.3. Skeletal Muscle mtDNA Content. As shown in Figure 4, in the LM, a significant interaction effect between BW and RSV was observed in mtDNA copy number ($P < 0.05$); RSV alleviated the diminished mtDNA content induced by IUGR ($P < 0.05$).

3.4. Skeletal Muscle Mitochondrial Redox Status. As shown in Figure 5, compared with the NBW, IUGR piglets exhibited mitochondrial OS in the LM evidenced by the increased MDA ($P < 0.05$) and PC ($P < 0.05$) levels as well as the reduced activities of GPX ($P = 0.068$) and GR ($P < 0.05$). The amount of mitochondrial PC in the LM of piglets was decreased by RSV treatment ($P = 0.095$). An interaction between BW and RSV was observed in GPX activity ($P < 0.05$), and amounts of PC ($P = 0.073$) and MDA ($P < 0.05$) in the LM mitochondria of piglets. Resveratrol suppressed the elevated MDA contents in the LM mitochondria induced by IUGR ($P < 0.05$). However, no differences were found in the LM mitochondrial Mn-SOD activity and GSH level of piglets among 4 groups ($P > 0.05$).

3.5. Skeletal Muscle Mitochondrial ETC Complexes Activities. The effects of BW and RSV on mitochondrial ETC complexes activities in the LM of piglets was shown in Figure 6. Compared with the NBW, IUGR resulted in the decreased complex I activity in the LM mitochondria of piglets ($P = 0.082$). Resveratrol elevated the activity of complex V in the LM mitochondria of piglets ($P < 0.05$). However, the activities of complex II, III, and IV in the LM mitochondria were not affected by BW or/and RSV ($P > 0.05$).

3.6. Skeletal Muscle Genes Expression Related to Mitochondrial Biogenesis. The effects of BW and RSV on the mRNA expression of mitochondrial biogenesis in the LM of piglets was shown in Figure 7. The profile of estrogen-related receptor alpha (ERRα, $P = 0.068$) and polymerase gamma (POLG, $P < 0.05$) mRNA in the LM piglets was decreased by IUGR. In contrast, RSV increased the mRNA level of ERRα ($P = 0.054$) and POLG ($P < 0.05$) in the LM of piglets. An interaction between BW and RSV was found in the mRNA expression of peroxisome proliferation activated receptor gamma coactivator-1 alpha ($P = 0.079$),

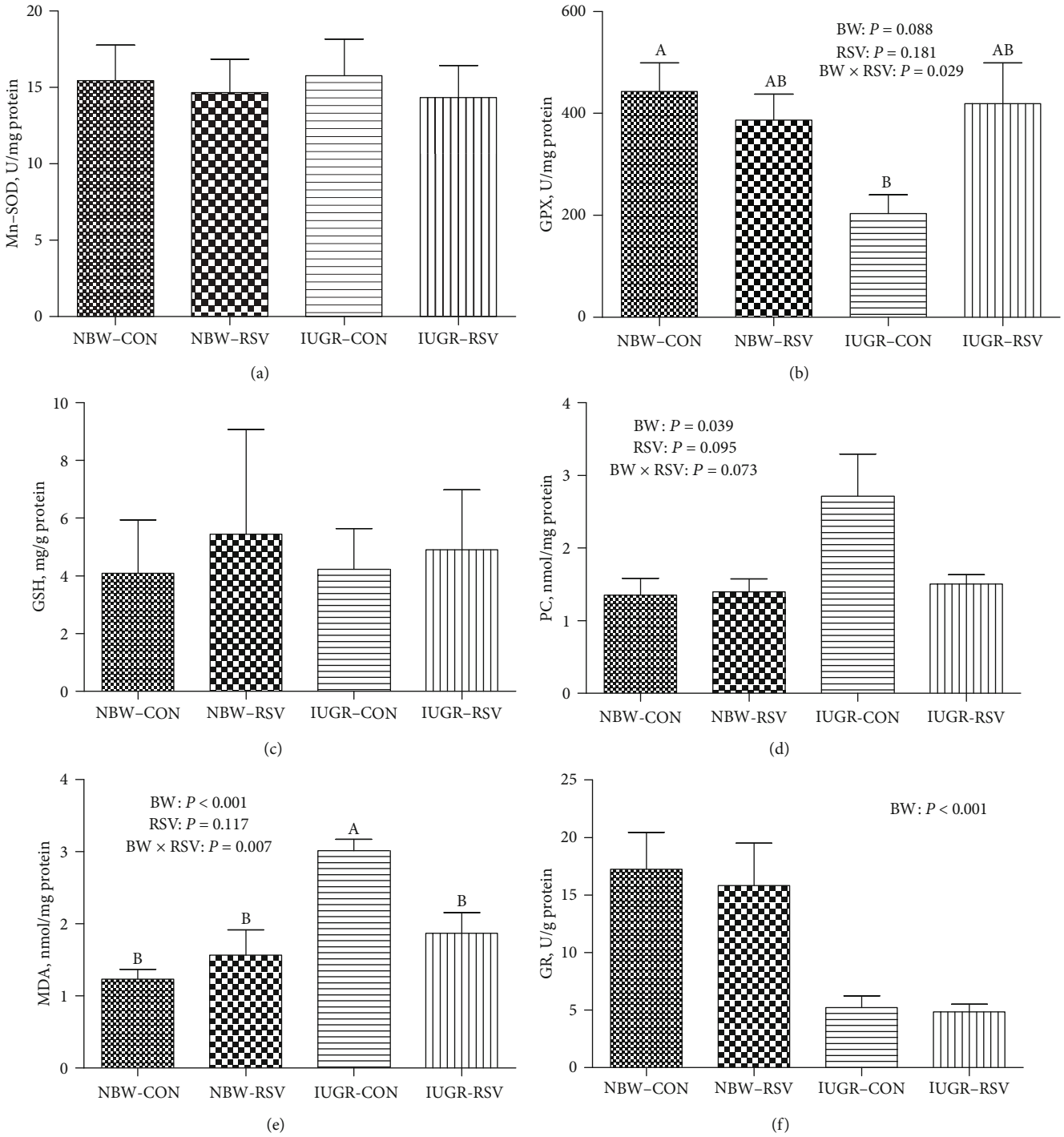

Figure 5: The mitochondrial redox status of longissimus dorsi muscle in piglets at 21 days of age. (a) Mn-SOD: manganese superoxide dismutase; (b) GPX: glutathione peroxidase; (c) GSH: glutathione; (d) PC: protein carbonyl; (e) MDA: malondialdehyde; (f) GR: glutathione reductase. BW: birth weight; RSV: resveratrol; NBW-CON: normal birth weight piglets were orally fed with 0.5% carboxymethylcellulose sodium; NBW-RSV: normal birth weight piglets were orally fed with 80 mg resveratrol/kg body weight/d; IUGR-CON: intrauterine growth-retarded piglets were orally fed with 0.5% carboxymethylcellulose sodium; IUGR-RSV: intrauterine growth-retarded piglets were orally fed with 80 mg resveratrol/kg body weight/d. Results are expressed as mean ± standard error, $n = 6$. Mean Values with unlike superscript were significantly different ($P < 0.05$).

mitochondrial transcription factor A (TFAM, $P < 0.05$), and nuclear respiratory factor 1 (NRF1, $P < 0.05$). Resveratrol increased ($P = 0.091$) the inhibited expression of NRF1 mRNA in the LM of piglets induced by IUGR. No difference in gene expression of sirtuin 1 was observed in the LM of piglets among these groups ($P > 0.05$).

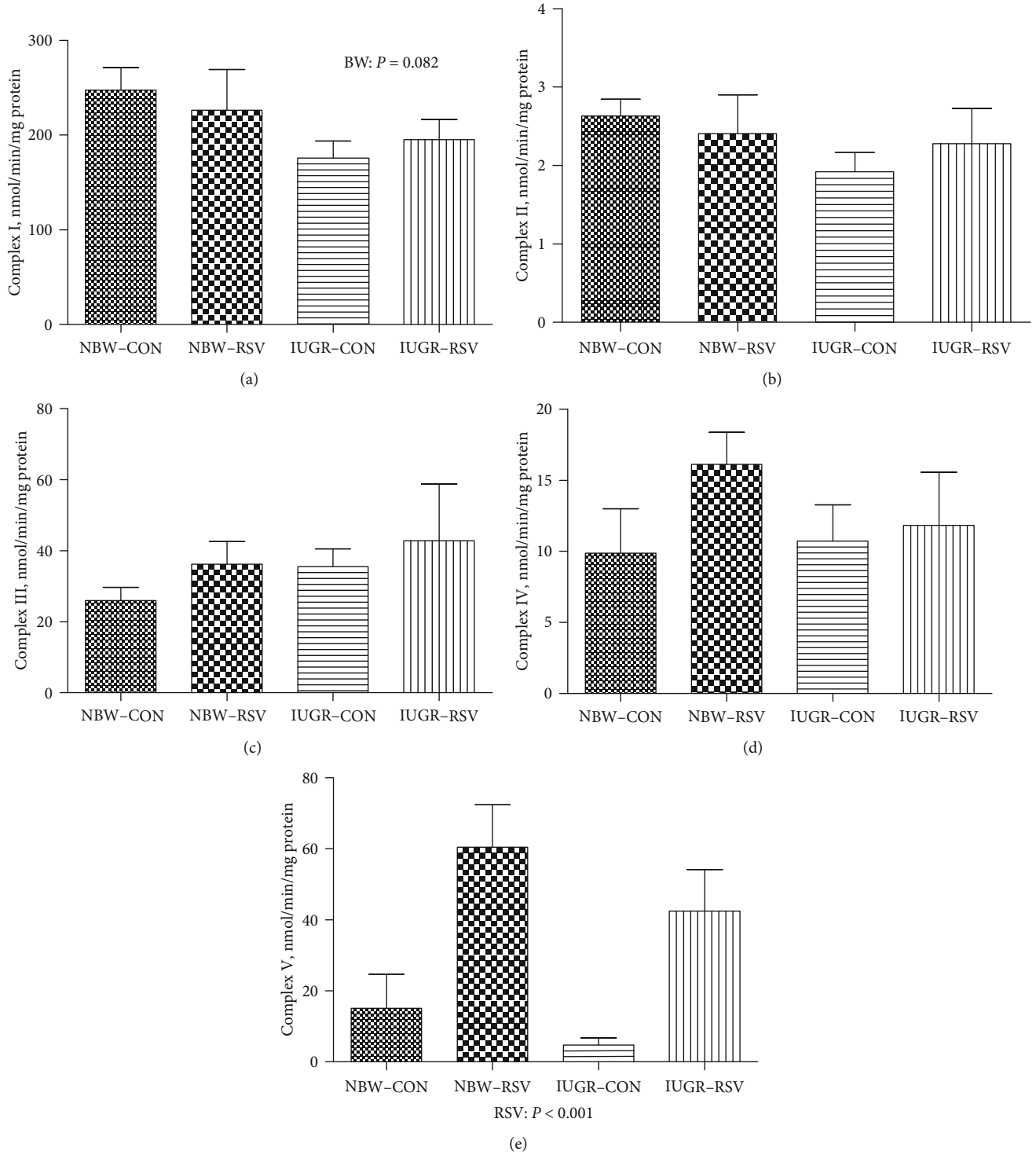

Figure 6: The mitochondrial respiratory chain complexes I (a), II (b), III (c), IV (d), and V (e) activities of longissimus dorsi muscle in piglets at 21 days of age. BW: birth weight; RSV: resveratrol; NBW-CON: normal birth weight piglets were orally fed with 0.5% carboxymethylcellulose sodium; NBW-RSV: normal birth weight piglets were orally fed with 80 mg resveratrol/kg body weight/d; IUGR-CON: intrauterine growth-retarded piglets were orally fed with 0.5% carboxymethylcellulose sodium; IUGR-RSV: intrauterine growth-retarded piglets were orally fed with 80 mg resveratrol/kg body weight/d. Results are expressed as mean ± standard error, $n = 6$. Mean Values with unlike superscript were significantly different ($P < 0.05$).

3.7. Skeletal Muscle Genes Expression Related to Energy Metabolism. As shown in Figure 8, IUGR led to the reduced gene expression of NADH dehydrogenase (ubiquinone) 1 alpha subcomplex 4 (NDUFA4, $P = 0.074$), NADH dehydrogenase (ubiquinone) 1 beta subcomplex 1 (NDUFB1, $P = 0.097$), succinate dehydrogenase complex flavoprotein

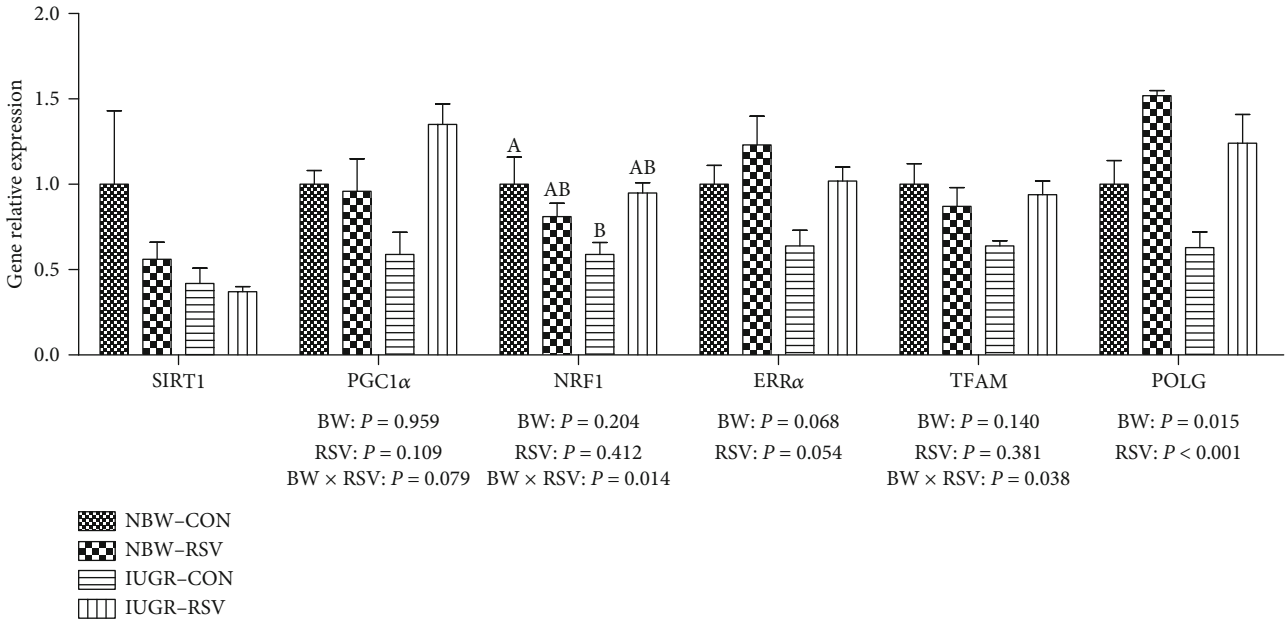

Figure 7: The genes expression related to mitochondrial biogenesis of longissimus dorsi muscle in piglets at 21 days of age. BW: birth weight; RSV: resveratrol; NBW-CON: normal birth weight piglets were orally fed with 0.5% carboxymethylcellulose sodium; NBW-RSV: normal birth weight piglets were orally fed with 80 mg resveratrol/kg body weight/d; IUGR-CON: intrauterine growth-retarded piglets were orally fed with 0.5% carboxymethylcellulose sodium; IUGR-RSV: intrauterine growth-retarded piglets were orally fed with 80 mg resveratrol/kg body weight/d. Results are expressed as mean ± standard error, $n = 5$. Mean Values with unlike superscript were significantly different ($P < 0.05$).

subunit A ($P = 0.063$), cytochrome c oxidase V (COXV, $P = 0.058$), ATP synthase alpha subunit (ATP5A1, $P < 0.05$), and ubiquinol-cytochrome c reductase binding protein (UQCRB, $P < 0.05$) in the LM of piglets compared with the NBW. However, there was no significant interaction between the effects of BW and RSV treatment on the mRNA abundance of these genes in the LM, except on NDUFA1 ($P < 0.05$). Resveratrol restored ($P = 0.074$) the suppressed expression of muscular NDUFA1 at the transcriptional level of IUGR piglets. In addition, the gene expression of NDUFA6, NDUFA13, succinate dehydrogenase complex iron sulfur subunit B, COXIV, ATP synthase beta polypeptide, ATP synthase F0 complex subunit C1, and cytochrome C in the LM of piglets was not altered among these groups ($P > 0.05$).

4. Discussion

To the best of our knowledge, this is the first study to determine the negative influence of IUGR on the mitochondrial function and redox status in skeletal muscle of neonatal pigs, and the therapeutic effect of RSV. Notably, novel and important findings from the present study are that reduced ATP production, decreased glycogen storage and NAD^+/NADH ratio, altered mitochondrial biogenesis and redox homeostasis, and diminished ETC complexes activities in skeletal muscle of the sucking IUGR piglets were mitigated to some extent by early RSV intervention.

Skeletal muscle is the main component of total body mass, and it can absorb circulatory glucose and synthesize glycogen, being responsible for metabolic homeostasis [3, 24]. But ATP is necessary for growth and glycogen synthesis, and IUGR animals exhibit reduced postnatal muscular growth [25, 26] and glycogen storage [6, 8]. These findings were corroborated by the present study that IUGR diminished ATP and glycogen contents in the LM of piglets. The deficiency of muscular energy of IUGR piglets in this study may be associated with impaired mitochondrial antioxidant defense system and decreased mitochondrial biogenesis.

In the present study, IUGR piglets had inhibited GR and GPX activities and increased MDA and PC concentrations in the LM mitochondria. MDA and PC are products of lipid and protein oxidation by superfluous free radicals, respectively, all of which are regarded as important markers of OS [27]. The occurrence of OS is due to the fact that the production of free radicals exceeds the scavenging capacity of antioxidants [28]. Both GR and GPX play a critical role in scavenging free radicals. The impairment of antioxidant enzymes activities in this study further confirmed that IUGR led to OS in the LM mitochondria. In the present study, the loss of complex I activity in the LM mitochondria of IUGR could be induced by OS, which could result in a shutdown of mitochondrial energy generation. Similar results were observed in hepatic mitochondria of piglets that IUGR increased MDA content and reduced complex I and III activities due to the increased production of superoxide radicals, and consequently inhibited ATP level [21]. Additionally, the lower NAD^+/NADH ratio in this study may be explained by the reduced activity of complex I, which couples electron from NADH to quinone with translocation of proton across the inner mitochondrial membrane for ATP production [29], thereby increasing NADH relative to NAD^+. Moreover, a

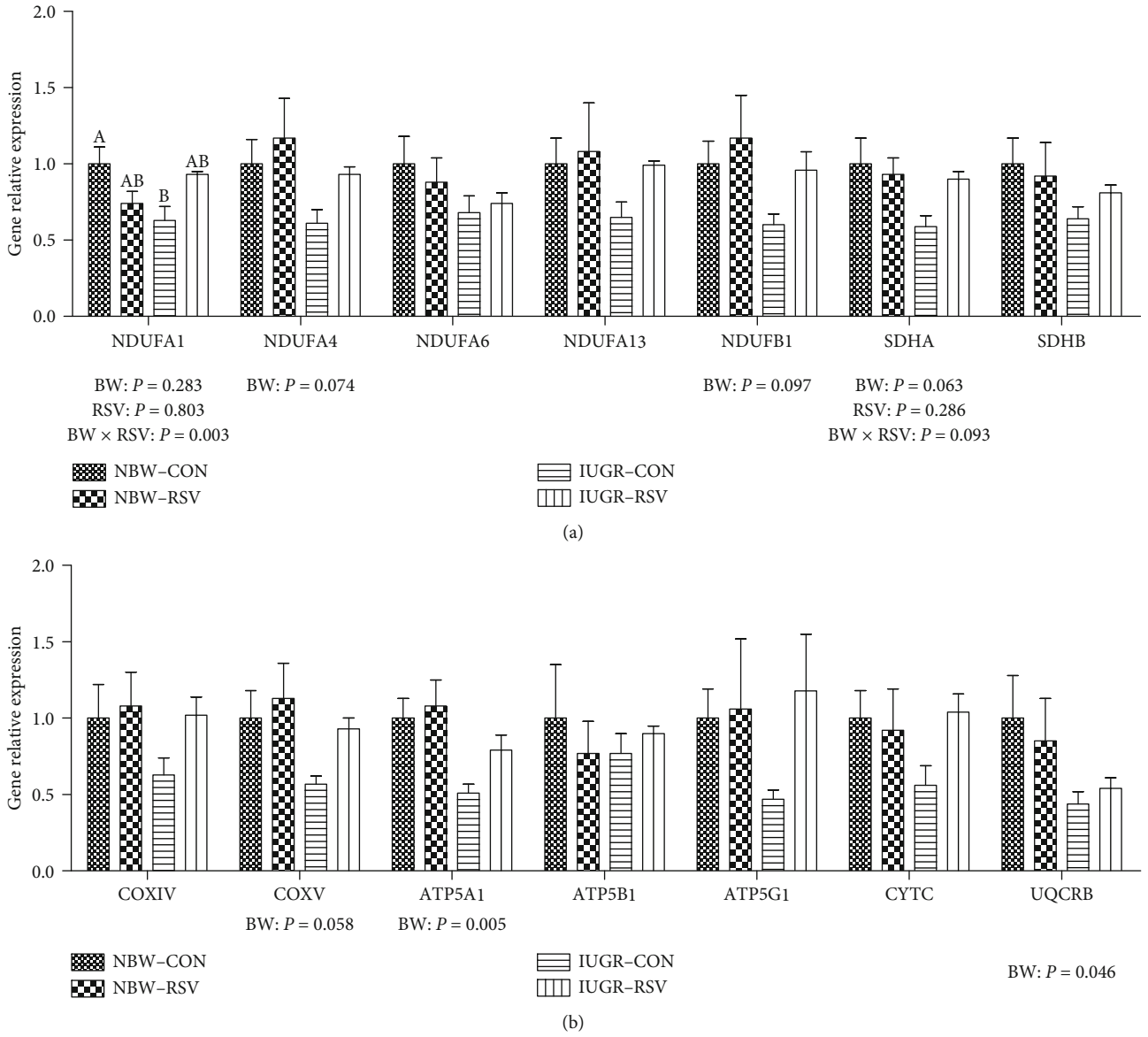

Figure 8: The genes expression related to mitochondrial energy metabolism of longissimus dorsi muscle in piglets at 21 days of age. BW: birth weight; RSV: resveratrol; NBW-CON: normal birth weight piglets were orally fed with 0.5% carboxymethylcellulose sodium; NBW-RSV: normal birth weight piglets were orally fed with 80 mg resveratrol/kg body weight/d; IUGR-CON: intrauterine growth-retarded piglets were orally fed with 0.5% carboxymethylcellulose sodium; IUGR-RSV: intrauterine growth-retarded piglets were orally fed with 80 mg resveratrol/kg body weight/d. Results are expressed as mean ± standard error, $n = 5$. Mean Values with unlike superscript were significantly different ($P < 0.05$).

decrease in NAD^+/NADH ratio inhibits the flux of glycolytic and tricarboxylic acid cyclic metabolites through the mitochondria, in turn, resulting in reduced ATP production [8]. Thus, in this study, the OS-reduced complex I activity due to impaired antioxidant defense system in the LM mitochondria of IUGR piglets may contribute to muscular energy deficiency.

Mitochondrial ATP production is related to the mitochondrial number, which could be determined quantitatively by mtDNA copy number [30]. Mitochondrial DNA content is regulated by mitochondrial biogenesis [31]. Mitochondrial biogenesis is under the regulation of some transcriptional factors such as NRF1 [32]. In the current study, we also found that IUGR reduced the genes expression of NRF1, ERRα, and POLG in the LM, involving in the compromised mtDNA level. The suppression of mitochondrial biogenesis may explain the reduced genes expression of NDUFA1, NADUFA4, NADUFB1, SDHA, UQCRB, COXV, and ATP5A1 in this study. NDUFA1, NADUFA4, and NADUFB1 are key components of complex I, and their inhibited mRNA abundance may be associated with the reduced activity of complex I in this study. Similar results in piglets model have shown that IUGR-diminished hepatic ATP generation is also associated with compromised mitochondrial biogenesis [21, 33]. Therefore, the lower mitochondrial number associated with inhibited mitochondrial

biogenesis in the LM of IUGR piglets might also be an important factor leading to the diminished production of ATP in this study.

As expected, in the present study, administration of RSV to IUGR piglets enhanced the synthesis of ATP and glycogen, and normalized NAD^+/NADH ratio and mtDNA content in skeletal muscle, which directly or indirectly indicated that RSV improved mitochondrial dysfunction and energy deficiency in the LM of IUGR piglets. We found that RSV reduced the elevated MDA and PC concentrations in the LM mitochondria of IUGR piglets but had no effects on antioxidants levels, suggesting that RSV alleviated the LM mitochondrial OS by the compromised free radical levels rather than the enhancement of antioxidant defense system. In this case, on the one hand, RSV can directly scavenge free radicals (e.g., superoxide anion and hydrogen peroxide) due to the presence of phenolic hydroxyl groups [12]; on the other hand, RSV indirectly inhibited the process of free radicals synthesis via enhancing mitochondrial function [21]. In the present study, we have also seen that an increase in complex V or ATP synthase activity in the LM mitochondria of IUGR-RSV piglets playing a major role in bioenergetics, which uses the exergonic proton backflow for ATP synthesis from ADP and inorganic phosphate in the matrix [34]. Of note, in this study, RSV increased the muscular NRF1, ERRα, and POLG gene expression of IUGR piglets. NRF1, a nuclear transcriptional factor, regulates the expression of TFAM and other nuclear-encoded mitochondrial subunits of ETC complexes such as ATP synthase. The increase of NRF1 gene expression may be related to the enhanced complex V activity in the present study. As a transcriptional factor, ERRα regulates the transcriptional expression of genes required for mitochondrial biogenesis and oxidative phosphorylation. Previous study reported that ERRα deficiency exacerbated the cisplatin-induced decrease in mtDNA and altered mitochondrial structure [35]. The POLG gene encodes the mitochondrial DNA polymerase, which is responsible for the replication of the mitochondrial genome. Mutations in POLG can cause early childhood mtDNA depletion syndromes or later-onset syndromes resulting from mtDNA deletions [36]. These results in this study indicated that the LM mitochondrial biogenesis of IUGR piglets was improved due to RSV administration. Similar results in diabetic mice [18] and obesity mice [17] have demonstrated that RSV treatment resulted in an increase in mitochondrial biogenesis in skeletal muscle. Also, Zhang et al. [21] found similar results in hepatic mitochondria of IUGR piglets fed with RSV. In addition, damage to mtDNA could lead to consecutive free radical bursts, which further exacerbated the mitochondrial dysfunction, setting a vicious cycle [37]. Therefore, the therapeutic and beneficial effects of RSV on the LM mitochondria of IUGR piglets may be associated with the improvement of mitochondrial biogenesis and/or diminished amounts of free radicals.

5. Conclusions

In conclusion, our results suggested that RSV alleviated the LM mitochondrial dysfunction of IUGR piglets, as evidenced by suppression of MDA and PC overproduction; maintenance of ATP, glycogen, and mtDNA levels; enhancement of ETC complex V activity, and mitochondrial biogenesis. These novel findings provide a new highly promising strategy for preventing the reduced growth of muscle and metabolic diseases of IUGR offspring after birth.

Data Availability

The data used to support the findings of this study are available from the corresponding authors upon request.

Conflicts of Interest

The authors declare that there is no conflict of interest.

Authors' Contributions

Authors' contributions are as follows: the conceptualization was worked by Kang Cheng, Zhihua Song, and Tian Wang; the investigation was explored by Kang Cheng, Ting Wang, and Simian Li; the validation was completed by Hao Zhang, and Lili Zhang; funding acquisition was supplied by Tian Wang; resources were provided by Tian Wang, and Lili Zhang; supervision was performed by Lili Zhang; Kang Cheng wrote the original draft; writing, reviewing, and editing were done by Kang Cheng, Zhihua Song, and Tian Wang. All authors read and approved the final version of this manuscript.

Acknowledgments

The present study was supported by the National Natural Science Foundation of China (grant no 31772634) and the Natural Science Foundation of Jiangsu Province (grant no BK20180531).

Supplementary Materials

Supplementary Table 1: primer sequences of the target and reference genes. *(Supplementary Materials)*

References

[1] C. Garcia-Contreras, M. Vazquez-Gomez, Z. Pardo et al., "Polyphenols and IUGR pregnancies: effects of maternal hydroxytyrosol supplementation on hepatic fat accretion and energy and fatty acids profile of fetal tissues," *Nutrients*, vol. 11, no. 7, article 1534, 2019.

[2] S. R. Thorn, P. J. Rozance, L. D. Brown, and W. W. Hay, "The intrauterine growth restriction phenotype: fetal adaptations and potential implications for later life insulin resistance and diabetes," *Seminars in Reproductive Medicine*, vol. 29, no. 3, pp. 225–236, 2011.

[3] L. Nastase, D. Cretoiu, and S. M. Stoicescu, "Skeletal muscle damage in intrauterine growth restriction," *Advances in Experimental Medicine and Biology*, vol. 1088, pp. 93–106, 2018.

[4] X. Yan, M. J. Zhu, M. V. Dodson, and M. Du, "Developmental programming of fetal skeletal muscle and adipose tissue development," *Journal of Genomics*, vol. 1, pp. 29–38, 2013.

[5] L. D. Brown and W. W. Hay Jr., "Impact of placental insufficiency on fetal skeletal muscle growth," *Molecular and Cellular Endocrinology*, vol. 435, pp. 69–77, 2016.

[6] M. A. Selak, B. T. Storey, I. Peterside, and R. A. Simmons, "Impaired oxidative phosphorylation in skeletal muscle of intrauterine growth-retarded rats," *American Journal of Physiology. Endocrinology and Metabolism*, vol. 285, no. 1, pp. E130–E137, 2003.

[7] Z. Ying, H. Zhang, W. Su et al., "Dietary methionine restriction alleviates hyperglycemia in pigs with intrauterine growth restriction by enhancing hepatic protein kinase B signaling and glycogen synthesis," *The Journal of Nutrition*, vol. 147, no. 10, pp. 1892–1899, 2017.

[8] R. H. Lane, A. K. Chandorkar, A. S. Flozak, and R. A. Simmons, "Intrauterine growth retardation alters mitochondrial gene expression and function in fetal and juvenile rat skeletal muscle," *Pediatric Research*, vol. 43, no. 5, pp. 563–570, 1998.

[9] C. Bonnard, A. Durand, S. Peyrol et al., "Mitochondrial dysfunction results from oxidative stress in the skeletal muscle of diet-induced insulin-resistant mice," *The Journal of Clinical Investigation*, vol. 118, no. 2, pp. 789–800, 2008.

[10] K. Cheng, Z. Song, S. Li et al., "Effects of resveratrol on intestinal oxidative status and inflammation in heat-stressed rats," *Journal of Thermal Biology*, vol. 85, article 102415, 2019.

[11] K. Cheng, E. Yan, Z. Song et al., "Protective effect of resveratrol against hepatic damage induced by heat stress in a rat model is associated with the regulation of oxidative stress and inflammation," *Journal of Thermal Biology*, vol. 82, pp. 70–75, 2019.

[12] K. Cheng, Z. Song, H. Zhang et al., "The therapeutic effects of resveratrol on hepatic steatosis in high-fat diet-induced obese mice by improving oxidative stress, inflammation and lipid-related gene transcriptional expression," *Medical Molecular Morphology*, vol. 52, no. 4, pp. 187–197, 2019.

[13] K. Cheng, Z. Song, Y. Chen et al., "Resveratrol protects against renal damage via attenuation of inflammation and oxidative stress in high-fat-diet-induced obese mice," *Inflammation*, vol. 42, no. 3, pp. 937–945, 2019.

[14] M. L. Chen, L. Yi, Y. Zhang et al., "Resveratrol attenuates trimethylamine-*N*-oxide (TMAO)-induced atherosclerosis by regulating TMAO synthesis and bile acid metabolism via remodeling of the gut microbiota," *MBio*, vol. 7, no. 2, pp. e02210–e02215, 2016.

[15] M. H. Farzaei, R. Bahramsoltani, and R. Rahimi, "Phytochemicals as adjunctive with conventional anticancer therapies," *Current Pharmaceutical Design*, vol. 22, no. 27, pp. 4201–4218, 2016.

[16] L. L. Chen, H. H. Zhang, J. Zheng et al., "Resveratrol attenuates high-fat diet–induced insulin resistance by influencing skeletal muscle lipid transport and subsarcolemmal mitochondrial β-oxidation," *Metabolism: Clinical and Experimental*, vol. 60, no. 11, pp. 1598–1609, 2011.

[17] M. Lagouge, C. Argmann, Z. Gerhart-Hines et al., "Resveratrol improves mitochondrial function and protects against metabolic disease by activating SIRT1 and PGC-1α," *Cell*, vol. 127, no. 6, pp. 1109–1122, 2006.

[18] D. Wang, H. Sun, G. Song et al., "Resveratrol improves muscle atrophy by modulating mitochondrial quality control in STZ-induced diabetic mice," *Molecular Nutrition & Food Research*, vol. 62, no. 9, article e1700941, 2018.

[19] L. Shen, M. Gan, S. Zhang et al., "Transcriptome analyses reveal adult metabolic syndrome with intrauterine growth restriction in pig models," *Frontiers in Genetics*, vol. 9, p. 291, 2018.

[20] T. Wang, Y. J. Huo, F. Shi, R. J. Xu, and R. J. Hutz, "Effects of intrauterine growth retardation on development of the gastrointestinal tract in neonatal pigs," *Neonatology*, vol. 88, no. 1, pp. 66–72, 2005.

[21] H. Zhang, Y. Li, W. Su et al., "Resveratrol attenuates mitochondrial dysfunction in the liver of intrauterine growth retarded suckling piglets by improving mitochondrial biogenesis and redox status," *Molecular Nutrition & Food Research*, vol. 61, no. 5, article 1600653, 2017.

[22] K. Cheng, Y. Niu, X. C. Zheng et al., "A comparison of natural (D-α-tocopherol) and synthetic (DL-α-tocopherol acetate) vitamin E supplementation on the growth performance, meat quality and oxidative status of broilers," *Asian-Australasian Journal of Animal Sciences*, vol. 29, no. 5, pp. 681–688, 2016.

[23] K. J. Livak and T. D. Schmittgen, "Analysis of relative gene expression data using real-time quantitative PCR and the $2^{-\Delta\Delta}$CT method," *Methods*, vol. 25, no. 4, pp. 402–408, 2001.

[24] Y. Quan, S. Hua, W. Li, M. Zhan, Y. Li, and L. Lu, "Resveratrol bidirectionally regulates insulin effects in skeletal muscle through alternation of intracellular redox homeostasis," *Life Sciences*, vol. 242, article 117188, 2020.

[25] F. Felicioni, A. D. Pereira, A. L. Caldeira-Brant et al., "Postnatal development of skeletal muscle in pigs with intrauterine growth restriction: morphofunctional phenotype and molecular mechanisms," *Journal of Anatomy*, vol. 236, no. 5, pp. 840–853, 2020.

[26] H. Wan, J. Zhu, G. Su et al., "Dietary supplementation with β-hydroxy-β-methylbutyrate calcium during the early postnatal period accelerates skeletal muscle fibre growth and maturity in intra-uterine growth-retarded and normal-birth-weight piglets," *British Journal of Nutrition*, vol. 115, no. 8, pp. 1360–1369, 2016.

[27] H. Zhang, Y. Chen, Y. Li, L. Yang, J. Wang, and T. Wang, "Medium-chain TAG attenuate hepatic oxidative damage in intra-uterine growth-retarded weanling piglets by improving the metabolic efficiency of the glutathione redox cycle," *British Journal of Nutrition*, vol. 112, no. 6, pp. 876–885, 2014.

[28] K. Cheng, M. Zhang, X. Huang et al., "An evaluation of natural and synthetic vitamin E supplementation on growth performance and antioxidant capacity of broilers in early age," *Canadian Journal of Animal Science*, vol. 98, no. 1, pp. 187–193, 2017.

[29] K. Fiedorczuk and L. A. Sazanov, "Mammalian mitochondrial complex I structure and disease-causing mutations," *Trends in Cell Biology*, vol. 28, no. 10, pp. 835–867, 2018.

[30] M. Pinto and C. T. Moraes, "Mechanisms linking mtDNA damage and aging," *Free Radical Biology & Medicine*, vol. 85, pp. 250–258, 2015.

[31] P. Puigserver and B. M. Spiegelman, "Peroxisome proliferator-activated receptor-γ coactivator 1α (PGC-1α): transcriptional coactivator and metabolic regulator," *Endocrine Reviews*, vol. 24, no. 1, pp. 78–90, 2003.

[32] J. V. Virbasius and R. C. Scarpulla, "Activation of the human mitochondrial transcription factor A gene by nuclear respiratory factors: a potential regulatory link between nuclear and mitochondrial gene expression in organelle biogenesis," *Proceedings of the National Academy of Sciences of the United States of America*, vol. 91, no. 4, pp. 1309–1313, 1994.

[33] H. Zhang, Y. Li, X. Hou, L. Zhang, and T. Wang, "Medium-chain TAG improve energy metabolism and mitochondrial biogenesis in the liver of intra-uterine growth-retarded and normal-birth-weight weanling piglets," *British Journal of Nutrition*, vol. 115, no. 9, pp. 1521–1530, 2016.

[34] F. Haraux and A. Lombes, "Kinetic analysis of ATP hydrolysis by complex V in four murine tissues: towards an assay suitable for clinical diagnosis," *PLoS One*, vol. 14, no. 8, article e0221886, 2019.

[35] K. Tsushida, K. Tanabe, K. Masuda et al., "Estrogen-related receptor α is essential for maintaining mitochondrial integrity in cisplatin-induced acute kidney injury," *Biochemical and Biophysical Research Communications*, vol. 498, no. 4, pp. 918–924, 2018.

[36] S. Rahman and W. C. Copeland, "*POLG*-related disorders and their neurological manifestations," *Nature Reviews Neurology*, vol. 15, no. 1, pp. 40–52, 2019.

[37] J. Zhang, K. W. Bai, J. He et al., "Curcumin attenuates hepatic mitochondrial dysfunction through the maintenance of thiol pool, inhibition of mtDNA damage, and stimulation of the mitochondrial thioredoxin system in heat-stressed broilers," *Journal of Animal Science*, vol. 96, no. 3, pp. 867–879, 2018.